NASA CR-121252
MDC J5738

DC-9/JT8D REFAN PHASE I
FINAL REPORT

by
DOUGLAS AIRCRAFT COMPANY
MCDONNELL DOUGLAS CORPORATION
LONG BEACH, CALIFORNIA

Prepared for
NATIONAL AERONAUTICS AND SPACE ADMINISTRATION
NASA LEWIS RESEARCH CENTER
Contract NAS 3-16814
Arthur A. Medeiros, Project Manager

1. Report No.	2. Government Accession No.	3. Recipient's Catalog No.
NASA CR-121252		

4. Title and Subtitle	5. Report Date
DC-9/JT8D REFAN PHASE I FINAL REPORT	November 1973
	6. Performing Organization Code
7. Author(s)	8. Performing Organization Report No. MDC J5738
	10. Work Unit No.
9. Performing Organization Name and Address Douglas Aircraft Company McDonnell Douglas Corporation Long Beach, California	11. Contract or Grant No. NAS 3-16814
	13. Type of Report and Period Covered Contractor Report
12. Sponsoring Agency Name and Address National Aeronautics and Space Administration Washington, D.C. 20546	14. Sponsoring Agency Code

15. Supplementary Notes

Project Manager, Arthur A. Medeiros, V/STOL and Noise Division
NASA Lewis Research Center, Cleveland, Ohio

16. Abstract

Analyses and design studies were conducted from August 1972 to June 1973 of the technical and economic feasibility of installing the JT8D-109 Refan engine on the DC-9 aircraft. Design criteria included minimum change to the airframe to achieve desired acoustic levels. Several acoustic configurations were studied with two selected for detailed investigations. The minimum selected acoustic treatment configuration results in an estimated aircraft weight increase of 608 kg (1,342 lb) and the maximum selected acoustic treatment configuration results in an estimated aircraft weight increase of 809 kg (1,784 lb). The range loss for the minimum and maximum selected acoustic treatment configurations based on long range cruise at 10 668 m (35,000 ft) altitude with a typical payload of 6 804 kg (15,000 lb) amounts to 54 km (86 n. mi.) respectively. Estimated reduction in EPNL's for minimum selected treatment show 8 EPNdB at approach, 12 EPNdB for takeoff with power cutback, 15 EPNdB for takeoff without power cutback and 12 EPNdB for sideline using FAR Part 36. Little difference was estimated in EPNL between minimum and maximum treatments due to reduced performance of maximum treatment. No major technical problems were encountered in the study. The Refan concept for the DC-9 appears technically feasible and economically viable at approximately $1,000,000 per airplane.

The four and one-half months study of the installation of JT3D-9 Refan engine on the DC-8-50/61 and DC-8-62/63 aircraft is included as an appendix. Three levels of acoustic treatment were suggested for DC-8-50/61 and two levels for DC-8-62/63. Results indicate the DC-8 technically can be retrofitted with Refan engines for approximately $2,500,000 per airplane.

17. Key Words (Suggested by Author(s))	18. Distribution Statement
McDonnell Douglas DC-9/DC-8 Airplanes, JT3D/JT8D Refan Engines, Acoustically treated nacelles, Fly-over noise reduction, Retrofit economics, Deep stall, Noise exposure forecast	Unclassified - unlimited

19. Security Classif. (of this report)	20. Security Classif. (of this page)	21. No. of Pages	22. Price*
Unclassified	Unclassified	332	

* For sale by the National Technical Information Service, Springfield, Virginia 22151

TABLE OF CONTENTS

SUMMARY

The purpose of the DC-9 Refan Program is to establish and demonstrate the technical and economic feasibility of significantly reducing the noise of existing JT8D powered DC-9 aircraft. The Refan Program is divided into two phases.

The objectives of Phase I were to provide engine and nacelle/airplane integration definition documents for installation of the JT8D-109 refan engine on the DC-9 series aircraft, prepare preliminary design of nacelle and airplane modifications, conduct model tests required to obtain design information, analyze the economic and retrofit considerations, and prepare and submit a detailed plan and proposal for Phase II work. Phase II will include detailed analyses, hardware design, fabrication and flight demonstration tests of a DC-9 airplane with modified engines and selected acoustically treated nacelles.

The work described in this report documents the results of the DC-9/JT8D Phase I analysis and design study effort carried out during the period from August 1972 to June 30, 1973, under Contract NAS 3-16814.

The JT8D-109, the refan derivative of the basic JT8D-9 engine, installed on a DC-9-32 airplane was selected for study. Since the Refan Program concept is to retrofit the existing fleet with quieter refan engines and acoustically treated nacelles, the DC-9 systems and structure were examined for minimum change or impact on retrofit while achieving a desired level of performance and noise.

Several acoustic treatment configurations were analyzed and two levels of acoustic treatment were selected for detailed investigation, and are reported herein. The minimum selected treatment has a 1 600.2 mm (63 in.) long inlet and a 1 854.2 mm (73 in.) tailpipe. The maximum selected treatment has a 1 905.0 mm (75 in.) long inlet and a 2 159 mm (110 in.) tailpipe.

The estimated EPNL's for the refanned DC-9-32 aircraft with the minimum selected treatment nacelle installed show a reduction of 8 dB at approach, 12 dB for takeoff with cutback, 15 dB for takeoff without cutback and 12 dB for sideline, using FAR Part 36 rules. There is little difference in the EPNdB between maximum and minimum treatment nacelles, particularly at takeoff, due primarily to the additional weight and thrust loss associated with the maximum treatment which reduces the height over the measuring station.

The installation of the JT8D-109 refan engine results in an operational weight increase of approximately 1 135 kg (2,500 lb) with an aft c.g. shift of 6 to 7 percent M.A.C. for the minimum selected treatment, and 1 360 kg (3,000 lb) operational weight increase for the maximum selected treatment with an aft c.g. shift of approximately 6.25 to 7.25 percent. The combined effects of increases in operational empty weight and improved engine SFC including the effect of nacelle and pylon drag changes based on long range cruise at 10 668 m (35,000 ft) results in a range loss of 54 km (29 n. mi.) and 159 km (86 n. mi.) on a typical payload mission for the minimum and maximum treatment respectively.

The retrofit and economic analysis indicates the unit price of the refan kit will be approximately $1,000,000 with about an equal split between the airframe and engine cost and that production kits could be made available by late 1975 or early 1976.

The work accomplished in Phase I indicated no major technical problems for installing the JT8D-109 refan engine on DC-9 aircraft; and that aircraft noise reduction using the refan concept is economically as well as technically feasible. Further, it was also concluded and proposed that the Phase II effort be directed toward design and fabrication of flightworthy hardware for the minimum acoustic treatment configuration and a flight demonstration program to substantiate the noise reduction capabilities of the refan concept.

Phase I also included the JT3D-9 refan engine installed on the DC-8 series 50/60 aircraft. All work on the DC-8 portion of the Refan Program was terminated after four and one-half months except for the high-speed wind tunnel test on the DC-8-50 and -61 models. This test was conducted and completed between January and April 1973, and reported in CR 121218.

Although the study was only approximately 65 percent complete several acoustic treatment configurations were selected for the preliminary design effort and are reported herein. The nacelle configurations identified for the DC-8 model 50 and 61 JT3D-9 refan engine installation covered three levels of acoustic treatment and are designated maximum, intermediate and minimum. Two levels of acoustic treatment, maximum and minimum, were identified for the DC-8-63/62 refan engine installation.

The retrofit and economic analysis estimated the retrofit costs between 2.3 and 2.5 million dollars per aircraft for the DC-8-61/-50's and between 2.1 and 2.3 million dollars per aircraft for the DC-8-63/-62's depending upon the noise treatment level desired.

The results (as of the program termination date) show that it is technically feasible and economically viable, assuming low cost financing and no spillover effects, to refan the DC-8 fleet provided that the noise reductions significantly contribute to improving the near airport noise environment.

INTRODUCTION

As a result of the continuing growth of the air transportation industry and the resulting increasing population density of communities near airports, numerous public actions have been initiated in an effort to control human exposure to aircraft noise. Some examples are: the enactment of Public Law 90-411; the issuance of new Part 36 of the Federal Aviation Regulations prescribing noise standards for new aircraft; the enactment of aircraft noise regulations by state and local governments; the adoption of operations curfews; limitations on expansions in the service at existing airports; and adverse public testimony in hearings related to proposals for new airports or expansion of existing ones. These actions can severely inhibit the continued growth of commercial aviation with its related national benefits. Government and industrial organizations have, therefore, agressively supported programs directed at producing airplane and engine designs offering meaningful reductions in airport community noise.

Research related to the generation of noise within the engine itself has developed effective principles for the design of reduced-noise-output turbofan engines. Research related to the absorption materials within the nacelle ducting has been similarly productive. These design principles are sufficiently refined to have been applied to the development of the quieter high by-pass ratio turbofan power plant installations for the new generation of wide-body commercial transports. The favorable public reaction to the lower noise levels of these new aircraft has been a gratifying result of these research programs.

However, the existing and expanding fleet of standard-bodied commercial transports powered by low by-pass ratio turbofan engines will continue to be the greatest contributor to the aircraft noise problem in the airport communities. These airplanes are noisier and far more numerous than the new generation wide-bodied high by-pass ratio turbofan powered, commercial transports.

Most of these commercial transports are powered by either JT3D or JT8D series engines. The low by-pass ratio turbofan engines and the standard-bodied transports have been continuously improved and updated such that those now coming from production lines are generally considered modern in every respect and are expected to remain in airline inventories as long as they remain economically competitive. Studies are therefore necessary to determine the technical and economic feasibility of reducing the noise of these transports.

There are four basic approaches or combinations of these approaches for reduction of existing commercial transport noise: (1) aircraft retirement, (2) nacelle acoustic treatment possibly including a jet noise suppressor, (3) engine and nacelle modifications, (4) a completely new engine and nacelle. Various studies by government and industry have considered all of these approaches. Approaches (1) and (4) are not competitive in terms of timeliness

or cost. Considerable effort has been applied to approach (2) and this solution is still being evaluated. Recent studies and technology work indicate that approach (3), engine and nacelle modifications, could be particularly attractive because the performance losses from nacelle treatment and jet noise suppression can be partially recovered due to improved thrust and SFC of the refanned engine, while not being as costly as a completely new engine.

Replacement of the present low by-pass ratio engine fans with larger quieter fans, while maintaining the hardware and general operating characteristics of the core engine, would shift the by-pass ratio in a direction toward the new high by-pass ratio engines which offer the unique advantages of: (1) substantial noise reduction, particularly jet exhaust noise for which other quieting methods have proved to be relatively ineffective or impractical, and (2) improved engine performance which would permit the use of nacelle modifications (addition of large areas of acoustic treatment) for further quieting without unacceptable airplane performance penalties.

The refanned JT8D and JT3D engines are designated JT8D-109 and JT3D-9 and will be referred to in this document by these designations and/or as refanned engines.

The purpose of this program is to develop and demonstrate the technical and economic feasibility of reducing noise by developing quieter engine and nacelle modifications in the form of flight hardware. The engine and aircraft that are covered are the JT3D engine and the airplanes it powers in the Douglas DC-8 series and the JT8D engine and the airplanes it powers in the Douglas DC-9 series. The program also covers Boeing 707, 727, and 737 airplanes powered by the JT3D and JT8D engines.

Under NASA Contract NAS 3-16814, the Douglas Aircraft Company was authorized to proceed with Phase I of a two-phase program. This contract was one of several independent Phase I contracts signed with Pratt and Whitney, The Boeing Company, United Air Lines, and American Airlines.

The objectives of the Phase I effort were to:

(1) Provide engine and nacelle/airplane integration definition documents for installation of the JT8D-109 engine on the DC-9 series airplanes and the JT3D-9 engine on the DC-8 series 50/60 airplanes.

(2) Prepare preliminary design of nacelle and airplane modifications for installing the JT8D-109 and JT3D-9 engines on the DC-9-32 and DC-8 series 50/60 airplanes, respectively.

(3) Initiate model tests of DC-9 and DC-8 nacelle and airplane configurations.

(4) Analyze the economic considerations of the JT8D-109 and JT3D-9 engines and the noise reduction tradeoffs in retrofitting these engines on the DC-9 series 10/30 and DC-8 series 50/60 airplanes, respectively.

(5) Prepare and submit a detailed plan and proposal for Phase II.

As originally conceived, Phase I included the JT3D-9 refanned engine mounted on the DC-8 series 50/60 airplanes; however, after approximately four and one-half months, all effort on the DC-8 series 50/60 airplanes (with the exception of the high-speed wind tunnel test) was terminated and a report submitted to NASA. A summary of this report is also presented in Appendix D.

This report is directed primarily at the DC-9-32 airplane with a takeoff gross weight of 48 989 kg (108,000 lb), a fuel capacity of 16 m^3 (4,259 gal), and JT8D-9 production engines modified to JT8D-109 refan engines. However, most descriptive material included herein is applicable to other versions of the basic DC-9 aircraft. All performance calculations presented are for the DC-9 equipped with JT8D-9 or JT8D-109 engines. Data for the refan JT8D-109 engine were obtained from Pratt and Whitney Aircraft, report PWATM-4713, 13 April 1973.

The results and conclusions from the Douglas Aircraft Company effort on objectives (1), (2), (3), and (4), are presented in this document. Objective (5) was completed when Douglas presented proposal documents which included a statement of work, schedule and costs for a Phase II flight demonstration of a DC-9 equipped with refanned engines and acoustically treated nacelles.

This report contains both U.S. Customary and SI Units; however, all calculations and measurements were made using the U.S. Customary Units.

DC-9 SERIES AIRPLANE DESCRIPTION

Figure 1 shows a simplified genealogy of the DC-9 family starting from the first models and showing the important changes made from model to model through the latest "stretched" versions. The most significant change in the DC-9 models was introduced with the initiation of the DC-9-30 Series. At that time, the fuselage was lengthened approximately 4 572 mm (179 in.), the wing span was increased 1 219 mm (48 in.) and full span leading edge slats were incorporated.

Table 1 shows the current disposition of the first 697 DC-9 production aircraft. On the basis of the numbers of aircraft (506) in service the DC-9-32 has been selected as the model to be studied. Other DC-9 models will be examined for differences that will affect the economics of retrofit or the amount of noise reduction available. Of the three engine models in service, the JT8D-11 is used exclusively in foreign service. The JT8D-9 is the higher thrust version used on the domestic aircraft and, therefore, constitutes a suitable study baseline engine.

The DC-9-32, shown in figure 2, is the "stretched" version of the DC-9 airplane using JT8D-9 engines installed in "long duct" pods. The pod is characterized by a full-length, annular fan exhaust duct supplied as an integral part of the engine. The duct mixes and discharges the fan air with the primary air at the aft end of the nacelle. It also features a single target-type reverser to reverse the fan and primary exhaust streams.

The DC-9 aircraft has established an excellent in-service record for maintainability, reliability, safety, economical and efficient service. The installation of the JT8D-109 engine must not compromise this record. The JT8D-109 refan engine offers improved engine performance and a substantial reduction in noise, particularly jet exhaust noise; however, the refan engine is also heavier and larger in diameter than the JT8D-9 engine. Therefore, the primary concerns for the installation of the refan engine on the DC-9 airplane involves the effects of the larger refan engine nacelle on airplane drag and deep stall recovery margin; the effects of the higher refan engine thrust on minimum control speeds and increased reverse thrust loads; the effects of the increased weight of the refan engine on airplane loads during hard landing and airplane aft c.g. limits; airplane stability and control characteristics; aerodynamic and inertia loads on wing flutter; and the incorporation of maintenance and access provisions for engine accessories.

The success of the refanning concept will depend, to a large extent, on the ability to design effective duct liners to capitalize on the noise reduction capabilities of the refan engine. Considerable effort must be directed towards the method by which nacelle treatment will be used to ensure that each nacelle configuration represents the most effective application of the amount of treatment contained in that particular design. This requires that the suppressed noise levels from the inlet and exhaust ducts be balanced or equal.

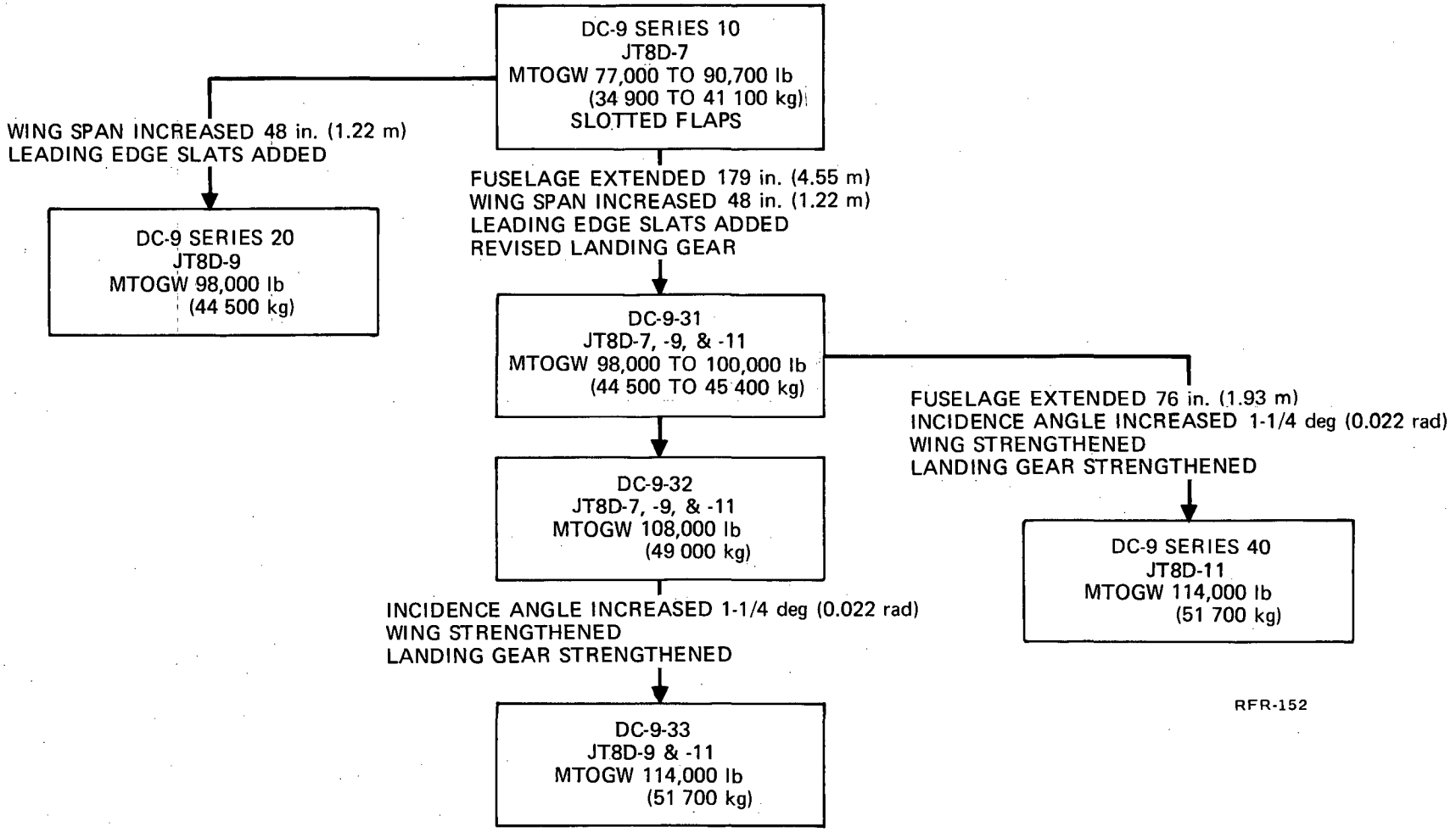

FIGURE 1. DC-9 GENEALOGY

TABLE 1

DC-9 FLEET THROUGH 1973

DC-9 MODEL	JT8D MODEL	DOMESTIC	FOREIGN	WORLD
EXPECTED FLEET THROUGH 1973:				
-10	-7	94	40	134
-20	-9	-	10	10
-31 AND -32	-7	246	117	363
-31 AND -32	-9	36	104	140
-31 AND -32	-11	-	3	3
-33	-9	2	16	18
-33	-11	-	3	3
-40	-11	-	26	26
TOTAL FLEET AT 12-31-73:		378	319	697

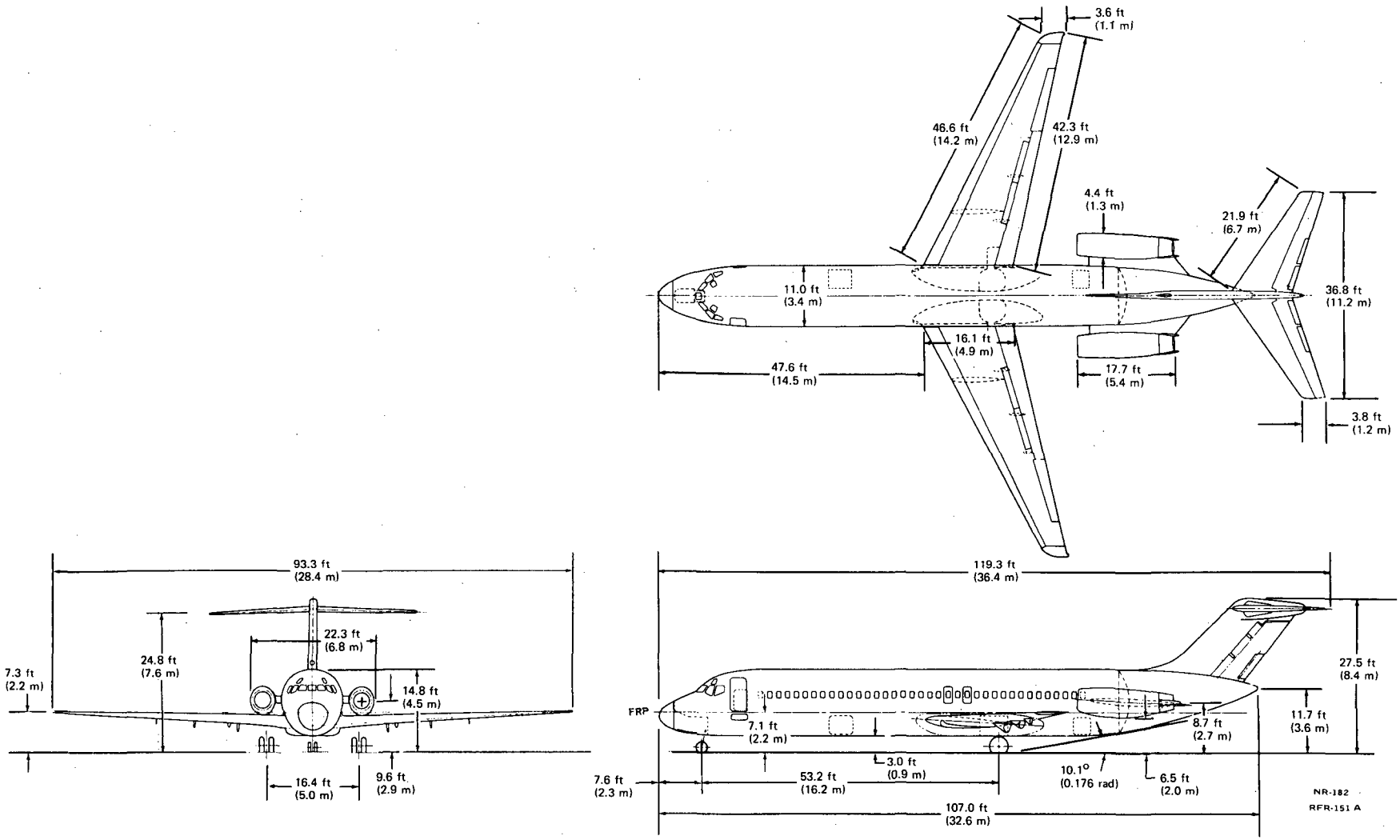

FIGURE 2. DC-9-32 THREE-VIEW

PRELIMINARY DESIGN

The modified refan nacelles, designed to achieve minimum and maximum noise suppression of the JT8D-109 refan engine, retain the existing installation concept of the DC-9 airplane.

The nacelle design selected to provide minimum noise suppression utilizes acoustically treated inlet and exhaust ducts, similar to the existing design. This design retains the "long duct" concept with mixed primary and fan air exhaust. The existing thrust reverser has been scaled up to accommodate the increased fan and primary duct areas and engine exhaust flow rates. Acoustic treatment has been incorporated in the nose cowl on the inner surface and in the exhaust duct on the inner walls of the tailpipe. Although the existing DC-9-32 major nacelle accessories have been retained with little or no modification, the increased fan case diameter of the refan engine necessitates redevelopment of much of the associated subsystem ducting, piping, and wiring.

The selected maximum noise suppression nacelle design differs from the minimum in that the inlet and exhaust ducts have been made longer to accept additional acoustic treatment. The engine and nacelle subsystems and accessories for the maximum treatment nacelle are essentially identical to the minimum treatment design. Figure 3 compares the existing JT8D-9 nacelle with the minimum and maximum acoustic treatment JT8D-109 refan engine nacelle.

The new nacelles, shown in figures 4 and 5 , each require a new pylon, a new nose cowl, a new thrust reverser, new upper and lower main access doors and a new pylon apron. Additional features of the new nacelle are summarized below:

- Fixed geometry minimum and maximum treatment inlets have been designed and sized to the flow requirements of the new fan and provided with a lip design (based on DC-10 experience) to prevent separation. The new inlets incorporate acoustic treatment along the inner flow surface of the duct walls.

- New engine mounts are required to accommodate the increased weight, increased engine diameter, and forward shift of the engine center of gravity.

- The radial growth of the refan engine necessitates new upper and lower access doors.

- The new minimum and maximum treatment ducts are sized for the larger flow of the JT8D-109, and incorporate acoustical treatment along the inner duct wall.

- The existing nacelle subsystems are retained with little or no modification to the components, but with extensive redevelopment of piping, ducting and wiring.

- The new thrust reverser is a scaled-up version of the existing DC-9 reverser.

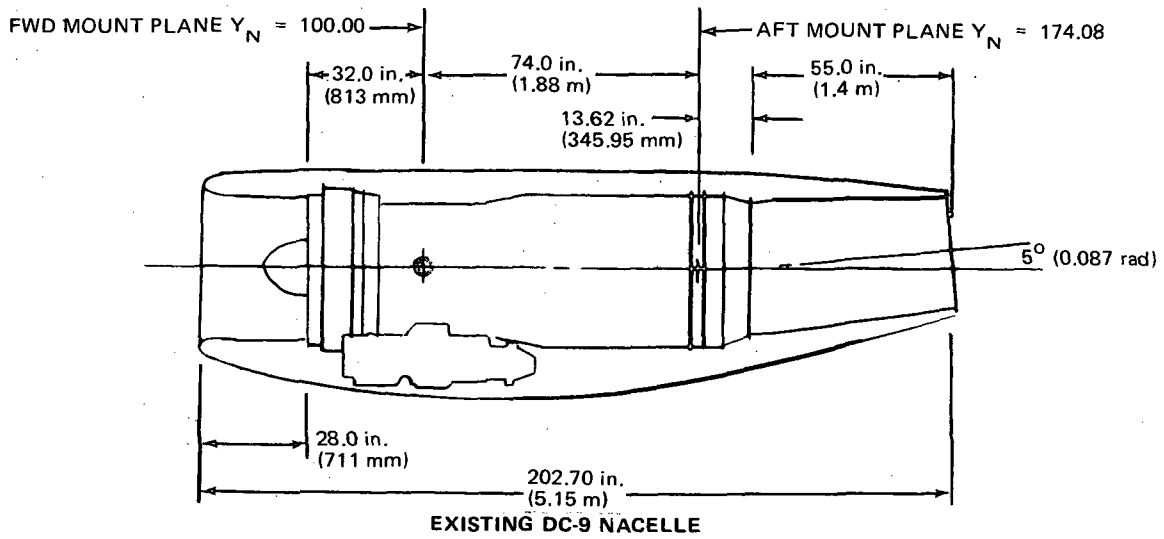

EXISTING DC-9 NACELLE

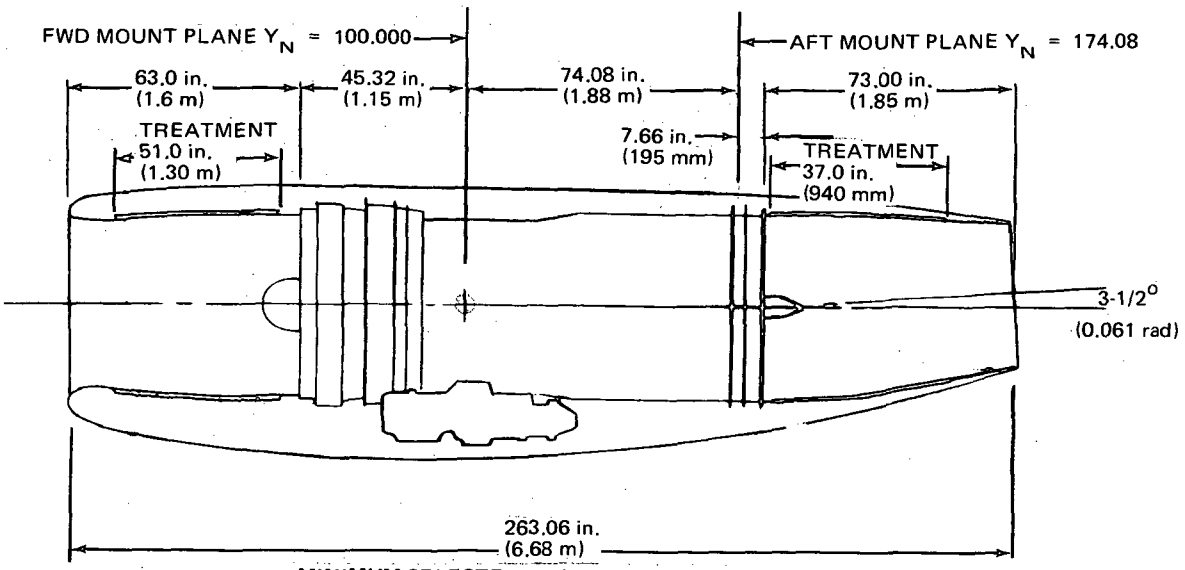

MINIMUM SELECTED ACOUSTIC TREATMENT

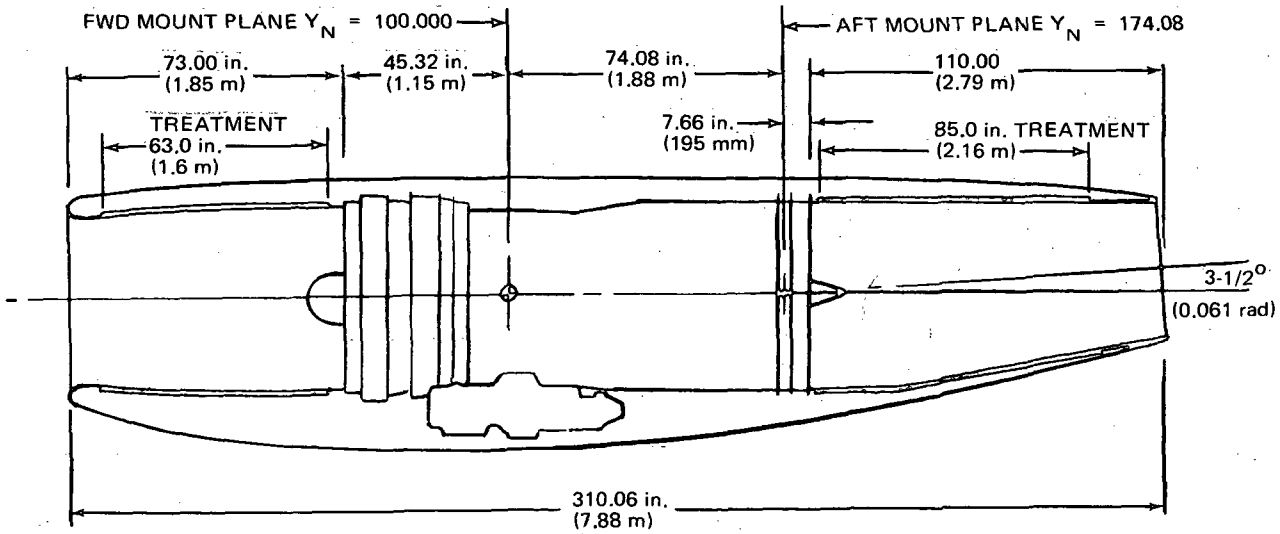

MAXIMUM SELECTED ACOUSTIC TREATMENT

RFR-014

FIGURE 3. DC-9 NACELLE COMPARISON

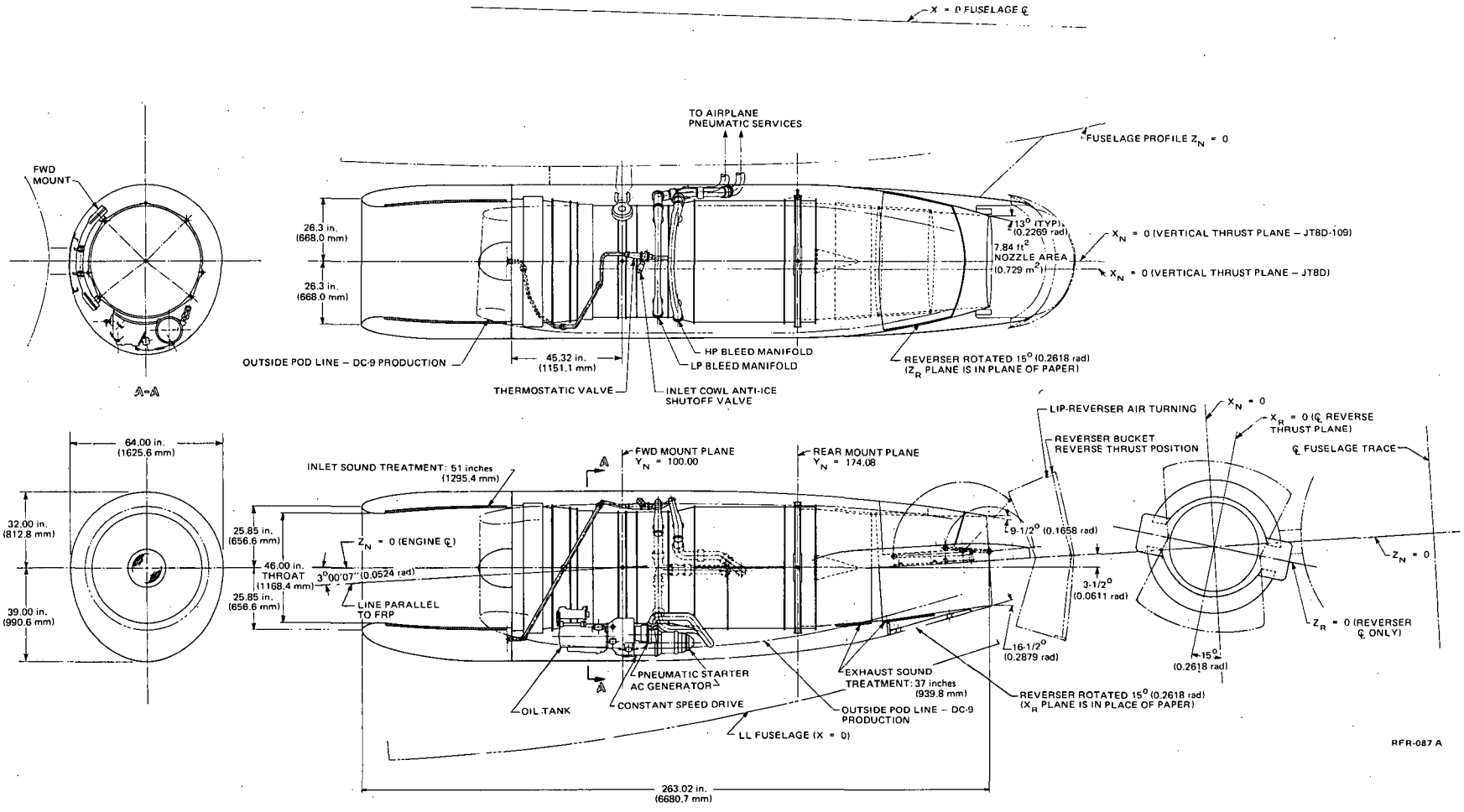

FIGURE 4. NACELLE GENERAL ARRANGEMENT – MINIMUM SELECTED ACOUSTIC TREATMENT, DC-9

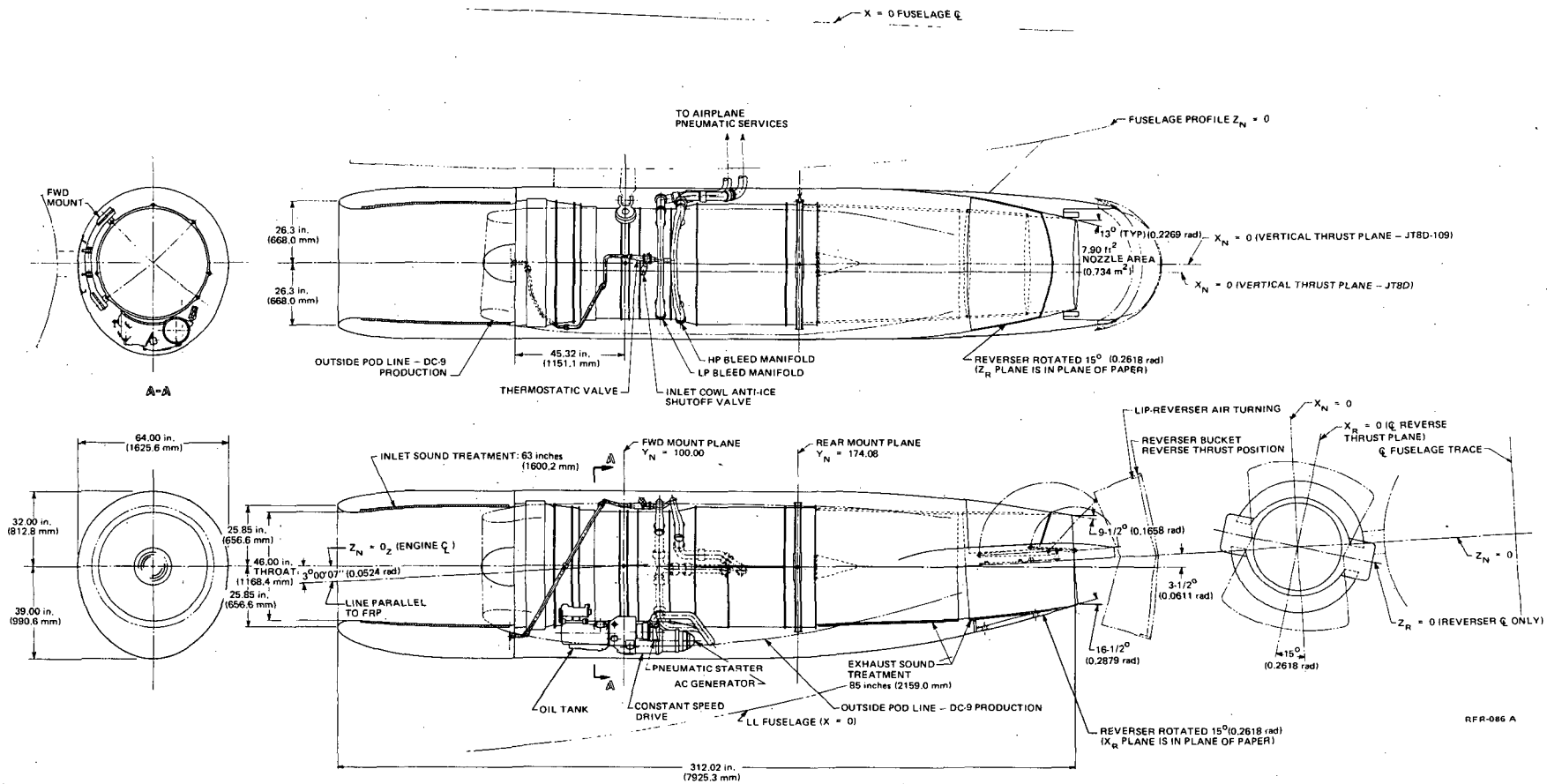

FIGURE 5. NACELLE GENERAL ARRANGEMENT – MAXIMUM SELECTED ACOUSTIC TREATMENT

Nacelle Aerodynamic Design

The aerodynamic design of the JT8D-109 inlet and nacelle is based on existing DC-9 lines and also on more recent DC-10 inlet and nacelle design information. Attached boundary layer flow with very low engine face distortion has been demonstrated with the DC-9 inlet. The JT8D-109 inlet has even less risk of separation due to thicker inlet lips, lower throat Mach numbers, and lower diffuser section wall angles.

DC-10 aerodynamic design information was used to achieve outstanding inlet crosswind capability, and to make possible a minimum frontal area nacelle with no inlet spillage drag. Wind tunnel tests have demonstrated excellent nacelle drag characteristics for the JT8D-109 installation.

External aerodynamic design. - The geometric characteristics of the minimum treatment JT8D-109 nacelle, the maximum treatment nacelle and the existing DC-9 nacelle are compared in figure 6 and table 2. The maximum treatment nacelle dimensions are the same as those of the minimum treatment nacelle except that the overall nacelle length is longer by 1.244 m (49 in.).

The new JT8D-109 minimum and maximum selected noise suppression nacelles are designed to enclose the engine and accessories with a minimum nacelle size. Therefore, the cowl frontal area has been set by engine and accessory packaging requirements rather than by inlet spillage drag considerations. Inlet spillage drag will not occur at cruise conditions.

The JT8D-109 cowling design is based on DC-10 cowl development test data obtained at the Calspan 8-foot wind tunnel and correlated with DC-10 flight test data. This cowling has a more efficient shape than the existing DC-9 cowling allowing larger inlet areas and lip thicknesses to be used for a given nacelle frontal area and spillage drag divergence Mach number.

The cowl afterbody boattail angles were made equal to the boattail angles of the existing DC-9 nacelle. Also, the rates of curvature on the afterbody are approximately the same as those on the existing DC-9 nacelle to minimize the possibility of strong shock waves or boundary layer separation on the cowl afterbody at cruise conditions.

On the existing DC-9 nacelle, the reverser bucket trailing edge forms the nacelle trailing edge. This results in a large base area and measurable base drag penalty since the trailing edge of the reverser buckets is blunt. For the JT8D-109 nacelle, the trailing edge of the reverser buckets has been located upstream of the nacelle trailing edge, with a fixed fairing between the bucket and nacelle trailing edge. This allows the nacelle base area and consequent base drag to be minimized.

Wind tunnel tests (ref. 1) in the NASA Ames 11-foot wind tunnel have shown that for the JT8D-109 nacelle installed on the DC-9 boundary layer separation or strong shock waves do not occur on the nacelle at cruise conditions. Force measurements showed that the incremental drag due to installation of the nacelles was equal to the estimated incremental skin friction and form drag for waves. Moreover, this increment existed only at low Mach numbers. At a

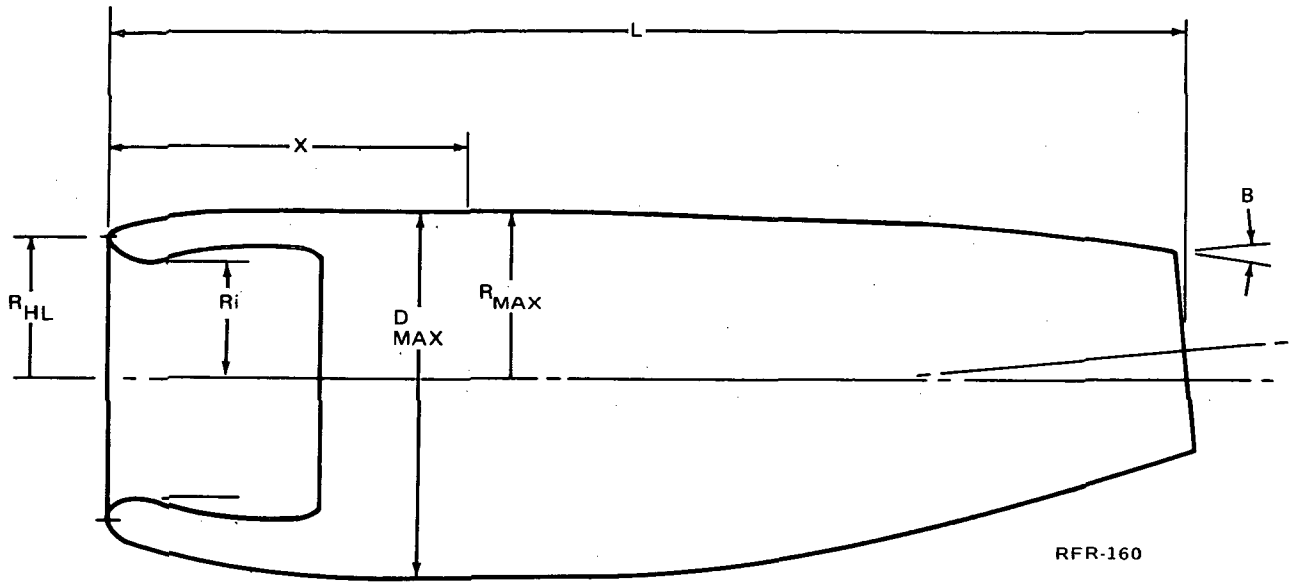

FIGURE 6. NACELLE - AERODYNAMIC SCHEMATIC

TABLE 2

NACELLE AERODYNAMIC DESIGN SUMMARY

		EXISTING JT8D-9	MINIMUM SUPPRESSION JT8D-109	MAXIMUM SUPPRESSION JT8D-109
A. Cowl:				
(1) Nacelle Length, L	in. mm	201.5 (5118)	263.02 (6681)	312.02 (7925)
(2) Maximum Diameter In Plan View ($D_{max} = 2R_{max}$)	in. mm	53.0 (1346)	64.0 (1626)	64.0 (1626)
(3) Maximum Area, A_{max}	ft^2 m^2	17.1 (1.589)	24.8 (2.304)	24.8 (2.304)
(4) Diameter at Exhaust Nozzle	in. mm	31.5 (800)	38.5 (978)	38.5 (978)
(5) Cowl Radius Ratio, R_{HL}/R_{max}				
Top		0.798	0.808	0.808
Side		0.788	0.822	0.822
Bottom		0.620	0.663	0.663
(6) External Cowl Length, X				
Top	in. mm	54.0 (1372)	34.0 (864)	34.0 (864)
Side	in. mm	34.0 (864)	34.0 (864)	34.0 (864)
Bottom	in. mm	54.0 (1372)	60.0 (1524)	60.0 (1524)
B. Afterbody:				
(1) Exhaust Boattail - Angle B	deg rad	13.0 (.227)	13.0 (.227)	13.0 (.227)

typical cruise Mach number (M_0 = 0.78) there was a favorable drag effect, that resulted from a change in the wing pressure distribution due to the presence of the larger entering stream tube and the more forward location of the JT8D-109 inlet.

The wind tunnel tests were conducted with a nacelle configuration that did not conform exactly to the JT8D-109 nacelle lines. However, the test configuration was similar enough that the wind tunnel results could be applied to the JT8D-109 minimum or maximum treatment nacelles. A comparison of the JT8D-109 minimum treatment nacelle configuration and the wind tunnel configuration is shown in figure 7.

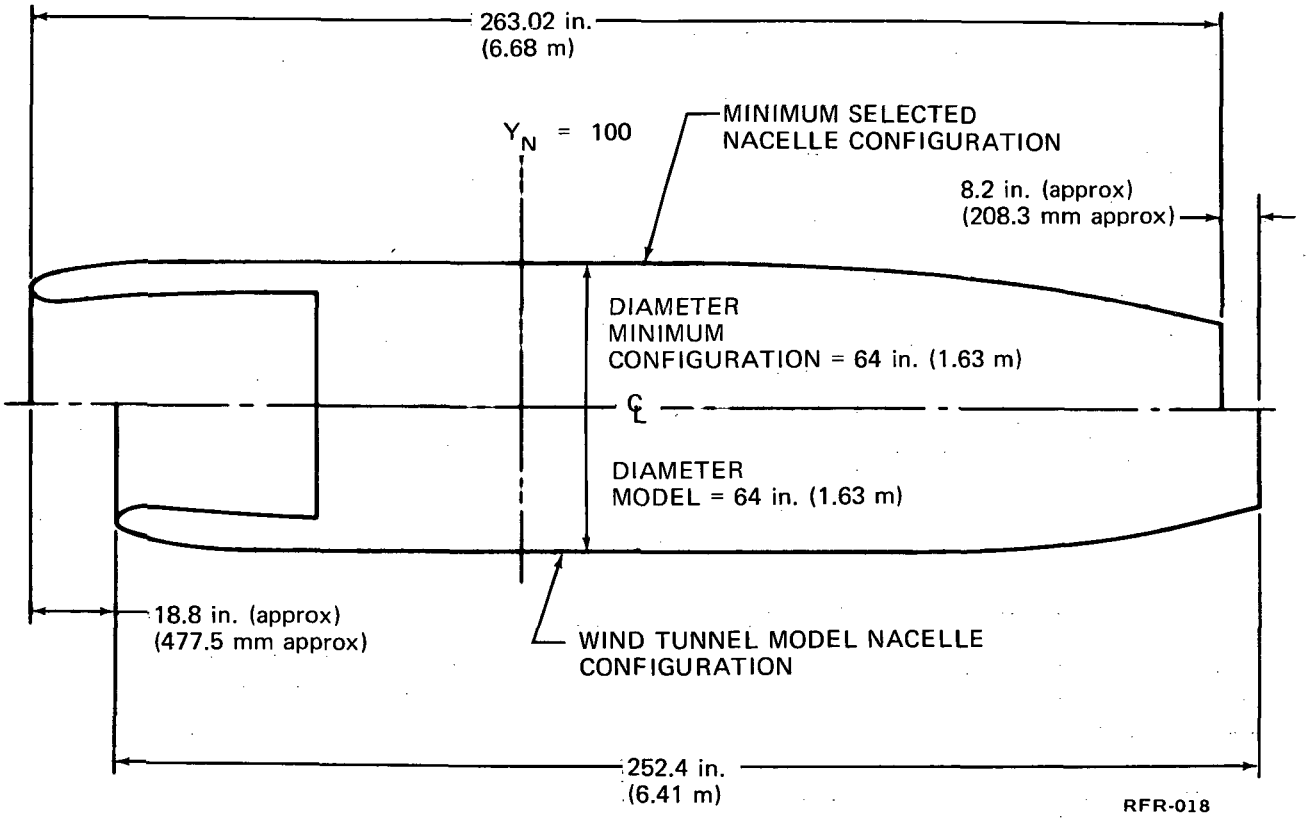

FIGURE 7. NACELLE COMPARISON

Inlet system aerodynamic design.. - The inlet diffuser section geometry was defined by acoustic and economic considerations rather than aerodynamic (Nacelle Acoustic Treatment Cost Trade Study Appendix B). The minimum treatment inlet for the JT8D-109 engine has wall treatment only, a long diffuser section and low divergent wall angles. The diffuser section area distribution is shown in figure 8. The maximum treatment inlet is the same as the minimum treatment inlet except for an additional 305 mm (12 in.) length of cylindrical duct section at the end of the diffuser section.

Other inlet configurations with an acoustically treated bullet and/or rings were considered. These inlets have shorter diffuser sections for a given level of inlet noise attenuation, but were slightly more expensive in conversion cost and operating cost than the baseline configurations.

The inlet throat area is 1.072 m^2 (11.54 ft^2) compared to 0.693 m^2 (7.44 ft^2) for the existing DC-9 inlet. The JT8D-109 inlet Mach numbers are lower than those for the existing DC-9 inlet as shown by table 3. The inlet was sized for relatively low throat Mach numbers to allow for possible engine airflow growth. The inlet lip thickness varies with circumferential location and is thicker on the sides of the inlet as shown by figure 9. The minimum lip thickness is 11 percent of the highlight radius, the maximum lip thickness is 12.5 percent. For the existing DC-9 inlet, the lip thickness is constant at all circumferential locations and equal to 11 percent of the lightlight radius.

The inlet lip thickness is larger on the side of the JT8D-109 inlet for additional operating margin in crosswind without inlet boundary layer separation. DC-10 full scale tests and model scale tests have shown considerable improvement in crosswind capability with this type of inlet lip design. Inlet operation at takeoff power with crosswinds of 40 knots have been demonstrated.

It was possible to design the JT8D-109 inlet with thicker inlet lips and lower inlet Mach numbers because the maximum frontal area of the nacelle, which was dependent on engine and accessory packaging requirements, was large enough for zero inlet spillage drag at cruise conditions. The inlet for the JT8D-109 engine will not have significant boundary layer separation inside the inlet for any flight test or operational conditions.

TABLE 3

INLET THROAT MACH NUMBERS

FLIGHT CONDITION	THROAT MACH NUMBER M_i	
	JT8D-9	JT8D-109
Sea Level Static Takeoff	0.63	0.58
M_o = 0.8 at 30,000 ft (9 144 m) Maximum Cruise Power	0.64	0.61

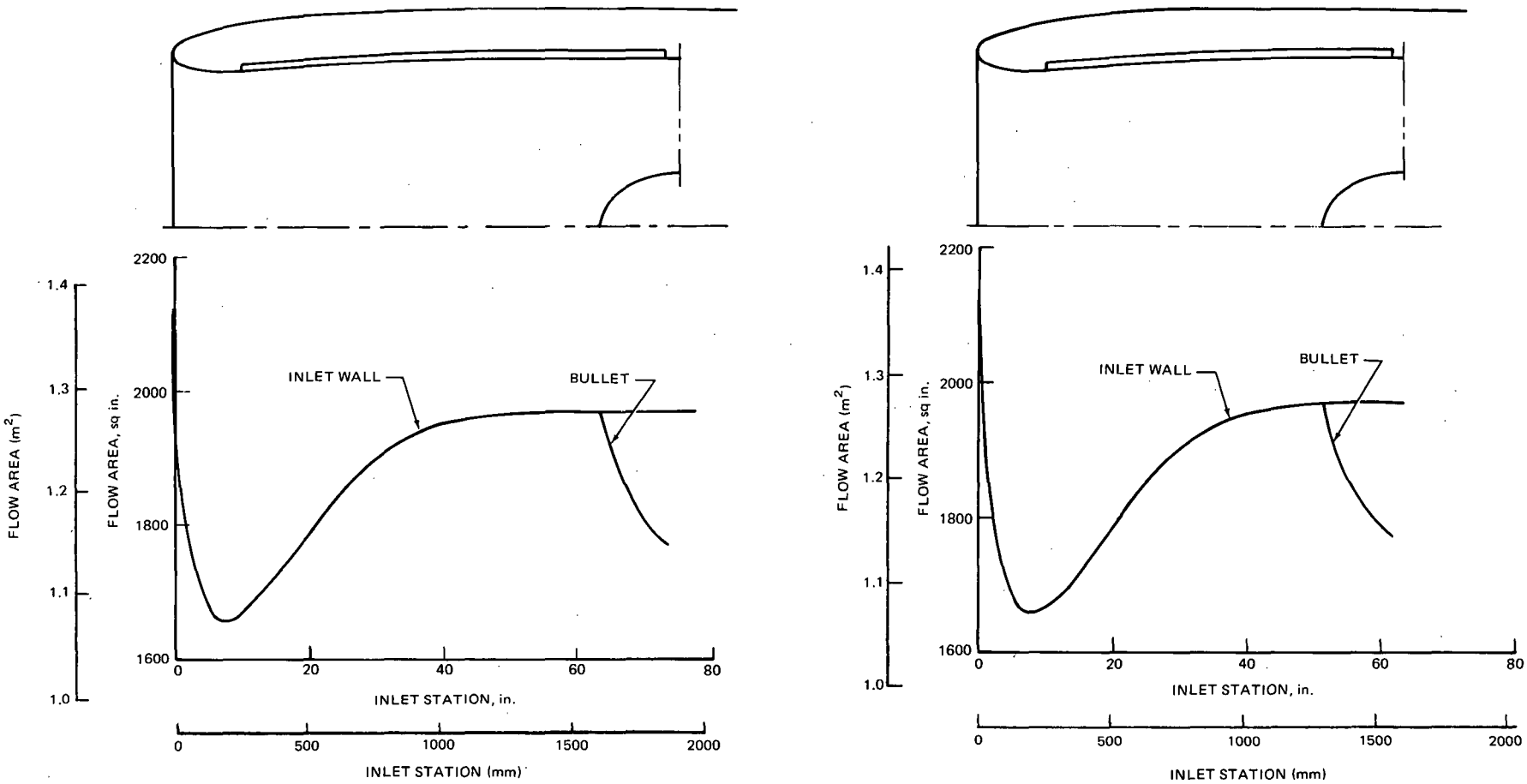

FIGURE 8. DC-9-32 INLET DIFFUSER AREA DISTRIBUTION

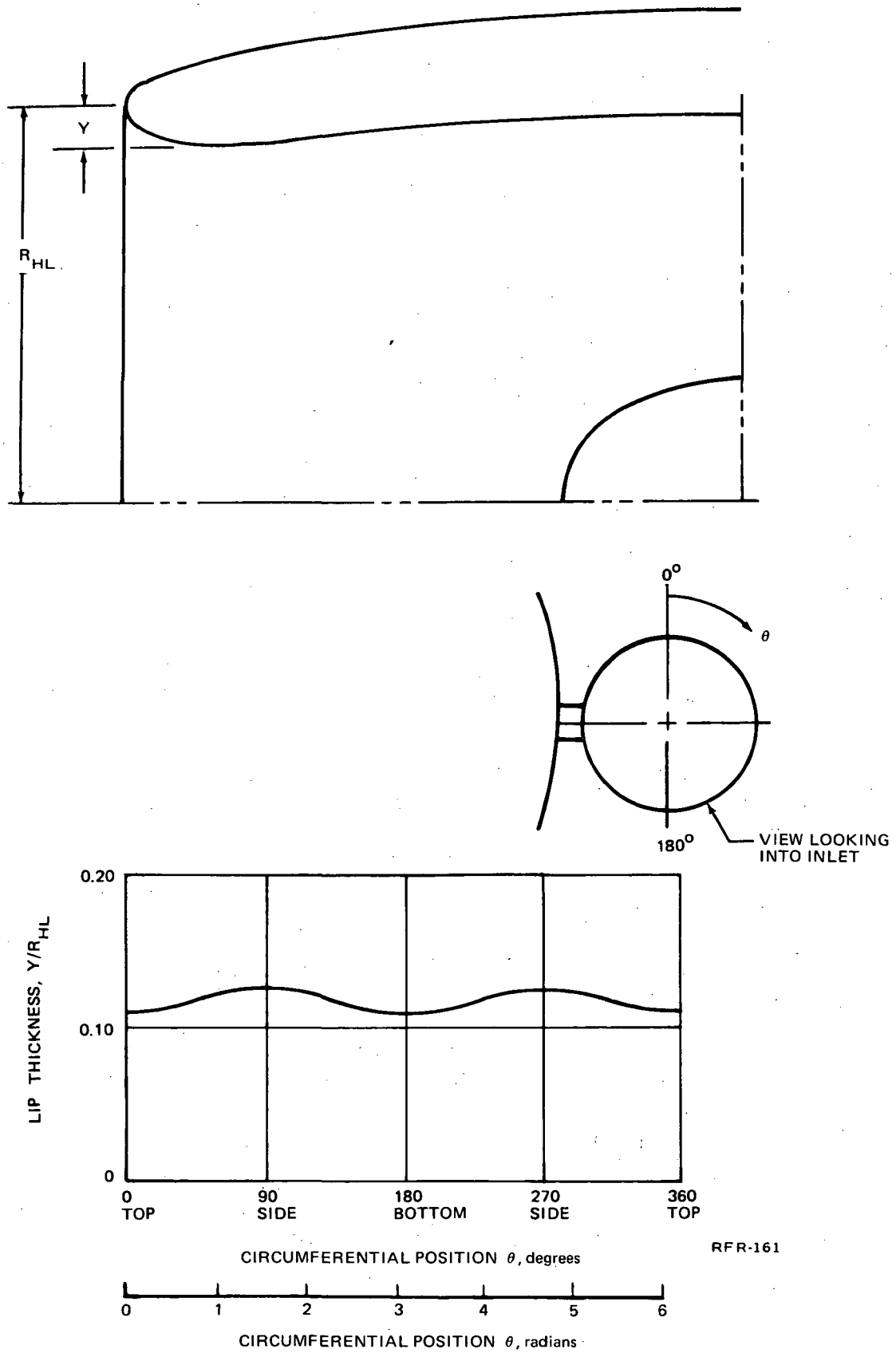

FIGURE 9. DC-9 (JT8D-109 ENGINE) INLET LIP THICKNESS CIRCUMFERENTIAL VARIATION

Exhaust system aerodynamic design. - The exhaust duct is designed to retain the proper wall curvature for minimum external boattail angle and low duct Mach numbers, aiding the sound attenuation characteristics and yielding good performance. The duct throat area is sized to provide an engine match at takeoff power.

The flow area distribution for the minimum and maximum treatment exhaust ducts are shown in figure 10. Those area distributions were calculated using a duct design definition computer program which estimates the flow area distribution from the duct geometry and calculates the one-dimensional flow properties based on the estimated flow areas. Estimated distributions in flow velocity, temperature, and Mach numbers near the treated surface for the minimum and maximum treatment configurations are shown in Appendix A.

The final lines of the exhaust system will be selected with the aid of the analytical methods described below. In particular, these methods will be used to help define the shape of the splitter that divides the fan and core streams up to the entrance of the exhaust nozzle, the contour of the outer nozzle wall in that region of the duct, and the plug.

The overall procedure involves making detailed flow calculations to define the wall surface pressure distributions and use those pressure distributions in conjunction with boundary layer analysis to evaluate the configuration for regions of possible flow separation. The process is cycled to arrive at a configuration that is free of separation problems.

The Douglas developed Neumann potential flow program is being used to estimate the flow field in the vicinity of the trailing edge of the core/fan splitter in the exhaust duct. This program represents the shape to be analyzed by a system of sources and sinks, and solves for the source density distribution necessary to make the normal velocities on the surface zero. In addition to the flow field in the duct, the program also computes surface pressure distributions.

Surface pressure distributions from the Neumann program are used with the Cebeci boundary layer program to calculate boundary layer properties. That program calculates the structure of compressible turbulent boundary layers using a finite difference calculation technique and predicts boundary layer separations as dictated by the pressure distribution.

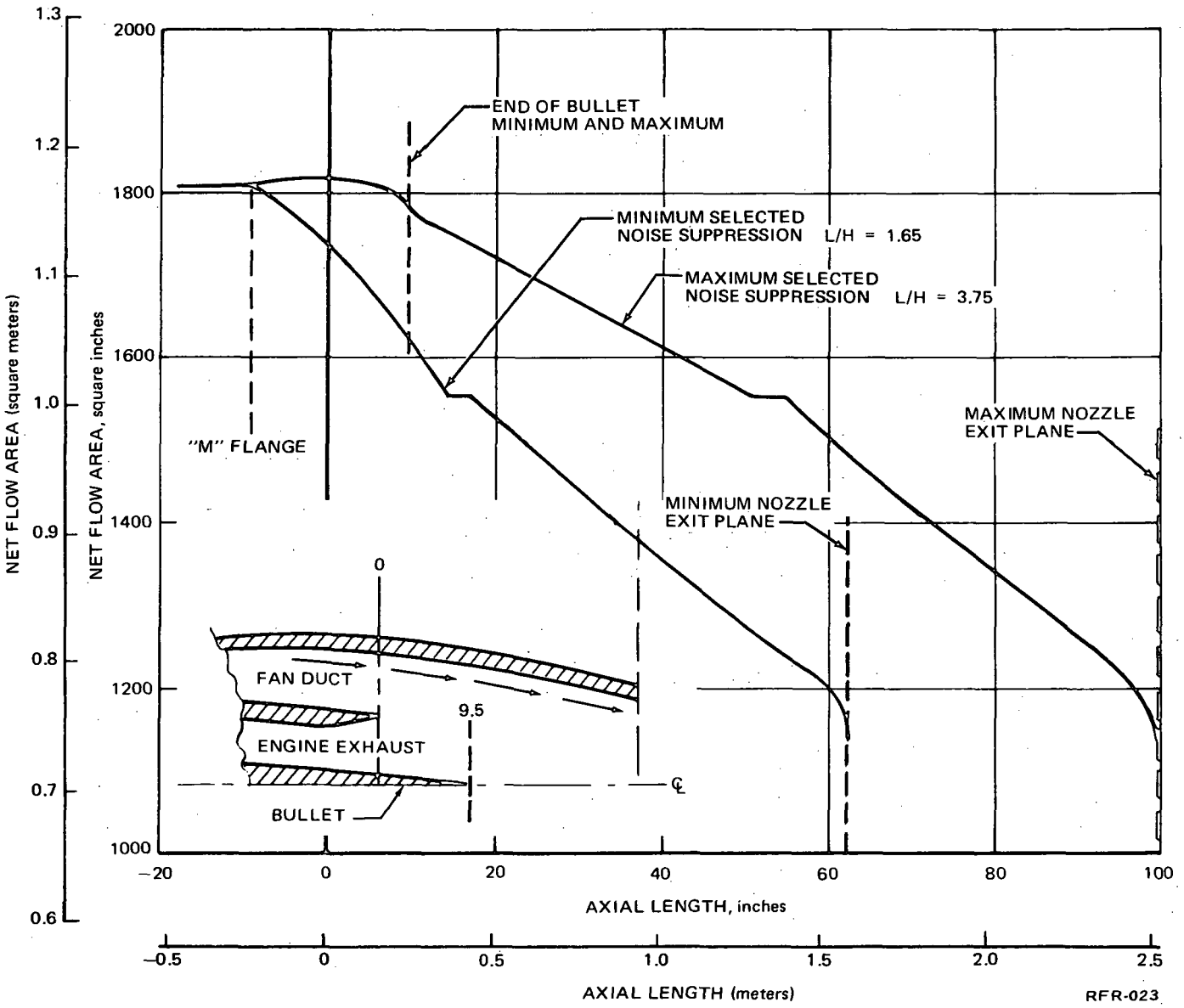

FIGURE 10. EXHAUST DUCT AIR FLOW DISTRIBUTION

Acoustic Design

This section presents the acoustic rationale for the inlet and tailpipe configuration selection, the definition of the detailed acoustic treatment and the flyover noise level predictions. The procedure in the inlet and tailpipe selection was to estimate the various untreated engine component noise sources (fan inlet and exhaust, turbine, low frequency core, and primary and bypass jet noise) for the FAR Part 36 0.052 rad (3 deg) approach, cutback, and sideline conditions. These noise predictions and acoustic treatment designs are based on Douglas prediction methods and Pratt and Whitney supplied engine cycle parameters.

An acoustic design chart was prepared to aid in the selection of inlet and tailpipe (exhaust nozzle) acoustic treatment. This chart, figure 11, is based on approach conditions and relates the inlet and tailpipe noise reduction to the amount of acoustic treatment. The tailpipe treatment is determined as a function of the ratio of the treated duct length to the channel height (L/H) and the inlet treatment is referenced to the length of the treated cowl wall and the bullet and ring configuration.

The design chart is configured to give approximately balanced configurations, that is, tailpipe and inlet scales are adjusted vertically so as to give equal inlet and aft fan flyover noise if both the inlet and tailpipe are chosen to give the same PNdB (Perceived Noise Level) from the chart. The exhaust nozzle intercepts 11 PNdB at zero treated length. This 11 PNdB is the attenuation of the fan noise by the treated fan duct supplied with the engine. Treatment in the tailpipe gives attenuations additive to that of the fan duct. The inlet treatment curves intercept 5 PNdB at zero treated length. This 5 PNdB results from the engine case treatment forward of the rotor (about 1 PNdB) and the predicted relative level of the untreated inlet noise below the aft radiated untreated fan noise during flyover approach conditions.

The minimum level of selected treatment resulted directly from the minimum aerodynamic tailpipe length. This gave a treated tailpipe L/H of 1.65. Several inlets were investigated for this tailpipe in the "Nacelle Acoustic Treatment Cost Trade Study" and an inlet with 1.3 m (51 in.) of cowl treatment only was chosen. Tailpipe L/H values up to 5.3 were investigated in selecting the maximum configuration. The final selection for the maximum treatment was a tailpipe L/H = 3.75 and an inlet with 1.6 m (63 in.) of cowl wall only treatment.

The acoustic treatment for the minimum and maximum inlet and tailpipe configurations is described in table 4 and the treatment details in the fan case and fan discharge ducts supplied with the engine are described in figure 12. All inlet acoustic treatment is perforated aluminum sheet bonded to honeycomb core. Welded steel and Inconel construction is used in the exhaust duct. The details of the acoustic treatment were determined by means of a design procedure based primarily on empirical data from DC-9 flyover noise tests, JT8D static engine tests, and laboratory flow duct transmission loss (TL) tests. This design procedure predicts the attenuation spectra for each

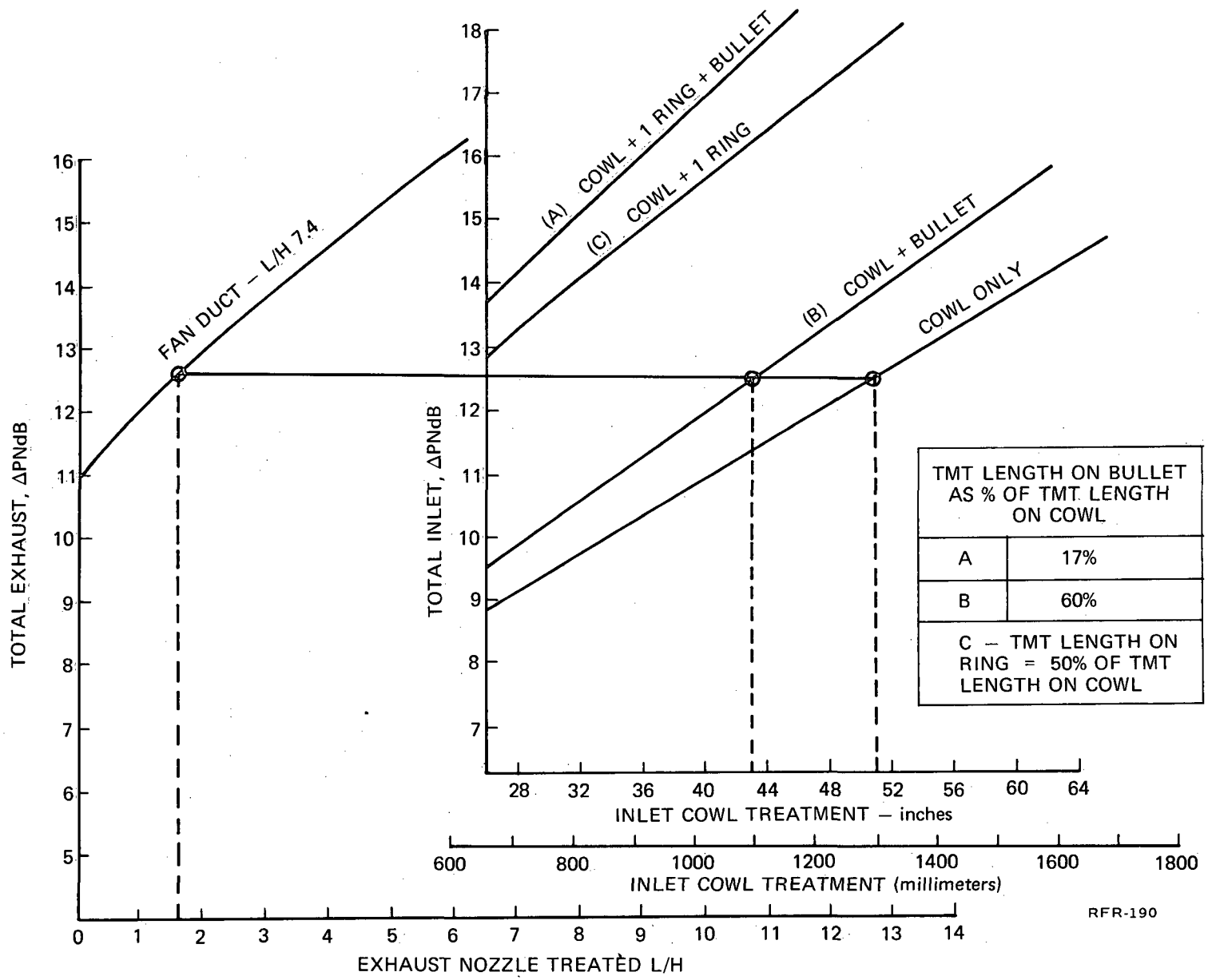

FIGURE 11. JT8D-109 ACOUSTIC DESIGN CHART FOR APPROACH

TABLE 4

ACOUSTIC TREATMENT DETAILS FOR THE MINIMUM AND MAXIMUM NOISE SUPPRESSION CONFIGURATIONS*

ITEM NO.	DUCT PARAMETER	MINIMUM INLET TREATMENT	MAXIMUM INLET TREATMENT	FAN CASE TREATMENT		FAN-DISCHARGE DUCT TREATMENT	MINIMUM TAILPIPE TREATMENT	MAXIMUM TAILPIPE TREATMENT
				FORWARD OF ROTOR	AFT OF ROTOR			
1	TREATMENT LENGTH	51 IN. 1295 (MM)	63 IN. 1600 (MM)	6.5 IN. 16.5 (MM)	6.2 IN. 158 (MM)	INNER WALL – 22.2 (IN.) 564 (MM) OUTER WALL – 85.2 (IN.) 2164 (MM)	37 IN. 940 (MM)	85 IN. 2159 (MM)
2	CHANNEL HEIGHT	24 IN. 610 (MM) RADIUS	24 IN. 610 (MM) RADIUS	33.2 IN. 843 (MM)	14.8 IN. 376 (MM)		22.5 IN. 572 (MM)	22.5 IN. 572 (MM)
3	TREATED (L/H)	2.10	2.60	0.2	0.4	6.8	1.65	3.75
4	CAVITY DEPTH	0.56 IN. 14.2 (MM)	0.56 IN. 14.2 (MM)	1.0 IN. 25.4 (MM)	0.50 IN. 12.7 (MM)	(**)	0.35 IN. 8.9 (MM)	0.40 IN. 10.2 (MM)
5	CELL SIZE	0.375 IN. 9.5 (MM)	0.375 IN. 9.5 (MM)	0.75 IN. 19.0 (MM)	0.375 IN. 9.5 (MM)	(**)	0.25 IN. 6.4 (MM)	0.25 IN. 6.4 (MM)
6	FACE SHEET POROSITY (PERCENT)	6	6	20	12	(**)	12	12
7	TUNING FREQUENCY OF ACOUSTIC TREATMENT	100% OF TREATMENT TUNED TO 3150 Hz	100% OF TREATMENT TUNED TO 3150 Hz	100% OF TREATMENT TUNED TO 1250 Hz	100% OF TREATMENT TUNED TO 3150 Hz	75% OF TREATMENT TUNED TO 3150 Hz 25% OF TREATMENT TUNED TO 6300 Hz	100% OF TREATMENT TUNED TO 6300 HZ	100% OF TREATMENT TUNED TO 6300 Hz

(*) ALL ACOUSTIC TREATMENT IS HONEYCOMB CORE ON PERFORATED PLATE. THE HOLE DIAMETER OF ALL PERFORATED PLATE IS 0.050 INCH 1.27 (MM).

(**) SEE FIGURE 12.

RFR-017

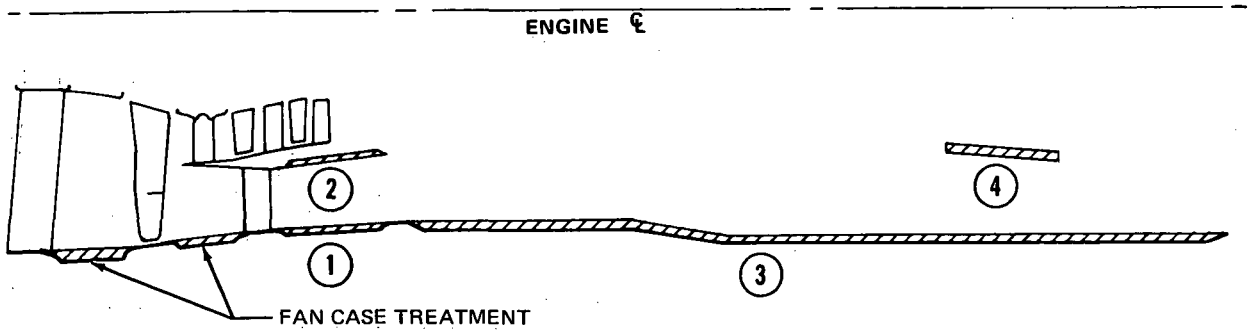

FAN DUCT LOCATION	ESTIMATED EFFECTIVE AREA		ESTIMATED DEPTH HONEYCOMB		% OPENING FACE SHEET	TREATED LENGTH/ EFFECTIVE DUCT HEIGHT (L/H)
	ft^2	(m^2)	in.	(mm)		
1	11.75	1.1	0.25	6.4	12	0.94
2	8.5	0.8	0.25	6.4	12	0.94
3	66.7	6.2	0.5	12.7	12	3.6
4	8.2	0.8	0.5	12.7	12	1.34

FIGURE 12. ACOUSTIC TREATMENT DETAILS FOR FAN DISCHARGE DUCT

piece of nacelle acoustic treatment as a function of duct height-to-length ratio, tuning frequency, duct sound pressure level (SPL), and the duct static temperature, velocity, and Mach number. The duct internal Mach number, temperatures, and velocities used to design the treatment are presented in Appendix A.

The predicted approach spectra and duct conditions were used as the basis of the treatment design. The tailpipe treatment was optimized by assuming that various portions of the treatment were tuned to the blade passage frequency (3 150 Hz) with the remainder tuned to the harmonic (6 300 Hz). As shown on figure 13, both the minimum and maximum length tailpipes optimize with all of the tailpipe treatment tuned to 6 300 Hz. This high frequency tuning is also effective in attenuating turbine noise. Figure 14 shows the turbomachinery SPL and NOY weighted spectra used to design the tailpipe. This figure shows the progressive attenuations of the fan duct and the minimum and maximum length tailpipes. The non-turbomachinery noise floor is shown as line 2 and consists of jet, core, and aft radiated inlet noise. This noise floor defines the level that would be obtained if the aft radiated turbomachinery noise was completely suppressed.

Multiple pure tone or buzzsaw noise caused by the high tip speeds of the refanned JT8D engine was not directly addressed by the inlet treatment design. This was done because the inlet treatment was designed to give maximum EPNL attenuation at approach and also because no method currently exists which enables the subjective annoyance of buzzsaw to be evaluated. Buzzsaw noise affects frequencies lower than the blade passage frequency tone which controls the flyover EPNL noise. A buzzsaw contingency plan was developed which will allow minimum cost changes to the inlet acoustical treatment if subsequent testing shows the buzzsaw noise to be significantly annoying. This plan allows space free from mechanical interference for thicker acoustical treatment in the inlet cowl wall. A section of thick acoustical treatment, tuned for multiple pure tone noise, is supplied with the engine case. This treatment is between the inlet guide vanes and the rotor.

The fan duct, inlet and tailpipe treatment was then re-evaluated for the spectra and flow environment at cutback and takeoff/sideline conditions and the attenuation characteristics were applied to the component noise sources at these higher power settings. Noise estimates for a 0.102 rad (6 deg) approach were determined in a similar manner. The untreated and treated spectra along with the flyover noise directivity for each source were then extrapolated for distance by the inverse square law and standard values for air attenuation to develop flyover time histories and curves of effective perceived noise level as a function of distance for engine power settings from takeoff to 0.102 rad (6 deg) approach. The EPNL distance curves for the existing DC-9-32 with JT8D-9 engines and the DC-9-31 with JT8D-7 engines are shown on figures 15 and 16. Figures 17 and 18 show the EPNL distance curves for the modified DC-9 with JT8D-109 engines for the two levels of nacelle acoustic treatment. Detail flyover time histories and spectra as well as a discussion of the noise prediction procedure are presented in Appendix A.

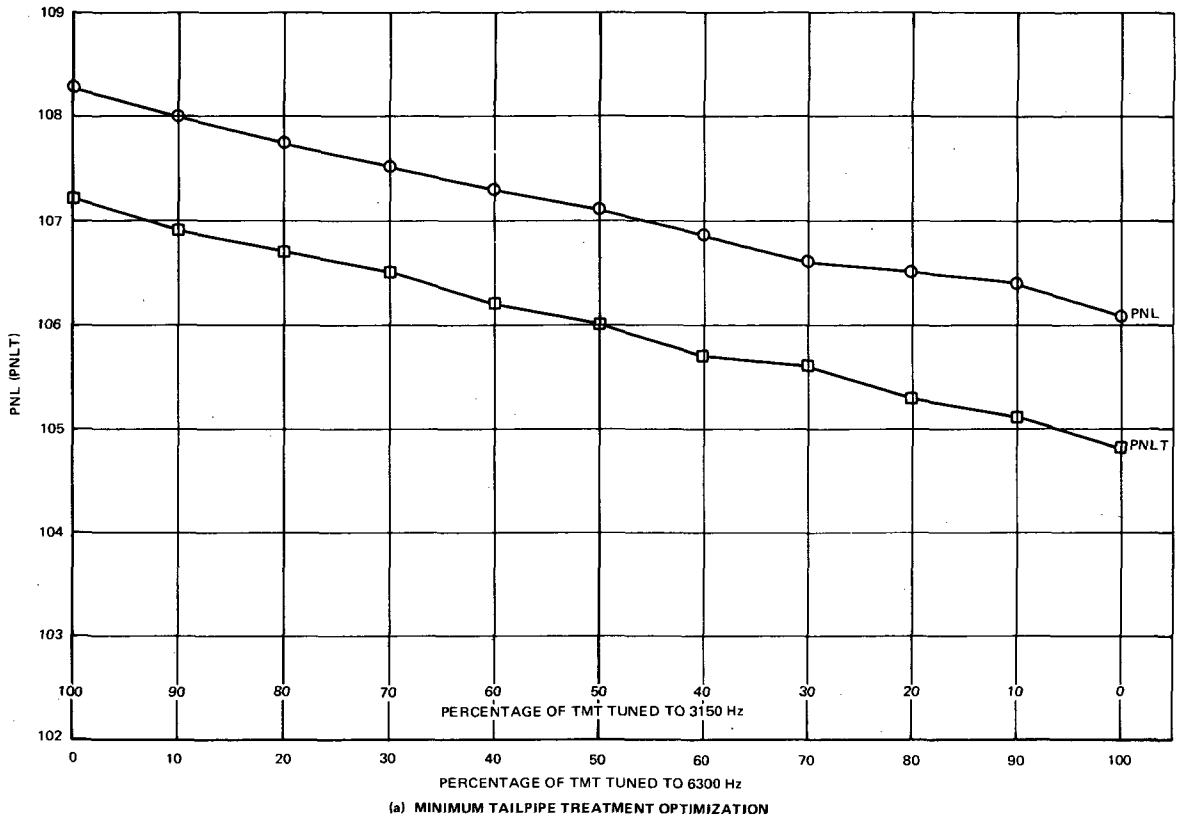

(a) MINIMUM TAILPIPE TREATMENT OPTIMIZATION

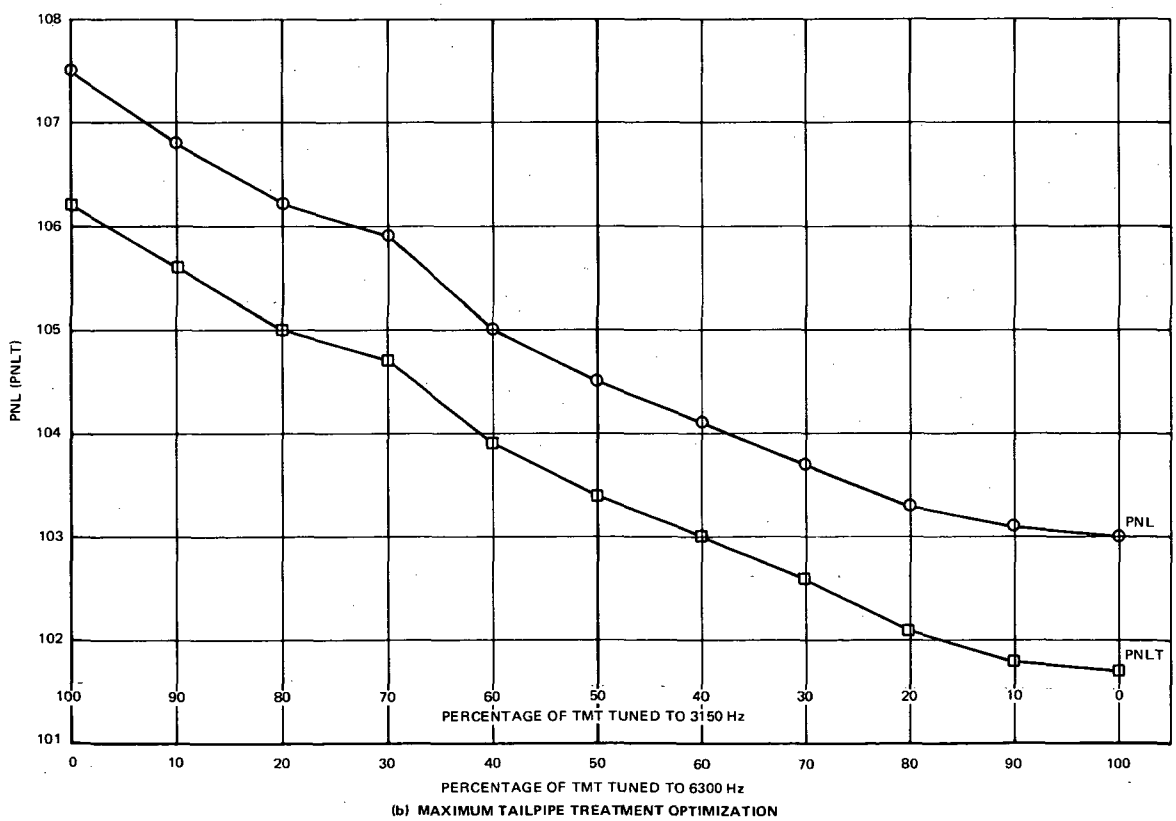

(b) MAXIMUM TAILPIPE TREATMENT OPTIMIZATION

FIGURE 13. TAILPIPE OPTIMIZATION PLOTS FOR FAR 36 APPROACH CONDITIONS

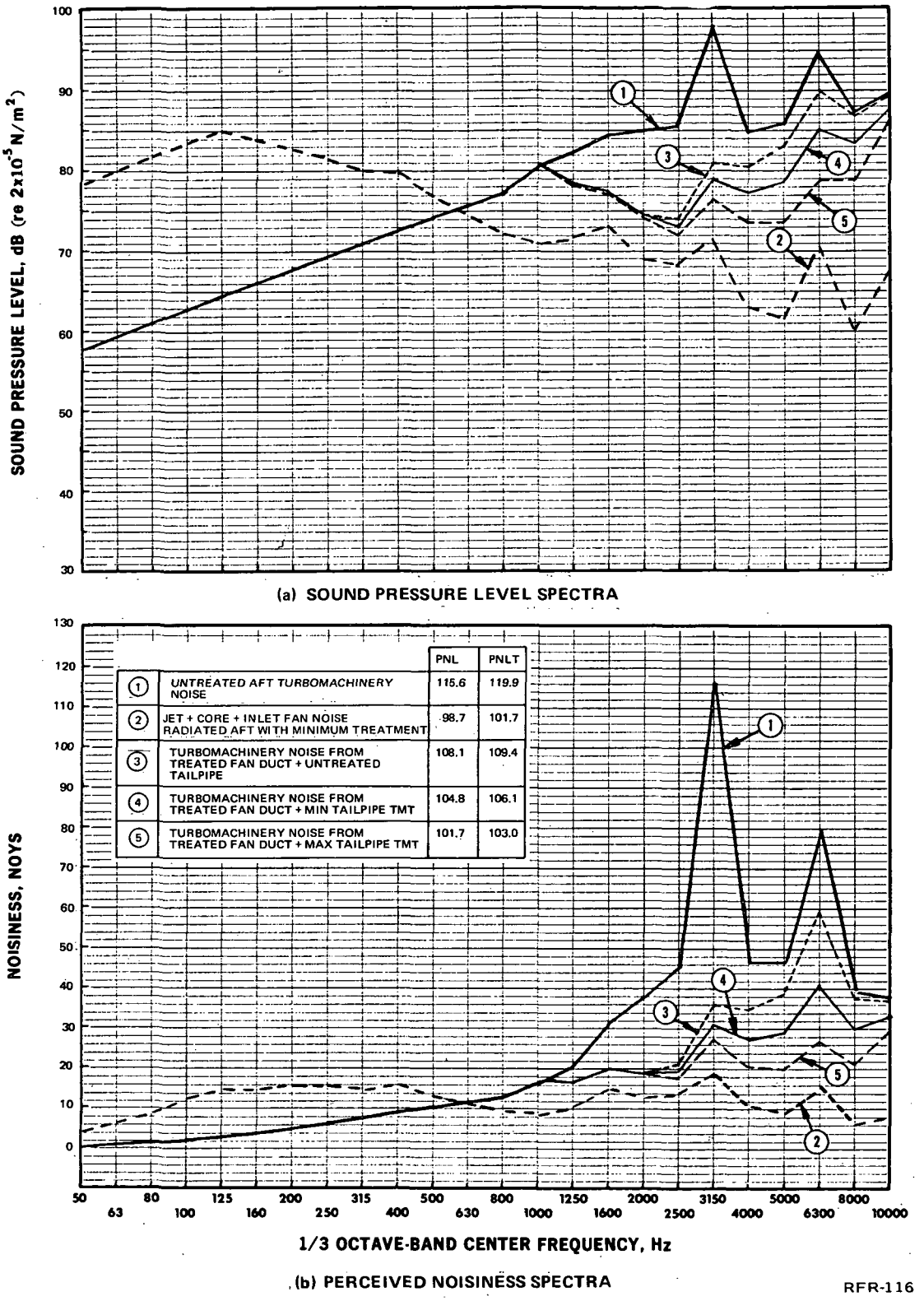

FIGURE 14. PEAK EXHAUST SPECTRA FOR UNTREATED AND TREATED NACELLE FAR PART 36 APPROACH CONDITION

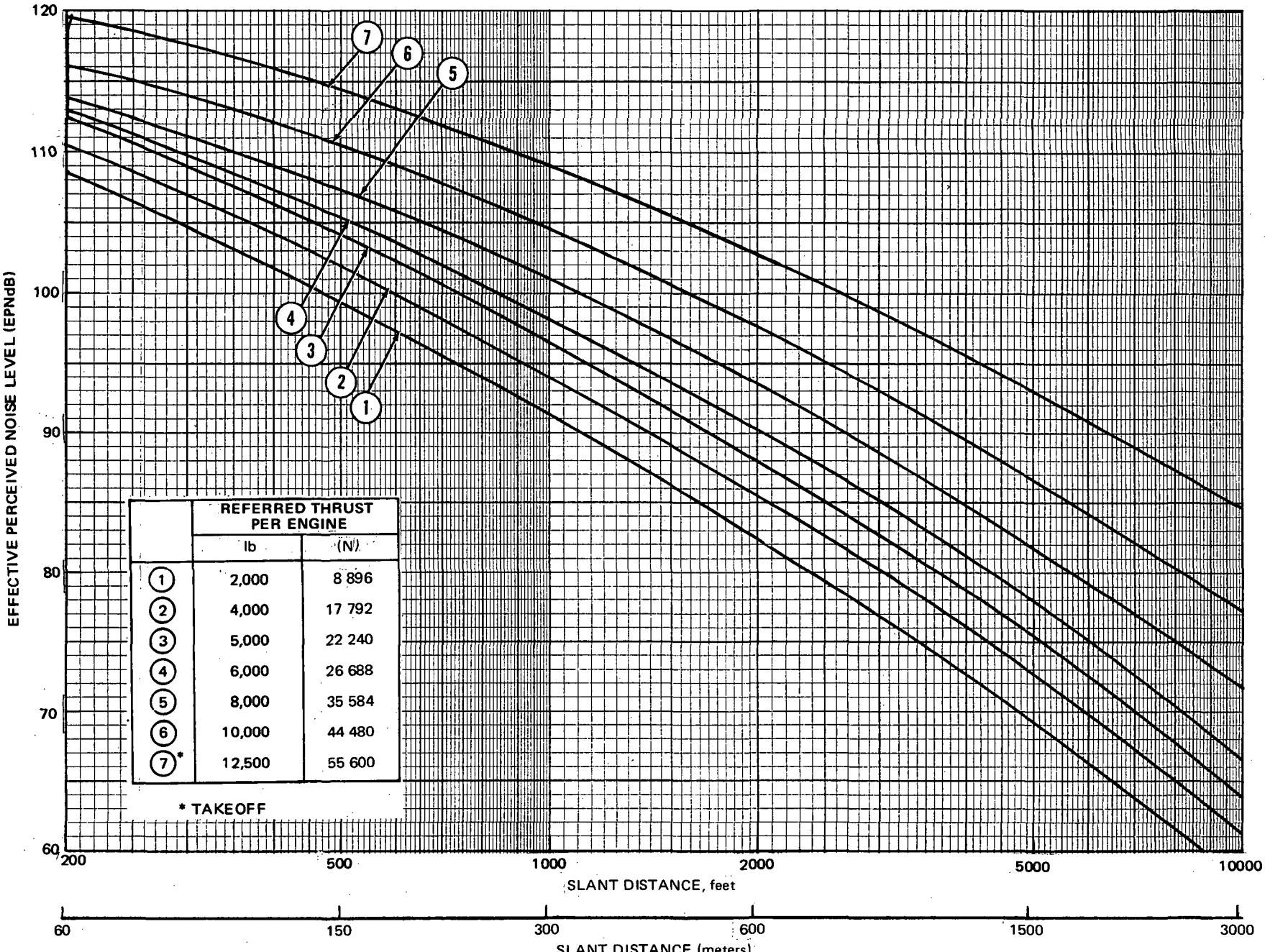

FIGURE 15. EPNL-DISTANCE MAP FOR EXISTING DC-9-32 AIRCRAFT WITH JT8D-9 ENGINES

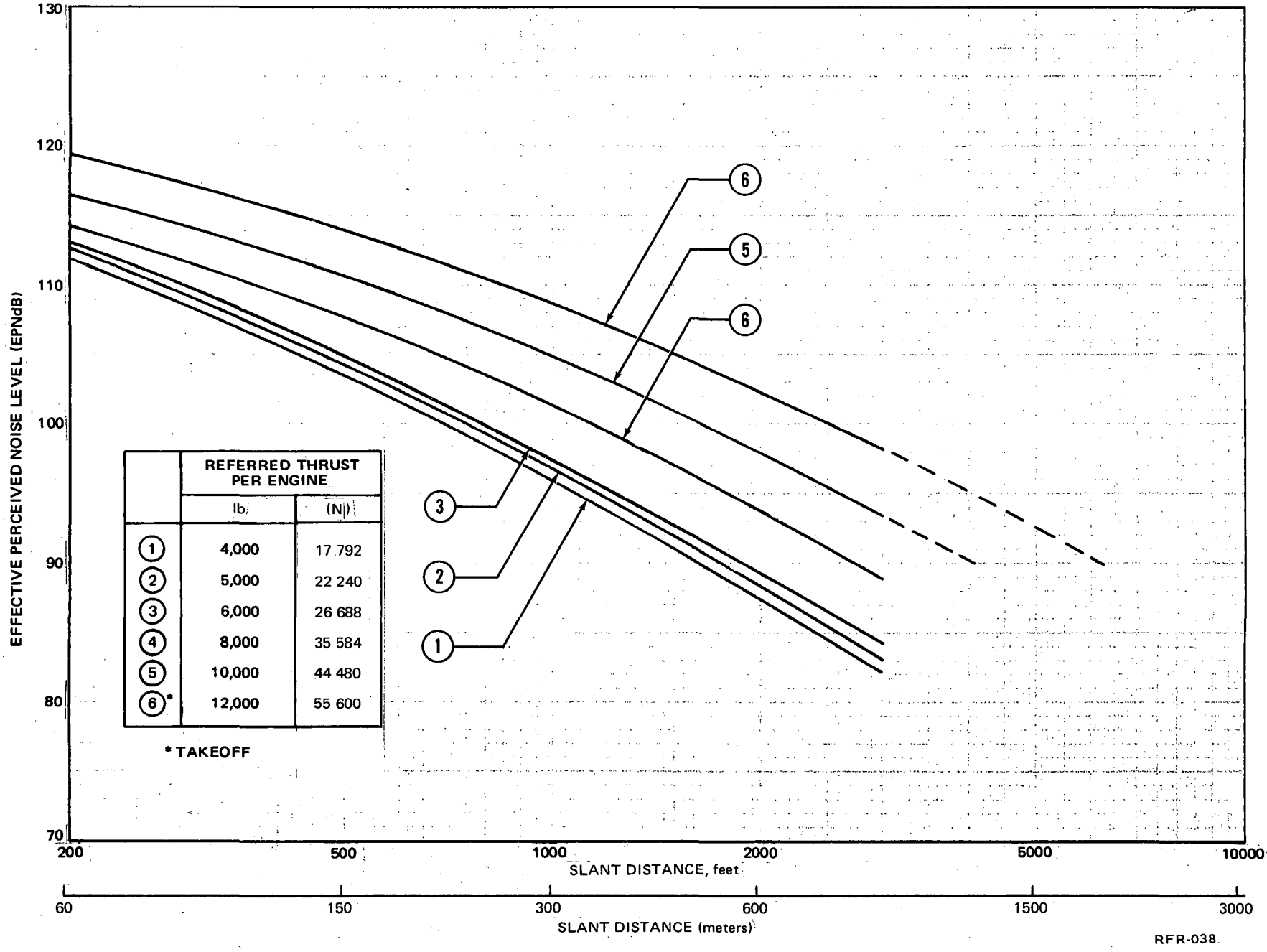

FIGURE 16. EPNL-DISTANCE MAP FOR EXISTING DC-9-15 AND DC-9-31 AIRCRAFT WITH JT8D-7 OR -7A ENGINES

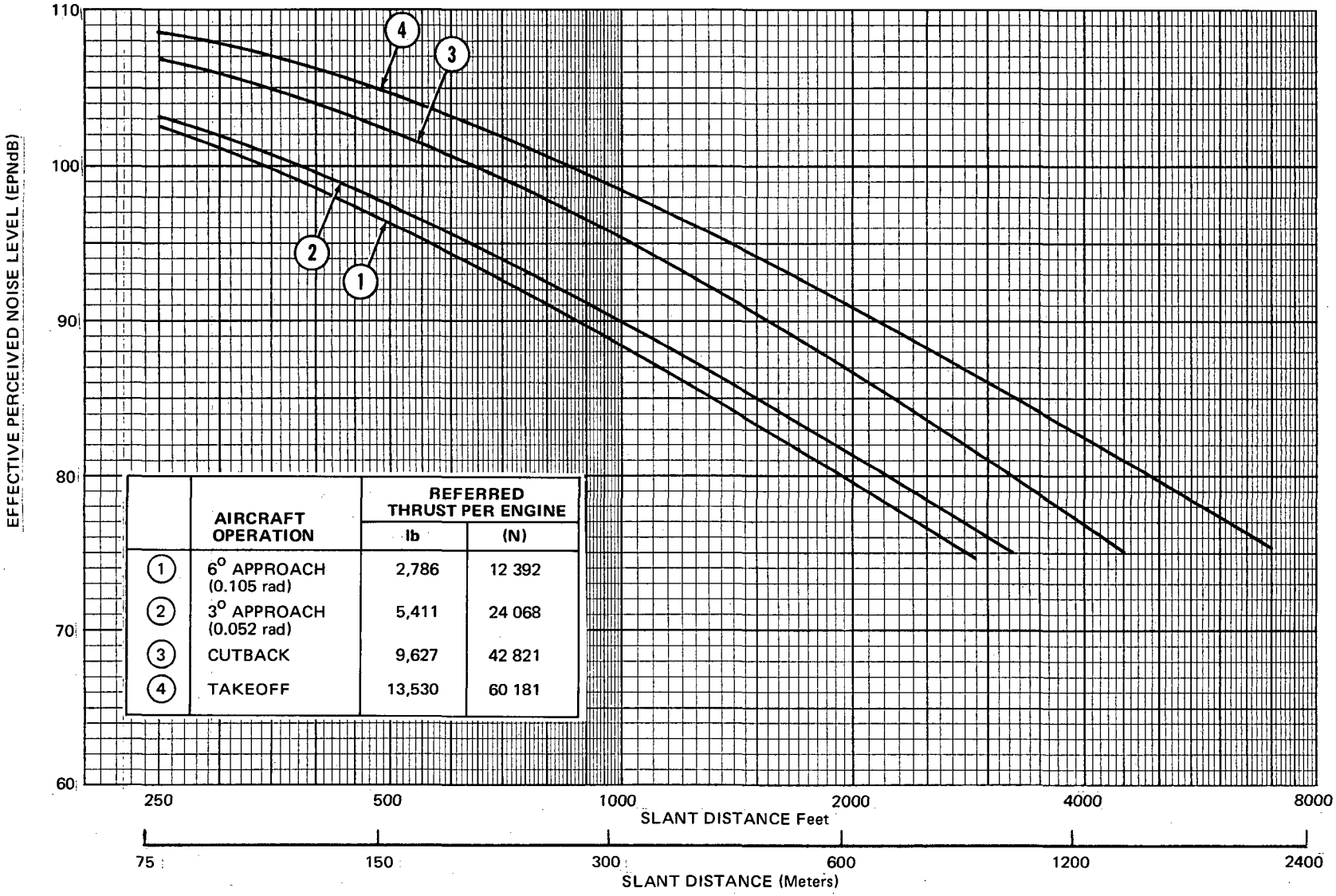

	AIRCRAFT OPERATION	REFERRED THRUST PER ENGINE lb	(N)
1	6° APPROACH (0.105 rad)	2,786	12 392
2	3° APPROACH (0.052 rad)	5,411	24 068
3	CUTBACK	9,627	42 821
4	TAKEOFF	13,530	60 181

FIGURE 17. EPNL-DISTANCE MAP FOR MODIFIED DC-9-32 AIRCRAFT FOR MINIMUM ACOUSTIC TREATMENT

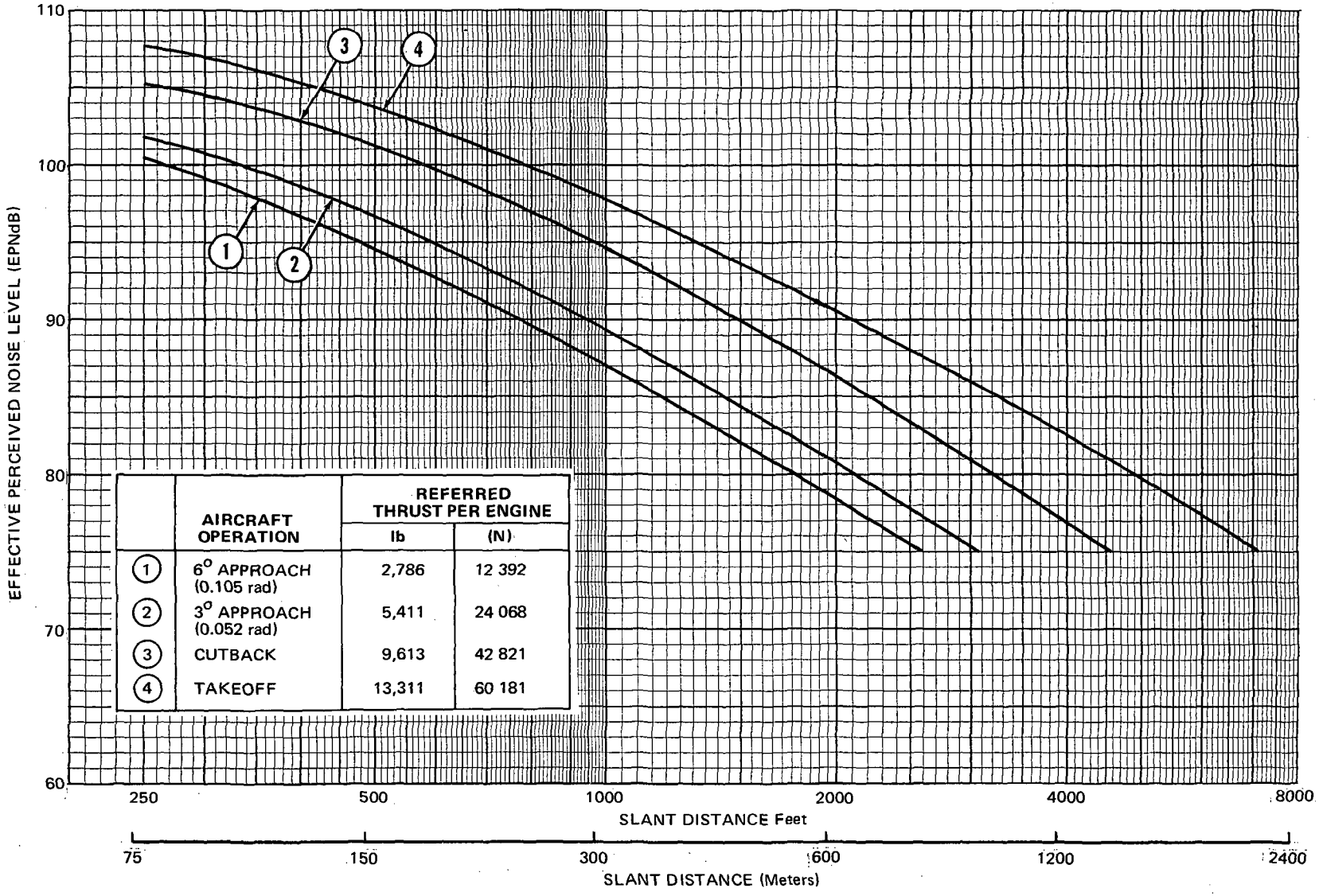

FIGURE 18. EPNL-DISTANCE MAP FOR MODIFIED DC-9-32 AIRCRAFT FOR MAXIMUM ACOUSTIC TREATMENT

Airframe Structural Design

The installation of the JT8D-109 refan engine requires structural modification or redesign in four areas. These areas are:

- Pylon
- Aft Fuselage
- Forward Fuselage
- Engine Mount System

No structural changes have been identified for the empennage.

Pylon. - Four pylon configurations were initially chosen and evaluated for aerodynamic, accessibility, cost, weight, and structural integrity considerations. During the trade studies a fifth pylon configuration developed, which met all the above requirements and is the pylon which will be designed and built during Phase II of this program. A detailed summary of the pylon trade study is presented in Appendix B.

The refan engine pylon shown in figure 19, is completely redesigned to reduce its width from 425.45 mm (16.75 in.) to 204.47 mm (8.05 in.), measured at fuselage station 969 on the pylon upper surface, and to increase its load carrying capabilities to accommodate the heavier JT8D-109 engine and nacelle. The reduction in pylon width results from a combination of the engine centerline 81.28 mm (3.2 in.) closer to the fuselage and increase in engine diameter of 279.4 mm (11 in.) and shown as configuration (5) of Appendix B.

The new pylon is structurally similar to the present JT8D-9 engine pylon, with front and rear engine mount spars, a closing rib adjacent to the nacelle apron, a fully skinned upper surface, and access panels in the aft lower surface. The existing JT8D-9 engine pylon secondary firewall, positioned approximately 102 mm (4 in.) from the fuselage (not required by FAA regulations), is deleted, and a thicker titanium fuselage skin panel will serve as the firewall for the refan engine installation. In the area adjacent to the engine burner cans, a columbium burn-through barrier will be attached approximately 12.7 mm (1/2 in.) outboard of the fuselage skin. The pylon leading and trailing edge fairings are constructed similarly to the existing units; i.e., upper and lower skins, attach angles, a closing rib, and longitudinal formers.

Openings, in the fuselage for the engine systems, remain unchanged in size and location with the exception of the fuel shutoff and the power control.

Aft fuselage. - The fuselage titanium skin panel which extends from longeron 14 down to the floor and over the whole length of the pylon will be removed and replaced with a heavier gauge.

The fuselage frames adjacent to the pylon and between pylon front spar and rear spar will require reinforcing (figure 20).

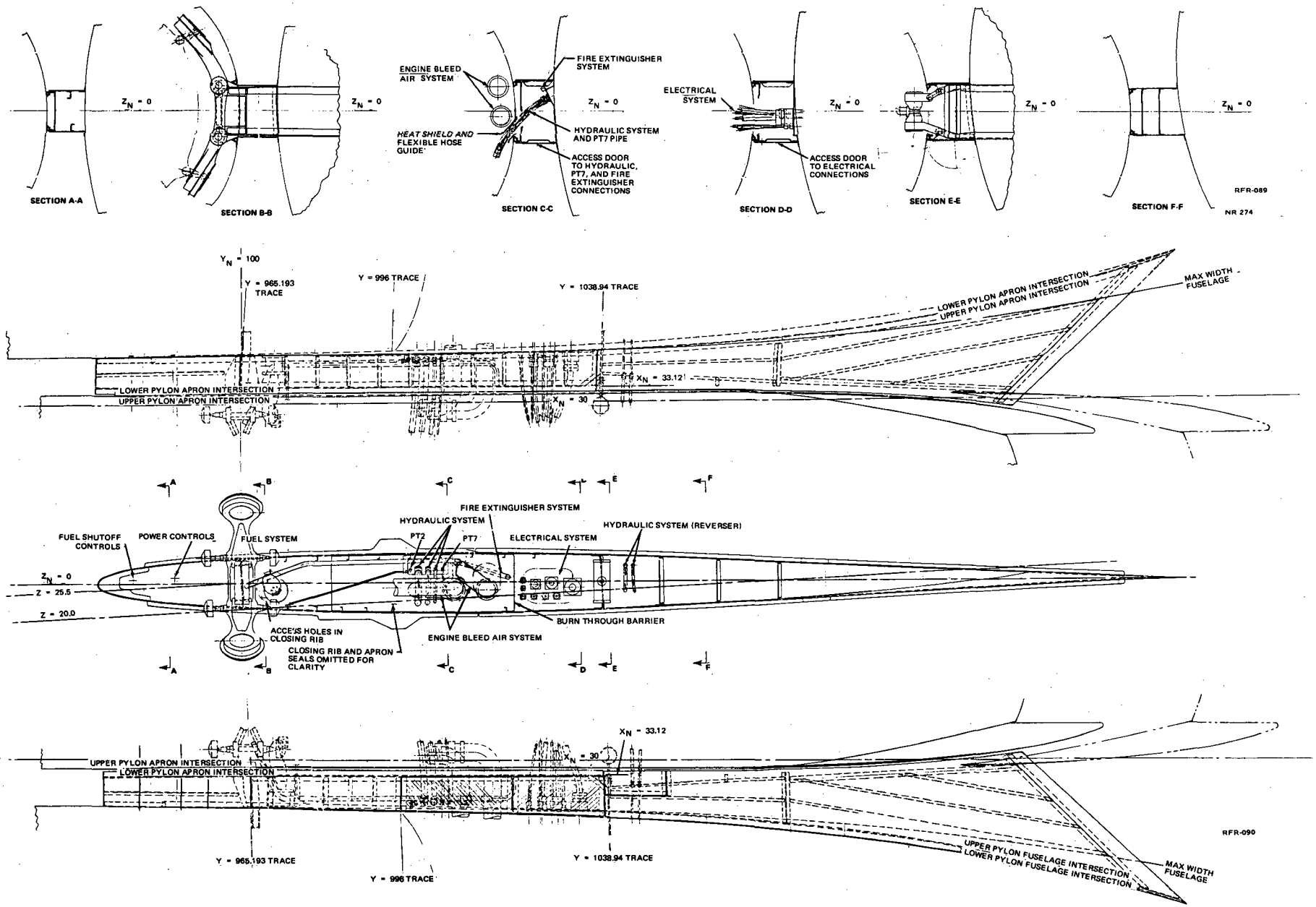

FIGURE 19. 8-INCH PYLON COMPARISON – MAXIMUM AND MINIMUM SELECTED ACOUSTIC TREATMENTS.

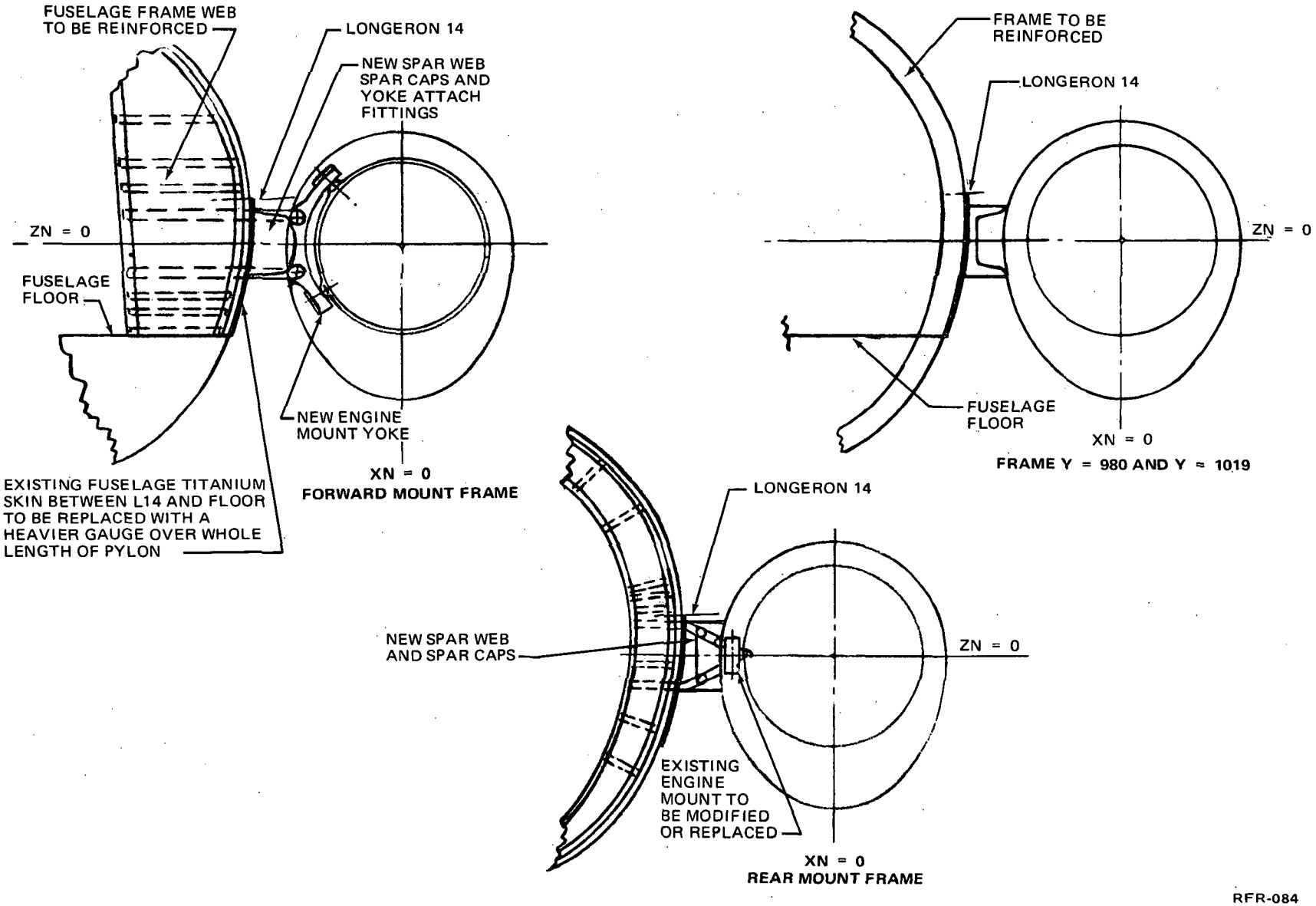

FIGURE 20. AFT FUSELAGE FRAME MODIFICATIONS

Fuselage keel. - Because of overall bending, the lower fuselage keel caps adjacent to the main landing gear wells require the addition of reinforcing members and skin doublers (figure 21).

Forward fuselage. - Ballast may be required to maintain the aircraft center of gravity within the aft limit. If permanent ballast is required, it will be installed in the nose of the aircraft, adjacent to the forward landing gear well.

Engine mount system. - The engine mount system is a three-point system utilizing two mounts at the same fuselage station on the forward end of the engine, and one mount at the aft end (figure 22).

The three attachments are made by cone bolts installed on the engine flanges and mated to the airframe structure. Although the basic system in use today remains unchanged in design concept, additional reinforcement is required at the forward end to accommodate the higher loads of the JT8D-109 engine. The forward mount yoke, while similar in design to the production yoke, will be manufactured from a new larger forging. The existing aft engine mount will be retained and used for the refan installation.

Vibration isolators are attached to the pylon in positions corresponding to the engine mounted cone bolts (figure 23). The two forward vibration isolators are installed in the mount yoke, while the aft vibration isolator is attached directly to the pylon. The forward and aft vibration isolators presently used will be used for the flight demonstration aircraft but will require modification to provide longer service life for retrofit.

Tuned vibration absorbers, installed on the forward mount yoke, were developed on the present DC-9 for reduction of cabin noise induced by engine rotor vibration (figure 22). For the JT8D-109 installation, the present vibration absorbers will be used on a restricted flight demonstration basis. If the cabin noise level is unacceptable during flight demonstration, a vibration absorber development program will be required. There are no absorbers used on the aft mount for the JT8D-9 or planned for the JT8D-109.

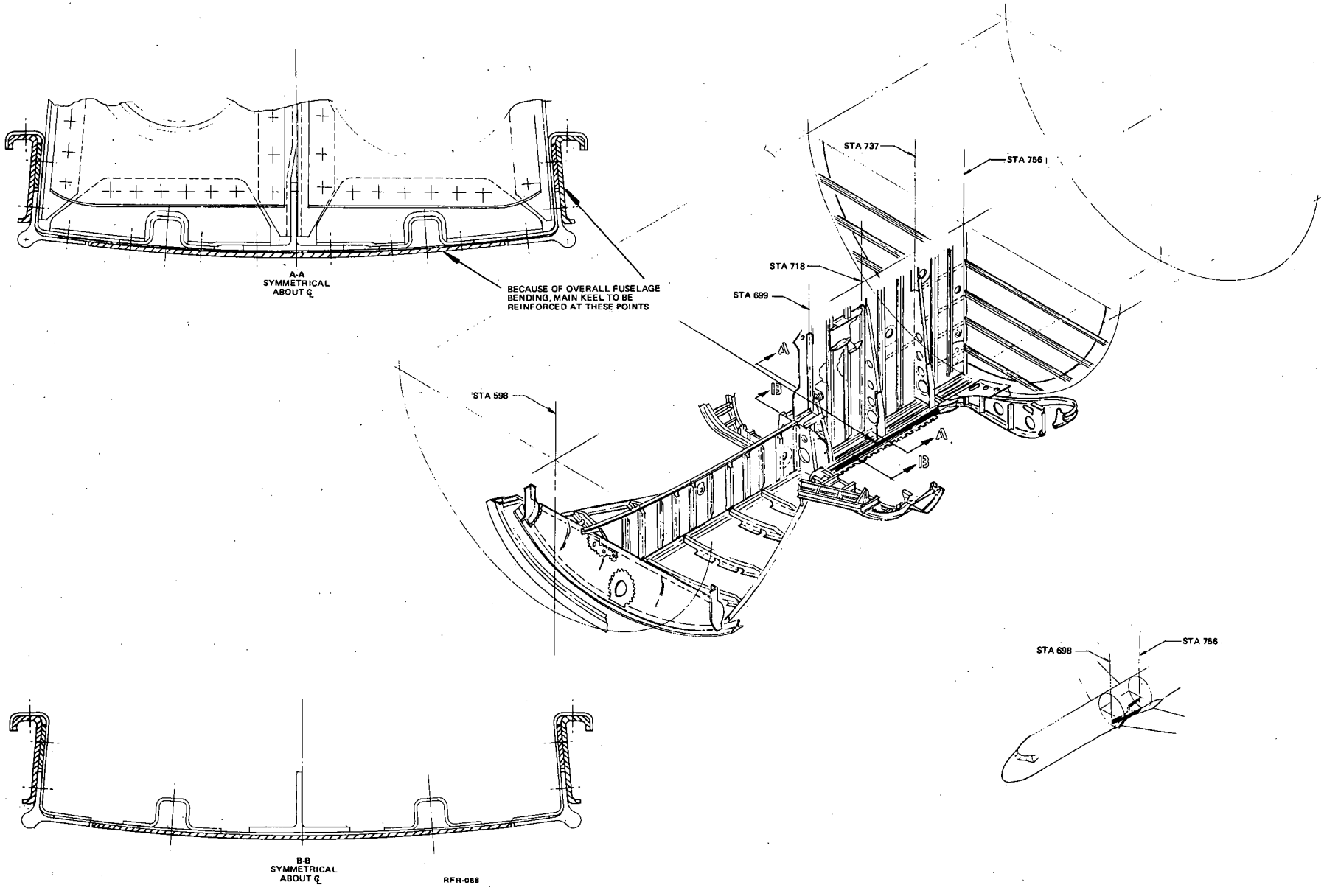

FIGURE 21. DC-9-32 REINFORCING AT FUSELAGE KEEL

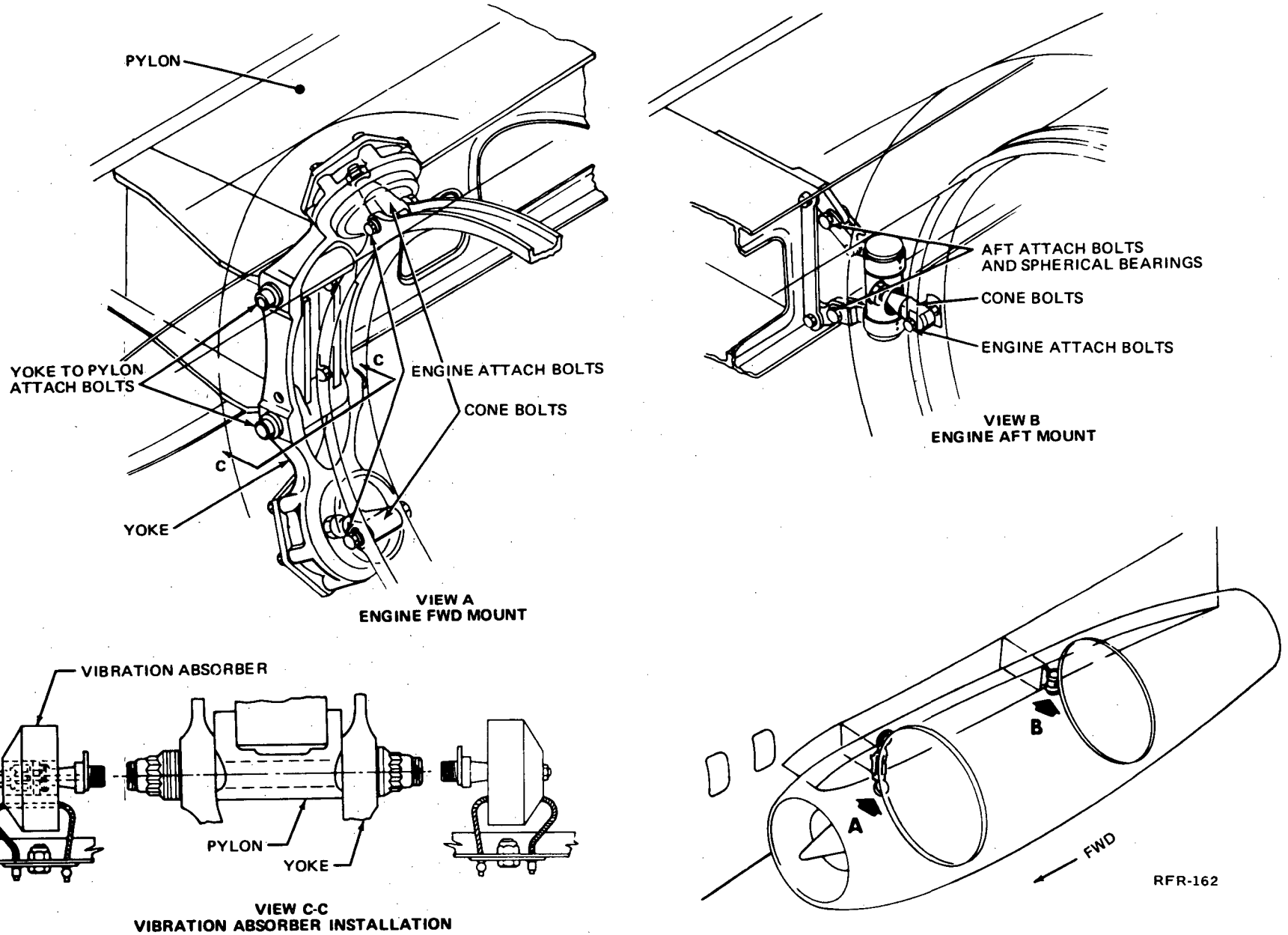

FIGURE 22. DC-9-32 ENGINE MOUNTS

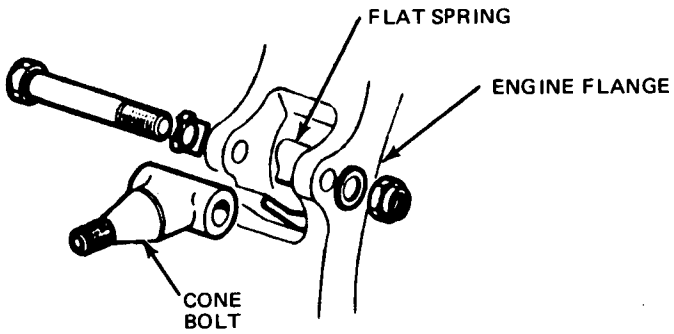

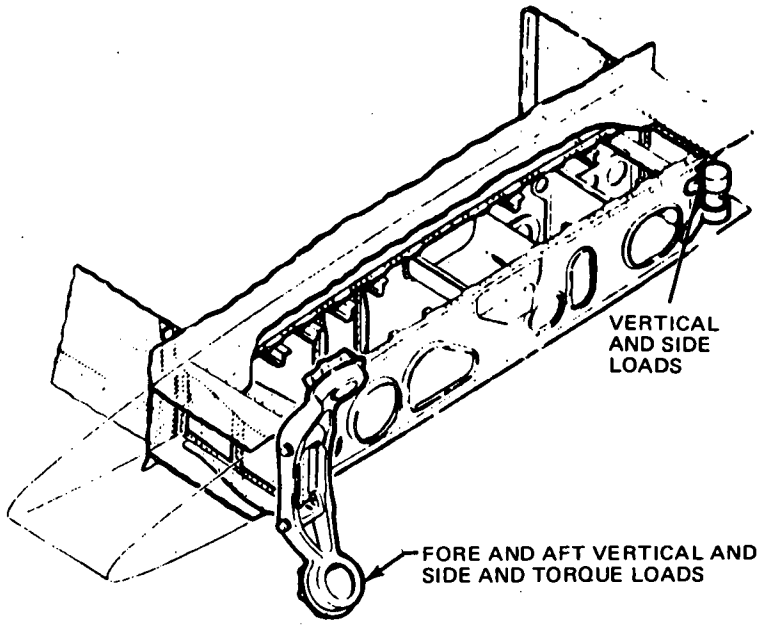

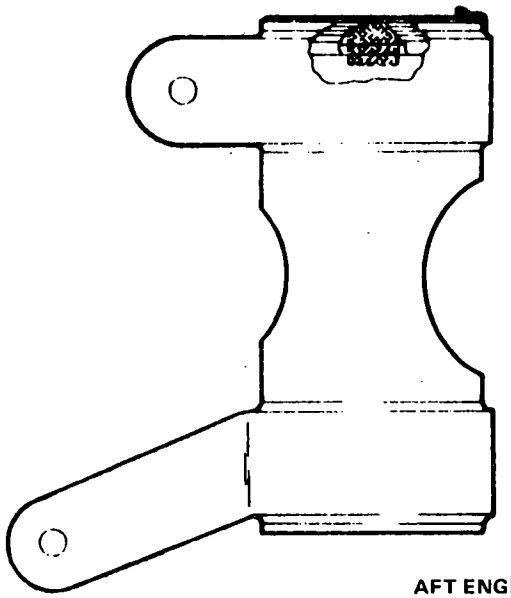

AFT ENGINE VIBRATION ISOLATOR

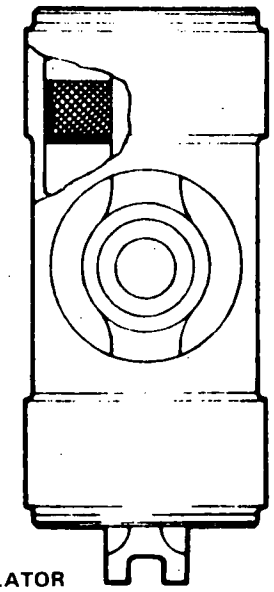

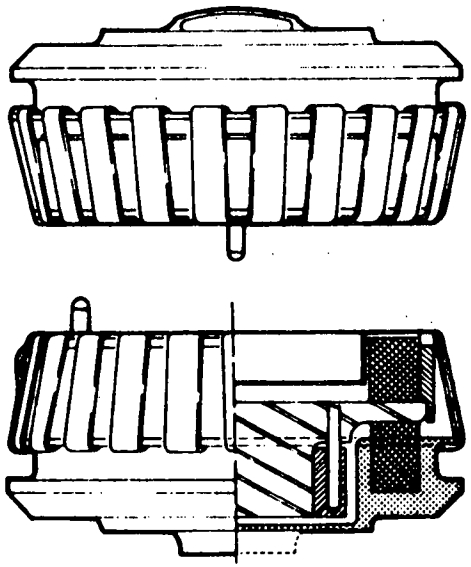

FWD ENGINE VIBRATION ISOLATOR

FIGURE 23. ENGINE METAL-FLEX VIBRATION ISOLATOR MOUNTS

RFR-163

Loads, Strength, and Dynamic Analyses

To install the refanned JT8D-109 engines on the DC-9 aircraft, redesign or modification of the following structure is required:

- Nacelle

  Inlet Duct
  Access Doors and Pylon Apron
  Exhaust Nozzle
  Thrust Reverser and Linkage
  Pneumatic Duct System

- Pylon

  Pylon and Fuselage Support Structure
  Engine Mounts

- Fuselage

  Fuselage Keel
  Fuselage Forward Frames

As design configurations were established during Phase I for the above structure, the pertinent design criteria were reviewed and loads and strength analyses initiated. Dynamic analyses were also performed for airplane flutter, gust loads, and landing loads. The following is a summary of the analyses accomplished during the Phase I Program.

Inlet duct. - Design of the inlet duct of the Refanned JT8D is similar to the existing DC-10-10 inlet duct. The running load on the inner barrel acoustic sandwich is within the limits for the DC-10-10. Bonded aluminum sandwich has been selected for the JT8D-109 inlet duct acoustic treatment as a result of the Structural/Acoustical Materials Trade Study (Appendix B). Douglas Aircraft Company sonic fatigue tests and DC-10-10 service experience show the bonded aluminum acoustic sandwich to be capable of withstanding the acoustical environment of the JT8D-109 inlet. The critical loads for the nose cowl attachment to the engine inlet flange result from a Douglas requirement that the nose cowl withstand the high vibration loading imposed by an engine failure. A 20g vibration load was assumed in lieu of a rational dynamic analysis. The bolt pattern of the engine inlet flange and the acoustic sandwich close-out structure were strength checked for a maximum bolt load of 5 604 N (1,260 lb).

Access doors and pylon apron. - The access doors and apron are being designed for the following load conditions:

(1) A limit differential pressure of 17.2 kPa (2.5 psi), internal greater than external, or 12.1 kPa (1.75 psi), external greater than internal applied uniformly over the entire surface. This condition encompasses the maximum aerodynamic pressures obtainable for any point on the nacelle surface from pressure coefficients corrected for V_D at sea level.

(2) Pressure loads resulting from failure in the pneumatic system which will be relieved by blowing open a pressure relief door. This door will be designed to blow open within a range of ultimate pressures from 25.5 kPa (3.7 psi) to 43.1 kPa (6.25 psi). The instantaneous peak pressure will not cause loads sufficient to fail any latch or hinge, and subsequently cause the loss of an access door.

(3) Limit aerodynamic loads from a 38.2 m/s (65 knot) ground gust applied normal to the door in the open position.

(4) A limit load on door hinges and latches of 2/3 of the rated latch strength, 20.76 kN (4,667 lb), applied in the principal load direction.

Exhaust nozzle. - Preliminary exhaust system design loads at the JT8D-109 attach flange are shown in table 5. These loads were calculated for a conservative exhaust system weight of 388 kg (856 lb). Loads and strength analysis of the exhaust nozzle will be performed when aerodynamic loads data for the exhaust nozzle and thrust reverser become available. As a result of the Structural/Acoustical Materials Trade Study (Appendix B), brazed Inconel 625 acoustic sandwich has been recommended for the JT8D-109 exhaust nozzle. However, for the flight demonstration airplane, welded Inconel 625 (Stresskin) will be substituted due to economic considerations.

Thrust reverser and linkage. - The structural design criteria for the thrust reverser and supporting linkage will include requirements for strength to withstand:

(1) The loads imposed to deploy or stow the thrust reverser at an airplane velocity of 89.25 m/s (175 KEAS) under maximum takeoff power.

(2) The effects due to a 2 ± 1 second time to deploy or stow, where zero time is coincident with full actuation of the thrust reverser valve.

(3) Landing, aborted takeoff, and inadvertent inflight deployment conditions.

Although the final design configuration of the thrust reverser and linkage has not been established, preliminary loads investigations have been performed. A structural idealization of the preliminary thrust reverser bucket was generated as a procedural checkout and a computer program developed to panel point external loads for input to the analysis model. To support the design of the linkage configuration, a computer program was written to calculate four-bar linkage loads. Operational loads for the proposed linkage configuration are shown in table 6. The condition analyzed is stowing at 92.5 m/s (170 KEAS) with the engine at idle thrust.

The thrust reverser four-bar linkage couples the buckets to the actuator and carries the weight and reverser thrust loads of the buckets in both the faired and reverse thrust positions. The driver link is an over-center type, preloaded in the locked (faired) position. Deflection of the driver link

TABLE 5

JT8D-109 EXHAUST NOZZLE ATTACH FLANGE DESIGN LOADS

		LOAD COMPONENTS					RESULTANT LOADS		
COND.	DESCRIPTION	F_x lb (N)	F_y lb (N)	F_z lb (N)	M_x in-lb (N·m)	M_z in-lb (N·m)	MOMENT in-lb (N·m)	SHEAR lb (N)	AXIAL lb (N)
1	Max. continuous thrust + max. inertia (limit)	571 (2 540)	16,000 (71 168)	-4,565 (-20 305)	-182,890 (-20 663)	-22,861 (-2 583)	184,312 (20 823)	4,601 (20 465)	16,000 (71 168)
2	Max. reverse thrust + inertia (limit)	856 (3 807	44,762 (199 101)	-3,424 (-15 223)	-137,166 (-15 497)	34,292 (3 874)	141,387 (15 974)	3,529 (15 697)	44,762 (199 101)
3	Crash (ultimate)	-	-10,272 (-45 690)	(-15 223)	-	-	-	-	-10,272 (-45 690)
4	Fail safe - one bucket extended (ultimate)	-	30,381 (135 135)	-	287,620 (32 495)	-	287,620 (32 495)	-	30,381 (135 135)

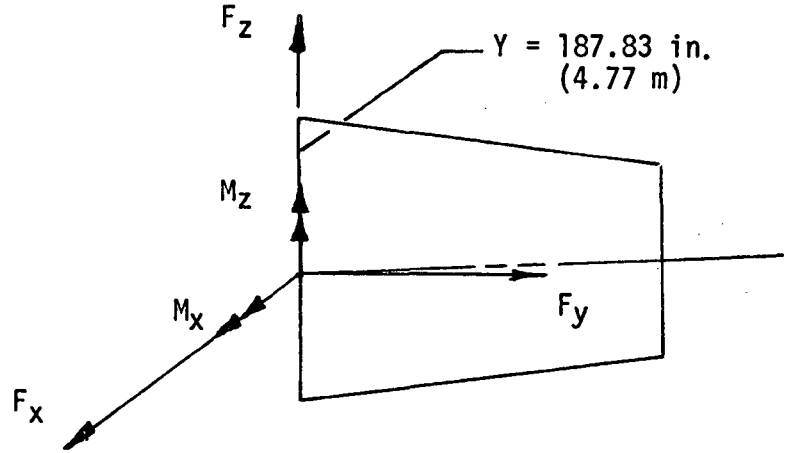

LOADS POSITIVE AS SHOWN - R.H. RULE FOR MOMENTS

NOTES:

LOADS ASSUMED TO ACT ON CENTERLINE

ANALYSIS WEIGHTS AND c.g.

EXHAUST NOZZLE 516 lb (234 kg) Y = 1084 in. (27.53m)

THRUST REVERSER 340 lb (154 kg) Y = 1111 in. (28.22m)

TABLE 6

THRUST REVERSER LINKAGE LOADS

STOWING LOADS AT 170 KNOTS (92.5 m/s)-IDLE THRUST

				DRIVER LINK			IDLER LINK
DRIVER ANGLE Deg (rad)	BUCKET LOAD lb (kN)	LOAD ANGLE Deg (rad)	LOAD CP % LENGTH	MOMENT in-lb (N·m)	AXIAL lb (N)	SHEAR lb (N)	AXIAL LOAD lb (N)
0	250 (1.120)	7.4 (1.292)	.632 -	-6,960 (-786.34)	81 (360.29)	-238 (-1 058.62)	-215 (-956.32)
5.5 (.0960)	650 (2.912)	72 (1.257)	.628 -	17,843 (2 015.92)	87 (386.98)	609 (2 708.83)	-399 (-1 774.75)
15.5 (.2705)	860 (3.853)	70 (1.222)	.616 -	23,946 (2 705.42)	-77 (-342.50)	818 (3 638.46)	-253 (-1 125.34)
45.5 (.7941)	1,020 (4.570)	59 (1.030)	.590 -	29,976 (3 386.69)	-18 (-80.06)	1,024 (4 554.75)	-27 (-120.09)
65.5 (1.1432)	1,095 (4.906)	51 (0.890)	.573 -	31,351 (3 542.04)	177 (787.30)	1,071 (4 763.81)	23 (102.30)
75.5 (1.3177)	1,130 (5.062)	46 (0.803)	.562 -	31,332 (3 539.89)	278 (1 236.54)	1,070 (4 759.36)	45 (200.16)
95.5 (1.6668)	1,210 (5.421)	35 (0.611)	.537 -	30,390 (3 433.46)	478 (2 126.14)	1,038 (4 617.02)	89 (395.87)
115.5 (2.0156)	1,310 (5.869)	23 (0.401)	.504 -	27,007 (3 051.25)	647 (2 877.86)	922 (4 101.06)	198 (880.70)
136.21 (2.3773)	1,725 (7.728)	13 (0.227)	.471 -	21,843 (2 467.82)	912 (4 056.58)	734 (3 264.83)	555 (2 468.64)

develops the over-center locking load and results in the critical design loads. Since the preload requirements for the faired reverser buckets have not been determined, this condition is not shown.

The design load for the idler link is produced in the fully deployed position with the engine developing maximum reverse thrust. The preliminary ultimate design load in the link is 75.6 kN (17.006 lb) tension.

Pneumatic duct system. - No loads or strength analyses have been performed on the pneumatic duct system. As pressure and temperature data becomes available for the JT8D-109 system, these analyses will be performed.

Pylon and fuselage support structure. - Redesign of the DC-9 pylon and supporting structure for the refan engine required that external and internal loads be calculated for the increased weight of the JT8D-109. The external loads analysis of the existing DC-9 pylon was reviewed and an envelope of critical conditions identified. The following airplane conditions were found to be most critical:

(1) Positive and negative symmetrical vertical gust.

(2) One wheel landing.

(3) Taxi turn.

The loads calculated include the gust and landing conditions. Analysis of the taxi turn conditions is in progress. A description of the conditions analyzed is shown in table 7. Airloads calculations were based on DC-9-30 aerodynamic coefficients scaled to the refan nacelle and pylon areas. The engine analysis parameters were determined as shown in table 8. The sign conventions for loads analyses are shown in figure 24.

Dynamic gust loads on the nacelle/pylon were calculated for the positive and negative symmetrical vertical gusts. The gust conditions (101 through 106) are described in table 7. Dynamic landing loads on the nacelle/pylon were calculated assuming a rigid airplane and flexible gear structure. The airplane weight used was the DC-9-32 maximum landing weight. The dynamic landing conditions (107 through 111) are described in table 7. Dynamic landing loads for the DC-9-32 airplane assuming a flexible airplane and flexible landing gear structure were also calculated. These dynamic landing conditions (112 through 117) are described in table 7. The dynamic responses of the engine for dynamic landing are given in table 9.

To compare with the dynamic gust loads, discrete symmetrical gust loads were calculated. Conditions 121 through 130 described in table 7 give the maximum discrete up gust and down gust loads at the nacelle and engine c.g. Conditions 201 through 204 in table 7 are the airplane gust and maneuver conditions analyzed for input to the fuselage/pylon internal loads analysis. These conditions produce critical aft fuselage bending and were used to determine if any structural modification to the fuselage shell was required.

It was necessary to define an envelope of design conditions to provide internal loads required for preliminary design of the pylon and fuselage

TABLE 7 CONTINUED

DC-9-32 NACELLE/PYLON LOADS ANALYSIS CONDITIONS

COND NO.	DESCRIPTION	ALT ft (m)	MACH	SPEED	V KEAS (m/s)	WT lb (kg)	CG % (M.A.C.)	I_p 10^6 SLUG ft^2 (Ggm^2)	THRUST lb (N)	α deg (rad)	N_{Z_a} (AT ENGINE c.g.)	N_{X_a}	N_{Y_a}	$\ddot{\theta}$ rad/sec^2
101	PSD Vert. Up Gust + (Bal. 1G)	22,000 (6 706	.814	V_C	350 (179)	70,273 (31 876)	11.67		10,849 (48 256)	0.17 (0.003)	3.77			
102	↓	22,000 (6 706)	.814	V_C	350 (179)	66,219 (30 037)	2.30		10,799 (48 034)	0.10 (0.002)	3.77			
103	↓	22,000 (6 706)	.814	V_C	350 (179)	66,219 (30 037)	36.00		10,709 (47 636)	-0.02 (0)	3.77			
104	PSD Vert. Down Gust + (Bal. 1G)	22,000 (6 706)	.814	V_C	350 (179)	70,273 (31 876)	11.67		10,849 (48 256)	0.17 (0.003)	-1.77			
105	↓	22,000 (6 706)	.814	V_C	350 (179)	66,219 (30 037)	2.30		10,799 (48 034)	0.10 (0.002)	-1.77			
106	↓	22,000 (6 706)	.814	V_C	350 (179)	66,219 (30 037)	36.00		10,709 (47 636)	-0.02 (0)	-1.77			
107	2 Whl Ldg. Dynamic A/P & Gear	S.L.		V_{SI}	150 (76.5)	94,184 (42 722)	6.2				3.90		+0.24	
108	↓	S.L.		V_{SI}	150 (76.5)	70,273 (31 876)	37.8				3.90		+0.80	
109	↓	S.L.		V_{SI}	150 (76.5)	70,273 (31 876)	37.8				2.72		-0.54	
110	↓	S.L.		V_{SI}	150 (76.5)	70,273 (31 876)	37.8				1.38		-0.02	
111	↓	S.L.		V_{SI}	150 (76.5)	70,273 (31 876)	37.8				2.12		+0.05	

TABLE 7 CONTINUED
DC-9-32 NACELLE/PYLON LOADS ANALYSIS CONDITIONS

COND NO.	DESCRIPTION	ALT ft (m)	MACH	SPEED	V KEAS (m/s)	WT lb (kg)	CG % (M.A.C)	I_p 10^6 SLUG ft^2 (Ggm^2)	THRUST lb (N)	α deg (rad)	N_{Z_a} (AT ENGINE c.g.)	N_{X_a}	N_{Y_a}	$\ddot{\theta}$ rad/sec^2
112	2 Whl Ldg. Rigid A/P & Dyn. Gear	S.L.		V_{S_1}	150 (76.5)	99,000 (44 906)					3.323		+0.303	
113	↓	S.L.		V_{S_1}	150 (76.5)	99,000 (44 906)					2.442		-0.593	
114	↓	S.L.		V_{S_1}	150 (76.5)	99,000 (44 906)					2.797		+0.709	
115	1 Whl Ldg. Rigid A/P & Dyn. Gear	S.L.		V_{S_1}	150 (76.5)	99,000 (44 906)					2.579	-0.110	+0.171	
116	Lat. Drift Ldg., Rigid A/P, Dyn. Gear	S.L.		V_{S_1}	150 (76.5)	99,000 (44 906)					1.683	-0.611	+0.043	
117	↓	S.L.		V_{S_1}	150 (76.5)	99,000 (44 906)					1.683	+0.611	-0.043	
121	Discrete Up Gust	20 000 (6 096)	0.636		285 (145)	70,312 (31 894)	3.8	1.71 (2.32)	5,790 (25 754)	7.35 (0.128)	4.055		-0.041	-0.5799
122	↓		0.754		338 (172)	70,312 (31 894)	3.8	1.71 (2.32)	8,419 (37 448)	4.21 (0.073)	4.009		-0.037	-0.5199
123	↓		0.754		338 (172)	67,616 (30 671)	33.2	1.55 (2.10)	8,367 (37 216)	4.01 (0.070)	3.779		-0.011	-0.1517
124	↓		0.636		285 (145)	64,740 (29 366)	26.0	1.51 (2.05)	5,771 (25 669)	7.04 (0.123)	4.021		-0.023	-0.3284
125	↓		0.754		333 (170)	64,740 (29 366)	26.0	1.51 (2.05)	8,349 (37 136)	3.95 (0.069)	3.979		-0.018	-0.2602

TABLE 7 CONCLUDED
DC-9-32 NACELLE/PYLON LOADS ANALYSIS CONDITIONS

COND NO.	DESCRIPTION	ALT ft (m)	MACH	SPEED	V KEAS (m/s)	WT lb (kg)	CG % (M.A.C.)	I_p 10^6 SLUG ft^2 (Ggm^2)	THRUST lb (N)	α deg (rad)	N_{Z_a} (AT ENGINE c.g.)	N_{X_a}	N_{Y_a}	$\ddot{\theta}$ rad/ sec^2
126	Discrete Down Gust	20,000 (6 096)	0.636		285 (145)	70,312 (31 894)	3.8	1.71 (2.32)	5,790 (25 754)	-4.97 (-0.087)	-2.055		-0.041	0.5799
127			0.754		338 (172)	70,312 (31 894)	3.8	1.71 (2.32)	(37 448)	-3.67 (-0.064)	-2.009		-0.037	0.5199
128			0.754		338 (172)	67,616 (30 671)	33.2	1.55 (2.10)	8,367 (37 216)	-3.83 (-0.067)	-1.779		-0.011	0.1517
129			0.636		285 (145)	64,740 (29 366)	26.0	1.51 (2.05)	5,771 (25 669)	-5.28 (-0.092)	-2.021		-0.023	0.3284
130			0.754		333 (170)	64,740 (29 366)	26.0	1.51 (2.05)	8,349 (37 136)	-3.85 (-0.067)	-1.979		-0.018	0.2602
201	Positive Vert. Gust		0.64		285 (145)	70,312 (31 894)	3.8		5,790 (25 754)	7.45 (0.130)	3.564		0	
202	Positive Bal. Maneuver	10,000 (3 048)	0.76		416 (212)	99,000 (44 906)	4.3		13,118 (58 349)	2.89 (0.050)	2.5		+0.099	
203	Negative Bal. Maneuver	25,850 (7 879)	0.85		332 (169)	107,240 (48 644)	6.79		9,886 (43 973)	-2.24 (-0.039)	-1.0		-0.093	
204	Yaw Maneuver	25,850 (7 879)	0.69		274 (140)	107,240 (48 644)	27.94		9,684 (43 074)	2.62 (0.046)	1.0		+0.074	

TABLE 8

REFANNED JT8D LOADS ANALYSIS PARAMETERS

ANALYSIS WEIGHT AND c.g.	WEIGHT lb	WEIGHT (kg)	Y (c.g.) in	Y (c.g.) (m)
JT8D-17 (basic demountable engine plus nacelle)	4,699	(2 133)	989	(25.12)
Weight increment for refan	570	(259)	942	(23.93)
Weight increment for acoustically treated nacelle	655	(297)	1 000	(25.40)
JT8D-117 Engine and nacelle	5,924	(2 689)	990	(25.15)
Add 5% for Contingencies	296	(134)	990	(25.15)
JT8D-117 Analysis Weight and c.g.	6,220	(2 823)	990	(25.15)

ANALYSIS FORWARD AND REVERSE THRUST

JT8D-117 Net Installed Forward Thrust F_T = 17 500 lb (77.84 kN)

Reverse Thrust per Engine and Nacelle:

$F_R = \xi F_T + D_{RAM} + D_{BASE} + P_{REV}dA_{FR} + D_{NAC}$

ξ = .4 (assumed efficiency for design)

D_{RAM} = 4,470 lb (19.88 kN)(ram drag at 175 KEAS (89.95 m/s)

D_{BASE} = 2,751 (12.24 kN)(base drag at 175 KEAS (89.95 m/s)

$P_{REV}dA_{FR}$ = -460 lb (-2.05 kN)(induced pressure force)

D_{NAC} = 104 lb (462 N)(nacelle drag at 175 KEAS (89.95 m/s)

F_R = 13,865 lb (61.67 kN)

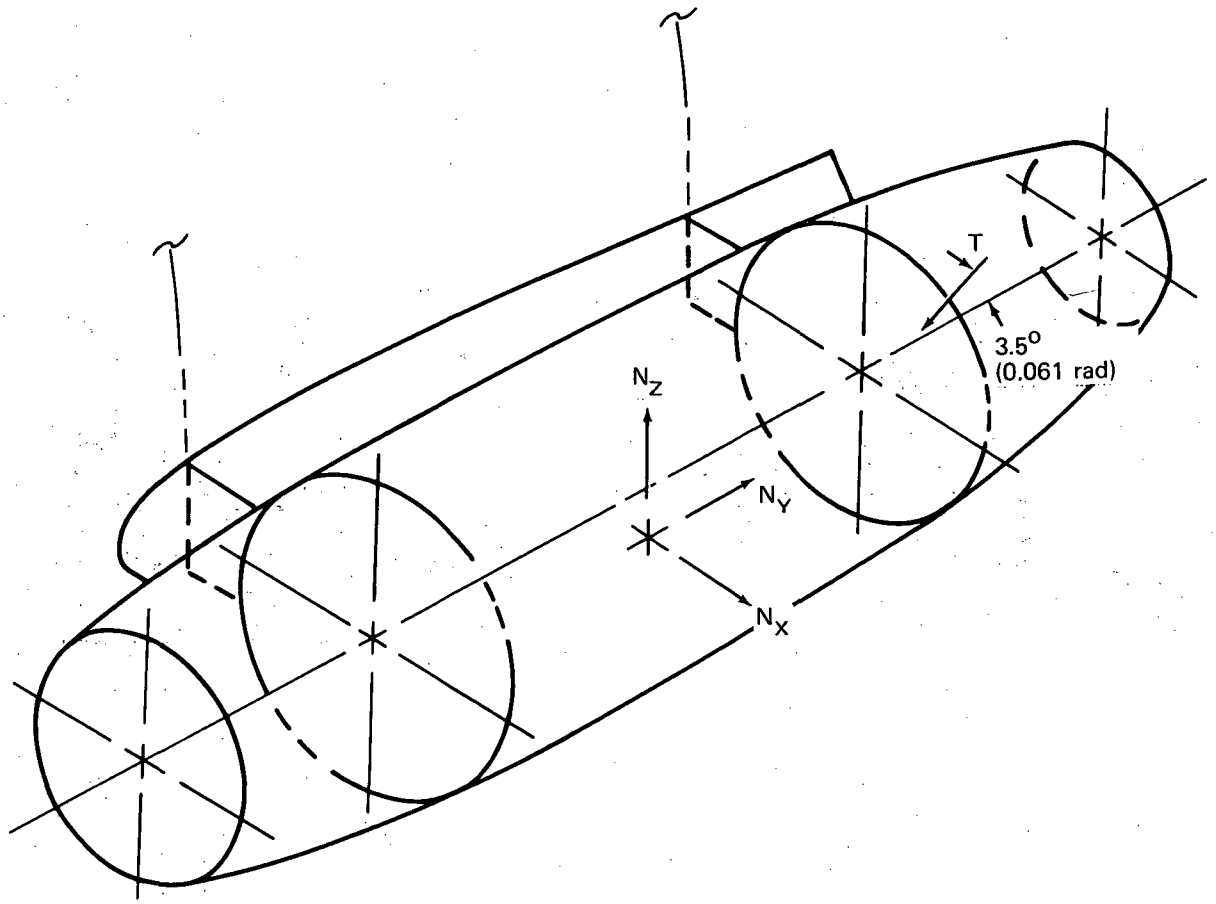

N_X, N_Y, AND N_Z – ACCELERATION LOAD FACTORS AT ENGINE CG

T – ENGINE THRUST

AIRPLANE SIGN CONVENTION:

N_{X_a}, N_{Y_a}, AND N_{Z_a} – ACCELERATION LOAD FACTORS AT AIRPLANE CG (SEE DIAGRAM ABOVE FOR POSITIVE SENSE)

α – AIRPLANE ANGLE OF ATTACK (+ NOSE UP)

$\ddot{\theta}$ – AIRPLANE PITCHING ACCELERATION (+ NOSE UP)

RFR-131

FIGURE 24. SIGN CONVENTIONS FOR LOADS ANALYSES

TABLE 9

DC-9-32 REFAN DYNAMIC LANDING LOAD CONDITIONS

(FLEXIBLE AIRPLANE AND GEAR)

AIRPLANE CONFIGURATIONS		
CONFIGURATION	1	2
Gross Weight lb (kg)	70,273 (31 876)	94,184 (42 722)
c.g. (% MAC)	37.8	6.2
Fuel lb (kg)	4,000 (1 814)	4,000 (1 814)
Payload lb (kg)	2,877 (1 305)	26,260 (11 912)

ENGINE LIMIT LANDING RESPONSES

CONF.	LOAD FACTORS (G's) N_Z	LOAD FACTORS (G's) N_Y	PITCHING MOMENT in lb (N·m)	REMARKS (1)
2	3.90	0.240	86,419 (9 764)	Max. Vert. Load Factor
1	3.29	0.80	-19,464 (-2 199)	Max. Aft Load Factor
1	2.72	-0.54	125,210 (14 146)	Max. Fwd Load Factor
1	1.38	-0.02	193,715 (21 886)	Max. Nose Up Moment
1	2.12	-0.05	-233,040 (-26 329)	Max. Nose Down Moment

(1) Values in each row occur at same time

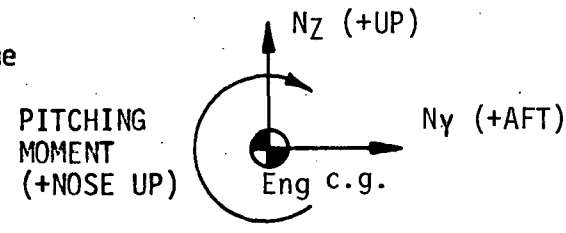

support structure. Load factors and thrust for these conditions are shown in table 10. As the external loads analysis progressed during Phase I, it was shown that the design conditions encompass the airplane flight and landing conditions.

The internal loads for the pylon and fuselage support structure were analyzed using a computer idealization of the preliminary structure. The analysis technique used was the Douglas developed FORMAT Combined Method of Analysis program which is a computerized solution of internal loads and deflections combining both the force and displacement methods. An existing idealization model of the DC-9-30 fuselage in the ventral stair configuration was modified to accept the refan pylon. This model which includes the engine, pylon, aft fuselage section and wing stubs was analyzed using the refan preliminary weights, c.g., and thrust. The structural idealization labeled the fuselage/pylon model, is shown in figures 25, 26 and 27. For preliminary design loads, the load conditions shown in table 10 were used. The initial analysis of the fuselage/pylon model indicated that the internal loads distribution varied from the existing DC-9 and caused overloading of the pressure bulkhead frame. This was primarily caused by a change in the system of lateral restraints between the pylon and fuselage. The existing DC-9 pylon has a flexible attachment to the pressure bulkhead frame whereas the refan model had a rigid attachment. This additional load path was provided in the structural idealization because the refan pylon width was reduced to 204.47 mm (8.05 in.). It was estimated that the most efficient pylon design would shear out the thrust loads in the forward portion between the front spar frame at Station 965 and the pressure bulkhead frame at Station 996. To study this design problem, a separate model of the pylon and engine was developed. This small model of the pylon which is shown in figure 28 permitted efficient iteration of the loads and deflection analysis and minimized the computing costs. As the analysis progressed, the pylon model was modified to give an improved representation of the pylon-to-fuselage attachment structure. This modified model is shown in figure 29. The analyses of these models are described with their significant results in table 11 in the sequence of their development.

In general, the results of the first five runs (1 through V) of the pylon model gave lateral loads that the fuselage frames were unable to support. When these frames were disconnected (lateral restraint cut) and the pylon supported at the front and rear spar frames, the lateral deflections of the pylon exceeded the limits of good fatigue design. An effort to stiffen the pylon to reduce the lateral deflection resulted in an excessive weight penalty. Table 12 gives a summary of the fuselage frame and bulkhead lateral restraints for each of the configuration investigated.

The final pylon-to-fuselage configuration resembles the existing DC-9 design. The frames at Stations 980 and 1019 were given a rigid attachment and the pressure bulkhead a flexible attachment. Excessive pressure bulkhead lateral loading was considered undesirable from a fatigue loading standpoint. Also, since there are two DC-9 pressure bulkhead configurations, with and without a ventral stair opening, minimizing the lateral load at the pressure bulkhead eliminates the need for two refan retrofit designs. Run (5) of the modified pylon model and Run C of the fuselage/pylon model which is presently in progress.

TABLE 10

DC-9 REFAN PYLON ARBITRARY DESIGN CONDITIONS

LOAD FACTORS AND THRUST ARE ULTIMATE
(SEE FIGURE 24 FOR SIGN CONVENTION)

CONDITION NUMBER	N_X	N_Y	N_Z	THRUST lb K_N	COMMENTS
1		12			CRASH
2		12	6		
3	-1.5		6	-24,000 (-106.8)	REPRESENT DYNAMIC VERTICAL GUST AND DYNAMIC LANDING
4	1.5		6	-24,000 (-106.8)	
5	-1.5		-3	-24,000 (-106.8)	
6	1.5		-3	-24,000 (-106.8)	
7	- 1		8	26,250 (116.8)	
8	1		8	26,250 (116.8)	
9	- 1		-5	26,250 (116.8)	
10	1		-5	26,250 (116.8)	
11	- 5				REPRESENT DYNAMIC LATERAL GUST
12	5				
13			3	52,500 (233.5)	FATIGUE DESIGN
14			3	-48,000 (-213.5)	

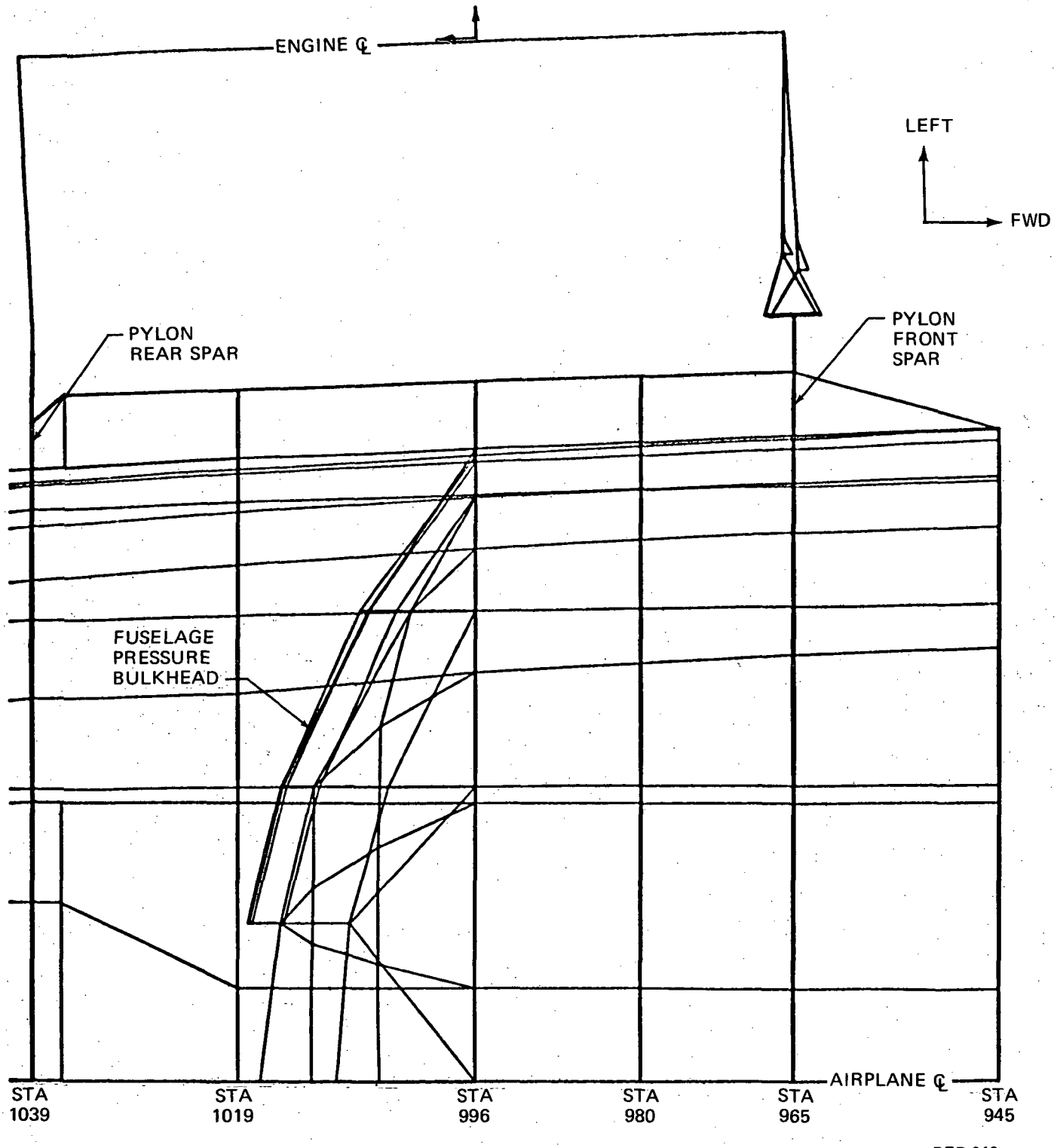

FIGURE 25. FUSELAGE/PYLON MODEL STRUCTURAL IDEALIZATION – PLAN VIEW

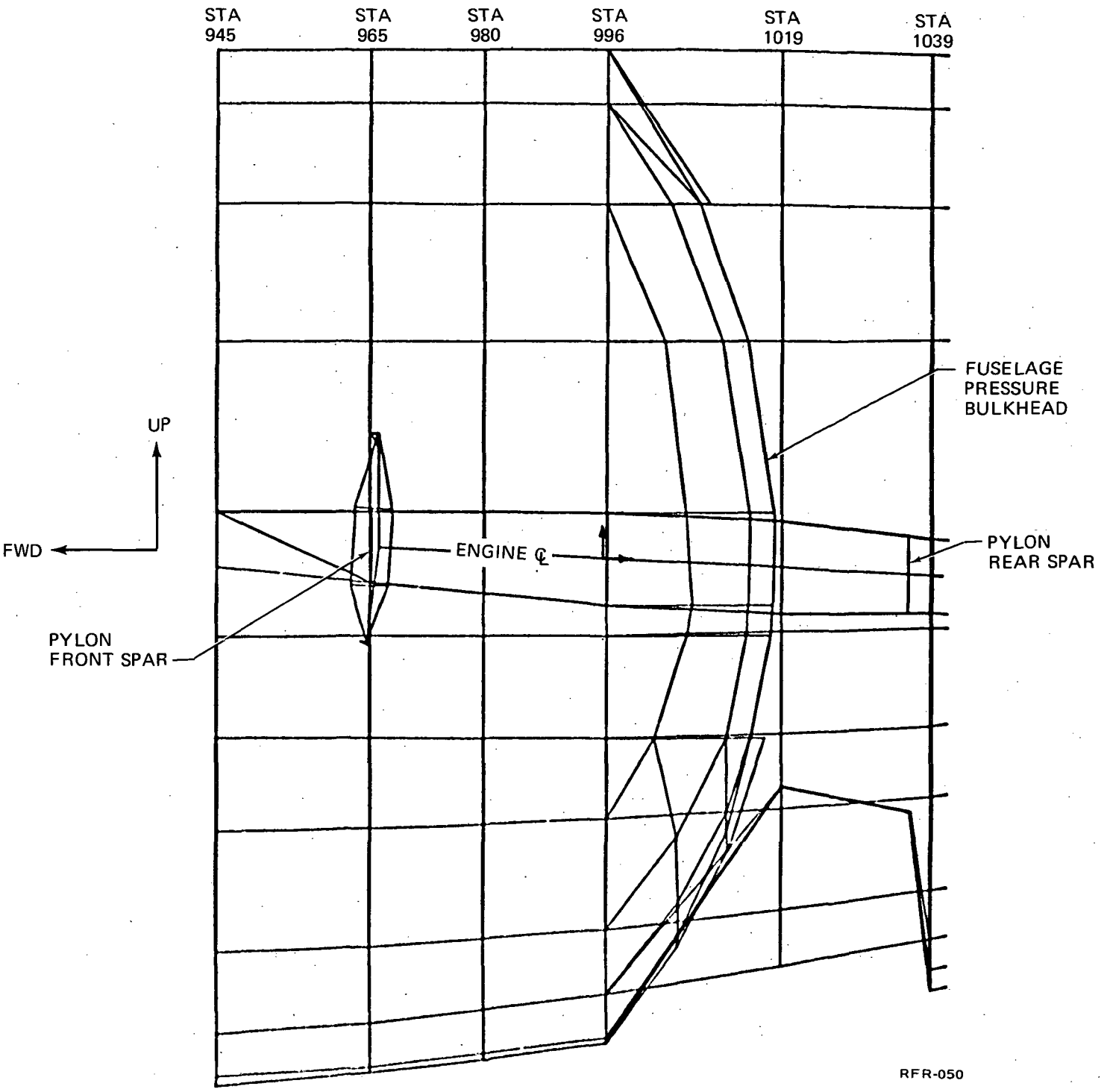

FIGURE 26. FUSELAGE/PYLON MODEL STRUCTURAL IDEALIZATION – SIDE VIEW

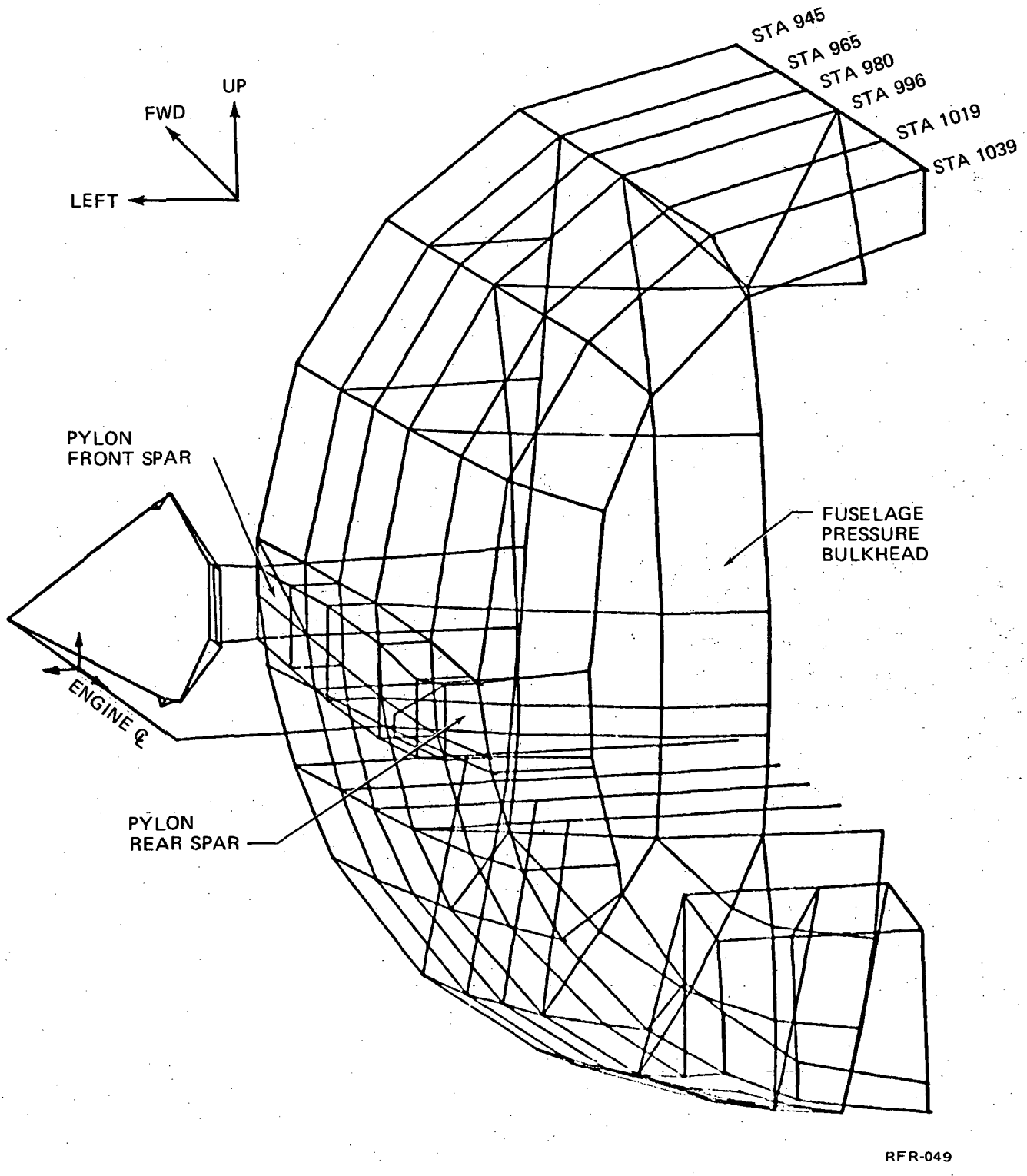

FIGURE 27. FUSELAGE/PYLON MODEL STRUCTURAL IDEALIZATION – REAR VIEW

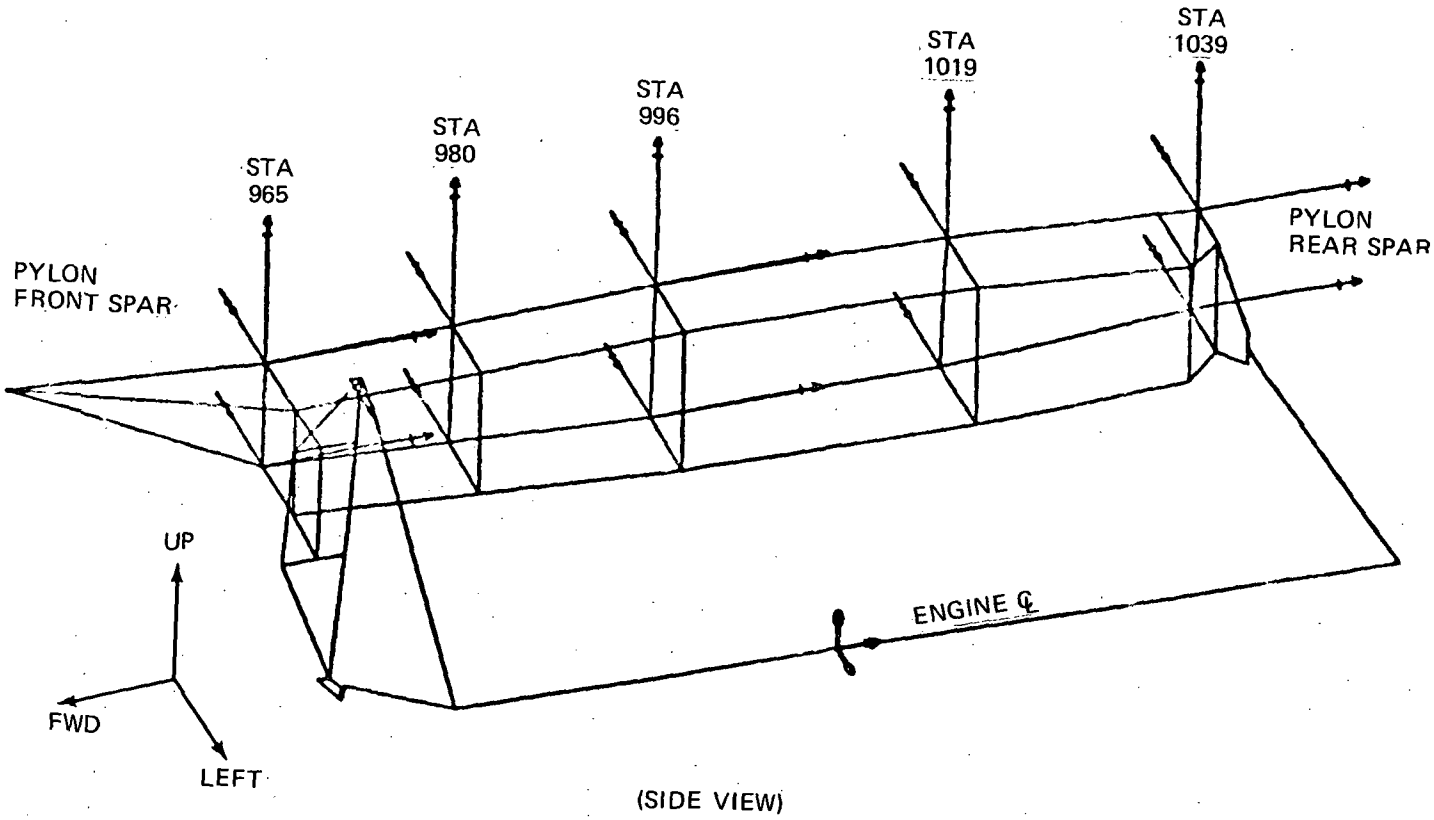

(SIDE VIEW)

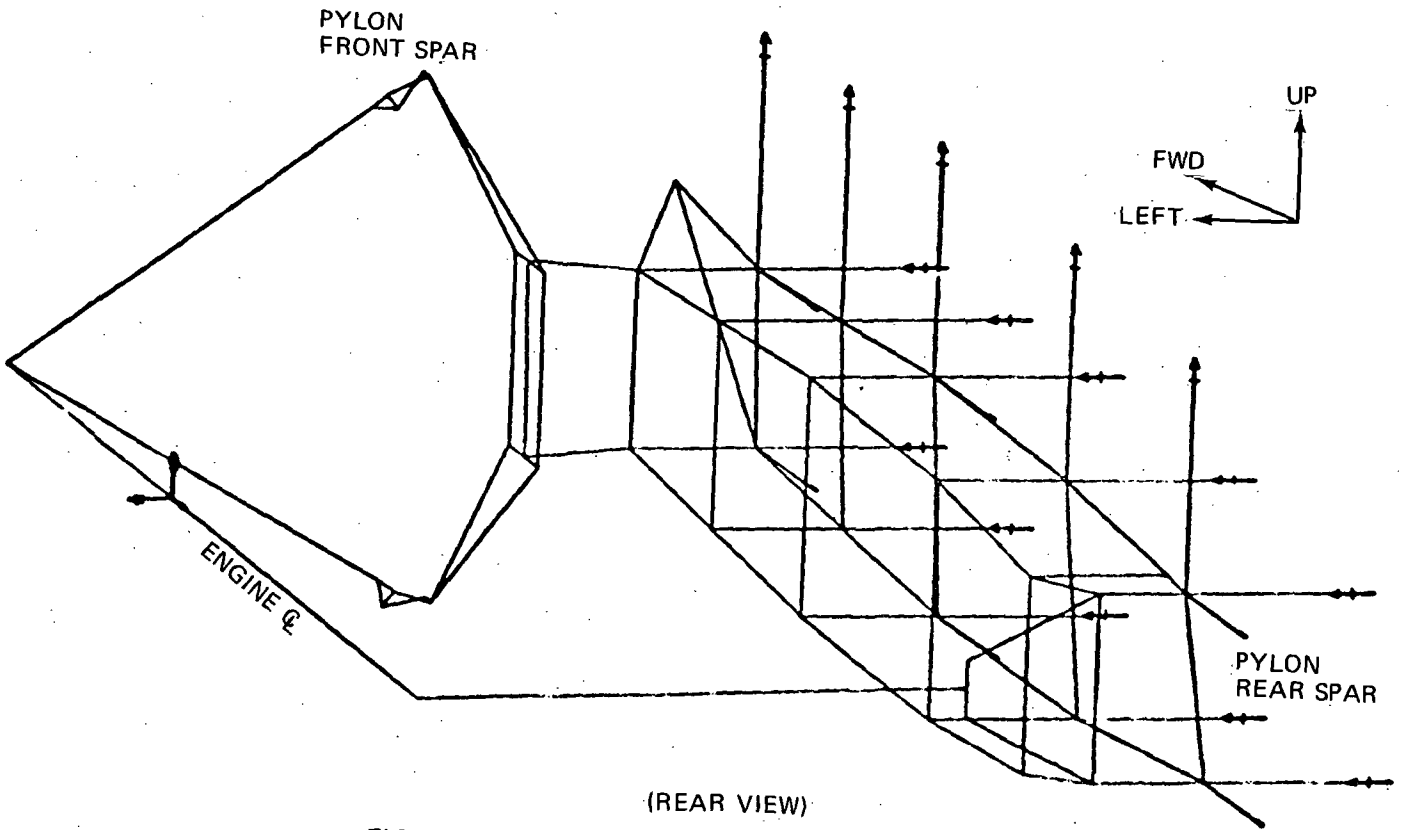

(REAR VIEW)

FIGURE 28. PYLON MODEL STRUCTURAL IDEALIZATION

RFR-047

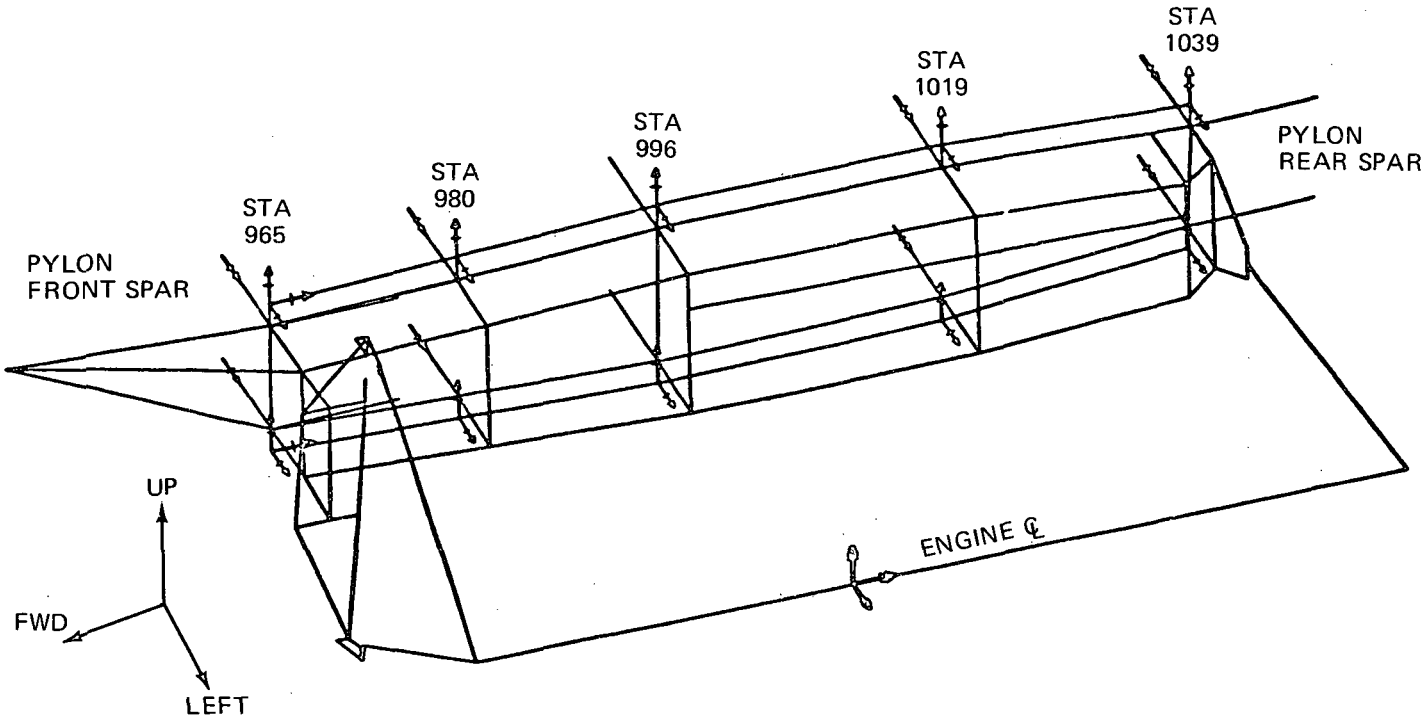

(SIDE VIEW)

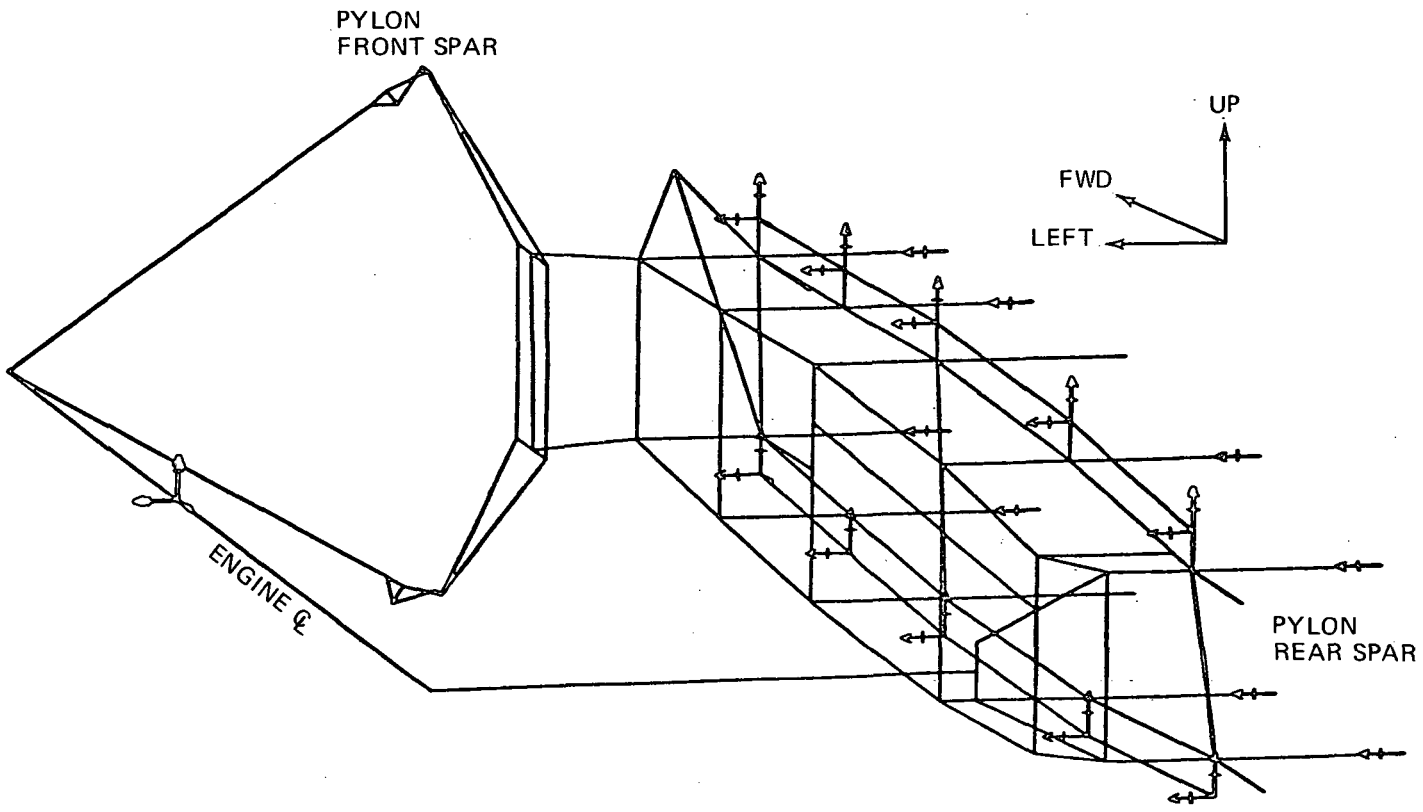

(REAR VIEW)

RFR-046

FIGURE 29. PYLON MODEL STRUCTURAL IDEALIZATION (REVISED BOUNDARIES)

TABLE 11 CONTINUED

DEVELOPMENT OF FUSELAGE AND PYLON STRUCTURAL MODELS

MODEL	RUN IDENTIFICATION	DESCRIPTION	SIGNIFICANT RESULTS
Fuselage/Pylon (with Engine)	A	Initial run with intermediate frames (Sta. 980 and 1019) and pressure bulkhead (Sta. 996) joined to pylon to give lateral restraint.	Pylon front spar shear was low due to redistribution through pylon to Sta. 996. Loads at pressure bulkhead were excessive.
Pylon (with Engine)	I	Removed pylon center shear web at Sta. 996.	Pylon front spar shear corrected, however, pressure bulkhead lateral loads remained excessive.
	II	Same as I with Sta. 996 lateral restraints cut.	High lateral loads at Sta. 980; would require auxiliary frame.
	III	Same as II with continuous shear panels in pylon closing rib.	Closing rib shears high for structure available. Load at Sta. 980 reduced, but marginal for single frame.
	IV	Same as III. with lateral restraints cut at Sta. 980, 996 and 1019.	Relative deflections between pylon and fuselage were excessive.
	V	Same as IV. with revised spring rates at engine shock mounts and engine weight and c.g.	Relative deflections between pylon and fuselage were excessive.

TABLE 11 CONCLUDED

DEVELOPMENT OF FUSELAGE AND PYLON STRUCTURAL MODELS

MODEL	RUN IDENTIFICATION	DESCRIPTION	SIGNIFICANT RESULTS
Modified Pylon (with Engine)	(1)	Pylon re-idealized to be more representative. Lateral restraints cut at Sta's. 980, 996 and 1019.	Relative deflections between pylon and fuselage were excessive. Engine bending deflection also was excessive.
	(2)	Same as (1) with increased engine stiffness.	Relative deflections between pylon and fuselage were excessive; engine bending deflection was satisfactory.
	(3)	Same as (2) with pylon center shear web at Sta. 996.	Relative deflections between pylon and fuselage were excessive, but center shear web made pylon upper and lower surface deflections uniform.
	(4)	Same as (3) with pylon upper surface bending stiffness 3 times greater.	The attempt to reduce pylon deflections was unsuccessful. Deflections were still too high for fatigue design.
	(5)	Same as (3) with lateral restraint provided at Sta's. 980 and 1019.	Pylon to fuselage deflections and load distribution were within acceptable limits.
Fuselage/Pylon (with Engine)	B	Same as A. with fuselage and pylon structure resized for the load distribution of Run I. Current engine weight, c.g.,and bending stiffness.	Pylon front spar shear was increased from Run A. This run gives the correct loads distribution for the configuration with lateral restraint at all frames.
	C	Model revised to the pylon configuration of Run (5) with lateral restraint at Sta's. 980 and 1019 and cut at Sta. 996.	Analysis in progress.

TABLE 12

FUSELAGE AND PYLON STRUCTURAL MODELS
SUMMARY OF FRAME AND BULKHEAD RESTRAINTS (1)

MODEL	RUN IDENTIFICATION	FRONT SPAR BULKHEAD	FRAME	PRESSURE BULKHEAD	FRAME	REAR SPAR BULKHEAD
		STATION 965	STATION 980	STATION 996	STATION 1019	STATION 1039
FUSELAGE/ PYLON	A	X	X	X	X	X
PYLON	I	X	X	X	X	X
	II	X	X	CUT	X	X
	III	X	X	CUT	X	X
	IV	X	CUT	CUT	CUT	X
	V	X	CUT	CUT	CUT	X
MODIFIED PYLON	1	X	CUT	CUT	CUT	X
	2	X	CUT	CUT	CUT	X
	3	X	CUT	CUT	CUT	X
	4	X	CUT	CUT	CUT	X
	5	X	X	CUT	X	X
FUSELAGE/ PYLON	B	X	X	X	X	X
	C	X	X	CUT	X	X

(1) X - indicates a lateral load path exists between the pylon and fuselage.

CUT - indicates removal of lateral load path.

Engine mounts. - Details of the engine mount system were included in the internal loads analysis models. Table 13 gives the ultimate engine mount loads from the pylon model, Run (5). The sign convention for JT8D-109 engine mount loads is shown in figure 30. These loads were provided to the manufacturer of the engine mount vibration isolators and cone bolts for the strength checks. A summary of the margins of safety from that analysis are shown in table 14. Structurally, the existing mounts will be adequate for the refanned DC-9.

Fuselage keel. - The lower center fuselage shell in the keel wheel well area has been modified (on a rework basis) to be capable of sustaining the refan loads. The rework basically consists of straps and nested angles added to longeron #29 and the addition of an external doubler to the lower fuselage shell between the rear spar and the main landing gear wheel well, aft bulkhead, figure 21. The strength analysis of the keel structure has been completed for the DC-9-10, -31 and -32 models. The DC-9-40 Series will also require a rework to sustain the required loads. The strength analysis verifying the structure will be performed upon completion of the rework design. Internal loads used for this analysis were taken from the DC-9 hard landing study which produces 1 370 kN (308,000 lb) through the lower shell structure of the center fuselage keel area. This load is based on a hard landing condition of 4.57 m/s (15 ft/sec) sink speed and an external fuselage bending moment of 5.197 MN·m (46×10^6) in.-lb).

Fuselage forward frames. - The maximum ballast required for any refanned DC-9 airplane is 408 kg (900 lb), figure 46. The installation will be similar to an existing 318 kg (700 lb) ballast installation for the DC-9-30 aircraft shown in figure 31. An additional tray to support lead "pigs" will be added to each side of the aircraft to accommodate the increased weight for refan.

The strength of the ballast installation has been checked for 635 kg (1,400 lb). The acceleration load factors were taken from the existing DC-9-30 analysis which are conservative since the refanned DC-9 results in lesser acceleration. The ultimate load factors are as follows:

- N_Z = 6.6 and -3.6
- N_Y = 1.44
- $N_X = \pm 0.75$

Flutter and Vibration. - Preliminary model vibration and flutter analyses have been performed in support of the DC-9 refan study. DC-9-32 airplane modes have been computed for the basic and the refan study configurations for use in flutter and dynamic loads analyses. The analytical modes for the basic configuration compare well with measured modes determined from past ground vibration tests. The basic airplane modes were modified analytically to represent the refan configurations. The analyses accounted for the change in engine weight, inertia and c.g. location, and changes in pylon geometry. Configurations analyzed include the refan nacelle with incremental weights of 759.8 kg (1,675 lb) per nacelle on a 203.2 mm (8 in.) pylon. Appropriate modifications were made to the pylon stiffness to reflect the decrease in pylon length. Symmetric and antisymmetric orthogonal modes

TABLE 13

JT8D-109 ULTIMATE ENGINE MOUNT LOADS

PYLON MODEL, RUN 5

(SEE FIGURE 30 FOR SIGN CONVENTION AND LOAD LOCATION)

COND.	P_{65}	P_{67}	P_{69}	P_{72}	P_{73}	P_{76}	P_{47A}	P_{47S}
SEE TABLE	lb (kN)	lb (kN)	lb (kN)	lb (kN)	lb (kN)	lb (kN)	lb (kN)	lb (kN)
1	34,650 (154)	-11,256 (-50)	11,684 (52)	-8,976 (-40)	-3,928 (-17)	42,470 (189)	23,054 (103)	1,535 (7)
2	35,053 (156)	28,644 (127)	-8,959 (-40)	-50,237 (-223)	-18,340 (-82)	40,890 (182)	22,195 (99)	17,640 (78)
4	-10,213 (-45)	39,933 (178)	-20,741 (-92)	-40,524 (-180)	-13,953 (-62)	-14,958 (-67)	-11,537 (-51)	14,710 (65)
7	12,113 (54)	52,548 (234)	-26,891 (-120)	-57,465 (-256)	-20,760 (-92)	12,466 (55)	9,128 (41)	22,993 (102)
8	11,997 (53)	50,619 (225)	-25,245 (-112)	-62,601 (-278)	-24,013 (-107)	12,280 (55)	4,744 (21)	22,983 (102)
10	11,123 (49)	-35,831 (-159)	19,482 (87)	26,796 (119)	7,212 (32)	15,704 (70)	6,607 (29)	-11,908 (-53)

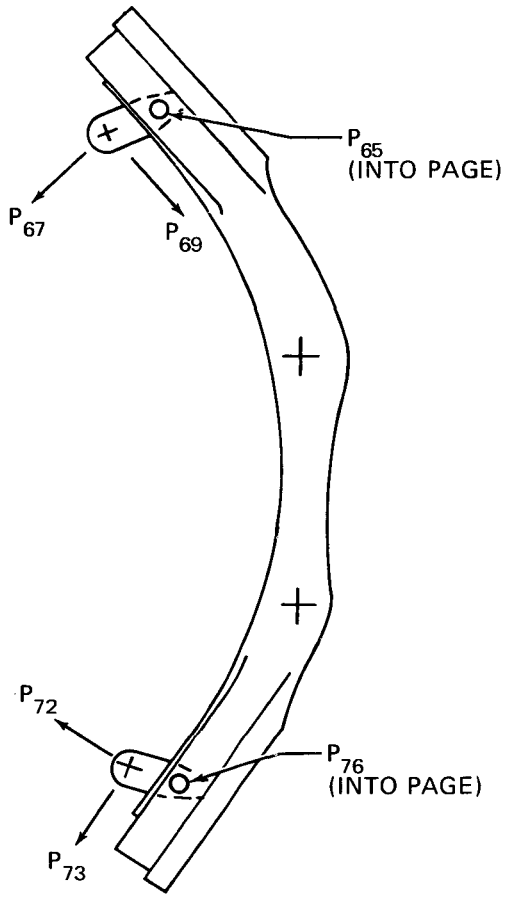

FORWARD MOUNT YOKE
(VIEW LOOKING FORWARD)

FORCES ARE NORMAL AND PARALLEL TO VIBRATION ISOLATORS

AFT MOUNT
(VIEW LOOKING FORWARD)

FORCES ARE NORMAL AND PARALLEL TO VIBRATION ISOLATORS

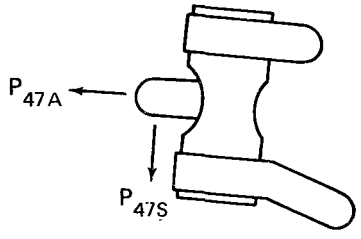

RFR-065

FIGURE 30. JT8D-109 ENGINE MOUNT LOADS (SIGN CONVENTION)

TABLE 14

DC-9 VIBRATION ISOLATOR AND CONE BOLT STRESS ANALYSIS RESULTS

	LOCATION	LOAD COND. SEE TABLE 10	MARGINS OF SAFETY DC-9	MARGINS OF SAFETY DC-9 REFAN(1)
Front Cone Bolt R18210-2	A-A B-B C-C D-D	7 7 6 2	.90 1.06 .96 1.89	.06 .46 .04
Aft Cone Bolt R18211-2	A-A	7	.51	
Front Inner Housing KR 4129-1		8	.14	.073
Aft Outer Housing R18227-2	A-A B-B C-C D-D Lwr. Lug E-E Upr. Lug	7 7 7 7 7 7 7	.50 4.58 1.72 2.18 1.44 2.50 .53	.77
Threaded Cap KR 4141-1		7	.16	
Aft Inner Housing KR 4140-1	A-A B-B C-C D-D	7 7 7 7	.78 .14 .29 .62	.40 .06 .09 .02
Link, Aft Mount KR 4111-1	Lug Shear Bearing Tension	7 7 7	.23 .35 .33	
Front Cushion Retainer KR 4131-1		2	.96	
Link, Aft Mount R18132-2	Lug Shear Bearing Tension	7 7 7	.11 .21 .20	

(1) Where no figure appears, Margin of Safety is taken to be satisfactory by inspection.

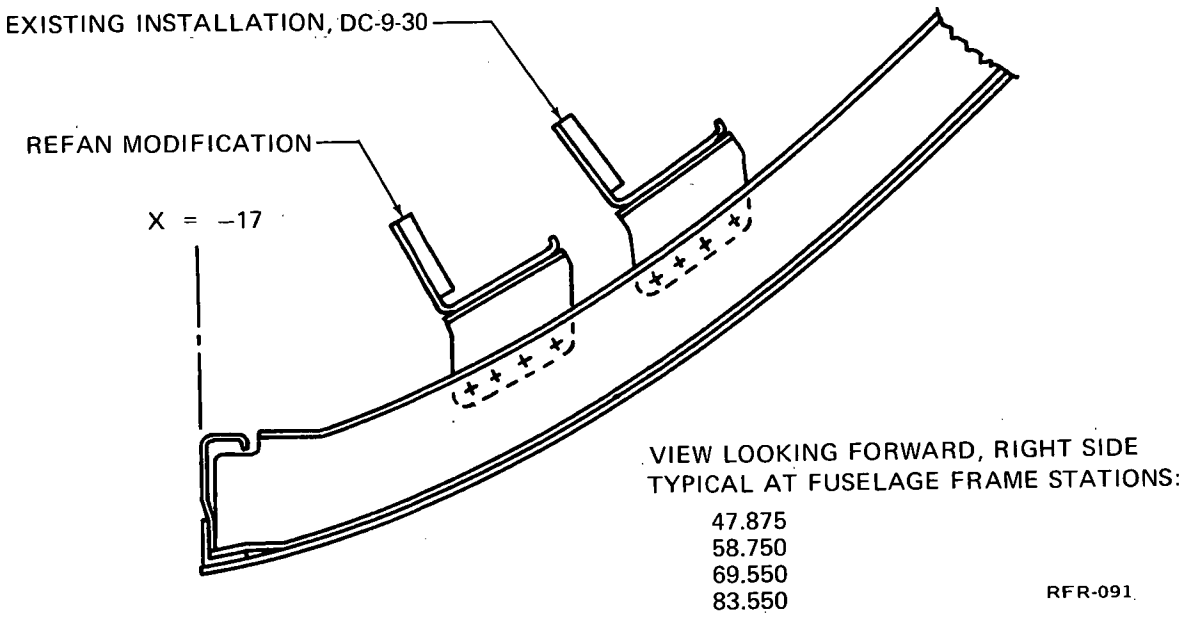

FIGURE 31. FUSELAGE BALLAST INSTALLATION

were computed for 6 payloads and 4 fuel load variations. A comparison of modal frequencies for the basic and refan configurations is presented in table 15. All modal data are available on magnetic tapes.

A flutter analysis was performed to determine the change in airplane flutter characteristics when configured with the refan engines using incremental weights up to 759.8 kg (1,675 lb) per nacelle. The unsteady aerodynamic coefficients have shown good correlation with previously obtained DC-9 flutter flight test results. The critical flutter model of the DC-9 is the 3.2 H_Z antisymmetric T-tail mode. The analysis showed the additional nacelle weight and pylon length changes to have no significant affect on the T-tail flutter mode. Therefore, structural changes for flutter prevention are not required for the refan configuration. Based upon these results, the expense of a flutter model program was deemed unnecessary and model tests were not performed.

TABLE 15

DC-9-32 ORTHOGONAL MODE FREQUENCY COMPARISON

NOTE: PAYLOAD = 27,000 lb (12 247 kg)

FULL FUEL LOAD

ANTISYMMETRIC MODES

DESCRIPTION	FREQUENCY - Hz	
	EXISTING ENGINE	REFAN ENGINE
FIN BENDING	2.501	2.508
FIN TORSION	3.041	3.044
ENGINE ROLL	4.033	4.144
1st WING BENDING	5.188	5.270
FUSELAGE BENDING	5.721	5.680
2nd WING BENDING	6.274	6.238
2nd FIN BENDING	8.142	8.126
WING FORE AND AFT	10.746	10.259
ENGINE PITCH	10.994	10.880
2nd H.S. BENDING	15.279	15.294
FUSELAGE BENDING	16.305	16.419
1st WING TORSION	16.693	16.830

SYMMETRIC

DESCRIPTION	FREQUENCY - Hz	
	EXISTING ENGINE	REFAN ENGINE
1st WING BENDING	2.955	2.956
1st H.S. BENDING	4.145	4.149
ENGINE ROLL	5.794	5.824
1st FUSELAGE BENDING	7.026	7.577
1st WING FORE AND AFT	8.730	8.615
2nd WING BENDING	9.097	8.704
ENGINE PITCH	9.217	9.128
1st V.S. FORE AND AFT	12.337	12.639
1st H.S. FORE AND AFT	15.316	15.336
1st WING TORSION	16.905	16.904
3rd WING BENDING	18.039	17.711
2nd H.S. BENDING	19.117	19.171
1st H.S. TORSION	23.171	23.171

Nacelle Design

Detailed structural design criteria was developed for the minimum and maximum noise suppression nacelle design. The purpose of this criteria was to identify and define the loads and environment that would be used to perform loads analyses. Aerodynamic loads, inertia loads, thermal effects, pneumatic, acoustic, and handling loads were identified. The results from the load analyses were used to size the nacelle structure and nacelle systems. The structural design criteria also defined the requirements of the nose cowl, nacelle upper and lower access doors, thrust reverser, and exhaust duct.

Nose cowl. - The minimum and maximum noise suppression treatment nose cowl design for the JT8D-109 refan engine has an inner barrel fabricated from bonded aluminum honeycomb sandwich and its outer skin and leading edge lip are fabricated from formed aluminum sheet. The honeycomb sandwich is structured with a porous face sheet on the inner duct airflow side for sound attenuation. The effective treatment length is 1.3 m (51 in.) for the minimum treatment and 1.6 m (63 in.) for the maximum treatment (figure 32). The inner and outer skins are supported by circumferential frames and bulkheads. The barrel functions as the principal load carrying component. At the aft end of the barrel is a nose cowl attach ring which transfers the load into the engine fan case. A double wall leading edge lip and closing bulkhead are attached to the forward end of the barrel forming a D-duct. The leading edge is anti-iced by ducting hot air into the D-duct. An aft bulkhead located forward of the nose cowl attach ring closes the nose cowl inner and outer skins and forms a land for the forward edge of nacelle upper and lower access doors.

Access doors. - New nacelle access doors are required for the JT8D-109 refan engine installation. Although the doors will be similar to the existing DC-9 nacelle door (figure 33), the structure will be simplified for the flight demonstration program to minimize tooling fabrication and assembly costs.

Fewer frames and heavier skins will be used to reduce the number of detail parts and the small access door normally used for daily maintenance will be eliminated; however, there will be a pressure relief door in each upper access door and a fire fighting door in each lower access door.

Thrust reverser. - The thrust reverser for the JT8D-109 refan engine is a scaled-up version of the present production DC-9 reverser and the control system of the reverser is unchanged. The thrust reverser is designed to produce essentially the same total retarding effect on the airplane during normal landing roll deployment as on the present production DC-9 (figure 34).

The reverser assembly is oriented on each of the two pods such that the upper reverse gas efflux is directed 15° from the vertical toward the airplane centerline while the lower reverse gas efflux is directed 15° from the vertical away from the airplane centerline. This outward direction alleviates the problem of ingestion of particles blown-up off the ground by reverser efflux.

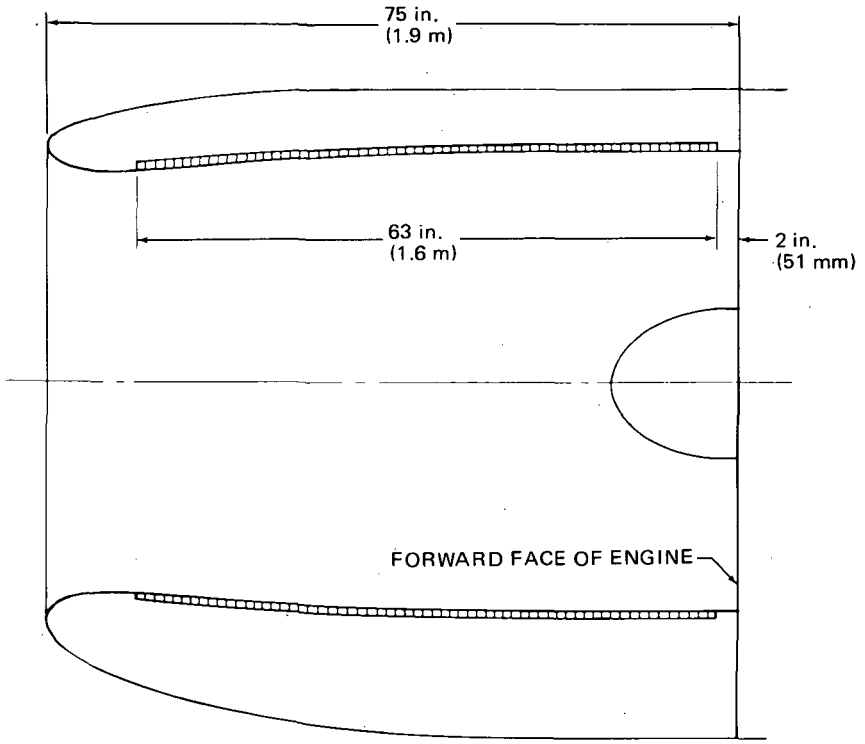

(a) MAXIMUM SELECTED ACOUSTIC TREATMENT

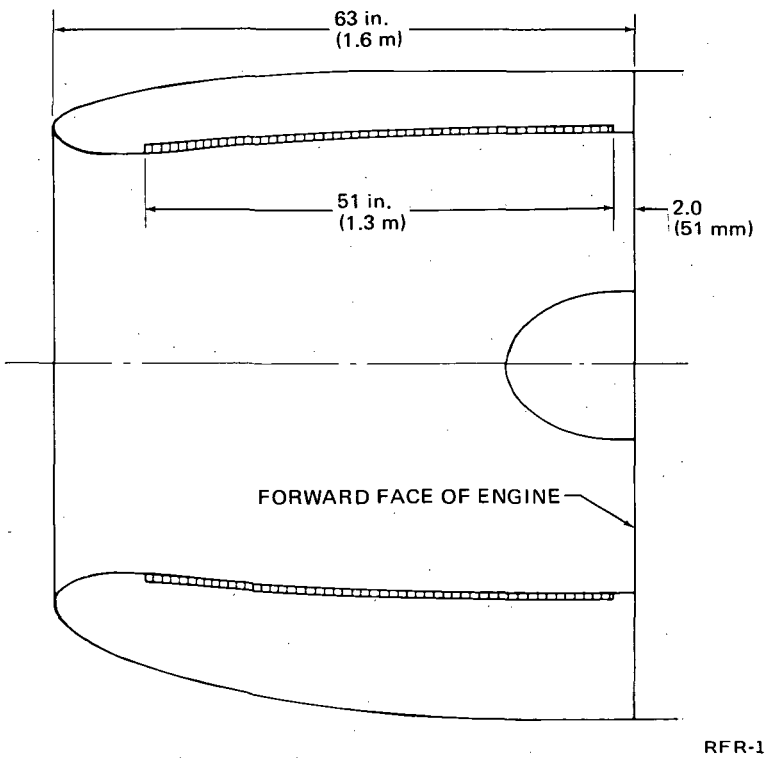

(b) MINIMUM SELECTED ACOUSTIC TREATMENT

FIGURE 32. NOSE COWL – MAXIMUM AND MINIMUM SELECTED ACOUSTIC TREATMENT

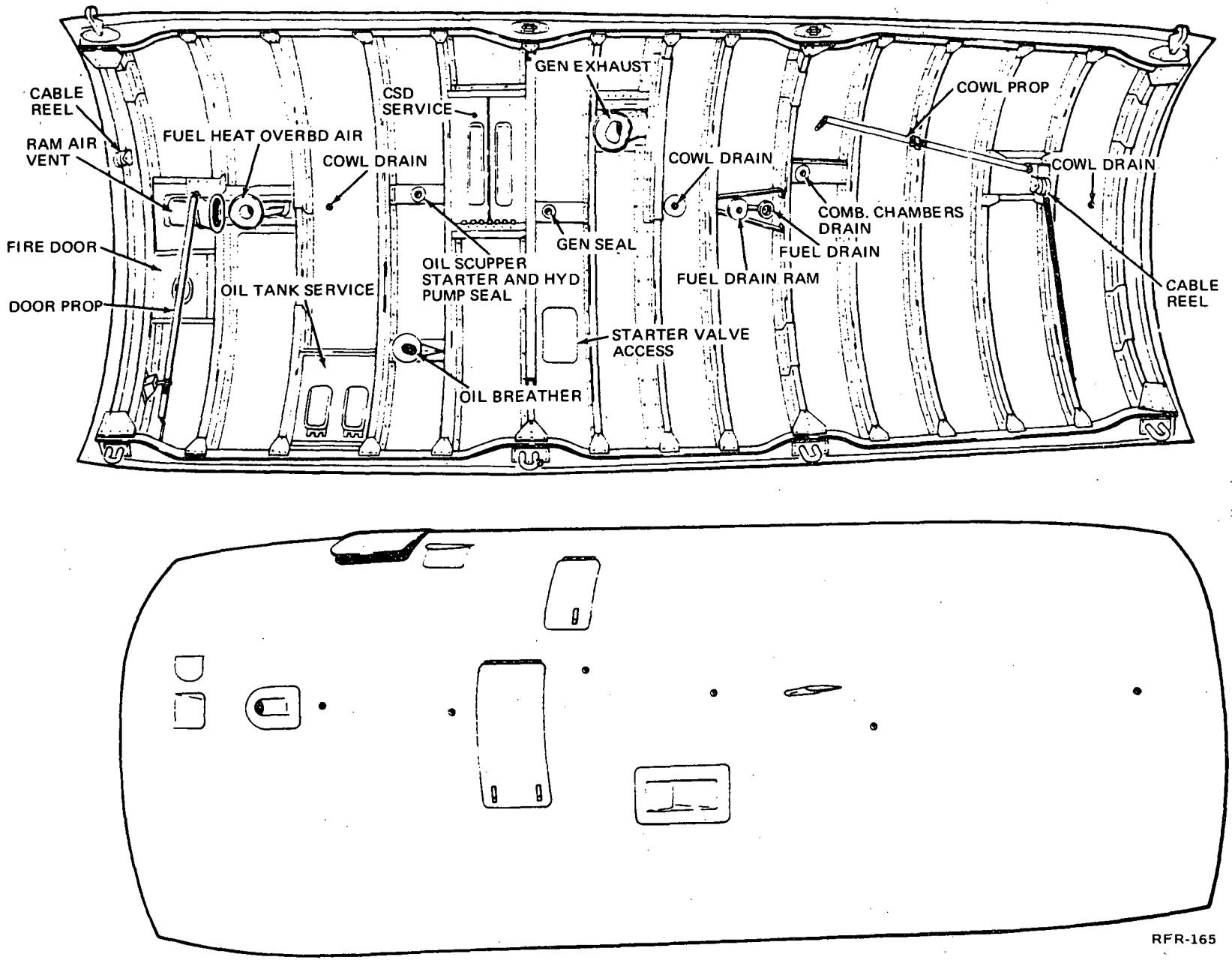

FIGURE 33. DC-9-32 ENGINE NACELLE DOOR

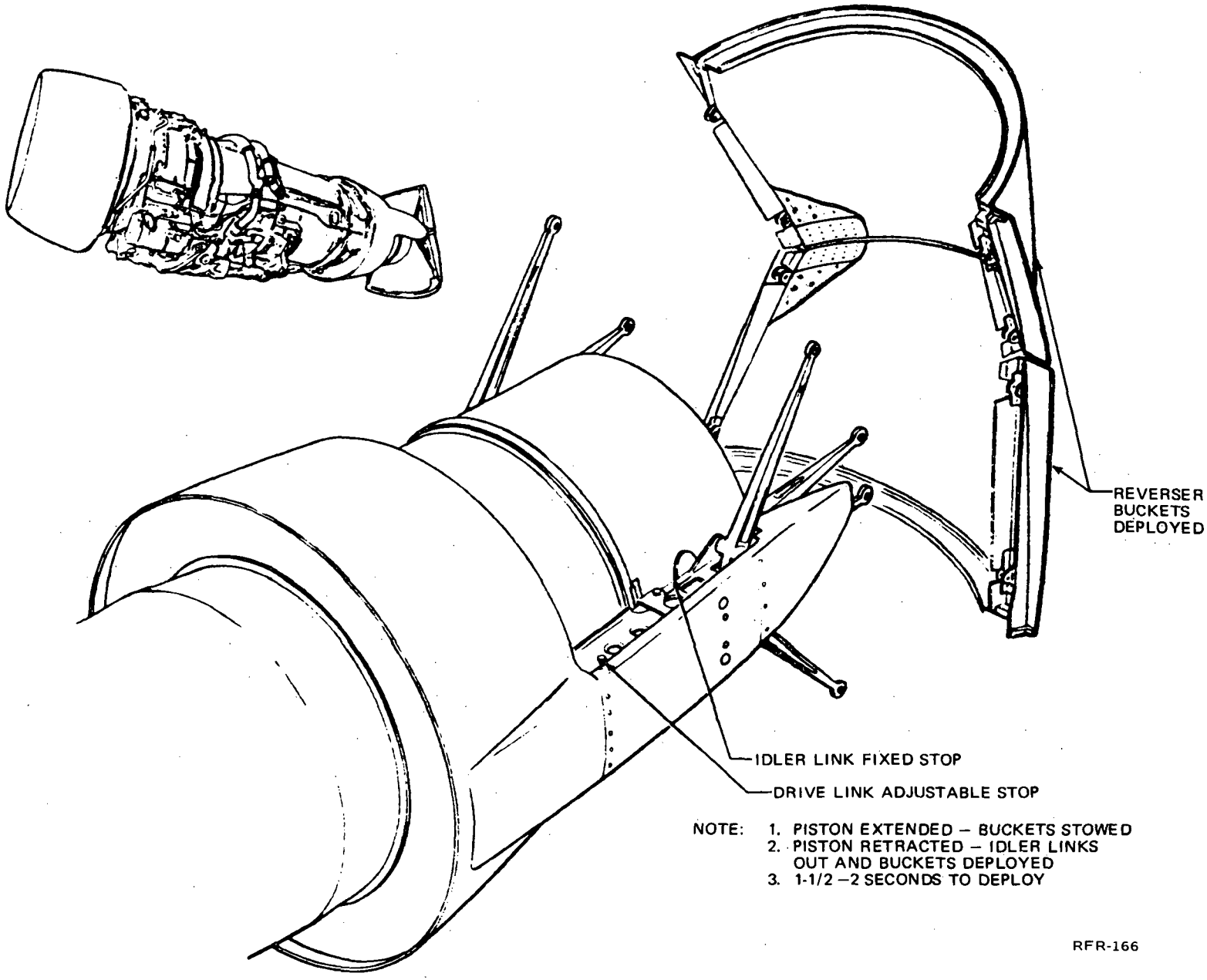

FIGURE 34. DC-9-32 THRUST REVERSER BUCKETS

The refan reverser is designed so that the same assembly will be used on both left and right pods. A bolted flange in the exhaust duct just forward of the reverser bucket leading edge will be used to achieve the proper reverser clocking for right or left side installation.

Exhaust duct. - The minimum and maximum noise suppression exhaust ducts, shown in figure 35 are similar in concept to the exhaust ducts used on production DC-9 aircraft. To achieve the desired installed performance with an acoustic treatment ratio of (treatment length/average channel height) L/H = 1.65 for the minimum case and L/H = 3.75 for the maximum case, the exhaust duct is increased in overall length from the existing 1.37 m (54 in.) to 1.85 m (73 in.) and 2.79 m (110 in.), respectively. The maximum treatment is measured lengthwise starting 30.48 mm (1.2 in.) from the engine "M" flange. The minimum treatment duct contains 939.8 mm (37 in.) of treatment starting 208.28 mm (8.2 in.) from the engine "M" flange.

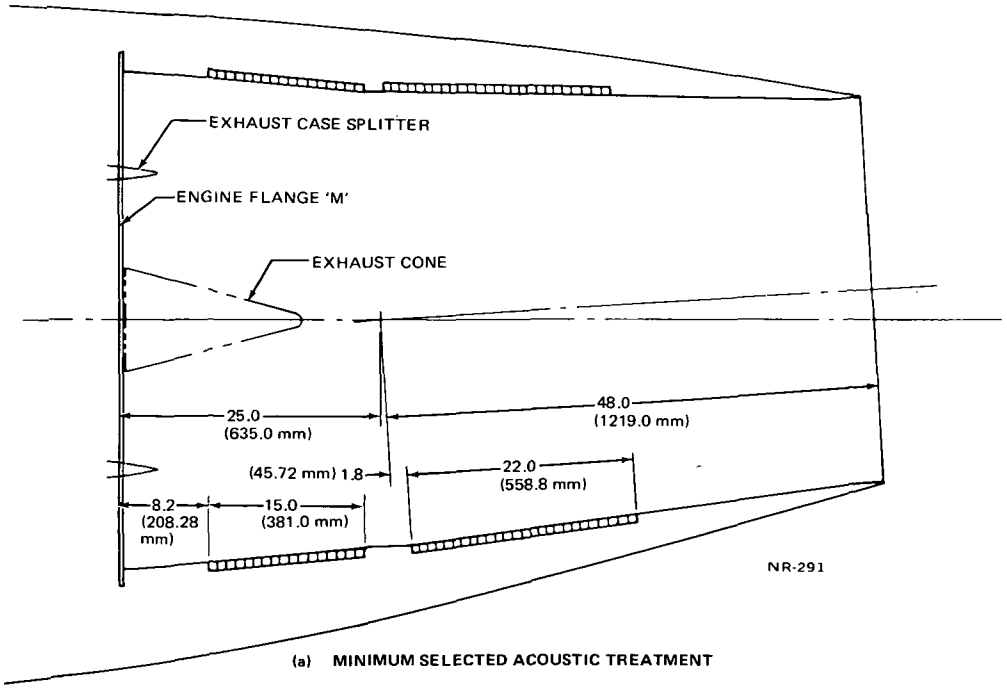

(a) MINIMUM SELECTED ACOUSTIC TREATMENT

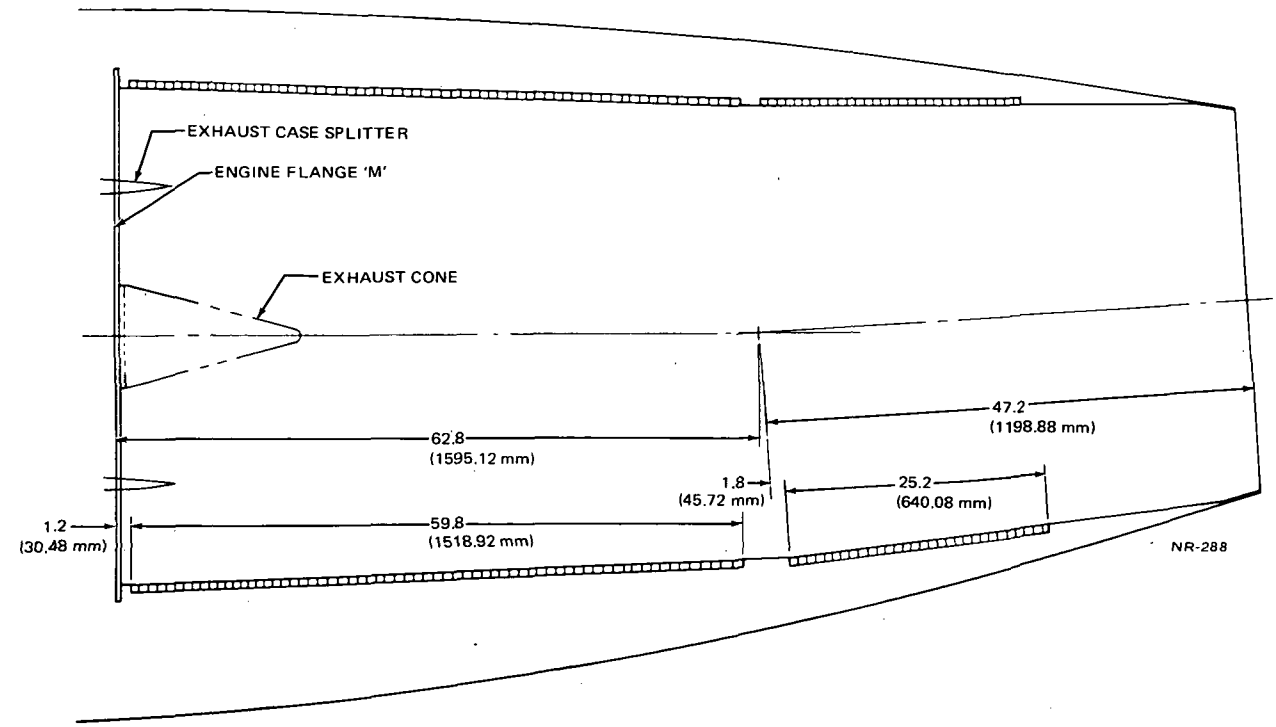

(b) MAXIMUM SELECTED ACOUSTIC TREATMENT

FIGURE 35. EXHAUST DUCTS – MINIMUM AND MAXIMUM SELECTED ACOUSTIC TREATMENT

Engine and Nacelle Subsystems

Preliminary analysis on the engine and nacelle subsystems for the JT8D-109 refan engine has identified the subsystem modifications required for the preliminary nacelle design activity. However, as additional refan engine performance data becomes available detailed analysis will be required to verify subsystem function. Piping and wire harness redevelopment will be required for the nacelle subsystems because of the increased engine diameter. The following engine and nacelle subsystems modifications have been identified:

Cooling and ventilation. - The refan engine cooling and ventilation system will remain schematically similar to the existing JT8D-9 engine nacelle system. Detailed analysis will be conducted in Phase II to optimize the size and location of the cooling air inlets and exits.

Fire protection. - The basic DC-9-32 fire protection system will be modified for the refan nacelle. The existing pylon utilizes a secondary firewall (not required by FAA regulations) positioned 101 mm (4 in.) from the fuselage. Due to the decrease in pylon width, the pylon for the refanned DC-9 will delete the secondary firewall and a thicker titanium fuselage skin panel will serve as the firewall. In the area adjacent to the engine burner cans, a columbium burn-through barrier will be attached approximately 12.7 mm (1/2 in.) outboard of the fuselage skin. Additional local fire protection is provided on the fuselage side of the burn-through barrier, in the form of sealed non-metallic boots around the electrical connectors.

Preliminary analysis indicates that the slight increase in the volume of the fire protected zone will not require any more fire extinguishing agent than is currently available in the existing DC-9 agent containers.

Engine controls. - Due to the decrease in space between the refan engine and the fuselage, a study was made to evaluate deleting the fuel shutoff push-pull cable system and replacing it with a push rod and torque tube system. However, after constructing a mock-up for checking clearances, function, and conducting preliminary tests, it was concluded that a possible mass imbalance and response frequency vibration problem existed. Therefore, the push-pull cable system will be replaced with a linear electric actuator on the engine operated by a switch on the fuel shutoff handle.

With the removal of the fuel shutoff push-pull cable, ample space is provided to allow replacement of the existing fuel control push-pull cable with a new cable, the engine mounting bracket, and the fuel control cranks as required for the refan engine installation.

The reverser latch/interlock subsystems require longer cable, clipping modifications, and redesign of the cam and bracket in order to be compatible with the refan engine installation.

Constant speed drive. - The constant speed drive currently used on the JT8D-9 will be used on the refan engine installation. Preliminary analysis indicates

that the existing constant speed drive oil cooler capacity may be marginal for the refan engine installation; however, additional detailed refan engine fan duct performance data cooler analysis will be required to verify the oil cooler compatibility with 100 percent generator load.

Engine bleed air. - The engine bleed air system picked for the JT8D-109 engine, installed in either the minimum or maximum noise suppression nacelles, is schematically identical to the DC-9-32 production aircraft system (figure 36). Changes are limited to the details of component relocation and to modifications of duct routing within the nacelle and pylon areas as dictated by the increase in engine physical size. There has been no change in the portion of the bleed air system currently installed in the fuselage area.

The ice protection controls and indicator lights are identical to the DC-9-32. These include the following:

- Valves for the inlet cowl lip and inlet vanes.
- Switches on the ice protection panel in the flight compartment for each nacelle.
- Amber disagreement lights for discrepancies between selected and actual shutoff valve positions.
- Blue lights for valve position within 0.087 rad (5°) of full open.
- Ice detection probe located in left hand engine nose cowl.
- Caution light for ice detection located on annunciator panel in the flight compartment.

The preliminary investigation of the bleed airflow capability of the JT8D-109 engine shows that sufficient bleed air is available to supply the air conditioning, anti-icing and pressurization requirements. There is no change from the DC-9-32 in the flow requirements for air conditioning, airframe anti-icing and pressurization.

Ice protection. - The ice protection system picked for the nacelle inlet on the JT8D-109 engine, installed in either the minimum or maximum noise suppression nacelles, is schematically identical to the existing DC-9-32 production aircraft system (figure 37). Changes are limited to the details of component relocation and to modifications of duct sizing and routing within the nacelle as dictated by the increase in engine physical size.

The preliminary investigation of the bleed airflow capability of the JT8D-109 engine shows that sufficient bleed air is available to supply the increased anti-icing air requirement necessitated by the increase in engine physical size.

The design of the anti-icing system for the nacelle minimum and maximum treatment inlet cowl lip is identical to the DC-9-32 except for the increased diameter of the inlet and the provision of acoustical treatment on the nacelle inlet duct wall (figure 38). The same "ejector" principle, for mixing 13th

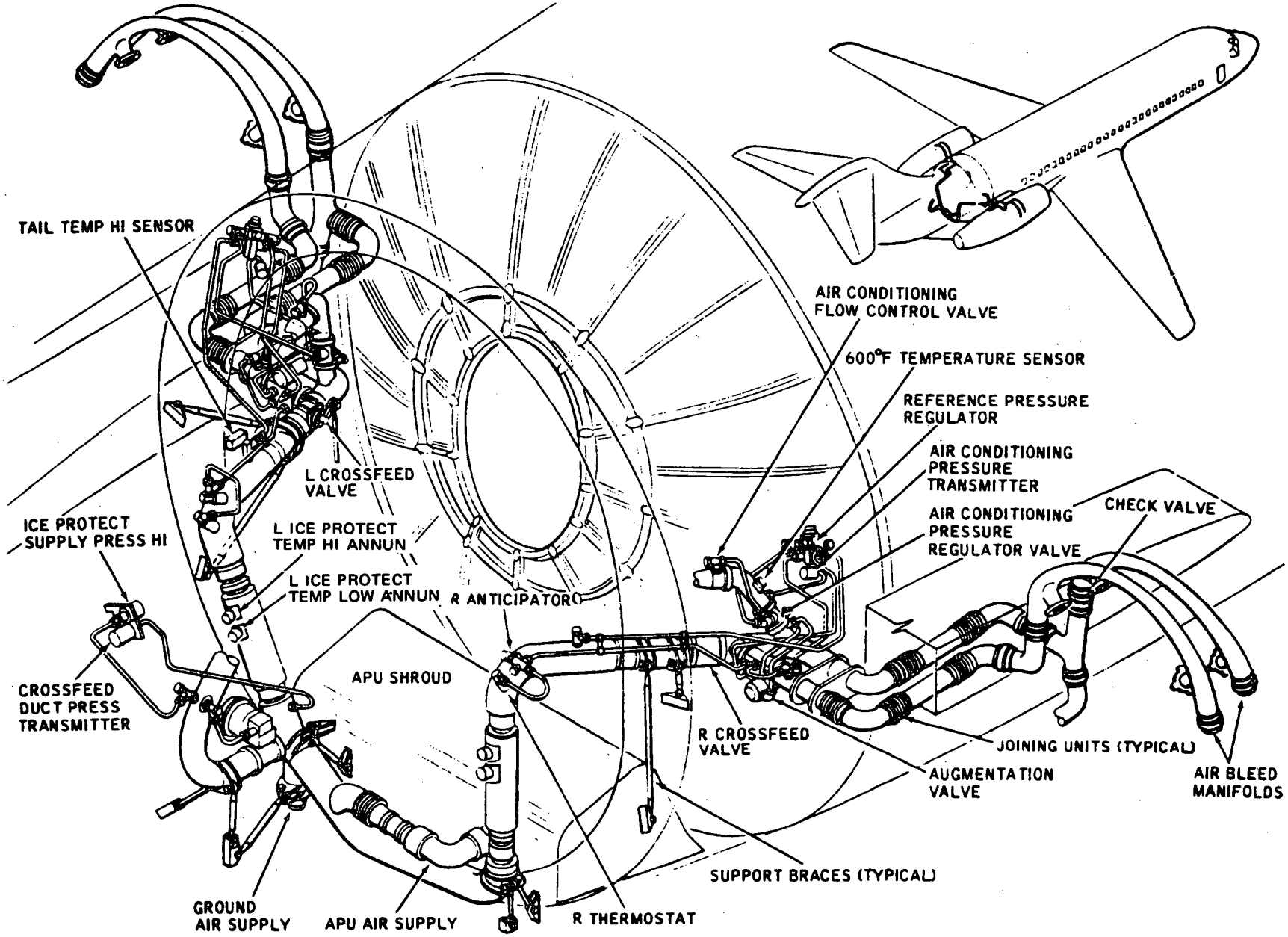

RFR-167

FIGURE 36. PNEUMATIC SYSTEM GENERAL LAYOUT

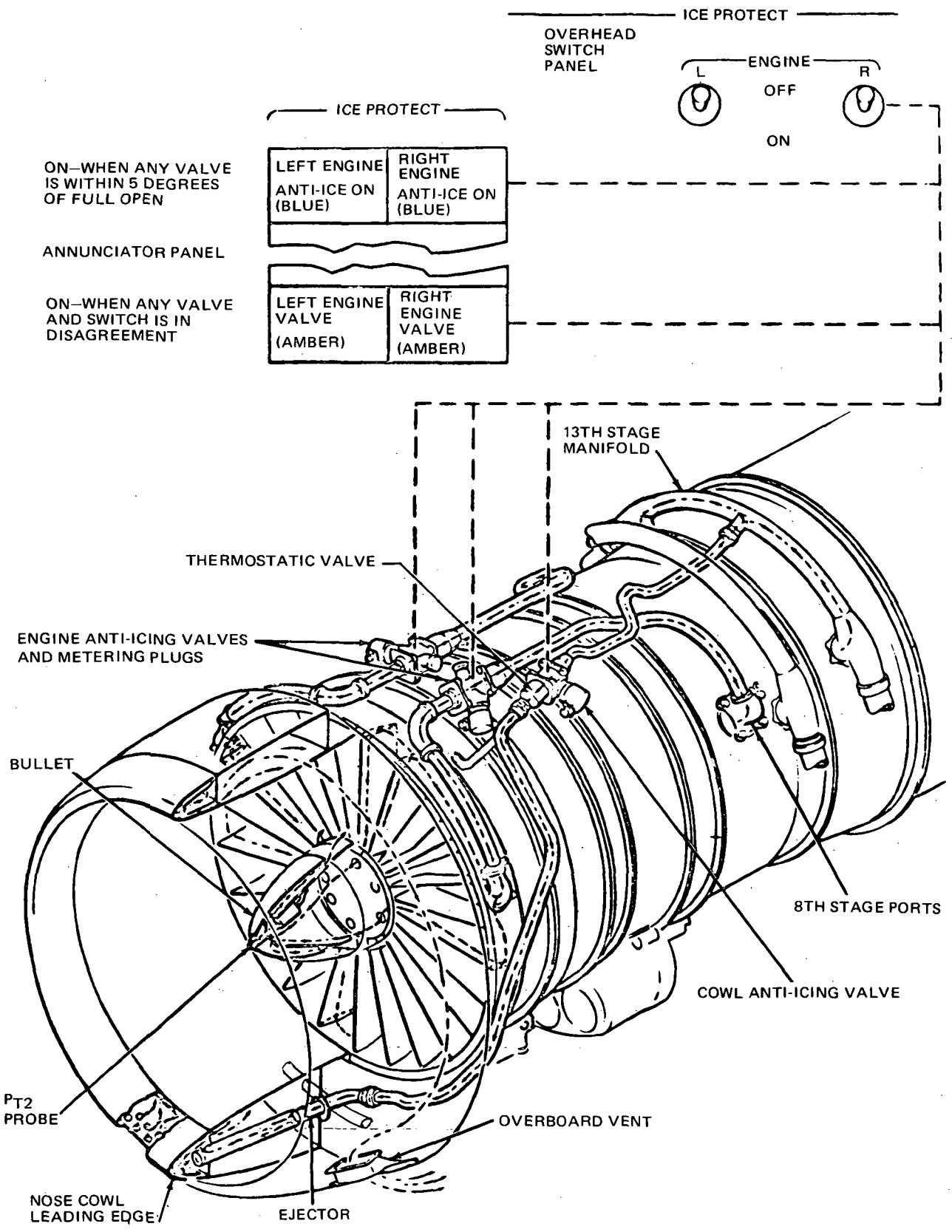

FIGURE 37. NACELLE INLET AND ENGINE ICE PROTECTION SYSTEMS

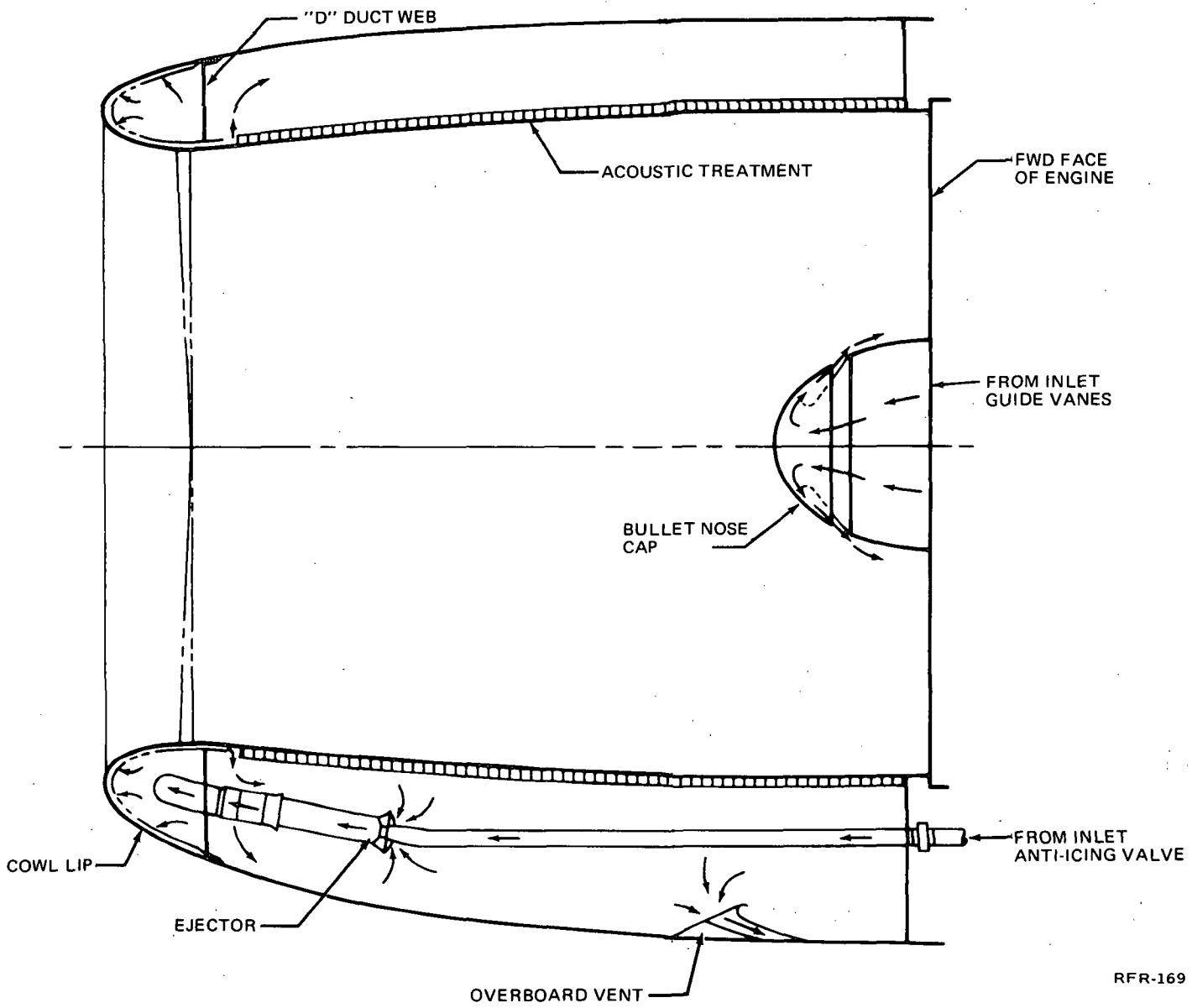

FIGURE 38. NACELLE INLET ICE PROTECTION SYSTEM

stage bleed air and secondary air drawn from the nose cowl cavity, is used in the anti-icing air supply line.

The surface of the nacelle wall from the inlet cowl lip to the engine fan face is protected by heat conduction through the metallic acoustically treated inner wall from the hot exhaust air inside the cowl cavity.

The engine inlet guide vanes are anti-iced by a system supplied by Pratt and Whitney. The system is identical to other JT8D engines except for the physical size of the engine. The bullet is anti-iced by the air exhausting from the inlet guide vanes in the same manner as the DC-9-32 production aircraft.

Hydraulic system. - The installation of the JT8D-109 refan engines will require moderate modifications of the hydraulic system. The hydraulic system pump supply and return installation will be made compatible with the new nacelle by re-routing the lines and providing new attach fittings.

The thrust reverser hydraulic subsystem requires modification due to the increased actuation loads. Based on the preliminary estimates of these loads, system and component design studies have been made to evaluate the modification requirements for the thrust reverser actuator, the control valve, the reservoir, and the system performance.

A new thrust reverser actuator is required to meet the increased actuator load and stroke requirements for the refan thrust reverser. The new actuator design is similar to the existing unit, thus requiring minimum development and qualification testing. The existing actuator control valve design has been modified to meet the larger flow requirements of the new actuator by resizing the internal porting. The basic valve design will be retained to minimize development and qualification testing. Additional accumulator capacity is required to satisfy the performance requirements of the refan actuator stroke.

A design evaluation of the reservoir shows that the existing unit is of sufficient size to meet all system requirements.

A hydraulic system performance study was performed to determine the compatibility of a new thrust reverser subsystem with the system performance requirements. The following performance levels were established:

- The control valve modification will provide thrust reverser operational time within the design limits for the normal deployment cycle.
- The new actuator snubbing cycle will provide optimum thrust reverser bucket deceleration and terminal velocities.
- Subsystem line sizes were increased where existing sizes were not compatible with the new actuator flow rates.

The reverser latch/interlock subsystems require longer cables, clipping modifications, and redesign of the cam and bracket in order to be compatible with the refan engine installation.

Instrumentation. - Installation of the refan engine results in minor changes to the existing DC-9-32 aircraft indicating systems.

The tachometer output gearing used on the JT8D-109 refan engine will be the same as for production JT8D engines, therefore, the indicators must be recalibrated for the refan engine installation; the Ram Air Temperature (RAT)/Engine Pressure Ratio (EPR) indicator EPR limitation scales on the current production indicators must be changed to display the new values applicable to the refan engine; and a new location for the flag detent, mask and revised stall warning switch is required.

[illegible] of the [illegible] engine results in minor changes
[illegible] indicating systems.

[illegible] requiring use of the [illegible] will be
[illegible] engine. Therefore, the following must be
[illegible] engine modification: the Tach Adjustment
[illegible] Selective Pitch (SPP) Governor EPP Modification supplies on the
[illegible] instructions must be changed to display the new values
[illegible] engine; and a new location for the flag decent.
[illegible] starting switch is required.

ENGINE PERFORMANCE

The refanned JT8D-109 engine is a derivative of the basic Pratt and Whitney Aircraft JT8D turbofan engine. The JT8D-109 engine is a two spool turbofan engine with a mechanically coupled fan and low pressure compressor. It has a single stage fan, six low compressor stages and seven high compressor stages. The compressor system generates a takeoff compression ratio of approximately 15.6 and a 2.03 bypass ratio. The burner section consists of nine separate chambers in an annular array. The JT8D-109 derivative of a particular engine model uses the air-cooled or uncooled single stage high pressure turbine applicable for the rating of the particular current engine model, and three stage low pressure turbine. A cross-section comparison of the JT8D-109 and JT8D-9 engine is depicted in figure 39. The general performance, physical characteristics and features of the JT8D-109 and the JT8D-9 are compared in table 16.

Direct comparison of bare engine performance is based on conditions at the reference nozzles for the JT8D-109 and JT8D-9 engines. All performance estimates are based on data supplied by the engine manufacturer (Pratt and Whitney), using a fuel lower heating value of 10 224 kg cal/kg (18,400 Btu/lb). Figures 40 and 41 compare the JT8D-9 and JT8D-109 performance with Pratt and Whitney reference nozzles.

The engine performance of the JT8D-109 refan engine and the basic Pratt and Whitney JT8D-9 turbofan engine installed on the production DC-9-32 airplane is compared in figures 42 and 43. Curves are shown for the minimum and maximum noise suppression configurations at takeoff and cruise conditions. A direct comparison can be made between the JT8D-9 and JT8D-109 engine installation because Pratt and Whitney used identical reference nozzles for the engine performance. The data presented include all installation effects for normal operation. The installation losses applied to the JT8D-9 and JT8D-109 engines include the effects of internal losses such as inlet, bleed, power extraction, nozzle and duct effects and external losses from pylon, nacelle, and wing/nacelle interference effects.

The inlet loss is estimated by calculating the internal drag of the components of the inlet and then changing these values into the form of equivalent pressure loss coefficients. Inlet total pressure losses for the minimum and maximum selected noise suppression configurations are shown in figure 44. Bare engine performance demonstrations are made with a bellmouth installed and no correction is made by the engine manufacturer for bellmouth loss, therefore, only the difference between the inlet and bellmouth loss is applied for the calculation of installed engine performance.

The estimated performance of the minimum and maximum selected noise suppression exhaust nozzle is shown in figure 45. The velocity coefficient for the takeoff condition is 0.9765 and for the cruise condition is 0.9827 at 9 144 m (30,000 ft) and 0.78 Mach number for the minimum treated nacelle. These values include 1/2 of the nozzle lip base drag, nozzle duct total pressure loss, and nozzle exit flow angularity loss. The remaining 1/2 of the nozzle lip base drag is accounted for in the nacelle drag.

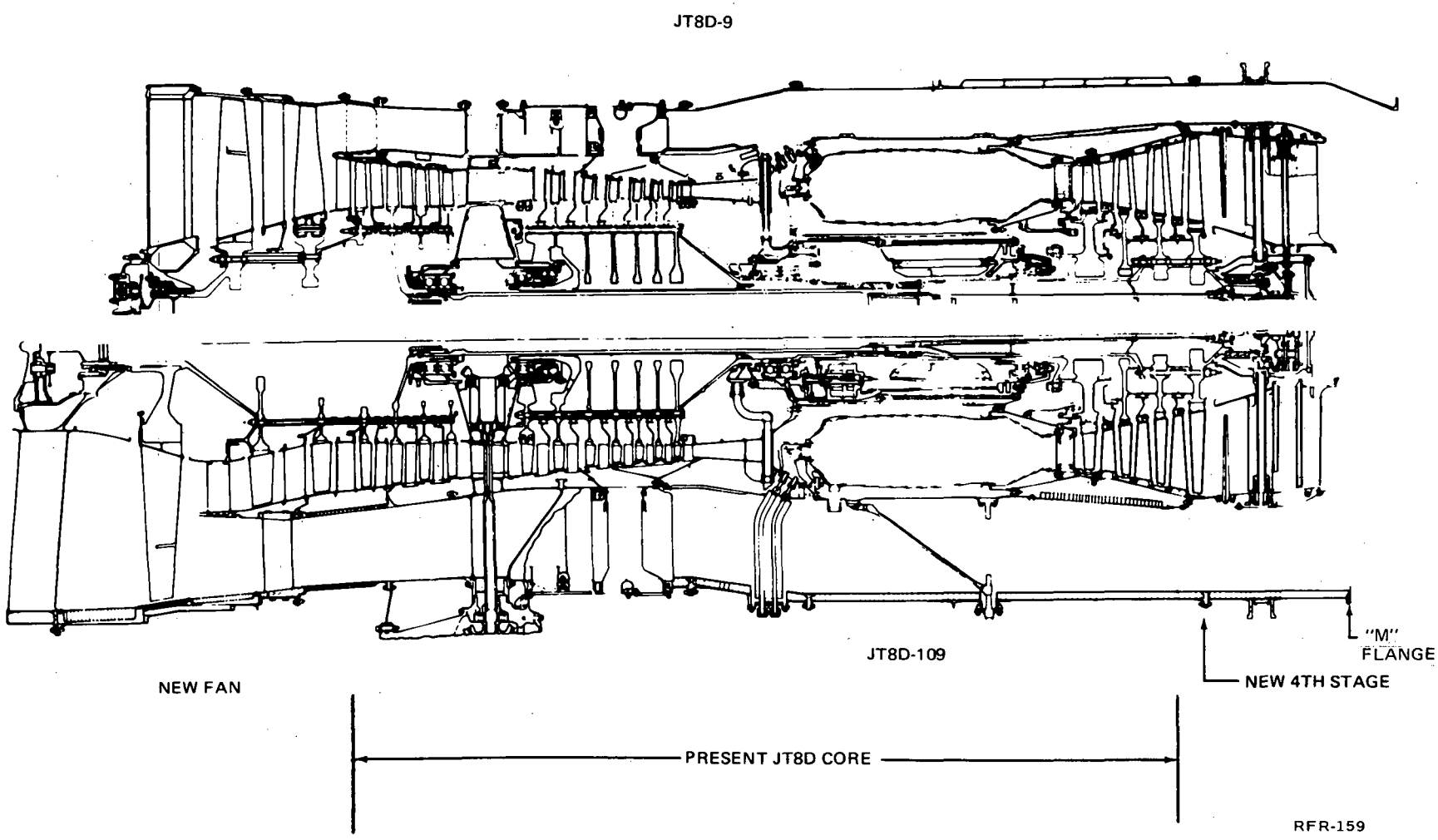

FIGURE 39. ENGINE CHARACTERISTICS COMPARISON

TABLE 16

ENGINE CHARACTERISTICS COMPARISON

		JT8D-9	JT8D-109
TAKEOFF THRUST (Sea Level Static, Standard Day)	lb N	14,500 (64 500)	16,600 (73 840)
FAN TIP SPEED, SEA LEVEL STATIC TAKEOFF	ft/sec m/sec	1,420 (432.8)	1,600 (487.7)
BYPASS RATIO		1.05	2.03
FAN PRESSURE RATIO		1.97	1.67
MAXIMUM CRUISE THRUST - 30,000 ft (9 144 m), 0.80 Mach	lb N	4,540 (20 195)	4,720 (20 996)
CRUISE TSFC-30,000 ft (9 144 m), 0.80 Mach, 4,400 lb (19 571 N) THRUST	lb/hr/lb kg/hr/N	0.799* (0.082)	0.766* (0.078)
FAN TIP DIAMETER	in. m	40.5 (1.03)	49.2 (1.25)
OVERALL BARE ENGINE LENGTH (LESS SPINNER)	in.	119.97 (3.047)	127.19 (3.231)
BARE ENGINE WEIGHT	lb kg	3,218 (1 460)	3,788 (1 718)

*BASED ON PRATT & WHITNEY AIRCRAFT REFERENCE NOZZLES

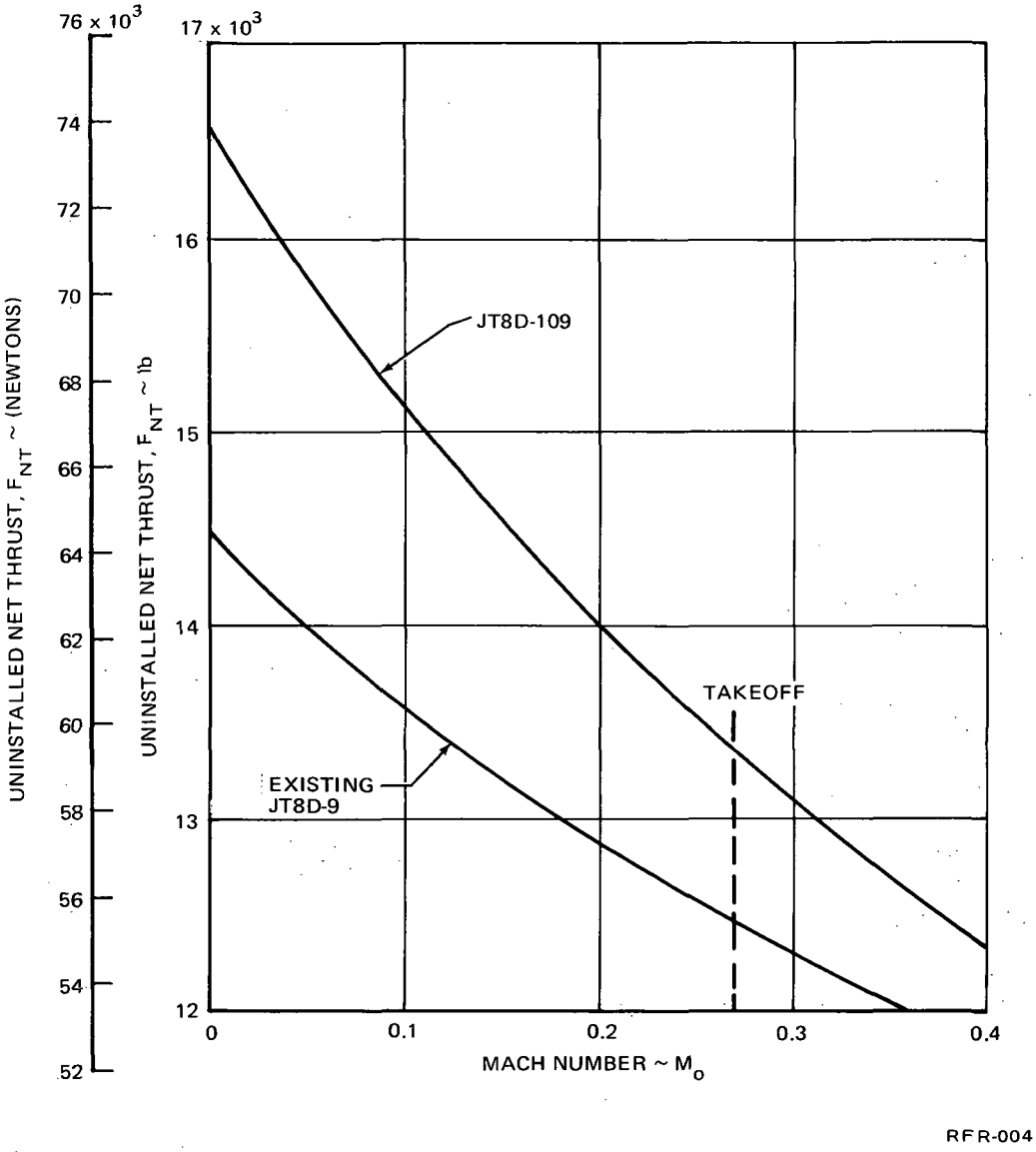

FIGURE 40. BARE ENGINE TAKEOFF PERFORMANCE – JT8D-9 AND JT8D-109 WITH PWA REFERENCE NOZZLES, SEA LEVEL, STANDARD DAY

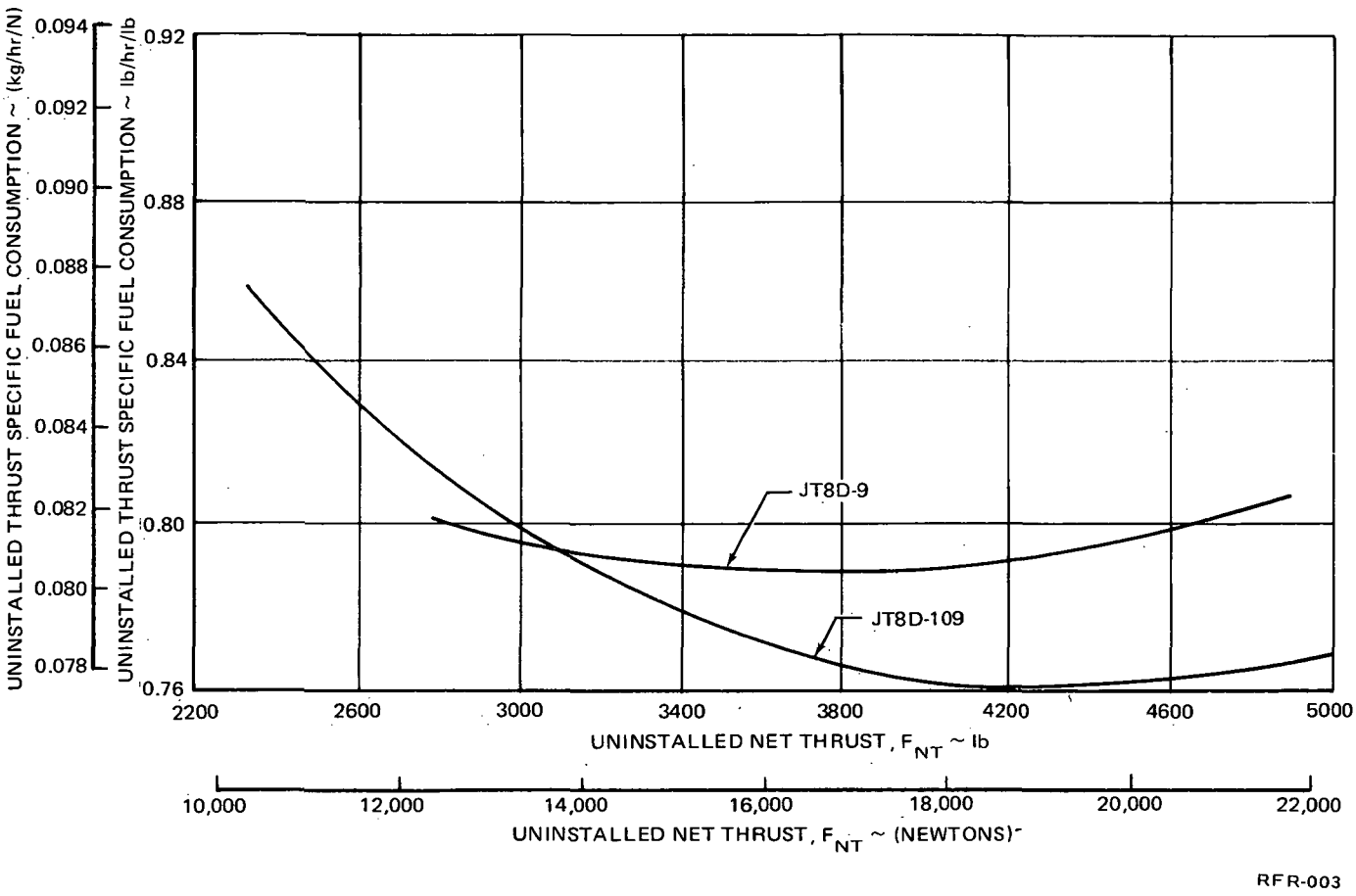

FIGURE 41. BARE ENGINE CRUISE PERFORMANCE – JT8D-9 AND JT8D-109 WITH PWA REFERENCE NOZZLES, M = 0.78, h_p = 30,000 ft (9 144 m), STANDARD DAY

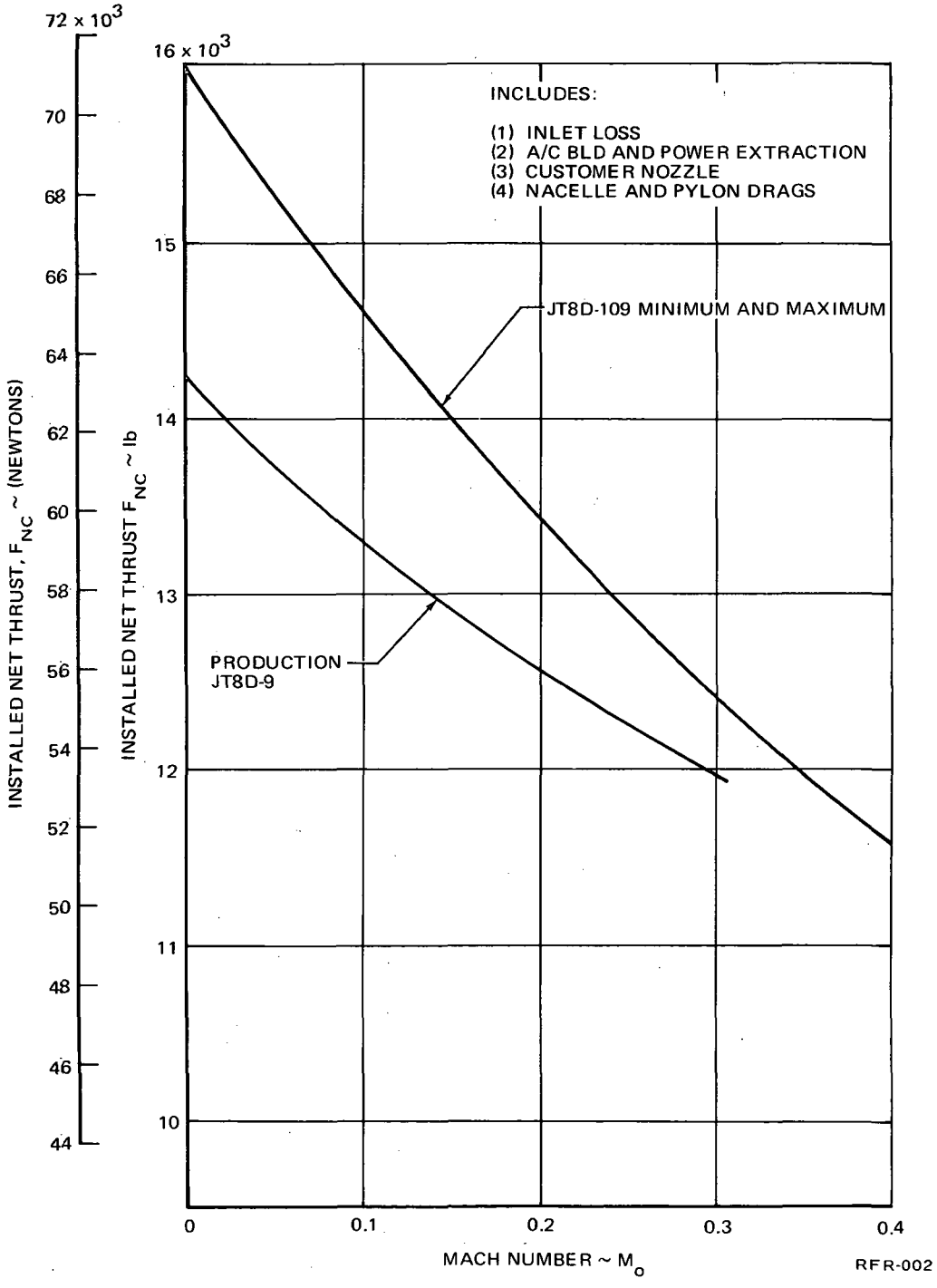

FIGURE 42. DC-9-32 MINIMUM AND MAXIMUM SELECTED NOISE SUPPRESSION TAKEOFF THRUST LAPSE RATE FOR SEA LEVEL, STANDARD DAY

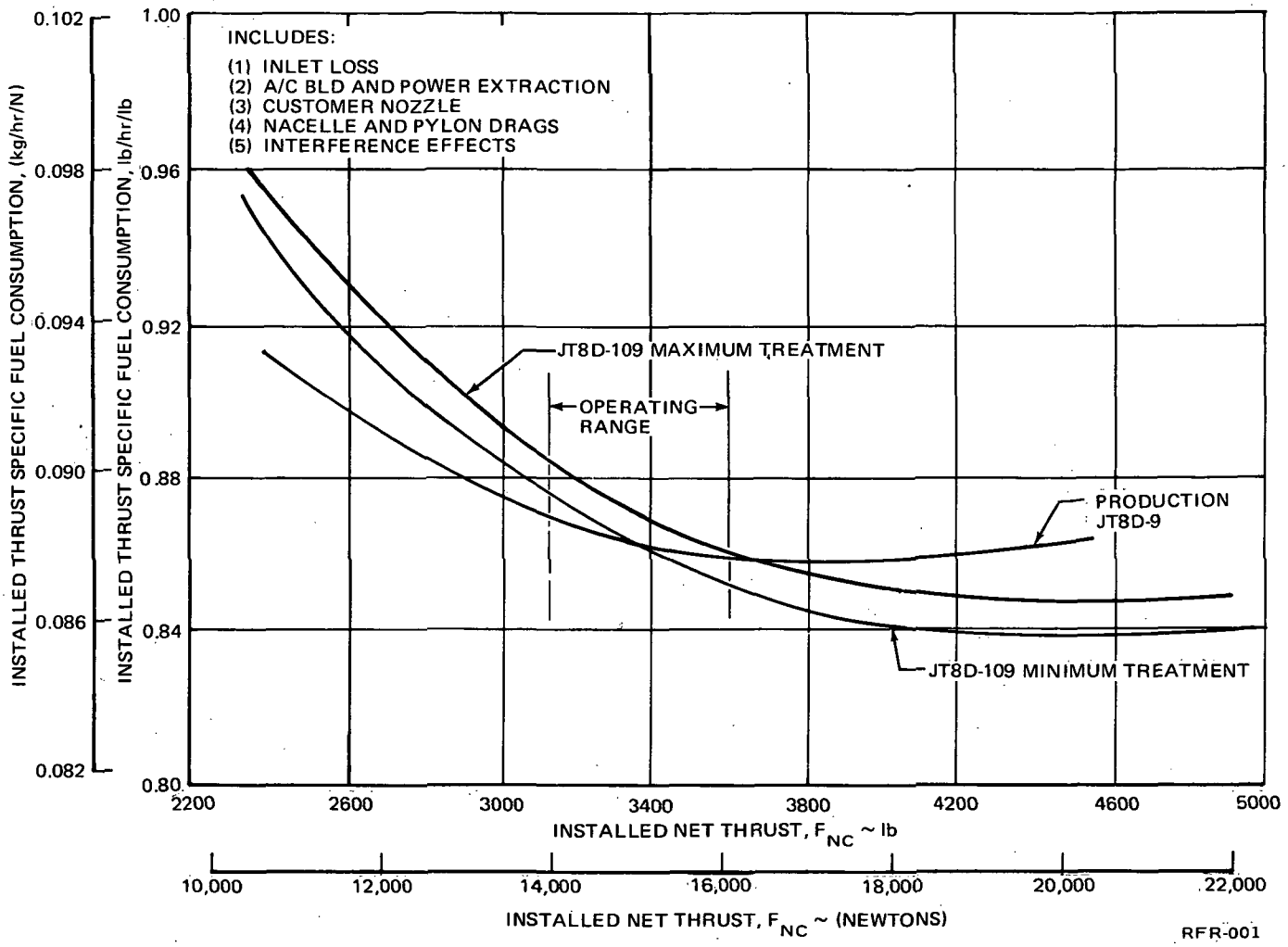

FIGURE 43. MINIMUM AND MAXIMUM SELECTED NOISE SUPPRESSION ESTIMATED CRUISE PERFORMANCE AT M = 0.78, hp = 30,000 ft (9 144 m), STANDARD DAY

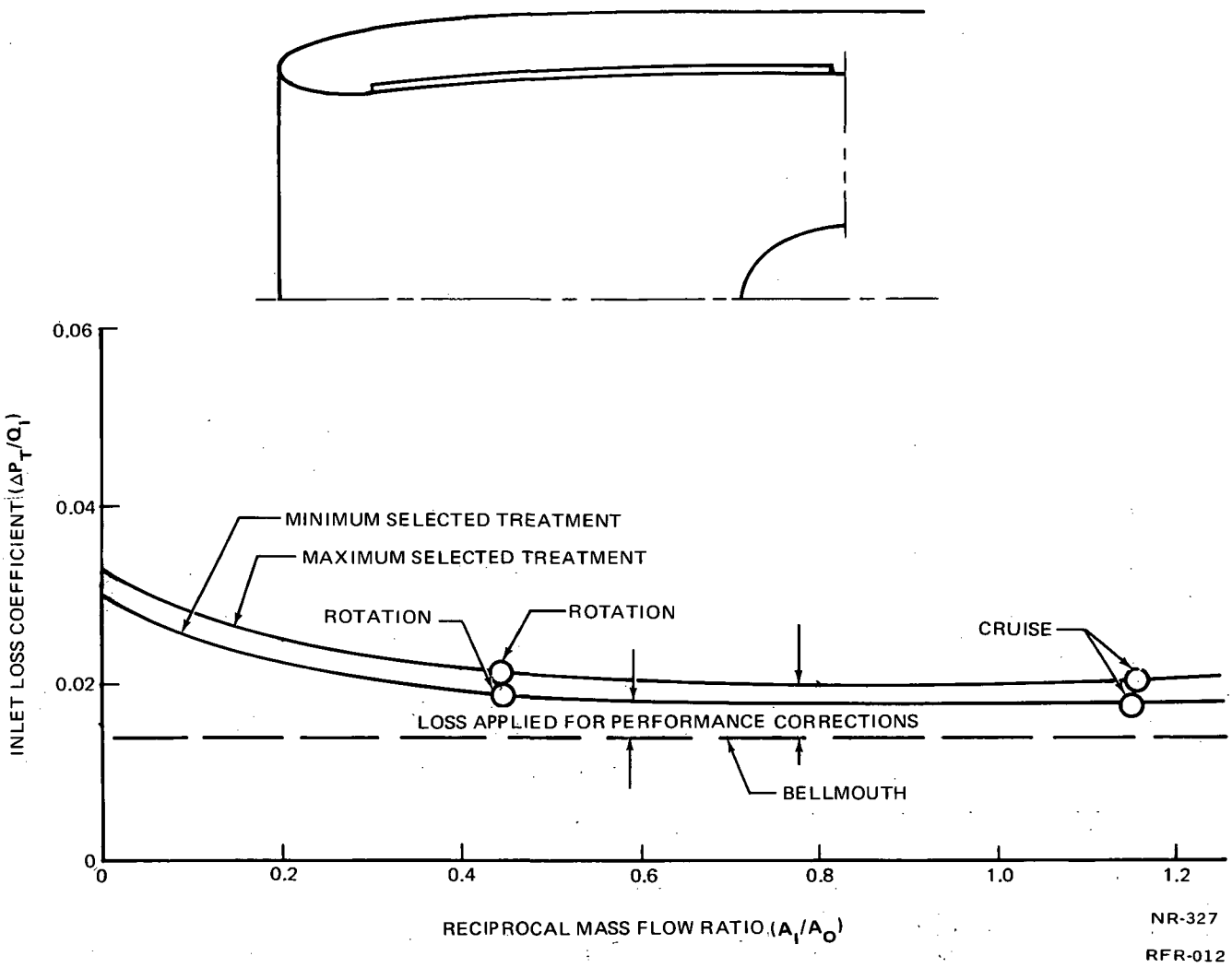

FIGURE 44. DC-9-32 MINIMUM AND MAXIMUM SELECTED TREATMENT INLET TOTAL PRESSURE LOSS

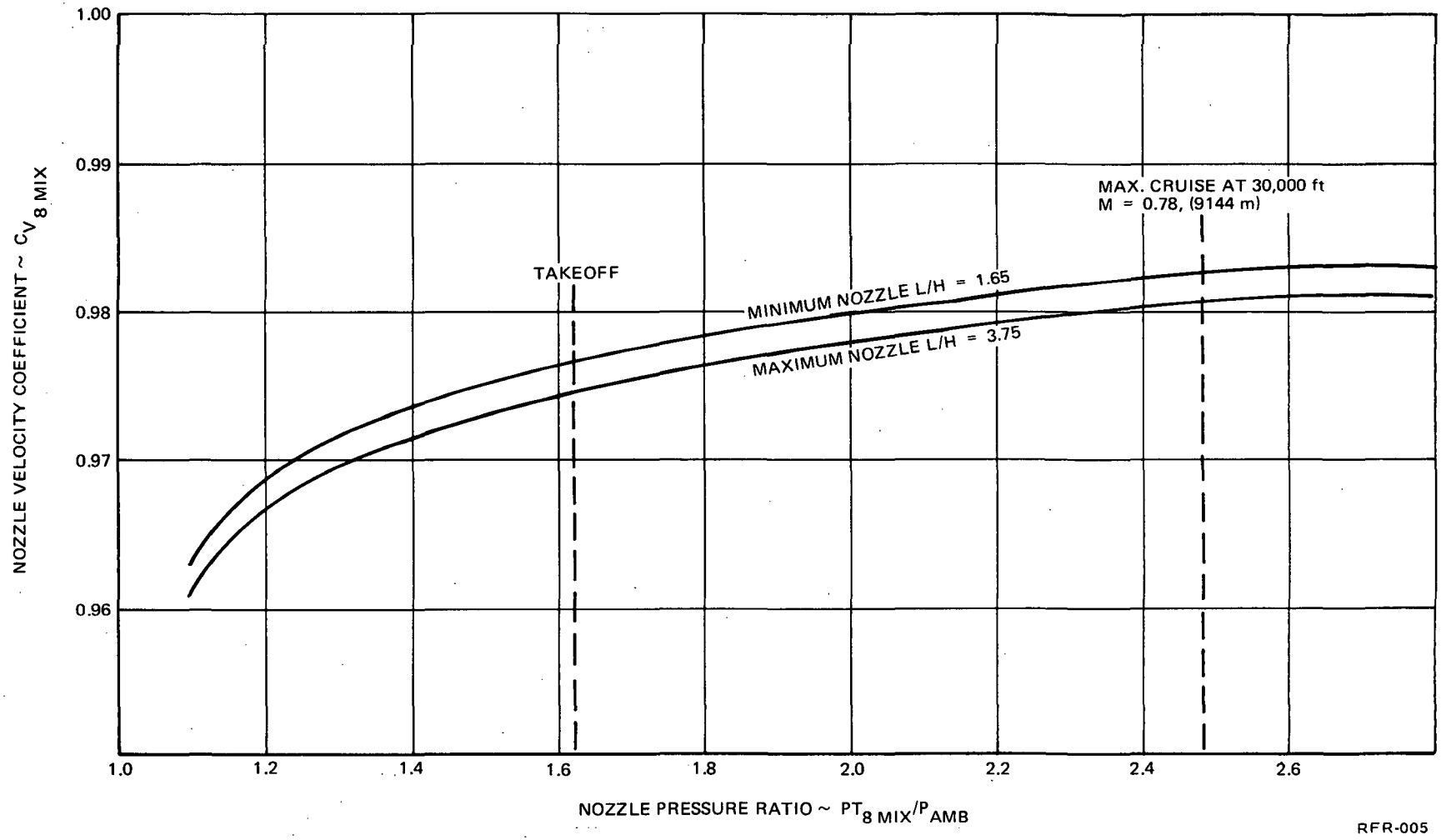

FIGURE 45. ESTIMATED EXHAUST NOZZLE PERFORMANCE – JT8D-109

Table 17 shows the installation loss comparison for the minimum and maximum noise suppression nacelles at a typical takeoff condition of Mach number 0.27, sea level standard day, and table 18 compares the losses at a typical cruise condition of Mach number 0.78, 9 144 m (30,000 ft) and 16 014 N (3,600 lb) installed thrust per engine.

TABLE 17

INSTALLATION LOSS COMPARISON DC-9-32

MINIMUM AND MAXIMUM SUPPRESSION NACELLES

TAKEOFF M = 0.27, SEA LEVEL, STD. DAY				
	ENGINE	JT8D-9	JT8D-109 MINIMUM TREATMENT	JT8D-109 MAXIMUM TREATMENT
	F_{NR} (PWA Ref. Nozzle) lb	12,450	13,325	13,325
	N	(55 380)	(59 273)	(59 273)
$\frac{\Delta F_N}{F_{NR}}$ - THRUST CHANGE DUE TO	C_V (DAC Nozzle Coefficient)	+0.0070	-0.0104	-0.0130
	Inlet Loss	0.0	-0.0010	-0.0020
	Nacelle & Pylon Drags	-0.0070	-0.0077	-0.0085
	Interference Effects	0.0	0.0	0.0
	Bleed & Power Extraction	-0.019	-0.0214	-0.0214
	Total	-0.019	-0.0405	-0.0449
	F_{NC} (Installed) lb	12,200	12,775	12,700
	N	(54 268)	(56 826)	(56 492)

$$F_{NC} = F_{NR} \times \left(1 + \left(\frac{\Delta F_N}{F_{NR}}\right)_{TOTAL}\right)$$

TABLE 18

INSTALLATION LOSS COMPARISON DC-9-32 MINIMUM AND MAXIMUM SUPPRESSION NACELLE

TYPICAL CRUISE PERFORMANCE

F_{NC} = 3,600 lb, (16 014 N), M = 0.78, h_p = 30,000 ft (9 144 m), STD. DAY

		$\frac{\Delta F_N}{F_{NR}}$ — THRUST CHANGE DUE TO INSTALLATION				$\frac{\Delta SFC}{TSFC_R}$ — SFC CHANGE DUE TO INSTALLATION		
	ENGINE	JT8D-9	JT8D-109 MINIMUM TREATMENT	JT8D-109 MAXIMUM TREATMENT		JT8D-9	JT8D-109 MINIMUM TREATMENT	JT8D-109 MAXIMUM TREATMENT
1	F_{NR} (PWA Ref. Nozzle) - lb N	3,975 (17 682)	4,085 (18 171)	4,145 (18 438)	1	3,975 (17 682)	4,085 (18 171)	4,145 (18 438)
2	$TSFC_R$ (PWA Ref. Nozzle) lb/hr/lb kg/hr/N	0.788 (0.080)	0.760 (0.078)	0.760 (0.078)	2	0.788 (0.080)	0.760 (0.078)	0.760 (0.078)
3	C_V (DACo Nozzle Coefficient)	+0.008	-0.0230	-0.0268	3	-0.008	+0.0235	+0.0275
4	Inlet Loss	BASE	-0.0015	-0.0030	4	BASE	+0.0010	+0.0020
5	Nacelle & Pylon Drags	-0.0570	-0.0720	-0.0790	5	+0.0676	+0.0790	+0.0857
6	Interference Effects	BASE	+0.0170	+0.0163	6	BASE	-0.0172	-0.0165
7	Bleed & Power Extraction	-0.0455	-0.0391	-0.0391	7	+0.0288	+0.0344	+0.0344
8	Total	-0.0945	-0.1186	-0.1316	8	+0.0884	+0.1207	+0.1331
9	F_{NC} (Installed Net Thrust) - lb N	3,600 (16 014)	3,600 (16 014)	3,600 (16 014)	9	3,600 (16 014)	3,600 (16 014)	3,600 (16 014)
10	SFCC (Installed SFC) lb/hr/lb kg/hr/N				10	0.858 (0.075)	0.852 (0.087)	0.861 (0.088)

NOTE: $F_{NC} = F_{NR} \times \left(1 + \left(\frac{\Delta F_N}{F_{NR}}\right)_{TOTAL}\right)$; $SFCC = TSFC_R \times \left(1 + \left(\frac{\Delta SFC}{TSFC_T}\right)_{TOTAL}\right)$

AIRCRAFT PERFORMANCE

The installation of the JT8D-109 refan engine results in an operational weight increase of approximately 1 135 kg (2,500 lb) and an aft Operational Empty Weight (O.E.W.) center of gravity shift of 6 to 7 percent M.A.C. for the minimum selected treatment, and 1 360 kg (3,000 lb) operational weight increase for the maximum selected treatment with an aft center of gravity shift of approximately 6.25 to 7.25 percent. The preliminary weight breakdown is presented in table 19 for an existing DC-9-32 airplane and a refanned DC-9-32 airplane with the minimum and maximum selected treatment configuration.

A review of the DC-9 Series 30 and 10 "In-Service Fleet" has been made to survey the loadability changes associated with the aft c.g. movement. Results of this study are presented in figures 46 and 47. The figures indicate the wide range in O.E.W. and c.g. among basic customer configurations. The ballast weight range and number of aircraft in each group is shown. For this study the ballast was assumed to be located in the nose gear wheel well.

Many of these configurations require no ballast; in fact, the loadability will be improved by the refan engine installation. Other operators will use no ballast, but will choose other methods, which are technically feasible, to correct any adverse balance effect on their operations.

A review of the ground handling characteristics during maintenance for the DC-9 Series 30 and 10 fleet disclosed that the majority of the aircraft configurations are not balance critical with the refan engine installation. For those configurations which may be subjected to a tip-over condition in ground gusts, snow loads, towing, maintenance, etc., several alternative corrections are readily available. One simple method used at the Douglas Aircraft Company, is to install water ballast tanks at hard points located on the forward fuselage. Since these hard points exist, no fuselage modification is required for their use.

A comparison of DC-9-32 FAA takeoff field length as a function of takeoff weight is shown in figure 48 for the JT8D-109 and the JT8D-9 engine installations. Figure 49 presents a similar comparison for a DC-9-15 with JT8D-109 and JT8D-7A engine installations. The minimum required field length, as limited by airplane minimum control speed, is indicated in figure 48.

Preliminary takeoff flight path comparisons of the DC-9-32 using the JT8D-9 and the JT8D-109 engines have been made. Figure 50 compares the two engines for a maximum design takeoff gross weight condition, while figure 51 presents a similar comparison for the takeoff weights associated with a typical mission of 694 km (375 n. mi.). Figures 52 and 53 present similar comparisons for the DC-9-15 aircraft. Flight paths are presented, both with and without cutback to the thrust required for 5.1 m/s (1,000 ft/min) rate of climb for the typical mission case. The maximum design takeoff weight condition shows thrust cutback 610 m (2,000 ft), prior to a horizontal distance of 6.5 km (3.5 n. mi.) from brake release; the typical mission takeoff weights are cutback at 457 m (1,500 ft) altitude.

TABLE 19

WEIGHT COMPARISON $\frac{lb}{(kg)}$ - EXISTING AND REFANNED DC-9-32

AIRPLANE	DC-9-32	DC-9-32 REFAN	DC-9-32 REFAN	DC-9-15	DC-9-15 REFAN
ENGINE	JT8D-9	JT8D-109	JT8D-109	JT8D-7A	JT8D-109
TREATMENT LEVEL	NONE	MINIMUM	MAXIMUM	NONE	MINIMUM
NOSE COWL	106 (48)	322 (146)	377 (171)	106 (48)	322 (146)
ACCESS DOORS	218 (99)	280 (127)	280 (127)	218 (99)	280 (127)
THRUST REVERSER	245 (111)	340 (154)	340 (154)	245 (111)	340 (154)
ENGINE MOUNTS	50 (23)	60 (27)	60 (27)	50 (23)	60 (27)
EXHAUST SYSTEM	141 (64)	324 (147)	490 (222)	141 (64)	324 (147)
APRON STRUCTURE	60 (27)	80 (36)	80 (36)	60 (27)	80 (36)
PYLONS	225 (102)	193 (88)	193 (88)	225 (102)	193 (88)
FUSELAGE	0 (0)	105 (48)	105 (48)	0 (0)	105 (48)
ACCESSORIES	240 (109)	240 (109)	240 (109)	240 (109)	240 (109)
SYSTEMS	325 (147)	337 (153)	337 (153)	325 (147)	337 (153)
TOTAL WEIGHT PER NACELLE	1,610 (730)	2,281 (1 035)	2,502 (1 135)	1,610 (730)	2,281 (1 035)
TOTAL WEIGHT PER AIRCRAFT	3,220 (1 461)	4,562 (2 069)	5,004 (2 270)	3,220 (1 461)	4,562 (2 069)
ENGINE 2 PER P&WA WEIGHT	6,436 (2 919)	7,576 (3 436)	7,576 (3 436)	6,310 (2 862)	7,576 (3 436)
MANUFACTURER'S EMPTY WEIGHT	55,216 (25 046)	57,698 (26 171)	58,140 (26 372)	47,648 (21 613)	50,256 (22 796)
OPERATIONAL EMPTY WEIGHT	59,076 (26 797)	61,558 (27 922)	62,000 (28 123)	50,248 (22 792)	52,856 (23 975)
MAXIMUM ZERO FUEL WEIGHT	87,000 (39 463)	87,000 (39 463)	87,000 (39 463)	74,000 (33 566)	74,000 (33 566)
MAXIMUM LANDING WEIGHT	99,000 (44 906)	99,000 (44 906)	99,000 (44 906)	81,700 (37 058)	81,700 (37 058)
MAXIMUM TAKEOFF WEIGHT	108,000 (48 988)	108,000 (48 988)	108,000 (48 988)	90,700 (41 140)	90,700 (41 140)
MAXIMUM TAXI WEIGHT	109,000 (49 442)	109,000 (49 442)	109,000 (49 442)	91,500 (41 504)	91,500 (41 504)

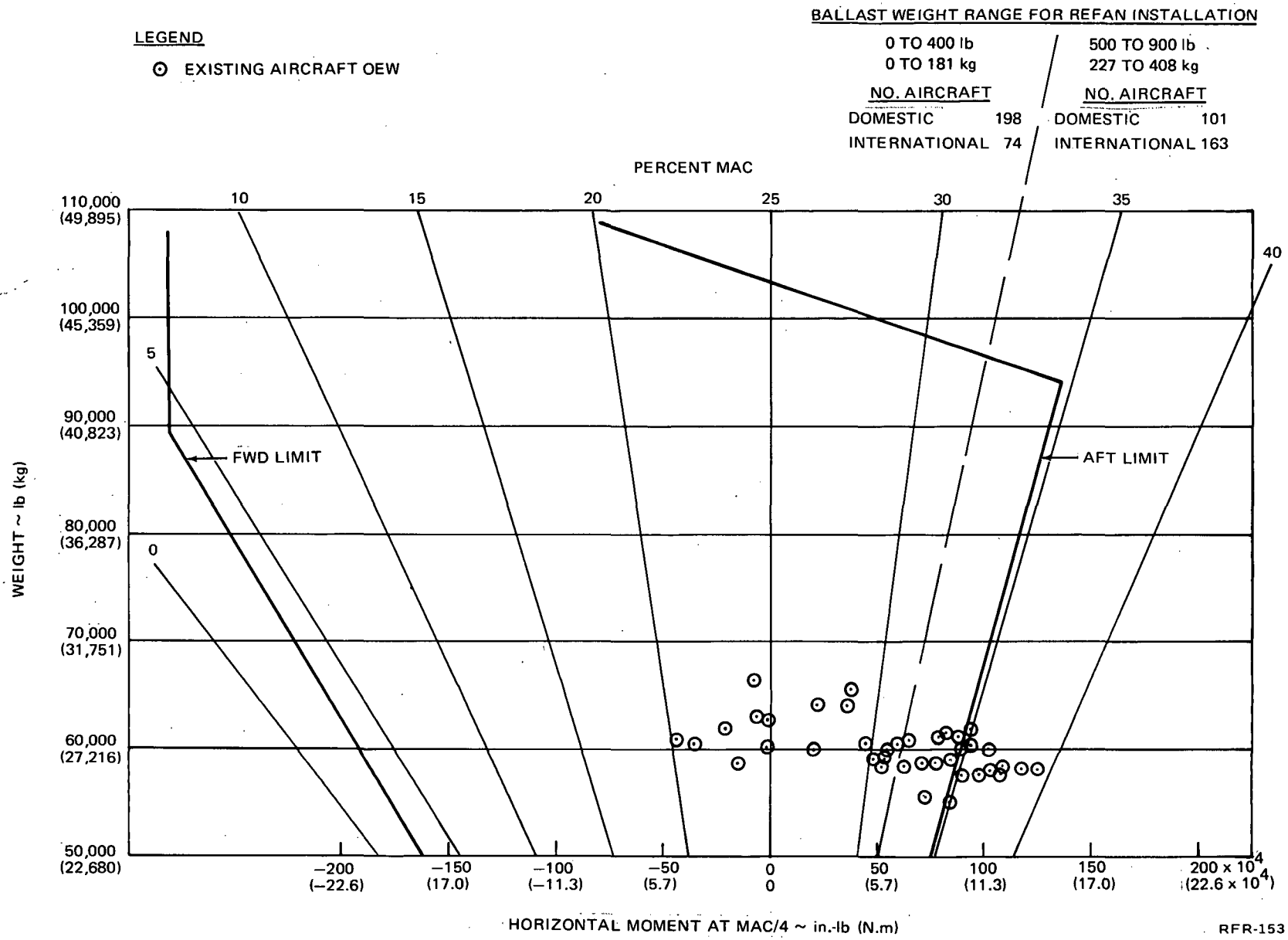

FIGURE 46. HORIZONTAL MOMENT AT MAC/4 VERSUS BASIC AIRCRAFT OEW FOR DC-9-30 SERIES

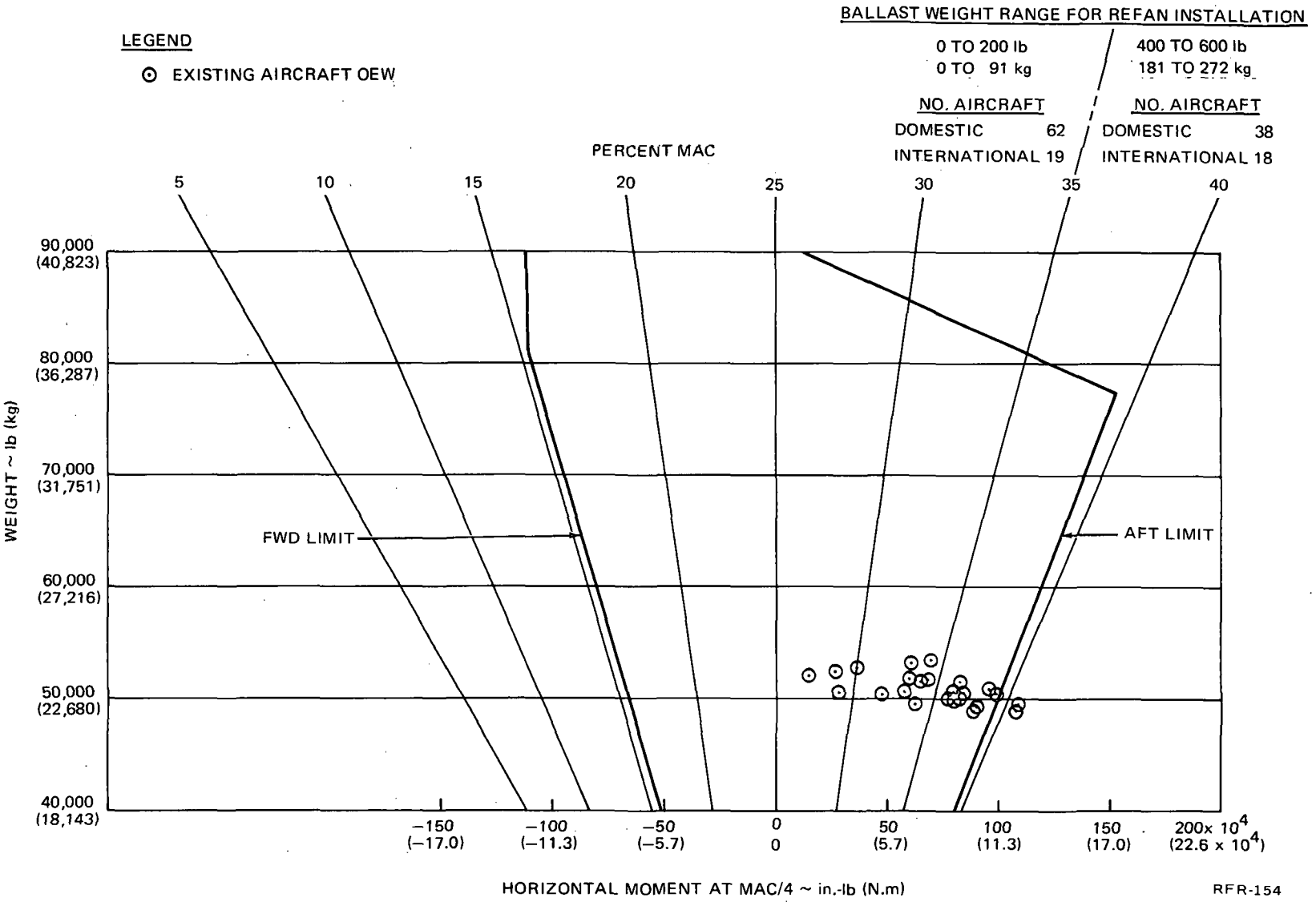

FIGURE 47. HORIZONTAL MOMENT AT MAC/4 VERSUS BASIC AIRCRAFT OEW FOR DC-9-10 SERIES

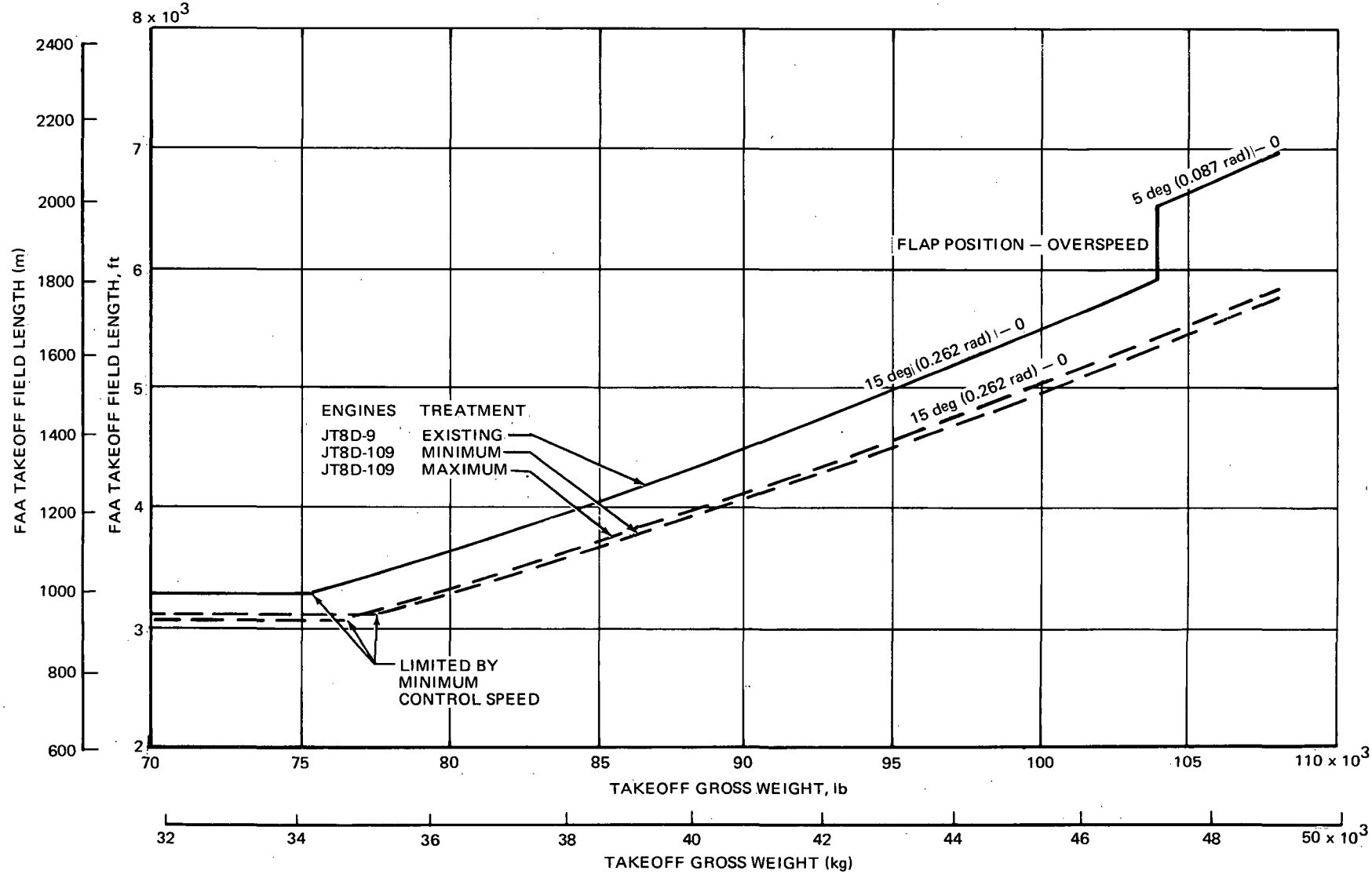

RFR-008

FIGURE 48. DC-9-32 FAA TAKEOFF FIELD LENGTH COMPARISON

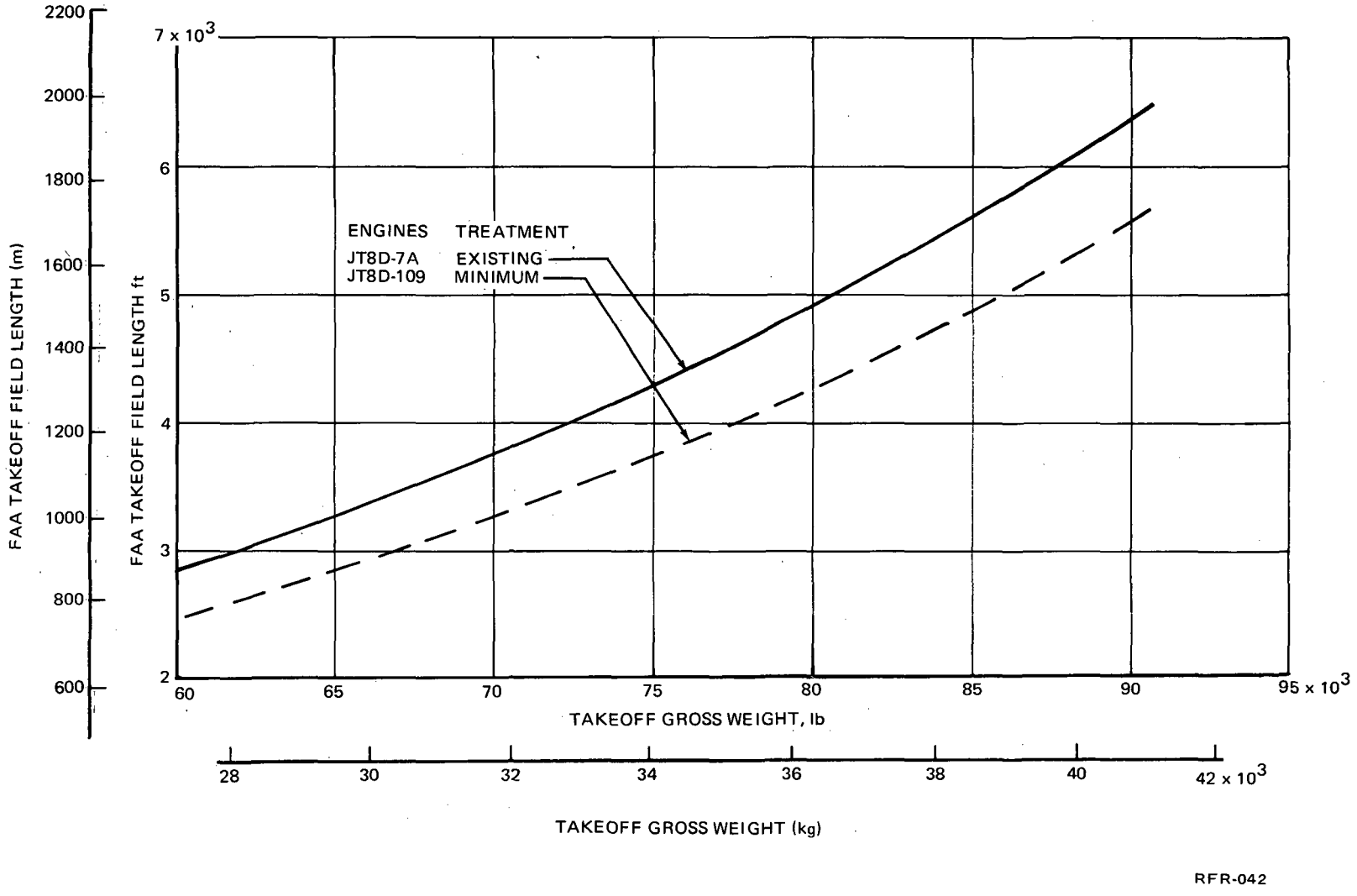

FIGURE 49. DC-9-15 FAA TAKEOFF FIELD LENGTH COMPARISON AT SEA LEVEL, STANDARD DAY, FLAP POSITION = 20 deg (0.350 rad)

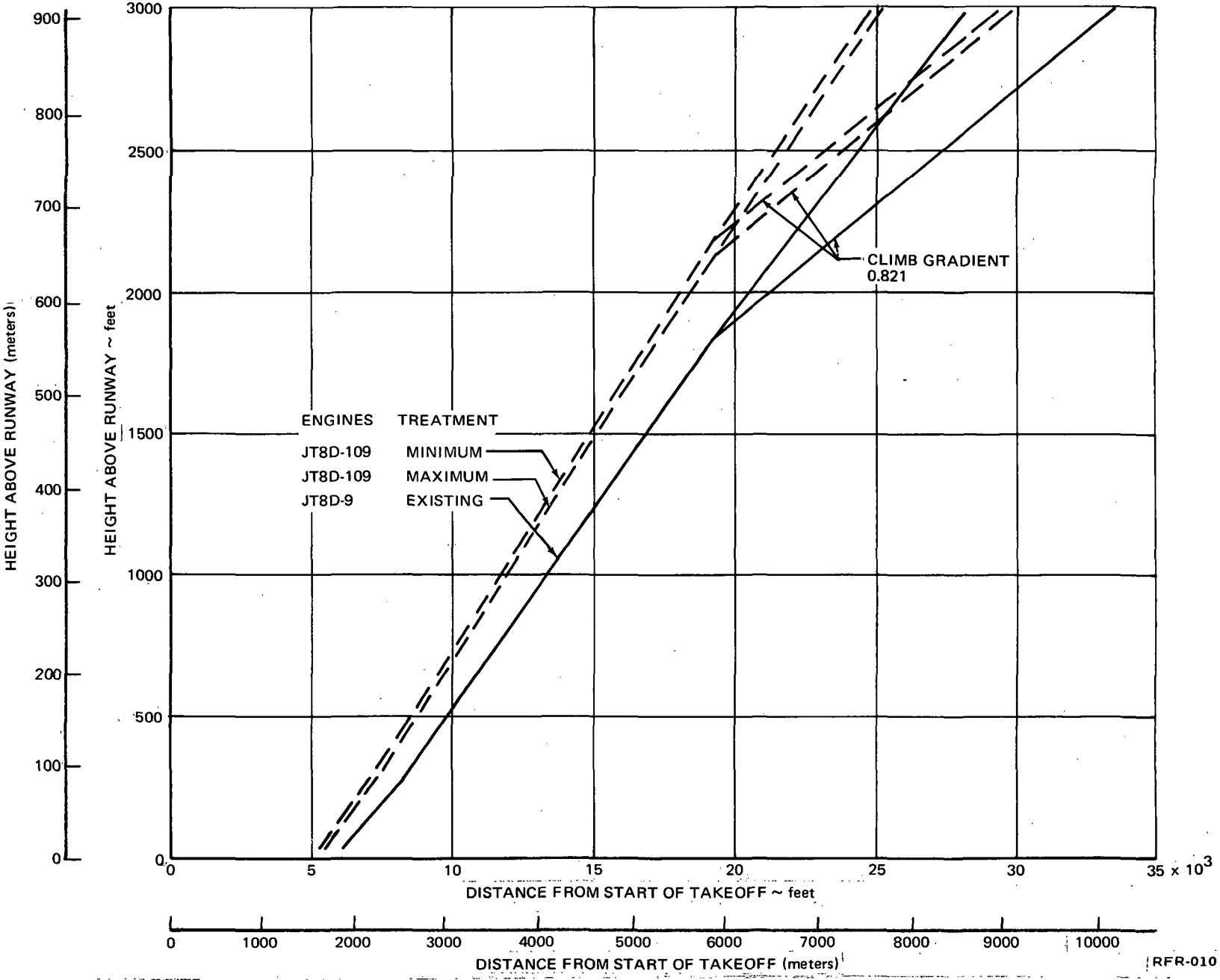

FIGURE 50. DC-9-32 TAKEOFF FLIGHT PATH COMPARISON – ALL ENGINE, MAXIMUM TOGW = 108,000 lb (48 988 kg) SEA LEVEL, 25°C (298.15 °K) DAY, FLAP POSITION = 5 deg (0.087 rad), ZERO OVERSPEED

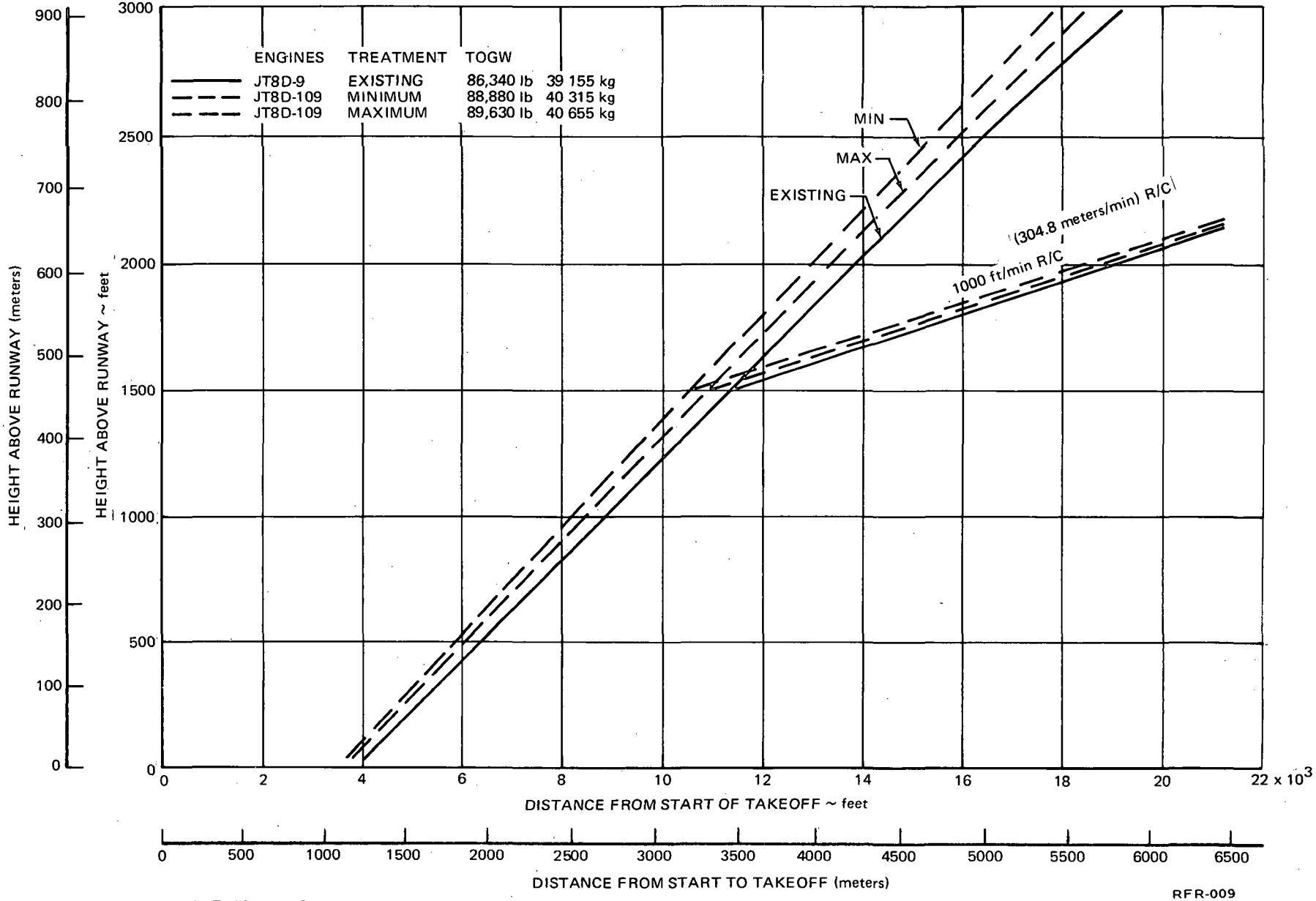

FIGURE 51. DC-9-32 TAKEOFF FLIGHT PATH COMPARISON – ALL ENGINE, TYPICAL MISSION AT SEA LEVEL, 25°C (298.15 °K) DAY, FLAP POSITION = 5 deg (0.087 rad), ZERO OVERSPEED

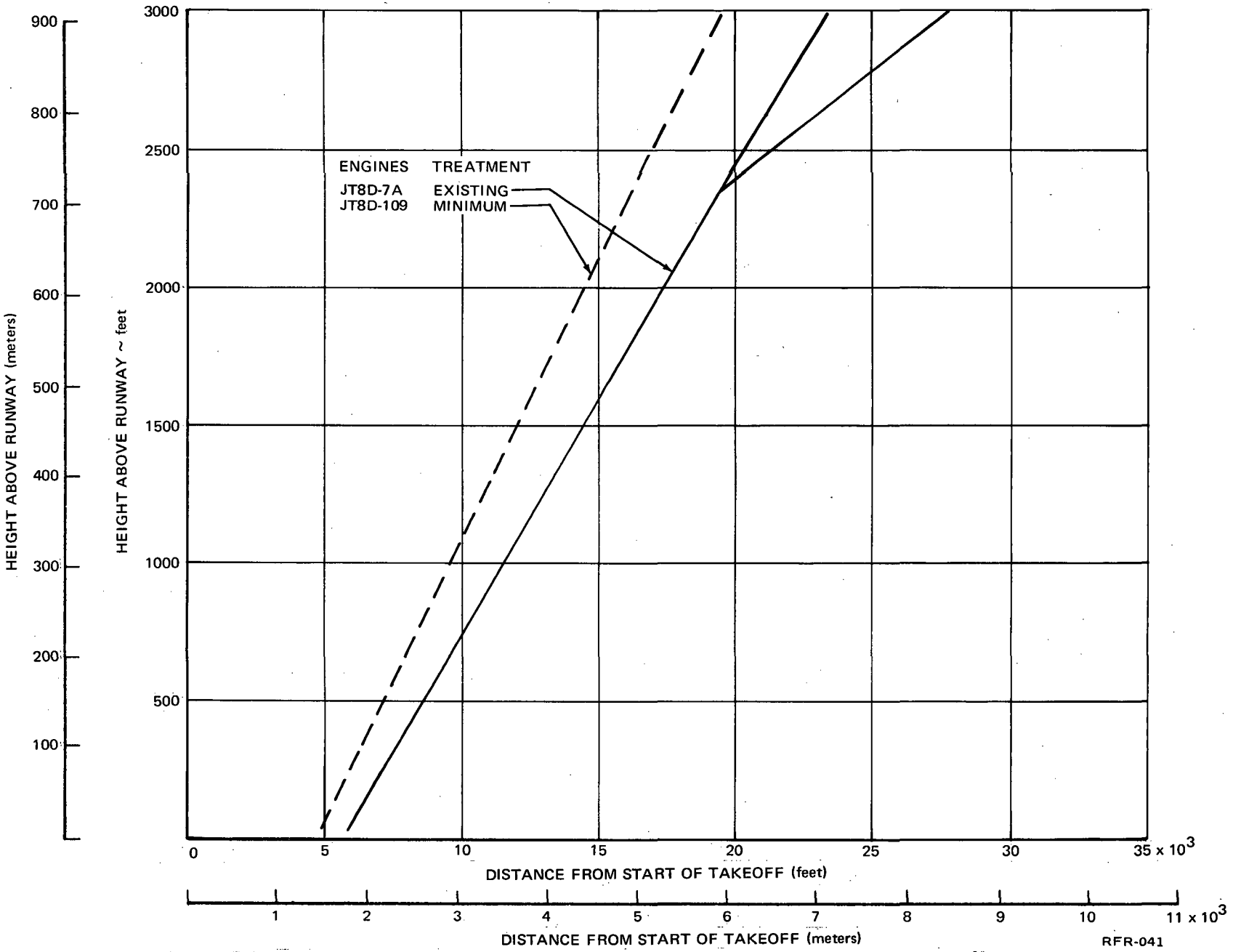

FIGURE 52. DC-9-15 TAKEOFF FLIGHT PATH – ALL ENGINE, MAXIMUM TOGW AT SEA LEVEL, 25°C (298.15°K) DAY, FLAP POSITION = 10 deg (0.175 rad), TOGW = 90,700 lb (41 141 kg)

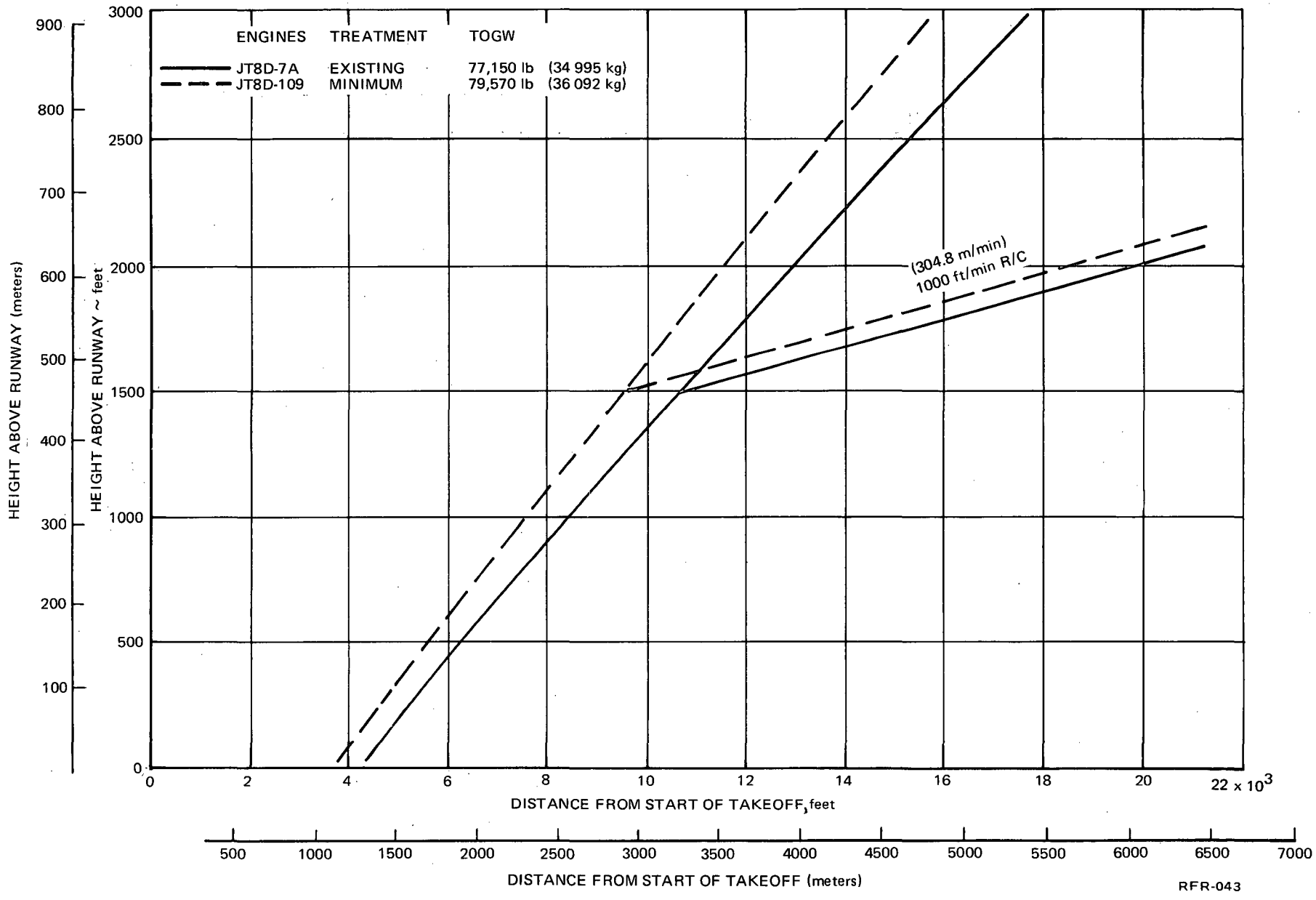

FIGURE 53. DC-9-15 TAKEOFF FLIGHT PATH – ALL ENGINE, TYPICAL MISSION AT SEA LEVEL, 25°C (298.15°K) DAY, FLAP POSITION = 10 deg (0.175 rad)

A comparison of the DC-9-32 payload range characteristics, based on long range cruise at 10 668 m (35,000 ft altitude) for the production JT8D-9 engines in the production nacelles and the JT8D-109 engines installed in the minimum noise suppression nacelles, is presented in figure 54. As shown in the figure, with a typical payload of 6 804 kg (15,000 lb), the range difference for the minimum configuration amounts to a 54 km (24 n. mi.) reduction, and with a weight limited payload of 11 540 kg (25,442 lb), the range difference amounts to a 394 km (213 n. mi.) reduction. For the maximum selected configuration, the range difference amounts to a 159 km (86 n. mi.) reduction with a typical payload of 6 804 kg (15,000 lb) and a 542 km (293 n. mi.) reduction with a weight limited payload of 11 340 kg (25,000 lb).

A breakdown of the components affecting maximum range for these payload points is shown in table 20.

TABLE 20

DC-9-32 PAYLOAD RANGE COMPONENTS

LONG RANGE CRUISE AT 35,000 ft (10 668 m)

COMPONENTS AFFECTING MAXIMUM RANGE	RANGE CHANGE FOR THE JT8D-109 INSTALLATION			
	TYPICAL MISSION PAYLOAD		WEIGHT LIMITED PAYLOAD	
	MAXIMUM SUPPRESSION 15,000 lb (6 804 kg)	MINIMUM SUPPRESSION 15,000 lb (6 804 kg)	MAXIMUM SUPPRESSION 25,000 lb (11 340 kg)	MINIMUM SUPPRESSION 25,442 lb (11 540 kg)
SFC (including effect of nacelle and pylon drag changes.	-33 n. mi. (-61 km)	+21 n. mi. (+39 km)	-20 n. mi. (-37 km)	+14 n. mi. (+26 km)
Weight Increase	-53 n. mi. (-98 km)	-50 n. mi. (-93 km)	-273 n. mi. (-505 km)	-227 n. mi. (-420 km)
Total Change	-86 n. mi. (-159 km)	-29 n. mi. (-54 km)	-293 n. mi. (-542 km)	-213 n. mi. (-394 km)

A comparison of the DC-9-32 payload range characteristics, based on high speed cruise at 9 144 m (30,000 ft altitude), is presented in figure 55. As shown in the figure, with a typical payload of 6 804 kg (15,000 lb), the range difference for the minimum suppression configuration amounts to a 30 km (16 n. mi.) reduction, and with weight limited payload of 11 540 kg (25,442 lb), the range difference amounts to a 352 km (190 n. mi.) reduction. For the maximum suppression configuration, the range difference amounts to a 121 km (65 n. mi.) reduction with a typical payload of 6 804 kg (15,000 lb), and a 482 km (260 n. mi.) reduction with a weight limited payload of 11 340 kg (25,000 lb). A breakdown of the components affecting maximum range for the payload points is shown in table 21.

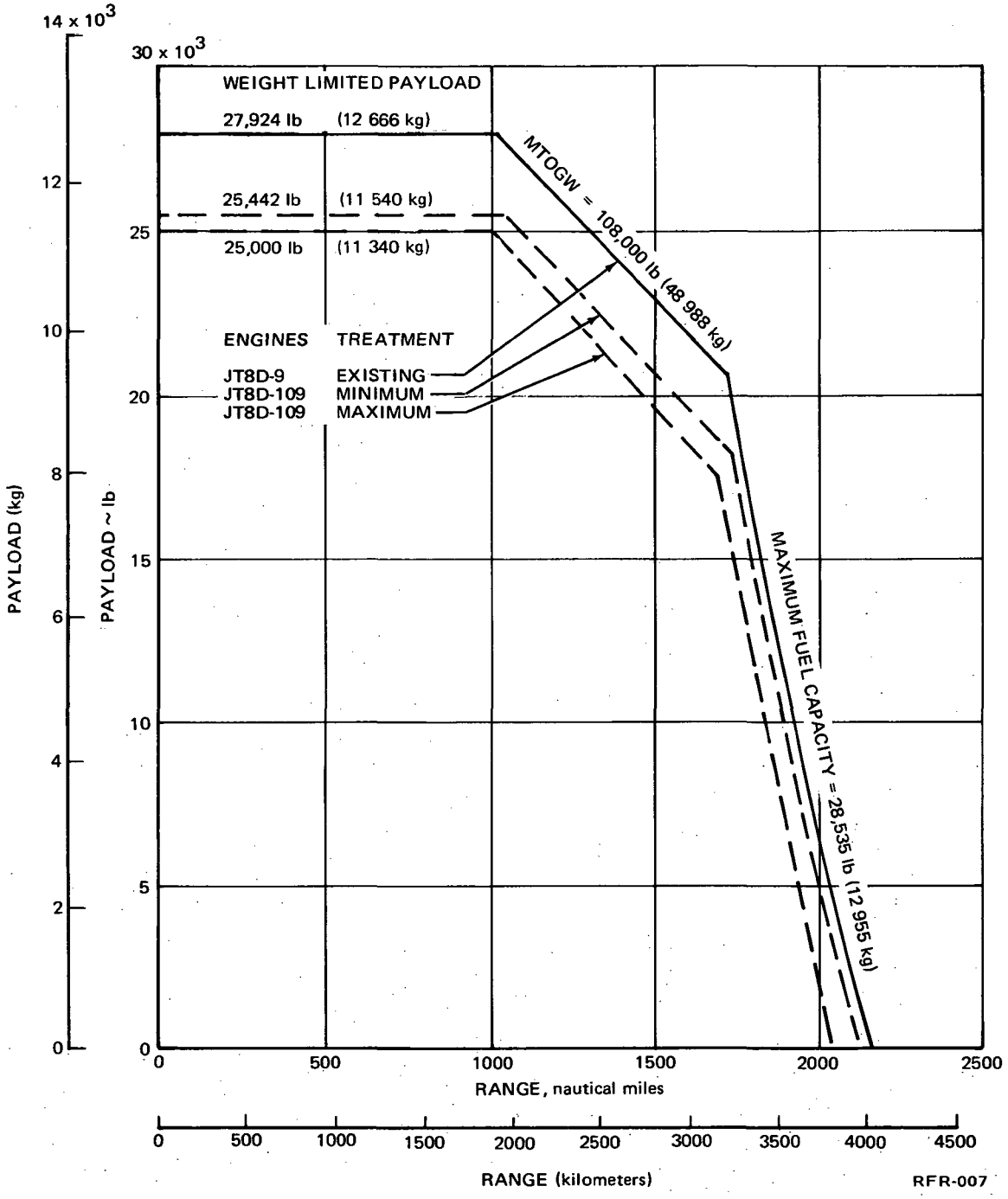

FIGURE 54. DC-9-32 PAYLOAD RANGE CAPABILITY COMPARISON – LONG RANGE CRUISE AT 35,000 ft (10 668 meters) ALTITUDE

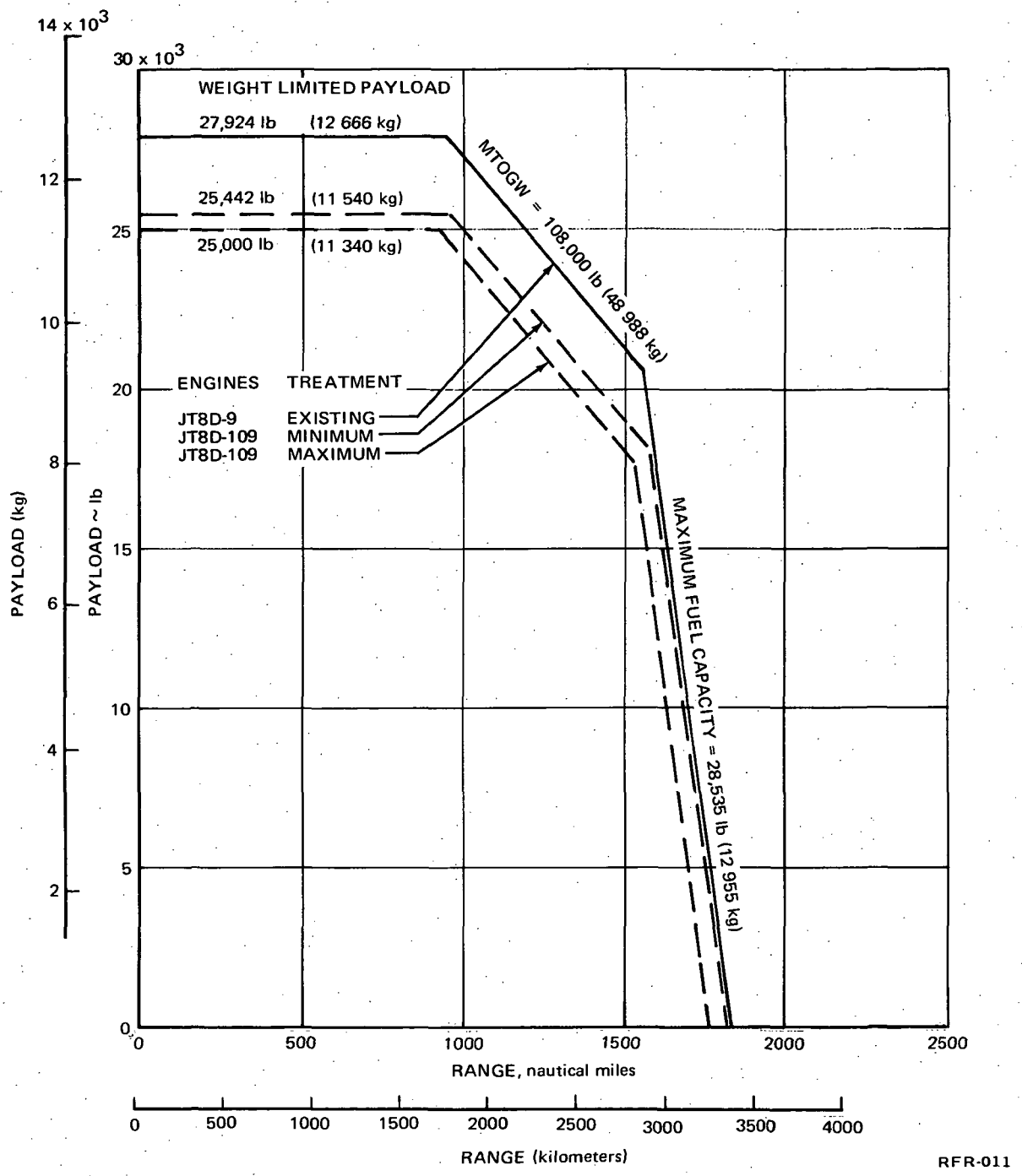

FIGURE 55. DC-9-32 PAYLOAD RANGE CAPABILITY COMPARISON – HIGH SPEED CRUISE AT 0.78 MACH NO., 30,000 feet (9 144 meters) ALTITUDE

TABLE 21

DC-9-32 PAYLOAD RANGE COMPONENTS

HIGH SPEED CRUISE AT 30,000 ft (9 144 m)

COMPONENTS AFFECTING MAXIMUM RANGE	RANGE CHANGE FOR THE JT8D-109 INSTALLATION			
	TYPICAL MISSION PAYLOAD		WEIGHT LIMITED PAYLOAD	
	MAXIMUM SUPPRESSION 15,000 lb (6 804 kg)	MINIMUM SUPPRESSION 15,000 lb (6 804 kg)	MAXIMUM SUPPRESSION 25,000 lb (11 340 kg)	MINIMUM SUPPRESSION 25,442 lb (11 540 kg)
SFC (including effect of nacelle and pylon drag changes.)	-28 n. mi. (-52 km)	+19 n. mi. (+35 km)	-17 n. mi. (-32 km)	+13 n. mi. (+24 km)
Weight Increase	-37 n. mi. (-69 km)	-35 n. mi. (-65 km)	-243 n. mi. (-450 km)	-203 n. mi. (-376 km)
Total Change	-65 n. mi. (-121 km)	-16 n. mi. (-30 km)	-260 n. mi. (-482 km)	-190 n. mi. (-352 km)

A comparison of the DC-9-15 payload characteristics, based on long range cruise at 10 668 m (35,000 ft altitude) for the production JT8D-7A engines in production nacelles and the JT8D-109 engines installed in the minimum suppression nacelles, is presented in figure 56. As shown in the figure, with a typical payload of 6 804 kg (15,000 lb), the range difference amounts to a 246 km (133 n. mi.) reduction, and with a weight limited payload of 9 591 kg (21,114 lb), the range difference amounts to a 376 km (203 n. mi.) reduction. A breakdown of the components affecting maximum range for the payload points is shown in table 22.

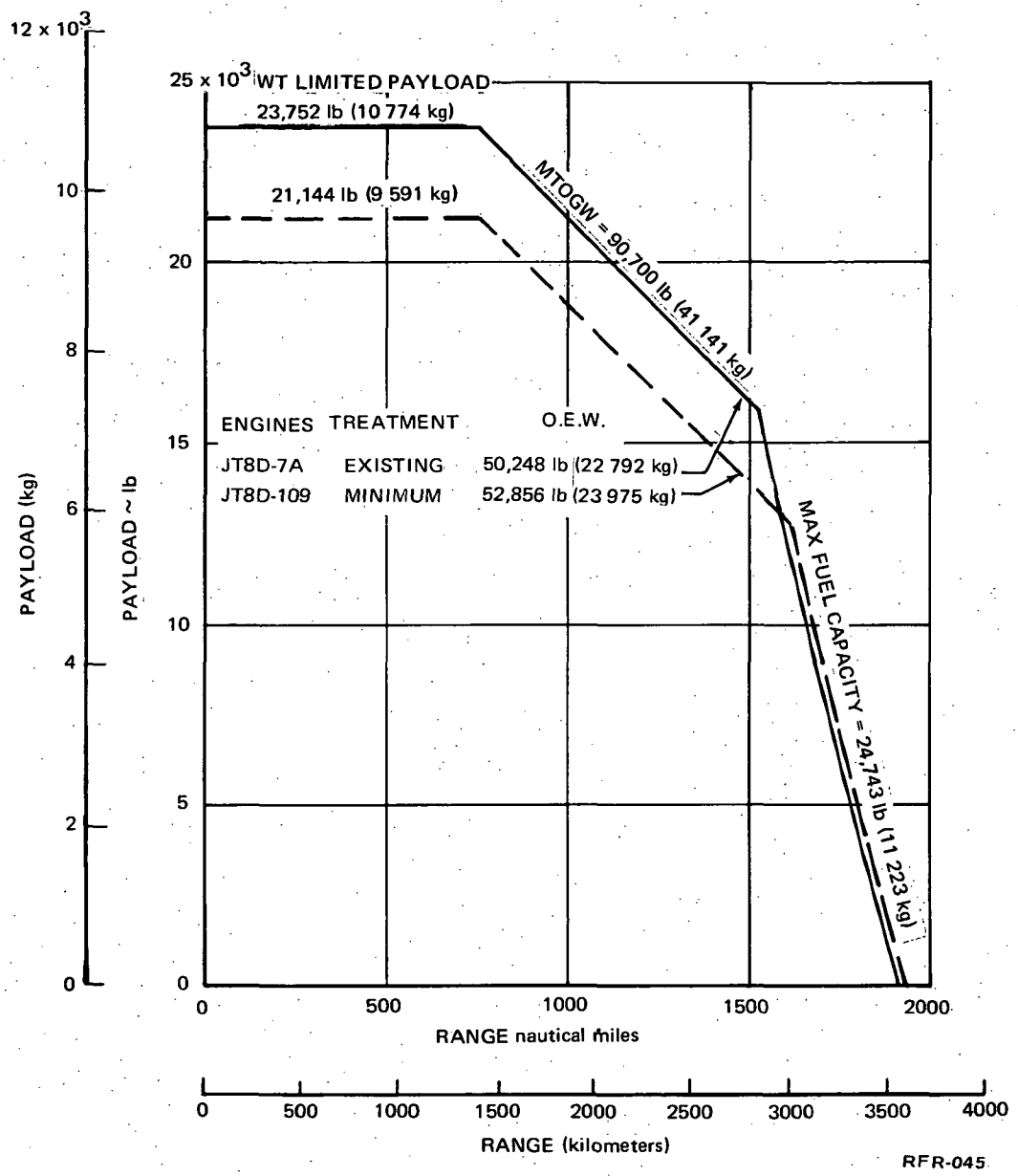

FIGURE 56. DC-9-15 PAYLOAD RANGE CAPABILITY – LONG RANGE CRUISE AT 35,000 feet (10 668 meters) ALTITUDE

TABLE 22

DC-9-15 PAYLOAD RANGE COMPONENTS

LONG RANGE CRUISE AT 35,000 ft (10 668 m)

COMPONENTS AFFECTING MAXIMUM RANGE	RANGE CHANGE FOR JT8D-7A TO JT8D-109	
	MINIMUM SUPPRESSION 15,000 lb (6 804 kg) PAYLOAD	MINIMUM SUPPRESSION 21,144 lb (9 591 kg) PAYLOAD
SFC (including effect of nacelle and pylon drag changes.)	+70 n. mi. (+130 km)	+43 n. mi. (+80 km)
Weight Increase	-203 n. mi. (-376 km)	-246 n. mi. (-456 km)
Total Change	-133 n. mi. (-246 km)	-203 n. mi. (-376 km)

A comparison of the DC-9-15 payload range characteristics, based on high speed cruise at 9 144 m (30,000 ft) altitude is presented in figure 57. As shown in the figure, with a typical payload of 6 804 kg (15,000 lb), the range difference amounts to a 211 km (114 n. mi.) reduction, and a weight limited payload of 9 591 kg (21,144 lb), the range difference amounts to a 343 km (185 n. mi.) reduction. A breakdown of the components affecting maximum range for the payload points is shown in table 23.

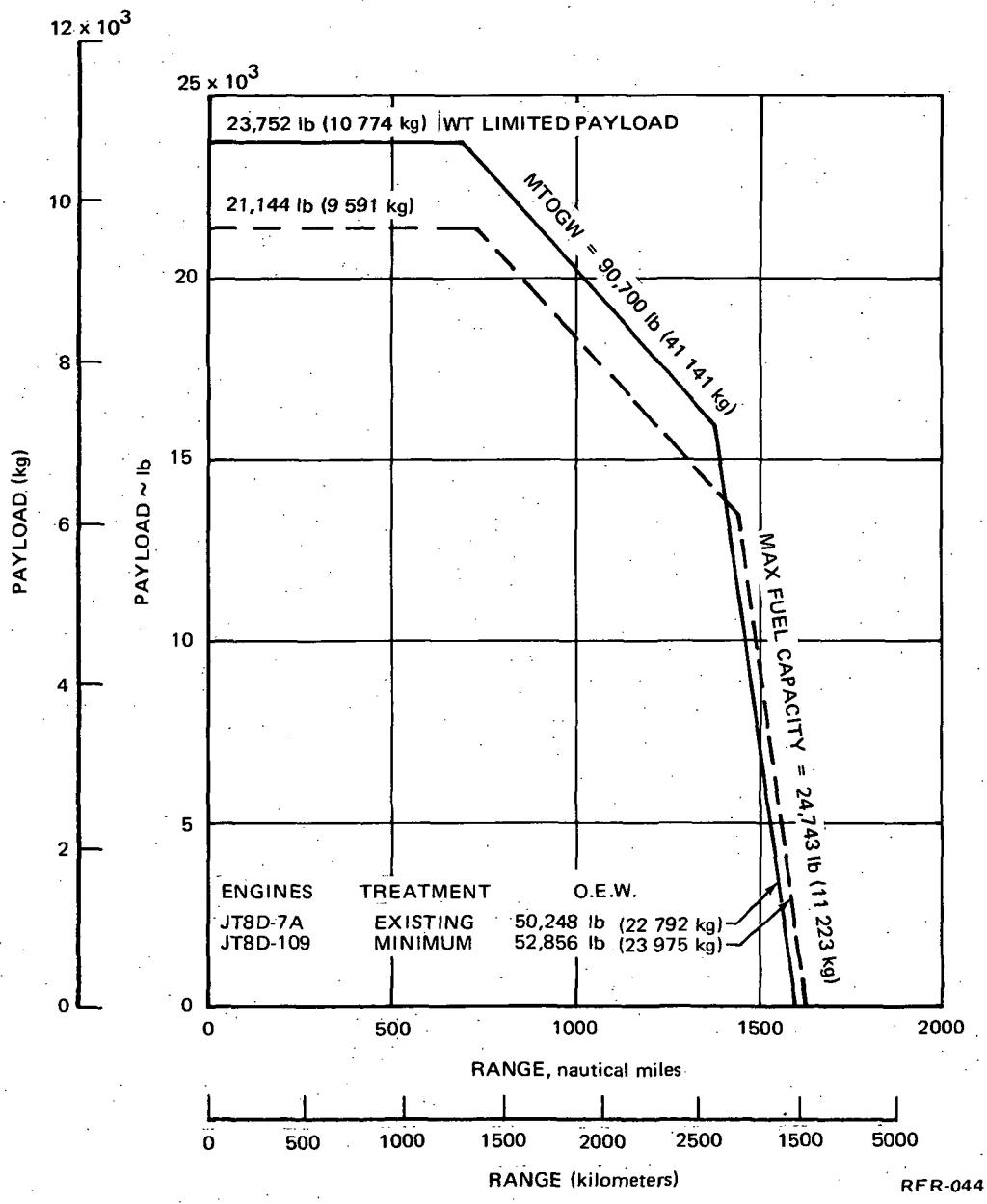

FIGURE 57. DC-9-15 PAYLOAD RANGE CAPABILITY – HIGH SPEED CRUISE AT 0.78 MACH NO., 30,000 ft (9 144 meters) ALTITUDE

TABLE 23

DC-9-15 PAYLOAD RANGE COMPONENTS

HIGH SPEED CRUISE AT 30,000 ft (9 144 m)

COMPONENTS AFFECTING MAXIMUM RANGE	RANGE CHANGE FOR JT8D-7A TO JT8D-109	
	MINIMUM SUPPRESSION 15,000 lb (6 804 kg) PAYLOAD	MINIMUM SUPPRESSION 21,144 lb (9 591 kg) PAYLOAD
SFC (including effect of nacelle and pylon drag changes.)	+63 n. mi. (+117 km)	+38 n. mi. (+70 km)
Weight Increase	-177 n. mi. (-328 km)	-223 n. mi. (-413 km)
Total Change	-114 n. mi. (-211 km)	-185 n. mi. (-343 km)

The significant changes in airplane performance parameters are shown in table 24 for the DC-9-32 and in table 25 for the DC-9-15. The flight condition is a typical route of 695 km (375 n. mi.) with a 6 804 kg (15,000 lb) payload at Mach number = .78 and 9 144 m (30,000 ft) altitude for minimum Direct Operating Costs.

The installation of JT8D-109 engines in either minimum or maximum noise suppression treatment nacelles results in a slight increase in ground minimum control speeds and air minimum control speeds (table 26) which are within acceptable limits.

TABLE 24

PERFORMANCE CHANGE FOR THE JT8D-109 RELATIVE TO JT8D-9 ON THE DC-9-32 FOR MINIMUM DIRECT OPERATING COST

		MAXIMUM SUPPRESSION	MINIMUM SUPPRESSION
Fuel Burned	lb kg	+145 (+66)	+25 (+11)
Takeoff Gross Weight	lb kg	+3,290 (+1 492)	+2,540 (+1 152)
Block Speed	n. mi./hr km/hr	-1 (-2)	-1 (-2)
Takeoff Field Length Required at Sea Level on a Standard Day	ft m	-80 (-24)	-200 (-61)
Total Fuel Burned	lb kg	+6,450 (+2 926)	+6,330 (+2 871)
Base Fuel Burned 6,305 lb (2 860 kg)			

TABLE 25

PERFORMANCE CHANGE FOR THE JT8D-109 RELATIVE TO JT8D-7A ON THE DC-9-15 FOR MINIMUM DIRECT OPERATING COST

		MINIMUM SUPPRESSION
Fuel Burned	lb kg	+100 (+45)
Takeoff Gross Weight	lb kg	+2,680 (+1 215)
Block Speed	n. mi./hr km/hr	-4 (-7)
Takeoff Field Length Required at Sea Level on a Standard Day	ft m	-290 (-88)
Total Fuel Burned	lb kg	+6,340 (+2 876)
Base Fuel Burned 6,240 lb (2 831 kg)		

TABLE 26

MINIMUM CONTROL SPEED DIFFERENTIAL - JT8D-109

MINIMUM AND MAXIMUM NACELLES

	DC-9-32 MINIMUM SELECTED ACOUSTIC TREATMENT RELATIVE TO JT8D-9	DC-9-32 MAXIMUM SELECTED ACOUSTIC TREATMENT RELATIVE TO JT8D-9	DC-9-15 MINIMUM SELECTED ACOUSTIC TREATMENT RELATIVE TO JT8D-7A
Air Minimum Control Speed (V_{MCA})	+1.5 to 2.0 Knots +0.772 to 1.029 m/s	+1.0 to 1.5 Knots +0.514 to 0.772 m/s	+7.0 Knots +3.601 m/s
Ground Minimum Control Speed (V_{MCG})	+1.5 Knots +0.772 m/s	+1.0 Knots +0.514 m/s	+5.0 Knots +2.514 m/s

Water ingestion from wet runways can be a critical factor of engine performance during airplane takeoff and landing operations. The principle cause for water ingestion is water and/or slush spray from the landing gear wheels. As water ingestion increases, engine performance degrades to the level where complete engine flame-out occurs.

Figure 58 shows the angle of spray tolerable before water ingestion occurs on the existing DC-9 airplane. The spray angle shown is without the landing gear spray deflector installed. As shown in figure 58, the refan configurated airplane is more tolerant to these conditions since a larger angle of spray is required before water ingestion occurs. Therefore, no change is required to make the existing spray deflector system compatible with the new refan nacelle configuration.

NOTES:

1. ANGLE OF SPRAY SHOWN IS WITHOUT SPRAY DEFLECTORS INSTALLED.
2. NO CHANGE IN THE SPRAY DEFLECTOR SYSTEM IS REQUIRED AS THE RESULT OF THE REFAN ENGINE INSTALLATION.

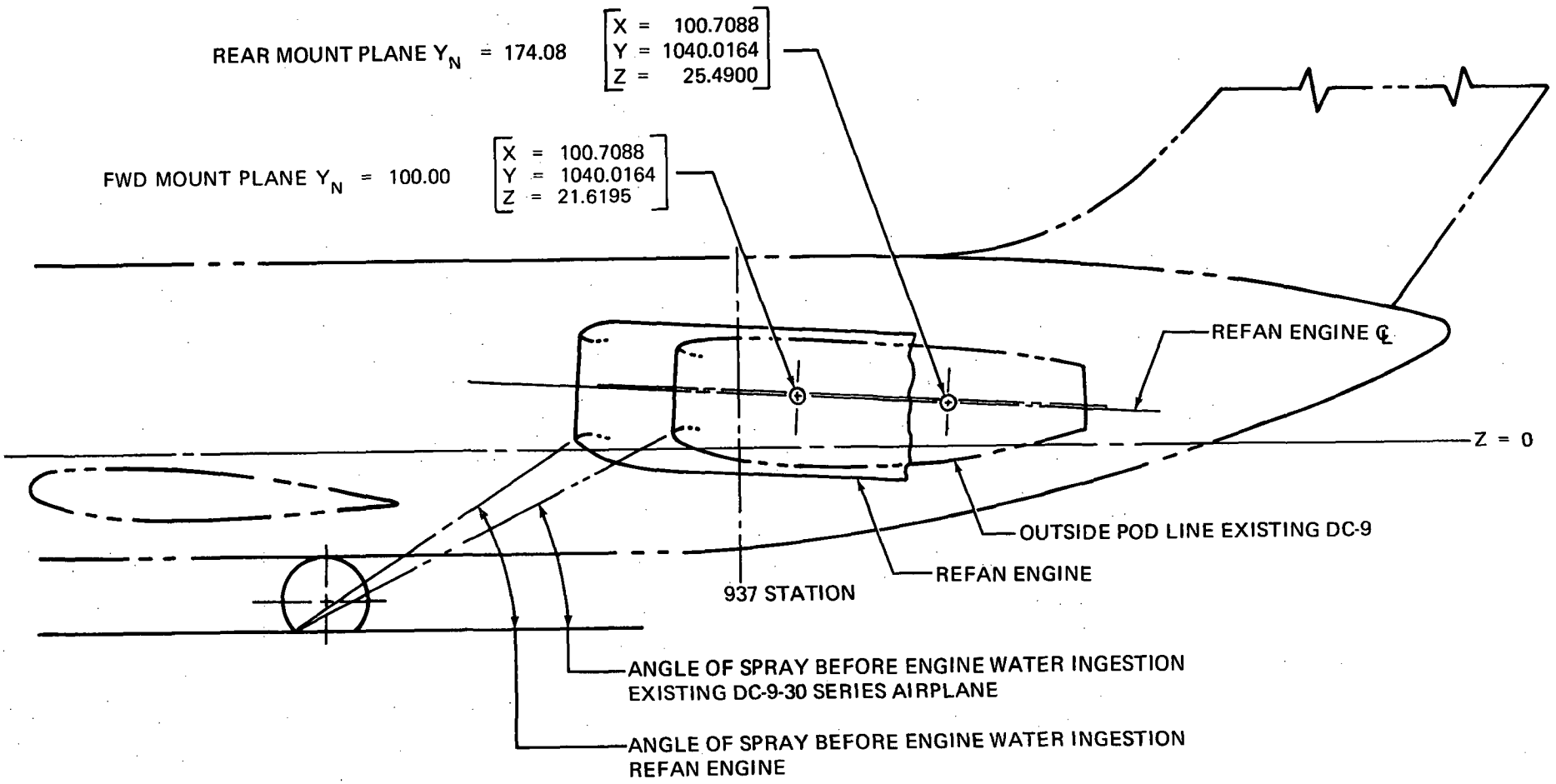

FIGURE 58. DC-9 REFAN SLUSH AND WATER SPRAY PATTERN

ACOUSTICAL CHARACTERISTICS

The JT8D refan program engine and nacelle modifications are designed to reduce the dominant jet noise source on the JT8D engine-by-engine cycle modifications which remove energy from the jet exhaust and transfer this work to the fan. A new, large diameter, single stage fan is used to absorb this increased work and increase the bypass ratio or the fan airflow relative to the primary core airflow. The engine modifications effectively reduce primary jet exhaust velocity at takeoff power and therefore reduce jet noise, but also tend to increase fan and turbine noise because of the higher fan tip speed on the refanned engine.

The fan noise is effectively suppressed by engine case and nacelle acoustic treatment. The refanned engine comes with an extensively lined fan duct and inlet acoustic treatment between the inlet guide vanes and the fan rotor. A treated inlet and tailpipe is added by the airframe manufacturer. Varying levels of inlet and tailpipe treatment were investigated to determine the most cost effective configurations. Suggested approach noise goals for inlet and tailpipe design were FAR Part 36, Part 36 minus 5, and Part 36 minus 10 noise levels. The chosen inlet and tailpipe configurations approach the intermediate goal of Part 36 minus 5 noise levels.

The final selected nacelle inlet and tailpipe configurations for the refanned DC-9 compared to the existing DC-9 nacelle are shown on figure 3 . These configurations were chosen following the nacelle trade study (Appendix B). This study, using Douglas estimates of the untreated JT8D-109 refanned engine noise levels, traded the weight, performance, external drag, development cost and risk, and acoustical characteristics of several refanned nacelle inlet and tailpipe configurations. These configurations include long and short inlets and tailpipes, and treated rings, splitters, plugs, and bullets. The chosen inlets and tailpipes of figure 3 , titled "minimum" and "maximum" treatment, utilize relatively long inlets and tailpipes without rings, treated bullets, or plugs. The acoustic procedure used to choose the inlets and tailpipes is described in the Acoustic Design Section.

Detailed noise estimates including spectra and flyover time histories were made by Douglas for the untreated JT8D-109 engine and for the JT8D-109 engine together with the minimum and maximum nacelle treatment. Details of this procedure along with the resulting spectra and time histories are presented in Appendix A. The results of this analysis were combined with the estimated aircraft performance to determine FAR Part 36 noise levels. Table 27 presents a comparison of FAR Part 36 noise levels for the existing and refanned DC-9-32. The estimated EPNL's for the refanned aircraft, together with the minimum nacelle acoustic treatment is lower than FAR Part 36 noise levels by 3 EPNdB at approach, 10 at takeoff with cutback and 13 at sideline, and achieves reductions from the existing DC-9 of 8 EPNdB at approach, 12 at takeoff, and 12 EPNdB at sideline. Table 28 presents a comparison for the DC-9-15. The existing DC-9-15 uses JT8D-7 or -7A engines, but uses the JT8D-109 engine in the refanned configuration.

TABLE 27

ESTIMATED EPNLS FOR EXISTING AND REFANNED DC-9-32 AIRCRAFT

AIRCRAFT	APPROACH			TAKEOFF WITH CUTBACK			TAKEOFF WITHOUT CUTBACK			SIDELINE		
		ΔEPNdB			ΔEPNdB			ΔEPNdB			ΔEPNdB	
	EPNdB	RELATIVE TO UN-TREATED REFANNED AIRCRAFT	RELATIVE TO EXISTING AIRCRAFT	EPNdB	RELATIVE TO UN-TREATED REFANNED AIRCRAFT	RELATIVE TO EXISTING AIRCRAFT	EPNdB	RELATIVE TO UN-TREATED REFANNED AIRCRAFT	RELATIVE TO EXISTING AIRCRAFT	EPNdB	RELATIVE TO UN-TREATED REFANNED AIRCRAFT	RELATIVE TO EXISTING AIRCRAFT
EXISTING AIRCRAFT	108	–	–	97	–	–	103	–	–	102	–	–
FAR PART 36 RULE	103.1	–	–	95.6	–	–	95.6	–	–	103.1	–	–
UNTREATED REFANNED*	112	–	-4**	92	–	5	94	–	11	97	–	5
MINIMUM TREATMENT REFANNED	100	12	8	85	7	12	88	6	15	90	7	12
MAXIMUM TREATMENT REFANNED	99	13	9	84	8	13	88	6	15	90	7	12

*ASSUMES AERO PERFORMANCE OF UNTREATED REFANNED AIRCRAFT IS THE SAME AS THE MINIMUM TREATED REFANNED AIRCRAFT.
**NOISE INCREASE.

TABLE 28

ESTIMATED EFFECTIVE PERCEIVED NOISE LEVELS AT FAR PART 36 CONDITIONS FOR EXISTING AND REFANNED DC-9-15 AIRCRAFT WITH MINIMUM TREATED NACELLE

	APPROACH	TAKEOFF WITHOUT CUTBACK	TAKEOFF WITH CUTBACK	SIDELINE
EXISTING AIRCRAFT	107	99	90	100
FAR PART 36 RULE	102.5	94.3	94.3	102.5
REFANNED AIRCRAFT (UNTREATED)	112	89	85	96
REFANNED AIRCRAFT (TREATED)	100	84	79	90
NOISE REDUCTION RELATIVE TO UNTREATED REFANNED AIRCRAFT	12	5	6	6
NOISE REDUCTION RELATIVE TO EXISTING AIRCRAFT	7	15	11	10

RFR-129

EPNL noise contours were calculated for the existing and refanned DC-9-32. The resulting areas of these contours are summarized in figure 59 as a function of EPNL contour level. The refan configurations achieve an 80 to 90 percent reduction in contour area and the area differences between minimum and maximum nacelle treatment are very small. Representative 90 and 95 EPNdB contour comparisons between an existing and modified DC-9 are shown on figures 60 through 67 for both typical mission operation 6 804 kg (15,000 lb) payload, 694 km (375 n. mi.) range, and for FAR Part 36 operation. Typical mission operation gives a steeper climbout path and lower approach thrust than does FAR Part 36 certification weight. Typical mission operation is believed to better reflect the day-to-day airline operating environment. The effect of takeoff with cutback and two-segment 0.105/0.052 rad (6/3 deg) approaches are also shown on figures 60 through 67.

The contour shape lateral to the runway is based on empirically derived factors which reflect ground attenuation, the time duration increase during ground roll, and the increased inlet and jet noise at low forward velocities. There is little difference on the takeoff noise contour between minimum and maximum treatment; both these configurations are dominated by jet noise because, at takeoff power, the fan noise is treated below the jet noise. At typical mission operation the maximum treatment has a higher gross weight than the minimum treatment and this is reflected in slightly shallower climbout gradients and slightly larger takeoff noise contours. This takeoff contour area increase for the maximum treatment is compensated for by a smaller approach contour. The two-segment approach in general does not improve the modified DC-9 contour area for the 90 and 95 EPNdB contours except it does affect the minimum treatment 90 EPNdB contour at FAR Part 36 weights enough to offset the area benefit between the minimum and maximum configurations on figures 60 and 67 . Additional contours for the DC-9-15 modification are presented in Appendix A.

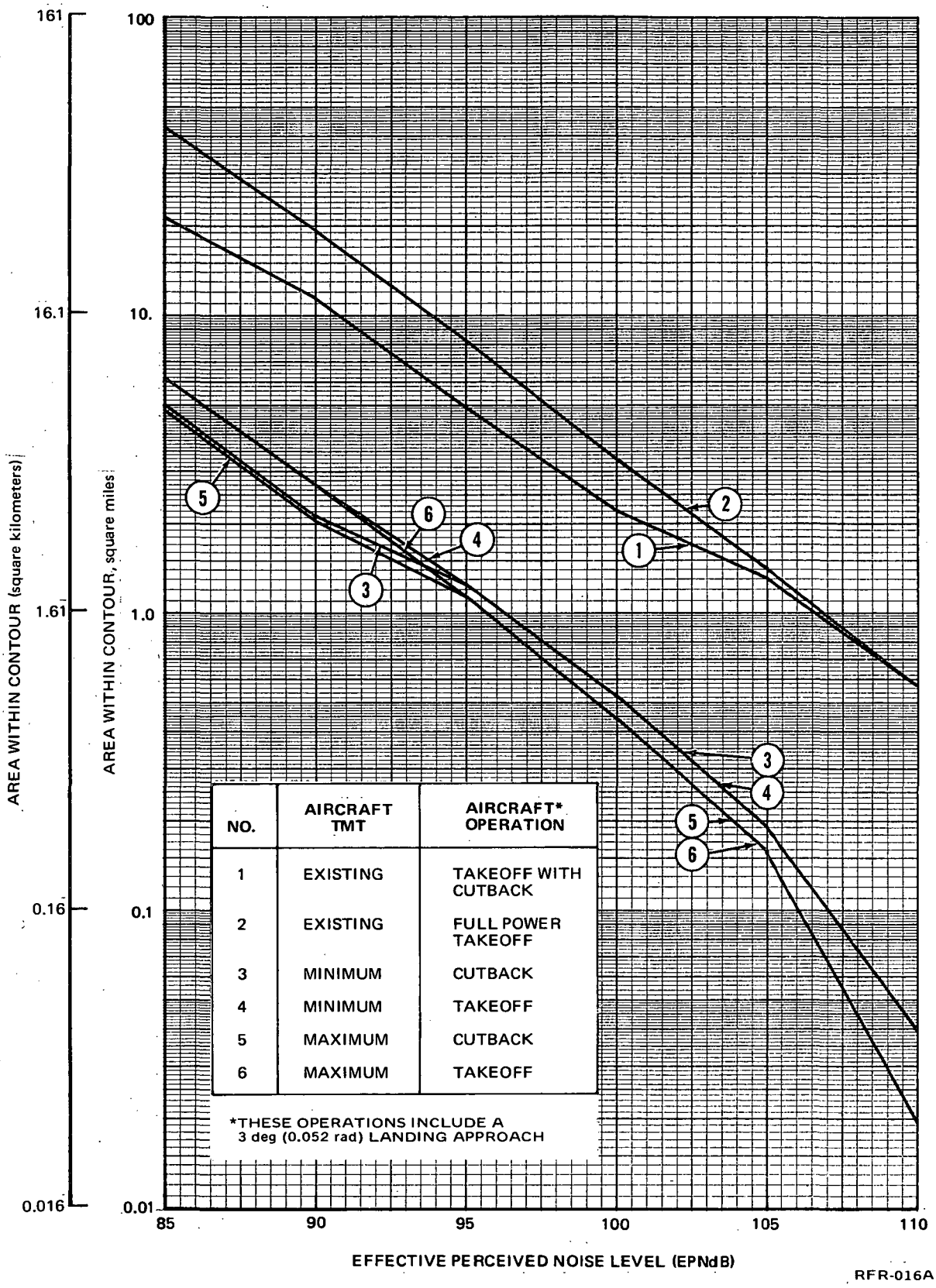

FIGURE 59. EPNL-AREA CONTOUR MAP FOR EXISTING AND MODIFIED DC-9-32 AIRCRAFT FOR TYPICAL MISSION OPERATION WITH SINGLE SEGMENT APPROACH

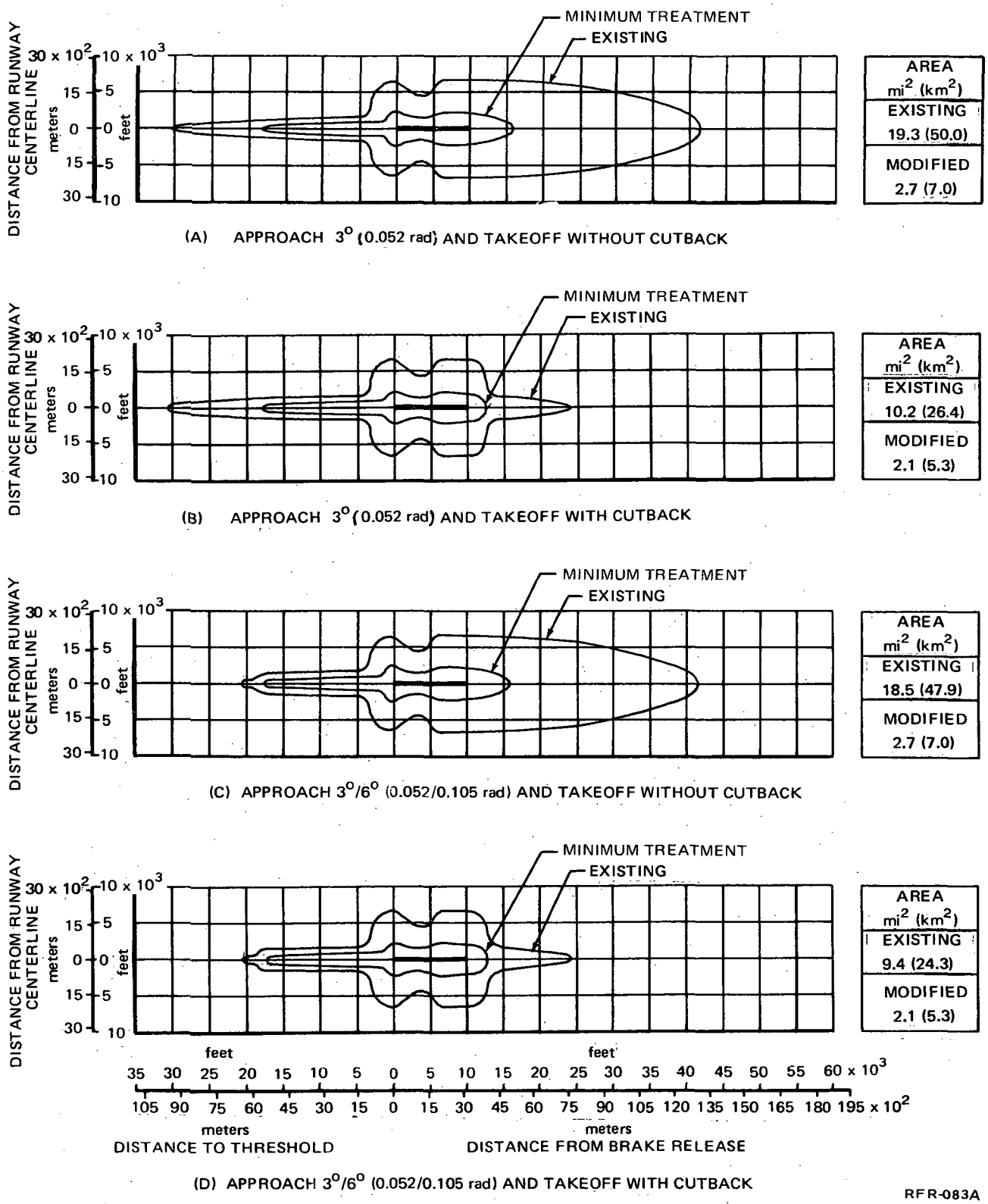

FIGURE 60. 90-EPNdB NOISE CONTOURS FOR EXISTING AND MODIFIED DC-9-32 AIRCRAFT (MINIMUM TREATMENT) FOR TYPICAL MISSION OPERATION

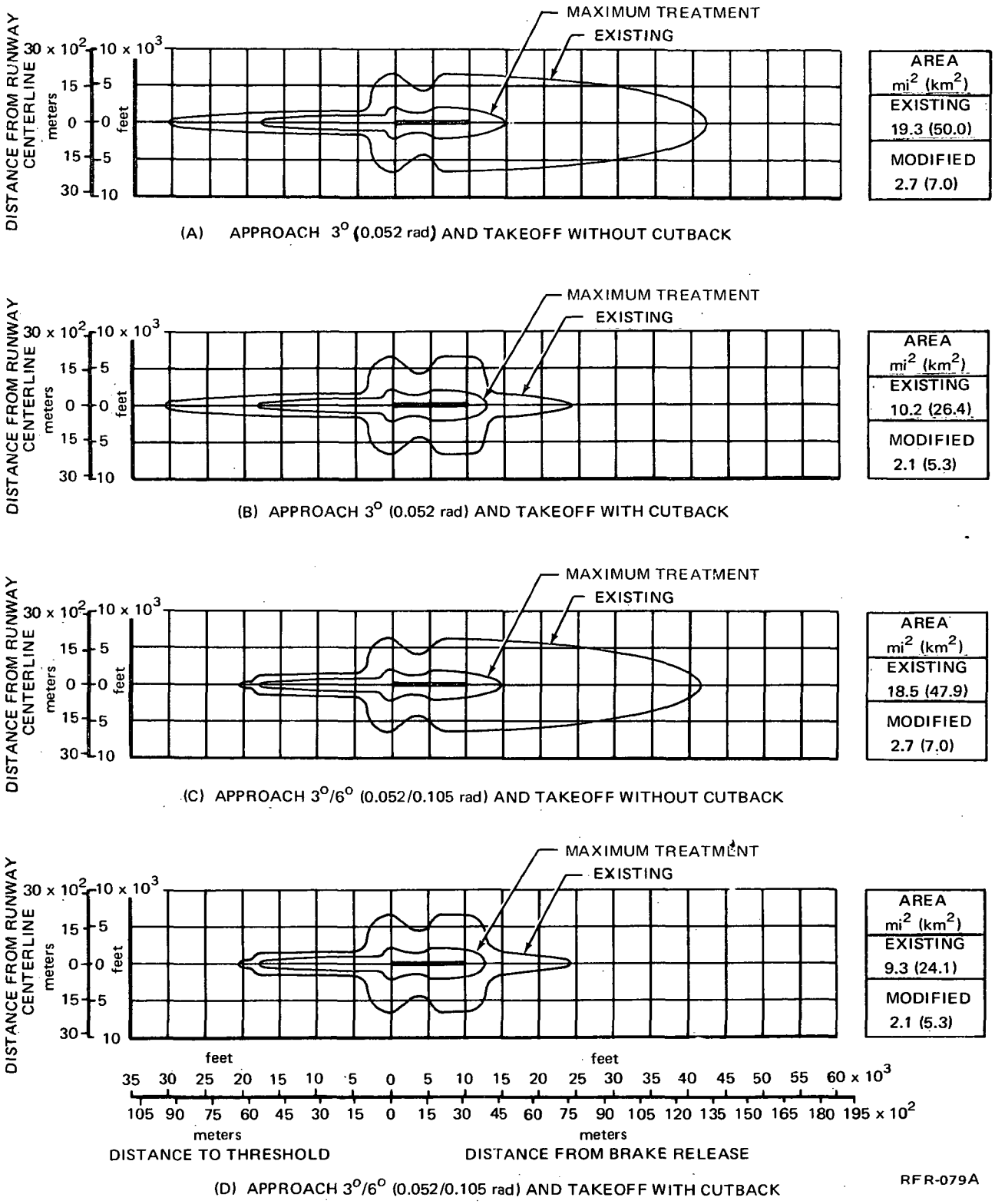

FIGURE 61. 90-EPNdB NOISE CONTOURS FOR EXISTING AND MODIFIED DC-9-32 AIRCRAFT (MAXIMUM TREATMENT) FOR TYPICAL MISSION OPERATION

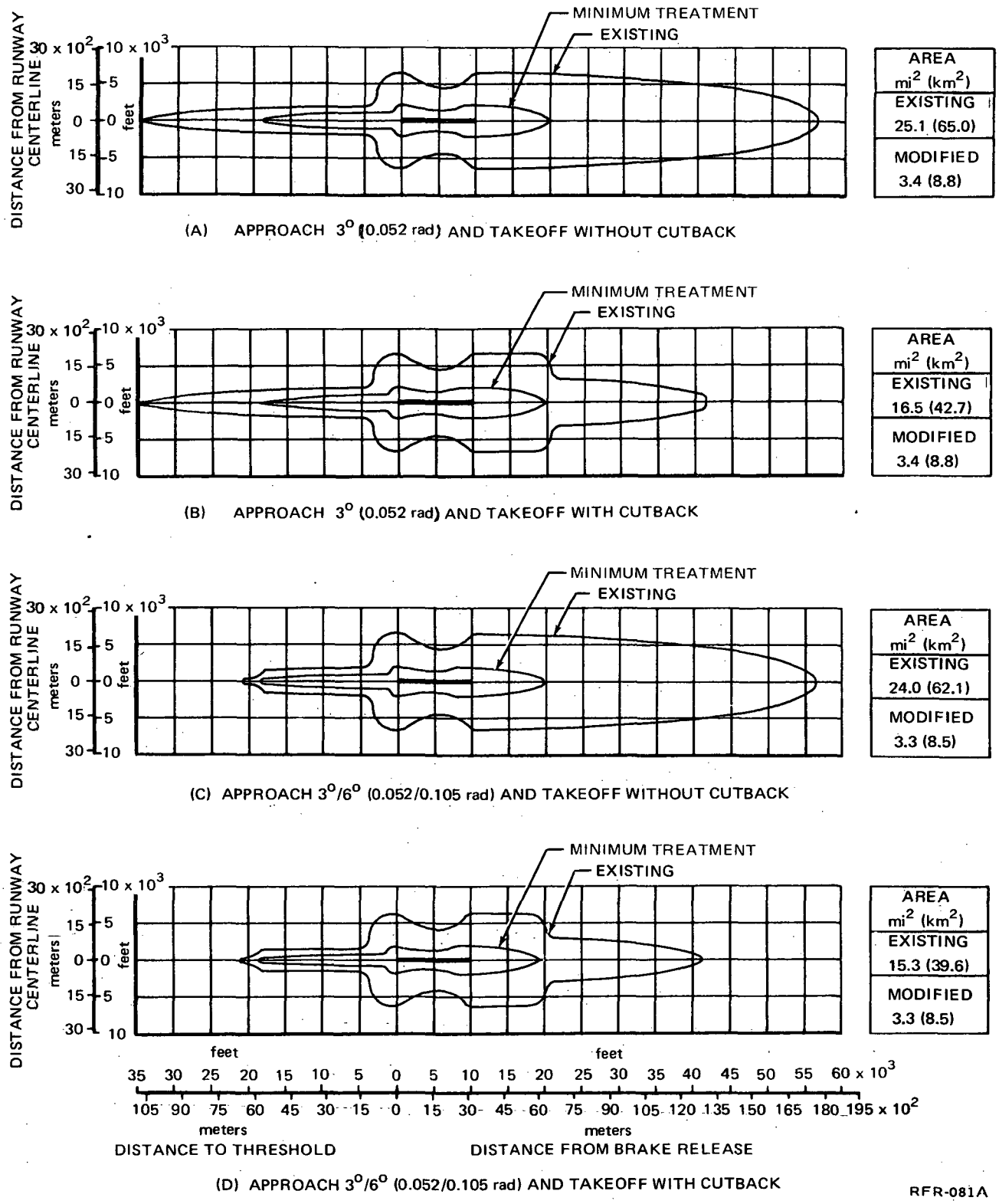

FIGURE 62. 90-EPNdB NOISE CONTOURS FOR EXISTING AND MODIFIED DC-9-32 AIRCRAFT (MINIMUM TREATMENT) FOR FAR PART 36 OPERATION

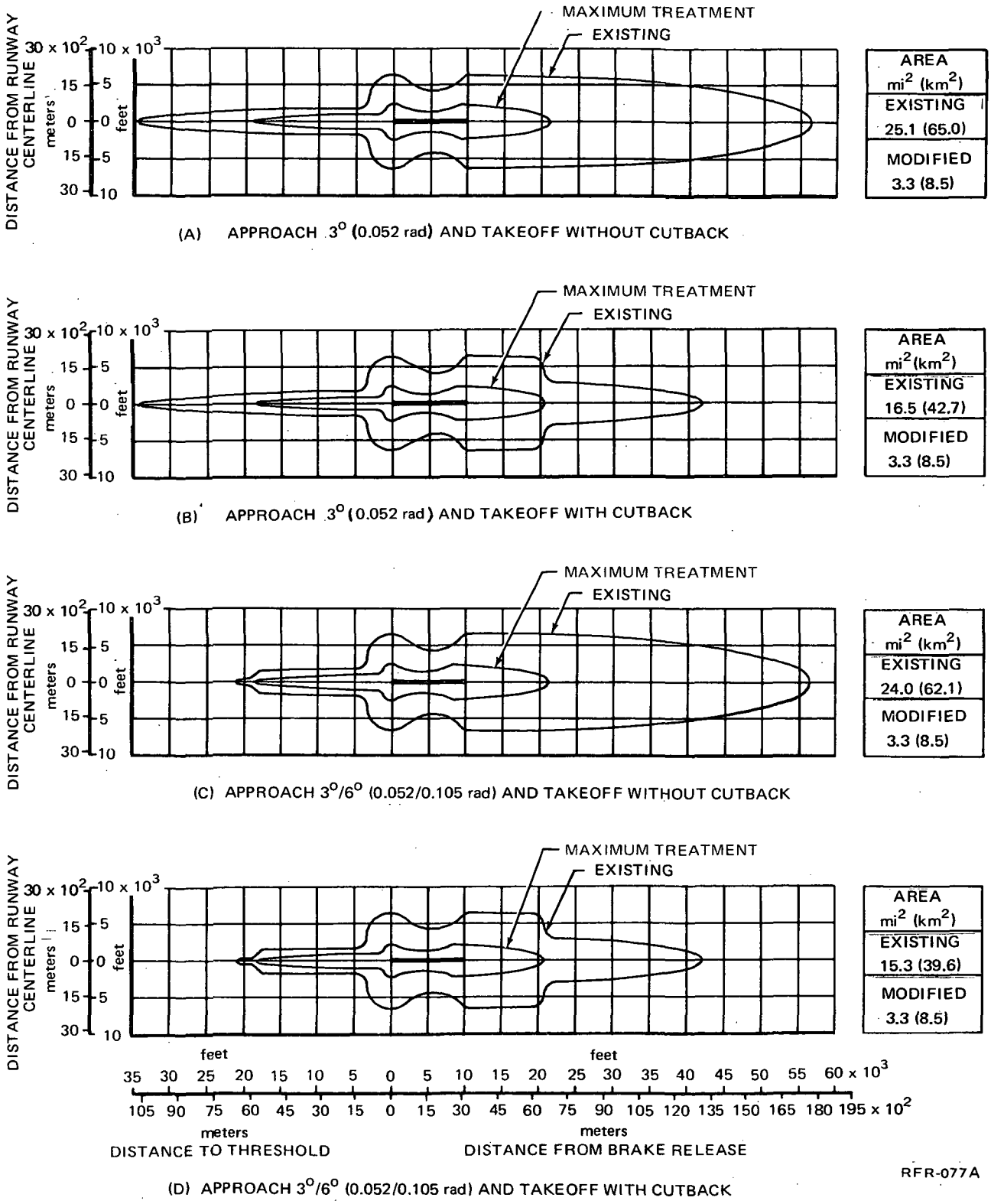

FIGURE 63. 90-EPNdB NOISE CONTOURS FOR EXISTING AND MODIFIED DC-9-32 AIRCRAFT (MAXIMUM TREATMENT) FOR FAR PART 36 OPERATION

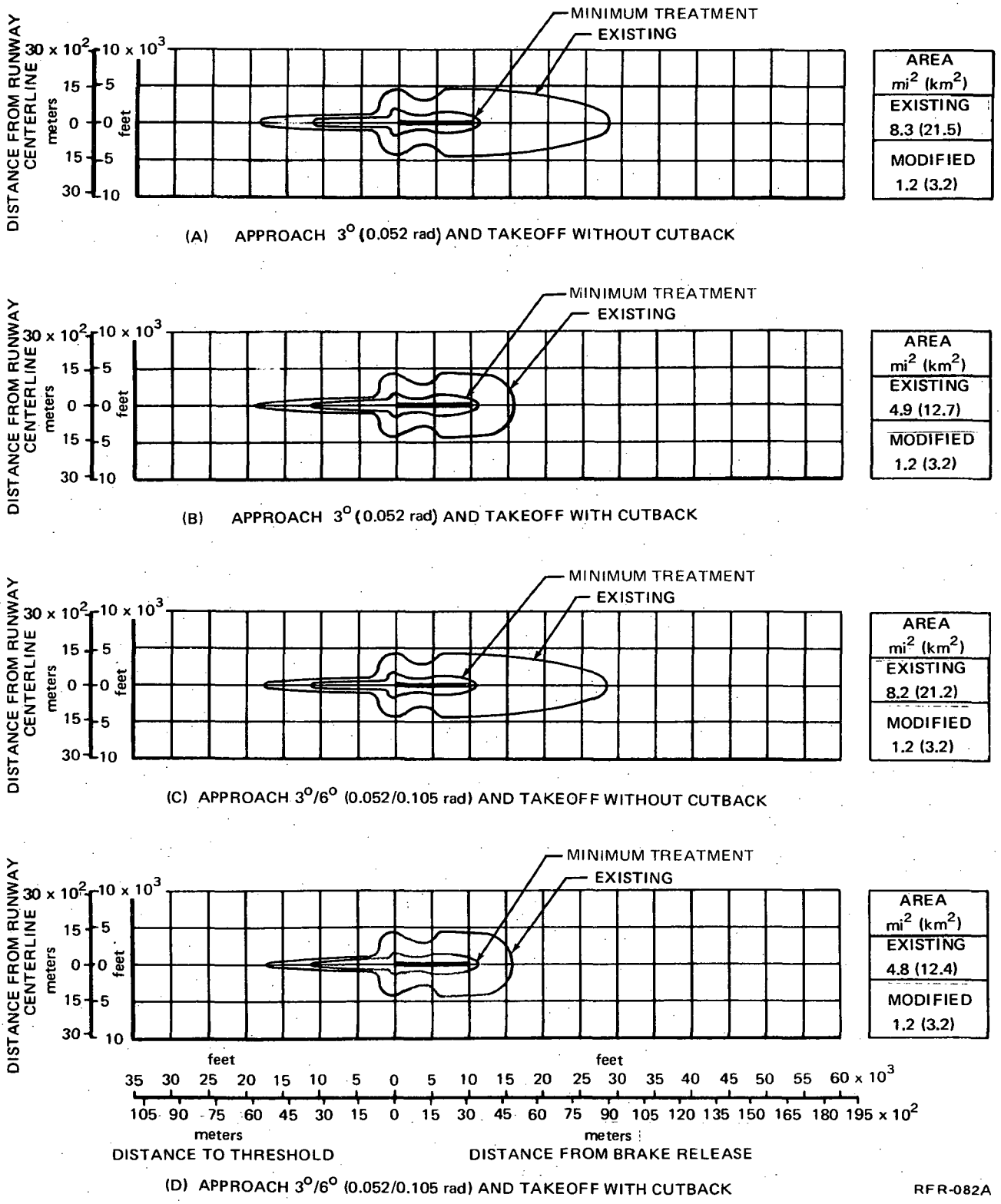

FIGURE 64. 95-EPNdB NOISE CONTOURS FOR EXISTING AND MODIFIED DC-9-32 AIRCRAFT (MINIMUM TREATMENT) FOR TYPICAL MISSION OPERATION

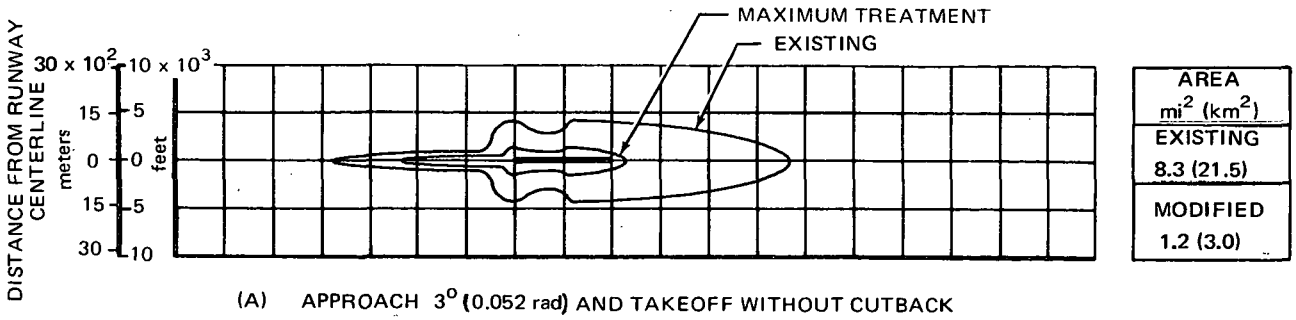

(A) APPROACH 3° (0.052 rad) AND TAKEOFF WITHOUT CUTBACK

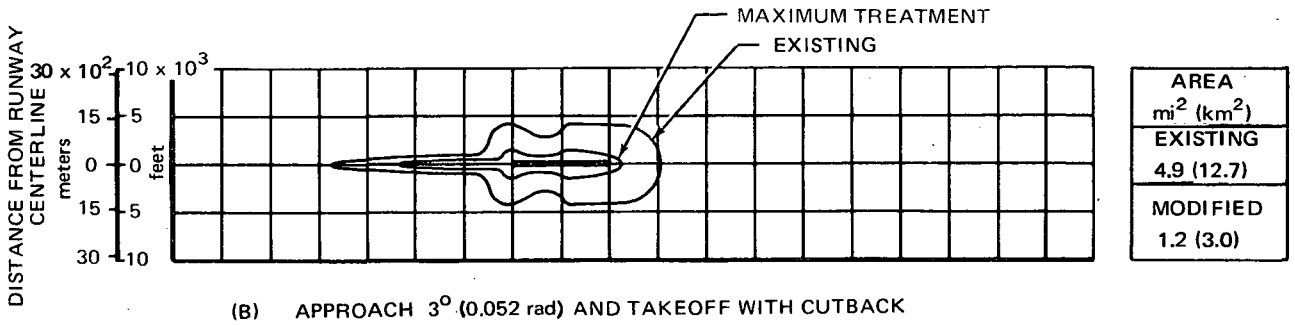

(B) APPROACH 3° (0.052 rad) AND TAKEOFF WITH CUTBACK

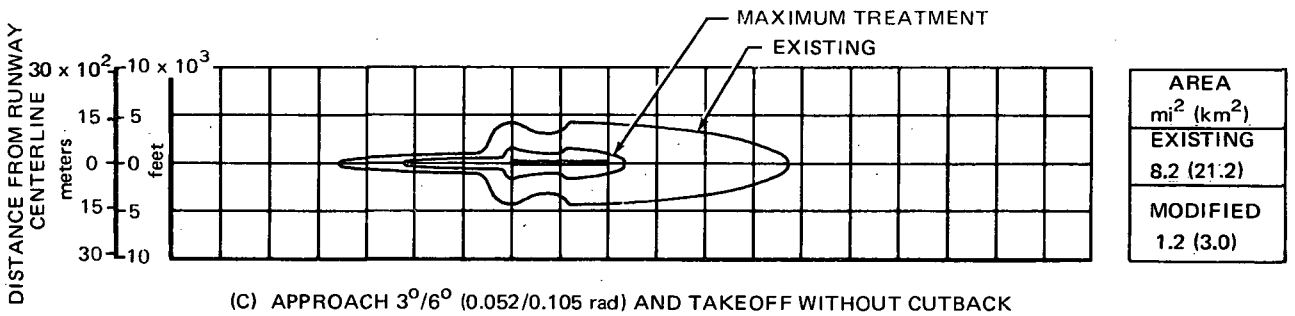

(C) APPROACH 3°/6° (0.052/0.105 rad) AND TAKEOFF WITHOUT CUTBACK

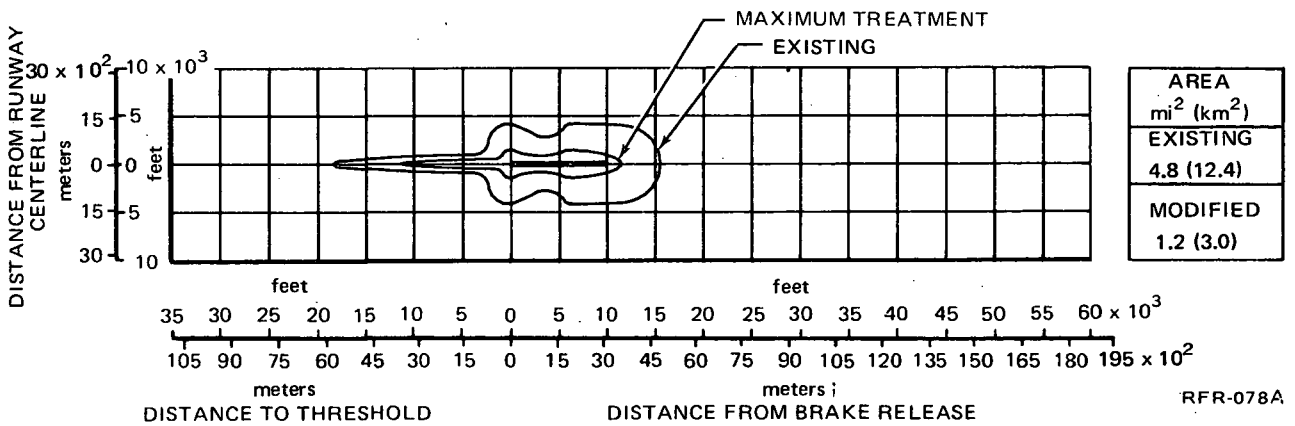

(D) APPROACH 3°/6° (0.052/0.105 rad) AND TAKEOFF WITH CUTBACK

FIGURE 65. 95-EPNdB NOISE CONTOURS FOR EXISTING AND MODIFIED DC-9-32 AIRCRAFT (MAXIMUM TREATMENT) FOR TYPICAL MISSION OPERATION

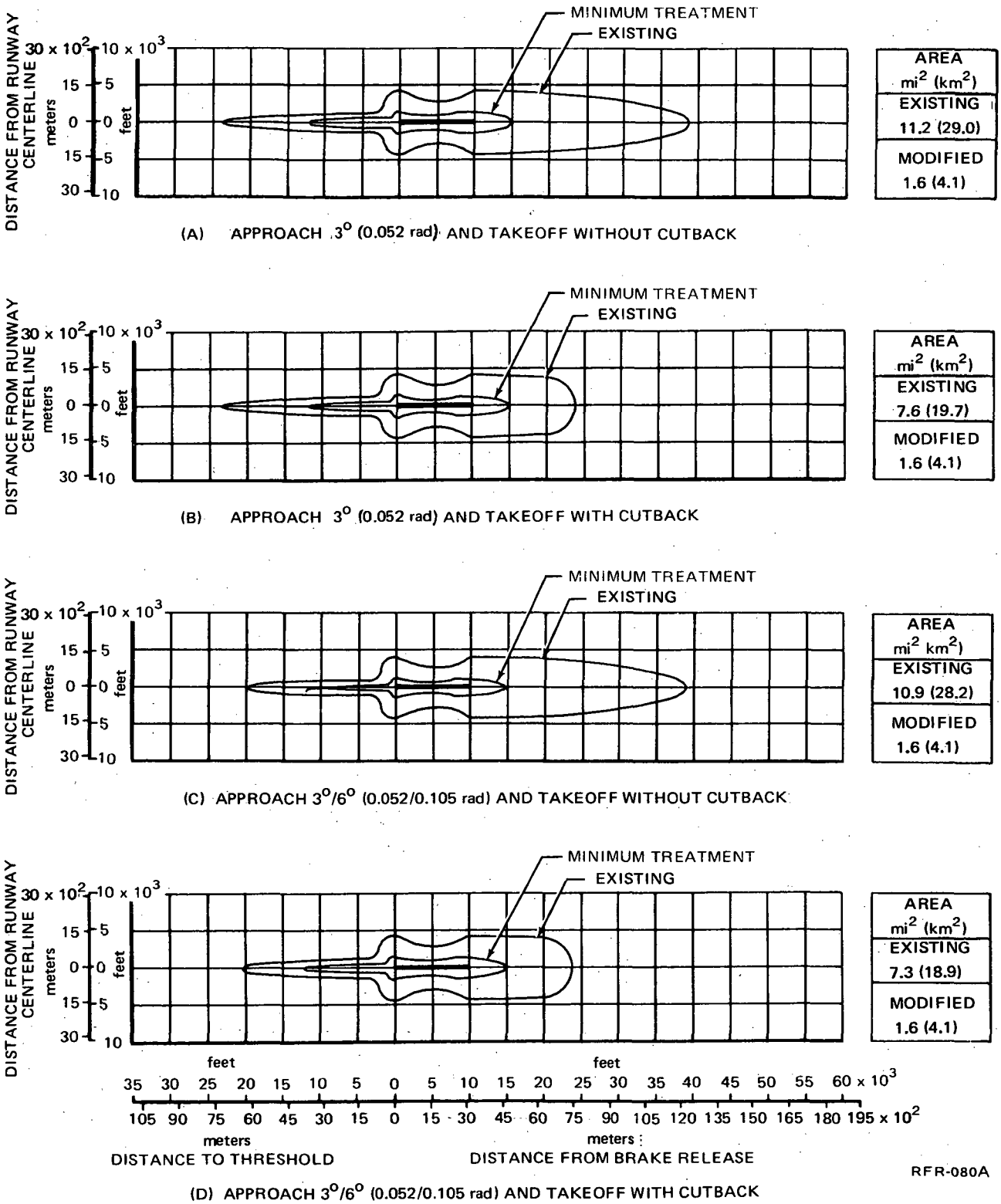

FIGURE 66. 95-EPNdB NOISE CONTOURS FOR EXISTING AND MODIFIED DC-9-32 AIRCRAFT (MINIMUM TREATMENT) FOR FAR PART 36 OPERATION

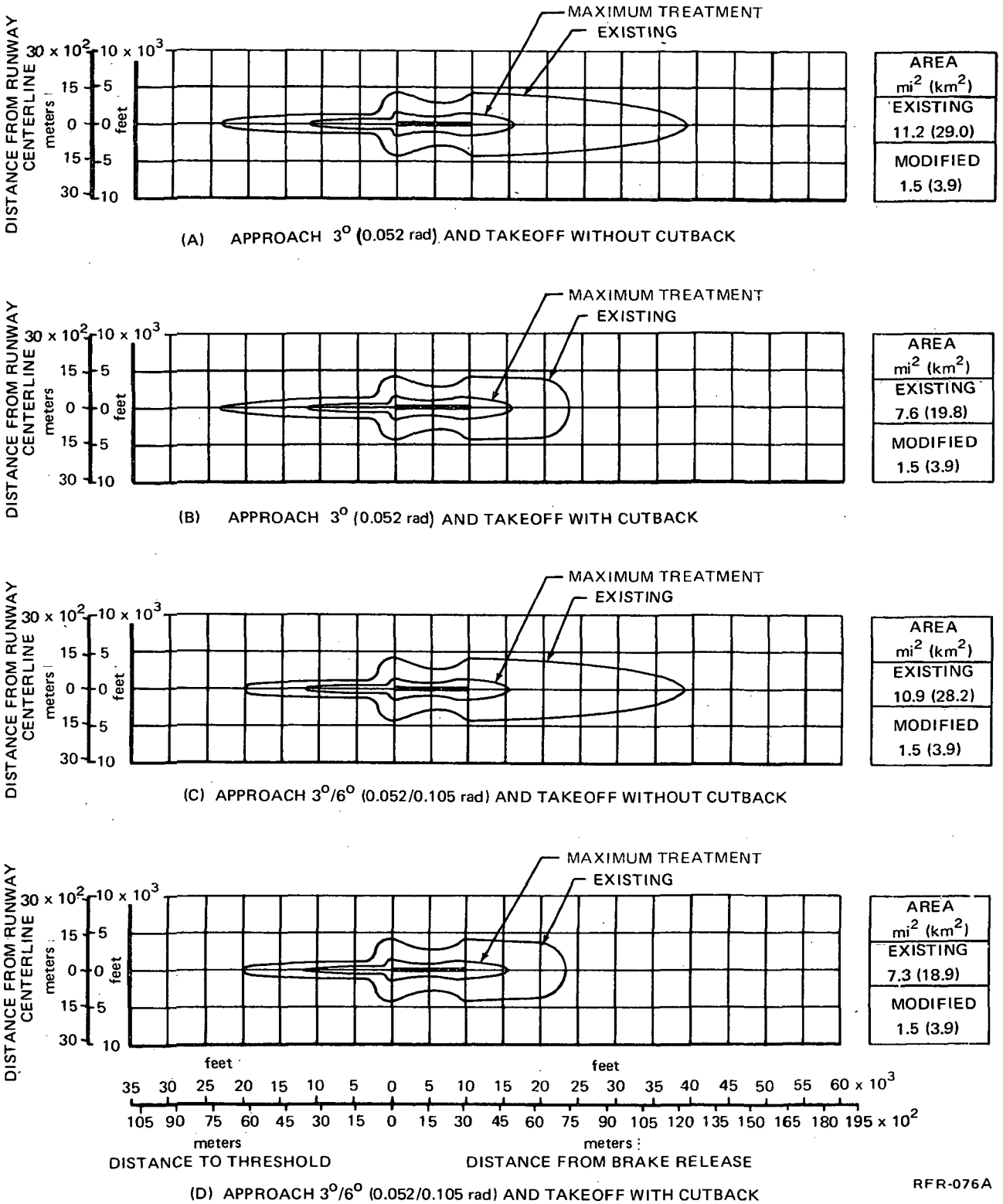

FIGURE 67. 95-EPNdB NOISE CONTOURS FOR EXISTING AND MODIFIED DC-9-32 AIRCRAFT (MAXIMUM TREATMENT) FOR FAR PART 36 OPERATION

MODEL TESTS

During the course of development of a new engine/nacelle installation, or a modification to an existing installation, much reliance is made on past experience and analytical analyses. However, some areas are not completely amenable to analytical analysis and require wind tunnel testing to determine design acceptability. In the case of installing refan nacelles on the DC-9 these areas were the high speed nacelle/fuselage interference drag and low speed deep stall characteristics.

The nacelle installation used on the DC-9 was developed with major consideration given to the effects of: (1) cruise drag, (2) deep stall recovery, (3) minimum control speeds, and (4) nacelle/pylon accessibility. The present installation is essentially interference-drag free, that is, there is little or no excess drag due to sonic velocities (wave drag) or excess adverse pressure gradients (pressure drag). The installed nacelle and pylon drag, therefore, consists almost entirely of basic skin friction and form drag.

For economic reasons it is desirable to install the larger diameter refan nacelle on the existing pylon, however, this method would increase the span of the nacelle/pylon combination, thus creating a potential low speed deep stall problem. With aft fuselage mounted nacelles and T-tails, there exists what is called a deep stall region where the wake from the wing, nacelles and pylons can blanket the horizontal tail and reduce its effectiveness and therefore reduce nose down pitch control. This phenomenon is illustrated in figure 68. While this happens well beyond the stall, and outside the normal operating envelope, it has been the position of the Douglas Company to provide positive aerodynamic recovery and not to rely on mechanical devices to prevent deep stall entry.

With the increased nacelle diameter associated with the refan engine ($\approx$22 percent), there was a concern that the larger nacelle on the existing pylon span would further reduce the tail effectiveness and decrease or negate the existing recovery margin. If there is a significant decrease in recovery margin an increase in horizontal tail area would be required. In addition, the increased thrust moment arm would tend to raise minimum control speeds. A solution for reducing the span would be to position the nacelle closer to the fuselage using a pylon of shorter span. The 292 mm (11.5 in.) increase in nacelle diameter could be offset by a shorter span pylon, thereby keeping the outer nacelle line the same as the existing nacelle, however, some reduction in pylon accessibility would result. The channel width would be reduced from 425 mm to 132 mm (16.7 in. to 5.2 in.). Figure 69 shows the change in channel area distribution with the snugged-in nacelle.

With the refan installation there was a concern for the possibility of interference drag at cruise speeds because of an increase in the degree of channel convergence and divergence. The higher degree of channel divergence could lead to increased adverse pressure gradients in the channel area. These increased gradients would increase the nacelle/fuselage/pylon boundary layer thickness with consequent drag increase due to momentum loss and possibly

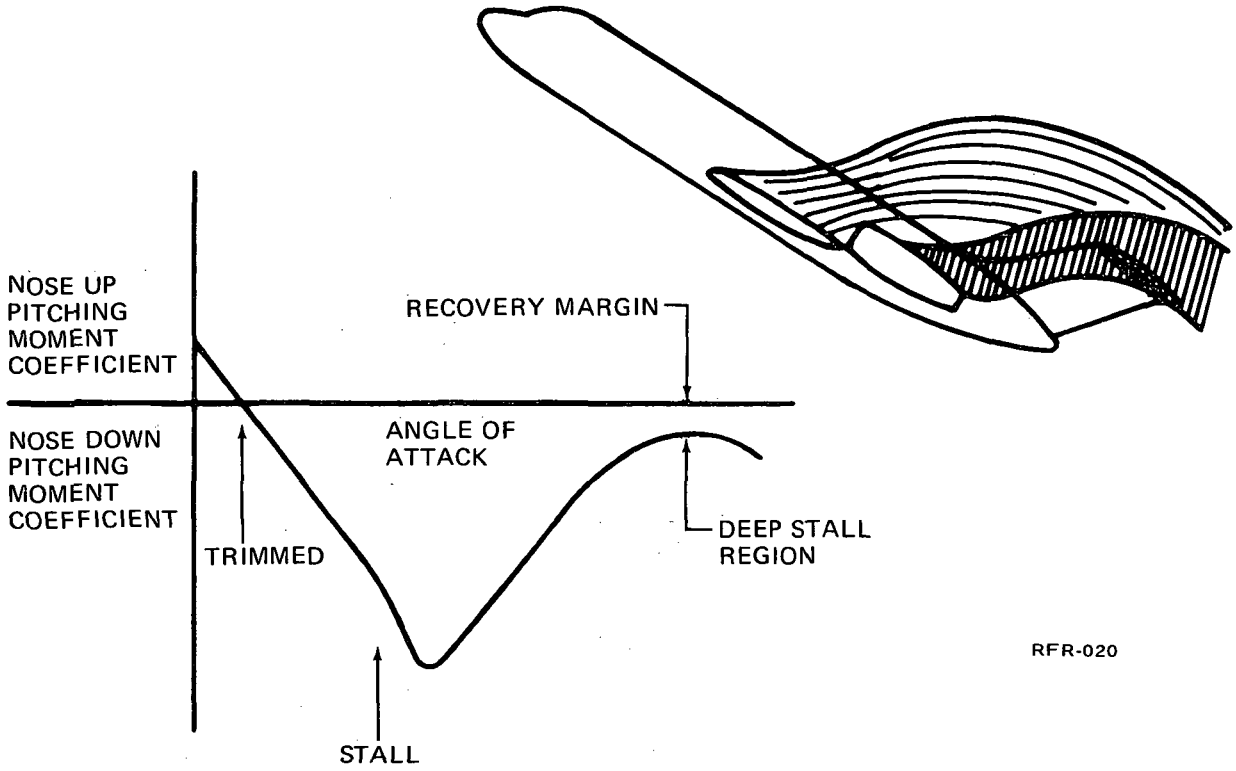

FIGURE 68. DEEP STALL RECOVERY

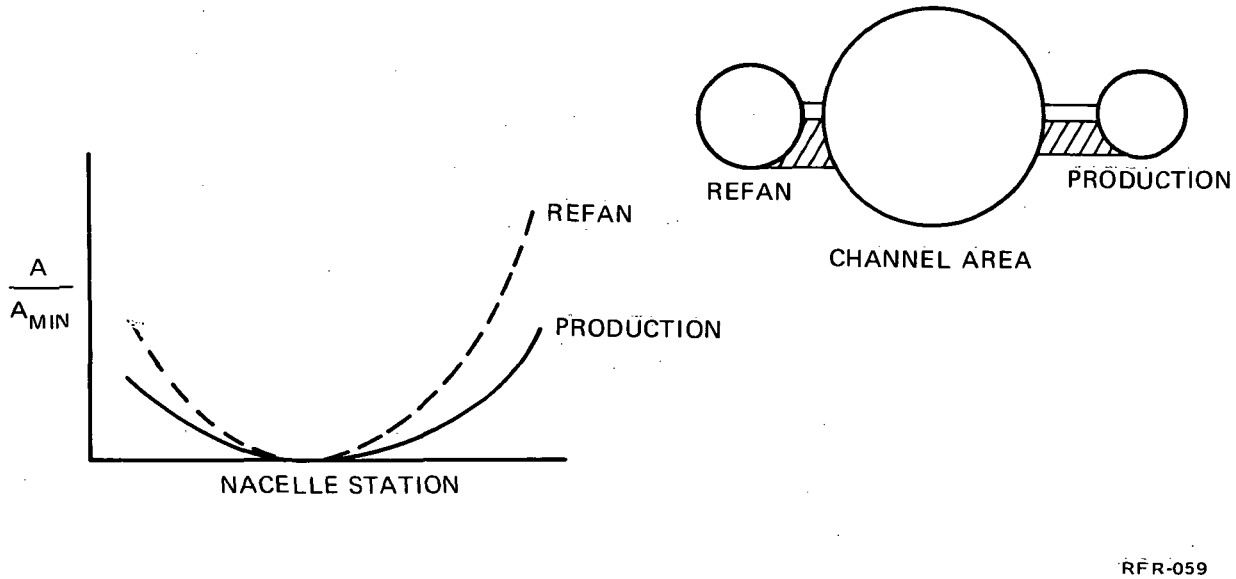

FIGURE 69. CHANNEL AREA DISTRIBUTION

boundary layer separation. A second source of interference drag may occur if the velocities in the channel become supersonic. This can result in shock wave drag and possible shock-induced boundary layer separation.

The effects of the larger nacelle and nacelle lateral spacing on aircraft cruise drag were examined in the NASA Ames 11-foot high speed wind tunnel during January 1973. The results from the high speed test and pylon accessibility trade studies were incorporated in the selection of pylon spacings tested in the low speed test at the NASA Ames 12-foot wind tunnel during February 1973. During the low speed test the effects of the refan engine installation on deep stall recovery characteristics were investigated.

The refan nacelle geometry simulated for the high speed and low speed tests has the following characteristics:

1. The inlet length from the engine face to the highlight is 1.093 m (43.0 in.).

2. The maximum nacelle diameter is 1.625 m (64.0 in.).

3. The nozzle L/H is 4.30.

4. The overall nacelle length is 6.44 m (253.0 in.).

5. The nacelle is of long duct design very similar in overall appearance to the existing nacelle.

6. The stang fairings required to enclose the thrust reverser operating linkage are simulated.

7. The afterbody boattail angle is .227 radians (13.0 degrees).

The installation of the refan nacelle compared to the existing nacelle is shown in figure 70. The refan inlet leading edge (highlight) is located 762 mm (30 in.) further forward and the refan nozzle is located 546 mm (21.5 in.) further aft.

The following two sections present a summary of the high speed and low speed wind tunnel tests. References 1 and 2 provide complete test results.

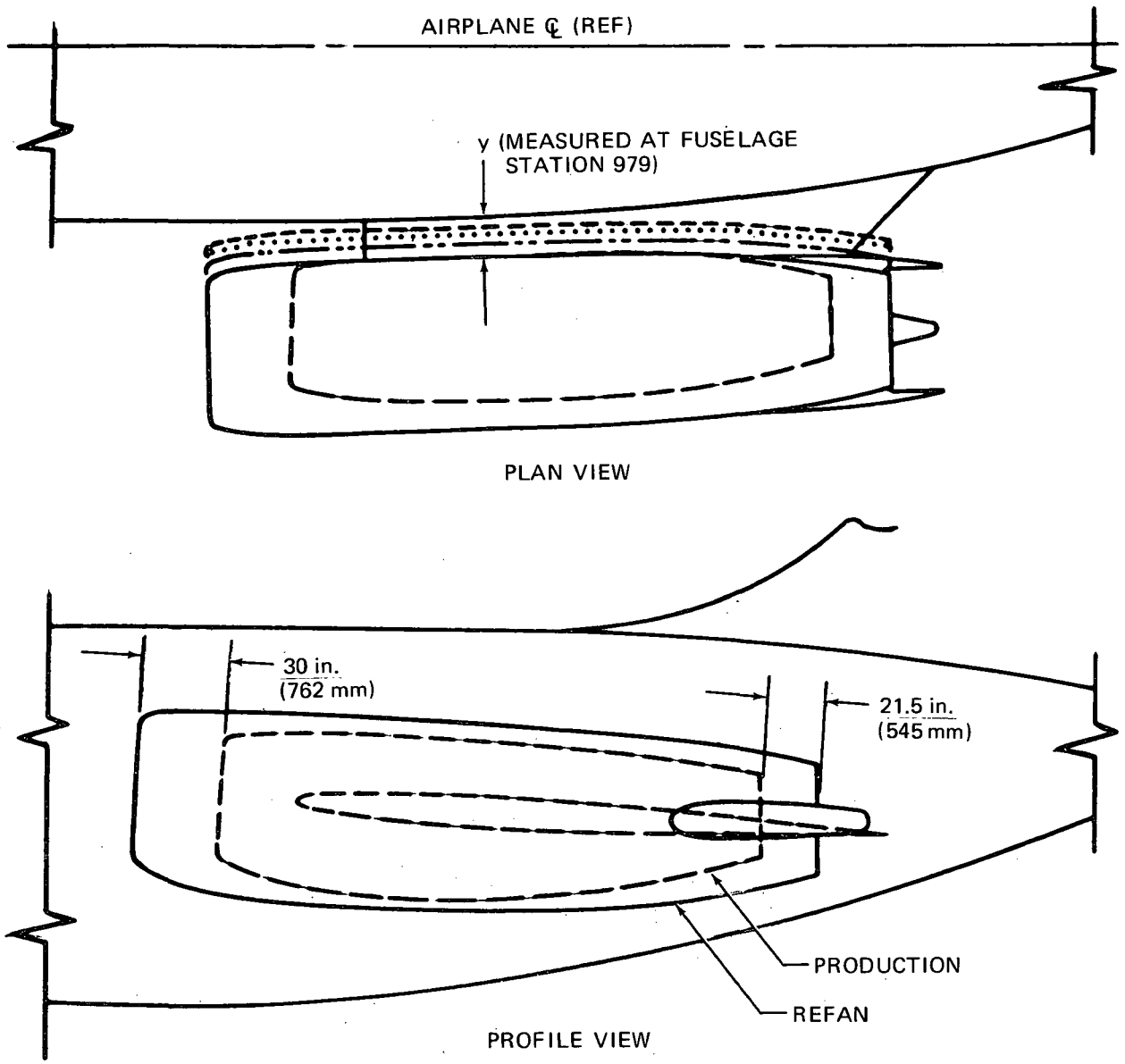

	NACELLE	PYLON SPAN y, inches (mm)
— — — —	EXISTING	16.7 (425)
———	REFAN	16.7 (425)
—··—	REFAN	11.0 (280)
- - - - - -	REFAN	5.2 (132)
·····	REFAN	7.5 (191)

RFR-060

FIGURE 70. NACELL NSTALLATION COMPARISON

High Speed Test

The model used in the high speed wind tunnel investigation was a 6 percent scale representation of the DC-9-30 and is designated LB-151M. The model was treated with the horizontal and vertical tail removed. The fuselage, wing and existing nacelles and pylons have been previously tested in the Ames Facility. The refan nacelles and pylons were fabricated for this test program. Figure 70 shows the nacelle installation comparison.

The high speed model provided for three nacelle/pylon spacings are described below:

1. y = 425 mm (16.7 in.) - existing pylon with the inside refan nacelle line coincident with the existing nacelle line.

2. y = 132 mm (5.2 in.) - stub pylon with the outside refan nacelle line coincident with the existing nacelle line. The planform span of the refan nacelle and pylon is the same as the production installation.

3. y = 280 mm (11.0 in.) - intermediate spacing to account for the possibility that: (1) the 132 mm (5.2 in.) pylon causes an excessive drag penalty, or (2) due to accessibility constraints the 132 mm (5.3 in.) pylon is not feasible to build.

Figure 71 shows the incremental drag difference between the refan installation and the existing installation. Two pylon spans for the refan nacelle are shown: y = 425 mm (16.7 in.) and y = 132 mm (5.2 in.). The increment is shown as a function of Mach number for the lift coefficients of operational interest (0.25 - 0.4). It can be seen that for the lower Mach numbers where the aircraft is free of compressibility effects (M_0<0.7), the measured increment agrees well with the estimation, considering only the internal and external skin friction and form drag of the larger flow-through nacelle. For Mach numbers greater than 0.7 the increment is less than the estimate. This trend is apparent over the operational range of lift coefficients. At a typical cruise condition of M_0 = 0.78, C_L = 0.35 the drag effect amounts to approximately 2 percent of the airplane drag (ΔC_D = 0.0005). This compares closely to the calculated penalty (due only to increased external wetted area) for the full scale minimum treatment configuration at flight cruise conditions, which would say that the refan nacelle can be installed without paying a drag penalty due to the larger nacelle. The fact that figure 71 still shows a small penalty for the refan nacelle at this condition is due to the increased skin friction drag at the model Reynolds number and the incremental internal drag of the flow-through nacelle.

Figure 72 shows that there is little effect of pylon spacing on the drag increment. For M_0 = 0.78 the drag increment exists for all three pylon spacings, and is slightly greater for the 425 mm (16.7 in.) spacing (about one drag count, ΔC_D = 0.0001).

The fact that the drag reduction is Mach number dependent indicates that it must be a reduction in compressibility drag. Wing surface pressures were measured at two semi-span locations: (1) 17 percent b/2 (inboard of the

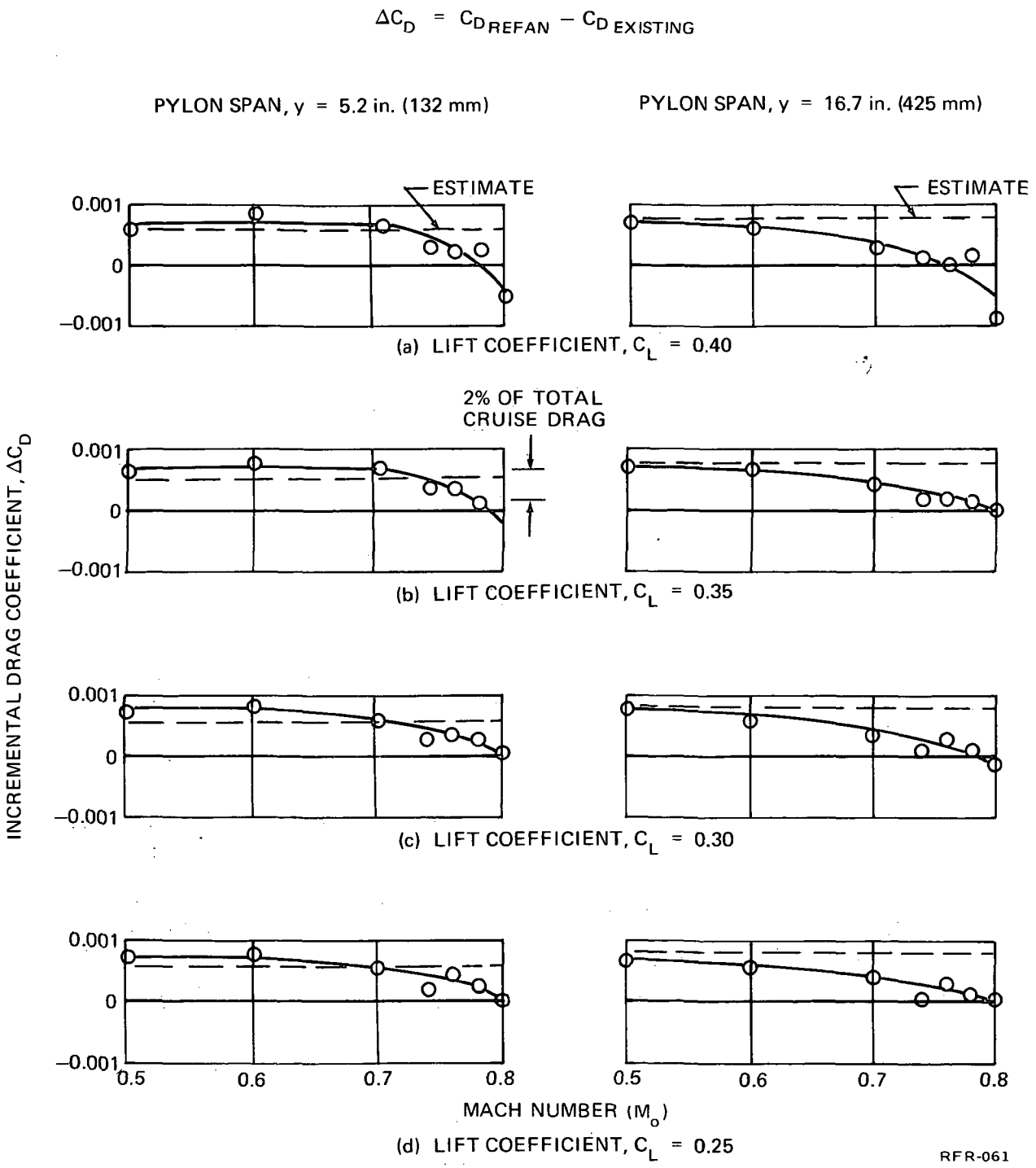

FIGURE 71. INCREMENTAL DRAG COEFFICIENT FOR REFAN NACELLE

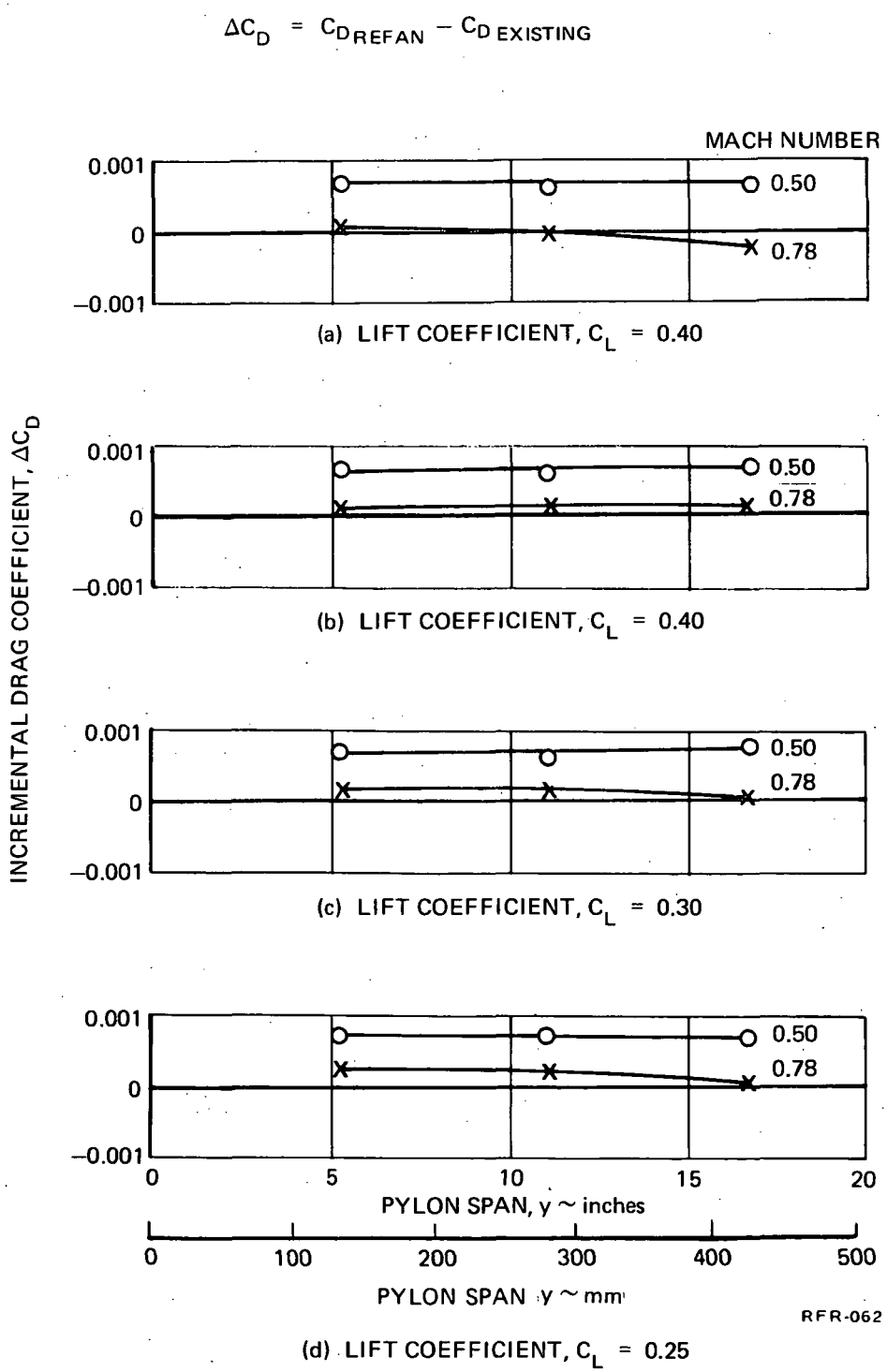

FIGURE 72. EFFECT OF PYLON SPAN ON INCREMENTAL DRAG COEFFICIENT FOR REFAN NACELLE

nacelle location), and (2) 28 percent b/2 (outboard of the nacelle location). Figure 73 shows the upper surface wing pressures as a function of Mach number for the various nacelle configurations tested. While only the typical cruise lift coefficient (C_L = 0.35) is shown, the same general trends exist at other lift coefficients. Figure 73 shows that at the lower Mach numbers (M_0 = 0.5 shown) there is a general suppression of the upper surface pressures (velocities) with the refan installation relative to the existing installation. As the Mach number increases beyond 0.7, this suppression lowers the peak velocities ahead of the shock wave and moves the shock forward, thereby reducing the strength of the shock wave and hence the wing compressibility drag. Note also from figure 73 that the influence of the entering stream tube is felt considerably outboard indicating that it influences the shock over a significant portion of the wing. Figure 74 shows how the inlet can influence the wing pressures. The stream tube of air entering the inlet must slow down as it approaches the inlet since the inlet Mach number is less than the free stream Mach number. This requires positive pressures on the entering stream tube for the refan nacelle is larger in diameter (22 percent) and the inlet is considerably longer relative to the existing nacelle which places the positive pressures closer to the wing where they have a larger influence. Note from figure 74 there is some influence of the basic nacelle, but much less for the refan nacelle. These results are also substantiated by results from a recent flight test program for another DC-9 acoustic nacelle installation. The inlet was longer and the program was conducted on a Series 10 aircraft which has a shorter fuselage. While the nacelle was no bigger in diameter than the existing nacelle the inlet was closer to the wing relative to the refan installation. A favorable interference effect with Mach number was measured and was very similar in both magnitude and characteristics to that measured with the refan installation.

The favorable interference would be expected to be larger for a Series 10 aircraft (shorter fuselage placing the inlet closer to the wing) and slightly less for a Series 40 aircraft (longer fuselage placing the inlet farther from the wing). In addition, since the tested configuration was based on a ringed inlet, if a longer inlet is selected, the improvement will probably be slightly larger.

Figure 75 shows the pressure distributions in the lower nacelle/pylon/fuselage channel for Mach numbers of 0.7 and 0.78. The nacelle and fuselage pressure peaks at about Station 900 are due to the spillage around the cowling. The cowling is designed to spill flow with some supervelocities. While the peak velocities tend to be aggravated by the closer spacing, they are just sonic at 0.78 Mach number for the 132 mm (5.2 in.) spacing and are subsonic for both the 280 mm (11.0 in.) and 425 mm (16.7 in.) spacings.

The peak pressures on the inlet cowl are far enough forward that they do not add to the peak pressure on the pylon.

Also, note that the channel recompressions are all about the same and give no indication of any separation. The recompressions on the aft fuselage were essentially the same for all configurations tested. While figure 75 is shown only for C_L = 0.35, the pressure distributions for other lift coefficients of interest show the same general trends.

SYM	CONFIGURATION
○	NACELLES AND PYLONS OFF
△	EXISTING NACELLE
□	11.0 in. (280 mm) REFAN NACELLE
×	5.2 in. (132 mm) REFAN NACELLE

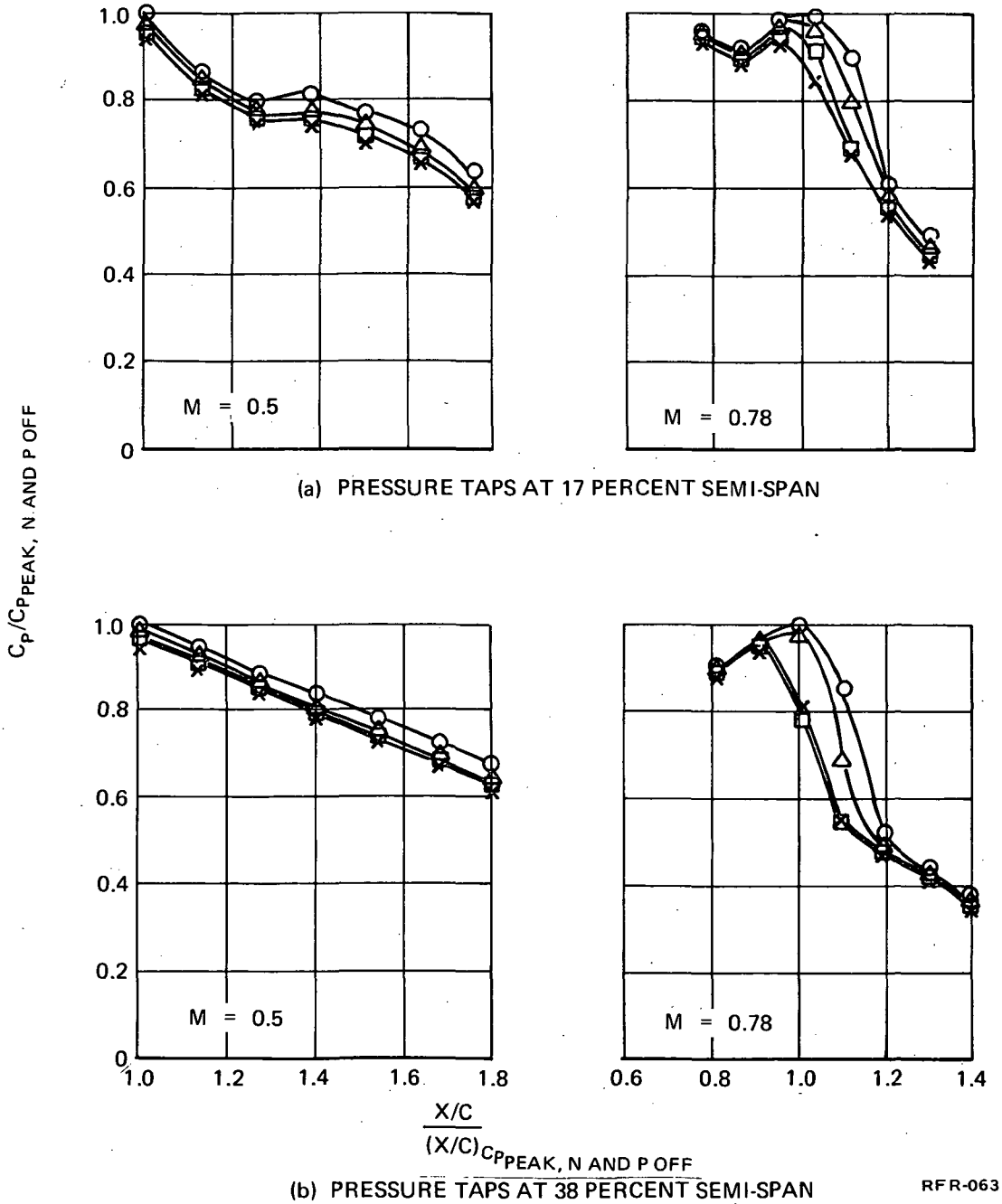

(a) PRESSURE TAPS AT 17 PERCENT SEMI-SPAN

(b) PRESSURE TAPS AT 38 PERCENT SEMI-SPAN

RFR-063

NOTE: SUBSCRIPT "PEAK, N AND P OFF" REFERS TO PEAK PRESSURE COEFFICIENT WITH NACELLES AND PYLONS OFF, LIFT COEFFICIENT, C_L = 0.35

FIGURE 73. WING UPPER SURFACE PRESSURE DISTRIBUTIONS

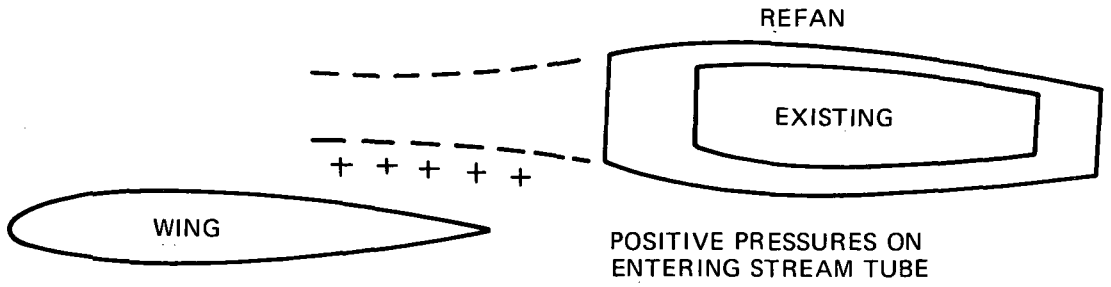

FIGURE 74. LOCATION OF INLET ENTERING STREAM TUBE RELATIVE TO WING

From the results of a high speed wind tunnel test conducted to assess the drag increments for installing a larger refan engine nacelle installation on the DC-9-30, the following conclusions are drawn:

1. At the lower Mach number ($M_0 < 0.7$), the drag increment of the refan installation relative to the production nacelle and pylon is equal to that calculated by considering only wetted area and form factor changes.

2. At typical cruise Mach number ($M_0 = 0.78$) there exists a favorable interference drag relative to the calculated difference between the refan and production installations. This amounts to about 2 percent of total airplane drag for the Series 30. Applying this favorable effect to the full scale minimum treatment installation, where the skin friction penalty due to the larger nacelle amounts to about 2 percent of total airplane drag, would result in the refan nacelle being installed without any drag penalty.

3. This favorable effect occurs because the positive pressures on the stream tube entering the engine suppress the wing upper surface velocities, thereby, moving the wing shock forward with subsequent reduction in wing compressibility drag (the stream tube is larger and located further forward with the refan installation). This effect would be expected to be larger for a Series 10 airplane (inlet located closer to wing) and slightly less for a Series 40 (inlet located farther aft of wing).

4. There is little effect of pylon span on the incremental drag of the refan installation. The incremental drags for the 132 mm (5.2 in.) and 280 mm (11.0 in.) span pylons are about the same while the 425 mm (16.7 in.) pylon is about one drag count ($\Delta C_D = 0.0001$) less at 0.78 Mach number.

5. The nacelle/pylon/fuselage channel does not exhibit any excess supervelocities or lack of recompression. The refan inlet is long enough to prevent superposition of the cowl- and pylon-peak pressure coefficients.

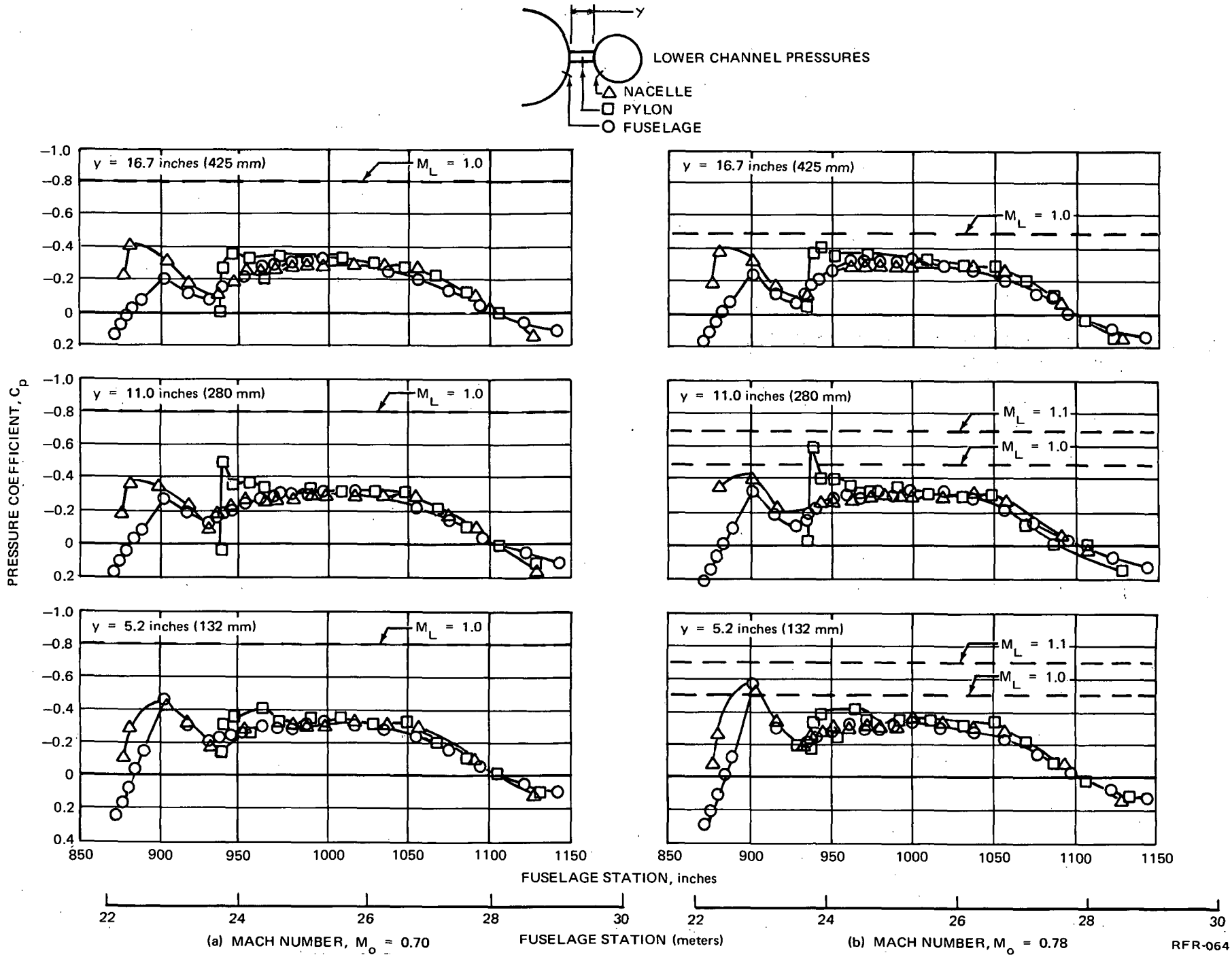

FIGURE 75. NACELLE/PYLON/FUSELAGE LOWER-CHANNEL PRESSURE DISTRIBUTIONS, LIFT COEFFICIENT, C_L = 0.35

Low Speed Test

The model used in this wind tunnel investigation was a 9 percent scale representation of the DC-9-30 and is designated LB-155U. The model was tested in the tail-on and tail-off configurations. The fuselage, wing, existing empennage, existing nacelles, and pylons have been previously tested in the Ames Facility. The refan nacelles and pylons and a larger horizontal tail were fabricated specifically for this test program.

During the course of the high speed testing it was learned that cruise drag considerations would permit close-in spacings. In addition, pylon accessibility studies indicated that a spacing in the order of 191 mm (7.5 in.) was the minimum that would be practical. Therefore, for the low speed test the 425 mm (16.7 in.) pylon was dropped and replaced with a 191 mm (7.5 in.) pylon.

In order to determine if a larger horizontal tail would be required due to any decrease in tail effectiveness, two horizontal tail configurations were tested.

Figure 76 shows the two horizontal tail configurations, the existing tail and an enlarged tail, which were tested during the low speed wind tunnel test. The enlarged tail has an increased span of 508 mm (20 in.) and an increased area of 4.13 m^2 (44.4 ft^2) relative to the basic DC-9-30 horizontal tail. The increased span is achieved by splitting the existing horizontal tail at the centerline and adding a 508 mm (20 in.) span center-section which extends the leading and trailing edge lines inboard. This increases the root chord from 3.371 m (132.7 in.) to 3.47 m (136.6 in.) and retains the tip chord of 1.189 m (46.8 in.). The quarter chord of the MAC for the modified tail is positioned at the same fuselage station as that of the existing tail. The new center-section does not have elevators, so the elevator geometry is identical to the existing tail except for the spanwise location.

The wind tunnel data in figure 77 show pitching moment coefficient (about the wing MAC quarter chord) versus angle-of-attack, and compare the existing DC-9-30 to the DC-9-30 with the refan nacelle and 191 mm (7.5 in.) pylon. These data are for a 0.873 rad (50 deg) flaps/slats extended configuration with the stabilizer set at -0.087 rad (-5 deg), and with the elevators at both 0 and +0.262 rad (+15 deg). The data, as shown, are not used directly to analyze deep stall recovery capability, but do illustrate the typical nature of the DC-9 longitudinal characteristics and the effects of the refan engine on those characteristics.

As can be seen in figure 77, the aircraft exhibits strong positive stability, increasing nose down C_m as α_F increases, throughout the angle-of-attack range for normal flight. The model displayed a good pitch-down at the stall. Beyond the stall, the data show a reversal in pitching characteristics which reflect instability. This instability is caused by the tail entering first the wing wake and later the nacelle/pylon wake. At approximately 0.79 rad (45 deg) angle-of-attack, positive stability is regained as the tail comes out of the bottom of the wake. The deep stall recovery margin is

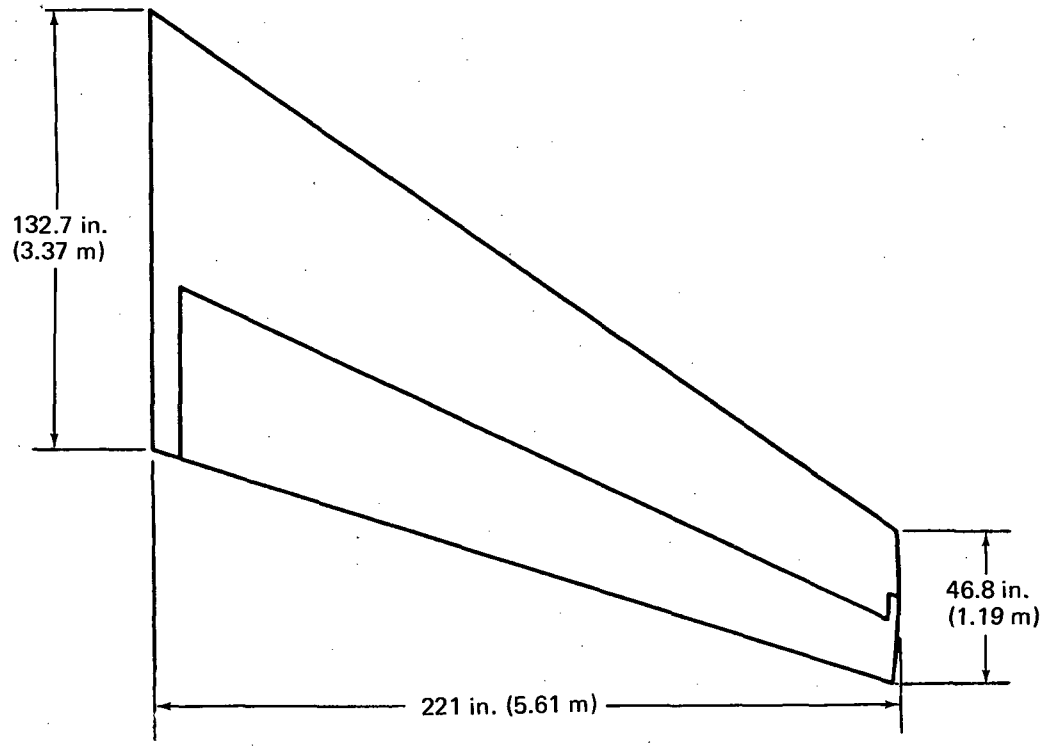

(a) BASIC HORIZONTAL TAIL
AREA = 275.5 sq ft (25.59 sq m)

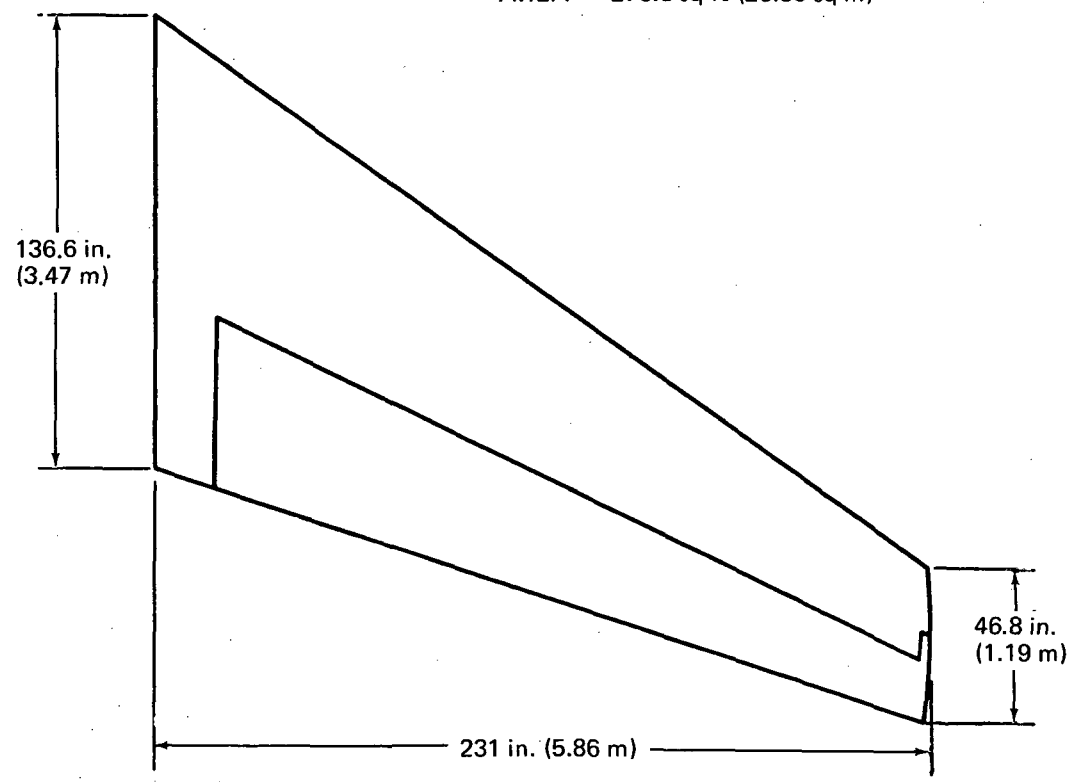

(b) LARGE HORIZONTAL TAIL
AREA = 294.1 sq ft (27.32 sq m)

RFR-052

FIGURE 76. HORIZONTAL TAIL GEOMETRY

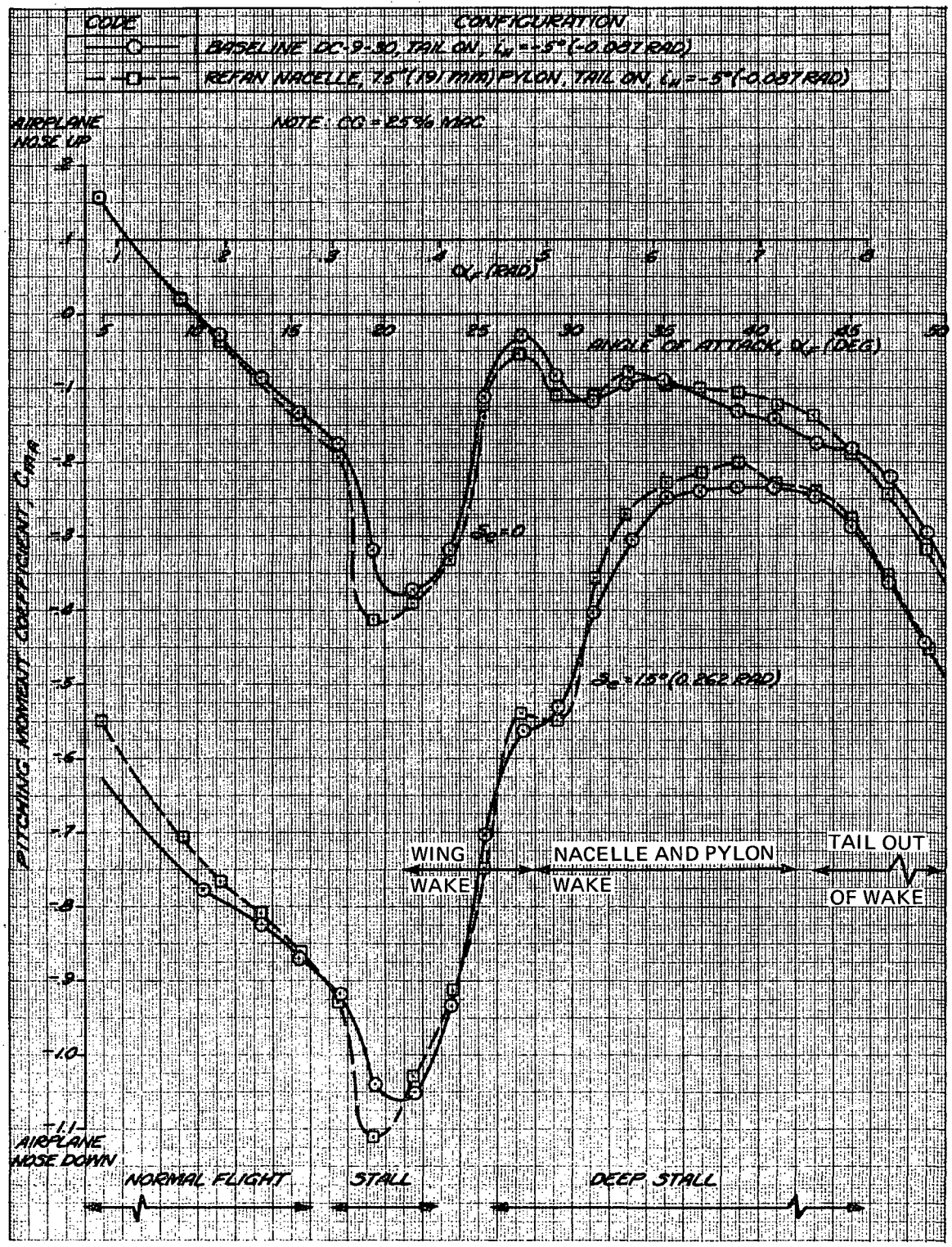

RFR-150

FIGURE 77. EFFECTS OF NASA REFAN ENGINES ON PITCHING MOMENT COEFFICIENT, FLAP POSITION = 50 deg (0.873 rad), SLATS EXTENDED

the minimum nose down pitching moment available with full down elevator deflection, occurring at approximately 0.68 rad (39 deg) angle-of-attack for the configuration and conditions shown in figure 77. The reduction in available nose down pitch control due to the refan engine can be seen by comparing the data for the two configurations with full-down elevator. The data for other configurations tested vary in detail, but the trends are basically the same as those of figure 77.

In order to evaluate deep stall recovery capability, the wind tunnel pitching moment data were adjusted to represent the aircraft trimmed at 1.3 V_S and the lift and drag data were used to correct the moment data center to the aft center of gravity limit for the DC-9-30 (34.7% MAC).

The summary of the deep stall recovery margins plotted as a function of flap deflection is presented for all configurations tested in figure 78. Examination of this figure shows the following:

1. Recovery margins are reduced somewhat with reduced flap setting. Slat position has a major effect on the recovery margins, showing significant gains in nose down pitching moment with slat retraction.

2. The refan installation causes a small reduction in deep stall recovery margin relative to the existing installation.

3. The deep stall recovery margins for the refan installation are essentially independent of pylon span.

4. The larger horizontal tail significantly increased the deep stall recovery margin.

The DC-9-30 elevator hinge moments at full down elevator become very large at high angles-of-attack for all configurations. Previous wind tunnel data, which also included testing of the elevator tab effectiveness, revealed that the elevator would tend to travel trailing edge up at very high angles-of-attack, even with full trailing edge up tab. Since full down elevator is required for positive recovery from critical deep stall conditions, an elevator power assist system is provided on all DC-9 aircraft. The data from this test show essentially no difference in the elevator hinge moment characteristics between the existing and refan DC-9-30 configurations. Based on these test results, it appears that the present authority of the power assist system will be adequate for the refanned DC-9-30.

The effects of the refan nacelles and 191 mm (7.5 in.) pylon on the DC-9-30 pitching moment characteristics for the normal operating envelope are shown in figure 79. Tail-off data are presented for four (4) flap/slat configurations: (1) up/retracted, (2) up/extended, (3) 0.436 rad (25 deg)/extended, (4) 0.873 rad (50 deg)/extended. The only tail-on configurations tested with the elevator undeflected were flap/slat configurations of (1) up/extended and (2) 0.873 rad (50 deg)/extended.

A comparison of the tail-off data reveals that the refan nacelle causes a positive (nose up) shift in the pitching moment coefficient at all flap settings. The effect was expected since the nacelles and pylons on the DC-9,

SYMBOL	CONFIGURATION
○	BASELINE DC-9-30, BASIC TAIL
△	REFAN NACELLE – 5.2 IN. (132 MM) PYLON, BASIC TAIL
□	REFAN NACELLE – 7.5 IN. (191 MM) PYLON, BASIC TAIL
⬭	REFAN NACELLE – 11.0 IN. (280 MM) PYLON, BASIC TAIL
◇	REFAN NACELLE – 7.5 IN. (191 MM) PYLON, LARGE TAIL

NOTE: 1. TRIMMED FOR AFT CG (34.7% MAC) AT $1.3V_S$

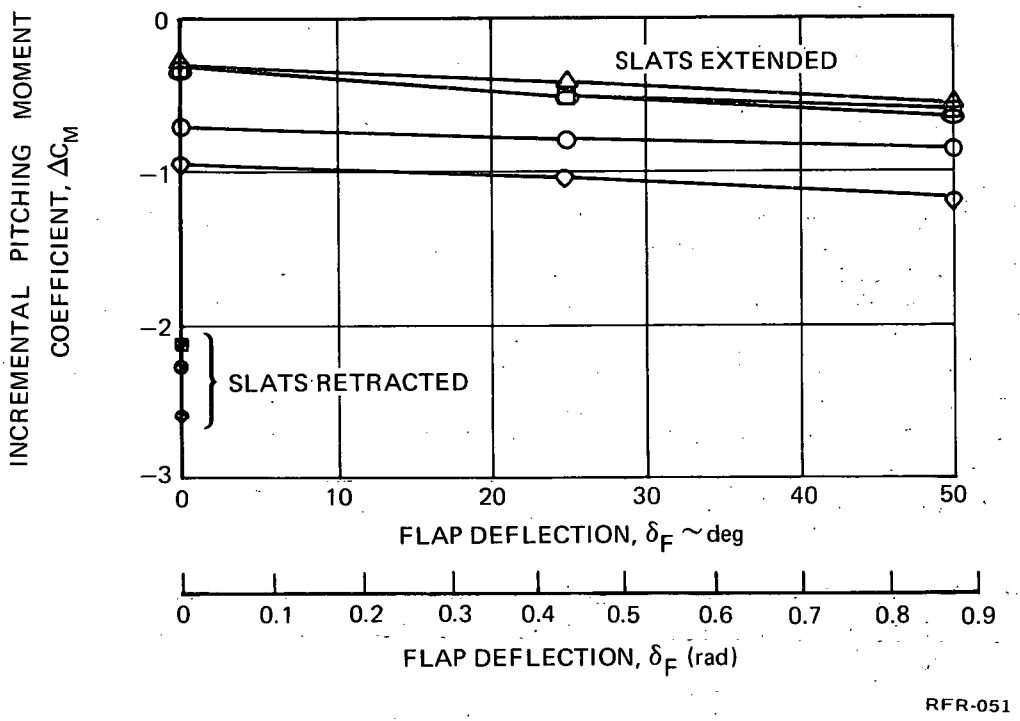

FIGURE 78. EFFECTS OF NASA REFAN ENGINES ON DEEP STALL RECOVERY MARGIN, ELEVATOR DEFLECTION, δ_e = 15 deg (0.262 rad)

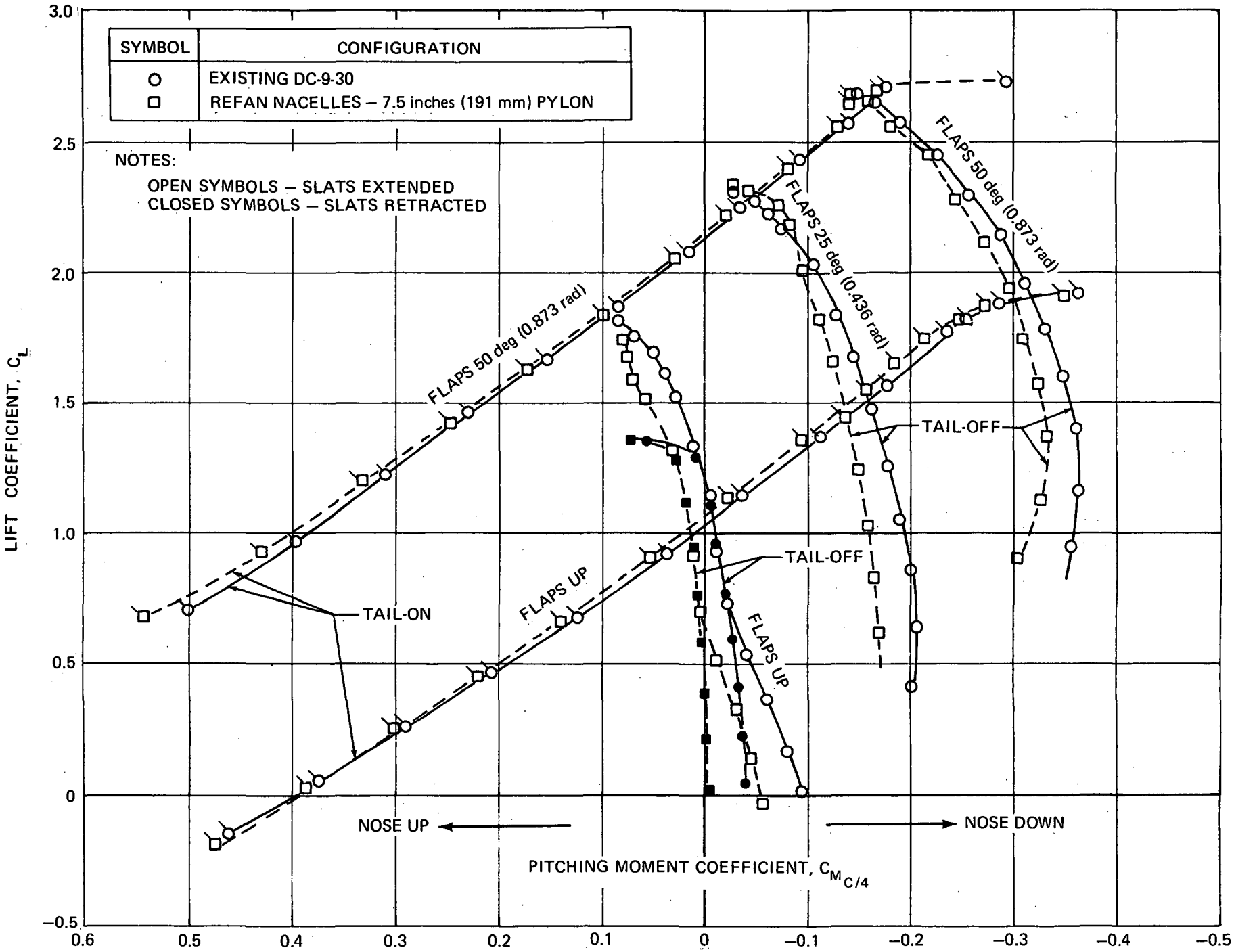

FIGURE 79. EFFECTS OF REFAN ENGINES ON PITCHING MOMENT CHARACTERISTICS

RFR-053

being in the region of high downwash, normally experience a negative angle-of-attack and a download. Since the download acts aft of the c.g. and the nacelles have some negative camber, they contribute a positive pitching moment to the tail-off airplane. The larger refan nacelles would therefore be expected to increase this nose up effect. The tail-off data also generally show that the refan nacelle/pylons have a mild stabilizing effect. This too is caused by the increased size of the refan nacelle and aft location of the DC-9 engines.

The tail-on data in figure 79 indicate that the shift in the tail-on pitching moments at a constant lift coefficient due to the refan engine is less than indicated with the tail-off. Also, the tail-on data show little effect of the refan nacelles on stability (increasing nose down C_m with increasing C_L). The nacelles and pylons reduce the downwash at the horizontal tail, and this reduction would be larger for the refan engine configuration. This reduction in downwash produces a nose down pitching moment increment which tends to offset the nose up moment with the tail-off. The conclusion drawn from these data is that the aircraft's longitudinal flight regime will be essentially unchanged by the refan modification.

The results of the low speed wind tunnel test to determine the impact of the refan engines on the DC-9-30 low speed stability and control characteristics lead to the following conclusions.

1. The refan installation has a small detrimental effect on the DC-9-30 deep stall recovery capability. However, the deep stall characteristics of the refan installation, within the range of pylon spans tested, are acceptable with no additional design changes anticipated.

2. The effects of pylon span on deep stall recovery margin is small, within the range of spans tested, 132 mm (5.2 in.) to 280 mm (11.0 in.).

3. A larger horizontal tail with area increased by 1.72 m^2 (18.6 ft^2) and an increased span of 508 mm (20 in.) significantly increased the deep stall recovery margin.

4. The refan installation has no significant effect on elevator hinge moment characteristics.

5. In the normal flight regime, the refan engines caused a positive (airplane nose up) increment in tail-off pitching moments and a slight increase in tail-off longitudinal stability.

6. In the normal flight regime, the refan engines do not significantly affect the DC-9 tail-on pitching moments. The refan engines alter the downwash at the horizontal tail such that the change in tail contribution essentially offsets the tail-off effects described above.

RETROFIT AND ECONOMIC ANALYSIS

The economic and benefit analysis were prepared using earlier design minimum, intermediate and maximum levels of acoustic treatment than are shown in figure 3. The elapsed time required to perform cost and acoustic analysis necessitated the use of these earlier designs to perform the complete costing and economic analysis.

Schedule and Market

The availability of DC-9 refan retrofit kits is paced by the availability of the first refanned engines for the flight demonstration program. The first flight is scheduled to take place in early 1975 beginning with a 1 July 1973 authority to proceed for Phase II. Following a 3 month flight demonstration program, the first production retrofit kits could be available in late 1975 based upon issuance of authority to proceed in early 1975. The retrofit modification program rate would build up through 1976 leading to high sustained rates in 1977, 1978 and 1979. The entire DC-9 fleet refan retrofit could be complete by 1 January 1980. Since the DC-9 refan market is a function of when retrofit can be accomplished, the market analysis projects a total of 555 retrofit DC-9 airplanes consisting of 395 domestic aircraft and 160 foreign aircraft.

The domestic market comprises all DC-9 aircraft which would be in service after 1981 while the foreign market is based upon 50% of the foreign airplanes. The total JT8D refanned program would require production of approximately 6,000 refan engine kits including spares and a modest number of refanned engines which would be incorporated into production airplanes at the factory. Retrofit of refanned JT3D engines into DC-8 airplanes could begin about 9 months later leading to a total DC-8 retrofit market of 255 airplanes. The market analysis indicates a total market for approximately 3,000 JT3D engine kits including spares.

Retrofit Unit Costs

The costs of refanning the DC-9 aircraft vary between $950,000 and $1,050,000 as shown in table 29. These costs include prorated research and development, the Pratt and Whitney engine rework activities, new nacelles, new pylons, local rework of the fuselage, ballast and installation. Douglas profit and NASA fee are included. The costs of the DC-8 retrofit are significantly higher, in part due to higher engine rework costs and in part due to the extensive modifications required to beef-up the pylon/wing attach points to carry the heavier loads. The DC-9 retrofit is relatively straightforward and can be accomplished in about 16-1/2 days based upon detailed task analyses. Comparable analyses for the DC-8 suggest an airplane would be out of service approximately 28 days.

TABLE 29

JT8D AND JT3D REFAN UNIT PRICE BREAKDOWN (MILLION DOLLARS)

No. of Domestic Aircraft Treatment Level Design Concept	DC-9 395			DC-8-50/61 80			DC-8-62/63 60	
	Min.	Int.	Max.	Min.	Int.	Max.	Min.	Max. Common
Non-Recurring	0.062	0.069	0.075	0.092	0.121	0.271	0.088	0.080
Engine Kits	0.492	0.492	0.492	1.144	1.144	1.144	1.144	1.144
Nacelles	0.297	0.309	0.357	1.140	1.260	1.052	1.114	1.000
Airframe Kits	0.041	0.042	0.043	0.035	0.035	0.174	0.028	0.028
Installation	0.065	0.067	0.069	0.102	0.102	0.095	0.097	0.097
TOTAL	0.957	0.979	1.036	2.513	2.662	2.736	2.471	2.349

In addition to the retrofit costs, the airplanes would incur additional costs for spares inventories, crew training and lost revenue over the period the airplanes would be out of service. The use of a variable domestic retrofit rate would minimize the impact of out of service losses by reducing the monthly rate during periods of peak demand and increasing it during periods of slack demand. Nevertheless, refanning the worldwide JT8D and JT3D fleets would probably require special modification centers. Retrofitting the DC-9 over a 3-1/2 year period would require a rate of approximately 16 airplanes a month or a little less than 4 airplanes per week. While this modification would be accomplished at a single facility, the addition of potential DC-8 modifications would seriously strain the capacity of almost any aircraft overhaul installation both in terms of area and labor force.

The total initial costs for refanning the domestic DC-9 fleet would amount to over 1/2 billion dollars when the financing charges are included, table 30. On the other hand, the incremental cash costs of operating refanned DC-9 airplanes would be relatively small, on the order of 10 dollars per block hour at an average stage length of 483 km (261 n. mi.). The annual cash operating cost increment would amount to about $10,000,000 for the 395 aircraft domestic DC-9 fleet at approximately 2,500 hours per year utilization.

The direct operating cost in terms of cost per kilometer (nautical mile) and cost per seat kilometer (nautical mile) are shown in figure 80. Typically, these show a 10% to 15% increase in direct operating cost at a 483 km (261 n. mi.) stage length most of which is accounted for by increased depreciation. Since it is doubtful that the airlines could by themselves finance a major refan retrofit program without government assistance, the primary impact would be seen in cash operating costs which would amount to only 2-1/2 to 4-1/2% at the average stage length of the DC-9, table 31.

The threshold costs of the minimum JT8D noise treatment for the DC-9 are relatively high. Increasing noise treatment to provide the maximum treatment level increases cash operating cost and depreciation only a relatively small amount. This insensitivity to increasing noise abatement treatment within the refanned concept suggests that noise treatment levels higher than the minimum could well be considered to provide maximum benefit.

Noise Abatement Benefits

The reduction in Noise Exposure Forecast (NEF) contour area was used as the basis of determining the acoustic benefit of refanning the JT8D and JT3D powered aircraft. Noise Exposure Forecast is readily translatable into community annoyance because it includes the effect of the number of flights and fleet mix between aircraft types as well as changes to the aircraft noise sources and flight paths. Two basic type of airports and fleet mixes were investigated. The first is the short haul airport, such as Washington National, where the commercial traffic is essentially JT8D powered. The second type is the major hubs, such as John F. Kennedy airport, where there is a wide range of JT8D, JT3D and high by-pass ratio engine powered aircraft. Refanning the JT3D as well as the JT8D aircraft was investigated at these major hubs. Washington National Airport was used to investigate the benefit of refanning

TABLE 30

DOMESTIC FLEETS RETROFIT INITIAL COSTS INCLUDING RETROFIT, SPARES, OUT OF SERVICE AND ROUTE FAMILIARIZATION

(DOLLARS IN MILLION)

	DC-9	DC-8-50/61	DC-8-62/63
NO. OF DOMESTIC AIRCRAFT	395	80	60
REFAN MINIMUM TREATMENT			
RETROFIT	378.0	201.0	148.3
SPARES	56.7	30.2	22.2
OUT OF SERVICE	4.7	4.3	3.7
ROUTE FAMILIARIZATION	5.4	2.3	1.8
TOTAL	444.8	237.8	176.0
REFAN - INTERMEDIATE TREATMENT			
RETROFIT	386.7	212.9	
SPARES	58.0	31.9	
OUT OF SERVICE	4.7	4.3	
ROUTE FAMILIARIZATION	5.4	2.3	
TOTAL	454.8	251.4	
REFAN MAXIMUM TREATMENT			
RETROFIT	409.2	218.8	140.9
SPARES	61.4	32.8	21.1
OUT OF SERVICE	4.7	4.3	3.7
ROUTE FAMILIARIZATION	5.4	2.3	1.8
TOTAL	480.7	258.2	167.5

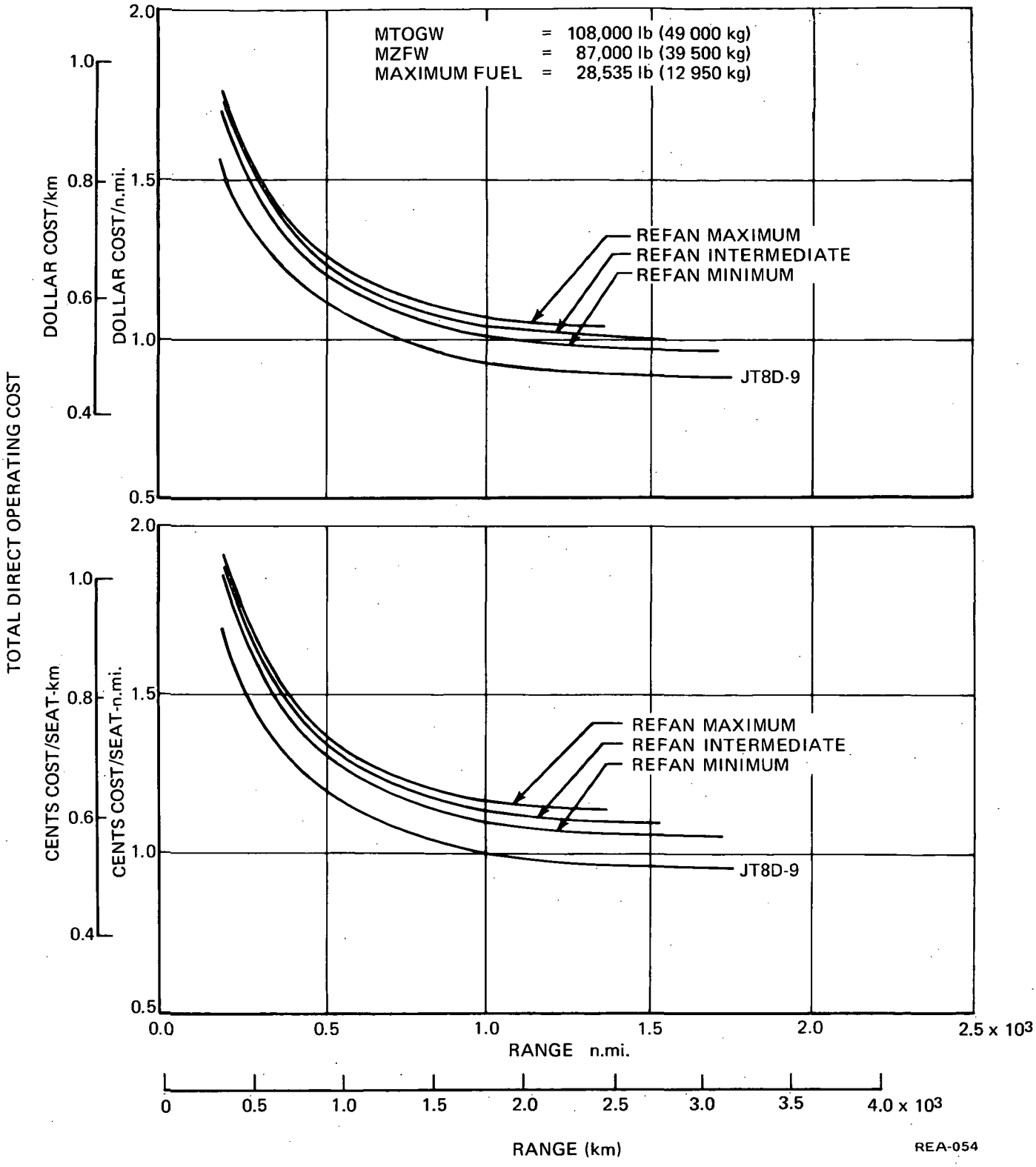

FIGURE 80. TOTAL DOC FOR LONG RANGE CRUISE AT 35,000 ft (10 668 m) at 99 PERCENT MAXIMUM n.mi./lb DOMESTIC RESERVES 200 n.mi. (370 km) ALTERNATE, ZERO WIND, STANDARD DAY

TABLE 31

DIRECT OPERATING COST-DOLLARS PER BLOCK HOUR

TYPICAL RANGE 261 n. mi. (483 km)

TREATMENT LEVEL	CASH DOC	*DOC DUE TO DEPRECIATION	TOTAL DOC
JT8D-9	394	103	497
JT8D-109			
MIN.	403	129	532
INT.	407	129	536
MAX.	412	131	543

*NOTE: The depreciation estimates are based on the adjusted original value; i.e., after reducing the original price by the value of the discarded engine and airframe components, and the capitalized value of the installed refan kits.

the JT8D aircraft in an environment dominated by this noise source. The NEF contours were based on "typical mission" gross weights and simulated operations for a given day rather than an average of yearly operations and runway utilization. Rapid climbout without cutback and a three degree glide flight path were used to calculate the contours.

It is not possible to assess the benefits of refanning only the domestic DC-9 fleet. The most predominant member of the JT8D fleet is the B-727. A retrofit program which would not provide a high noise treatment level for the B-727 and also the B-737 would vitiate the noise benefits which could be attained by refanning the DC-9. If all JT8D domestic airplanes were refanned, significant noise reductions would be observed at those airports presently, and in the future, served by JT8D powered airplanes and smaller general aviation aircraft. For example, refanning all JT8D powered airplanes and treating the nacelles to the intermediate level would reduce the calculated 1973 30 NEF contours at Washington National to approximately the area covered by the 1973 40 NEF contour. The refanned 40 NEF contour would be shrunk to an area approximately the size of Washington National Airport, see figure 81. Further, the 30 NEF contour primarily would be confined to the airport and river areas with only a small spillover into developed land areas.

At those airports which are used by wide mixture of airplanes, including JT3D and high bypass ratio as well as JT8D powered airplanes, the noise benefits from refanning the JT8D are much less marked than at Washington National. For example, refanning the JT3D powered domestic fleets alone would sharply reduce the noise under the John F. Kennedy Airport takeoff pattern but would hardly effect the noise environment under the approach pattern, figure 82. Significant JT3D noise treatment would be required to extend the benefits of the JT8D refan engine to residents living under the approach patterns of the major hub airports. The area of the NEF 30 to 45 contours for Washington National and John F. Kennedy Airports are plotted on figures 83 and 84. As shown by the NEF contour areas, the refan concept with nacelle acoustic treatment gives a large reduction in contour areas. The level of nacelle treatment, as shown by minimum, intermediate and maximum treatment, gives relatively smaller contour area reductions.

To provide a comprehensive single measure value of the benefits, the areas between the contours in 5 NEF increments were weighted for the average NEF level and summed. This value, called the "Total Weighted NEF Contour Area" was used to compare the various retrofit options. The weighing factor used doubled for an increase of 10 NEF. This is based on psycho-acoustic research which indicated, on the average, a doubling of annoyance for each 10 dB increase in noise level.

Table 32 presents the total weighted NEF areas as a percent of existing total weighted area for four airports. The remaining percentage of total weighted contour area is shown based on the absolute contour areas and also based on the contour areas less the airport area. This latter case was included because it can be debated that the land area within the airport boundaries is unaffected by community noise complaints and should, therefore, be excluded from calculations of community annoyance. Excluding the airport area has the effect of enhancing the appeal of quieter retrofit options because the airport area becomes a larger percentage of the noise impact area. The airport areas for Washington National, John F. Kennedy, O'Hare, and Atlanta, respectively, are: 1.0, 8.1, 14.1, and 6.5 square miles.

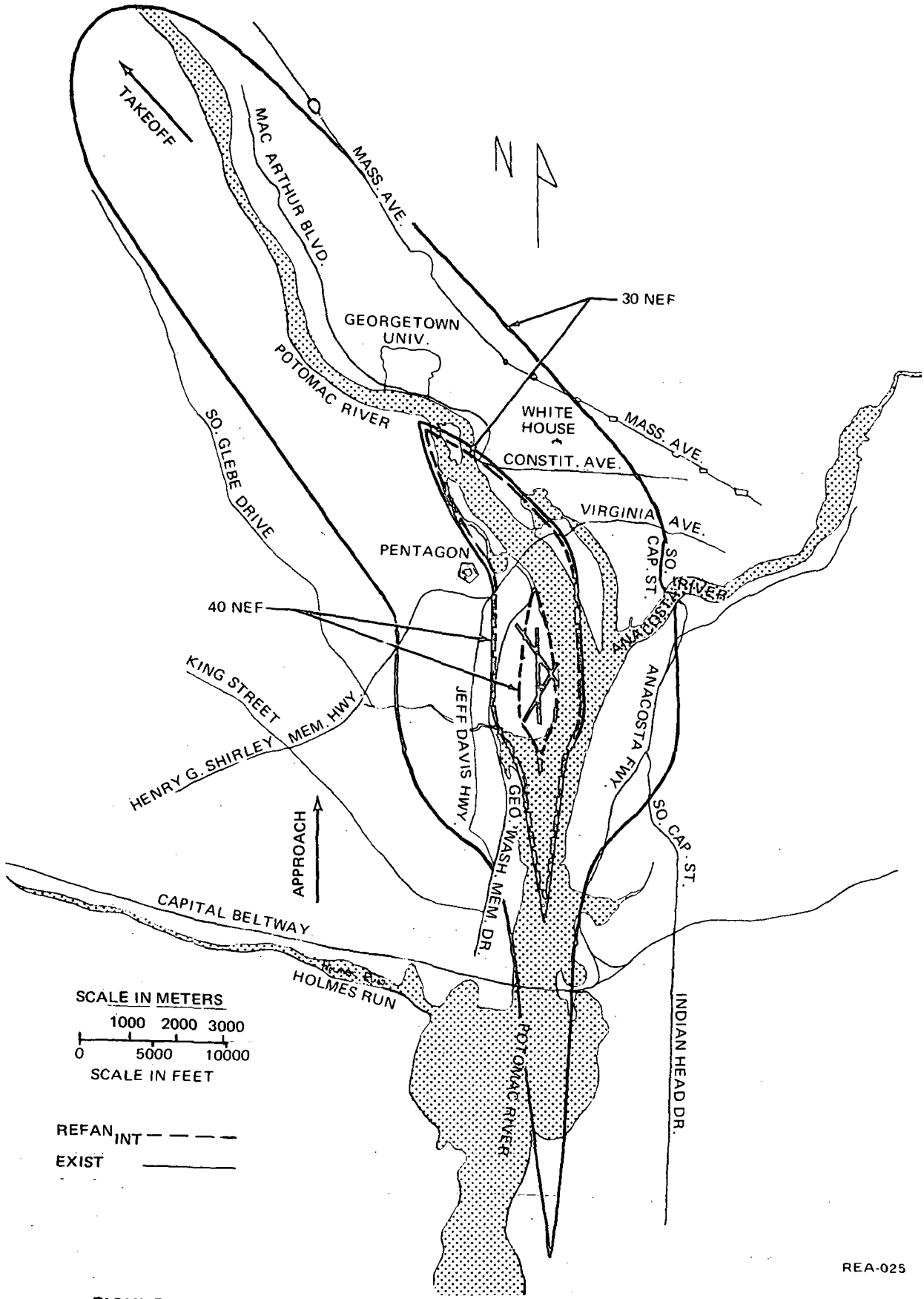

FIGURE 81. 30 AND 40 NEF CONTOURS AT WASHINGTON NATIONAL AIRPORT

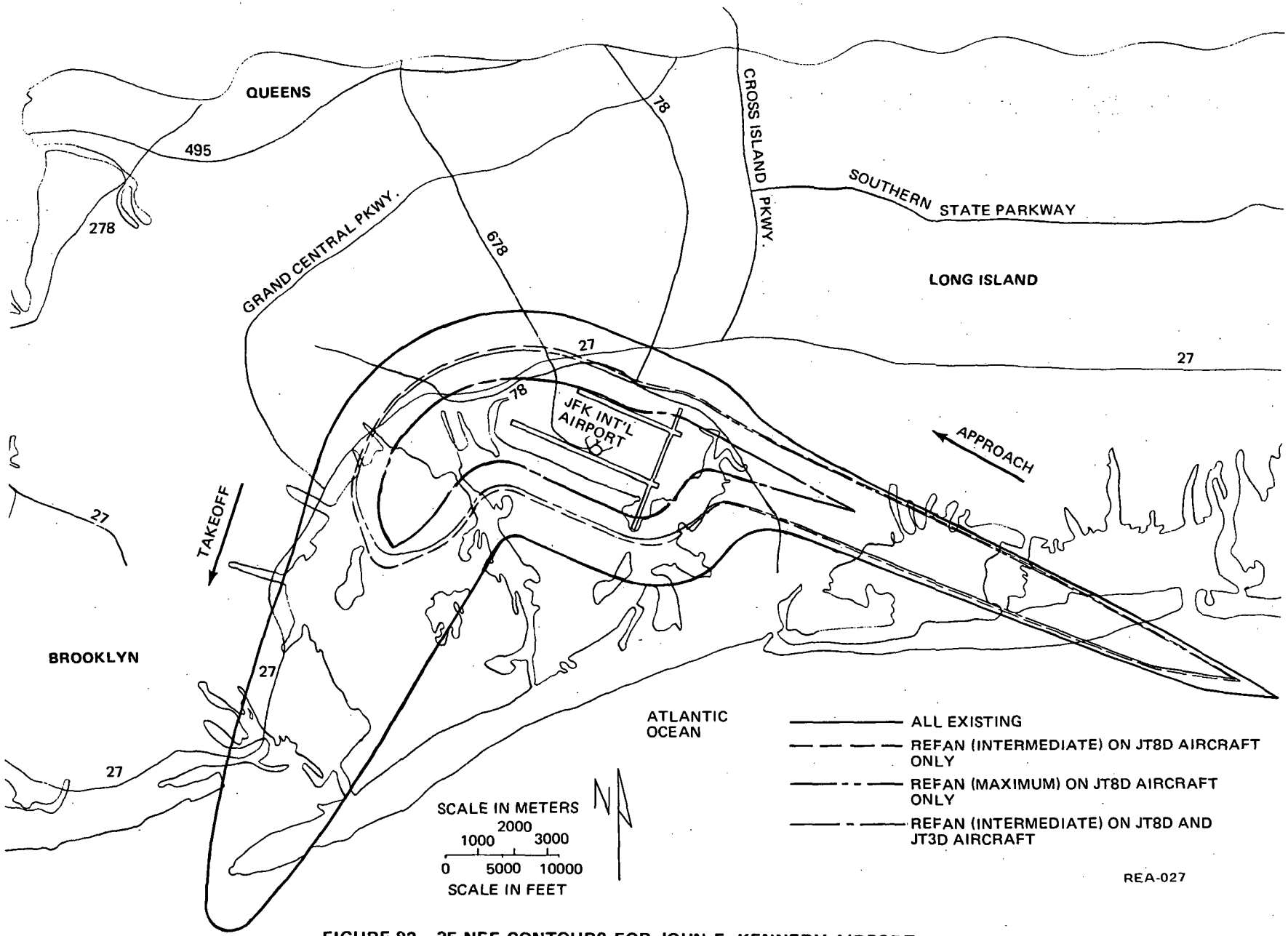

FIGURE 82. 35 NEF CONTOURS FOR JOHN F. KENNEDY AIRPORT

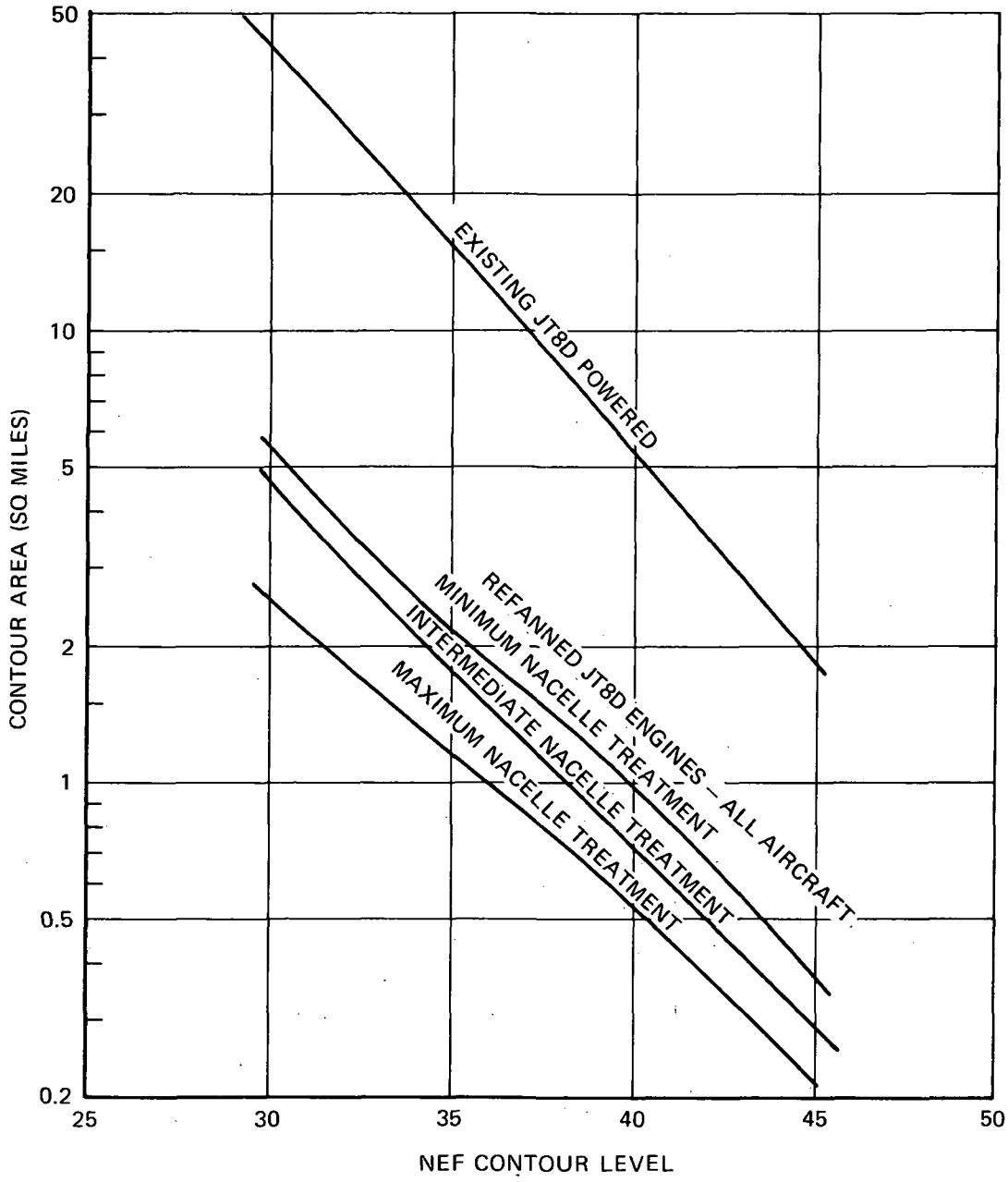

FIGURE 83. NEF CONTOUR AREAS FOR WASHINGTON NATIONAL AIRPORT

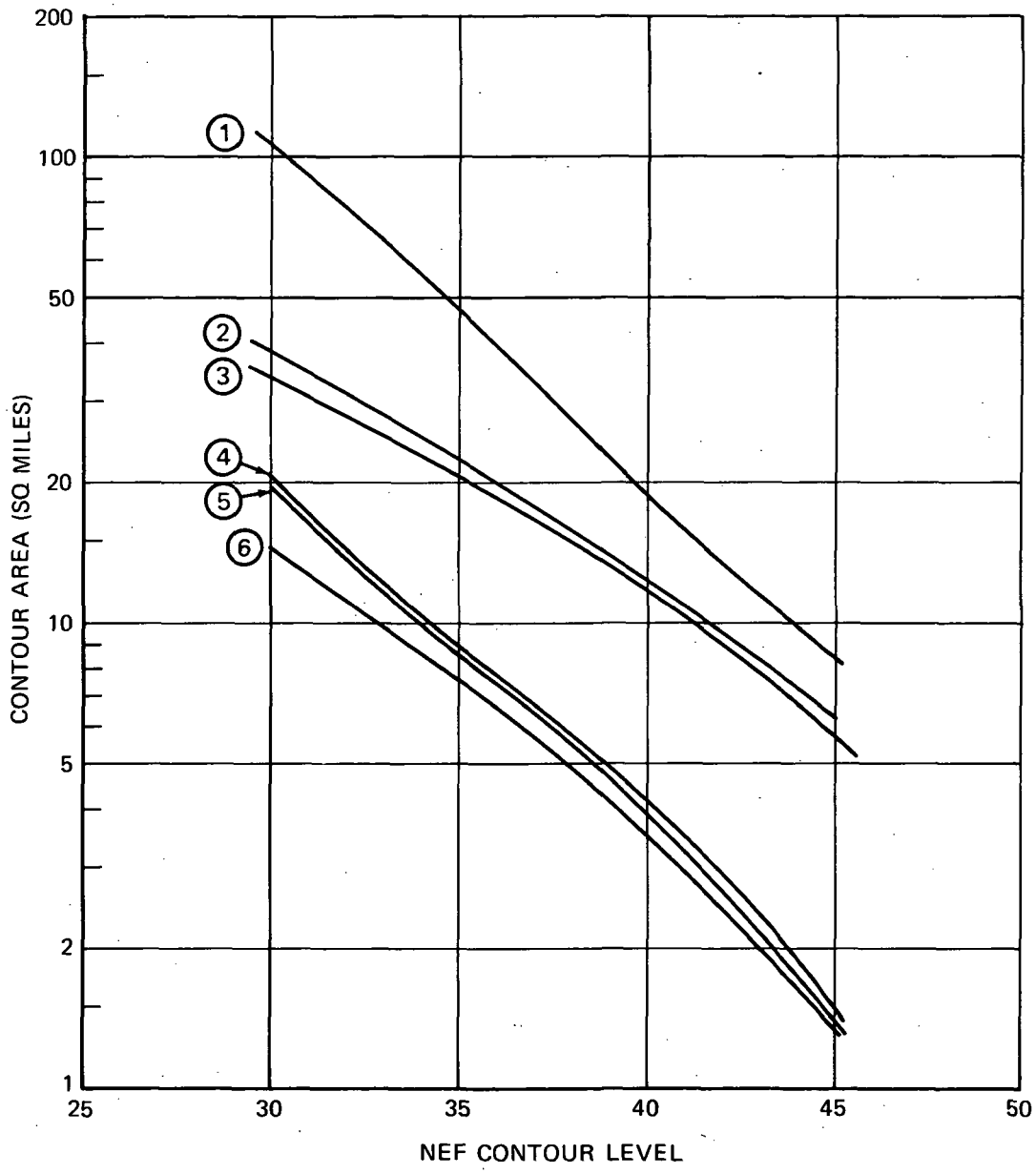

AIRCRAFT POWERED BY:

	JT8D	JT3D	HI BYPASS
1	EXISTING	EXISTING	EXISTING
2	$REFAN_{MIN}$	EXISTING	EXISTING
	$REFAN_{INT}$	EXISTING	EXISTING
3	$REFAN_{MAX}$	EXISTING	EXISTING
4	$REFAN_{MIN}$	$REFAN_{INT}$	EXISTING
5	$REFAN_{INT}$	$REFAN_{INT}$	EXISTING
6	$REFAN_{MAX}$	$REFAN_{INT}$	EXISTING

NOTE:

MIN, INT, MAX = LEVEL OF NACELLE ACOUSTICAL TREATMENT

REA-031

FIGURE 84. NEF CONTOUR AREAS FOR JOHN F. KENNEDY AIRPORT

TABLE 32

REFAN ACOUSTIC BENEFITS - SELECTED AIRPORTS

AIRPORT	OPERATING MIX % JT8D	JT3D	Other	PERCENT REDUCTION IN TOTAL WEIGHTED NEF CONTOUR AREA: TOTAL AREA EXCLUDING AIRPORT — NONE	REFAN - INT. JT8D ONLY	REFAN - INT. JT8D & JT3D	TOTAL AREA INCLUDING AIRPORT — NONE	REFAN - INT. JT8D ONLY	REFAN - INT. JT8D & JT3D
Washington National	100	0	0	0	88.5	NA	0	92.0	NA
John F. Kennedy	40	40	20	0	59.0	81.5	0	68.0	90.3
O'Hare International	63	27	10	0	63.0	81.3	0	77.4	93.9
Atlanta Municipal	84	15	1	0	65.0	83.0	0	72.0	89.2

Table 32 also shows the fleet mix between JT8D and JT3D powered aircraft and indicates that the fleet mix doesn't appear to have a major effect on the reduction in total weighted NEF contour area. For John F. Kennedy, O'Hare, and Atlanta airports, JT3D powered aircraft compose between 15 and 40 percent of the total aircraft operations. If only the JT8D powered aircraft are refanned, the reduction in Total Weighted NEF Contour Area varies only between 59 and 65 percent. This indicates that even a relatively modest number of untreated JT3D aircraft seriously dilute the noise benefits, as measured by NEF, of refanning the JT8D fleet.

Table 33 shows a comparison of the FAR Part 36 noise levels between the configurations used in this section and the configurations in figure 3. These differences are due inpart, to the depth of acoustic analysis as well as to the physical configurations. As shown in table 33 the intermediate level of treatment is equivalent to the selected configurations during approach. The selected configurations give slightly lower noise levels during takeoff. In general then, the selected configurations, in the predominately JT8D airports, would give equal or slightly improved noise reduction benefits compared to the configurations analyzed here.

TABLE 33

COMPARISON OF FAR PART 36 NOISE LEVELS FOR DC-9 REFANNED CONFIGURATIONS

	APPROACH	TAKEOFF		SIDELINE
		WITH CUTBACK	WITHOUT CUTBACK	
Acoustic Configurations used on NEF contours:				
Minimum	102	87	91	94
Intermediate	100	87	91	93
Maximum	97	88	92	92
Selected Acoustic Configurations:				
Minimum	100	85	88	90
Maximum	99	84	88	90

Feasibility

A program to refan all domestic JT8D and JT3D powered airplanes would increase total airline costs by about 4-1/2 billion dollars over an eight year period. Approximately 3-1/2 billion would be accounted for by initial costs with the other billion being the result of increased operating costs and interest on the indebtedness generated to accomplish the refan programs. Relief of this financial burden would probably be required to maintain the financial stability of the domestic airlines industry over this period. It would require approximately 60% of the ticket tax receipts generated by the narrow bodied fleets over the 8 year period to provide this financial relief. While this seems large, it would only amount to about 25% of total ticket tax collections. This rather modest amount suggests the refanned program lies in an economically feasible region even though this financing scheme is not recommended, although the government could subsidize a refan program with a wide variety of options, economic and political considerations suggest tax credits under pollution abatement legislation and/or direct subsidy would be among the more likely policies.

Significant noise abatement of at least JT8D powered fleets is almost essential for the continued long term viability and steady evolution of the domestic airline industry. Unless this can be accomplished there will be significant public opinion opposed to the expansion of scheduled air service. The dislocation affects of such opposition cannot adequately be estimated but would be felt over an extended period both in terms of airline financial stability and in terms of lack of responsiveness to growing demand for air transportation.

SUMMARY OF RESULTS AND CONCLUSIONS

The purpose of the Refan Program is to determine the technical and economic feasibility of reducing community noise of JT8D powered aircraft through modification of the existing engines and nacelle. Objective (1) required a definition of the nacelle modifications, an assessment of design variables on performance parameters, and a recommendation of engine and nacelle/airframe integration definition and characteristics.

The JT8D-109, the refan derivative of the basic JT8D-9 engine, was selected for study installed on a DC-9-32 airplane. Since the refan concept is to retrofit the existing fleet with quieter refan engines, the DC-9 systems and structure were examined for minimum change or economic impact on retrofit while achieving a desired level of performance and noise. Two levels of acoustic treatment were investigated in detail. The minimum selected treatment has a 1 600.2 mm (63 in.) long inlet and a 1 854.2 mm (73 in.) tailpipe. The maximum selected treatment has a 1 905.0 mm (75 in.) long inlet and a 2 159 mm (110 in.) tailpipe. Both of these configurations include wall treatment only to minimize performance penalties, external drag, development costs and risk.

The installation of the JT8D-109 results in an operational weight increase of approximately 1 135 kg (2,500 lb) with a c.g. shift of 6 to 7 percent MAC for the minimum selected treatment. The ground handling characteristics may require water ballast at hard points already located in the fuselage. Operationally an airline may require ballast up to 408 kg (900 lb). Since many of the configurations require no ballast, and in fact the loadability will be improved by the refan installation, many operators will choose other methods such as placement of baggage to correct adverse balance conditions.

The takeoff gross weight for a given field length is increased approximately 2 268 kg (5,000 lb), due to the increase in installed sea level static thrust of 71 168 N (16,000 lb) for the refan compared to 63 162 N (14,200 lb) for the basic JT8D-9. The payload ranges were determined for typical mission payloads of 6 804 kg (15,000 lb) and maximum payloads based on the zero fuel weight of 39 463 kg (87,000 lb). Long range cruise at an altitude of 10 668 m (35,000 ft) as well as the minimum direct operating cost operation at M_O 0.78 at 9 144 m (30,000 ft) were considered. The refan installed SFC effect shows a slight range improvement varying from 24 km (13 n. mi.) to 39 km (21 n. mi.) for the minimum suppression nacelle and a slight increase varying from -32 km (-17 n. mi.) to -61 km (-33 n. mi.) for the maximum suppression nacelle. The additional weight of the refan installation shows a range degradation varying from -65 km (-35 n. mi.) for the typical mission payload with minimum suppression to -505 km (-273 n. mi.) for the maximum payload with maximum suppression. The net effect of installed SFC and the additional weight of the refan installation can vary with minimum suppression from -30 km (-16 n. mi.) for a typical mission to -394 km (-213 n. mi.) for the maximum payload case and can vary, with maximum suppression, from -121 km (-65 n. mi.) for a typical mission to -542 km (-293 n. mi.) for the maximum payload case. The primary effect on range is, therefore, the additional weight of the refan installation and occurs at the higher payloads where the aircraft is gross weight limited.

The estimated EPNL's for the refanned DC-9-32 aircraft indicate a reduction from existing aircraft EPNL's of 7 at approach, 12 for takeoff with cutback, 14 for takeoff without cutback and 11 for sideline, using FAR Part 36 rules. There is little difference in the EPNdB between maximum and minimum treatment nacelles, due primarily to the additional weight and thrust loss associated with the maximum treatment that reduces the height over the measuring station.

The 90 EPNdB contours were calculated for typical mission and FAR 36 operation using two-segment approach and takeoff with and without cutback. Improvements in area reduction varied from a high of 87.5% for the Part 36 operation two-segment approach, maximum suppression, takeoff without cutback to a minimum reduction of 73% for the typical mission, two-segment approach, minimum suppression, takeoff with cutback (80% reduction of area is considered as typical).

Objective (2) required a preliminary design of nacelle and airplane modifications for installing the JT8D-109 and JT8D-9 engines on the DC-9-32 aircraft, and objective (3) required model tests to determine the optimum DC-9 pylon configuration.

The primary concerns for the installation of the refan engine on the DC-9 airplane involves the effects of the larger refan engine nacelle on airplane drag and deep stall recovery margin; the effects of the higher refan engine thrust on takeoff field length, minimum control speeds, and increased reverse thrust loads; the effects of the increased weight of the refan engine on airplane loads during hard landing and airplane aft c.g. limits; airplane stability and control characteristics; aerodynamic and inertia loads on wing flutter; and the incorporation of maintenance and access provisions for engine accessories.

Since it was desirable from a deep stall recovery and minimum control speed viewpoint to have a minimum pylon span, a high speed test was run with spans of 425 mm (16.7 in.) and 132 mm (5.2 in.) to determine the incremental drag difference. At a typical cruise Mach number (M_0 = 0.78) an improvement in interference drag compared to the existing DC-9 installation of about 2% of the total airplane drag was found. Since the skin friction penalties of the larger refan installation amounts to about 2% of the total airplane drag, this resulted in the refan nacelle being installed without penalty. A low speed test confirmed that the refan nacelle with pylon spans up to 280 mm (11 in.) has a small detrimental effect on deep stall margin and is within acceptable limits. Because of accessibility requirements the pylon span was designed to 204.47 mm (8.05 in.). Minimum control speeds were determined acceptable since the centerline of the higher thrust engines moves inboard by 31.3 mm (3.2 in.).

The increased weight of the refan nacelle configuration requires reinforcing at fuselage skin in the vicinity of the pylon, fuselage keel structure and the engine mount system. Loads, strength and dynamic analyses have been performed on the nacelles, pylon and fuselage structure.

Engine and nacelle subsystems have been investigated and the subsystem modifications identified. As additional refan engine data become available detailed analyses will be required to verify each subsystem function.

Objective (4) required an analysis of the economic considerations of the JT8D-109 and JT8D-9 engines and the noise reduction trade-offs in retrofitting these engines on the DC-9 Series 10/30 airplanes.

The retrofit analysis indicates the unit price of the refan kit would be approximately $1,000,000 with about an equal split between the airframe and the engine cost. NEF contour areas at Washington National, where a substantial number of JT8D powered airplanes operate, indicate reductions in 30 NEF contour areas of approximately 90% could be achieved. The schedule of the program indicates that production kits could be made available by late 1975 or early 1976, with a DC-9 market potential in the order of 555 airplanes.

No major technical problem was determined in Phase I for installing a refan JT8D-109 engine on a DC-9 airplane. The structural problems associated with the keel structure or fuselage rework appear to be well within the capability of a retrofit program. Performance losses, minimum control speeds, and stability and control problems associated with the larger nacelle are minimal. The results of the acoustical analysis inidicate the area within the confines of a 90 EPNdB contour could be reduced by 73 to 87% dependent on the level of treatment. Since there is little acoustic advantage for maximum acoustic treatment, the minimum treatment case is recommended for subsequent studies.

It is concluded that a Phase II flight demonstration program to substantiate the hardware design, obtain reliable acoustic data and determine more accurate retrofit costs, be undertaken.

APPENDIX A

ACOUSTICS

This appendix presents the following acoustic information:

- The Douglas Noise Prediction Procedure and the cycle data used in the calculations.
- The inlet and tailpipe internal flow conditions.
- Predicted flyover noise time histories and spectra.
- 90 and 95 EPNdB Noise Contours for the existing and refanned DC-9-15.

APPENDIX A

Noise Prediction Procedure

The aircraft flyover noise levels were calculated by predicting the component noise source levels and spectra for the fan, turbine, core engine, and jet. The component noise levels for the fan inlet and fan exhaust include broadband noise, discrete tones, and multipure tone inlet noise. Turbine noise includes high frequency broadband noise and discrete tones. Core noise, which includes combustion noise, consists of low frequency broadband noise resulting from the aerodynamic disturbances upstream of the primary nozzle. Jet mixing noise includes noise due to the bypass stream's mixing with both the surrounding environment and the hot primary stream.

The component SPL spectra were calculated using a computerized procedure called Gas Turbine Engine Noise (GTEN). GTEN utilizes procedures and data supplied by the engine manufacturers for calculating the noise spectra of individual components of aircraft gas turbine engines.

The program utilizes semi-empirical equations that relate the strength and the directivity of the FAR field noise levels to the appropriate aerodynamic and geometric variables of various components of a propulsion system. The program uses a stage-stacking or component building block approach to estimate the noise produced by 11 separate engine components. For a turbofan engine, the components are:

1. Inlet guide vanes.
2. Fan rotor.
3. Fan stator.
4. Fan outlet guide vanes at entrance to fan discharge ducts.
5. Fan outlet guide vanes at entrance to engine core compressor.
6. Core compressor rotor.
7. Core compressor stator.
8. Turbine rotor.
9. Turbine stator.
10. Fan exhaust nozzle.
11. Primary exhaust nozzle.

Exhaust nozzles can be convergent, convergent-divergent, or of the modified mixer type used as jet noise suppression devices.

The noise calculations procedure which treats each noise component generated by a blade row or a nozzle separately, requires a detailed description of the engine component geometry, cycle parameters, and aerodynamic performance parameters.

APPENDIX A

Three modes of program operation are available for calculating the engine component aerodynamic and geometric inputs to the acoustic equations. In the first mode, the program calculates the engine component geometry and the aerodynamic performance parameters from the engine design point cycle parameters, the engine configurations, and the flight condition. The off-design aerodynamic performance parameters are then calculated from the given geometry and the off-design cycle parameters. In the second mode, which was used for the study presented here, the cycle parameters and the component geometry parameters for a given engine are input and the aerodynamic performance parameters are calculated. In the third mode, all the geometry and aerodynamic performance parameters for a particular engine and power setting are input.

Once inputs to the acoustic equations have been defined for a given engine configuration and operating point, the program calculates broadband noise, discrete tone, and multiple pure tone frequency spectra as required for each engine component.

Each noise source prediction results in a matrix of one-third octave band SPL frequency spectra for angles between 0 and 3.14 rad (180 deg) from the inlet at a 30.48 m (100 ft) polar radius. Attenuation spectra for each source are from the untreated SPL spectra to obtain the treated SPL spectra. The treated SPL for each component are extrapolated to the desired distance by accounting for spherical divergence, atmospheric attenuation, and forward flight speed effects. The data are then combined to calculate the complete engine flyover noise time histories and the effective perceived noise levels.

To account for DC-9 installation effects, the EPNL at each power setting and altitude are adjusted to establish the EPNL distance maps and the FAR Part 36 flyover noise levels presented in this report. The data used to calculate the uninstalled JT8D-109 component noise levels are presented in table A-1. The engine power setting and aircraft altitudes for the refanned DC-9-32 and DC-9-15 are shown in tables A-2 and A-3.

The predicted noise levels of GTEN have been compared with measured test stand and flyover data wherever possible. Figure A-1 shows a spectral comparison with the JT8D-3B and figure A-2 shows a directivity comparison with the P&WA high tip speed fan rig. In general, the predicted values are very close to the measured, especially near the peak noise radiation angles and blade passing frequencies. Figure A-3 shows the predicted turbine noise of the refanned JT8D-109 and the existing JT8D engines along with a measured JT8D-9 spectra. The prediction, for the existing JT8D-9, shows good agreement with the measured data, and the refan cycle parameters cause the predicted increase in turbine noise. This point is made to illustrate the desirability of the airframe manufacturer performing the cycle noise calculations, in the absence of a running engine and test stand data, to ensure all of the engine noise sources are accounted and to enable comprehensive nacelle treatment and flyover noise calculations.

APPENDIX A

TABLE A-2

AERODYNAMIC DATA FOR DC-9-32 AIRCRAFT AT FAR PART 36 AIRCRAFT OPERATIONS

MTOGW 108,000 lb (49 000 kg) | 5 deg FLAPS (0.086 rad) | MLdGW 99,000 lb (45 000 kg)

ENGINE CONFIGURATION	PARAMETER	APPROACH		CUTBACK	TAKEOFF	SIDELINE
		3 deg (0.052 rad)	6 deg*** (0.105 rad)			
UNTREATED*		6,280	5,130	7,290	8,020	8,000
UNTREATED**	$N_1/\sqrt{\theta}$	5,340	4,260	6,530	7,370	7,370
MINIMUM TREATMENT**	rpm	5,340	4,260	6,530	7,370	7,370
MAXIMUM TREATMENT**		5,385	4,340	6,560	7,370	7,370
UNTREATED*		5,411 (24 068)	2,786 (12 392)	9,514 (42 318)	12,529 (55 729)	12,486 (55 538)
UNTREATED**	F_n/δ	5,411 (24 068)	2,786 (12 392)	9,627 (42 820)	13,530 (60 181)	13,490 (60 004)
MINIMUM TREATMENT**	lb/ENG (N/ENG)	5,411 (24 068)	2,786 (12 392)	9,627 (42 820)	13,530 (60 181)	13,490 (60 004)
MAXIMUM TREATMENT**		5,411 (24 068)	2,786 (12 392)	9,613 (42 759)	13,311 (59 207)	13,330 (59 158)
UNTREATED*		370 (113)	1,000 (305)	1,995 (608)	2,099 (640)	1,000 (305)
UNTREATED**	ALTITUDE	370 (113)	1,000 (305)	2,327 (709)	2,462 (750)	1,000 (305)
MINIMUM TREATMENT*	feet (meter)	370 (113)	1,000 (305)	2,327 (709)	2,462 (750)	1,000 (305)
MAXIMUM TREATMENT**		370 (113)	1,000 (305)	2,287 (697)	2,420 (738)	1,000 (305)

RFR-157

*ENGINES USED ARE JT8D-9
**ENGINES USED ARE JT8D-109
***THIS DATA IS TABULATED HERE FOR COMPARATIVE PURPOSES ONLY

TABLE A-1
DATA USED TO CALCULATE UNINSTALLED JT8D-109 COMPONENT NOISE LEVELS

CYCLE PARAMETERS

POWER SETTING	ALTITUDE ft	ALTITUDE (m)	rpm $N_1/\sqrt{\theta}$	FPR	EFF	BPR	TOTAL FAN INLET FLOW RATE, W_T LB/SEC	TOTAL FAN INLET FLOW RATE, W_T (N/SEC)	CORE FLOW RATE W_C lb/sec	CORE FLOW RATE W_C (N/sec)	PRIMARY VELOCITY V_{PRI} ft/sec	PRIMARY VELOCITY V_{PRI} (m/sec)	FAN FLOW VELOCITY V_{FAN} ft/sec	FAN FLOW VELOCITY V_{FAN} (m/sec)
TO/SL	2462/1000	750.2/304.8	7370	1.68	0.82	2.05	472.00	2099.46	154.75	688.33	1473.0	449.0	1006.0	306.6
CUTBACK	2327	712.1	6530	1.52	0.83	2.28	416.00	1850.37	126.83	564.14	1225.0	373.4	890.0	271.2
3 DEG (0.052 RAD) APPROACH	370	112.8	5340	1.32	0.86	2.64	342.00	1521.22	93.96	417.93	957.0	291.7	739.0	225.3
6 DEG (0.102 RAD) APPROACH	1000	304.8	4280	1.12	0.88	3.00	270.00	1200.96	67.50	300.24	700.0	213.4	592.0	180.4

TURBOMACHINERY*

COMPONENT	POWER SETTING	rpm $N_1/\sqrt{\theta}$	RELATIVE VELOCITY, V_{REL} HUB ft/sec	RELATIVE VELOCITY, V_{REL} HUB (m/sec)	RELATIVE VELOCITY, V_{REL} TIP ft/sec	RELATIVE VELOCITY, V_{REL} TIP (m/sec)	BLADE ROW RELATIVE INLET MACH NUMBER M_{REL} HUB	BLADE ROW RELATIVE INLET MACH NUMBER M_{REL} TIP	AVERAGE AXIAL MACH NUMBER M_{AXIAL}^{AVE}
IGV	TAKEOFF/SEA LEVEL	7370	551.91	168.22	551.91	168.22	0.50	0.50	0.50
	CUTBACK	6530	469.50	143.10	469.50	143.10	0.43	0.43	0.43
	3 deg (0.052 rad) APRCH	5340	376.74	114.83	376.74	108.9	0.34	0.34	0.34
	6 deg (0.102 rad) APRCH	4280	290.43	88.52	290.43	88.2	0.26	0.26	0.26
FAN ROTOR	TAKEOFF/SEA LEVEL	7370	964.96	294.12	1605.51	489.36	0.89	1.47	0.54
	CUTBACK	6530	832.68	253.80	1415.07	431.31	0.98	1.29	0.45
	3 deg (0.052 rad) APRCH	5340	675.82	205.99	1165.19	355.15	0.61	1.05	0.36
	6 deg (0.102 rad) APRCH	4280	528.48	161.08	924.69	281.85	0.48	0.83	0.27
FAN STATOR	TAKEOFF/SEA LEVEL	7370	793.68	241.91	648.33	197.61	0.68	0.54	0.41
	CUTBACK	6530	710.38	216.52	583.12	177.74	0.61	0.50	0.38
	3 deg (0.052 rad) APRCH	5340	570.25	173.81	479.82	146.25	0.50	0.42	0.33
	6 deg (0.102 rad) APRCH	4280	388.86	118.53	356.20	108.57	0.34	0.31	0.29
LPT 3RD STAGE	TAKEOFF/SEA LEVEL	7370	1105.00	336.80					
	CUTBACK	6530	1072.00	326.75					
	3 deg (0.052 rad) APRCH	5340	1018.00	310.29					
	6 deg (0.102 rad) APRCH	4280	949.00	289.26					
LPT 4TH STAGE	TAKEOFF/SEA LEVEL	7370	1130.00	344.42					
	CUTBACK	6530	1031.00	314.25					
	3 deg (0.052 rad) APRCH	5340	938.00	285.90					
	6 deg (0.120 rad) APRCH	4280	870.00	265.18					

RFR-158

APPENDIX A

TABLE A-3

AERODYNAMIC DATA FOR DC-9-15 AIRCRAFT AT FAR PART 36 AIRCRAFT OPERATIONS

MTOGW 90,700 lb (41 200 kg) | 10 deg FLAPS (0.174 rad) | MLdGW 81,700 lb (37 200 kg)

ENGINE CONFIGURATION	PARAMETER	APPROACH 3 deg (0.052 rad)	APPROACH 6 deg*** (0.105 rad)	CUTBACK	TAKEOFF	SIDELINE
UNTREATED*		6,170	5,250	6,980	7,970	7,960
UNTREATED**	$N_1/\sqrt{\theta}$	5,220	4,320	6,100	7,370	7,370
MINIMUM TREATMENT**	rpm	5,220	4,320	6,100	7,370	7,370
UNTREATED*		5,043 (22 431)	2,884 (12 828)	7,770 (34 561)	11,995 (53 354)	11,951 (53 158)
UNTREATED**	F_n/δ	5,043 (22 432)	2,884 (12 828)	7,923 (35 242)	13,369 (59 465)	13,346 (59 363)
MINIMUM TREATMENT**	lb/ENG (N/ENG)	5,043 (22 431)	2,884 (12 828)	7,923 (35 242)	13,369 (59 465)	13,346 (59 363)
UNTREATED*		370 (113)	1,000 (305)	2,498 (761)	2,667 (813)	1,000 (305)
UNTREATED**	ALTITUDE	370 (113)	1,000 (305)	3,100 (945)	3,305 (1 007)	1,000 (305)
MINIMUM TREATMENT**	feet (meter)	370 (113)	1,000 (305)	3,100 (945)	3,305 (1 007)	1,000 (305)

RFR-156

*ENGINES USED ARE JT8D-7A
**ENGINES USED ARE JT8D-109
***THIS DATA IS TABULATED HERE FOR COMPARATIVE PURPOSES ONLY

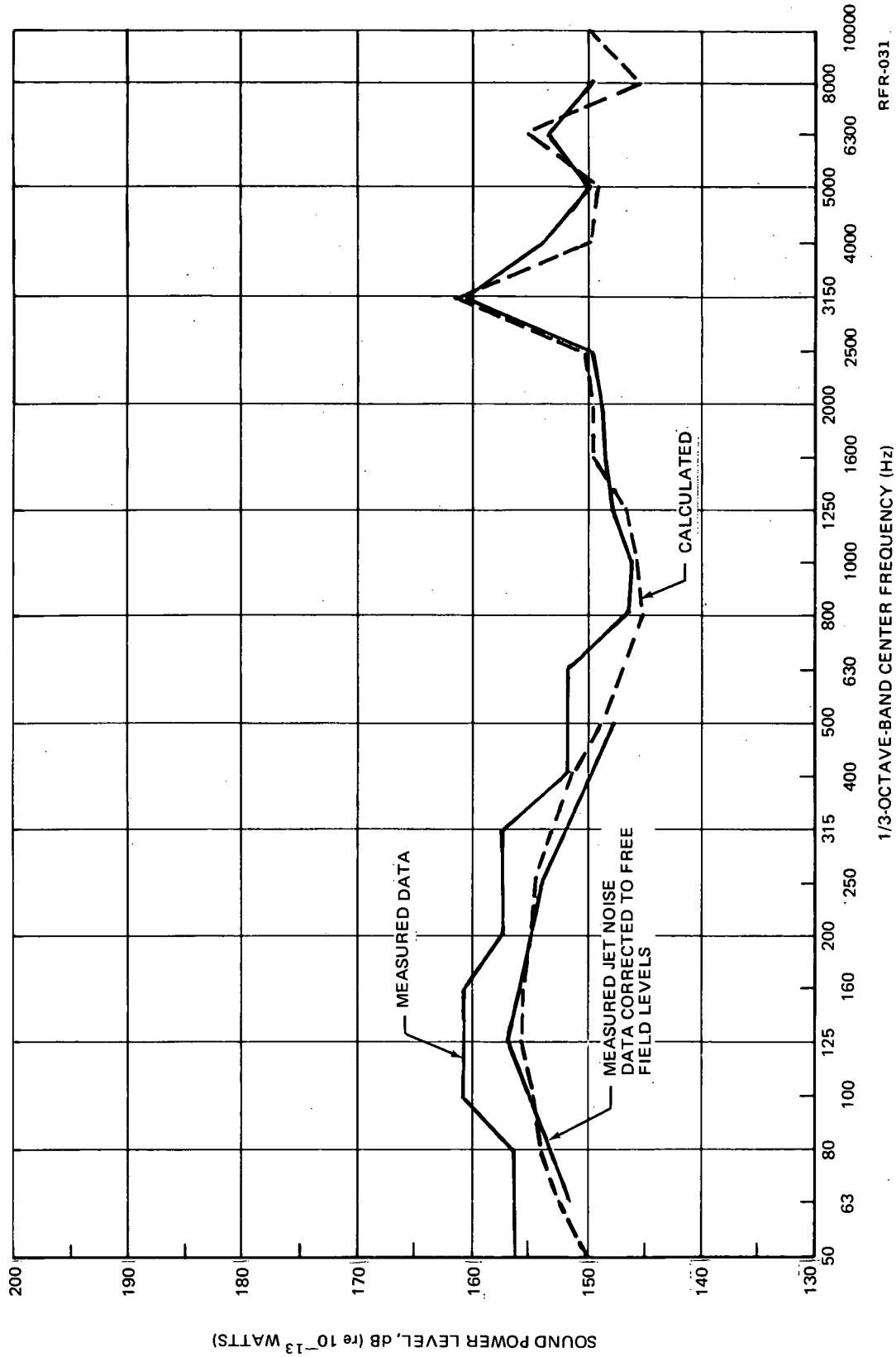

FIGURE A-1. JT3D-3B NOISE COMPARISON, SIDELINE DISTANCE = 155 ft (46 m), N_1 = 600 rpm, THRUST = 15,053 lb (66 956 N), ENGINE PRESSURE RATIO = 1.64

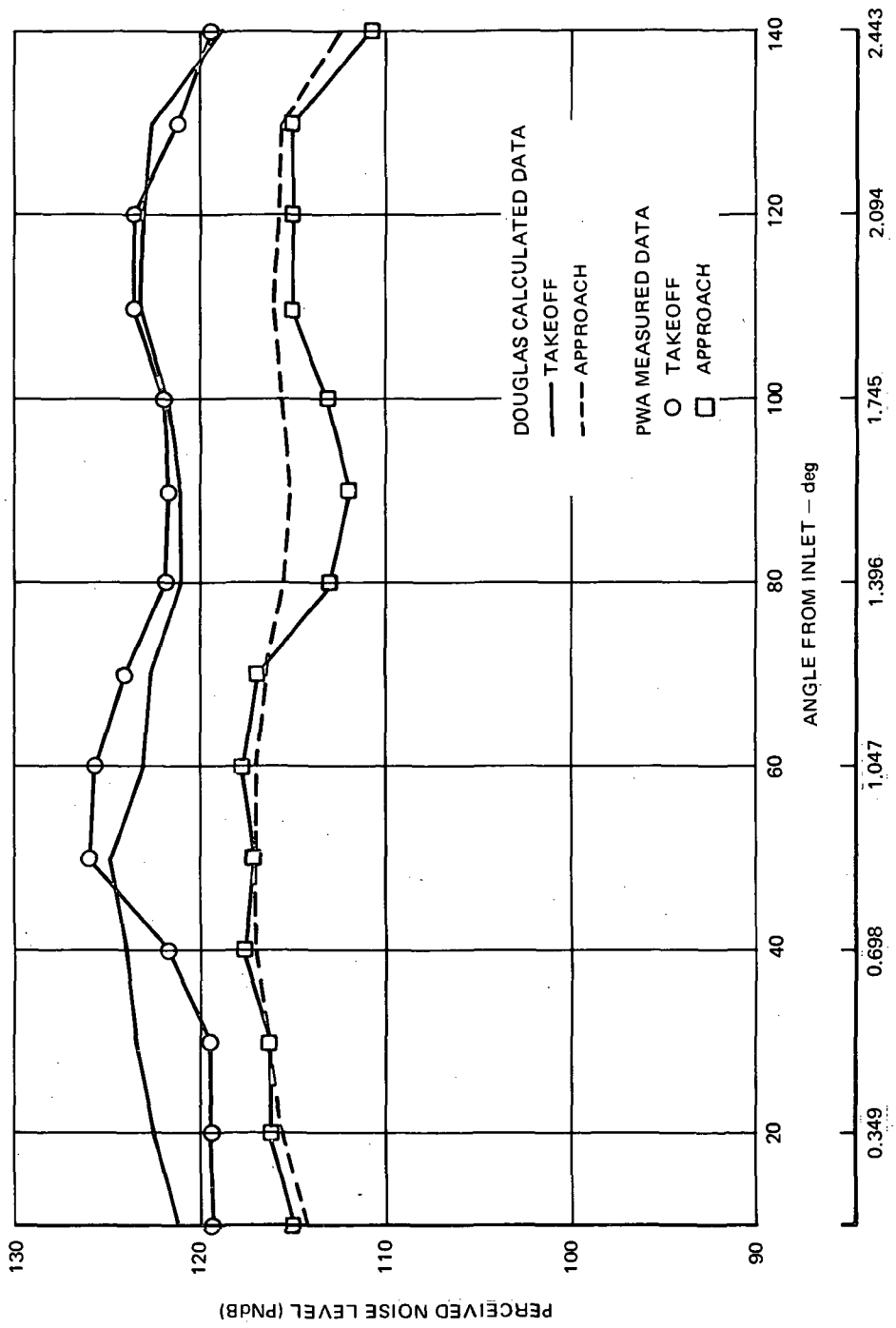

FIGURE A-2. PWA FAA HIGH TIP SPEED FAN NOISE COMPARISON, SEA LEVEL STATIC THRUST, 150 ft (46 m) RADIUS

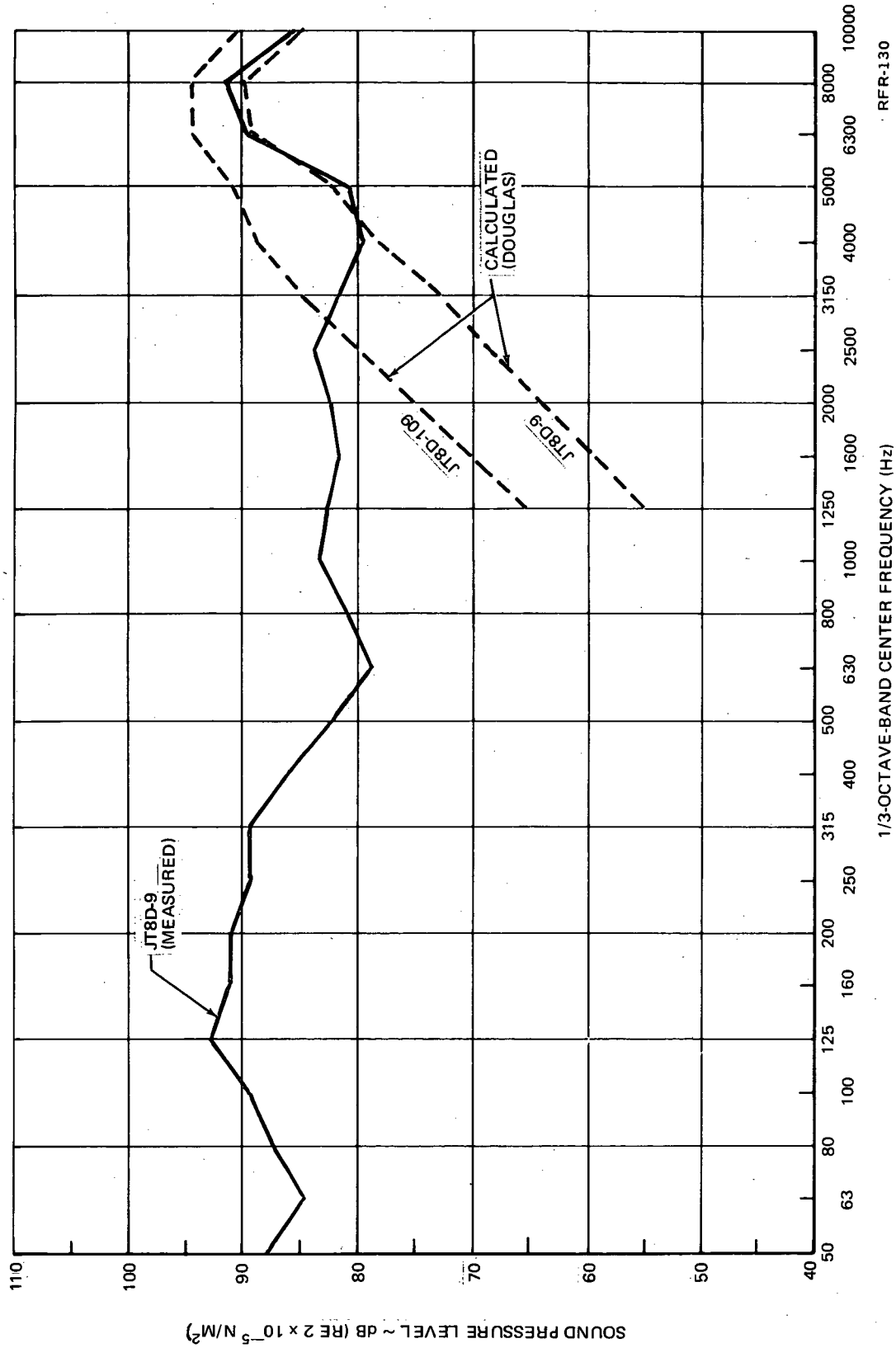

FIGURE A-3. JT8D TURBINE NOISE COMPARISON, ANGLE FROM INLET = 110 deg (1.920 rad), N_1 = 5337 rpm

APPENDIX A

Duct Internal Flow Conditions

Figures A-4 through A-12 describe the inlet and tailpipe internal flow conditions used as a basis for the acoustical treatment design. The maximum treated inlet is similar to the minimum treated inlet (figures A-4 to A-6) except for a 305 mm (12 in.) constant area extension near the fan face.

Predicted Flyover Noise Levels

This section presents selected predicted tone corrected perceived noise level flyover time histories and spectra for the untreated and treated refanned JT8D-109 engine. The FAR Part 36 approach condition is given the most attention because these spectra were used as the basis of the engine and nacelle acoustical treatment design. Spectra are also provided for the sideline condition to show the effect of engine thrust level on the relative levels of the noise sources.

The tone corrected perceived noise level (PNL_t) flyover time histories for the untreated refan noise sources at approach are shown on figure A-13 and the sound pressure level and NOY weighted spectra for the peak aft and forward radiated noise are shown on figures A-14 and A-15. These figures show that fan tones are the dominant noise source at approach. An exercise was performed to determine the percentage of fan duct treatment tuned to the blade passage frequency of 3150 Hz or to the harmonic of 6300 Hz to result in maximum fan duct PNL suppression. This optimization, figure A-16, shows that optimum suppression occurs with 60 percent of the fan duct treatment tuned to 3150 Hz. The fan duct treatment supplied with the engine has 75 percent of the treatment tuned to 3150 Hz. Figure A-16 shows this is a penalty of about 1 PNdB considering the fan duct alone. The tailpipe treatment, however, gives additional fan noise suppression, and was optimized together with the fan duct. Figure A-17 shows the minimum and maximum tailpipe optimization procedure for both the P&WA supplied fan duct and the independently optimized Douglas fan duct. The optimization showed that the tailpipes should be treated for the harmonic of 6300 Hz. As the minimum tailpipe is progressively treated for 6300 Hz, the overall tone corrected PNL becomes practically identical for both the P&WA supplied and the Douglas optimized fan ducts. The maximum tailpipe optimizes at 100 percent of the treatment tuned at 6300 Hz for the P&WA supplied fan duct and at 80 percent tuned to 6300 Hz for the independently optimized fan duct. The overall suppression at both of the optimums is nearly the same because the P&WA fan duct has more treatment tuned to 3150 Hz than does the optimized fan duct, the tailpipe corrects this imbalance by optimizing at different treatment splits for each fan duct. The tailpipes are also effective in attenuating the turbine noise which becomes dominant at high frequencies when the fan noise is suppressed.

Attenuation spectra for the minimum and maximum treated inlets and tailpipes are shown on figures A-18 and A-19. The total attenuation of the

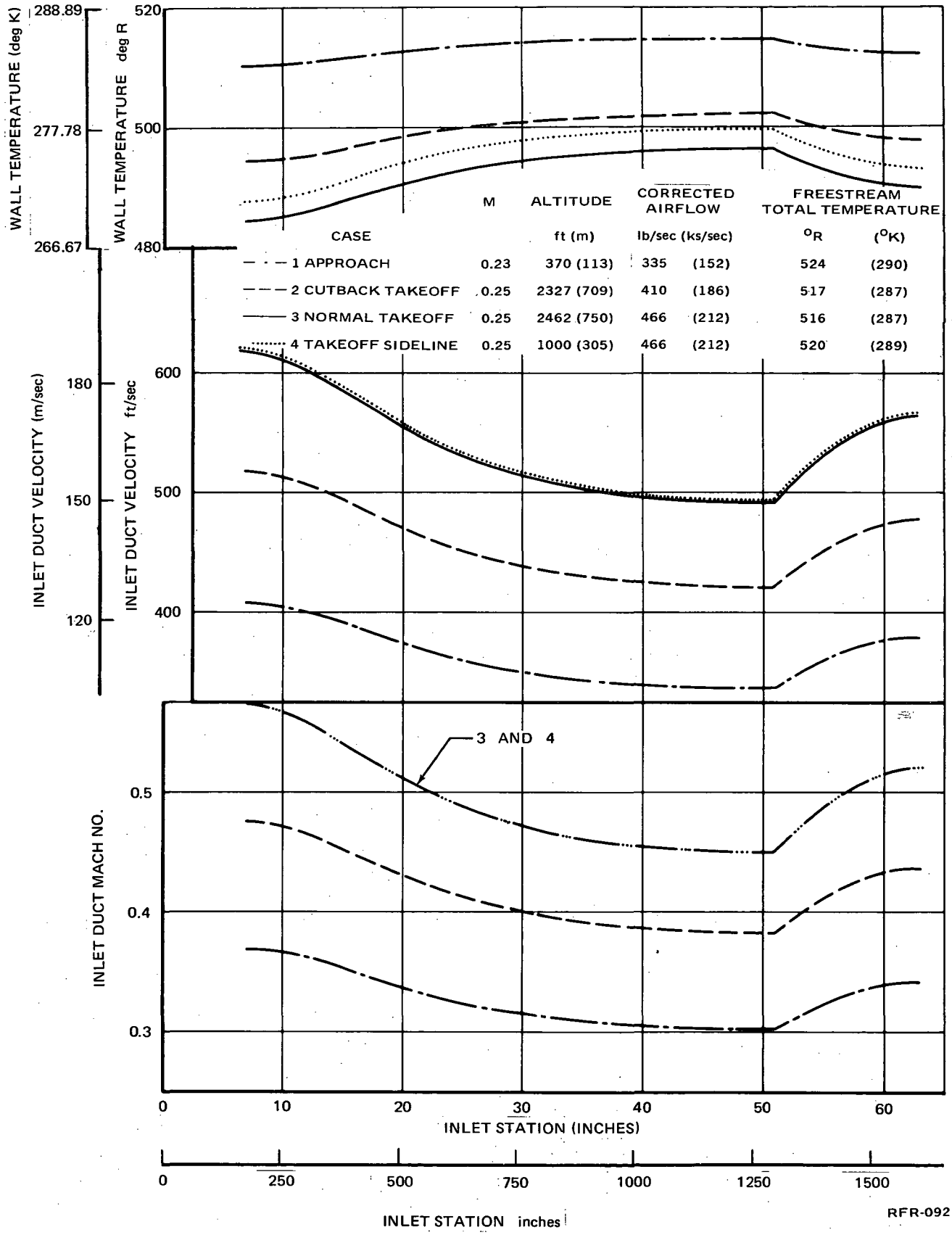

FIGURE A-4. ONE-DIMENSIONAL DUCT AIRFLOW PLOT FOR MINIMUM TREATED INLET

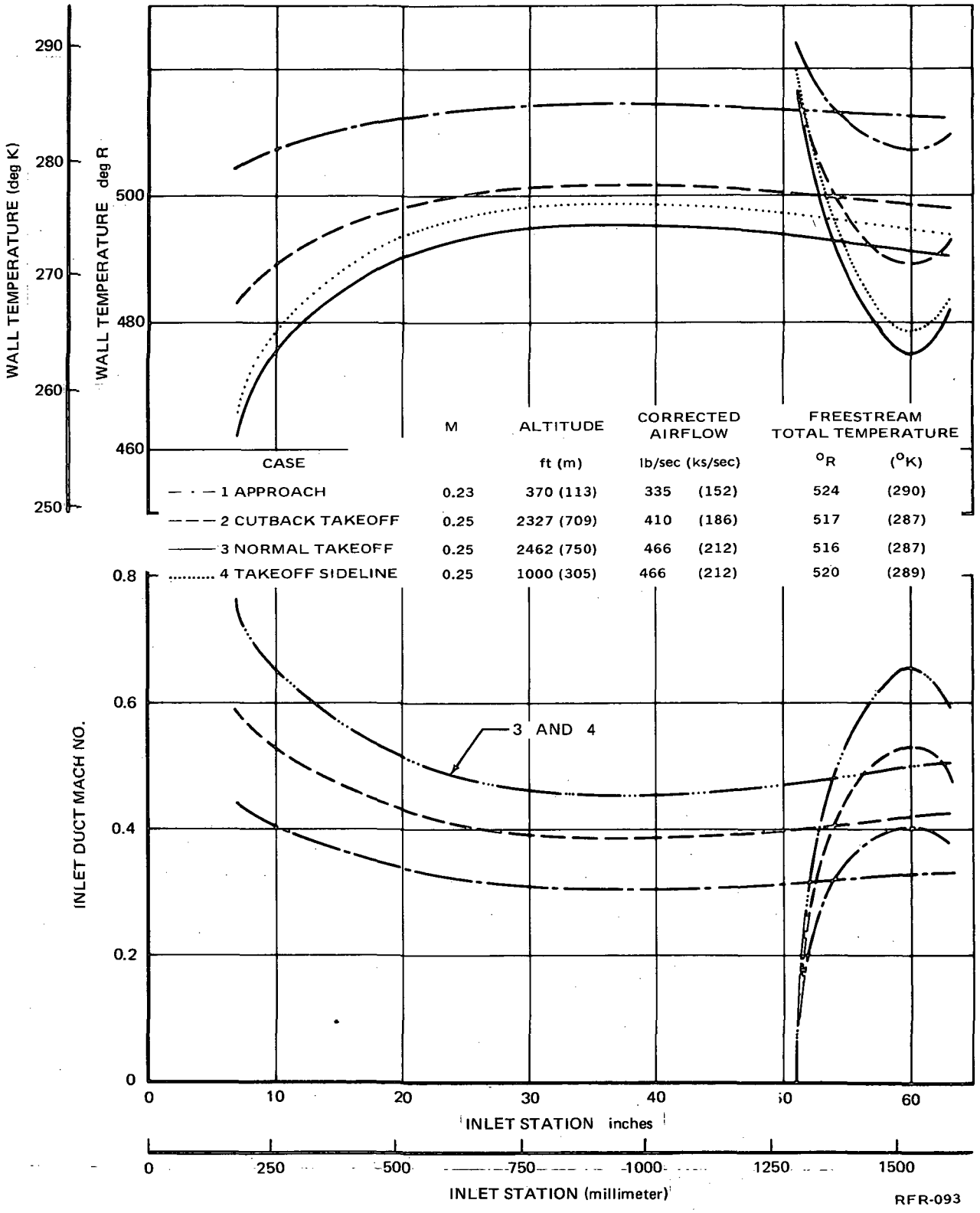

FIGURE A-5. AIRFLOW STATIC TEMPERATURE AND MACH NUMBER NEAR DUCT SURFACES FOR MINIMUM TREATED INLET

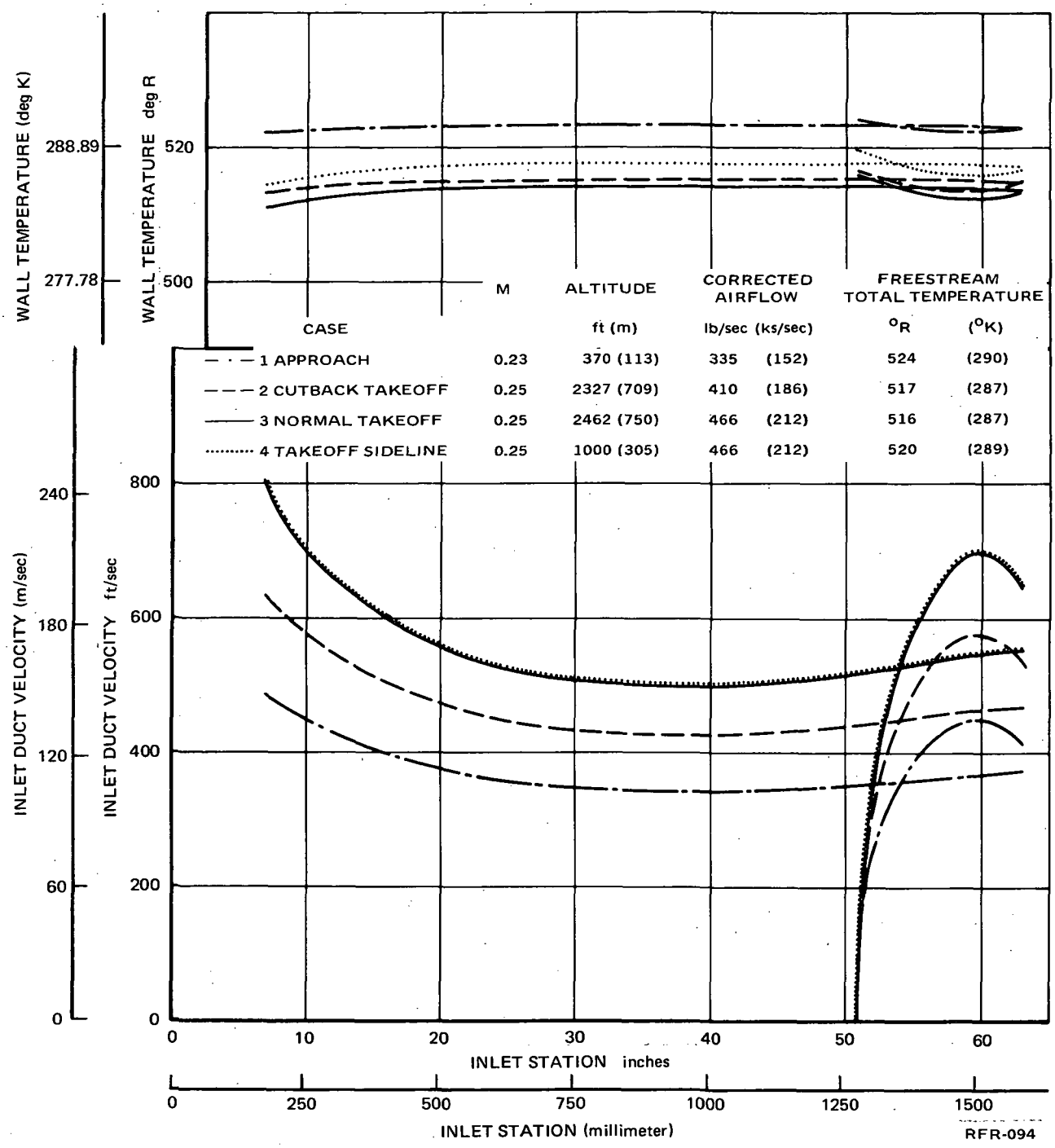

FIGURE A-6. WALL TEMPERATURE AND AIRFLOW VELOCITY NEAR DUCT SURFACES FOR MINIMUM TREATED INLET

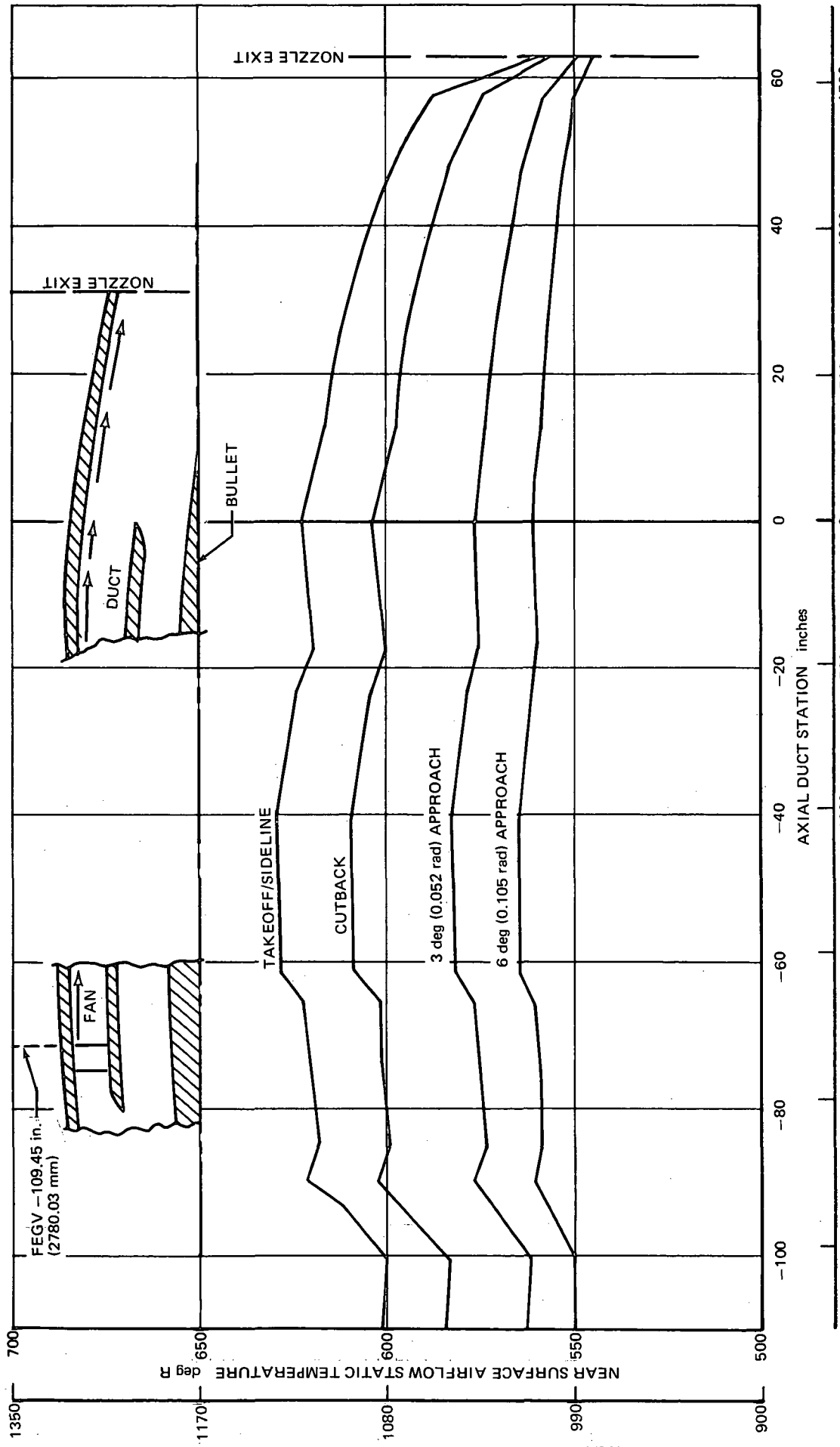

FIGURE A-7. FAN DUCT AND MINIMUM TAILPIPE AIRFLOW STATIC TEMPERATURE PLOT, TAILPIPE L/H = 1.65

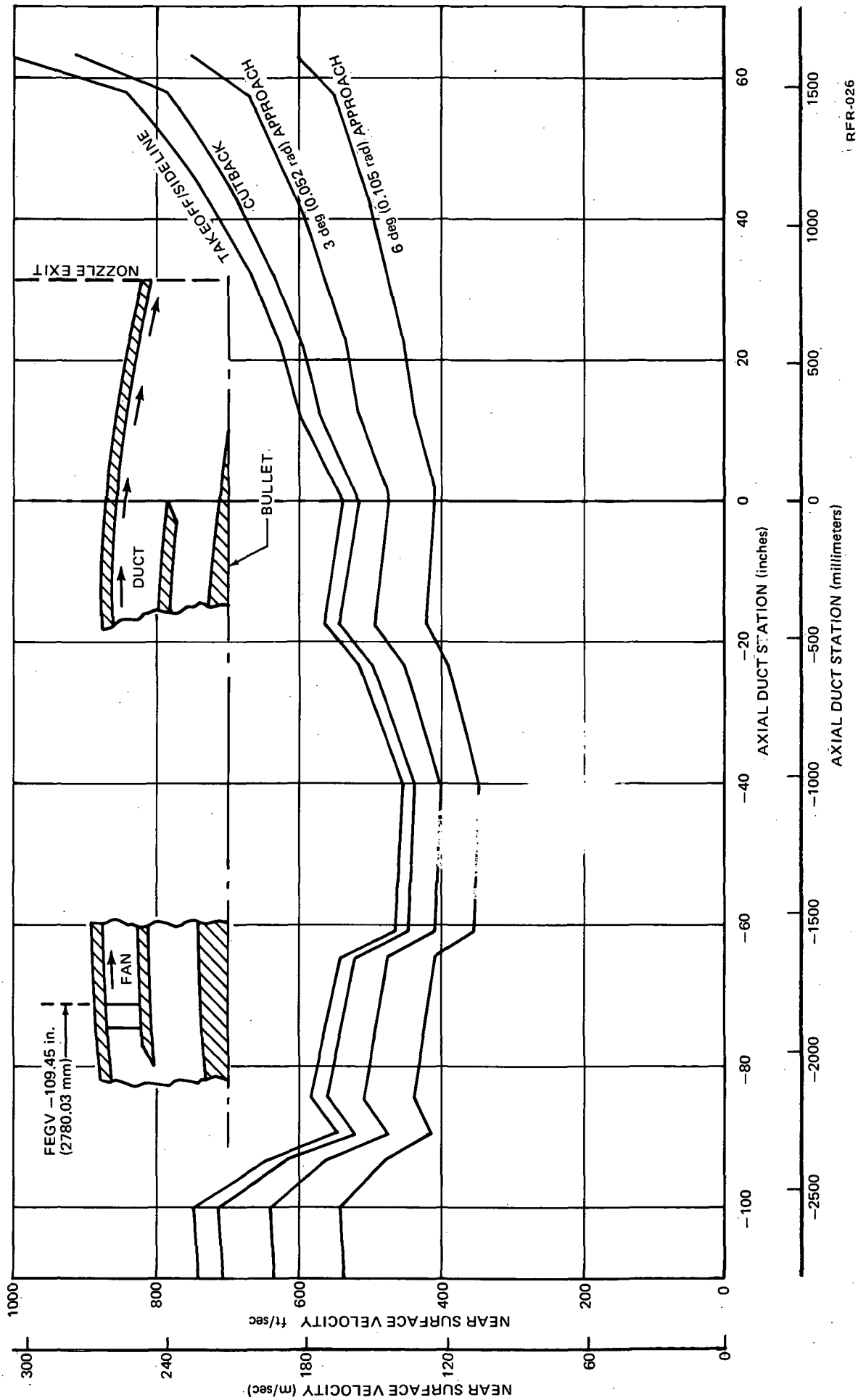

FIGURE A-8. FAN DUCT AND MINIMUM TAILPIPE AIRFLOW VELOCITY PLOT, TAILPIPE L/H = 1.65

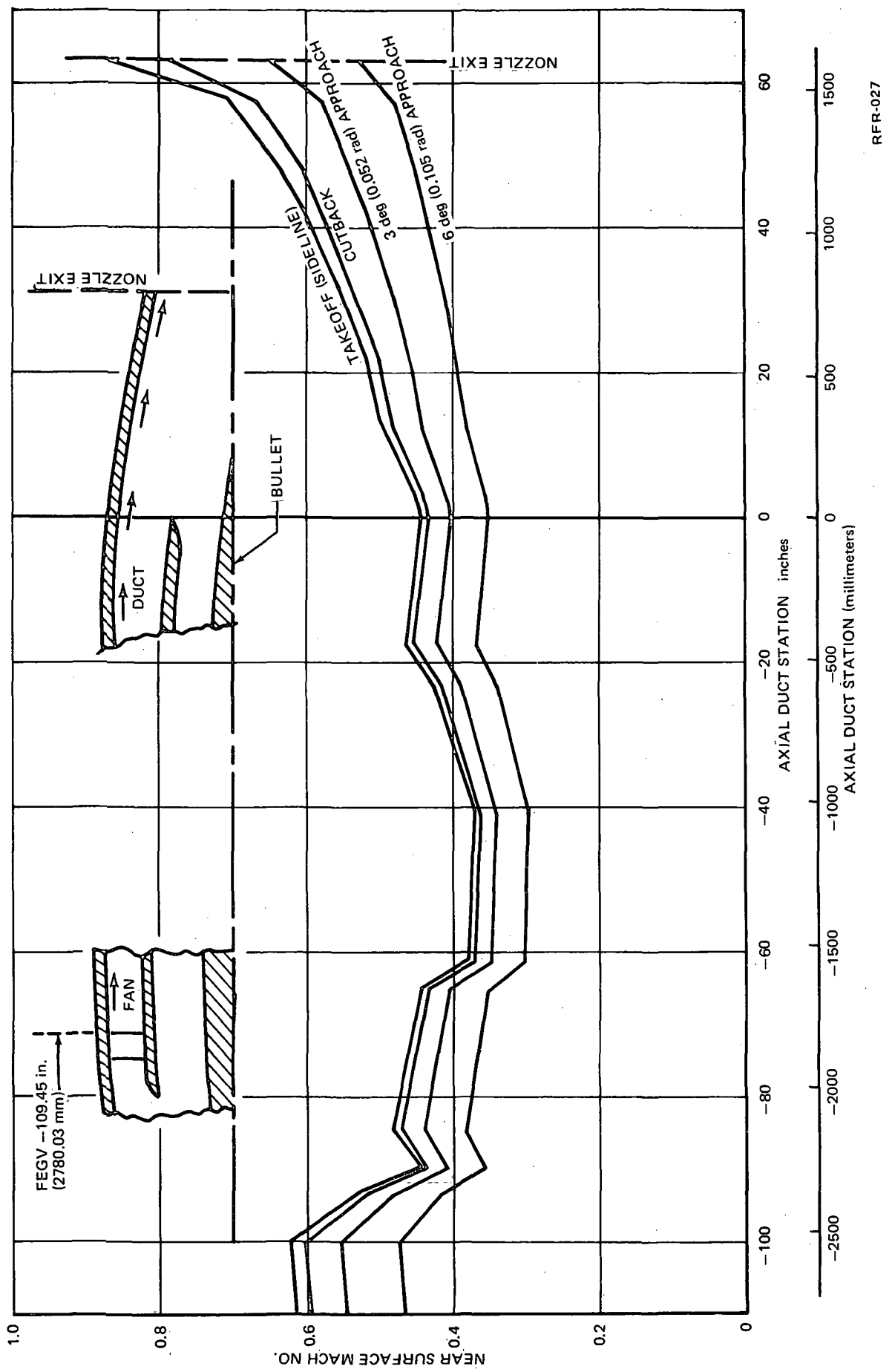

FIGURE A-9. FAN DUCT AND MINIMUM TAILPIPE AIRFLOW MACH NUMBER PLOT, TAILPIPE L/H = 1.65

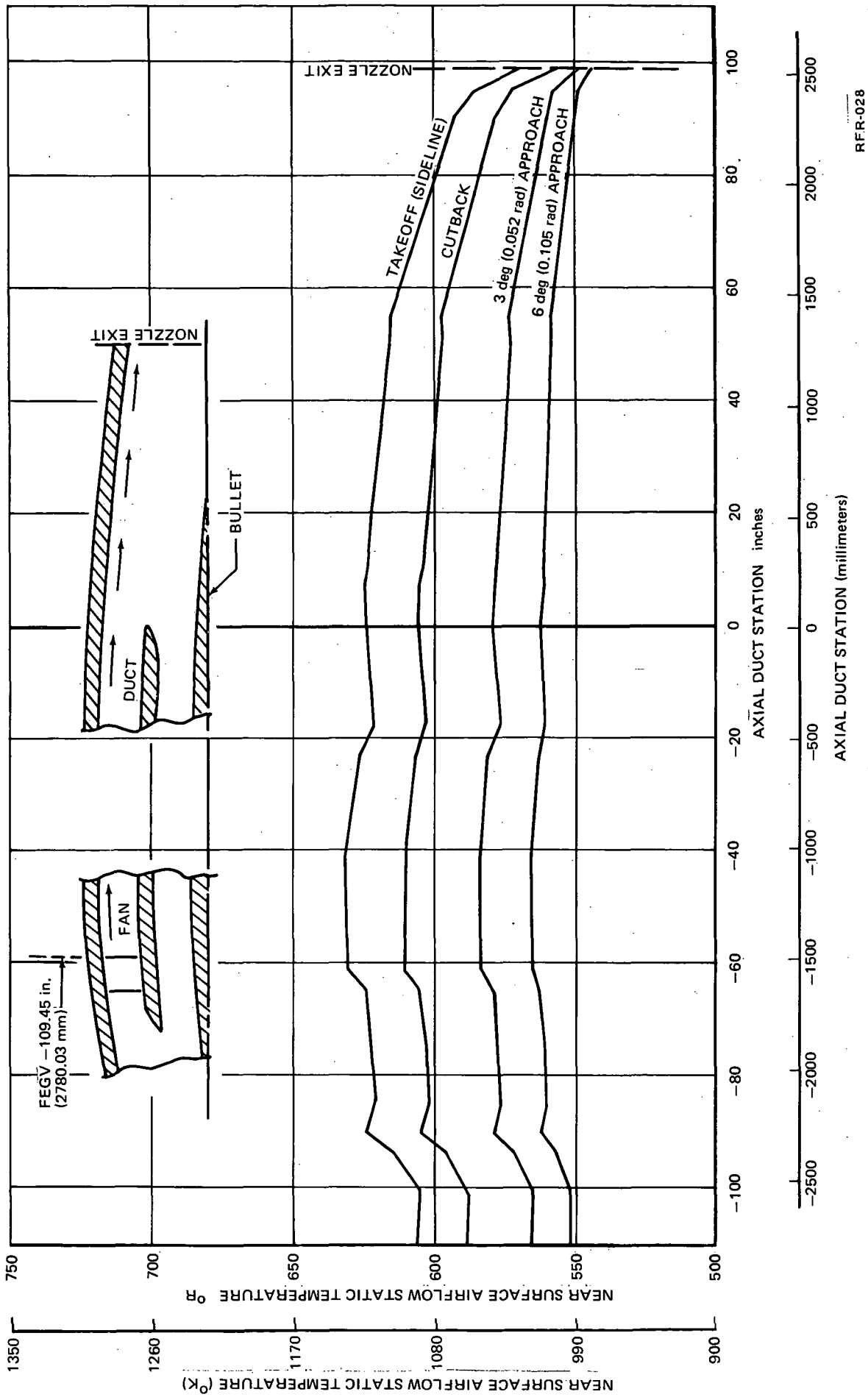

FIGURE A-10. FAN DUCT AND MAXIMUM TAILPIPE AIRFLOW STATIC TEMPERATURE PLOT, TAILPIPE L/H = 3.75

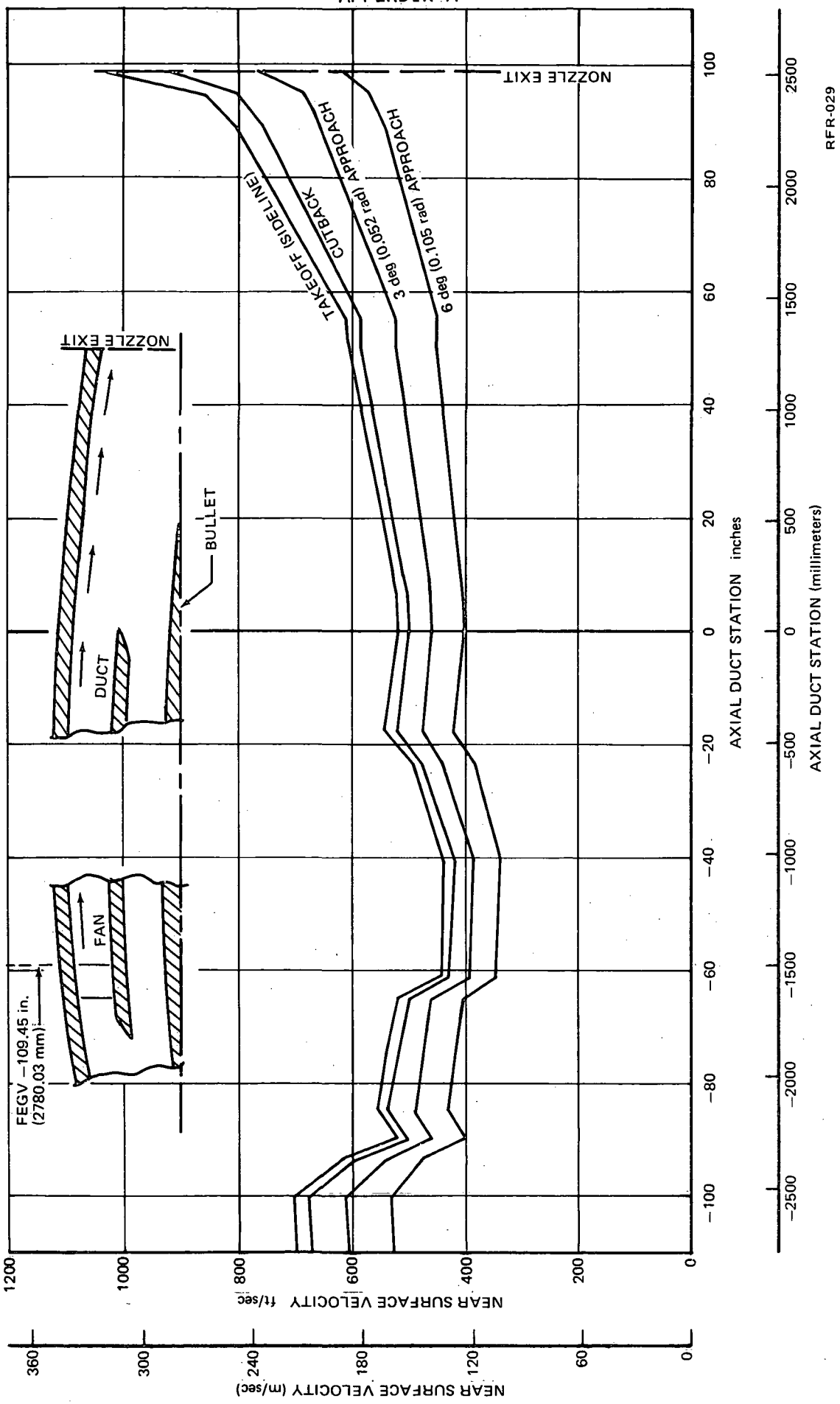

FIGURE A-11. FAN DUCT AND MAXIMUM TAILPIPE AIRFLOW VELOCITY PLOT, TAILPIPE L/H = 3.75

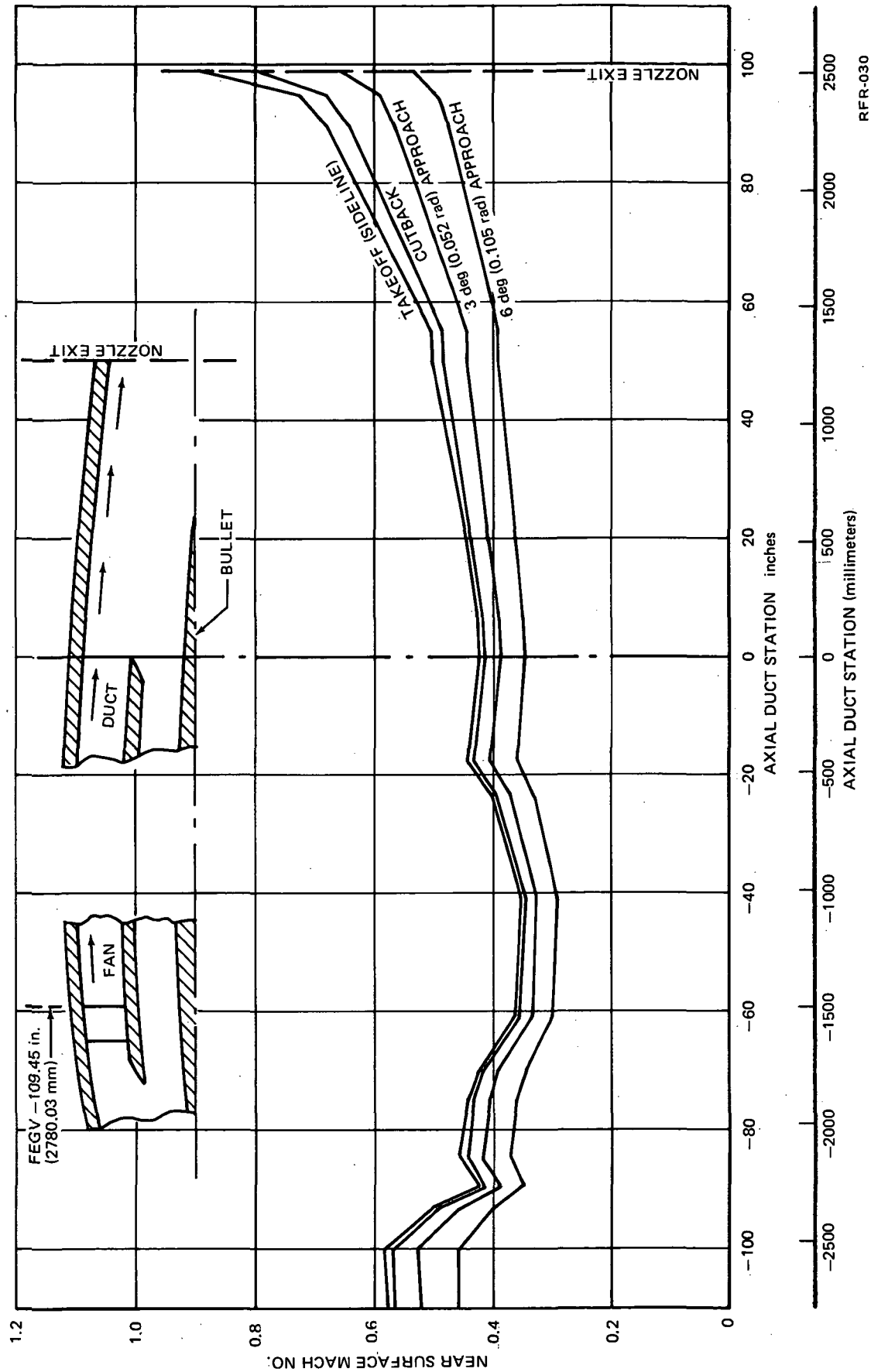

FIGURE A-12. FAN DUCT AND MAXIMUM TAILPIPE AIRFLOW MACH NUMBER PLOT, TAILPIPE L/H = 3.75

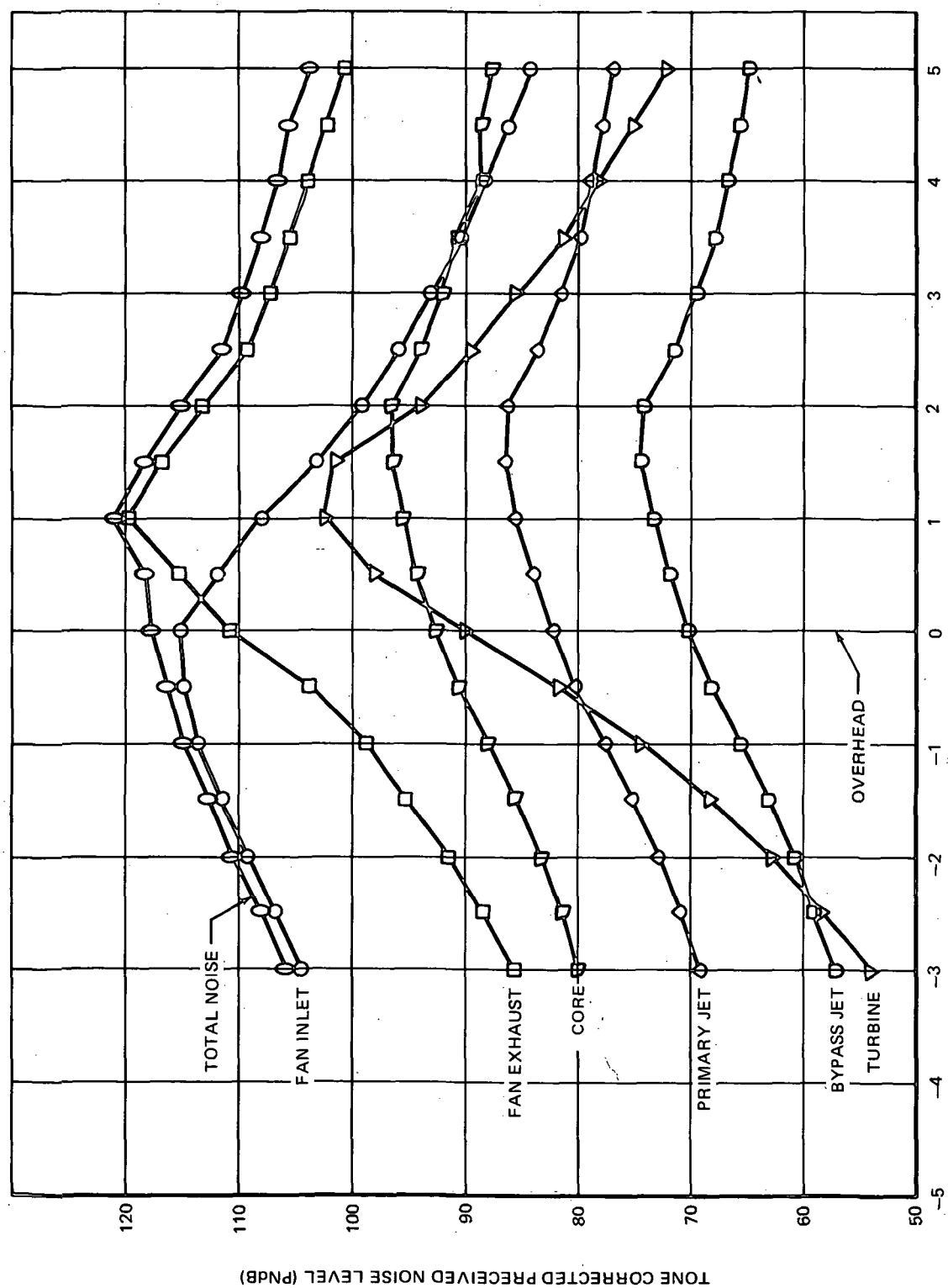

FIGURE A-13. PNLT VERSUS TIME AT FAR PART 36 APPROACH OPERATION FOR UNTREATED DC-9 AIRCRAFT WITH REFANNED JT8D ENGINES, ALTITUDE = 370 ft (113 m), N_1 = 5340 rpm

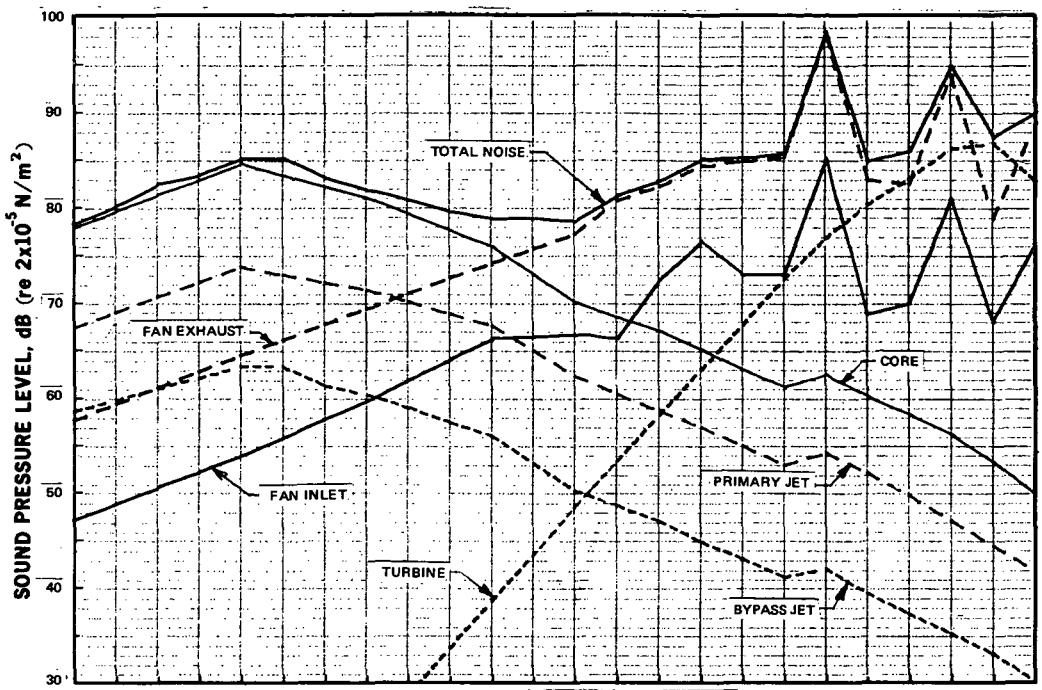

(a) SOUND PRESSURE LEVEL SPECTRA

NOISE SOURCE	PNL	PNLT
FAN INLET	103.0	107.7
FAN EXHAUST	115.3	120.0
TURBINE	102.7	102.7
CORE	95.8	95.8
PRIMARY JET	85.9	85.9
BYPASS JET	74.0	74.0
TOTAL	117.1	121.4

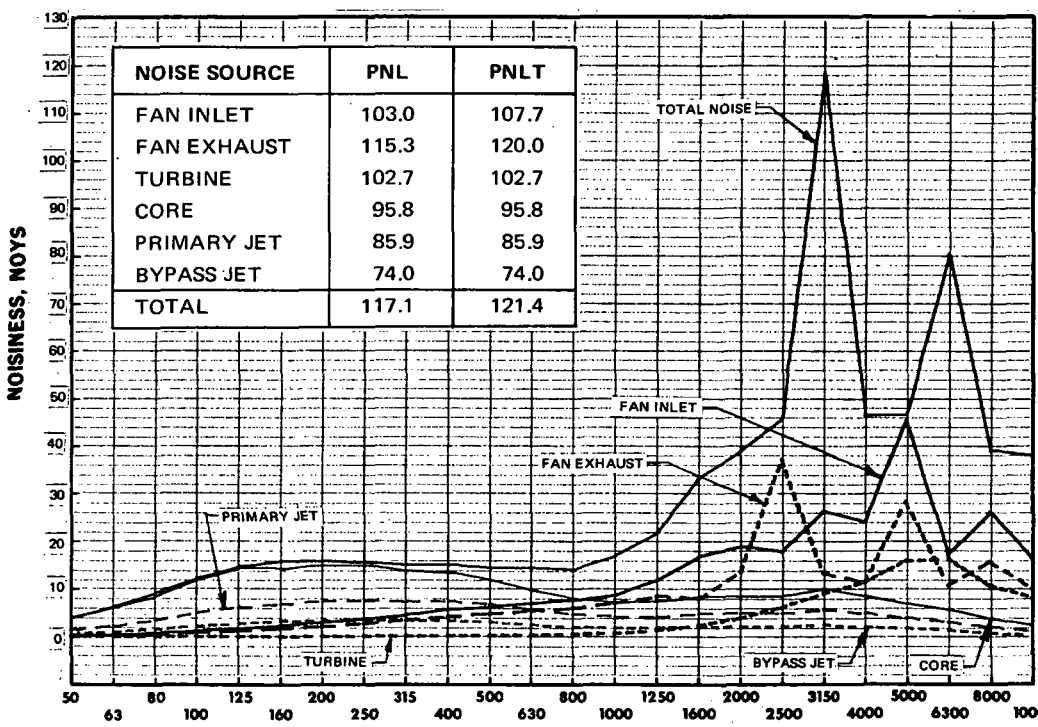

(b) PERCEIVED NOISINESS SPECTRA

RFR-108

FIGURE A-14. UNTREATED SPECTRA AT FAR PART 36 APPROACH OPERATION FOR ANGLE OF PEAK EXHAUST NOISE 109 deg (1.89 rad), ALTITUDE = 370 ft (113 m), N_1 = 5340 rpm, THRUST = 5411 lb (24 068 N)

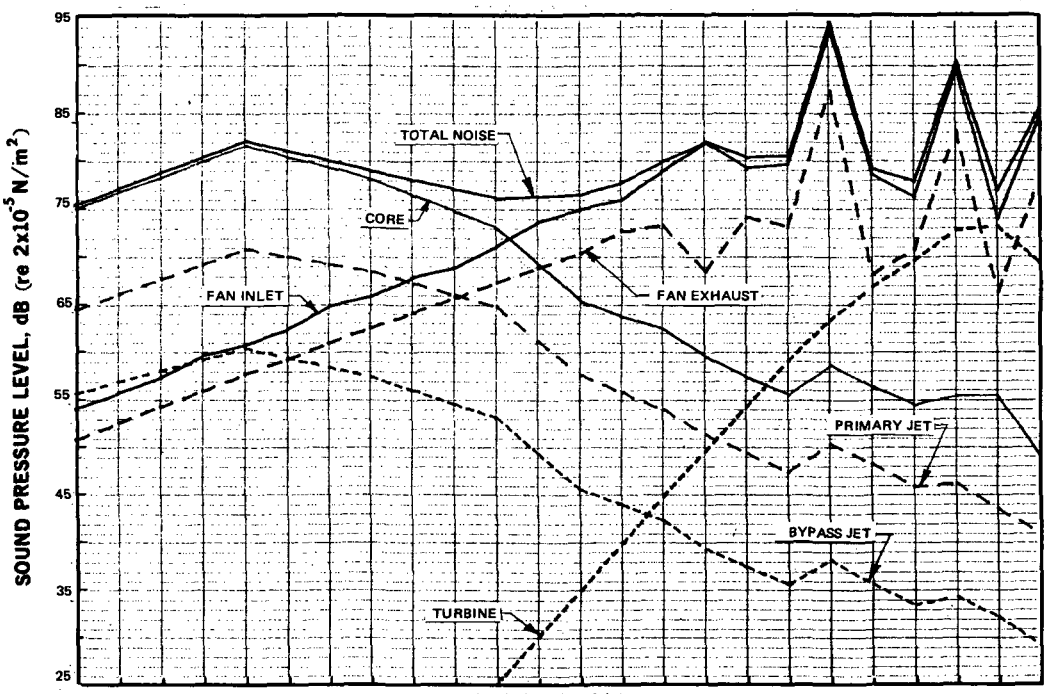

(a) SOUND PRESSURE LEVEL SPECTRA

NOISE SOURCE	PNL	PNLT
FAN INLET	110.3	115.6
FAN EXHAUST	104.9	104.9
TURBINE	89.1	89.1
CORE	92.4	92.4
PRIMARY JET	82.4	82.4
BYPASS JET	70.5	70.5
TOTAL	112.8	117.7

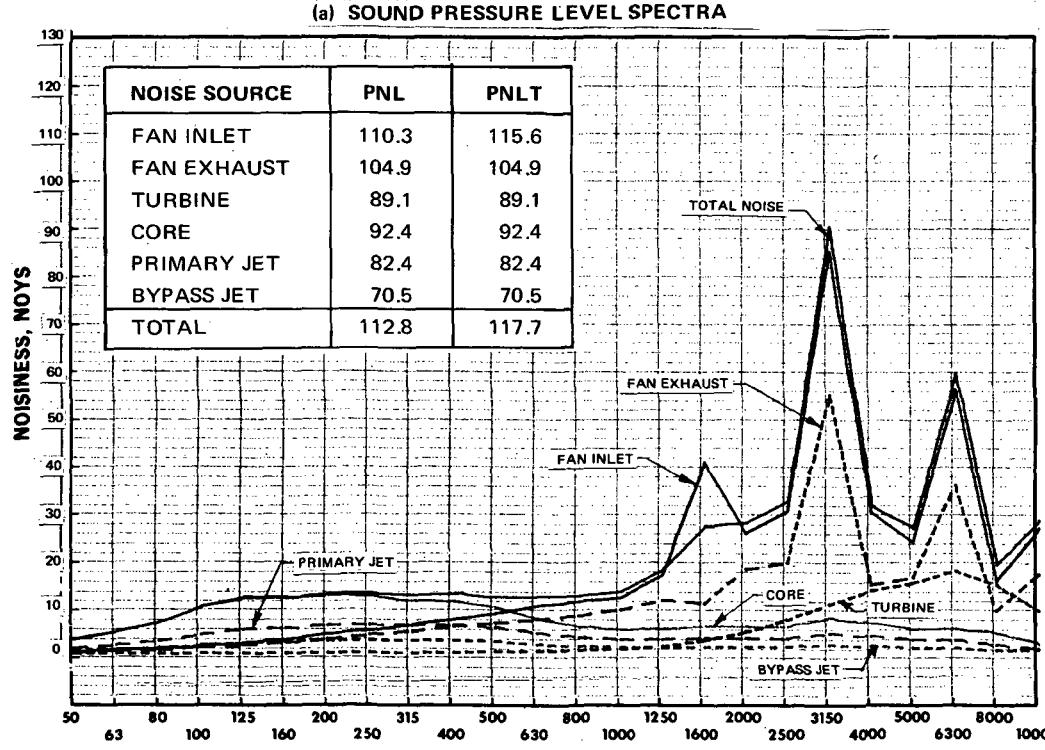

(b) PERCEIVED NOISINESS SPECTRA

RFR-110

FIGURE A-15. UNTREATED SPECTRA AT FAR PART 36 APPROACH OPERATION FOR ANGLE OF PEAK INLET NOISE 69 deg (1.204 rad), ALTITUDE = 370 ft (113 m), N_1 = 5340 rpm, THRUST = 5411 lb (23 752 N)

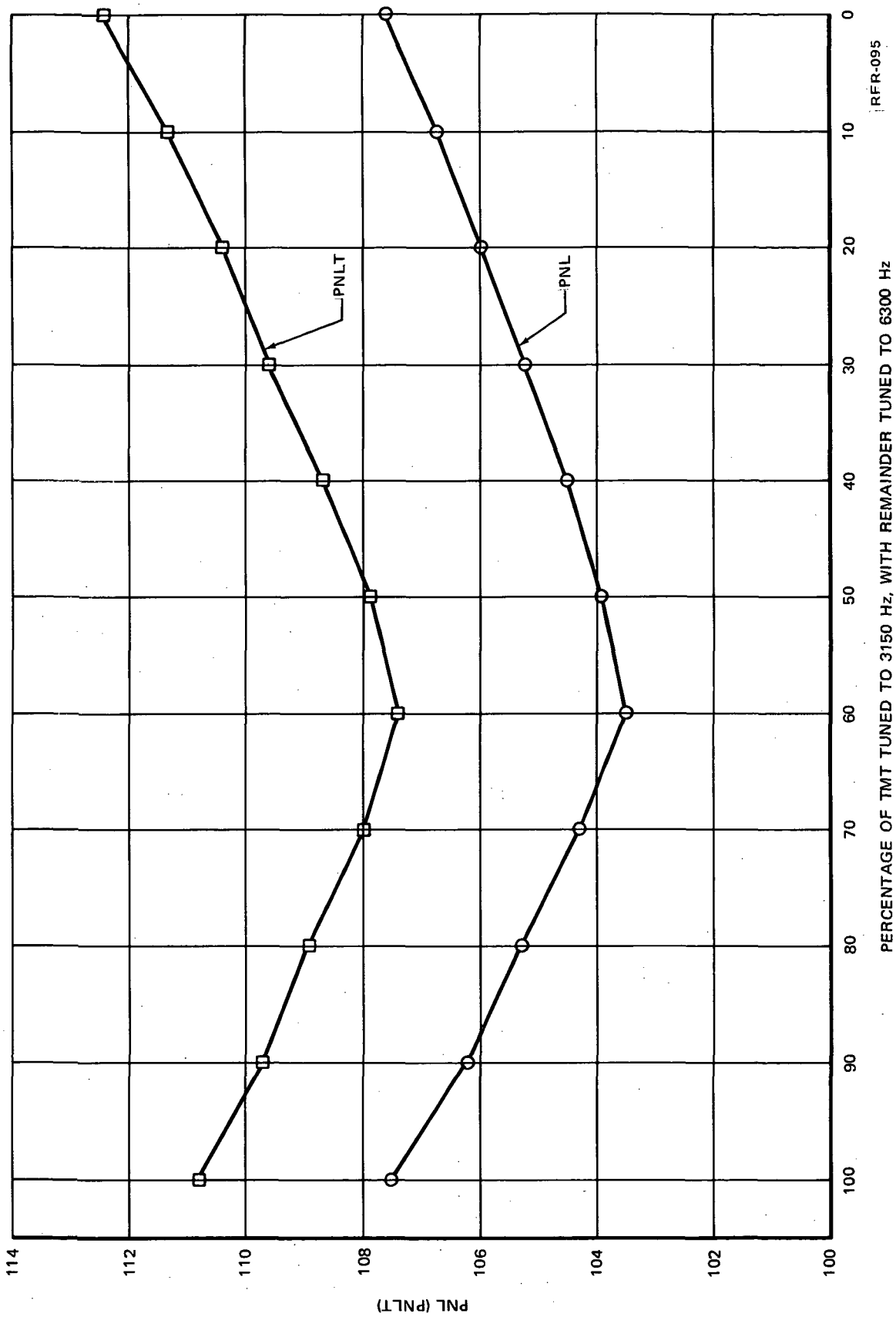

FIGURE A-16. FAN DUCT TREATMENT OPTIMIZATION PLOT FOR FAR PART 36 APPROACH OPERATION, TREATED FAN DUCT + UNTREATED TAILPIPE NOISE LEVELS, PNL = 115.3, PNLT = 120.0 FAN DUCT TREATMENT L/H = 7.2

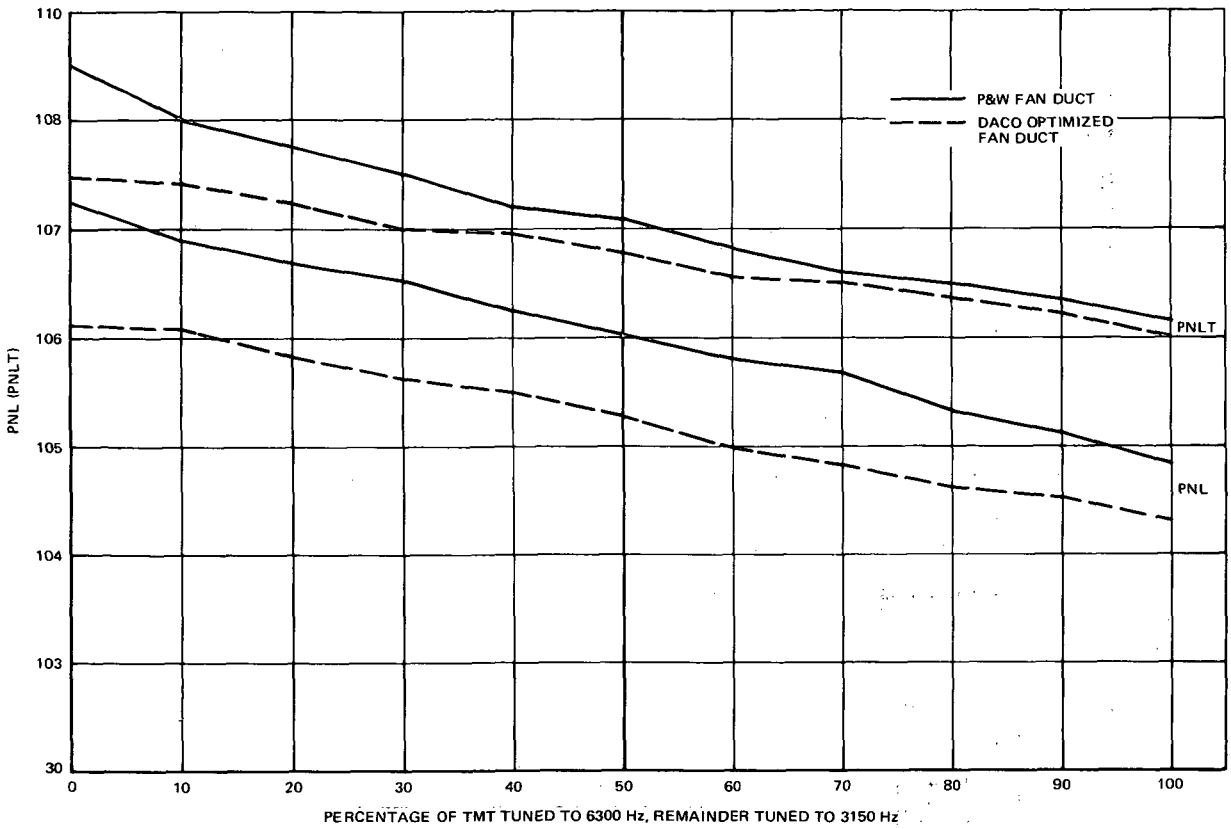

(a) MINIMUM TAILPIPE OPTIMIZATION, L/H = 1.65

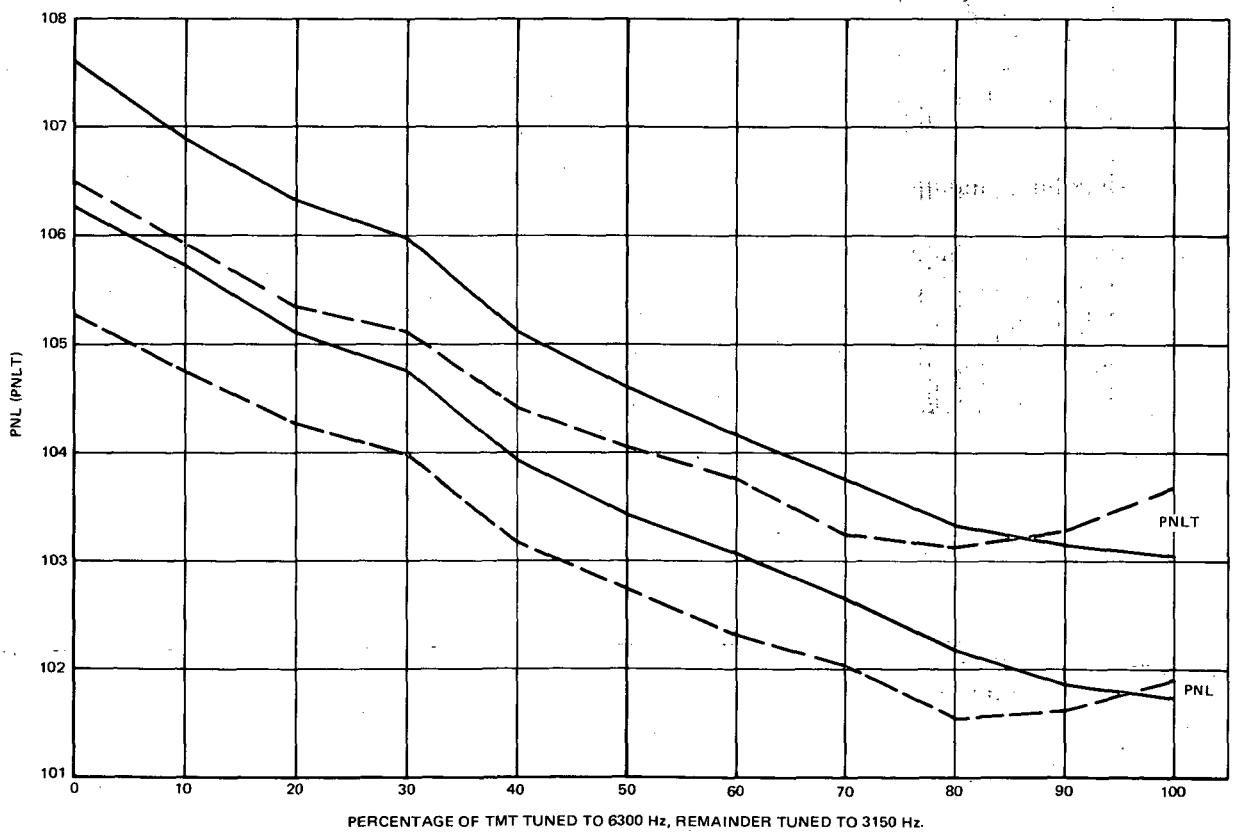

(b) MAXIMUM TAILPIPE OPTIMIZATION, L/H = 3.75

FIGURE A-17. TAILPIPE OPTIMIZATION PLOTS FOR FAR PART 36 APPROACH CONDITION

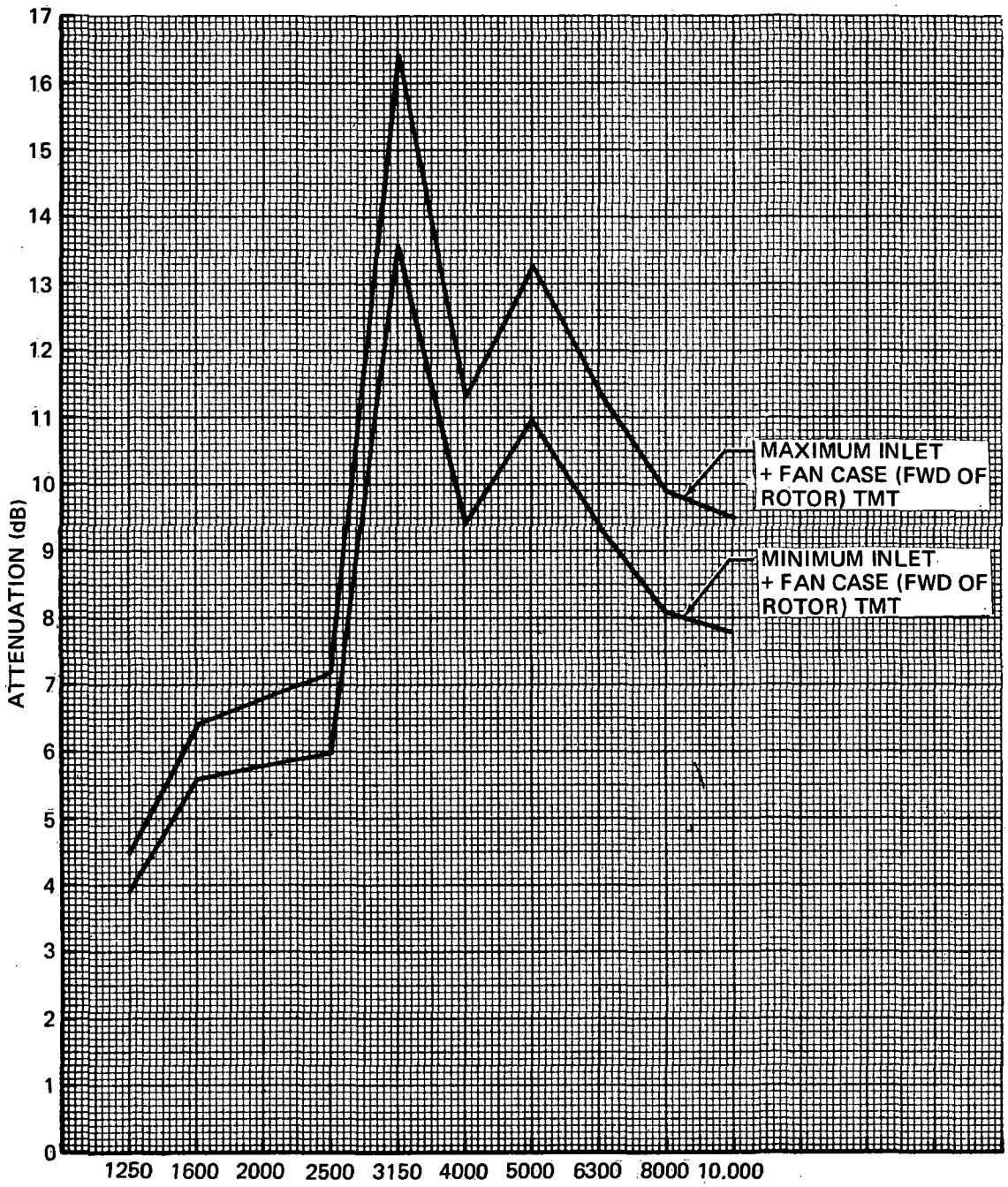

FIGURE A-18. ATTENUATION SPECTRA FROM MINIMUM AND MAXIMUM TREATMENT AT FAR PART 36 APPROACH OPERATION

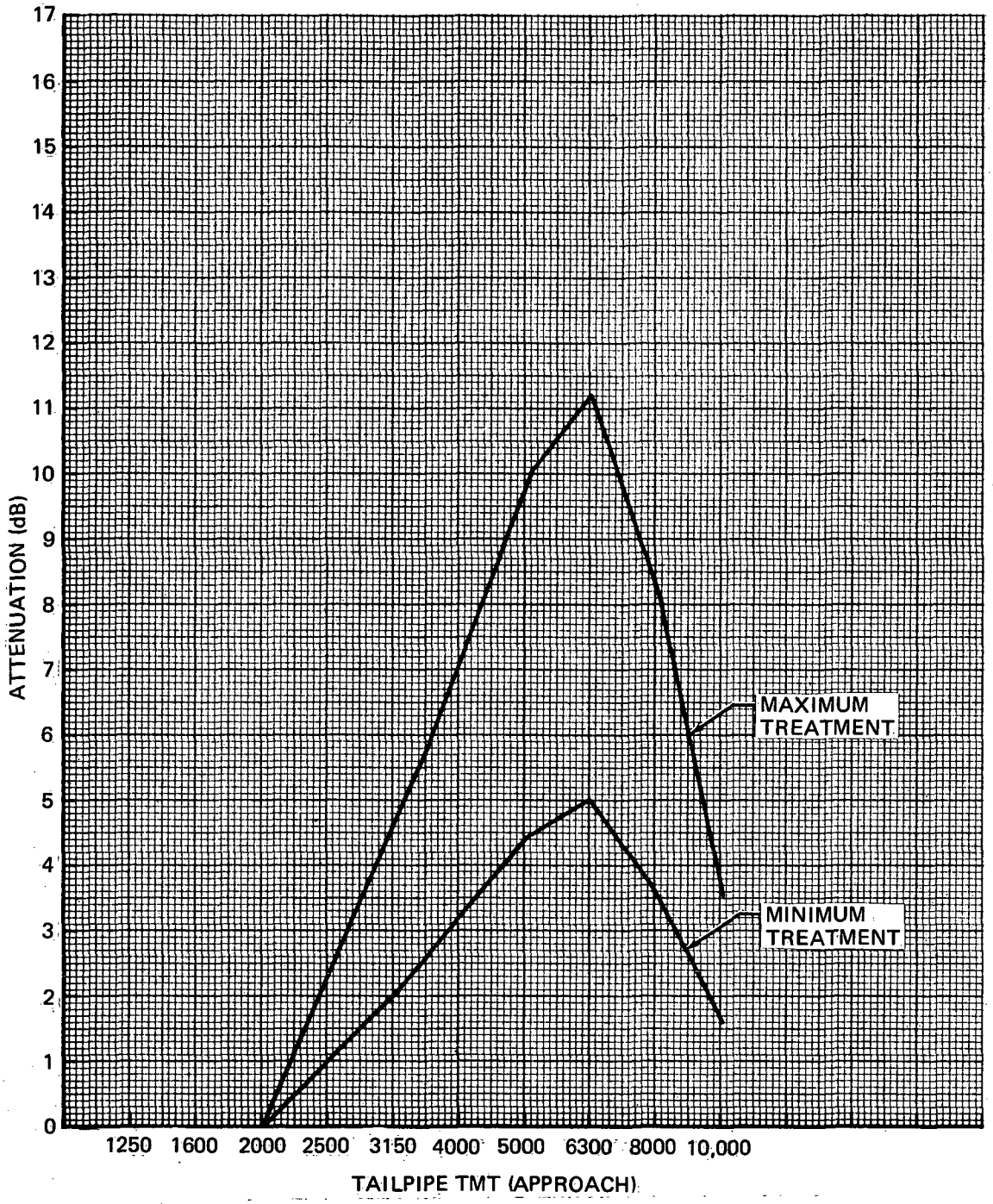

FIGURE A-19. ATTENUATION SPECTRA FROM MINIMUM AND MAXIMUM TAIL PIPE TREATMENT AT FAR PART 36 APPROACH OPERATION

treated fan duct, plus the maximum tailpipe, applied to fan discharge noise is shown on figure A-20. The tone corrected perceived noise level flyover time histories at approach for the minimum and maximum nacelle treatment are shown in figures A-21 and A-22. The approach spectra, for the minimum nacelle treatment, at angles of peak inlet and exhaust noise are shown on figure A-23. Comparing figures A-21 and A-22 shows that maximum nacelle treatment gives additional suppression from the minimum nacelle of about 1 PNdB on the inlet, 2.5 PNdB on the fan exhaust, and 4.5 PNdB on the turbine noise. The jet and core noise sources dilute the suppression on these turbomachinery noise sources to give lower overall noise reductions between the minimum and maximum level of treatment.

The prediction procedure for sideline, takeoff, cutback, and 0.104 rad (6 deg) approach was similar to the procedure used for the 0.052 rad (3 deg) FAR Part 36 approach, except the acoustic lining is in an off-design environment. The PNL_t time history for the untreated refanned DC-9 at the Part 36 cutback condition is shown on figure A-24. The spectra at peak exhaust and inlet noise level is shown on figures A-25 and A-26. The attenuation spectra at cutback power, figures A-27, A-28 and A-29, are similar to the approach spectra, except that the attenuation is slightly less effective than at approach because of the off-design conditions. The cutback PNL_t time history, with minimum and maximum levels of treatment, is shown on figure A-30. At this condition, the jet and core noise make a distinct contribution to the overall flyover noise. The spectra at the peak inlet and exhaust angle for cutback with the minimum nacelle treatment, figure A-31, show the relative levels of the turbomachinery, jet, and core noise sources.

PNL_t flyover time histories for the sideline and 0.104 rad (6 deg) approach conditions are shown on figures A-32 and A-33. The sideline noise, with the minimum nacelle treatment, is jet and core noise dominant. The 0.104 rad (6 deg) approach, with its very low power setting, is almost completely turbomachinery noise controlled.

DC-9-15 Refan Noise Contours

Noise contours of 90 and 95 EPNdB for the existing and refanned DC-9-15 with minimum nacelle treatment are shown on figures A-34 through A-37. The existing DC-9-15 uses JT8D-7 or -7A engines, and JT8D-109 engines are used on the refanned DC-9-15. The contour format is similar to the contour format used for the DC-9-32 contours presented under "Acoustic Characteristics." The contours show comparisons for both typical mission and FAR Part 36 certification weights and the effect of takeoff cutback and two-segment approach operational procedures.

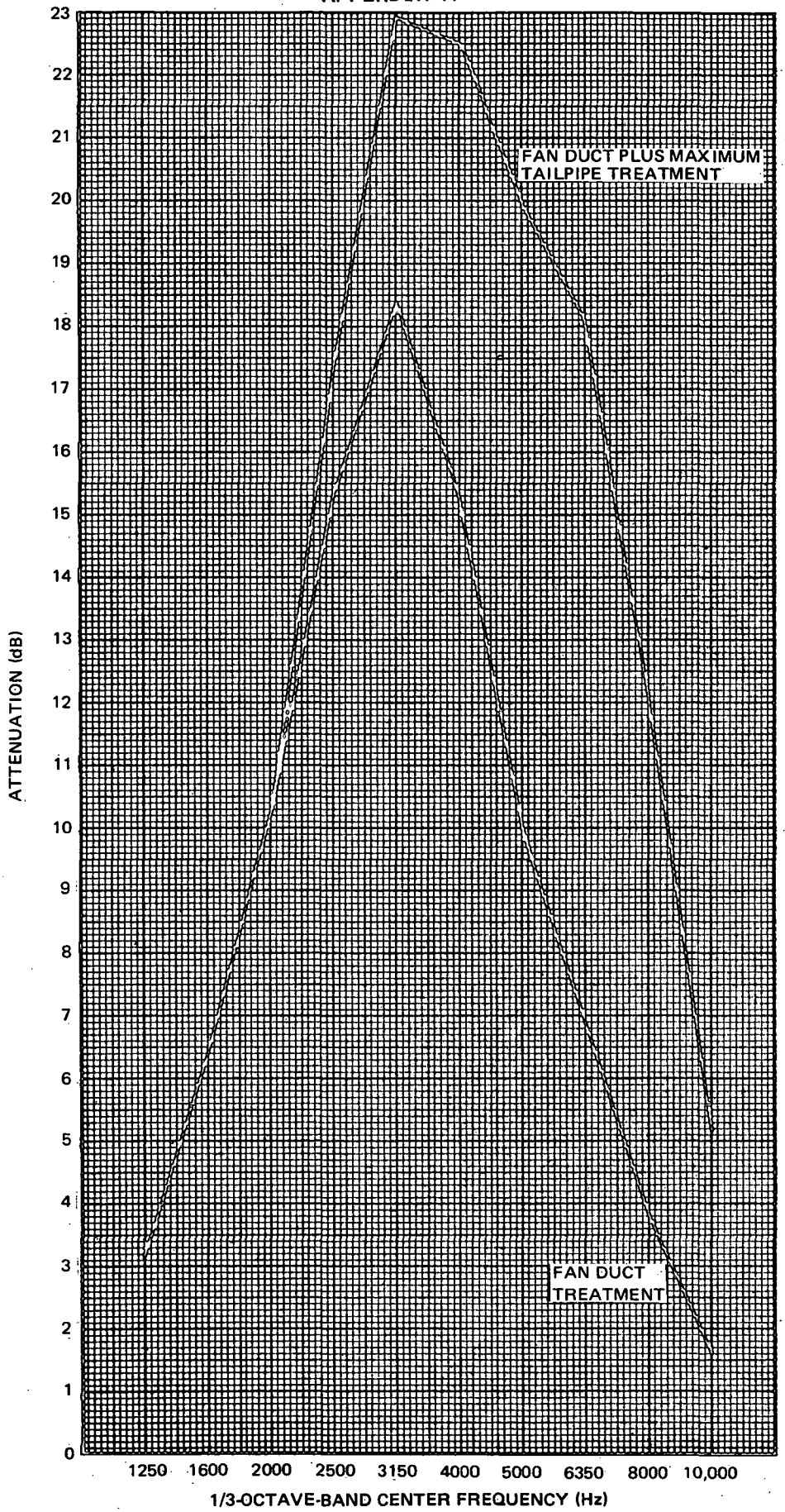

FIGURE A-20. ATTENUATION SPECTRA OF FAN EXHAUST NOISE FOR THE MAXIMUM TREATMENT CONFIGURATION AT FAR PART 36 APPROACH OPERATION

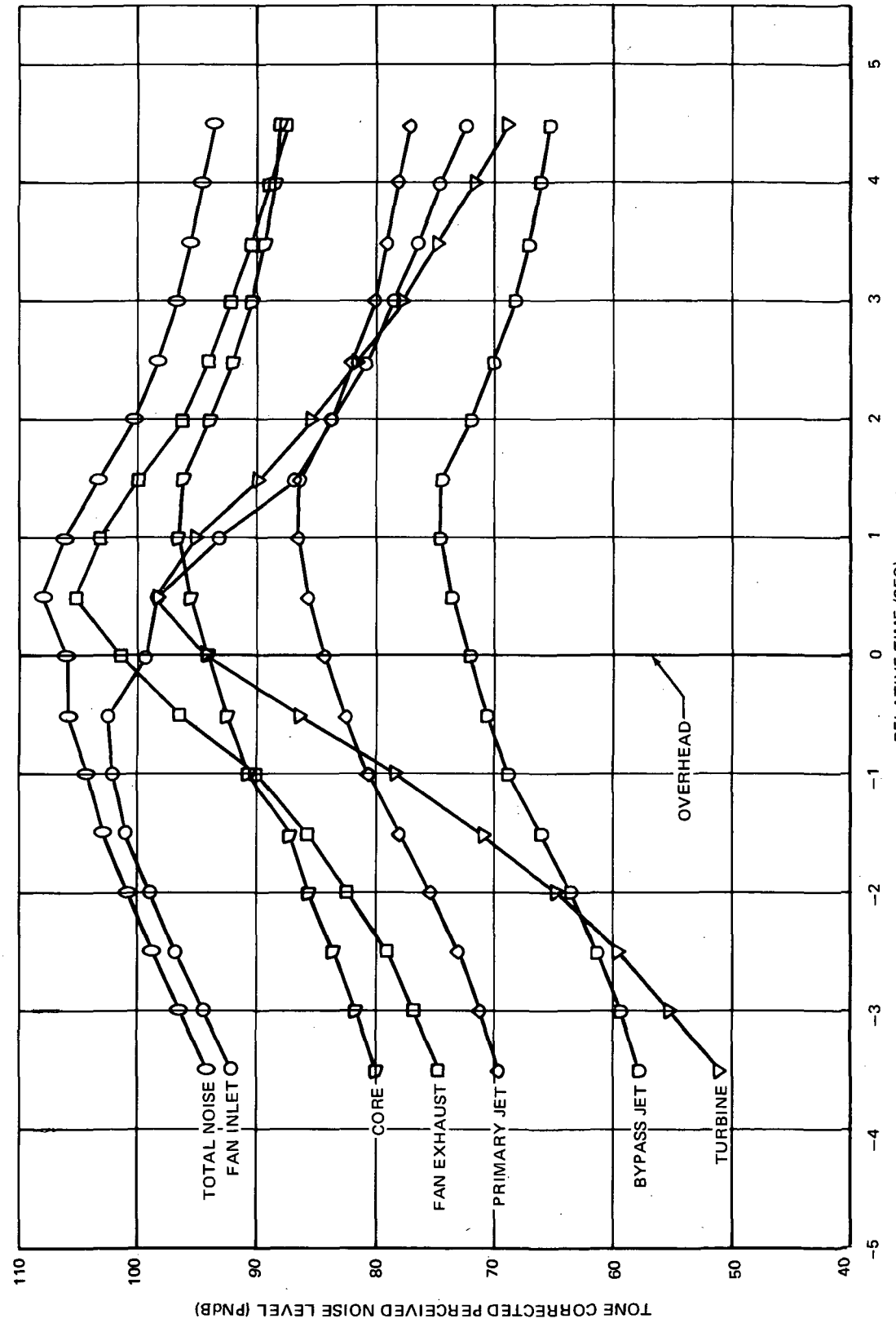

FIGURE A-21. PNLT VERSUS TIME AT FAR PART 36 APPROACH OPERATION FOR MINIMUM TREATED DC-9 AIRCRAFT, FOR ALTITUDE = 370 ft (113 m)

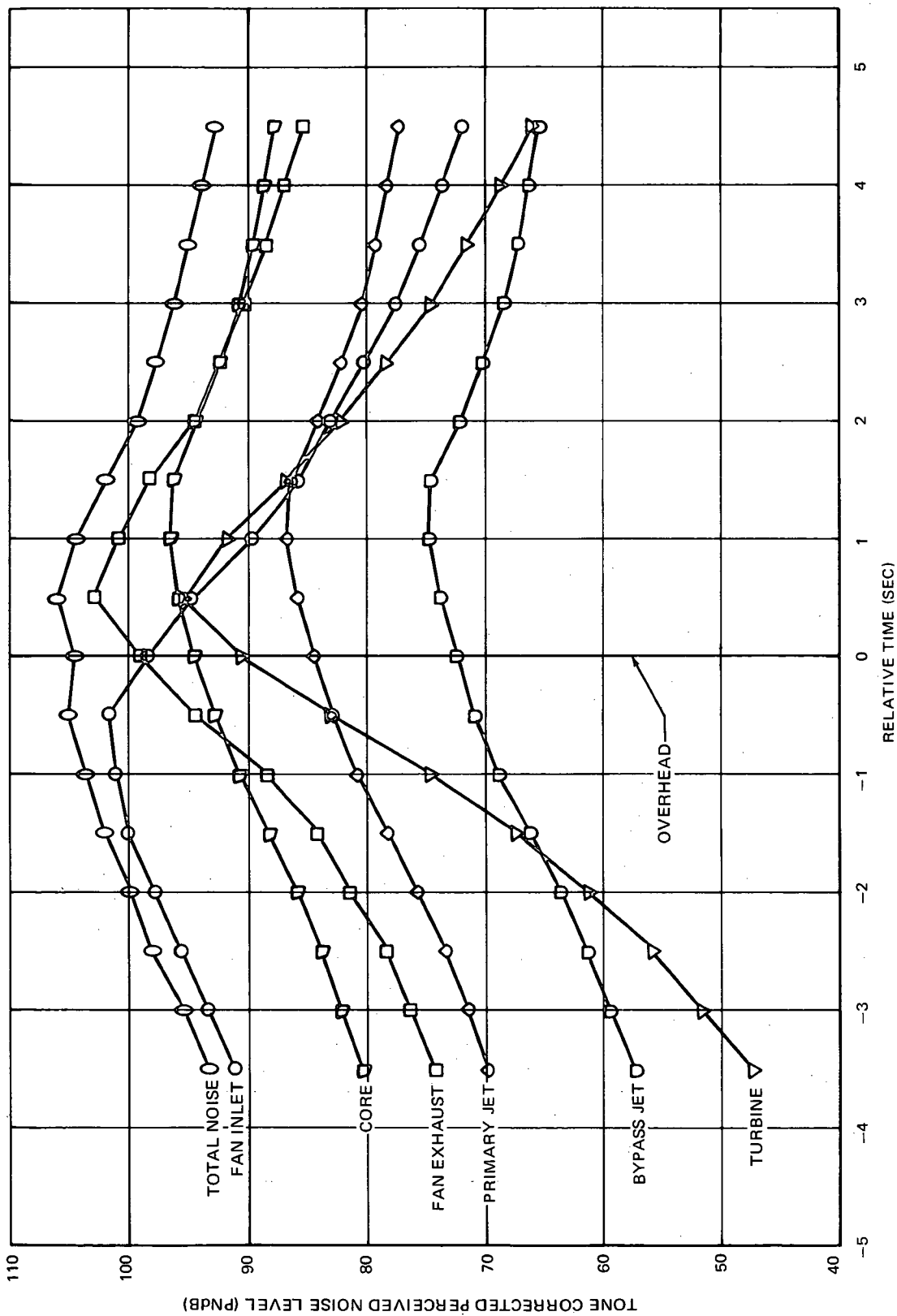

FIGURE A-22. PNLT VERSUS TIME AT FAR PART 36 APPROACH OPERATION FOR MAXIMUM TREATED DC-9 AIRCRAFT AT ALTITUDE = 370 ft (113 m), N_1 = 5385 rpm

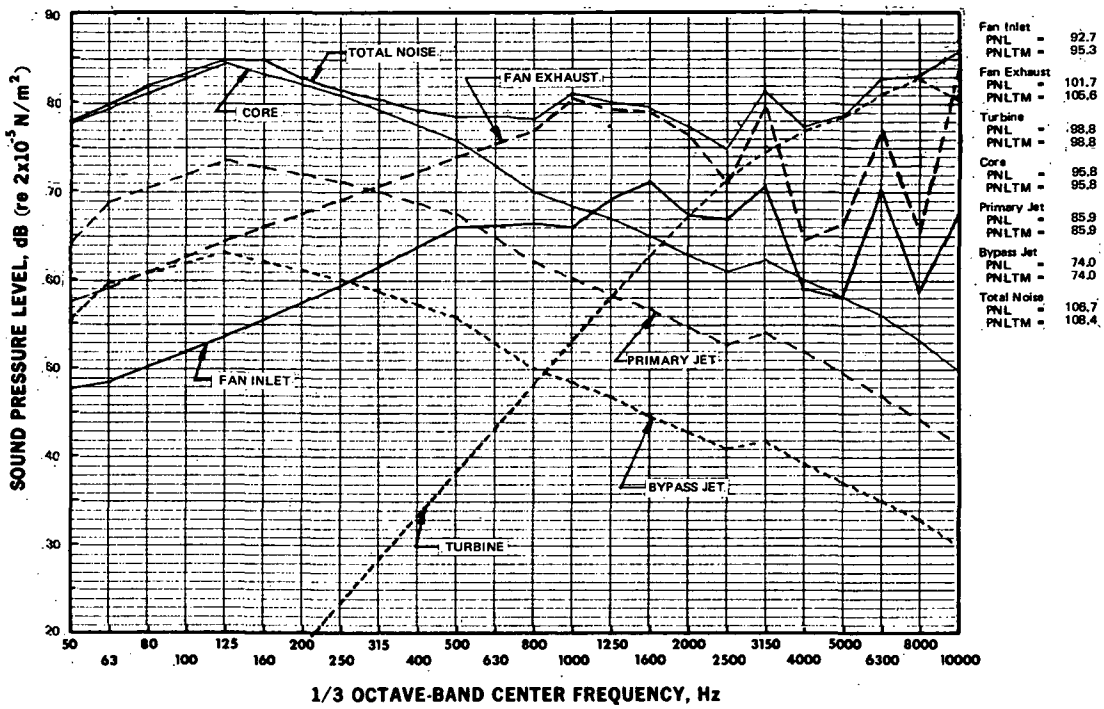

(a) PEAK INLET NOISE SPECTRA, ANGLE FROM INLET = 109 deg (1.89 rad)

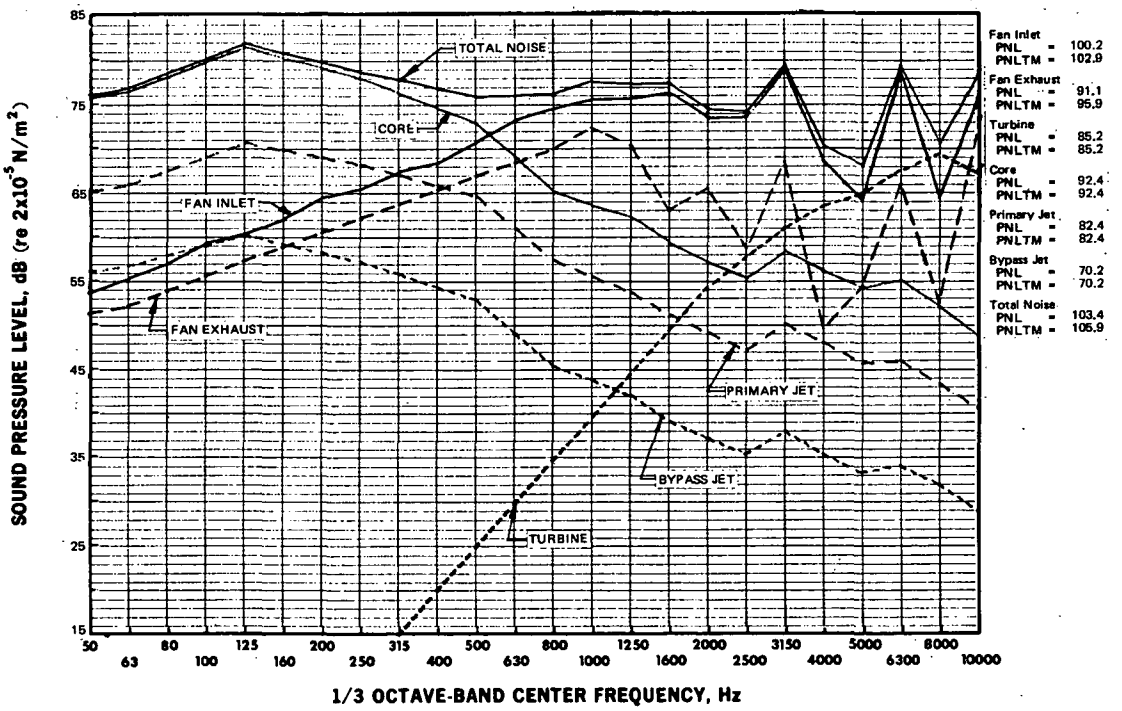

(b) PEAK EXHAUST NOISE SPECTRA, ANGLE FROM INLET = 69 deg (1.19 rad)

FIGURE A-23. SPL vs FREQUENCY FOR FAR 36 APPROACH FOR MINIMUM TREATED NACELLE AT ANGLE OF PEAK INLET AND EXHAUST NOISE FOR DC-9 REFAN AIRCRAFT, ALTITUDE = 370 ft (113 m), N_1 = 5340 rpm, THRUST = 5411 lb (24 068N)

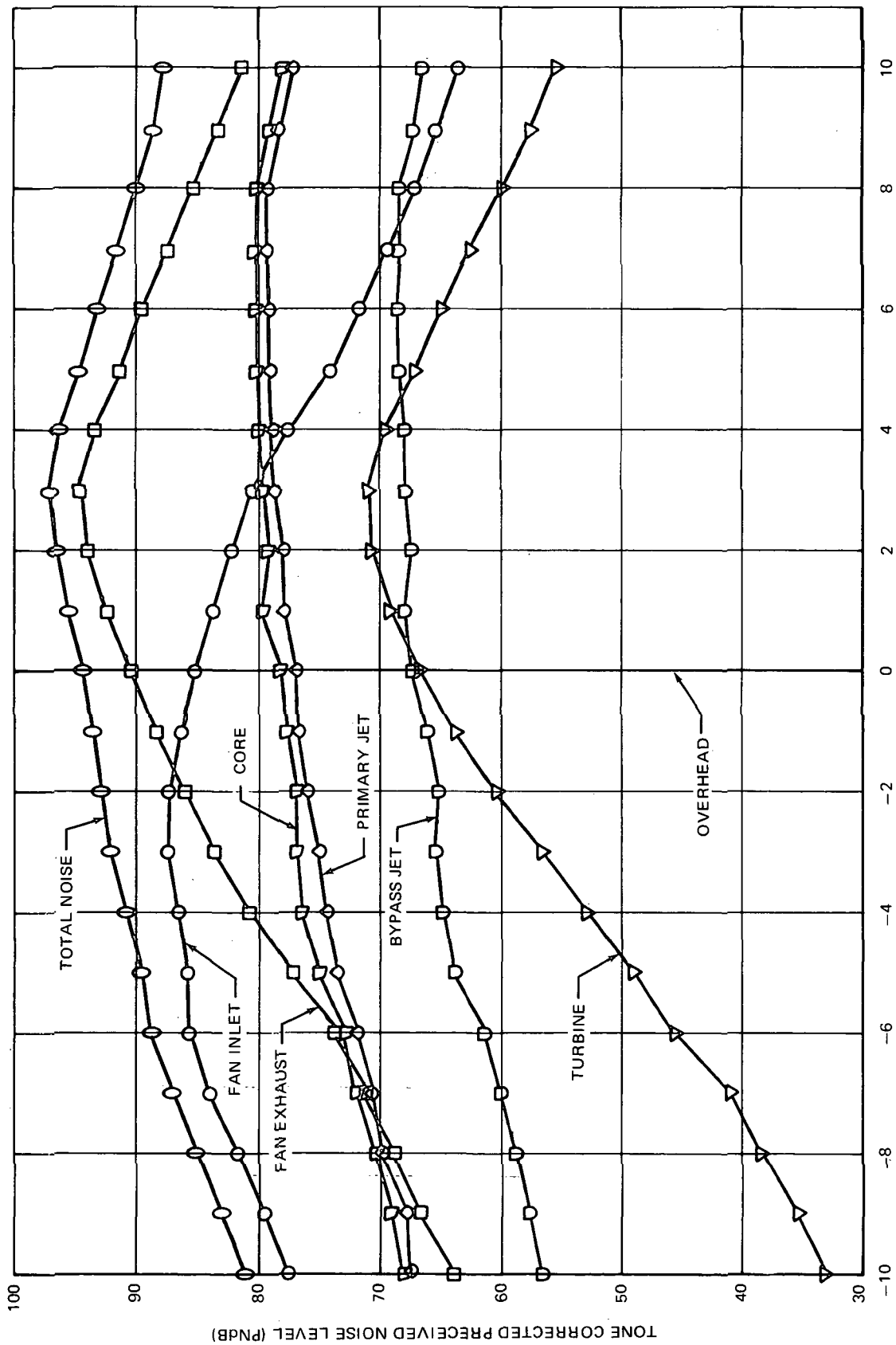

FIGURE A-24. PNLT VERSUS TIME FOR FAR PART 36 CUTBACK CONDITION, UNTREATED ENGINE AND NACELLE, ALTITUDE = 2327 ft (709 m), N_1 = 6530 rpm

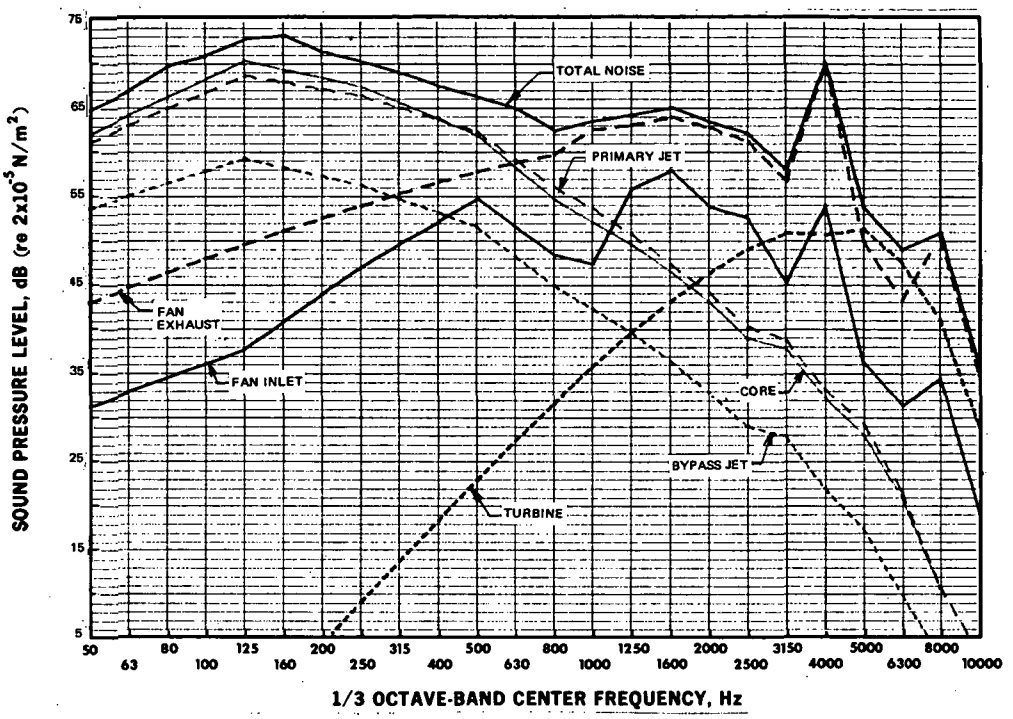

(a) SPL SPECTRA

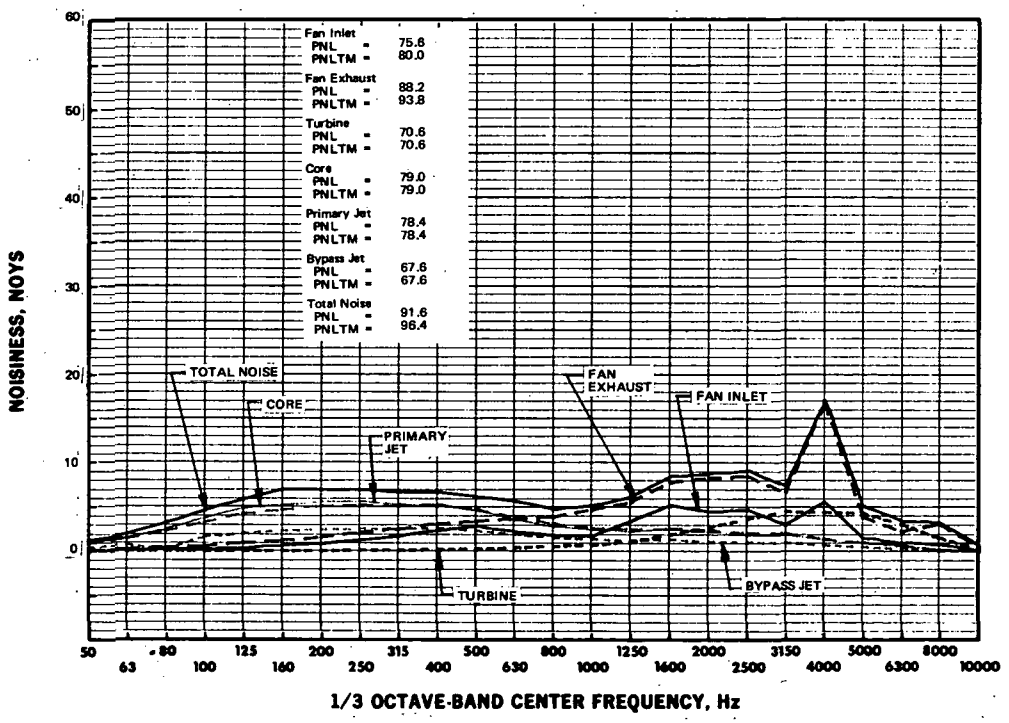

(b) NOY SPECTRA

FIGURE A-25. SPL AND NOY SPECTRA AT PEAK ANGLE OF NOISE FOR UNTREATED ENGINE AND NACELLE AT FAR PART 36 CUTBACK CONDITION, ALTITUDE 2327 ft (710 m), N_1 = 6530 rpm, THRUST = 9627 lb (42 900 N), ANGLE FROM INLET 108 deg (1.88 rad)

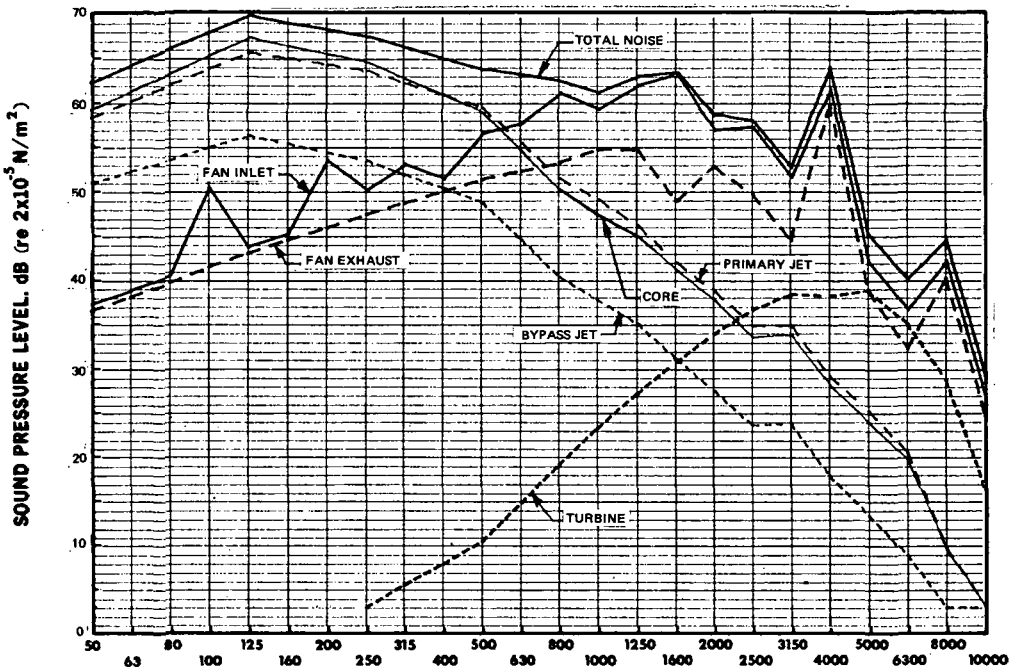

(a) SPL SPECTRA

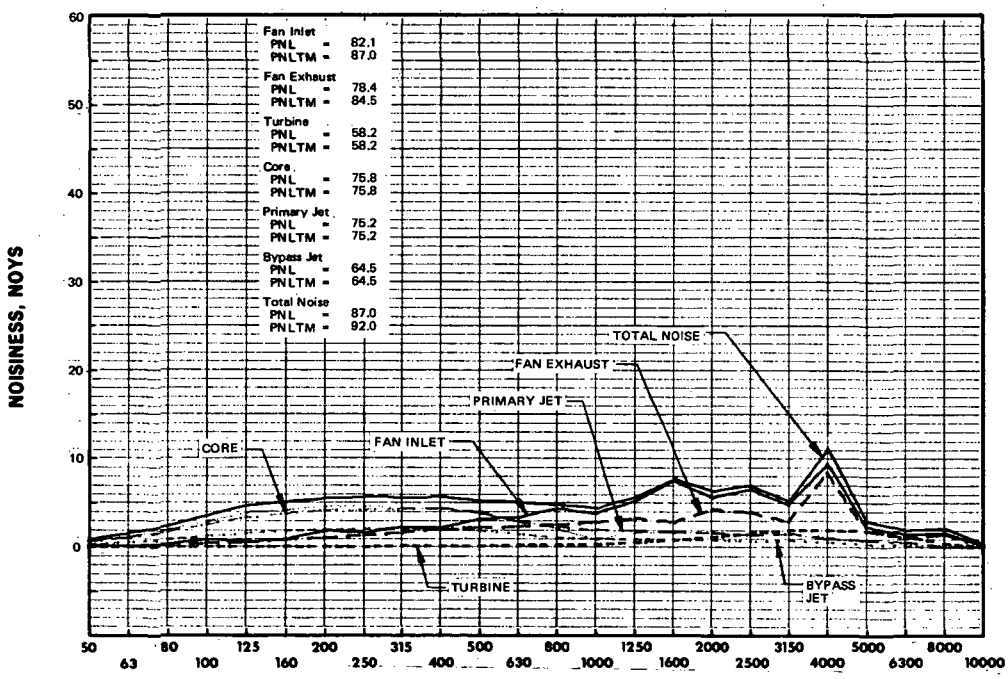

(b) NOY SPECTRA

FIGURE A-26. SPL AND NOY SPECTRA AT PEAK INLET ANGLE FOR UNTREATED ENGINE AND NACELLE AT FAR PART 36 CUTBACK CONDITION, ALTITUDE = 2327 ft (710 m), N_1 = 6530 rpm, THRUST = 9627 lb (42 900 N), ANGLE FROM INLET = 72 deg (1.25 rad)

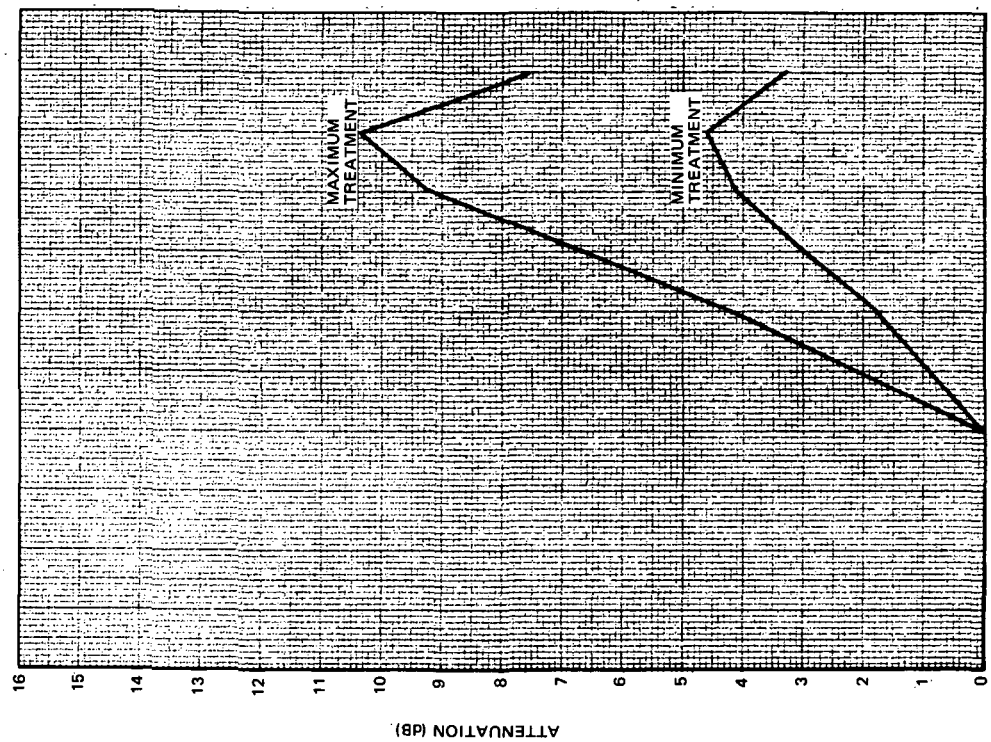

FIGURE A-28. ATTENUATION SPECTRA FROM TAILPIPE TREATMENT AT FAR PART 36 CUTBACK

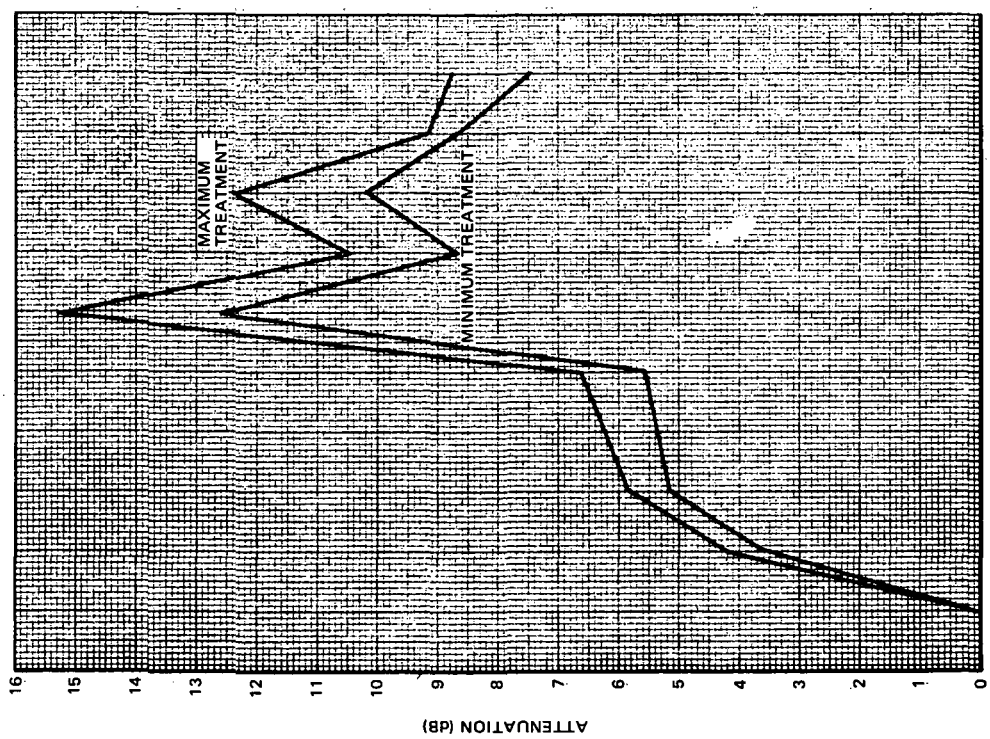

FIGURE A-27. ATTENUATION SPECTRA FROM INLET TREATMENT AT FAR PART 36 CUTBACK

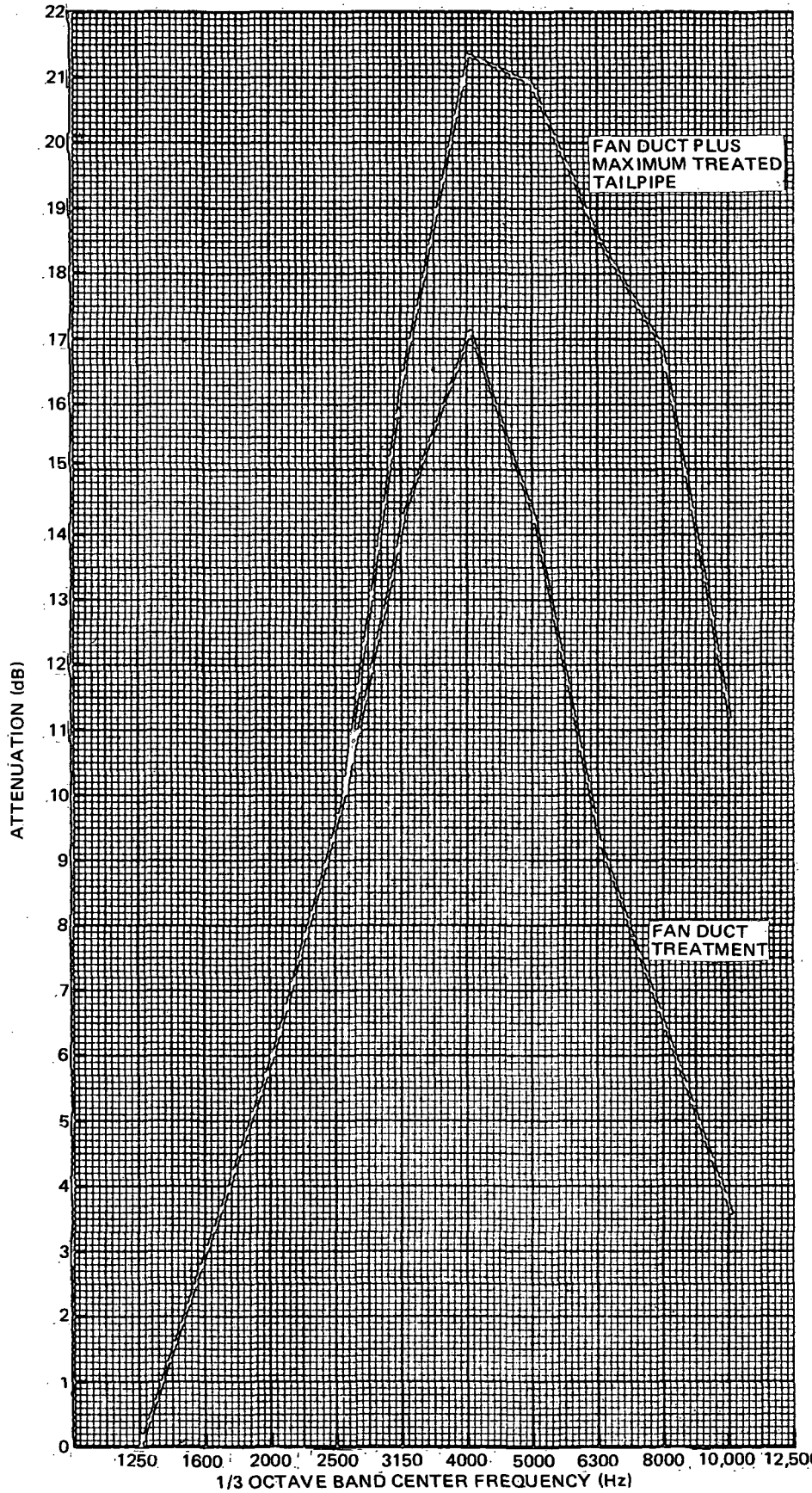

FIGURE A-29. ATTENUATION SPECTRA OF FAN EXHAUST NOISE FOR THE MAXIMUM TREATMENT CONFIGURATION AT FAR PART 36 CUTBACK OPERATION

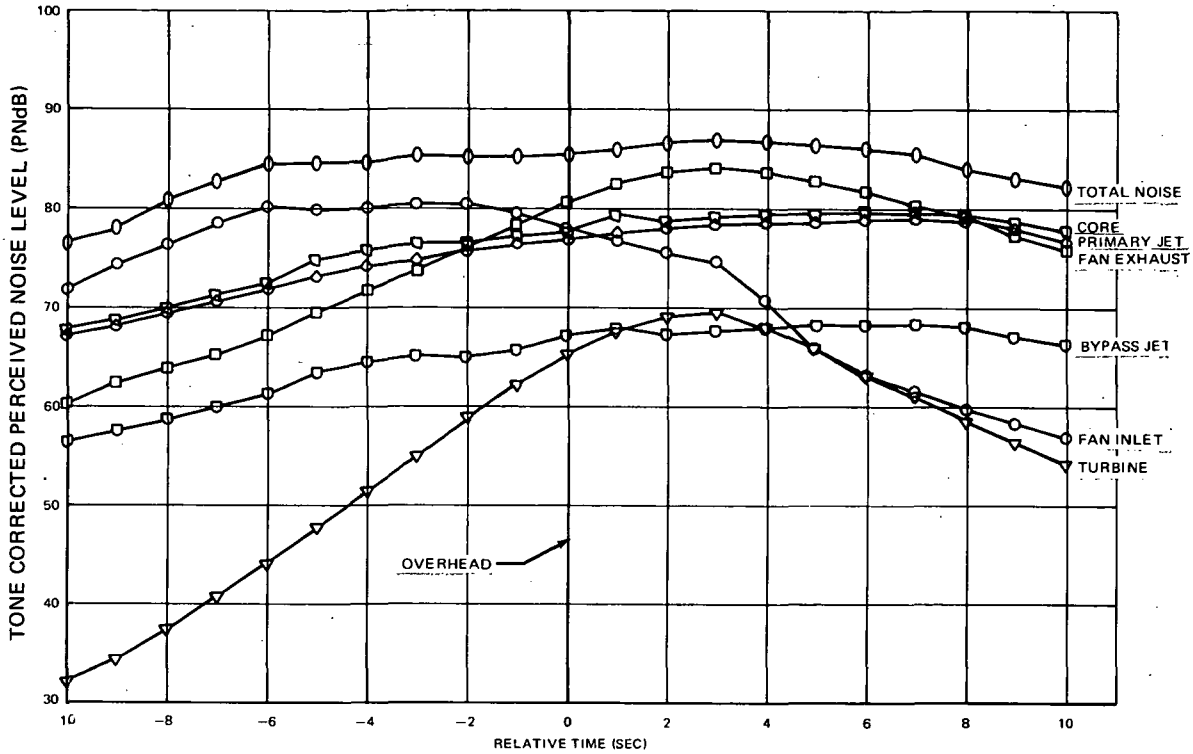

(a) MINIMUM NACELLE TREATMENT, ALTITUDE = 2327 ft (710 m), N_1 = 6530 rpm

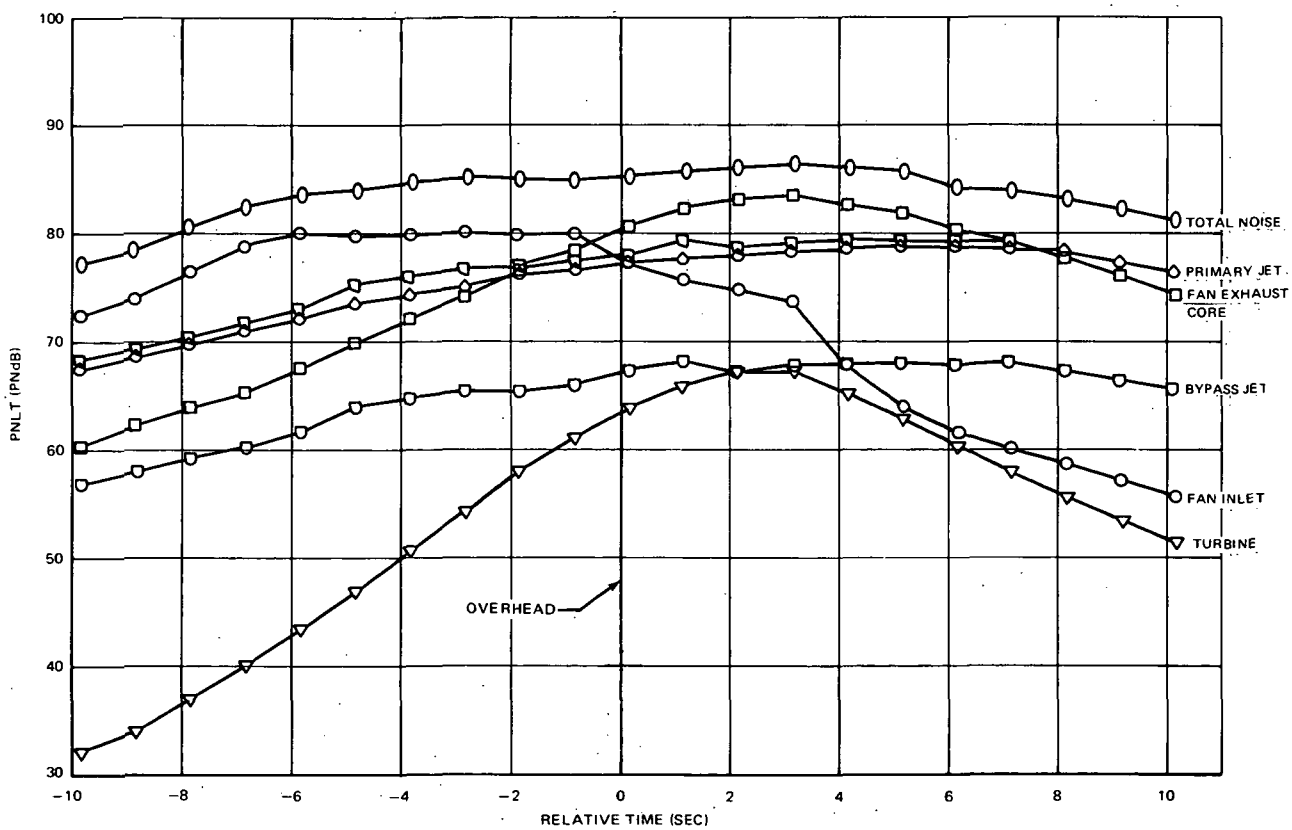

(b) MAXIMUM NACELLE TREATMENT, ALTITUDE = 2287 ft (697 m), N_1 = 6560 rpm

FIGURE A-30. PNLT VS TIME FOR FAR 36 CUTBACK OPERATION WITH MINIMUM AND MAXIMUM NACELLE TREATMENT FOR THE DC-4 REFAN AIRCRAFT

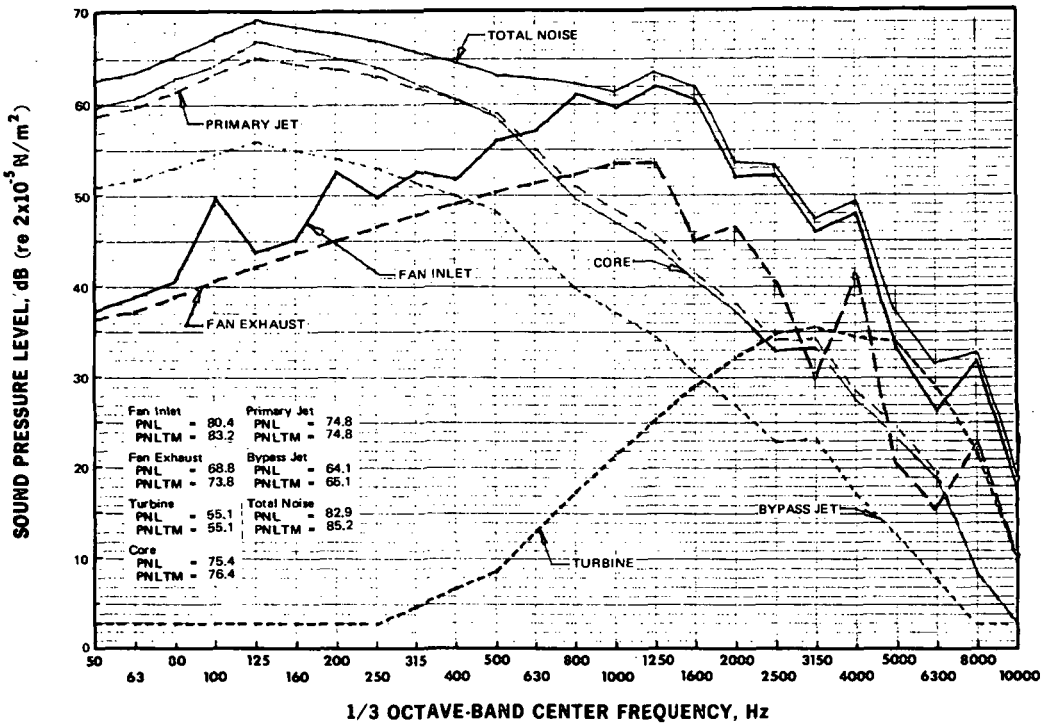

(a) PEAK INLET NOISE SPECTRA, ANGLE FROM INLET = 69 deg (1.2 rad)

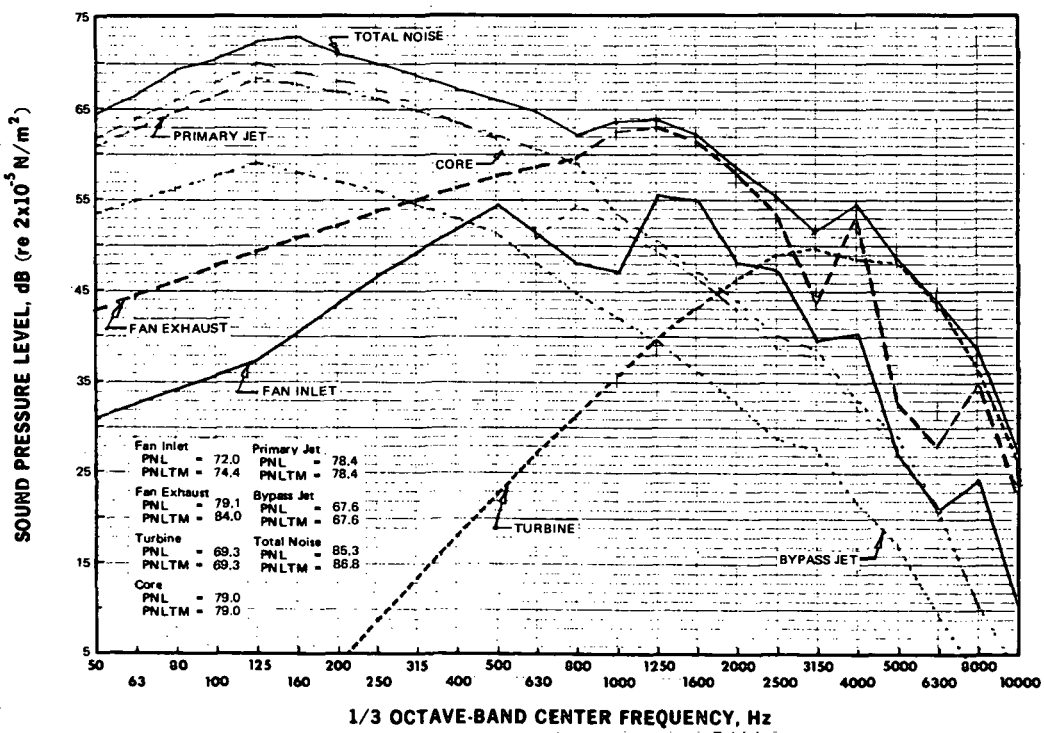

(b) PEAK EXHAUST NOISE SPECTRA, ANGLE FROM INLET - 108 deg (1.88 rad)

FIGURE A-31. SPL vs FREQUENCY FOR FAR 36 CUTBACK FOR MINIMUM TREATED NACELLE AT ANGLE OF PEAK INLET AND EXHAUST NOISE, ALTITUDE = 2327 ft (710 m) N_1 = 6530 rpm, THRUST = 9627 lb (42 900 N)

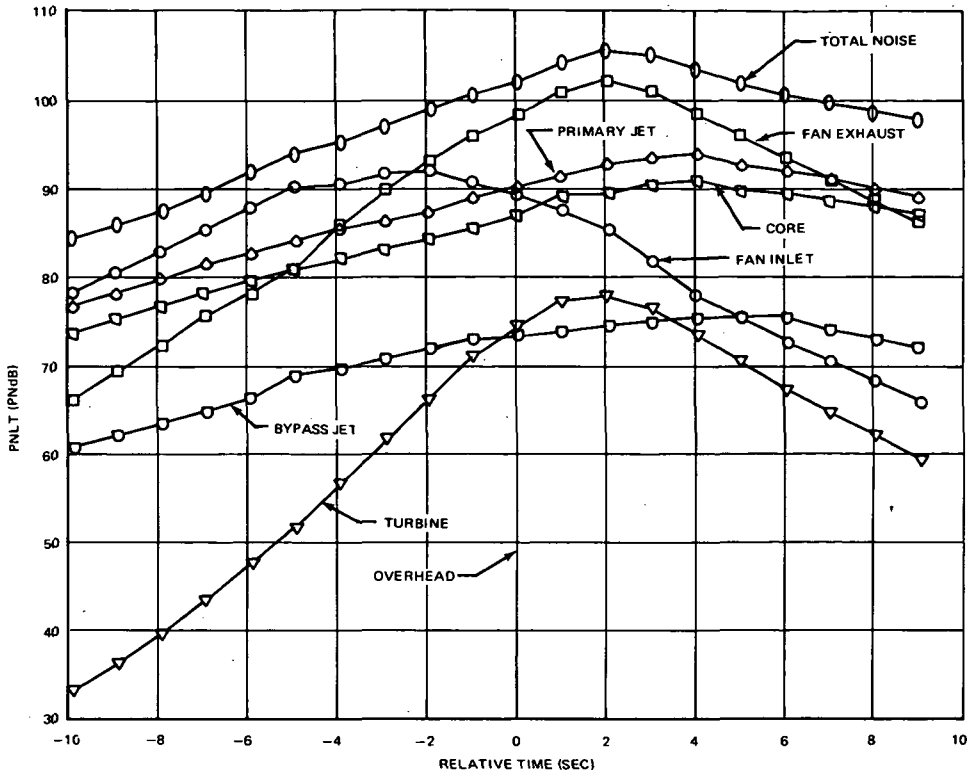

(a) UNTREATED ENGINE AND NACELLE, ALTITUDE = 1500 ft (457 m)

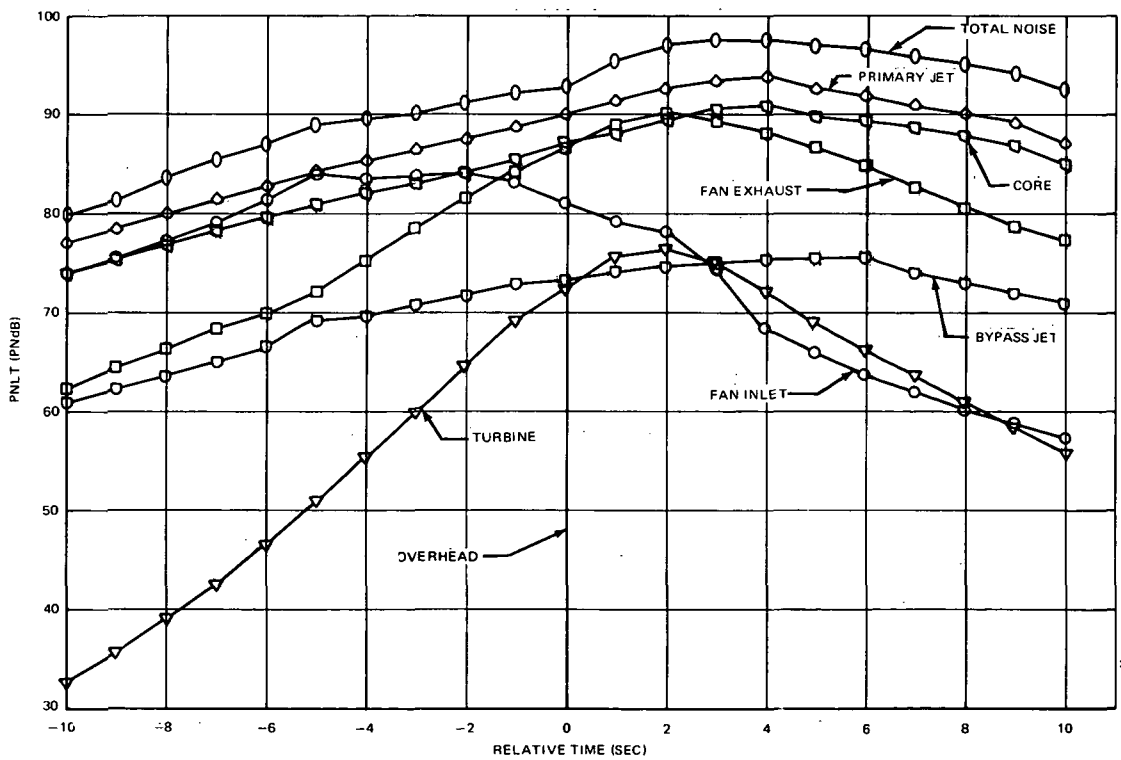

(b) MINIMUM TREATED NACELLE, ALTITUDE = 1000 ft (305 m)

FIGURE A-32. PNLT vs TIME FOR FAR 36 SIDELINE OPERATION WITH UNTREATED AND MINIMUM TREATED NACELLES FOR DC-9 REFAN, N_1 = 7370 rpm

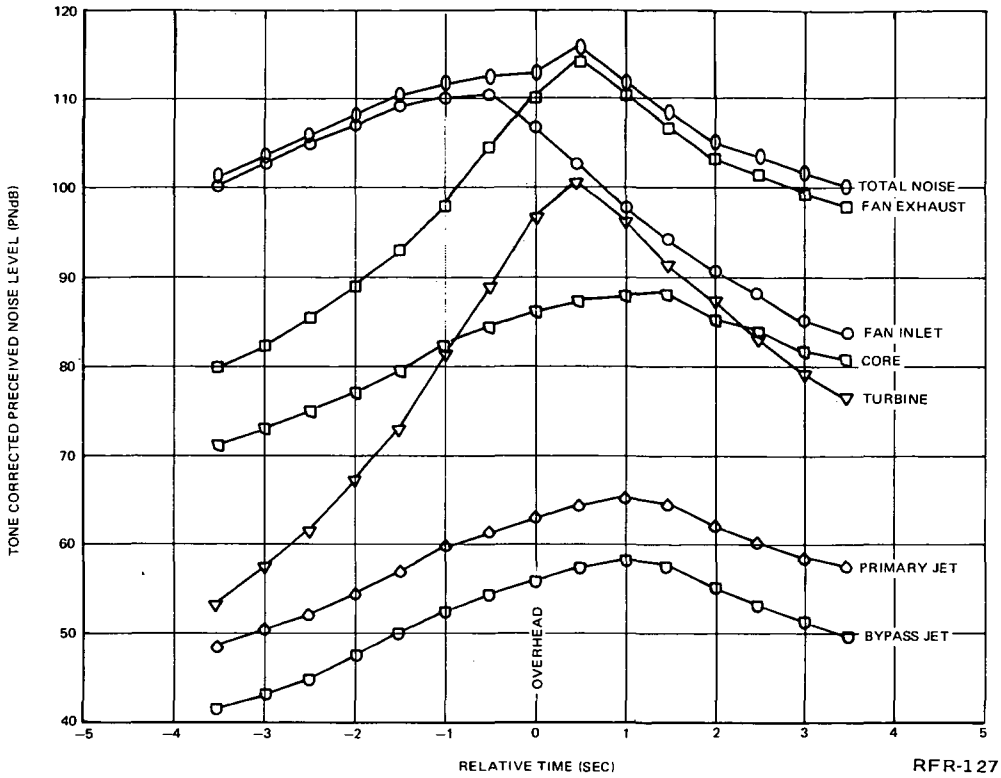

(a) UNTREATED AIRCRAFT

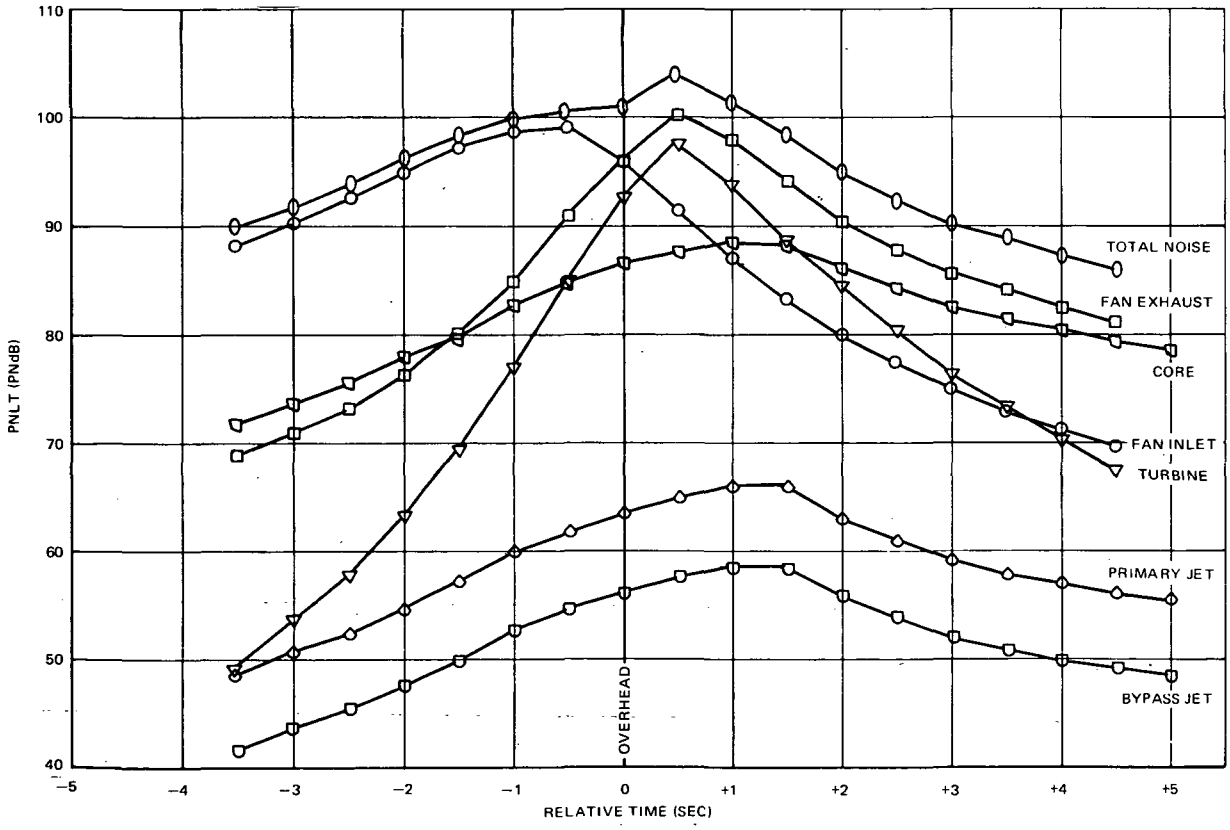

(b) MINIMUM TREATMENT

FIGURE C-21. PNLT VS TIME FOR 6°-APPROACH OPERATION

FIGURE A-33. PNLT VERSUS TIME FOR 6-DEGREE APPROACH FOR UNTREATED AND MINIMUM TREATED DC-9 REFAN AIRCRAFT, ALTITUDE = 370 ft (113 m)

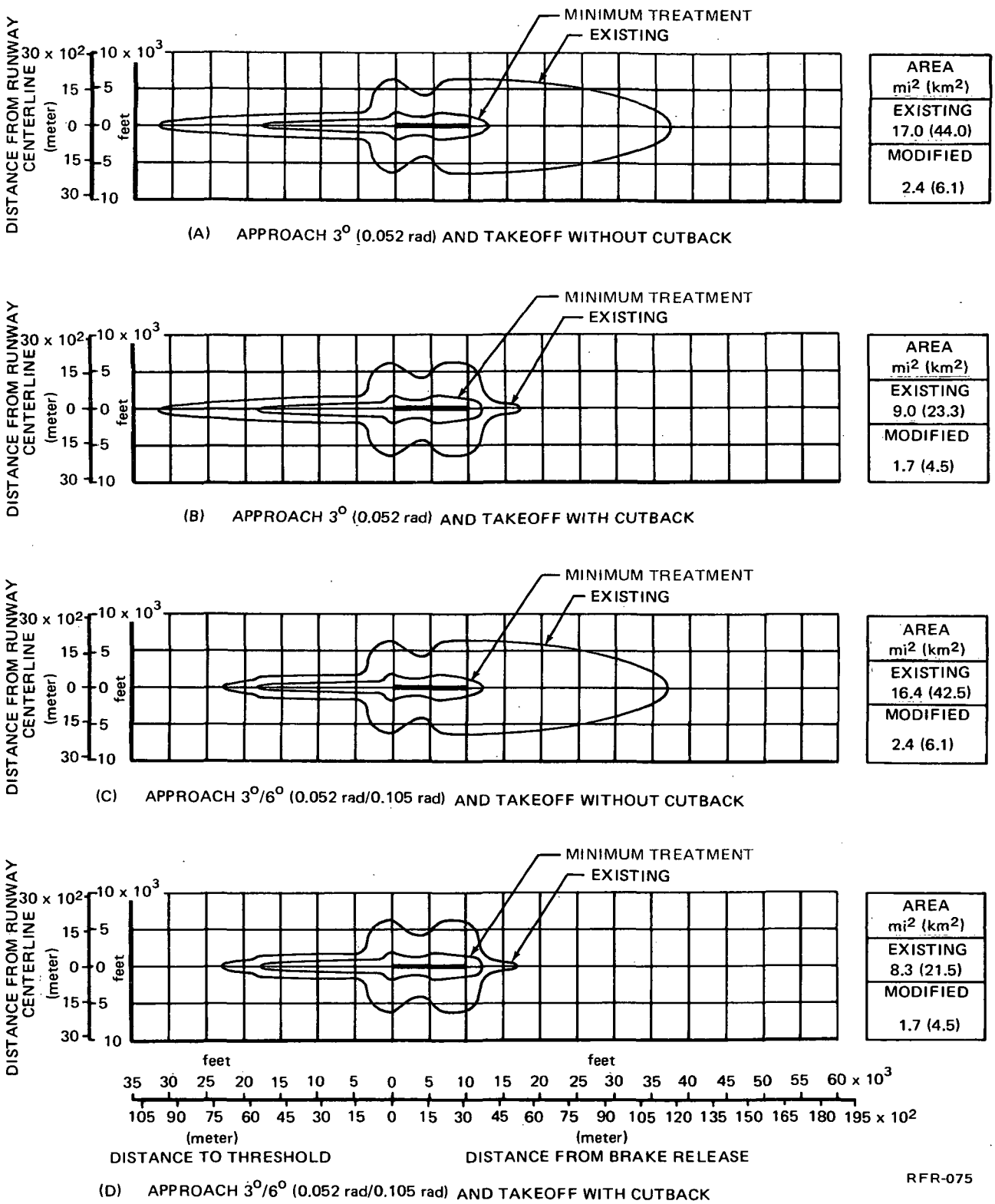

FIGURE A-34. 90-EPNdB NOISE CONTOURS FOR EXISTING AND MODIFIED DC-9-15 AIRCRAFT (MINIMUM TREATMENT) FOR TYPICAL MISSION OPERATION

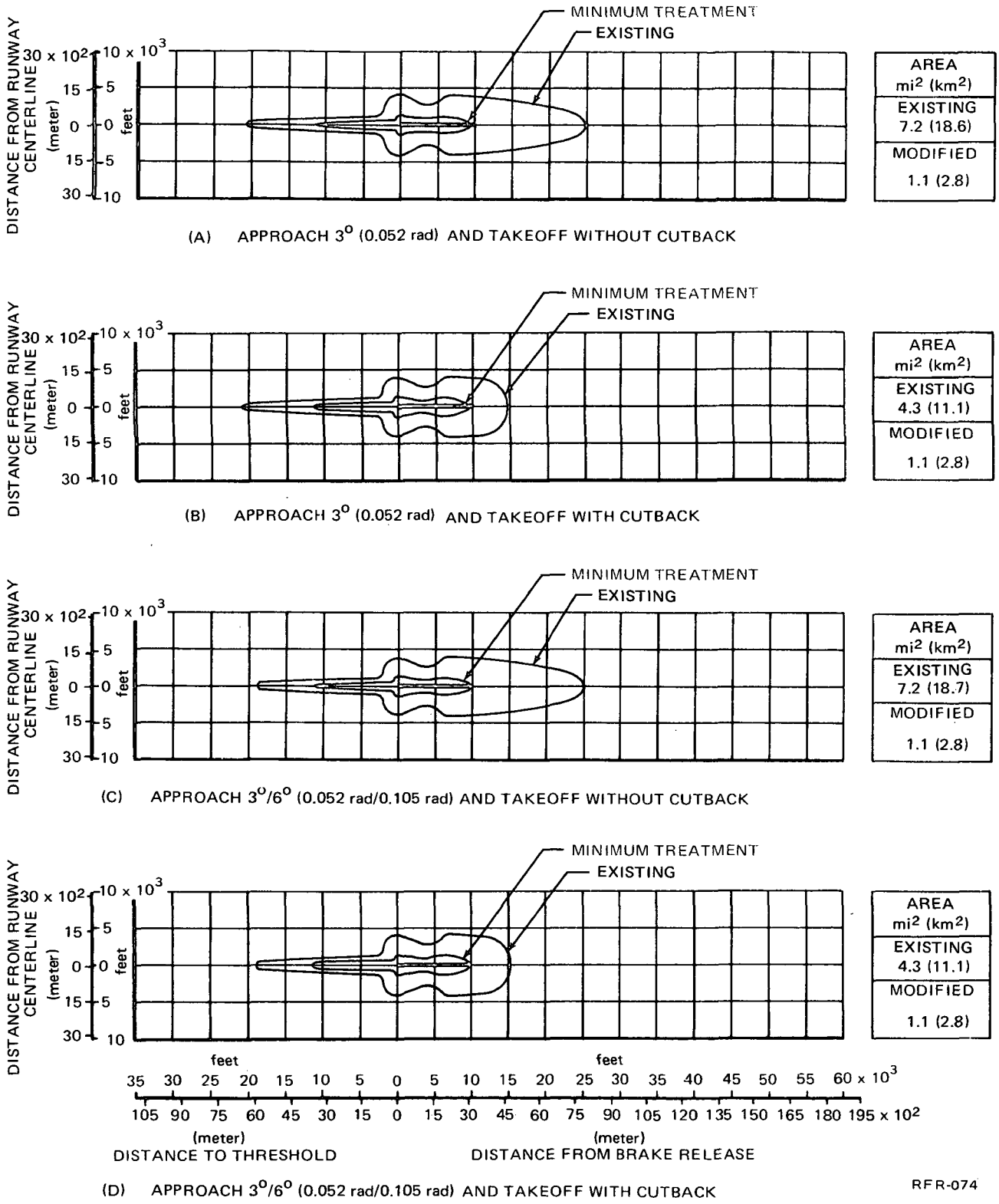

FIGURE A-35. 95-EPNdB NOISE CONTOURS FOR EXISTING AND MODIFIED DC-9-15 AIRCRAFT (MINIMUM TREATMENT) FOR TYPICAL MISSION OPERATION

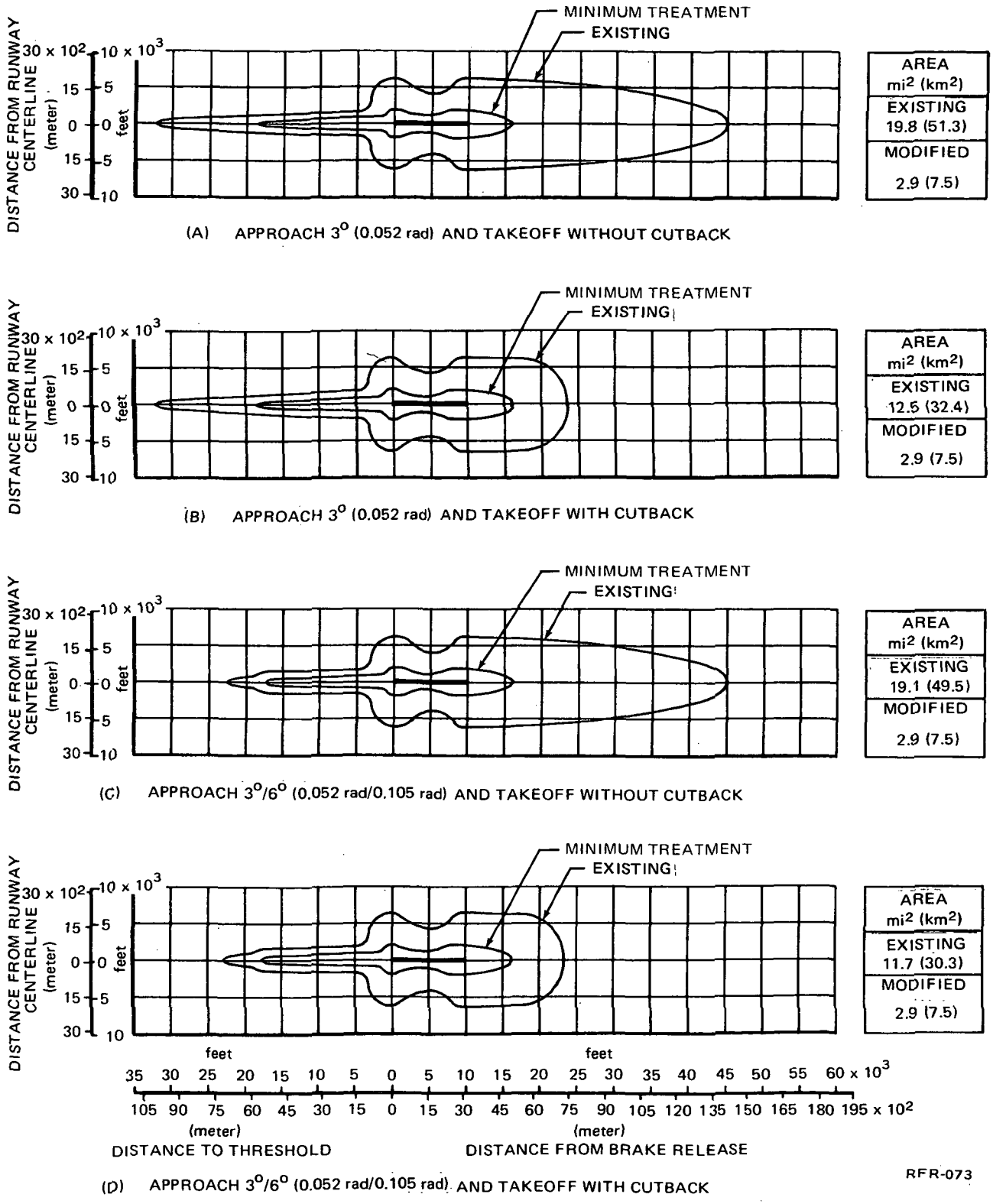

FIGURE A-36. 90-EPNdB NOISE CONTOURS FOR EXISTING AND MODIFIED DC-9-15 AIRCRAFT (MINIMUM TREATMENT) FOR FAR PART 36 OPERATION

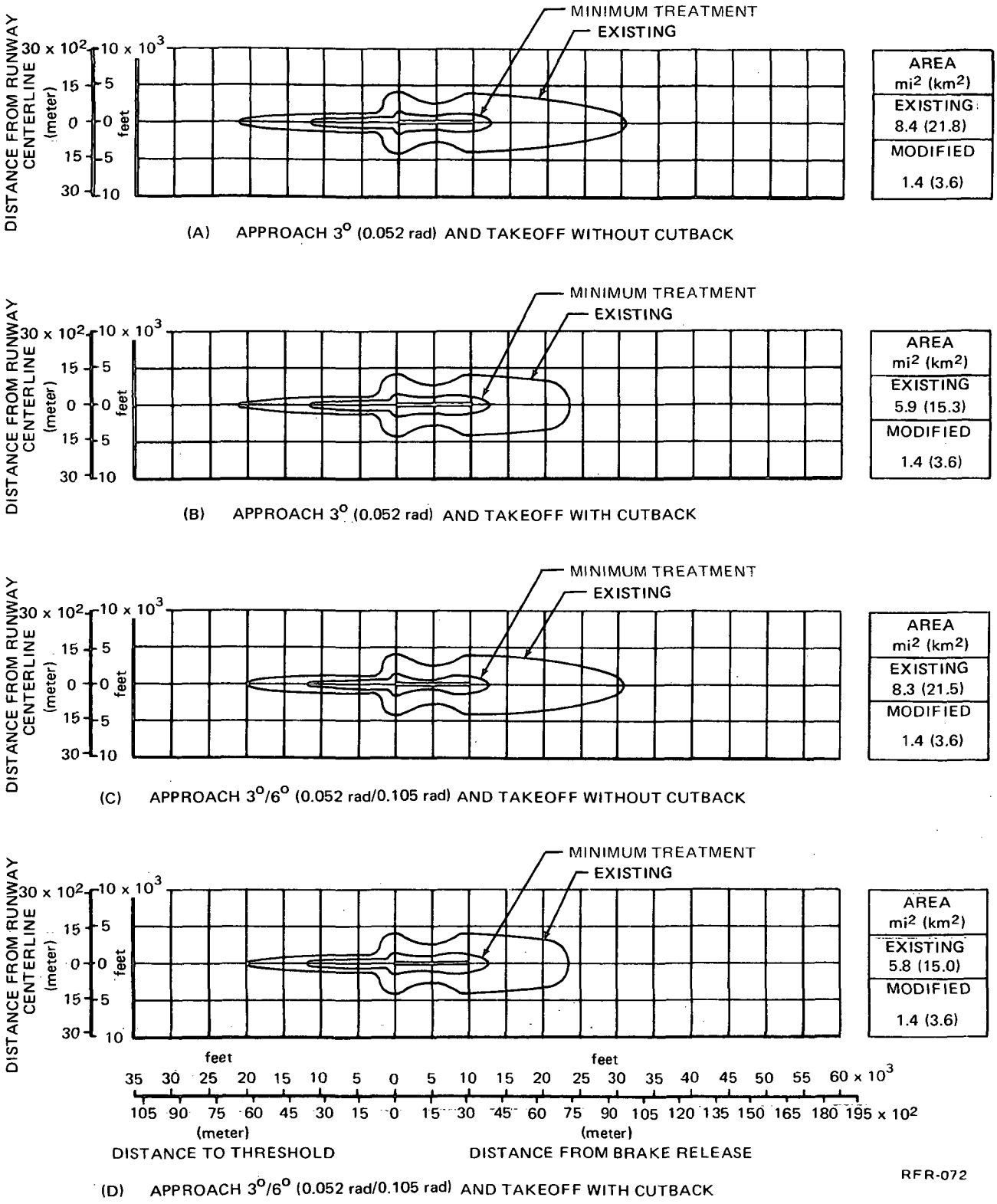

FIGURE A-37. 95-EPNdB NOISE CONTOURS FOR EXISTING AND MODIFIED DC-9-15 AIRCRAFT (MINIMUM TREATMENT) FOR FAR PART 36 OPERATION

APPENDIX B

TRADE STUDIES

This appendix presents summaries of the following trade studies conducted during Phase I of the DC-9 Refan Program:

APPENDIX B

NACELLE ACOUSTIC TREATMENT COST TRADE STUDY

The acoustic treatment trade study was conducted to determine the cost of candidate acoustic treatment configurations for the refanned engine installation on the DC-9 airplane. This study was developed using JT8D-109 data from the Phase I Engine Definition and Characteristics of the JT8D-100 Turbofan Engine Document, PWA^{TM}-4713, 13 April 1973, and involved sixteen acoustically balanced configurations.

Engine Acoustic Configuration

The JT8D-109 has acoustic treatment located along the fan exhaust duct. The effective length of fan exhaust duct acoustic treatment/average channel height (L/H value) has been calculated as 7.4. All nacelle configurations in this study assume the same engine fan duct acoustic treatment. However, some details of the engine manufacturer's acoustic treatment may change, notably core depth and face porosity, which will change the fan duct acoustic performance.

Acoustic Materials

To estimate weights for this study, all inlet acoustic treatment was assumed to be perforated aluminum sheet bonded to aluminum honeycomb core. Welded steel and Inconel construction was assumed for the refan nacelle exhaust duct treatment. This is the same type construction that will be used for the flight demonstration aircraft during Phase II. A thickness of 19.0 mm (0.75 in.) for both the inlet and exhaust system was used for this study. A change in core depth for any final selection would have a minor effect on the weight since the major weight is in the face sheets.

Inlet and External Duct Limits

A minimum length inlet was established by Douglas Aerodynamics with an overall length of 965.2 mm (38.0 in.). By layout, it was determined that wall treatment could be installed in 660.4 mm (26 in.) of this length, allowing for a heated inlet lip and flanges fore and aft. This allowance of 304.8 mm (12.0 in.) for the heated inlet lip and flanges was used as a constant in determining the overall length of all the inlets used in the trade study. No maximum inlet length was established.

The minimum length of the exhaust duct was established at 1.85 m (73.0 in.) by interior and exterior aerodynamic considerations. Acoustic treatment is not a factor in determining this minimum length. It was determined that 1.22 m (48.0 in.) of treatment could be installed along the length of the minimum tailpipe.

The maximum length exhaust duct was established by the ground clearance requirement during rotation for takeoff. The existing fuselage clearance was used as a limit. All exhaust ducts included in this study are of simple, conical shape. The previous trade study proposed centerbodies and/or rings in the exhaust duct for greater noise reduction. These have not been included in this study due to their high technical risk and the high costs of development and fabrication.

The important geometric characteristics of the sixteen study configurations shown in table B-1 were obtained from figure 11. The configurations using L/H values of zero and 1.65 were based on the minimum aerodynamic exhaust duct. The configurations with an L/H of 5.3 were designed around the maximum length exhaust duct, utilizing various inlet treatments which include rings and treated centerbodies. The remaining configurations were developed with L/H values of 3.75 and 4.3.

Table B-2 lists the component weights for each configuration. Weights were re-estimated for the selected configurations shown in table 19, including the engine weight and the totals are within 2%. The change in certain component weights, such as the engine weight of 509.84 kg (1124 lb), doors and apron of 56.35 kg (124 lb), pylon of 19.50 kg (43 lb), thrust reverser of 85.28 kg (188 lb), fuselage of 65.77 kg (145 lb), and systems of 11.79 kg (26 lb) for a total change in weight of 709.43 kg (1564 lb) were assumed constant for this trade study.

Trade factors were determined based on operating a DC-9-32 for an 8-year period with a utilization of 3170 hrs/yr. for a 694 km (375 n. mi.) range. An interest rate of 7% was used to determine the factor for conversion costs. The trade factors are as follows:

	Trade Factor (1973 Dollars)
$1 First Cost	1.43
0.454 kg (1 lb) Dead Weight	12.60
0.093 m^2 (1 sq ft) Equivalent Flat Plate Area	26,400
0.102 kg/hr/N (1 lb/hr/lb) Increase in SFC	2,330,000

Table B-3 lists the total system operating and conversion costs per airplane of the sixteen configurations. The maintainability was based on a detail study to determine the change in MMH/FH and material costs in $/FH for each configuration. The total system cost for maintainability is then based on a utilization of 3170 hrs/yr. for an 8-year period. The inlet cost includes the effect of SFC and external drag of the inlet and was obtained from figure B-1. The exhaust cost includes the effect of nozzle loss and external drag of the exhaust and was obtained from figure B-2. The system cost of weight and the conversion cost were determined using the trade factors.

APPENDIX B

TABLE B-1. GEOMETRIC CHARACTERISTICS

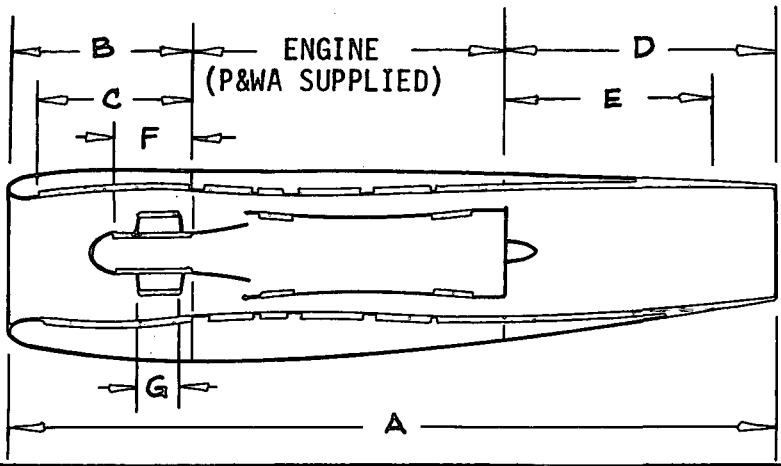

CONFIG. NO.	NACELLE, INLET AND EXHAUST LENGTHS LENGTHS - INCHES (m)						
	A	B	C	D	E	F	G
1	253.20 (6.43)	53.00 (1.35)	41.00 (1.04)	73.00 (1.85)	0	0	0
2	246.20 (6.25)	46.00 (1.17)	34.00 (0.86)	73.00 (1.85)	0	20.00 (0.51)	0
3	263.20 (6.69)	63.00 (1.60)	51.00 (1.30)	73.00 (1.85)	37.00 (0.94)	0	0
4	255.20 (6.48)	55.00 (1.40)	43.00 (1.09)	73.00 (1.85)	37.00 (0.94)	26.00 (0.66)	0
5	312.20 (7.93)	75.00 (1.91)	63.00 (1.60)	110.00 (2.79)	85.00 (2.16)	0	0
6	303.20 (7.70)	66.00 (1.68)	54.00 (1.37)	110.00 (2.79)	85.00 (2.16)	32.00 (0.81)	0
7	283.20 (7.19)	46.00 (1.17)	34.00 (0.86)	110.00 (2.79)	85.00 (2.16)	0	15.00 (0.38)
8	278.20 (7.07)	41.00 (1.04)	29.00 (0.74)	110.00 (2.79)	85.00 (2.16)	5.00 (0.13)	15.00 (0.38)
9	325.20 (8.26)	78.00 (1.98)	66.00 (1.68)	120.00 (3.05)	95.00 (2.41)	0	0
10	315.20 (8.01)	68.00 (1.73)	56.00 (1.42)	120.00 (3.05)	95.00 (2.41)	34.00 (0.86)	0
11	295.20 (7.50)	48.00 (1.22)	36.00 (0.91)	120.00 (3.05)	95.00 (2.41)	0	18.00 (0.46)
12	290.20 (7.37)	43.00 (1.09)	31.00 (0.79)	120.00 (3.05)	95.00 (2.41)	5.00 (0.13)	16.00 (0.41)
13	352.20 (8.95)	84.00 (2.13)	72.00 (1.83)	141.00 (3.58)	116.00 (2.95)	0	0
14	341.20 (8.67)	73.00 (1.85)	61.00 (1.55)	141.00 (3.58)	116.00 (2.95)	37.00 (0.94)	0
15	320.20 (8.13)	52.00 (1.32)	40.00 (1.02)	141.00 (3.58)	116.00 (2.95)	0	20.00 (0.51)
16	314.20 (7.98)	46.00 (1.17)	34.00 (0.86)	141.00 (3.58)	116.00 (2.95)	6.00 (0.15)	17.00 (0.43)

TABLE B-2 - continued

CONFIGURATION DESCRIPTION - DC-9 REFAN

COMPONENT WEIGHT lb (kg) PER AIRPLANE

CONFIG. NUMBER	EXHAUST NOZZLE L/H	PNdB (APPROACH)	INLET DUCT	INLET BULLET	INLET RING	EXHAUST NOZZLE	TOTAL WEIGHT PER A/C		[1]TOTAL WEIGHT CHANGE PER A/C
							EXISTING	REFAN	
1	0	11	356 (161.48)	-	-	440 (199.58)	9,493 (4 305.95)	11,853 (5 376.43)	2,360 (1 070.49)
2	0	11	318 (144.24)	38 (17.24)	-	440 (199.58)	9,493 (4 305.95)	11,853 (5 376.43)	2,360 (1 070.49)
3	1.65	12.6	452 (205.02)	-	-	433 (196.41)	9,493 (4 305.95)	11,942 (5 416.80)	2,449 (1 110.85)
4	1.65	12.6	419 (190.06)	45 (20.41)	-	433 (196.41)	9,493 (4 305.95)	11,954 (5 422.24)	2,461 (1 116.29)
5	3.75	14.4	576 (261.27)	-	-	795 (360.61)	9,493 (4 305.95)	12,428 (5 637.25)	2,935 (1 331.29)
6	3.75	14.4	542 (245.85)	52 (23.59)	-	795 (360.61)	9,493 (4 305.95)	12,446 (5 645.41)	2,953 (1 339.46)
7	3.75	14.4	341 (154.68)	-	125 (56.70)	795 (360.61)	9,493 (4 305.95)	12,318 (5 587.35)	2,825 (1 281.40)
8	3.75	14.4	309 (140.16)	24 (10.89)	125 (56.70)	795 (360.61)	9,493 (4 305.95)	12,310 (5 583.72)	2,817 (1 277.77)

[1]NOTE: Includes the engine, doors and apron, pylon, thrust reverser, fuselage, and systems at 709.43 kg (1564 lb) assumed constant for this study.

TABLE B-2 - concluded

CONFIGURATION DESCRIPTION - DC-9 REFAN

COMPONENT WEIGHT lb (kg) PER AIRPLANE

CONFIG. NUMBER	EXHAUST NOZZLE L/H	PNdB (APPROACH)	INLET DUCT	INLET BULLET	INLET RING	EXHAUST NOZZLE	TOTAL WEIGHT PER A/C		[1]TOTAL WEIGHT CHANGE PER A/C
							EXISTING	REFAN	
9	4.3	14.8	624 (283.04)	-	-	913 (414.13)	9,493 (4 305.95)	12,594 (5 712.54)	3,101 (1 406.59)
10	4.3	14.8	563 (255.37)	55 (24.95)	-	913 (414.13)	9,493 (4 305.95)	12,588 (5 709.82)	3,095 (1 403.87)
11	4.3	14.8	418 (189.60)	-	134 (60.78)	913 (414.13)	9,493 (4 305.95)	12,522 (5 679.88)	3,029 (1 373.93)
12	4.3	14.8	335 (151.95)	24 (10.89)	129 (58.51)	913 (414.13)	9,493 (4 305.95)	12,458 (5 650.85)	2,965 (1 344.90)
13	5.3	15.6	688 (312.07)	-	-	1,138 (516.19)	9,493 (4 305.95)	12,883 (5 843.63)	3,390 (1 537.68)
14	5.3	15.6	619 (280.77)	59 (26.76)	-	1,138 (516.19)	9,493 (4 305.95)	12,873 (5 839.09)	3,380 (1 533.14)
15	5.3	15.6	402 (182.34)	-	141 (63.96)	1,138 (516.19)	9,493 (4 305.95)	12,738 (5 777.86)	3,245 (1 471.91)
16	5.3	15.6	380 (172.37)	25 (11.34)	131 (59.42)	1,138 (516.19)	9,493 (4 305.95)	12,731 (5 774.68)	3,238 (1 468.73)

[1]NOTE: Includes the engine, doors and apron, pylon, thrust reverser, fuselage, and systems at 709.43 kg (1564 lb) assumed constant for this study.

TABLE B-3
MAINTAINABILITY – OPERATING AND CONVERSION COSTS PER AIRPLANE – DC-9 REFAN

CONFIGURATION NUMBER	MAINTAINABILITY PER AIRPLANE						DOLLAR COST IN MILLIONS PER AIRPLANE OVER 8-YEAR PERIOD						
	EXISTING		REFAN		Δ			OPERATING COSTS					
	MMH/FH	$/FH	MMH/FH	$/FH	MMH/FH	$/FH	INLET COST	EXHAUST COST	MAINTAINABILITY COST	WEIGHT COST	TOTAL OPERATING COST	CONVERSION COST	TOTAL COST
1	2.508	23.82	2.562	25.84	0.054	2.02	0.028	ZERO	0.051	0.030	0.109	1.680	1.789
2	2.508	23.82	2.563	25.85	0.055	2.03	0.024	ZERO	0.051	0.030	0.105	1.686	1.791
3	2.508	23.82	2.562	25.84	0.054	2.02	0.044	0.002	0.051	0.032	0.128	1.686	1.814
4	2.508	23.82	2.563	25.85	0.055	2.03	0.040	0.002	0.051	0.032	0.124	1.693	1.817
5	2.508	23.82	2.562	25.84	0.054	2.02	0.062	0.133	0.051	0.036	0.282	1.710	1.992
6	2.508	23.82	2.564	25.85	0.056	2.03	0.058	0.133	0.051	0.036	0.278	1.720	1.998
7	2.508	23.82	2.565	25.86	0.057	2.04	0.038	0.133	0.051	0.034	0.256	1.745	2.001
8	2.508	23.82	2.565	25.86	0.057	2.04	0.035	0.133	0.051	0.034	0.253	1.740	1.993
9	2.508	23.82	2.563	25.86	0.055	2.04	0.066	0.188	0.051	0.039	0.344	1.719	2.063
10	2.508	23.82	2.564	25.86	0.056	2.04	0.062	0.188	0.051	0.038	0.339	1.729	2.068
11	2.508	23.82	2.565	25.87	0.057	2.05	0.042	0.188	0.051	0.038	0.319	1.757	2.076
12	2.508	23.82	2.564	25.85	0.056	2.03	0.040	0.188	0.051	0.037	0.316	1.752	2.068
13	2.508	23.82	2.564	25.86	0.056	2.04	0.075	0.260	0.051	0.042	0.428	1.732	2.160
14	2.508	23.82	2.565	25.86	0.057	2.04	0.070	0.260	0.051	0.042	0.423	1.742	2.165
15	2.508	23.82	2.566	25.87	0.058	2.05	0.050	0.260	0.052	0.040	0.402	1.773	2.175
16	2.508	23.82	2.566	25.87	0.058	2.05	0.048	0.260	0.052	0.040	0.400	1.769	2.169

RFR-066

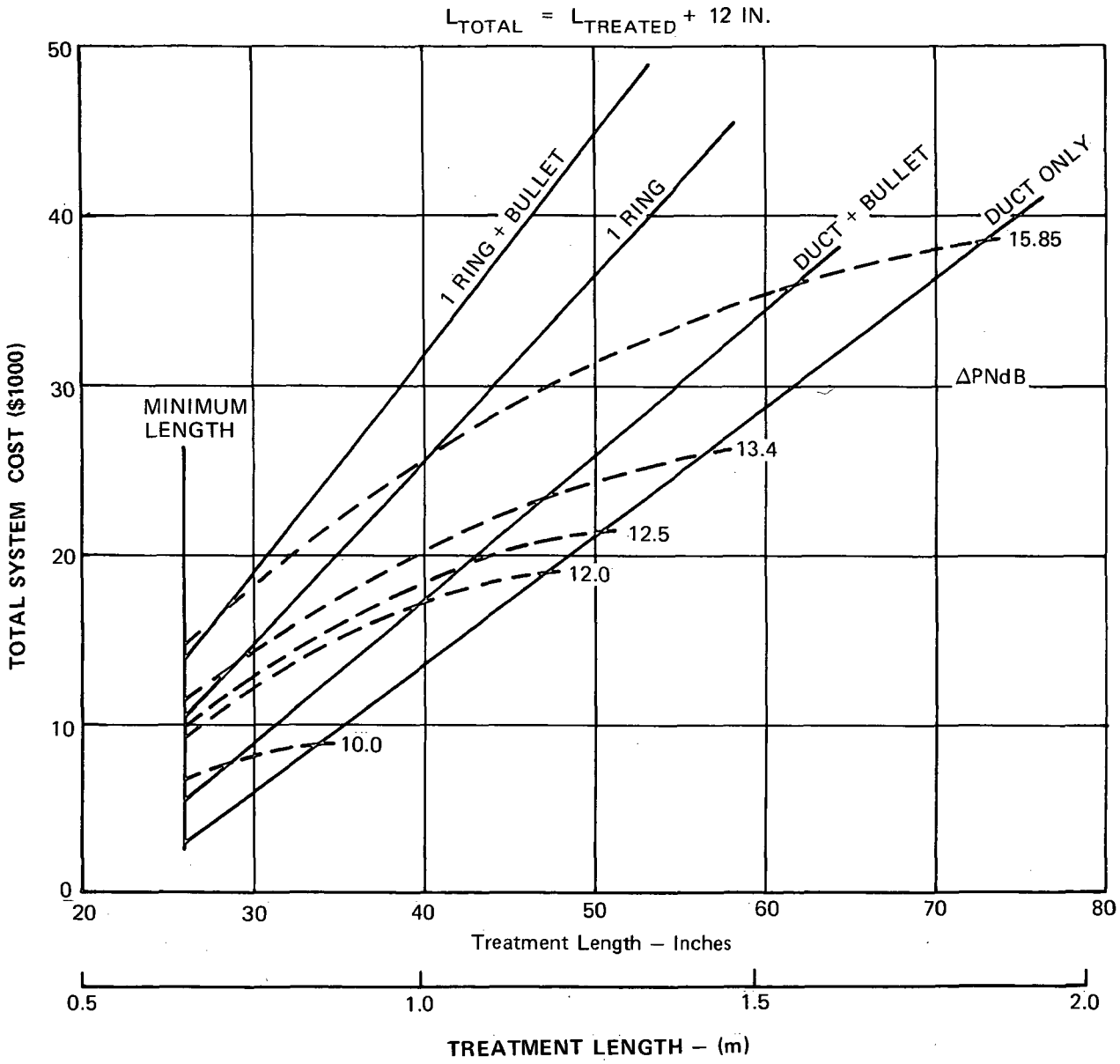

FIGURE B-1. DC-9 JT8D-109 REFAN INLETS TOTAL SYSTEM COSTS/INLET EFFECTS OF INLET LOSS, SFC AND EXTERNAL DRAG

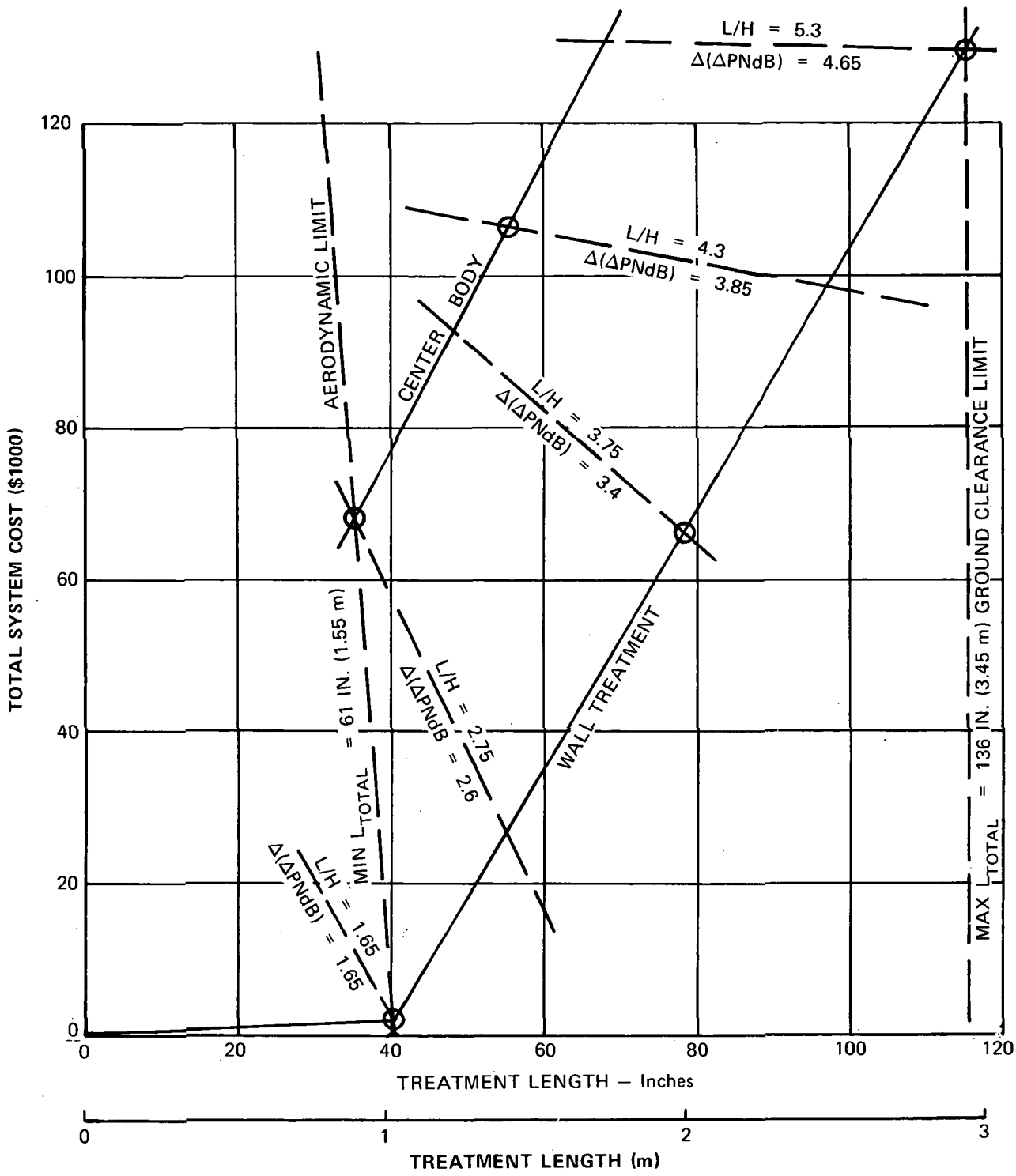

FIGURE B-2. DC-9 JT8D-109 NOZZLE TOTAL SYSTEM COSTS/EXHAUST EFFECTS OF NOZZLE LOSS AND EXTERNAL DRAG

Conclusion

Figure B-3 shows the total cost in dollars, including the conversion and operational costs for each of the sixteen study configurations plotted against the reduction in predicted noise (ΔPNdB). Note that the costs for configurations 3 and 5, identified as the Minimum and Maximum Selected Configurations, fall on either side of the knee in the curve.

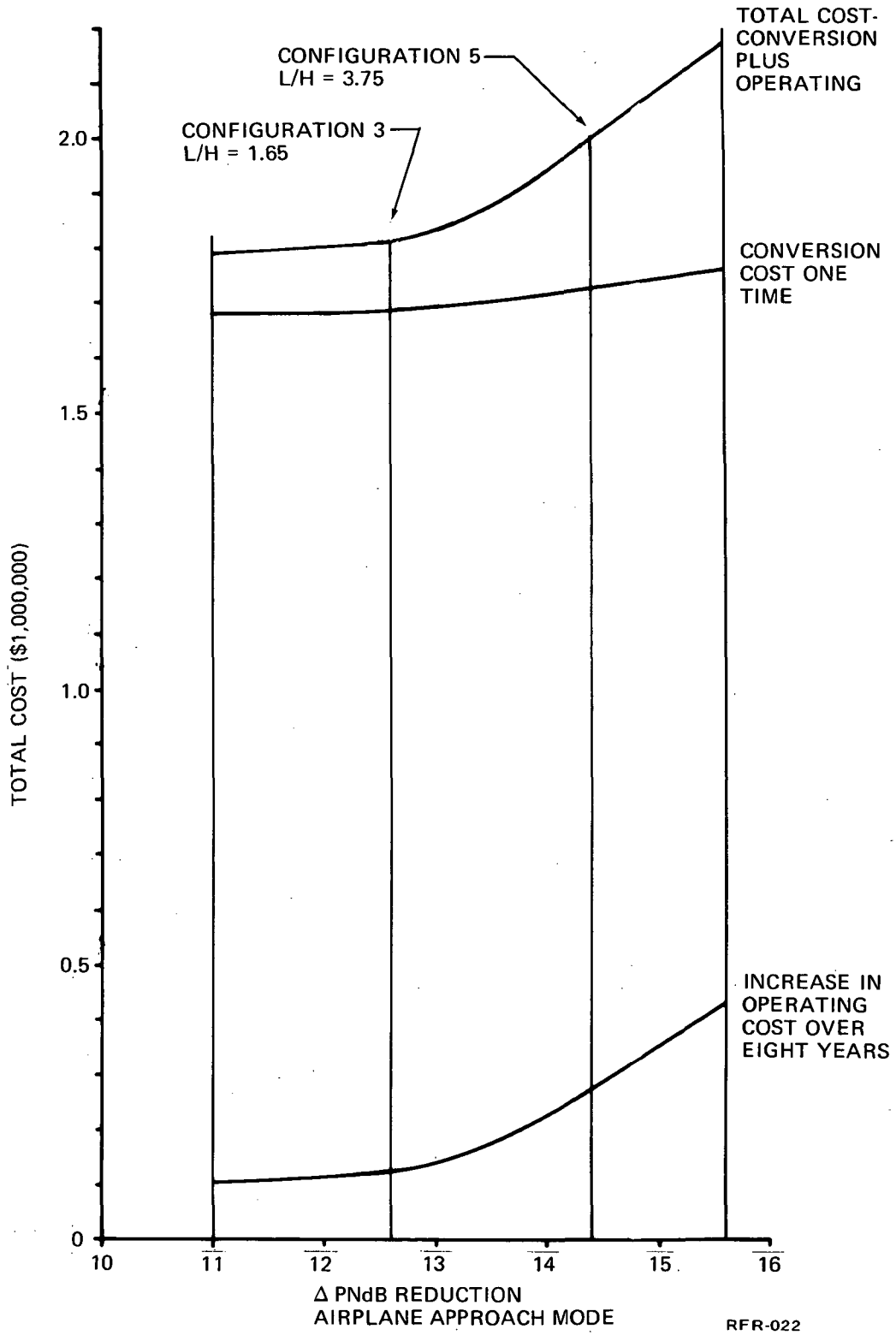

FIGURE B-3. DC-9 REFAN TRADE STUDY

APPENDIX B

PYLON CONFIGURATION TRADE STUDY

Optimization of the Refanned JT8D-109 Pylon on the DC-9 required detail study of two interrelated problems: (1) aerodynamic considerations of high speed cruise drag and low speed stall recovery; and (2) the physical constraints of pylon accessibility.

Pylon Configurations

At the start of Phase I four pylon configurations were chosen for study. This pylon configuration trade study was initiated to determine an optimum configuration that would meet the aerodynamic requirements and pylon accessibility.

The pylon configurations evaluated were (figure B-4):

Configuration 1: Pylon apron same relative position to fuselage as existing.

Configuration 2: Refan engine centerline same relative position to fuselage as existing.

Configuration 3: Outside refan engine nacelle contour same relative position to fuselage as existing.

Configuration 4: Pylon apron moved outboard 82.5 mm (3.25 in.).

Accessibility

The pylon minimum width is limited by the access requirements for the subsystems connections. The electrical system interfaces at the fuselage in a cluster of connectors as shown in figure B-5. The connectors must be accessible for individual installation and removal through the pylon access door. The hydraulic, fuel, fire extinguishing, PT_7, PT_2, and engine bleed air connections must also be accessible through these doors for installation and tightening with standard tools.

The aft engine mount utilizes three attach points within the pylon as shown in figure B-6. These bolts require adequate accessibility through the pylon to allow removal and installation with a standard torque wrench. The forward mount has no attach points within the pylon, and, therefore, requires no access door.

Aircraft maintenance and installation experience indicates the pylon access doors must be a minimum of 127.0 mm (5 in.) to provide adequate access

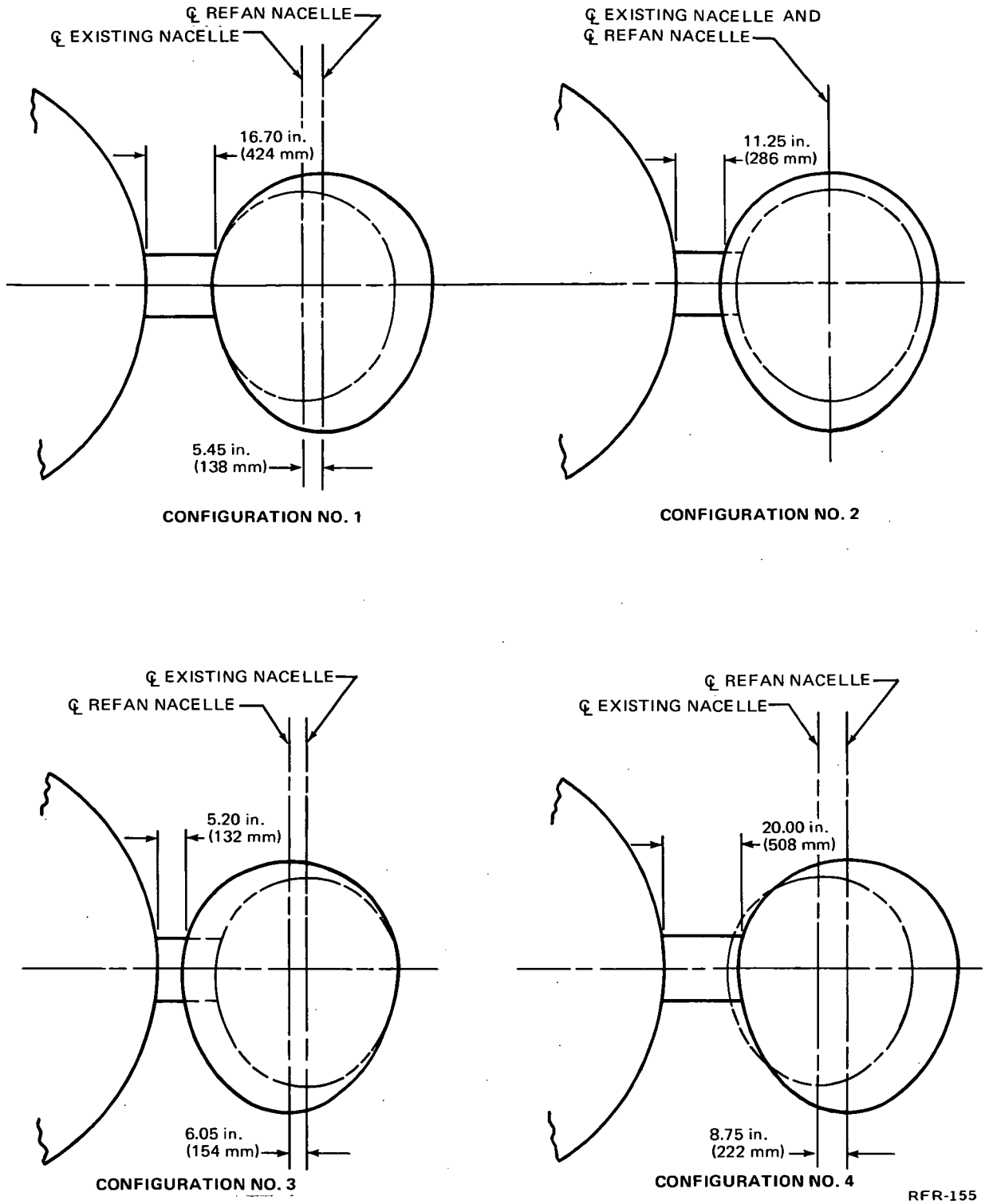

FIGURE B-4. PYLON STUDY CONFIGURATIONS

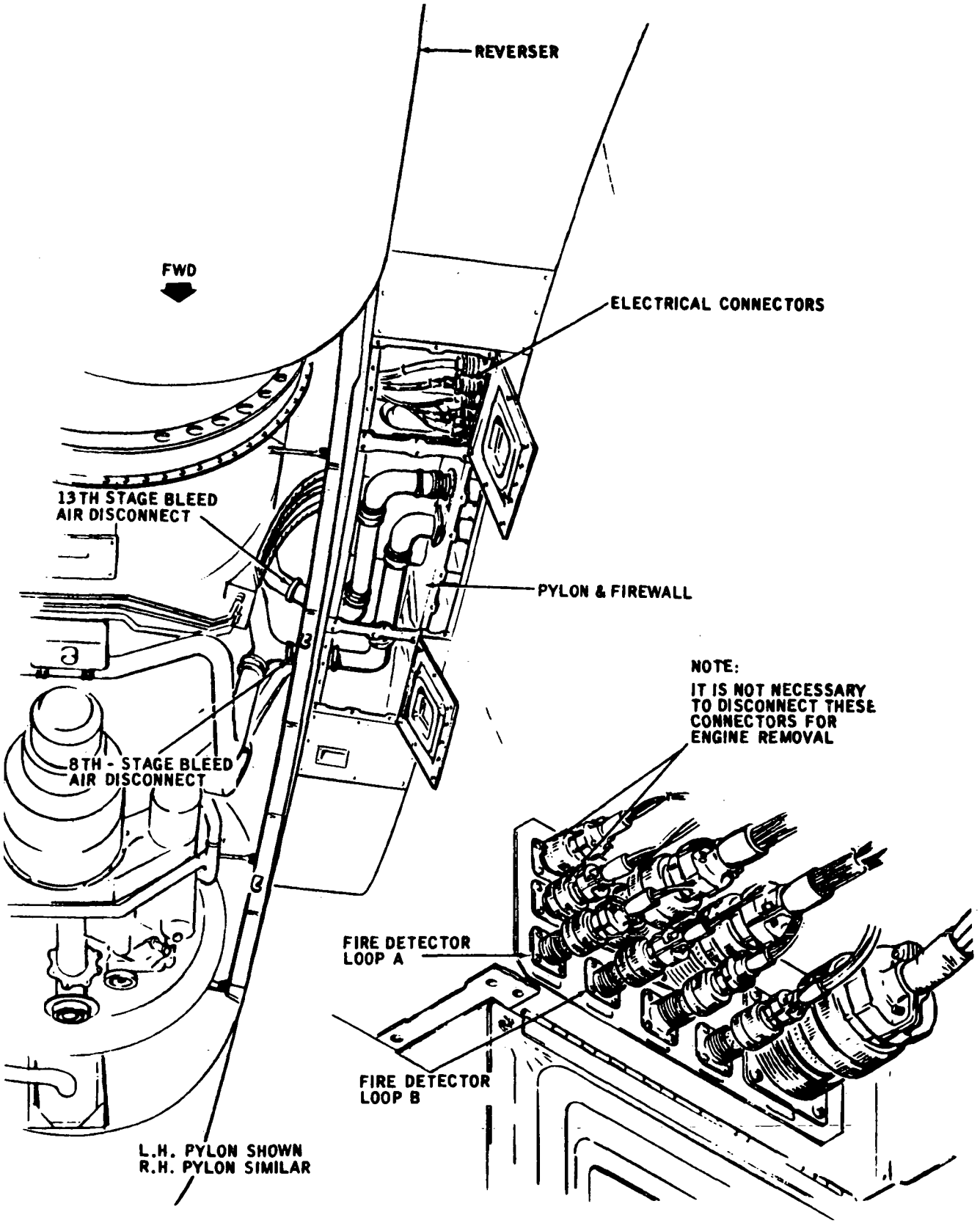

FIGURE B-5. EXISTING ENGINE DISCONNECT POINTS

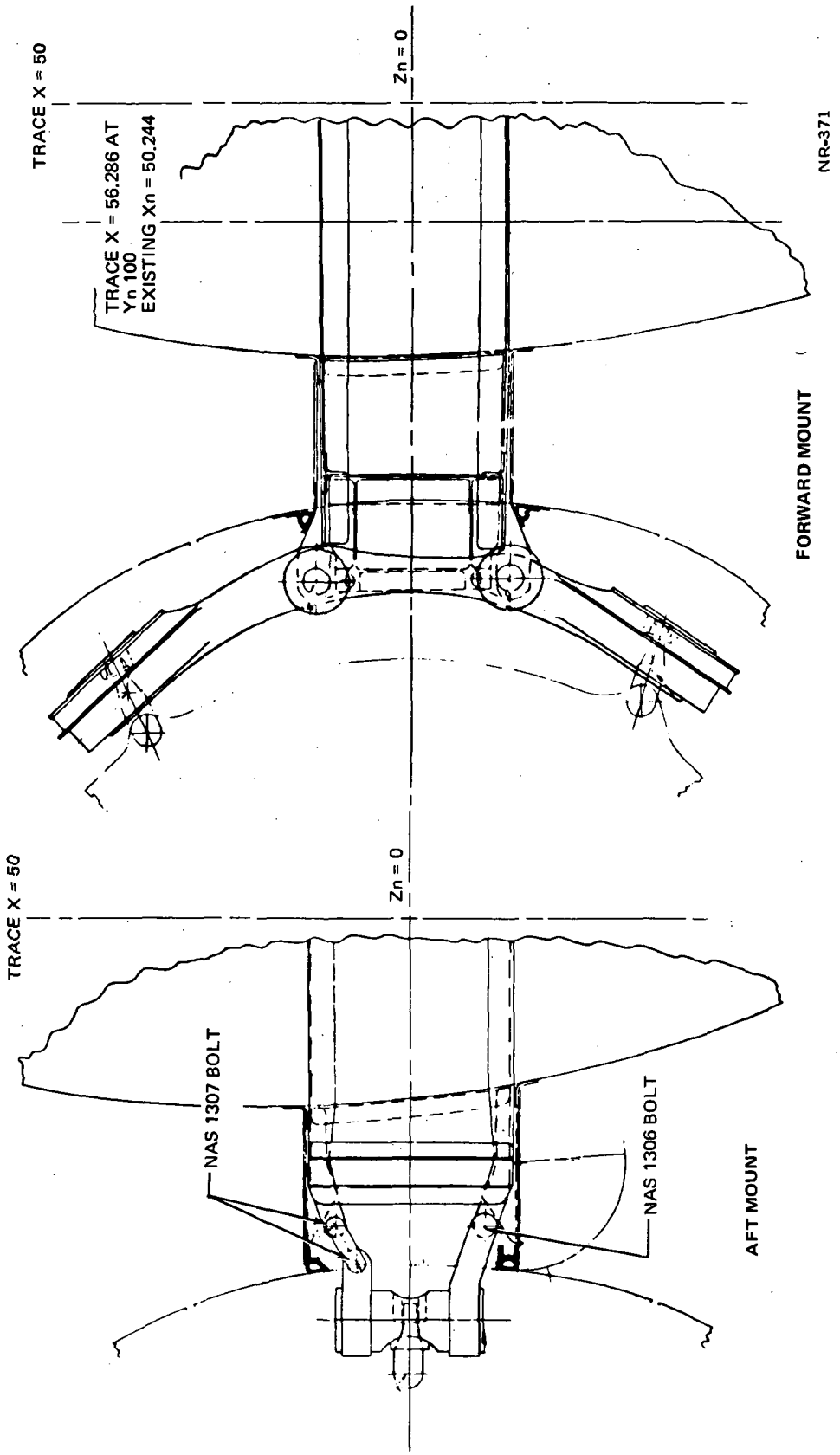

FIGURE B-6. ENGINE MOUNTS

in cold climates with a gloved hand and tools. In order to provide a 127.0 mm (5 in.) wide door with adequate support structure, the pylon width is restricted to a minimum of 191.0 mm (7.50 in.). Figure B-7 shows the door lands and minimum structure required on each side of the door.

From the results of the high and low speed testing (references 1 and 2), it was concluded that a Refan Nacelle could be installed on a pylon of from 132.0 mm (5.2 in.) to 279.0 mm (11.0 in.) in width without detriment to the aircraft performance or stability characteristics. By layout, mockup and shop experience, it was determined that the very short pylon width was too restrictive to allow adequate access to the engine systems passing through the pylon.

A fifth pylon (figure B-8) was sized approximately half-way between configuration (2) and (3) designated configuration (5) having the following characteristics:

- Outside nacelle contour 58.5 mm (2.3 in.) outboard of production nacelle contour.
- Engine centerline moved inboard 81.3 mm (3.2 in.) of production engine centerline.
- Pylon width at upper front spar 204.2 mm (8.05 in.)

Conclusion

Pylon configuration (5) meets all known requirements and will be designed and built during Phase II of the Refan Program (figure B-8).

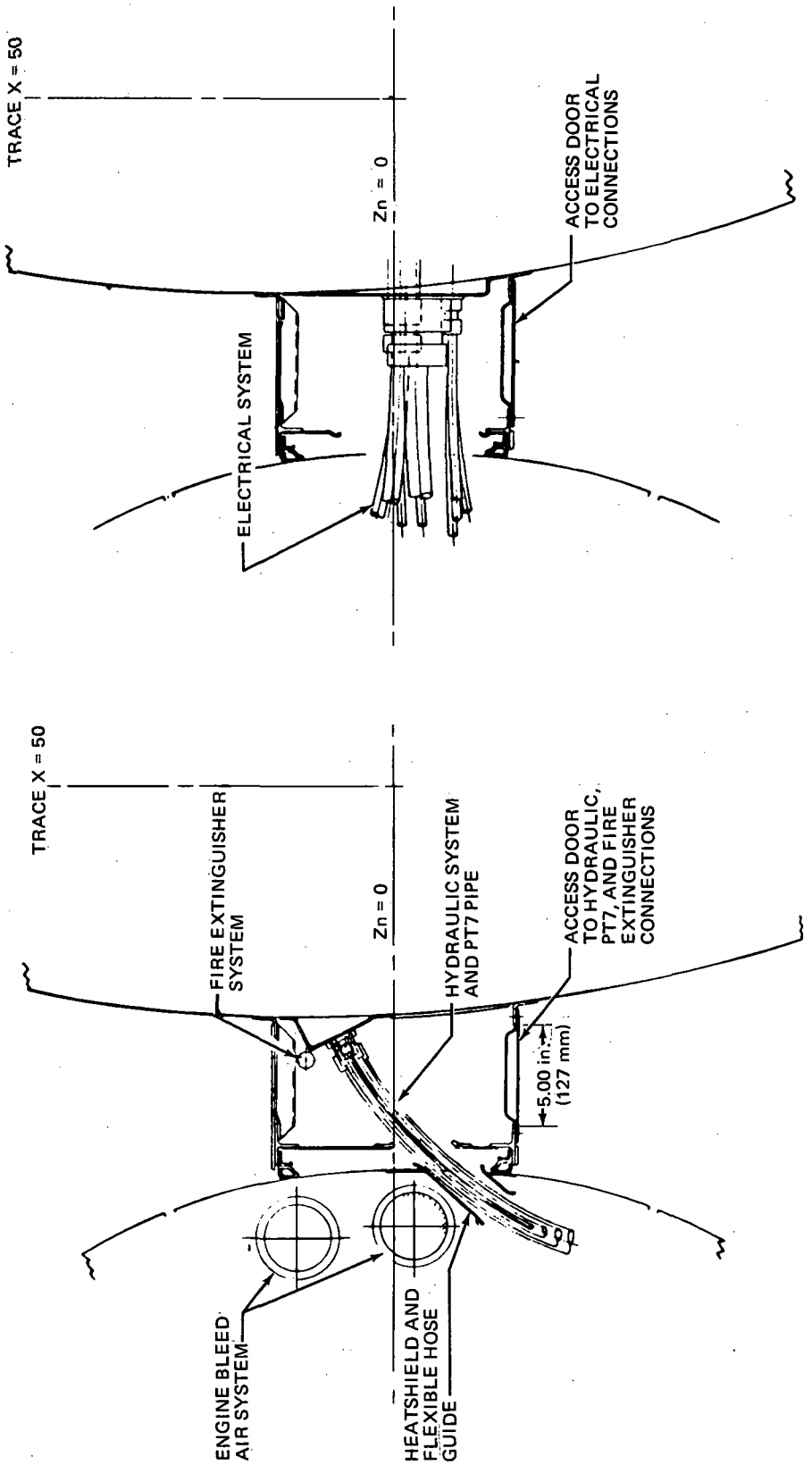

FIGURE B-7. ENGINE SUBSYSTEM CONNECTORS

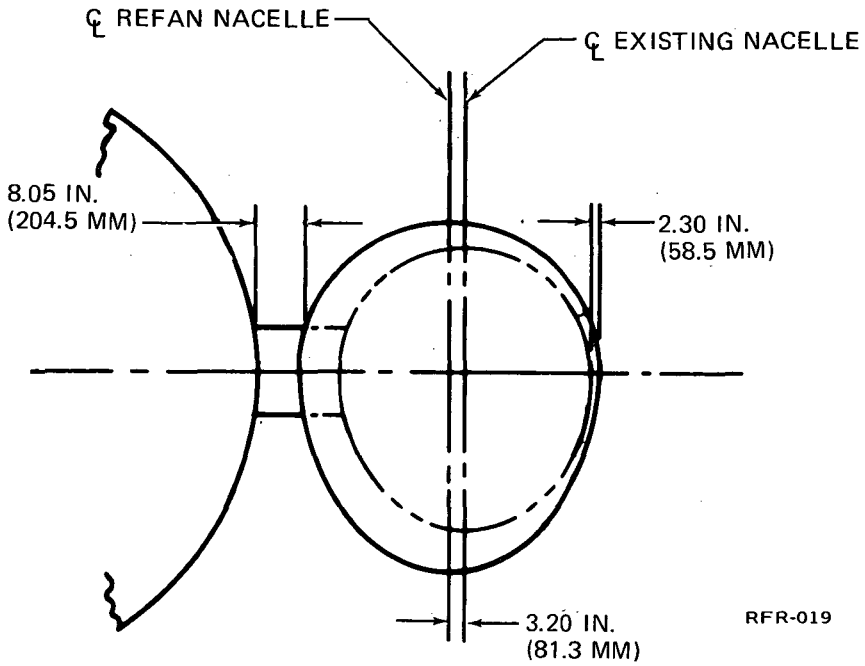

FIGURE B-8. CHOSEN PYLON CONFIGURATION

APPENDIX B

STRUCTURAL/ACOUSTICAL MATERIALS

A design study was conducted for the purpose of selecting the optimum material and cell construction for the acoustical attenuation treatment that would be used in the engine nacelle. This was a comprehensive study involving acoustic attenuation, strength, weight, and cost. The state of the art presently prescribes bonded aluminum to be used in the nacelle inlet and brazed Inconel for the exhaust nozzle.

Functional and Design Requirements

The noise attenuation treatments used in nacelles are subjected (depending upon the location in the nacelle) to varying levels of vibrations, elevated temperature, rain and sand erosion, and sonic fatigue. Since the treatments add weight and occupy additional space, substantial weight penalties are incurred unless the noise attenuation treatment is able to act as primary structure.

The Douglas Aircraft Company has acquired substantial structural test data and production experience in epoxy bonded aluminum sandwich, welded steel (Stresskin) sandwich, brazed Inconel sandwich, and integrally-woven glass/polyimide structures in previous Internal Research and Development, Contract Research and Development, and the DC-10 programs. However, many new materials, material applications, and processes with attractive design features are now available and can be considered.

Alternatives or Design Approaches

The sound suppression ability of the acoustic sandwich has been well demonstrated, however, some past designs have experienced sonic fatigue failures. To date, analytical study has not defined the local stresses within the cells which predicate cell fatigue life. Experimentally, difficulties occur in measuring the stress-strain inside the cell because of its smallness. As a result, the failure modes are not defined and the fatigue life data from one sandwich panel cannot be extrapolated to another of different or modified design. Depending on location within the nacelle, several sandwich materials have been studied for temperature and acoustic environment considerations.

APPENDIX B

Trade Study Evaluation Matrix

The structural/acoustical materials chosen for evaluation were:

(1) Bonded Aluminum
(2) Brazed Inconel
(3) Brazed Stainless Steel
(4) Brazed Aluminum
(5) Welded Stainless Steel
(6) Diffusion Bonded Titanium
(7) Integrally Woven Fiber Glass/Polyimide
(8) Sintered Stainless Steel

These materials have been selected to span a temperature range of 400 to 1100°K (250 to 1500°F). The purpose of the trade study was to determine the most effective use of each material relative to its strength retention and weight. The trade study was centered on a cell configuration, a 9.5 mm (3/8 in.) cell size and approximately 19 mm (3/4 in.) core height.

This trade study encompassed not only strength and weight studies, but also mechanical and acoustical fatigue, joints and closeouts, repairs, forming and cost considerations. Comparisons of typical room temperature mechanical properties and strength/mass ratios for selected sandwich panel construction are presented in tables B-4 and B-5. Formability and manufacturing costs are compared in table B-6. Bonded aluminum honeycomb was chosen as the basis for the table comparison because the current line of Douglas Aircraft Company nacelles utilize this treatment.

These tables represent only a brief summary of the data collected and do not reflect all possible relationships.

As a result of this materials trade study, the following recommendations are made for the JT8D-109 nacelle:

Inlet Inner Barrel (Estimated Temperature is 436°K (325°F).
Recommendations: Bonded Aluminum Sandwich using FM 150 adhesive.

Exhaust Nozzle (Estimated Temperature is 506°K (450°F).
Recommendations: Brazed Inconel 625 or 718 Sandwich.

TABLE B-4 - CONTINUED

TYPICAL MECHANICAL PROPERTIES OF SELECTED SANDWICH CONSTRUCTION

(ALL PROPERTIES AT ROOM TEMPERATURE)

SANDWICH CONSTRUCTION	FLATWISE TENSION F_{ft}, psi (kPa)	FLATWISE COMPRESSION F_{fc}, psi (kPa)	FLATWISE COMPRESSION MODULUS E_{fc}, psi (MPa)	EDGEWISE COMPRESSION F_{ec}, psi (MPa)	FLATWISE CORE SHEAR F_{fcs}, psi (kPa)	BEAM FLEXURE CORE SHEAR F_{bfcs}, psi (kPa)	CORE SHEAR MODULUS G_{cs}, psi (MPa)
BRAZED INCONEL 718							
Temp. Range: to 1200°F (922°K)	1,540 (10 610)	1,020 (7 028)	228,000 (1 570)	175,000 (1 205)	520 (3 582)	475 (3 272)	67,300 (464)
WELDED STAINLESS STEEL 316L (Stresskin)							
Temp. Range: to 700°F (644°K)	380 (2 618)	350 (2 411)	28,000 (193)	42,000 (289)	150 (1 033)	125 (861)	40,000 (275)
BONDED ALUMINUM (FM 150)							
Temp. Range: 300°F (422°K)	400 (2 756)	645 (4 444)	198,000 (1 364)	53,600 (369)	200 (1 378)	- -	29,000 (200)
BONDED ALUMINUM (FM 400) Per M.M.S. 307							
Temp. Range: to 450°F (505°K)	400 (2 756)	645 (4 444)	198,000 (1 364)	53,600 (369)	200 (1 378)	- -	29,000 (200)
BONDED ALUMINUM (Polyimide)							
Temp. Range: to 500°F (533°K)	400 (2 756)	645 (4 444)	198,000 (1 364)	53,600 (369)	200 (1 378)	- -	29,000 (200)

TABLE B-4 - CONCLUDED

TYPICAL MECHANICAL PROPERTIES OF SELECTED SANDWICH CONSTRUCTION

(ALL PROPERTIES AT ROOM TEMPERATURE)

SANDWICH CONSTRUCTION	FLATWISE TENSION F_{ft}, psi (kPa)	FLATWISE COMPRESSION F_{fc}, psi (kPa)	FLATWISE COMPRESSION MODULUS E_{fc}, psi (MPa)	EDGEWISE COMPRESSION F_{ec}, psi (MPa)	FLATWISE CORE SHEAR F_{fcs}, psi (kPa)	BEAM FLEXURE CORE SHEAR F_{bfcs}, psi (kPa)	CORE SHEAR MODULUS G_{cs}, psi (MPa)
INTEGRALLY WOVEN GLASS/ POLYIMIDE							
Temp. Range: to 500°F (533°K)	400 (2 756)	150 (1 033)	10,800 (74)	7,835 (54)	95 (654)	80 (551)	8,840 (61)
DIFFUSION BONDED TITANIUM 6Al-4V (Stresskin)							
Temp. Range: to 800°F (700°K)	720 (4 960)	580 (3 996)	- -	77,800 (536)	260 (1 798)	- -	- -
DIFFUSION BONDED TITANIUM 6Al-4V (Rohr Lid)							
Temp. Range: to 800°F (700°K)	1,000 (6 890)	700 (4 823)	150,000 (1 033)	- -	300 (2 067)	- -	44,000 (303)
BRAZED STAINLESS STEEL PH15-7MO							
Temp. Range: to 1000°F (811°K)	1,650 (11 368)	950 (6 545)	165,000 (1 136)	175,000 (1 205)	650 (4 478)	- -	42,000 (289)
BRAZED ALUMINUM 7106							
Temp. Range: to 600°F (589°K)	675 (4 650)	620 (4 271)	- -	38,700 (266)	305 (2 101)	525 (3 617)	90,250 (622)
SINTERED STAINLESS STEEL 347 S.S.							
Temp. Range: to 800°F (700°K)	630 (4 340)	- -	- -	- -	- -	- -	- -

TABLE B-5 - CONTINUED

TYPICAL STRENGTH/WEIGHT RATIOS OF SELECTED SANDWICH CONSTRUCTIONS

SANDWICH CONSTRUCTION	DENSITY SANDWICH ρ_s	DENSITY CORE ρ_c	STRENGTH/MASS RATIOS				
			FLATWISE TENSION F_{ft}/ρ_c	FLATWISE COMPRESSION F_{fc}/ρ_c	EDGEWISE COMPRESSION F_{ec}/ρ_s	FLATWISE CORE SHEAR F_{fcs}/ρ_c	BEAM FLEXURE CORE SHEAR F_{bfcs}/ρ_c
	10^{-3} slug/in^2 (kg/m^2)	10^{-3} slug/in^2 (kg/m^2)	$\frac{ksi}{slug/in^2}$ $\frac{kPa}{g/m^2}$	$\frac{ksi}{slug/in^2}$ $\frac{kPa}{g/m^2}$	$\frac{ksi}{slug/in^2}$ $\frac{kPa}{g/m^2}$	$\frac{ksi}{slug/in^2}$ $\frac{kPa}{g/m^2}$	$\frac{ksi}{slug/in^2}$ $\frac{kPa}{g/m^2}$
BRAZED INCONEL 718							
Temp. Range: to 1200°F (922°K)	.498 (11.26)	.100 (2.26)	15,400 (4.69)	10,200 (3.11)	351,406 (107.02)	5,200 (1.58)	4,750 (1.45)
WELDED STAINLESS STEEL 316L(Stresskin)							
Temp. Range: to 700°F (644°K)	.367 (8.30)	.100 (2.26)	3,800 (1.16)	3,500 (1.07)	114,441 (34.82)	1,500 (.46)	1,250 (.38)
BONDED ALUMINUM (FM 150)							
Temp. Range: to 300°F (422°K)	.233 (5.27)	.053 (1.20)	7,547 (2.30)	12,170 (3.70)	230,043 (70.02)	3,774 (1.15)	- -
BONDED ALUMINUM (FM 400) Per MMS 307							
Temp. Range: to 450°F (505°K)	.233 (5.27)	.053 (1.20)	7,547 (2.30)	12,170 (3.70)	230,043 (70.02)	3,774 (1.15)	- -
BONDED ALUMINUM (POLYIMIDE FM 34)							
Temp. Range: to 500°F (533°K)	.233 (5.27)	.053 (1.20)	7,547 (2.30)	12,170 (3.70)	230,043 (70.02)	3,774 (1.15)	- -

TABLE B-5 - CONCLUDED

TYPICAL STRENGTH/WEIGHT RATIOS OF SELECTED SANDWICH CONSTRUCTIONS

SANDWICH CONSTRUCTION	DENSITY SANDWICH ρ_s	DENSITY CORE ρ_c	STRENGTH/MASS RATIOS				
			FLATWISE TENSION F_{ft}/ρ_c	FLATWISE COMPRESSION F_{fc}/ρ_c	EDGEWISE COMPRESSION F_{ec}/ρ_s	FLATWISE CORE SHEAR F_{fcs}/ρ_c	BEAM FLEXURE CORE SHEAR F_{bfcs}/ρ_c
	10^{-3}slug/in^2 (kg/m^2)	10^{-3}slug/in^2 (kg/m^2)	$\frac{\text{ksi}}{\text{slug/in}^2}$ $\frac{\text{kPa}_2}{\text{g/m}^2}$	$\frac{\text{ksi}}{\text{slug/in}^2}$ $\frac{\text{kPa}_2}{\text{g/m}^2}$	$\frac{\text{ksi}}{\text{slug/in}^2}$ $\frac{\text{kPa}_2}{\text{g/m}^2}$	$\frac{\text{ksi}}{\text{slug/in}^2}$ $\frac{\text{kPa}_2}{\text{g/m}^2}$	$\frac{\text{ksi}}{\text{slug/in}^2}$ $\frac{\text{kPa}_2}{\text{g/m}^2}$
INTEGRALLY WOVEN GLASS POLYIMIDE							
Temp. Range: to 500°F (533°K)	.280 (6.33)	.121 (2.14)	3,306 (1.01)	1,240 (.38)	27,982 (8.53)	785 (.24)	661 (.20)
DIFFUSION BONDED TITANIUM 6Al-4V (Stresskin)							
Temp. Range: to 800°F (700°K)	.211 (4.77)	.081 (1.83)	8,889 (2.71)	7,160 (2.18)	368,720 (112.37)	3,210 (.98)	- -
DIFFUSION BONDED TITANIUM 6AL-4V (Rohr Lid)							
Temp. Range: to 800°F (700°K)	.211 (4.77)	.081 (1.83)	12,346 (3.77)	8,642 (2.64)	-	3,704 (1.13)	-
BRAZED STAINLESS STEEL PH15-7MO				-	-	-	-
Temp. Range: to 1000°F (811°K)	.498 (11.26)	.100 (2.26)	16,500 (5.03)	9,500 (2.90)	351,406 (107.02)	6,500 (1.98)	- -
BRAZED ALUMINUM 7106							
Temp. Range: to 600°F (589°K)	.519 (11.74)	.096 (2.17)	7,031 (2.14)	6,458 (1.97)	74,566 (22.66)	3,177 (.97)	5,469 (1.67)
SINTERED 347 S.S.							
Temp. Range: to 800°F (700°K)	.336 (7.60)	.100 (2.26)	6,300 (1.92)	- -	- -	- -	- -

TABLE B-6 - CONTINUED
FORMABILITY, TOOLING, MATERIAL AND LABOR
COST COMPARISON FOR SELECTED SANDWICH CONSTRUCTIONS

MATERIAL PROPOSED	FORM-ABILITY	TOOLING COSTS	MATERIAL and LABOR COSTS	REMARKS
Bonded Aluminum	1.0	1.0	1.0	Material established as a base for comparison. Basic tooling: SFD #1, and #2, Bonding fixture.
Brazed Inconel 718 or 625	4.0	4.0	7.0	Difficult to hold tolerance required between mating surfaces to ensure acceptable bonded interface. Basic tooling: SFD #1, and #2, Brazing fixture.
Welded Inconel 718 (Stresskin)	4.0	1.0	7.0	Material received in the past has been extremely difficult to form due to an inadequate thermal anneal condition. Redesign of the proposed configuration should be considered. Basic tooling: SFD #1.
Brazed Stainless Steel (300) Series)	3.0	4.0	6.0	The formability of this material is somewhat easier than that of Inconel. However, the brazing application still is the expensive item. Basic tooling: SFD #1, and #2, Brazing fixture.
Sintered Stainless Steel	2.5	1.0	6.0	The formability of this mat- is similar to stresskin; however, little is known on how well the bond will withstand the forming stresses. Basic tooling: SFD #1

TABLE B-6 - CONCLUDED

FORMABILITY, TOOLING, MATERIAL AND LABOR

COST COMPARISON FOR SELECTED SANDWICH CONSTRUCTIONS

MATERIAL PROPOSED	FORM-ABILITY	TOOLING COSTS	MATERIAL and LABOR COSTS	REMARKS
Welded Stainless Steel (Stresskin)	2.0	1.0	3.0	This material would have been the best chance to be formed into the desired shapes if both the core depth and cell size could be reduced. Basic tooling: SFD #1
Diffusion Bonded Titanium	2.5	5.0	6.0	The configuration would be possible if adequate tooling were built. Requiring a very sophisticated heating and protective inert gas purging system. Basic tooling: SFD #1
Integrally Woven Fiberglass/ Polyimide	--	--	--	The polyimide system requires very closs step control to produce acceptable end products. Hoever-virtually any shape is possible when tooled correctly. Basic Tooling: Lay-up tool, core mandrels, post curing fixture.

APPENDIX C

DOC'S AND ECONOMIC ASSUMPTIONS

The modified ATA direct operating cost formula was used to calculate relative cash operating cost increments as a result of refanning DC-9 and DC-8 aircraft. These relatives were then applied to 1972 reported direct operating cost data to estimate the actual cash operating costs increments anticipated as a result of refanning. The primary modifications to the 1967 ATA formula reflect current (1972/1973) cost levels. McDonnell Douglas historically based maintenance estimates were used in lieu of the parametric maintenance equations of the 1967 ATA.

This Appendix presents tables of 1967 ATA and Refan Domestic and International DOC Formulas. See table C-1 and C-2.

APPENDIX C

TABLE C-1

1967 ATA AND REFAN DOMESTIC DOC STUDY

	1967 ATA	ATA (1972 COEFFICIENT)
CREW PAY ($/BLK-HR)		
2-MAN JET	0.05 (TOGW/1000) + 100.00	$11.987 \left[\left(V_{cr} \frac{TOGW^{0.3}}{10^5}\right)\right] + 28.754$
3-MAN JET (SUBSONIC)	0.05 (TOGW/1000) + 135.00	$16.293 \left[\left(V_{cr} \frac{TOGW^{0.3}}{10^5}\right)\right] + 40.695$
FUEL ($/GAL)	0.10	0.12
NONREVENUE FACTOR ON FUEL	1.02	INCLUDED IN FUEL PRICE
AIRFRAME MAINTENCE – CYCLE		
MATERIAL ($/CYC)	$6.24\ (Ca/10^6)$	
DIRECT LABOR (MH/CYC)	$0.05\ (Wa/1000) + 6 - \frac{630}{(Wa/1000) + 120}$	DOUGLAS ESTIMATES
AIRFRAME MAINTENANCE – HOURLY		
MATERIAL ($/FH)	$3.08\ Ca/10^6$	
DIRECT LABOR (MH/FH)	$0.59\left[0.05\ (Wa/1000) + 6 - \frac{630}{(Wa/1000) + 120}\right]$	
ENGINE MAINTENANCE – CYCLE		
MATERIAL ($/CYC)	$20.0\ (Ce/10^6)\ Ne$	DOUGLAS ESTIMATES
DIRECT LABOR	$\left[0.3 + 0.03\ (T/10^3)\right] Ne$	
ENGINE MAINTENANCE – HOURLY		
MATERIAL	$25.0\ (Ce/10^6)\ Ne$	
DIRECT LABOR	$\left[0.6 + 0.027\ (T/10^3)\right] Ne$	
BURDEN MH/DIRECT LABOR MH	1.8	2.0
MAINTENANCE LABOR RATE ($/MH)	4.00	6.25
INSURANCE (PERCENT PRICE/YEAR)	2.0	1.0
INVESTMENT SPARES RATIO (PERCENT)		
AIRFRAME	10	6
ENGINE	40	30
DEPRECIATION SCHEDULE (YEARS/PERCENT RESIDUAL)		
SUBSONIC	12/0	14/10
UTILIZATION (HR/YEAR)	FORMULA: $U = \frac{4500}{1 + 1/(T_b + 0.30)} + 500$	FORMULA: $U = \frac{4500}{1 + 1/(T_b + 0.30)} + 500$

DEFINITIONS OF TERMS AND UNITS

TOGW – MAXIMUM TAKEOFF GROSS WEIGHT(LB)
Vcr – CRUISE SPEED (MPH)
Ca – AIRFRAME PRICE(S)
Ce – ENGINE PRICE(S)
Ne – NUMBER OF ENGINES
T – SEA LEVEL STATIC THRUST(LB)
Wa – AIRFRAME WEIGHT(LB)
M – MACH NUMBER
FH – FLIGHT HOURS
MH – MAN HOURS
CYC – CYCLE
T_b – BLOCK TIME (HR)

FOR 707/DC-8 TYPE AIRPLANES

RFR-187

APPENDIX C

TABLE C-2
1967 ATA AND REFAN INTERNATIONAL DOC STUDY

	1967 ATA	ATA (1972 COEFFICIENT)
CREW PAY ($/BLK-HR) 3 MAN JET (SUBSONIC)	$0.05\ (TOGW/1000) + 155.00$	$17.625\ [V_{cr}\ (TOGW/10^5]^{0.3} + 64.55$
FUEL ($/GAL) NONREVENUE FACTOR ON FUEL	0.11 1.02	0.12 INCLUDED IN FUEL PRICE
AIRFRAME MAINTENANCE CYCLE MATERIAL ($/CYC) DIRECT LABOR (MH/CYC) AIRFRAME MAINTENANCE HOURLY MATERIAL ($/FH) DIRECT LABOR (MH FH)	$6.24\ (Ca/10^6)$ $0.05\ (Wa/1000) + 6 - \frac{630}{(Wa/1000) + 120}$ $3.08\ (Ca/10^6)$ $0.59\left[0.05\ (Wa/1000) + 6 - \left(\frac{630}{(Wa/1000) + 120}\right)\right]$	DOUGLAS ESTIMATES
ENGINE MAINTENANCE – CYCLE MATERIAL ($/CYC) DIRECT LABOR ENGINE MAINTENANCE – HOURLY MATERIAL DIRECT LABOR	$20.0\ (Ce/10^6)\ Ne$ $[0.3 + 0.03\ (T/10^3)]\ Ne$ $25.0\ (Ce/10^6)\ Ne$ $[0.6 + 027\ (T/10^3)]\ Ne$	DOUGLAS ESTIMATES
BURDEN MH/DIRECT LABOR MH MAINTENANCE LABOR RATE ($/MH)	1.8 4.00	2.0 6.25
INSURANCE (PERCENT PRICE/YR)	2.0	1.0
INVESTMENT SPARES RATIO (PERCENT) AIRFRAME ENGINE	 10 40	 6 30
DEPRECIATION SCHEDULE (YEARS/PERCENT RESIDUAL) SUBSONIC	 12/0	 14/10
UTILIZATION (HR/YEAR)	FORMULA: $U = \frac{4500}{1 + 1/(T_b + 0.30)} + 500$	FORMULA: $U = \frac{4500}{1 + 1/(T_b + 0.30)} + 500$

DEFINITION OF TERMS AND UNITS

TOGW	MAXIMUM TAKEOFF GROSS WEIGHT (LB)	Wa	AIRFRAME WEIGHT (LB)	FOR 707/DC-8 TYPE AIRPLANES
Vcr	CRUISE SPEED (MPH)	M	MACH NUMBER	
Ca	AIRFRAME PRICE ($)	FH	FLIGHT HOURS	
Ce	ENGINE PRICE ($)	MH	MAN HOURS	
Ne	NUMBER OF ENGINES	CYC	CYCLE	
T	SEA LEVEL STATIC THRUST (LB)	T_b	BLOCK TIME (HR)	

RFR-186

APPENDIX D

This appendix presents a final summary of the status of the Douglas Aircraft Company effort to satisfy the objectives of the DC-8 Series 50 and 60/JT3D-9 refan engine portion of the NASA Phase I Refan Program at the time of termination. This appendix covers work from 17 August 1972 to 15 January 1973, except for the high speed wind tunnel test on the DC-8-50 and -61 models which was performed between January and April 1973 and is summarized in this appendix.

A report ("The Effects on Cruise Drag of Installing Long-Duct Refan Engine Nacelles on the McDonnell Douglas DC-8-50 and -61," J. T. Callaghan, J. E. Donelson, and J. P. Morelli.) NASA CR-121218 has been written and submitted to the NASA (reference 3).

APPENDIX D

DC-8-50/60 FINAL SUMMARY

TABLE OF CONTENTS

TABLE OF CONTENTS (Concluded)

APPENDIX D

PROGRAM DEFINITION

The objectives of this study were to:

(1) Provide nacelle and airplane integration documents for installation of the JT3D-9 engine on the DC-8 Series 50/60 airplanes.

(2) Prepare preliminary designs of nacelle and airplane modifications for installing the JT3D-9 engine on the DC-8 Series 50/60 airplanes.

(3) Initiate model tests of DC-8 nacelle and airplane configurations.

(4) Analyze the economic considerations of the JT3D-9 engine and the noise reduction trade-offs in retrofitting this engine on the DC-8 Series 50/60 airplanes.

(5) Prepare and submit a detailed plan and proposal for Phase II.

Objectives (1), (2), (3), and (4) had not been completed at the time of termination of the DC-8/JT3D-9 portion of Phase I and are summarized up to the termination point in this appendix. Objective (5) had been completed and proposals submitted.

DC-8 SERIES 50/60 AIRPLANE DESCRIPTION

The DC-8-61 was the last of the DC-8 airplanes using JT3D engines installed in "short duct" pods. This pod is characterized by a short 610 mm (24 in.), bifurcated fan exhaust duct which discharges the fan air at the sides of nacelle and utilizes separate fan and primary exhaust thrust reversers. The other DC-8 models which utilize the short duct JT3D engine installation are the -51, -52, -53, -54F, -55F, and -61F. All of these models feature the over-the-wing pylon (figure D-1) but differ widely in gross weights, fuel tank arrangements, wing skin thickness, and/or specific JT3D engine model. A total of 236 DC-8 Series 50 and DC-8-61 airplanes were manufactured with this nacelle/pylon design. Of these 236 airplanes 142 were sold to U.S. domestic operators.

The DC-8-63 was the last version of the DC-8 airplane produced and uses JT3D engines installed in "long duct" pods (figure D-1). This pod is characterized by a long 3.91 m (154 in.) fan exhaust duct, bifurcated for most of its length, which discharges the fan air at the aft end of the nacelle through an annular section surrounding the primary nozzle. It utilizes a single, target-type reverser to reverse both the fan and primary exhaust streams. The other DC-8 models which utilize the long duct JT3D engine installation are the -62, -62F and -63F. All of these models feature the

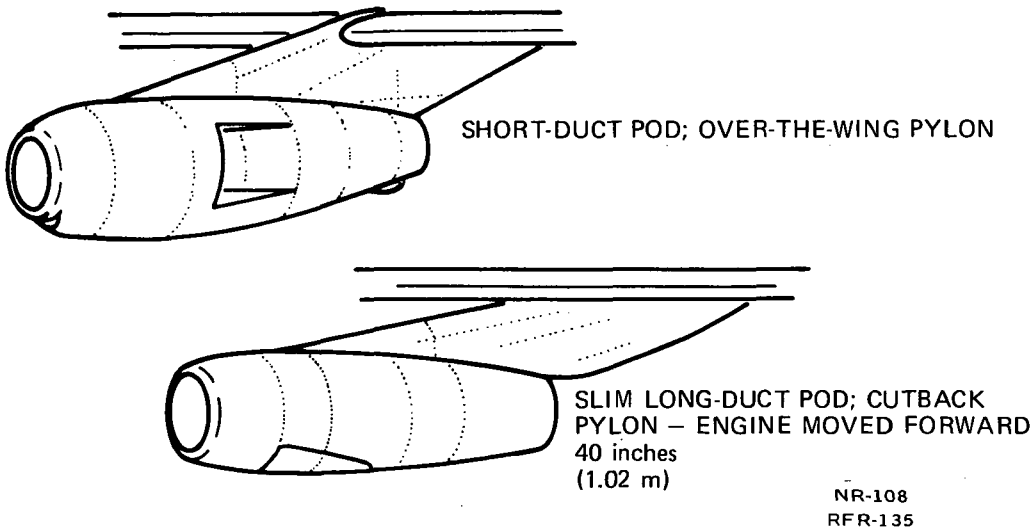

FIGURE D-1. SHORT AND LONG DUCT POD CONFIGURATIONS

under-cut pylon, but differ in gross weights, wing skin thickness, and/or specific JT3D engine model.

A total of 166 DC-8-62/-63 airplanes were manufactured with 72 of these being sold to U.S. domestic operators.

ENGINE DEFINITION

The Pratt & Whitney JT3D-9 is a derivative of the basic JT3D turbofan engine incorporating a new, larger diameter, single-stage fan with a 2.25:1 bypass ratio, a new super-charging low compressor stage, the existing 3-stage low pressure turbine incorporating a modified last stage blade and disk and the current high pressure spool and can-annular combustor without modification.

The general performance and physical characteristics and features of the JT3D-9 and JT3D-3B compared in figure D-2.

NACELLE PRELIMINARY DESIGN

Three levels of acoustic treatment were identified for the DC-8-61. The minimum treatment level utilized the short fan duct concept with a maximum utilization of existing hardware and acoustic treatment only on the walls of the inlet and fan exhaust duct (figure D-3). The intermediate level configuration was identified as the short duct concept treated as far as engineering judgment permitted. An acoustically treated splitter was added to the fan duct and a ring was installed in the inlet (figure D-4). For the maximum acoustic treatment it was necessary to install a long fan exhaust duct to achieve the required treated length/channel height relationship (figure D-5).

The installation of the JT3D-9 refan engine on the DC-8 Series 50 airplanes has been studied with a Delta DC-8 Model 51 and a United DC-8 Model 54F configuration using the intermediate level of noise suppression. These installations are basically identical to the DC-8 Model 61 airplane.

Two levels of acoustic treatment were identified for the long duct DC-8-63. The "minimum" treatment configuration utilized wall treatment only on an inlet sized for engine performance. Enough wall treatment was added to the fan exhaust duct to achieve a balanced configuration (figure D-6).

With the addition of a ring in the inlet and more fan duct treatment, a configuration was achieved which brought the noise level down to the jet floor. This was identified as a "maximum" treatment (figure D-7). No practical "intermediate" treatment was identified.

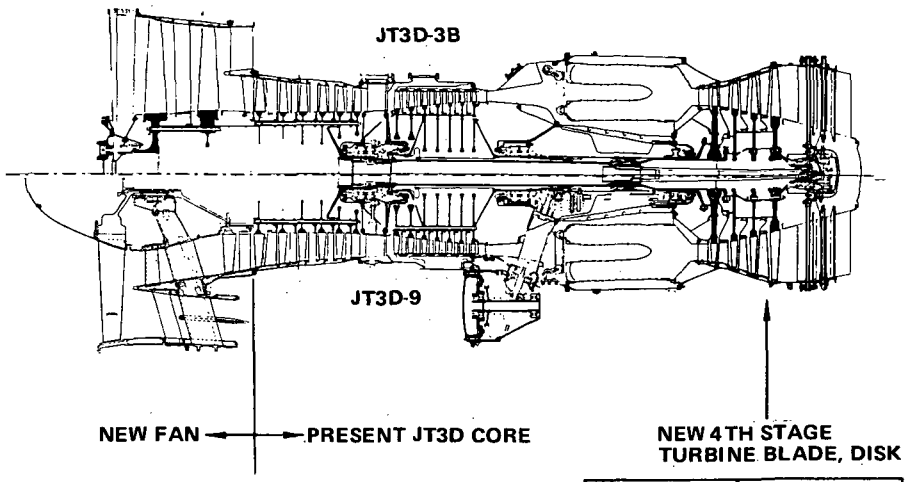

		JT3D-9	JT3D-3B
TAKEOFF THRUST (SEA LEVEL STATIC, STANDARD DAY)	lb N	20,750 (92,301)	18,000 (80,068)
FAN TIP SPEED, S.L.S.T.O.	ft/sec m/sec	1538 (468.8)	1423 (433.7)
BYPASS RATIO		2.25	1.36
FAN PRESSURE RATIO		1.66	1.75
CRUISE THRUST, 35,000 FT (10,668 M), 0.80 MACH	lb N	4712 (20,960)	4400 (19,572)
CRUISE TSFC, 35,000 FT (10,668 M), 0.80 MACH, 4400 LB (19,572 N) THRUST	lb/hr/lb kg/hr/N	0.745* (0.0760)	0.758* (0.0773)
FAN TIP DIAMETER	in. m	56.5 (1.435)	50.2 (1.275)
OVERALL BARE ENGINE LENGTH (LESS SPINNER)	in. m	135 (3.429)	134 (3.404)
BARE ENGINE WEIGHT	lb kg	4640 (2105)	4260 (1932)

*BASED ON A NOZZLE VELOCITY COEFFICIENT (C_V) OF 1.0 AT CUSTOMER FLANGE CONNECTIONS.

RFR-134

FIGURE D-2. ENGINE CHARACTERISTICS COMPARISON

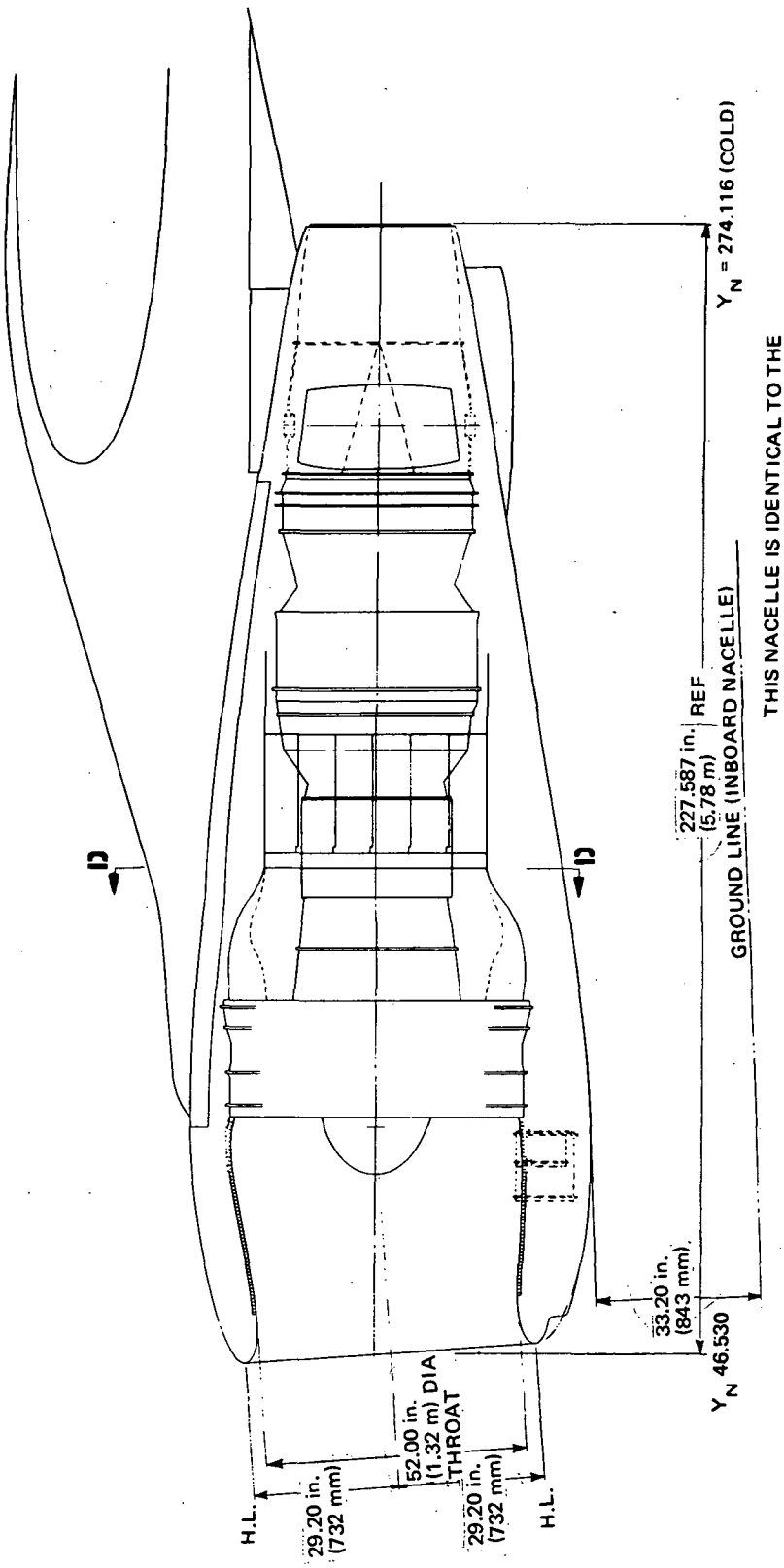

FIGURE D-3. DC-8-61 MINIMUM NOISE SUPPRESSION NACELLE GENERAL ARRANGEMENT – SIDEVIEW

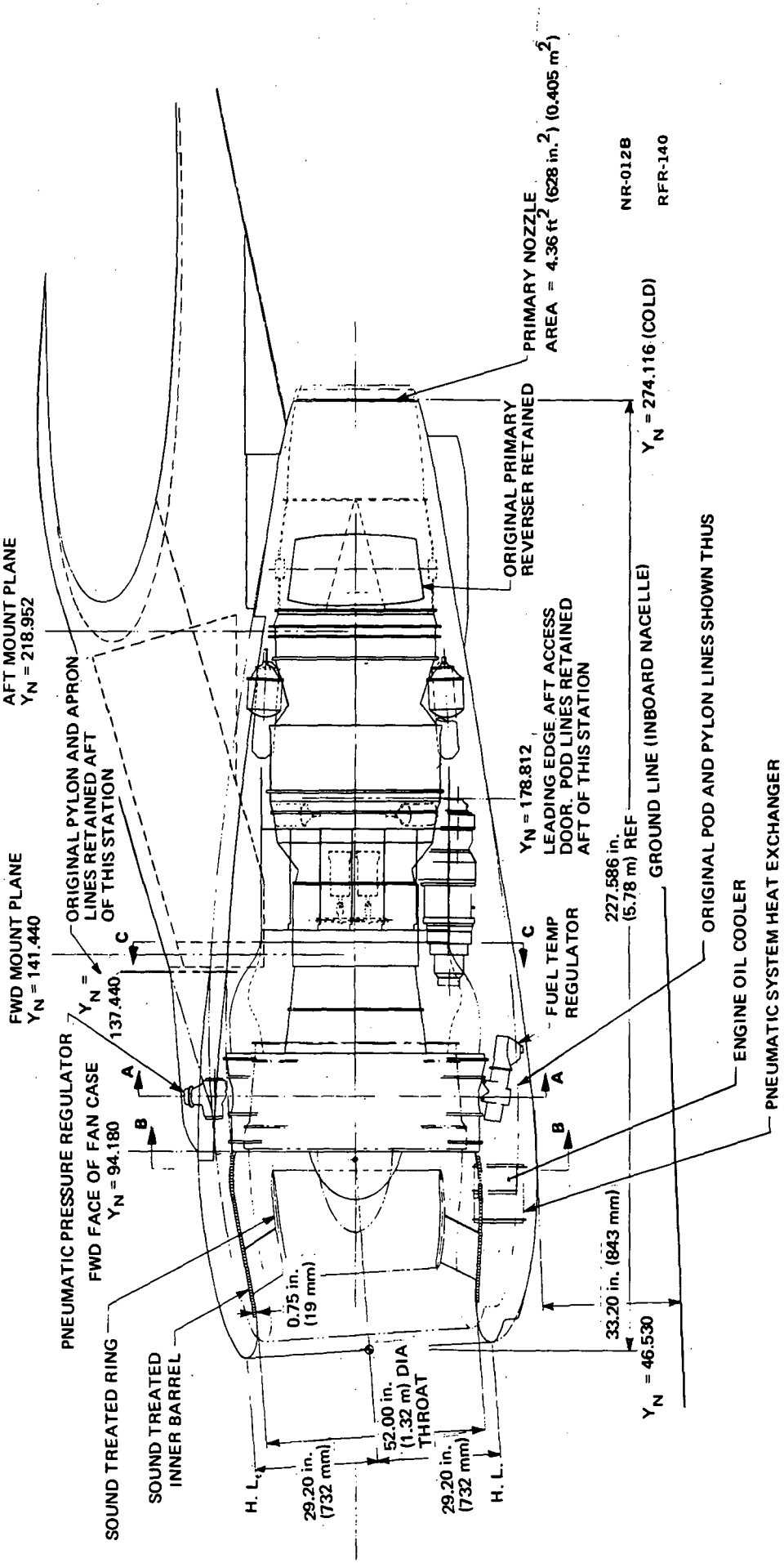

FIGURE D-4. DC-8-61 INTERMEDIATE NOISE SUPPRESSION NACELLE GENERAL ARRANGEMENT – SIDEVIEW

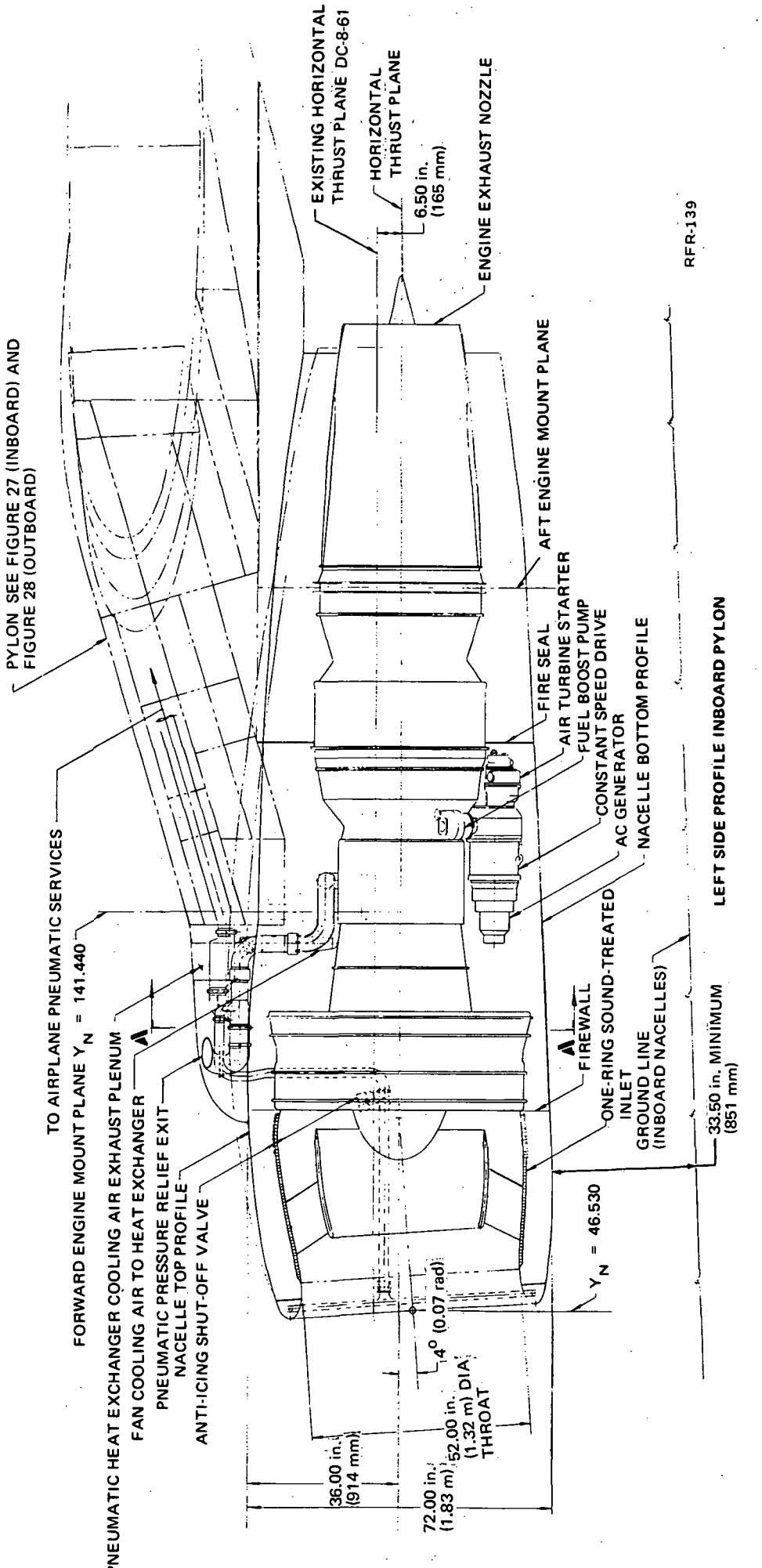

FIGURE D-5. DC-8-61 MAXIMUM NOISE SUPPRESSION NACELLE GENERAL ARRANGEMENT – SIDEVIEW

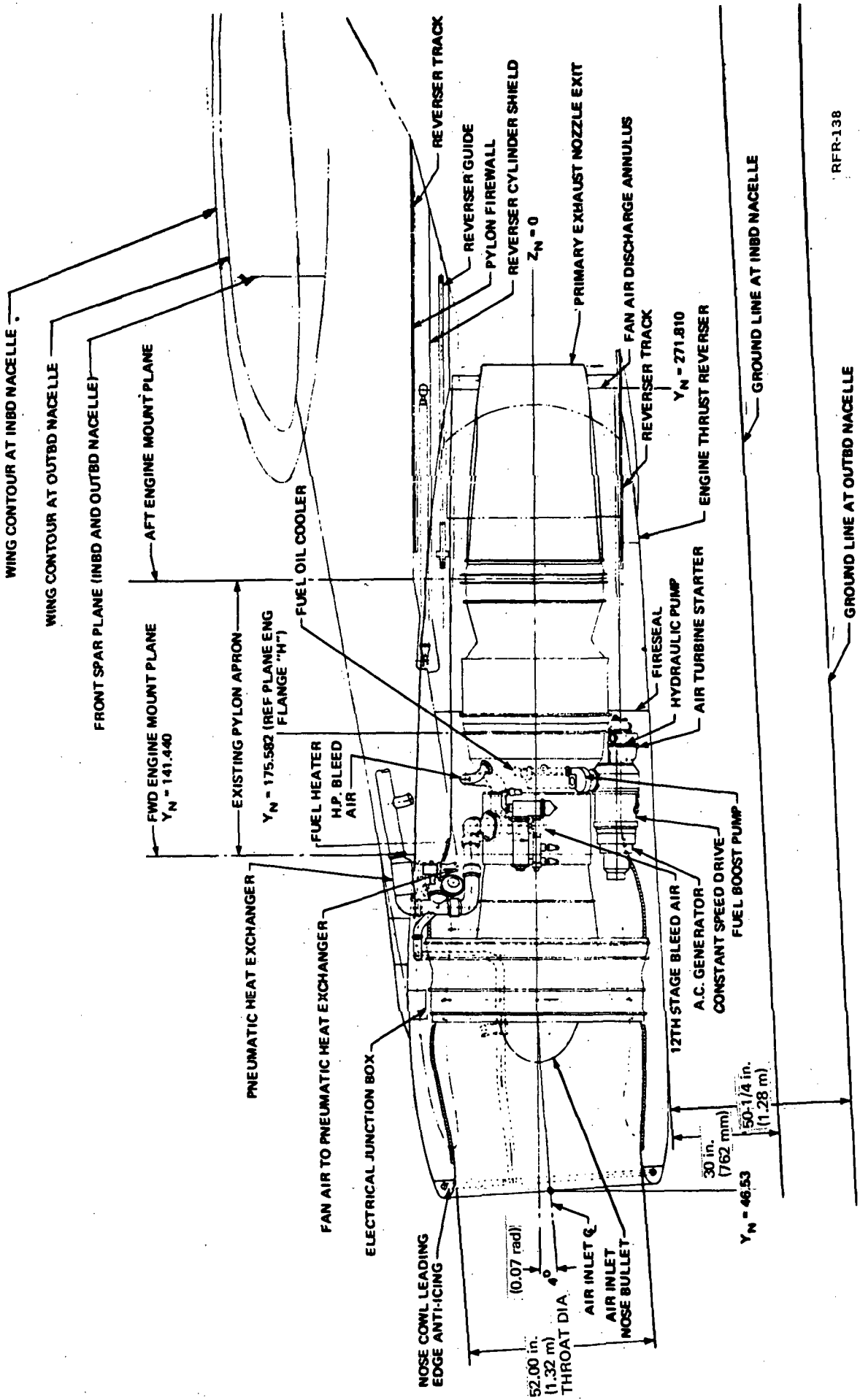

FIGURE D-6. DC-8-63 MINIMUM NOISE SUPPRESSION NACELLE GENERAL ARRANGEMENT – SIDEVIEW

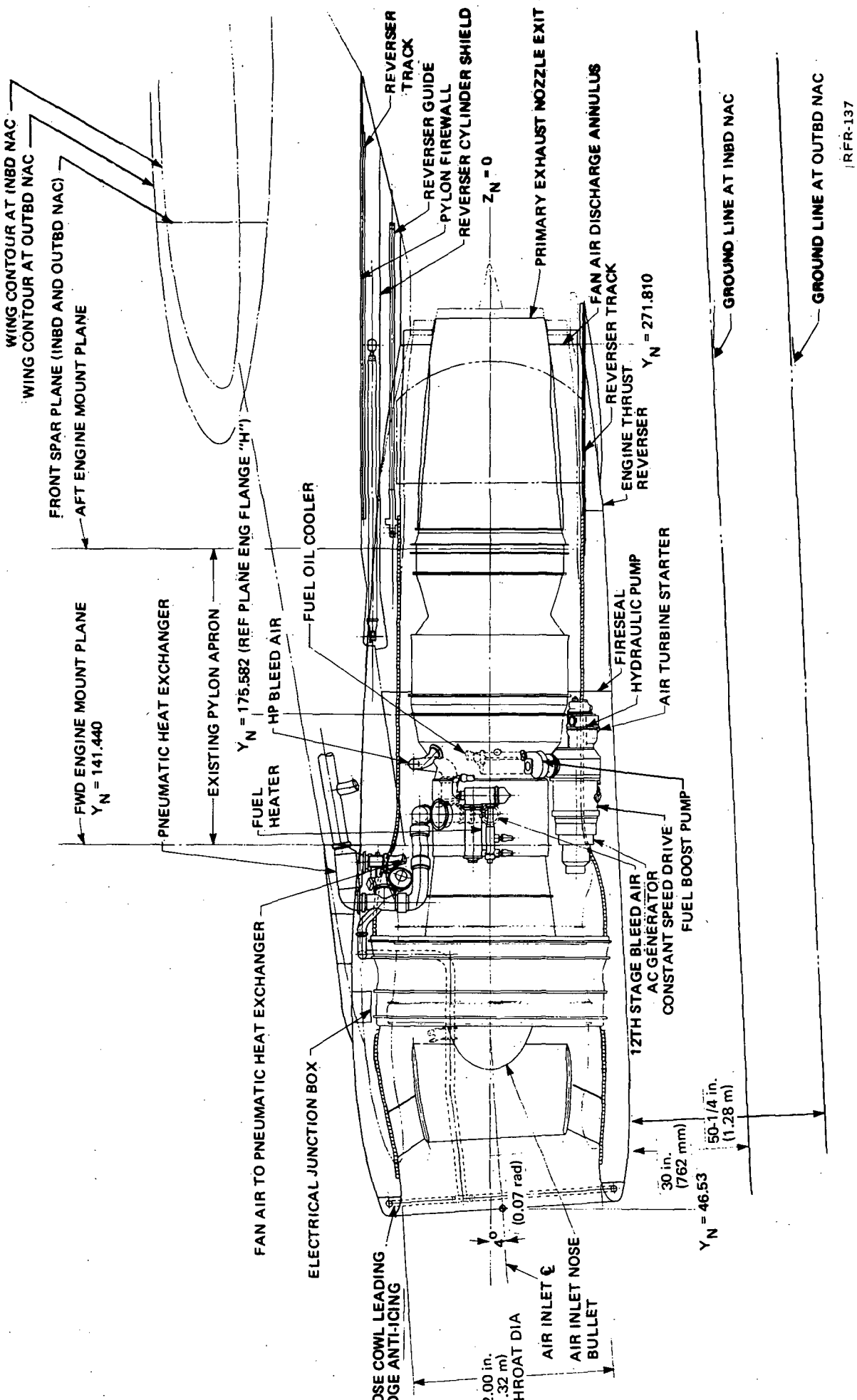

FIGURE D-7. DC-8-63 MAXIMUM NOISE SUPPRESSION NACELLE GENERAL ARRANGEMENT – SIDEVIEW

APPENDIX D

Fan Duct Lines

The following ground rules were used in the development of the short fan duct lines (DC-8 Model 61):

- The Pratt & Whitney fan reverser was retained essentially unchanged, as regards to matching the fan nozzle.
- The top, bottom and inner lines of the nozzle geometry were not changed; all increase in nozzle area was achieved by moving the outer line out board.
- The duct inner surface was at no point inboard of the original duct, to ensure clearance from systems, etc.

The final duct lines were evolved by reiteration of board lay-out, computer evaluation of flow areas and loft lay-out to establish corner radii and faired surfaces, station-to-station.

The first attempts at increasing the fan duct flow areas to suit the larger exit area of the new fan, maintained the inside lines at the same geometry as the existing DC-8-63 lines. The area increase was accomplished by pushing the outside duct lines further out and increasing the top and bottom radii. Figures D-6 and D-7 show the nacelle lines resulting from these duct lines. It was possible to keep the same ground clearance for both inner and outer pods. The distance between the top of the nacelle and the underside of the wing decreased slightly. Because of thrust reverser considerations, the aft end of the pod and the thrust reverser outline were changed. This change is not shown on figures D-6 and D-7.

Fan Reverser Design

For the minimum and intermediate treatment configuration of the short duct nacelle JT3D-9 installation, Douglas expected to retain the Pratt & Whitney fan reverser with minimum modification. It was considered acceptable if the total reverse thrust of the fan and primary reverser combined was no less than that of the original DC-8-61 design. Initial investigation indicated that the opening angle of the cascade assembly could be increased by no more than .053 rad (3°) without major interference between linkage elements in the area of the hinge line.

Further investigation proceeded on the following basis:

(1) Maximum opening angle would be 0.462 rad (26.50°).

(2) The leading edge of the cascade assembly would be modified to provide a spoiling effect on that amount of the fan air not accepted by the cascade assembly.

(3) The cascade shape and construction would be modified to provide sufficient flow area and to impart suitable direction to the reverse flow.

A test was planned using a configuration as defined above. The purpose being to determine the optimum leading edge shape and cascade shape and the reverser loads in relation to the existing actuation system. A schematic of the fan and primary reversers is shown in figure D-8.

The possibility existed that a modified version of the Pratt and Whitney reverser might be deficient in performance or economically undesirable when adapted to the JT3D-9 engine. In consideration of this possibility, a study was initiated to provide an alternate design. A reverser system, either the modified Pratt and Whitney or a new design, must maintain the existing aircraft performance envelope. This envelope dictates that a reversing system has the inherent design requirement that failure of the actuation system shall not prevent the removal of reversed thrust and add excessive drag. Several blocker door concepts were studied and each seemed mechanically complex. To meet the failure mode and simplify the mechanical complexity, a target type seemed the most promising. This concept was investigated in greater detail for feasibility and is shown in figure D-9.

A reverser of this concept would be a hydraulically actuated, single panel mounted in each fan stream. Loss of the actuation system would reduce movement of the reverser panel to a non-reversing position. However, the addition of a hydraulically actuated system places additional demands upon the aircraft hydraulic system. To meet this demand, the aircraft hydraulic system capacity would have to be increased.

The total evaluation of the feasibility of the Douglas fan reverser was not completed. The reverser system was to be mounted from the engine only. Also, the reverser panel track passed through the engine fire seal. Coordination with the engine manufacturer was not completed to verify the engine's capability to react the applied air loads and to approve the fire seal modification.

Engineering development tests would have to be performed to refine the reverser system air loads and verify anticipated failure mode.

Primary Duct and Primary Reverser Design

Development of the short duct (DC-8 Model 61) nacelle lines for the JT3D-9 installation sought to retain the original lines aft of $Y_N = 178.812$ and the original Pratt and Whitney primary reverser with minimum modification (figure D-4). Due to the increased volumetric flow through the primary exhaust, it was necessary to cut back the nozzle to increase the area and to provide for increased flow through the reverser.

On the DC-8-63 JT3D-9 long duct installation (figure D-10), the increased size of the fan duct and, consequently, the nacelle precluded the possibility of using the existing reverser in its entirety. The design of a new reverser was based on the following ground rules:

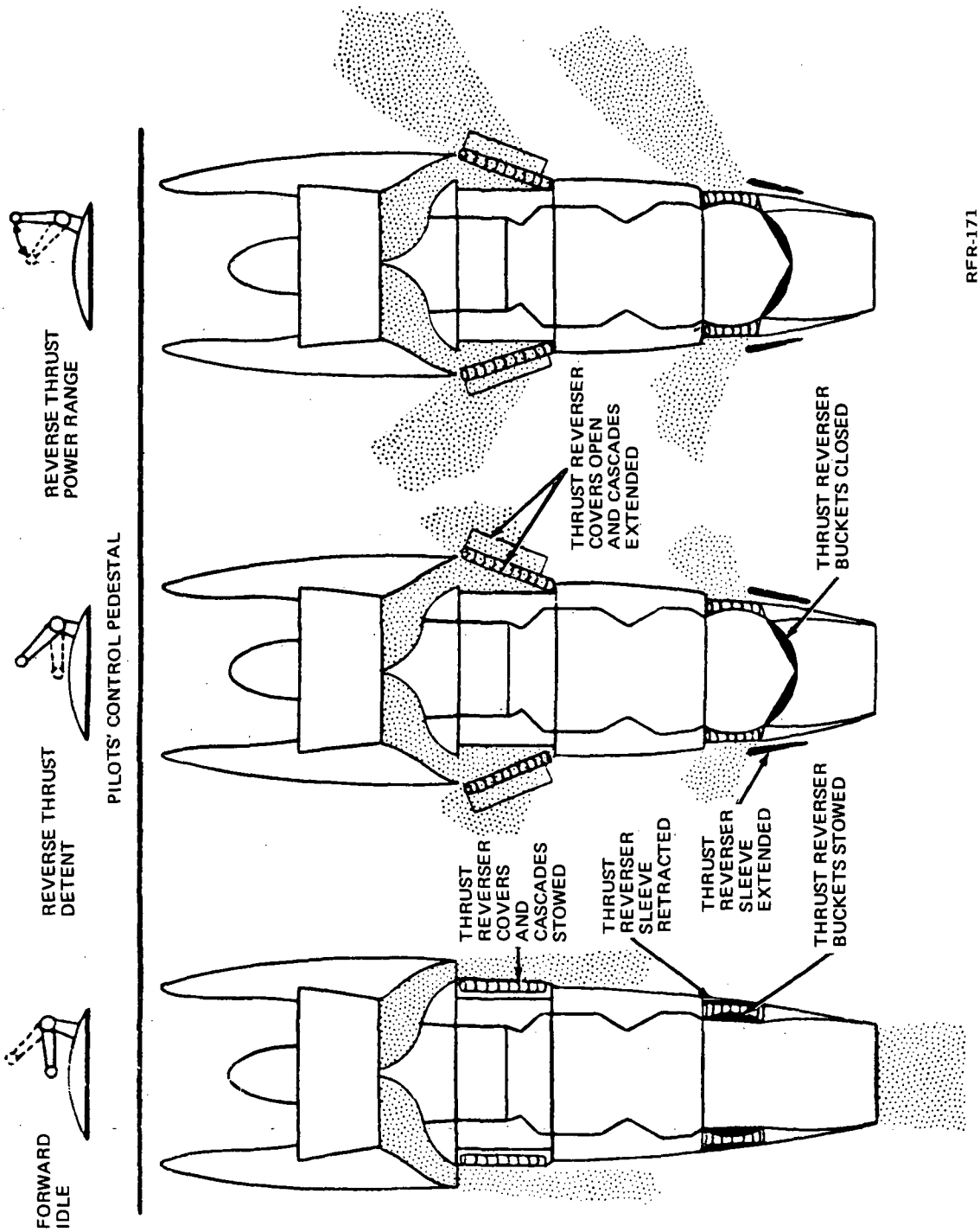

FIGURE D-8. DC-8-61 SHORT DUCT THRUST REVERSER SCHEMATIC

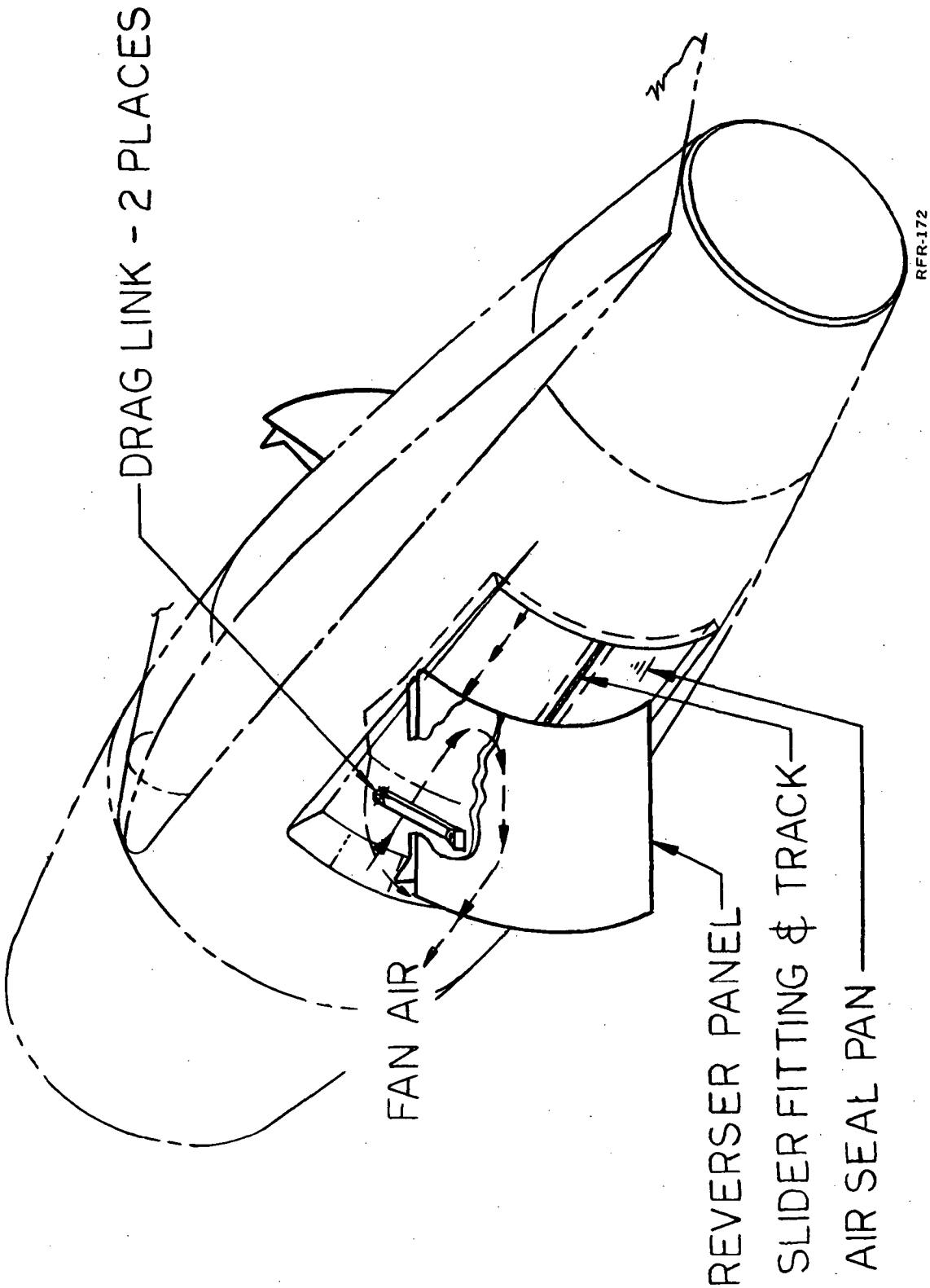

FIGURE D-9. ALTERNATE SHORT DUCT FAN REVERSER

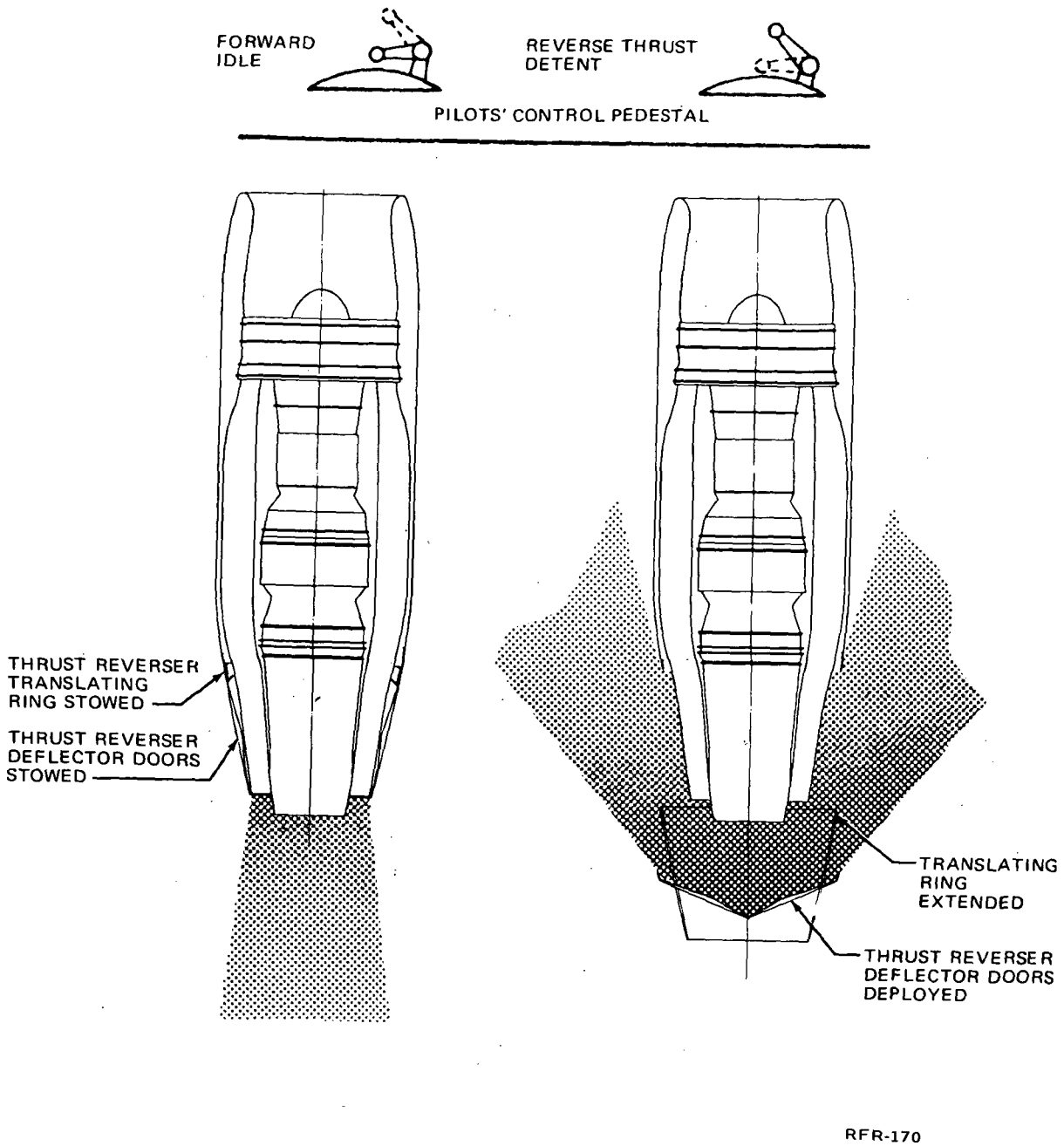

FIGURE D-10. DC-8-61 LONG-DUCT THRUST REVERSER SCHEMATIC

- The basic design concept would be retained.
- Existing hardware would be used where possible.
- Reverse thrust would be no less than that of the original DC-8-62.

Lay-out work determined the following:

- The original buckets could not be used without introducing "cusps" and discontinuities in the loft lines.
- If the nacelle grows radially, considerable changes to the reverser mechanism would be necessary. In addition, the aerodynamic characteristics of the nacelle in relation to the wing would be degraded.
- Restricting nacelle growth to a lateral direction, resulting in an elliptical duct and nacelle shape, would retain most of the reverser mechanism without degradation of aerodynamic characteristics.
- Some increase in bucket dimension fore and aft, combined with a relocation of the bucket hinge line, would result in geometry parameters (when deployed) comparable with those of the original DC-8-62 design.
- Some increase in nacelle length would be necessary to retain the structural integrity of the translating sleeve with the larger buckets.

AIRFRAME MODIFICATION

Pylons

For the DC-8 Model 61 maximum noise suppression configuration (figures D-11 and D-12), the main pylon structural boxes remain unchanged geometrically. The pylon structural box is bounded by the leading edge, the front mount bulkhead, the firewall, and sub-spar 2 for the inboard pylon, and by the leading edge, the front mount bulkhead, the firewall, and lower spar for the outboard pylon. Forward of the front mount bulkhead, the leading edge fairing is replaced by a new part which has been recontoured to accommodate the modified pod lines and re-routed environmental systems. The existing apron, together with its adjoining frames, hinges, junction boxes, etc., is replaced by a new redesigned unit, which includes a translating thrust reverser stang. At the forward end of the structural box, an extension is added to the bottom surface to enable lowering of modified existing engine mounts by the required 165 mm (6-1/2 in.) and also to provide space for the main service junction boxes which are located on either side. At the aft engine mount, pylon structure is modified to accommodate the revised aft engine mount upper fitting. The majority of existing junction boxes, installation bracketry, clips, etc., require modification.

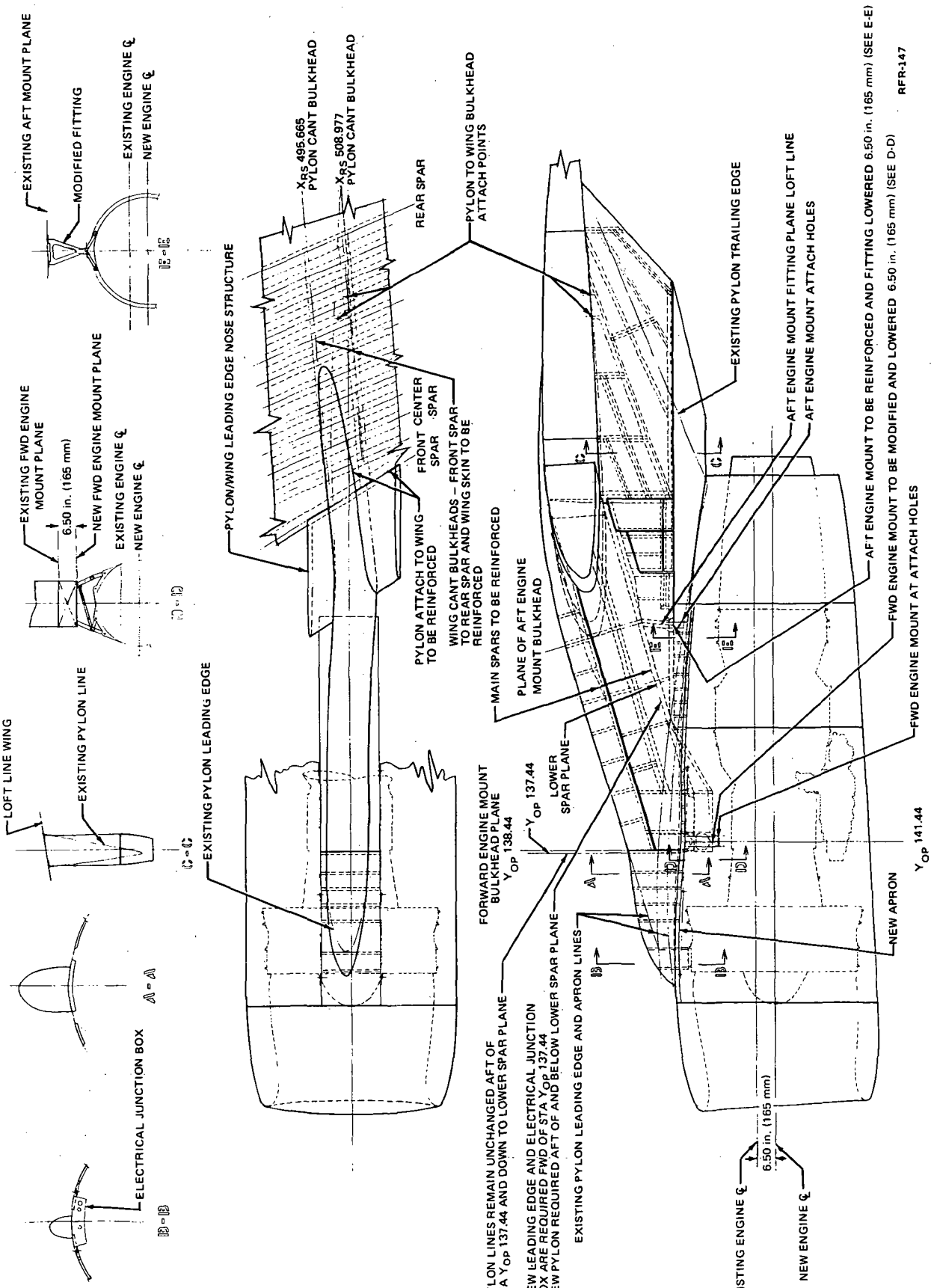

FIGURE D-11. DC-8-61 MAXIMUM TREATMENT STRUCTURAL CHANGES TO OUTBOARD OVERWING PYLON WITH LONG-DUCT POD

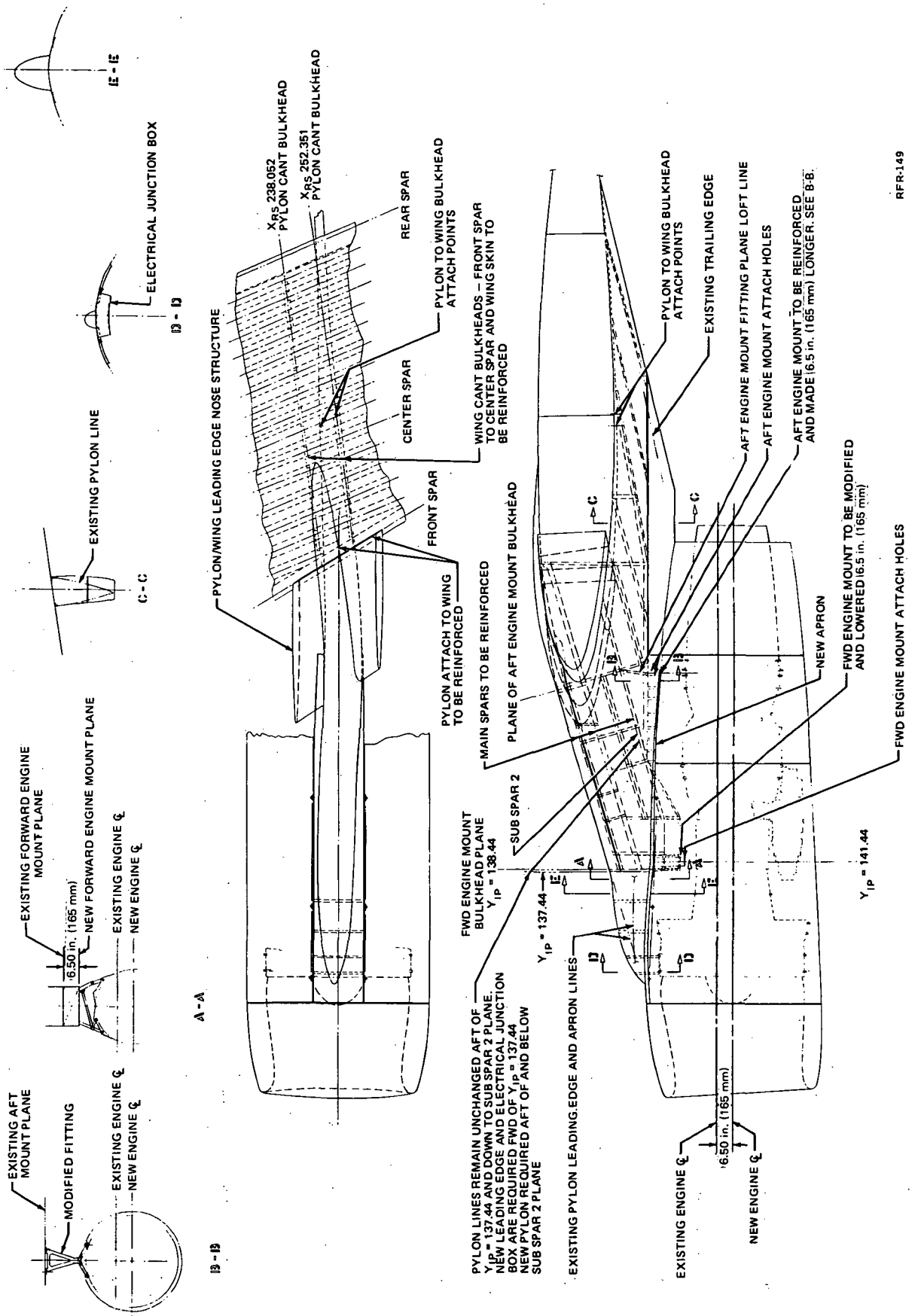

FIGURE D-12. DC-8-61 MAXIMUM TREATMENT STRUCTURAL CHANGES TO INBOARD OVERWING PYLON WITH LONG-DUCT POD

On the sides of the pylons, between the wing lower surface and pod upper surface, fairings may be required to minimize local velocities. The shape, size and amount of fairing were to be determined by wind tunnel tests (ref. 3).

Due to increased engine weight, downward movement of the center of gravity, flutter considerations, and high loads imposed by the actuator for the inflight operable target type thrust reverser, certain structural reinforcements may be necessary. These would include the main pylon spars together with their attachments to the wing, the lower firewall, the joint between pylon cant bulkhead and wing, the lower portion of the aft mount bulkhead, and the aft pylon to lower wing attachment.

For the DC-8 Model 61 intermediate and minimum noise suppression configurations, both inboard and outboard pylons, figures D-13 and D-14, respectively, will remain unchanged geometrically from the aft end to the forward engine mount bulkhead. Forward of this bulkhead, the existing apron, together with its adjoining frames, hinges, electrical junction boxes, and the forward leading edge fairing is replaced with a new apron and fairing which have been recontoured to accommodate the modified pod line and re-route environmental systems.

Due to increased engine weight, forward movement of the center of gravity, and flutter considerations, certain structural reinforcements may be necessary; these would include the main pylon spars together with their attachments to the wing, the joint between pylon cant bulkhead and wing, and the engine mount attachment points on the pylon lower surface.

The DC-8 Model 63 inboard and outboard pylons will remain unchanged geometrically from the aft end to the forward engine mount bulkhead (figure D-15). Forward of this bulkhead, the existing apron together with its adjoining frames, hinges, electrical junction boxes, and the forward leading edge fairing is replaced with a new apron and fairing which have been recontoured to accommodate the modified pod line and re-routed environmental systems. Due to increased engine weight, forward movement of the center of gravity and flutter considerations, the following changes to the structure may be necessary. The main pylon spars, the joints between pylon front spar bulkhead and wing, the pylon attach angles to lower wing skin, and also, engine mount attachment points on the pylon lower surface may all require reinforcing.

Wing

The current weight estimates for the DC-8-61 minimum noise suppression pod show an increase in weight of 284 kg (628 lb) and a forward center of gravity shift of 76 to 127 mm (3 to 5 in.) over the standard DC-8-61 short duct pod installation. Weight estimates for the DC-8-61 intermediate noise suppression pod show an increase in weight of 358 kg (789 lb) and a forward center of gravity shift of 76 to 127 mm (3 to 5 in.) over the standard DC-8-61 short duct pod installation. The present wing has adequate static strength, but the weight and center of gravity effects will significantly reduce the engine pylon pitch frequency as well as affecting the wing modes of vibration.

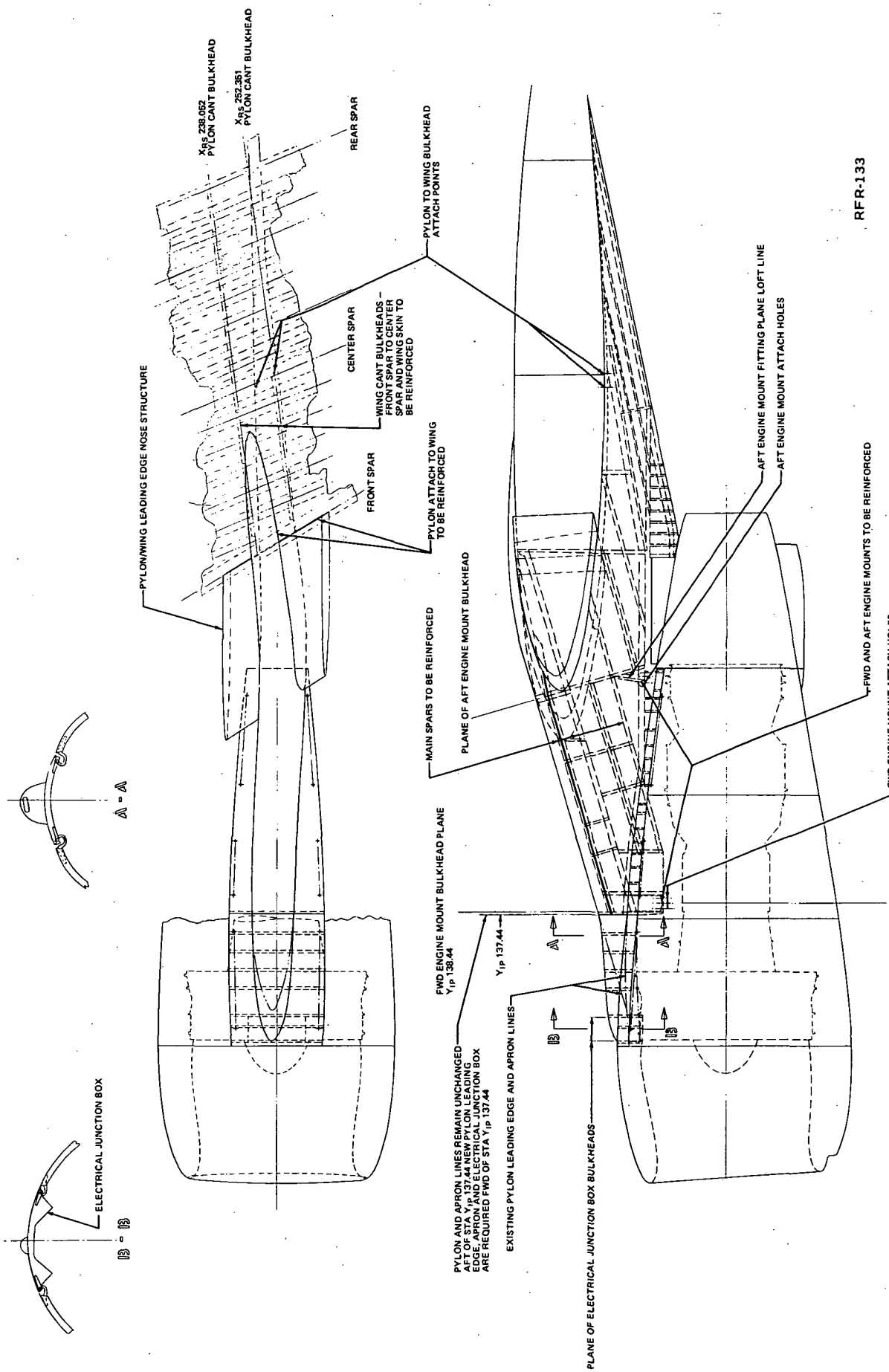

FIGURE D-13. DC-8-61 STRUCTURAL CHANGES TO INBOARD OVERWING PYLON WITH SHORT-DUCT POD

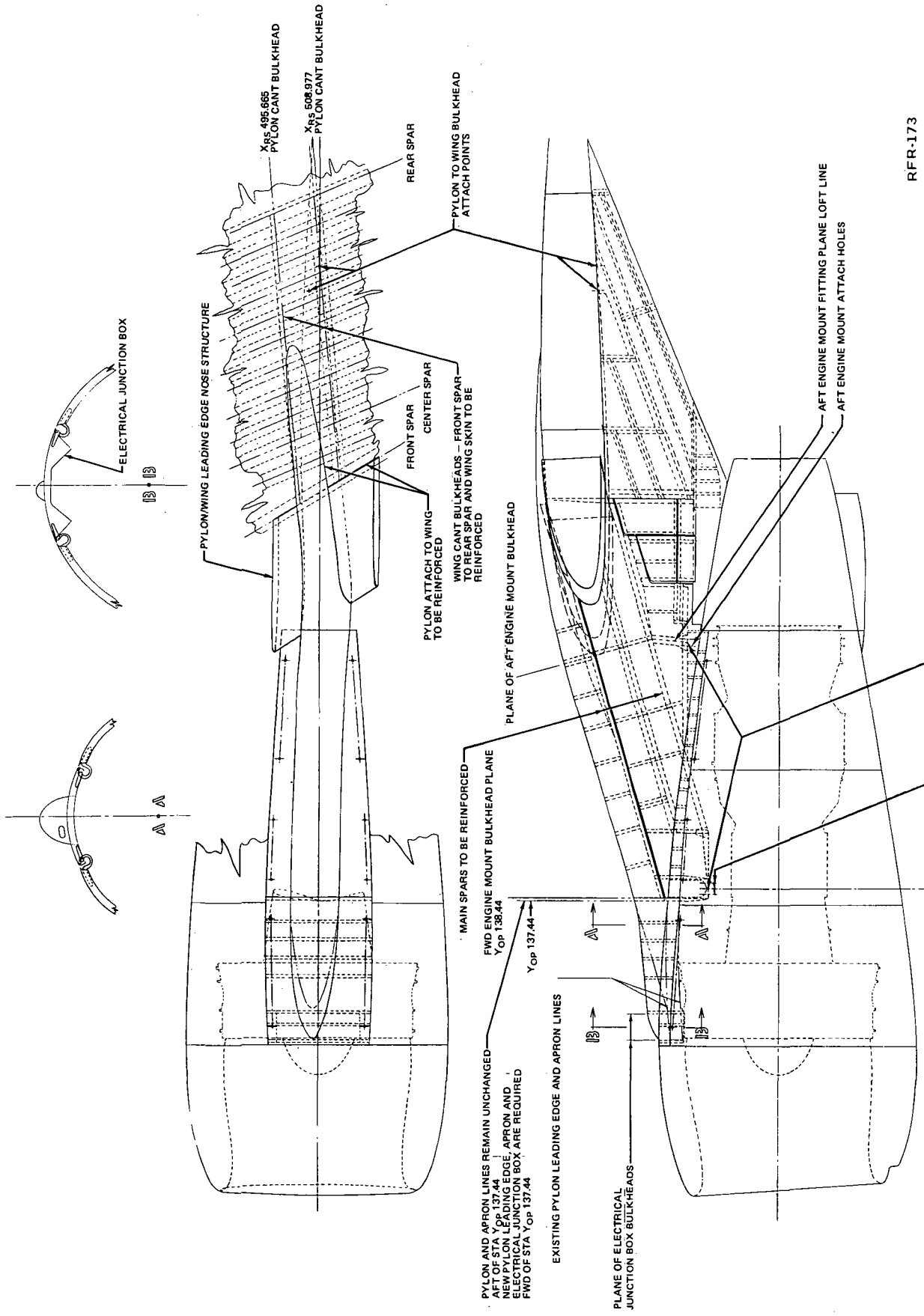

FIGURE D-14. INTERMEDIATE TREATMENT DC-8-61 STRUCTURAL CHANGES – OUTBOARD OVERWING PYLON

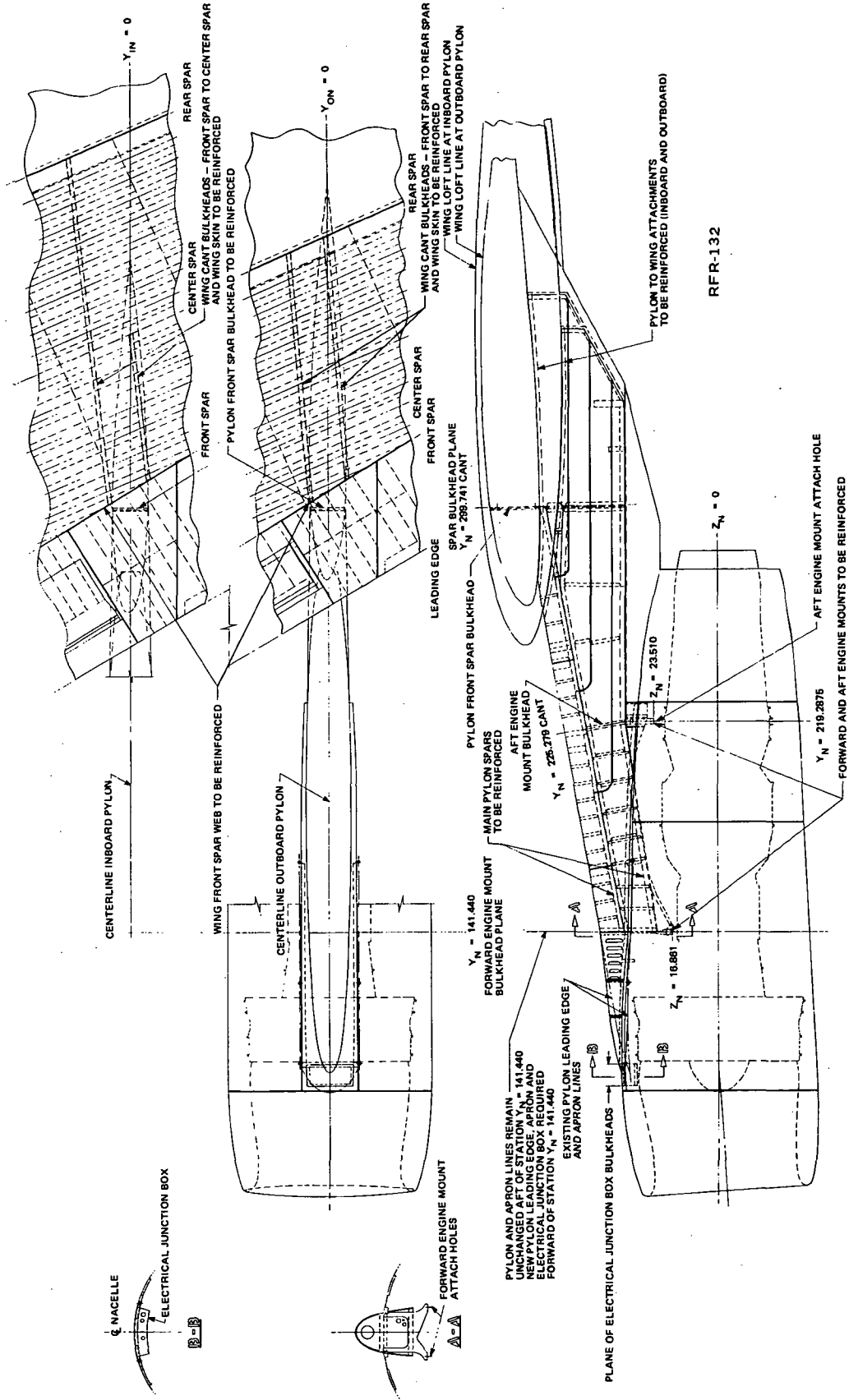

FIGURE D-15. INBOARD AND OUTBOARD PYLONS

Consequently, a flutter weight penalty in the form of wing stiffness may be necessary to maintain the required flutter margins. The required changes need to be determined on the basis of flutter analyses and low speed flutter model tests.

Weight estimates for the DC-8-61 maximum noise suppression long duct pod show an increase in weight of 489 kg (857 lb) and a center of gravity shift of 140 mm (5.5 in.) aft and 152 mm (6 in.) down over the standard DC-8-61 short duct pod installation. The reduction in engine pylon pitch frequency due to the increased engine weight, downward center of gravity movement and additional flexibility due to the downward extension of the engine mounts is partially offset by the aft center of gravity movement. However, a weight penalty to achieve wing stiffness may be necessary to maintain the required flutter margins. Static strength wing structural changes are not anticipated for this configuration (maximum noise suppression). The required changes, if necessary, need to be determined on the basis of flutter analyses and low speed flutter model tests.

Current weight estimates for the DC-8-63 long duct pod show an increase in weight of 311 and 372 kg (685 and 821 lb) and a center of gravity shift of approximately 178 and 203 mm (7 and 8 in.) forward, respectively, for the minimum and maximum suppression configuration over the standard DC-8-63 long duct installation. Both the increased weight and center of gravity movement will significantly reduce the engine pylon pitch frequency as well as affecting the wing modes of vibration. Consequently, a flutter weight penalty in the form of wing stiffness may be necessary to maintain the required flutter margins for both the minimum and maximum suppression configurations. The required changes, if necessary, need to be determined on the basis of flutter analyses and low speed flutter model tests.

Should strength analyses indicate that there is a need for structural revisions of the DC-8-50/61 or DC-8-62/63 aircraft, the changes will be of the following nature. Adjacent to the pylon, wing skins may have to be thickened, spars may have to be reinforced, and cant bulkhead fittings, which are required for pylon attachment, will have to be beefed-up.

Airframe Systems

Replacement of the stationary bullet with a spinner on the JT3D-9 refan engine necessitates redesign of the N_1 sensor and will require a new N_1 indicator on the instrument panel. This airframe system change is common to the three levels of noise suppression identified for the DC-8 Model 61 airplane. No hydraulic, electrical, control, firex, or fuel airframe system changes are anticipated for the minimum and intermediate suppression configurations. A new airframe hydraulic system will be required to actuate the maximum noise suppression (long duct) thrust reverser which is replacing the short duct pneumatic thrust reverser system. The new system shall be located in the main gear well and consist of an electric pump, fluid reservoir, isolation valve, and fluid lines interconnecting the reversers. Additional electrical systems are required to power and control the new hydraulic system.

APPENDIX D

Changes to the existing DC-8-63 airframe systems due to installing the JT3D-9 refan engine have not been determined. Changes, if any, are expected to be minor.

LOADS ANALYSES

Preliminary static and dynamic loads analyses were performed as indicated in support of the preliminary design effort on nacelles, pylons and supporting structure for the JT3D-9 refanned engine. The following dynamic loads analyses have been performed:

Vibration

DC-8 airplane vibration modes have been computed for various refanned engine configurations for use in flutter and dynamic loads analyses. All modal data are available on magnetic tapes. Coupled modes of each component were computed with the component cantilevered at an appropriate location. For example, the wing was cantilevered at the wing/fuselage intersection. Flexible root restraints at the intersections of major components were accounted for by placing rotation springs at these intersections to allow the components to undergo relative rigid body rotations. The cantilevered component modes were coupled together with appropriate rigid body modes to obtain orthogonal airplane modes. These analytical modes for the base (production) configuration compare well with measured modes determined from past ground vibration tests of the several aircraft. Over 1,500 DC-8 component modes have been computed. Complete airplane orthogonal modes are available for the following configurations:

MODEL	PAYLOAD	FUEL	ENGINE TREATMENT
-51	OWE	100%	None
			Min.
			Intermed.
			Max.
		Empty	None
-61	OWE	100%	None
			Min.
			Intermed.
			Max.
		Empty	None
-63	10,000	100%	None
			Min.
			Max.
	OWE	Empty	None
		61%	

APPENDIX D

Table D-1 presents a comparison of modal frequencies for the DC-8-51, -61 and -63 for several acoustic treatment levels. The comparison is shown for the antisymmetric full fuel configuration which is the critical flutter condition.

Flutter

Analyses have been performed to determine the changes in DC-8 airplane flutter characteristics when configured with various JT3D refanned engines. These preliminary analyses used unsteady aerodynamics based upon modified strip theory. Several acoustic treatment levels were analyzed to determine the effects of engine weight, inertia and c.g. location. The results are as follows:

DC-8 SERIES	$V_{FLUTTER}/V_{REF.}$ PRODUCTION NACELLE	MINIMUM TREATMENT	MAXIMUM TREATMENT
-51	1.0	0.95	0.95
-61	1.0	1.04	1.02
-63	1.0	0.98	0.97

The preliminary results shown above used unsteady aerodynamics on all lifting surfaces and engine based upon modified strip theory. The unsteady aerodynamics used for final design should be based upon lifting surface theory, such as the Doublet Lattice Method. The different trends shown above for the various DC-8 Series aircraft indicate the sensitivity of the flutter characteristics with engine weight and c.g. changes and show the need for a coordinated program of flutter analysis and flutter model tests for design verification.

Dynamic Loads

No power spectral density or dynamic landing analysis had as yet been performed since airplane orthogonal modes have just been completed. Estimations of loads on various portions of the nacelles were made for preliminary design of different candidate nacelles. For purposes of design, these loads were based on airframe critical considerations apart from engine critical parameters, even at engine mounting flanges. For example, the nose cowl loads are based on a 20g vibration load originating in a failing engine. It is Douglas policy that the nose cowl attachments shall be adequate to minimize the probability of nose cowl loss during severe engine vibration. In general, the loads on the various engine flanges, when finally calculated for engine-critical conditions for the selected nacelle configuration, will be within existing Pratt & Whitney limits.

TABLE D-1

DC-8 MODAL FREQUENCY COMPARISON BASED ON VARIOUS ENGINE CONFIGURATIONS (Hz)
(FULL FUEL ANTISYMMETRIC)

MODE DESCRIPTION	DC-8-51 PROD. ENGINE	DC-8-51 MIN. TREAT.	DC-8-51 MAX. TREAT.	DC-8-61 PROD. ENGINE	DC-8-61 MIN. TREAT.	DC-8-61 MAX. TREAT.	DC-8-63 PROD. ENGINE	DC-8-63 MIN. TREAT.	DC-8-63 MAX. TREAT.
Wing 1st Bending	1.896	1.872	1.863	1.983	1.959	1.950	1.818	1.788	1.784
O.B. Engine Yaw	2.509	2.383	2.341	2.548	2.445	2.414	2.169	2.066	2.050
I.B. Engine Yaw	2.801	2.773	2.725	2.734	2.649	2.614	2.214	2.131	2.117
Aft Fus. 1st Bending	2.848	2.835	2.829	2.255	2.224	2.210	2.386	2.372	2.370
Wing 1st Torsion O.B. Pitch	3.276	3.152	3.113	3.386	3.275	3.242	2.856	2.751	2.736
Fwd Fus. 1st Bending	5.126	5.116	5.112	3.149	3.071	3.044	3.149	3.106	3.098
Wing 2nd Bending, I.B. I.B. Eng. Pitch	4.456	4.333	4.286	4.685	4.543	4.489	3.356	3.242	3.227
Horizontal Stab. 1st Bending	4.025	4.023	4.022	3.992	3.989	3.989	3.956	3.955	3.955
Wing 2nd Torsion	-	-	-	-	-	-	5.108	5.085	5.080
Vertical Stab. 1st Bending	5.546	5.538	5.535	5.516	5.510	5.509	5.573	5.570	5.570

Front engine mount loads increase significantly over previous JT3D engines, primarily due to increased engine front end and nose cowl weight. The aft mount loads decrease slightly compared to identical conditions for the DC-8-50 and DC-8-62. Engine mount loads are summarized in Table D-2. The sign convention is shown in figure D-16.

Static Loads

Design static load emphasis was concentrated on limit and ultimate design loads. Fail safe loads are primarily evaluated after the final design has been selected; however, structural concepts are reviewed for fail safe characteristics. For initial fatigue considerations, a design ultimate load factor of 3 is used on thrust loading for critical engine support structure. The refan DC-8 static load analyses were based on the following considerations:

(1) Aerodynamic pressure distributions on the inlet cowl, inlet rings and struts calculated by Aerodynamics using their potential flow program did not correlate well with existing DC-8 wind tunnel model data. The JT3D refan program was terminated before pressures could be integrated to obtain final nose cowl shears and moments.

Side cowl door contours are similar to the existing nacelle contours, therefore, the external pressure distribution is expected to vary slightly, if at all, from existing pressures. Since the design pressure and temperature condition for the side cowl doors results from massive pneumatic duct rupture, the condition will not change significantly from the production version.

(2) Discrete gust and maneuvering conditions specified in CAR 04b were critical for design of the nacelles and pylons of the DC-8. For preliminary evaluation, these critical inertia loads were factored for changes in nacelle weight and c.g. location.

(3) Since the original pylon design criteria involved factored thrust loads to accommodate installation of a "growth" engine of 20,000 pounds static takeoff thrust, effects of increased thrust were not calculated.

(4) Engine thermal effects have been considered relative to material choice in the tail pipe and nose cowl leading edge and inner barrel.

(5) No ground handling loads analysis has been performed.

(6) The JT3D refanned engines could possibly increase the fuselage loads in the lateral gust and abrupt maneuver conditions. A survey of the external loads envelopes for the DC-8-61 and -63 aircraft shows that for these conditions and refanned engine, the loads are well within the design envelope. A possible increase of 1% in the vertical tail load resulting from engine flame-out would also fall within the design envelope.

TABLE D-2

JT3D-9 MAXIMUM ENGINE MOUNT LIMIT LOADS

COND NO.	D	V_R	S_R	V_L	S_L	V_A	S_A
DC-8-61	lb (kN)	lb (kN)	lb (kN)	lb (kN)	lb (kN)	lb (kN)	lb (kN)
111	18,845 (83.82)	7,259 (32.39)	1,796 (7.99)	-8,133 (36.18)	-2,138 (9.51)	14,342 (63.79)	4,679 (20.81)
147	21,721 (96.62)	5,555 (24.71)	-3,863 (-17.18)	-93 (-.41)	-21 (-.09)	12,102 (53.83)	4,702 (20.91)
340	4,945 (22.00)	-1,290 (-5.74)	-20,024 (-89.07)	7,501 (33.36)	2,029 (9.02)	5,365 (23.86)	11,415 (50.77)
351	19,684 (87.55)	-12,776 (-56.83)	-13,146 (-58.47)	7,171 (31.90)	1,192 (5.03)	13,167 (58.57)	3,325 (50.77)
522	-28,745 (-127.86)	7,301 (32.47)	14,723 (65.49)	4,413 (19.63)	1,160 (5.16)	-18,350 (-81.62)	-10,710 (-47.64)
541	-26,873 (-119.53)	11,851 (52.71)	19,584 (87.11)	7,353 (32.71)	1,935 (8.61)	-7,835 (-34.85)	-15,678 (-69.74)
557	0 (0)	16,453 (73.18)	17,194 (76.48)	-16,453 (-73.18)	-4,328 (-19.25)	0 (0)	2,437 (10.84)
563	-30,028 (-133.56)	17,425 (77.51)	18,011 (80.11)	5,985 (26.62)	1,576 (7.01)	-5,614 (-24.97)	-12,617 (-56.12)
565	-27,233 (-121.13)	18,992 (84.48)	17,414 (77.46)	10,894 (48.46)	2,868 (12.76)	-11,613 (-51.65)	-14,220 (-63.25)
664	-27,223 (-121.13)	6,436 (28.63)	-13,609 (-60.53)	22,318 (99.27)	5,779 (25.70)	-10,472 (-46.58)	1,593 (7.09)
DC-8-63							
03.32	13,002 (57.83)	-17,249 (-76.72)	-5,698 (-25.34)	15,437 (68.66)	10,777 (47.94)	12,965 (57.67)	1,874 (8.34)
25.42	12,539 (55.66)	-6,986 (-31.07)	-2,268 (-10.09)	20,949 (93.18)	8,805 (39.16)	14,610 (64.99)	-1,552 (-6.90)
41.12	6,725 (29.91)	21,598 (96.07)	7,179 (31.93)	-17,647 (-78.49)	17,774 (79.06)	6,749 (30.02)	-9,142 (-40.66)
46.11	20,082 (89.32)	4,136 (18.40)	1,369 (6.09)	1,000 (4.45)	-3,343 (-14.87)	10,203 (45.87)	6,954 (30.93)
57.20	0 (0)	19,137 (-85.12)	6,326 (28.14)	-19,096 (-84.94)	14,621 (65.03)	23 (.10)	8,308 (36.95)
58.20	0 (0)	-19,137 (-85.12)	-6,326 (-28.14)	19,096 (84.94)	-14,621 (-65.03)	-23 (-.10)	-8,308 (-36.95)

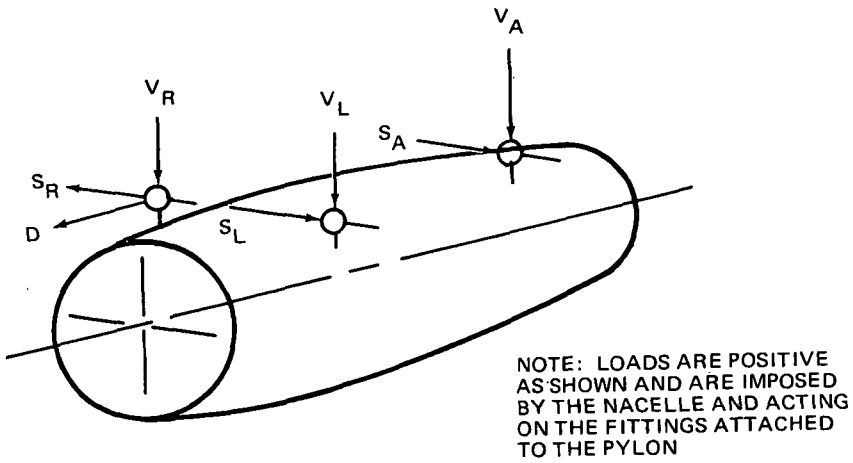

FIGURE D-16. - JT3D-9 ENGINE MOUNT LOAD SIGN CONVENTION

(7) Design loads for the DC-8-63 with the refanned engines indicated only local beef-up would be required for the wing-pylon intersection structure. Wing skin or stiffener changes were not indicated on the basis of this preliminary study.

STRESS ANALYSIS

Inlet Duct

It is a Douglas policy requirement that the nose cowl will not shake loose during high vibration loading imposed by failing an engine. A 20g vibration load was assumed in lieu of a rational dynamic analysis; the running load on inner barrel acoustic sandwich is within limits for DC-10 nose cowl. The attach bolt pattern to the engine inlet flange and the acoustic sandwich close-out structure were checked and are adequate. The inlet ring and strut leading edges are comparable to the Douglas Aircraft Company financed quiet engine study structure which is being tested for hail and bird impact resistance in February 1973.

Nacelle Doors

Proposed structure, contours and pressure are comparable to existing doors.

Thrust Reversers

The translating ring thrust reverser for the refanned DC-8-63 requires a broader "egg" shape to accommodate the increased air flow while maintaining adequate vertical clearance to the pylon firewall for the actuating mechanism. A strain energy analysis of the reverser door was begun to evaluate internal bending moments resulting from the revised contour.

Pylons and Engine Mounts

A review of the stress analysis reports for the pylons of the DC-8-50 and DC-8-62 airplanes was conducted to determine areas having low margins of safety and to verify that the critical conditions would be adversely affected by the refanned engine increase in weight and c.g. shift. Input data for generation of pylon load analysis data are available. Front engine mount loads increase sufficiently to require redesign; aft engine mounts are adequate unless relocation of the engine centerline, relative to the pylon firewall, is required. Critical design limit loads at the engine attach points are given in table D-2. The design conditions are defined in table D-3.

TABLE D-3

DC-8-61, -63 ENGINE MOUNT DESIGN LOAD CONDITIONS

COND. NO.	CONDITION TYPE	GROSS WEIGHT	N_Z	VELOCITY	MACH	ALTITUDE	THRUST	δ_{FLAP}	a	β
DC-8-61		lb (kg)		KEAS (m/s)		ft (km)		deg (rad)	deg (rad)	deg (rad)
111	Bal. Man	314,000 (142 556)	2.0	V_A 320 (165)	.35	SL	T.O.	20 (.349)	8.83 (.154)	0
522	Roll	138,940 (63 079)	0	V_D 406 (209)	.614	SL	Max. Cont.	0	-2.74 (-.048)	.33 (.006)
340, 541	Rudder Man	308,200 (139 923)	1.0	V_D 416 (214)	.93	20,000 (6.10)	Max. Cont.	0	1.16 (.020)	+2.45 (±.043)
351	Ground Turn	-	1.0	10 (5)	-	SL	T.O.	0	-	-
557	2g Side	-	-	-	-	-	-	-	-	-
563	Reverse Thrust	314,000 (142 556)	2.0	V_D 406 (209)	.614	SL	Max. Cont.	0	3.15 (.055)	3.2 (.056)
664, 565		308,000 (139 822)	2.0	V_D 416 (214)	.93	20,000 (6.10)	Max. Cont.	0	3.76 (.066)	+1.85 (±.032)
147	Spring Back	202,000 (91 708)	2.242	V_F 150 (77)	.23	SL	T.O.	0	-1.65 (-.029)	0
DC-8-63										
03.32	Bal. Man	349,000 (158 446)	2.5	V_A 264 (136)	.4	SL	Max. Cont.	0	12.9 (.225)	0
25.42	Roll	140,700 (63 878)	1.667	V_D 406 (209)	.614	SL	Max. Cont.	0	-.12 (-.002)	0
41.12	Rudder Man	327,000 (148 458)	1.0	V_D 416 (214)	.93	20,000 (6.10)	Max. Cont.	0	.87 (.015)	-2.45 (-.043)
46.11	Spin-up	240,006 (108 963)	2.368	V_F 190 (98)	.29	SL	T.O.	50 (.873)	-2.0 (-.035)	0
57.20	+2g Side	-	-	-	-	-	-	-	-	-
58.20	-2G Side	-	-	-	-	-	-	-	-	-

APPENDIX D

Pneumatic Duct System

No stress analysis has as yet been performed.

AIR LOADS ANALYSES

The aerodynamic data for stress analysis, scheduled prior to redirection of the JT3D refan effort, consisted of total loads on the nacelle and nacelle-pylon combinations, total loads on the inlet cowls, and pressure distributions over the inlet cowls, external nacelles, and pylons of both the long duct and short duct pods as applicable to the DC-8-61 and DC-8-63 airplanes, respectively.

Specifically, the aerodynamic loads analysis was to consist of estimation of the following data for both the long duct and short duct pods:

(1) Aerodynamic forces and moments on the inlet sections at the forward flanges for the following critical loading flight conditions:

   a. M = 0.422, Alt = S.L., V = 143.5 m/s (279 KEAS), F = 0.253 rad (14.5°), Windmilling (WM) and Maximum Continuous Power (MCT) settings.

   b. M = 0.83, Alt = 7.3 km (24,000 ft), V = 175.4 m/s (341 KEAS), F = 0.131 rad (7.5°), WM/MCT.

   c. M = 0.514, Alt = S.L., V = 201.6 m/s (392 KEAS), F = -0.122 rad (-7°), WM/MCT.

   d. M = 0.614, Alt = S.L., V = 208.8 m/s (406 KEAS), F = 0°, WM/MCT.

   e. M = 0.355, Alt = S.L., V = 120.9 m/s (235 KEAS), F = 0.105 rad (6°), = 0.349 rad (20°) WM/Takeoff Power (T.O.).

   f. Static, S.L., T.O. power.

   g. Static, S.L., 30 knot crosswind, T.O. power.

(2) Pressure distributions on all external and internal surfaces of the inlet section for flight conditions noted in item (1).

(3) Nacelle and nacelle/pylon total aerodynamic forces and moments on inboard and outboard nacelles as functions of Mach number, angle-of-attack, and angle-of-sideslip.

(4) External nacelle and pylon surface pressure distributions for flight conditions noted in item (1).

APPENDIX D

From its inception until the time the JT3D Refan Program was redirected, the Aerodynamics' loads analysis consisted of definition of the critical loading conditions, analysis of existing baseline data, definition of applicable loads methods, and JT3D refan nacelle geometry definitions required to accomplish the stated program objectives. No final aerodynamic data for stress analysis were generated.

ACOUSTIC DESIGN

Table D-4 summarizes the acoustic treatment configuration for the DC-8-61 and -63 aircraft installed with the JT3D-9. The inlet and exhaust L/H parameters (*i.e.*, the ratio of effective treated length to average duct height) were calculated to provide equal inlet and exhaust noise levels.

ENGINE AND NACELLE SUBSYSTEMS

A preliminary analysis indicates that the fuel, nacelle cooling and ventilation, generator, and constant speed drive systems will be essentially the same.

Starter System

The starting requirements of the JT3D-9 are identical to those of the JT3D-3. No modifications to the starting system, with the possible exception of piping redevelopment, were contemplated.

Hydraulic System

Changes required to the existing hydraulics systems were not identified. Changes would have been definitely required if the Douglas designed -61 fan reverser were employed.

Lubrication System

Because the engine oil heat rejection curves were not available, the maximum rate of heat rejection was estimated. If the maximum rate of heat rejection estimate is accurate, additional oil cooling capacity would be required of the airframe system.

APPENDIX D

TABLE D-4

DC-8/JT3D-9 ACOUSTIC TREATMENT CONFIGURATIONS

AIRCRAFT	SUPPRESSION LEVEL	FAN DISCHARGE DUCT LENGTH (EFFECTIVE)	AVG. L/H	FAN CASE	AVE. L/H	INLET	AVE. L/H
DC-8-61	Minimum	26 in. (660 mm)	3.0	Splitter + Wall Treatment	2.5	37 in. (940 mm) Cowl Wall	1.3
	Intermediate	26 in. (660 mm) +Splitter	5.0	Splitter + Wall Treatment	2.5	37 in. (940 mm) Wall +18-in. ring	2.8
	Maximum	110 in. (2.8 m)	8.8	Splitter + Wall Treatment	2.5	37 in. (940 mm) Cowl Wall	2.8
DC-8-63	Minimum	26 in. (660 mm)	2.1	Splitter + Wall Treatment	2.5	37 in. (940 mm) Cowl Wall	1.3
	Maximum	110 in. (2.8 m)	8.8	Splitter + Wall Treatment	2.5	37 in. (940 mm) Wall +18-in. ring	2.8

APPENDIX D

Fire Protection

The same general arrangement of fire detection, fire barriers and fire extinguishing would be used. Additional fire extinguishing agent would be required due to the increased nacelle volume.

Engine Controls

The mechanical controls remained unchanged except for possible revision to linkages in the nacelle. The replacement of the stationary bullet of the JT3D-3B with a spinner on the JT3D-9 necessitated a change in the N_1 indicating system. The JT3D-9 system used a magnetic fan rotor speed sensor located in the fan case.

AIRCRAFT PERFORMANCE

The changes in DC-8-61 airplane performance resulting from the JT3D-9 installation are limited to takeoff field length, flight path, and payload range characteristics. These three performance parameters are all affected, regardless of noise suppression configuration, with only small differences showing up as a function of noise treatment level. Takeoff field length and flight paths are slightly improved using the maximum treated JT3D-9 installation and payload range suffers only a minimal increase.

For the intermediate treatment level, takeoff field length, flight paths and the payload range are slightly improved. For the minimum treatment level, takeoff field length and flight path improvements are comparable to the maximum suppression values as is the payload range. The significant changes in aircraft payload and performance parameters are shown in table D-5 for a typical mission of 2.8 Mm (1,500 n. mi.) with a 55 percent load factor.

A comparison for the payload range characteristics of the DC-8-62 with the production JT3D-3B engines in the production long duct nacelle and the new JT3D-9 installed in the noise suppression nacelle is presented in table D-6. As shown in the table at a 55 percent load factor, the range difference amounts to a 241 km (130 n. mi.) reduction. A breakdown of the components affecting maximum range for the 55 percent load factor point is also shown in table D-6.

For a typical route of 2.3 Mm (1,250 n. mi.) with a typical payload of 26 672 kg (58,800 lb), the changes in significant airplane performance parameters for the DC-8-54F are shown in table D-7.

For a typical route of 2.3 Mm (1,250 n. mi.) with a 55 percent load factor, the changes in significant airplane performance parameters for the DC-8-51 are shown in table D-8.

APPENDIX D

TABLE D-5

CHANGE FOR JT3D-9 RELATIVE TO JT3D-3B ON DC-8-61

FOR A 55 PERCENT LOAD FACTOR

	MAXIMUM SUPPRESSION	INTERMEDIATE SUPPRESSION	MINIMUM SUPPRESSION
Fuel Burned, lb (kg)	-111 (-50)	+474 (+215)	-338 (-153)
Takeoff Gross Weight, lb (kg)	+3580 (+1625)	+3706 (+1682)	+1962 (+890)
Block Speed, knots (km/hr)	+1 (+2)	+1 (+2)	+1 (+2)
Takeoff Field Length Required Sea Level on a Standard Day, ft (m)	-80 (-24)	-190 (-58)	-285 (-87)
Range, n. mi. (km) due to SFC	+73 (+135)	+10 (+18)	+73 (+135)
Range, n. mi. (km) due to Weight	-53 (-107)	-60 (-111)	-33 (-61)
Total Range, n. mi. (km)	+15 (+28)	-50 (-93)	+40 (+74)

TABLE D-6

CHANGE FOR JT3D-9 RELATIVE TO JT3D-3B ON DC-8-62

FOR A 55 PERCENT LOAD FACTOR

	MAXIMUM SUPPRESSION
Fuel Burned, lb (kg)	+766 (+347)
Takeoff Gross Weight, lb (kg)	+4340 (+1968)
Block Speed, knots (km/hr)	+1 (+2)
Takeoff Field Length Required Sea Level on a Standard Day, ft (m)	0* (0*)
Range, n. mi. (km) due to SFC	-62 (-114)
Range, n. mi. (km) due to Weight	-68 (-125)
Total Range, n. mi. (km)	-130 (-239)

*V_{MC} limited.

TABLE D-7

CHANGE FOR JT3D-9 RELATIVE TO JT3D-3B ON DC-8-54F

	MAXIMUM SUPPRESSION
Fuel Burned, lb (kg)	+316 (+143)
Takeoff Gross Weight, lb (kg)	+3550 (+1610)
Block Speed, knots	0
Takeoff Field Length Required Sea Level on a Standard Day, ft (m)	-330 (-101)
Range due to SFC, n. mi. (m)	+12 (+22)
Range due to Weight, n. mi. (m)	-122 (-226)
Total Range, n. mi. (m)	-110 (-204)

TABLE D-8

CHANGE FOR JT3D-9 RELATIVE TO JT3D-3B ON DC-8-51

	INTERMEDIATE SUPPRESSION
Fuel Burned, lb (kg)	+280 (+127)
Takeoff Gross Weight, lb (kg)	+3525 (+1599)
Block Speed, knots	0
Takeoff Field Length Required Sea Level on a Standard Day, ft (km)	0
Range due to SFC, n. mi. (km)	+15 (+28)
Range due to Weight, n. mi. (km)	+70 (+130)
Total Range, n. mi. (km)	+85 (+158)

APPENDIX D

The changes in basic DC-8-63 airplane performance are limited to takeoff field length, flight path and payload range characteristics. These three performance parameters are all affected, regardless of noise suppression configuration, with only small differences showing up as a function of noise treatment level. Takeoff field length and flight paths are slightly improved through use of the maximum treated JT3D-9 installation and payload range suffers only a minimal reduction. Takeoff field length and flight path improvement for the minimum treatment level are comparable to those of the maximum treatment case; however, the payload range reduction is not as great.

The significant changes in aircraft payload and performance parameters are shown in table D-9 for a typical mission of 2.8 Mm (1,500 n. mi.) with a 55 percent load factor for a DC-8-63.

TABLE D-9

CHANGE FOR JT3D-9 RELATIVE TO JT3D-3B ON DC-8-63

	MAXIMUM SUPPRESSION	MINIMUM SUPPRESSION
Fuel Burned, lb (kg)	+1224 (+555)	+943 (+428)
Takeoff Gross Weight, lb (kg)	+4804 (+2179)	+3919 (+1778)
Block Speed, knots (km/hr)	+1 (+2)	+1 (+2)
Takeoff Field Length Required Sea Level on a Standard Day, ft (m)	-2400 (-73)	-150 (-46)
Range due to SFC, n. mi. (km)	-40 (-74)	-32 (-59)
Range due to Weight, n. mi. (km)	-160 (-296)	-118 (-218)
Total Range, n. mi. (km)	-200 (-370)	-150 (-277)

APPENDIX D

AIRPLANE ACOUSTIC CHARACTERISTICS

The DC-8-61 maximum noise suppression configuration requires the use of a long duct nacelle (figure D-17) to achieve the desired reduction in EPNL's. This represents a completely new nacelle and extensive modification to the over-the-wing pylon. The inlet incorporates acoustic treatment on the duct inner wall and a single concentric ring, while the long fan ducts have acoustic treatment on both walls. A new thrust reverser similar in concept to the DC-8-62/63 design is required, along with substantial changes to the existing engine and nacelle subsystems and accessories.

The DC-8-61 intermediate noise suppression configuration retains the short fan duct concept and the over-the-wing pylon (figure D-17). The existing Pratt & Whitney manufactured fan thrust reversers have been modified to accommodate the increased diameter fan and its higher flow rate. The primary exhaust nozzle exit area was increased to match the primary flow of the JT3D-9 engine, but the existing primary thrust reverser has been retained with only minor changes. Acoustic treatment has been incorporated in the wall treatment with one circumferential splitter in the fan discharge duct. Major nacelle accessories and subsystems of the existing DC-8-61 have been retained with little or no modification.

The minimum noise suppression nacelle configuration is very similar to the intermediate treatment design, differing basically in the elimination of the treated rings in the inlet and fan discharge duct (figure D-17). Engine and nacelle subsystems and accessories for this nacelle are essentially identical to the intermediate treatment design, except for the ice protection system simplification resulting from elimination of the inlet ring.

The acoustic treatment for the maximum, intermediate, and minimum treated nacelles is summarized in table D-10. All acoustic treatment is perforated aluminum sheet bonded to honeycomb core.

The estimated EPNL's for the maximum, intermediate, and minimum noise suppression nacelles (and reduction in EPNL's relative to the untreated modified aircraft and the existing aircraft) at FAR Part 36 conditions are summarized in table D-11. These estimates are for an aircraft with a maximum takeoff gross weight of 158 760 kg (350,000 lb), and a maximum landing gross weight of 117 029 kg (258,000 lb).

Figure D-18 presents 90 EPNdB noise contours and areas within the contours for the existing and modified (maximum, intermediate and minimum levels of treatment) aircraft, for typical mission operations. A typical mission is defined here as a 55 percent payload and 2.8 Mm (1,500 n. mi.) mission. Noise contours are presented in figure D-10 for the following power settings and flight paths: (1) approach and takeoff without cutback, and (2) approach and takeoff with cutback.

Estimated noise levels at FAR Part 36 conditions are presented in tables D-12 and D-13 for the Delta DC-8-51 and UAL DC-8-54F, respectively. The estimates for the Delta DC-8-51 are for an aircraft with a maximum takeoff

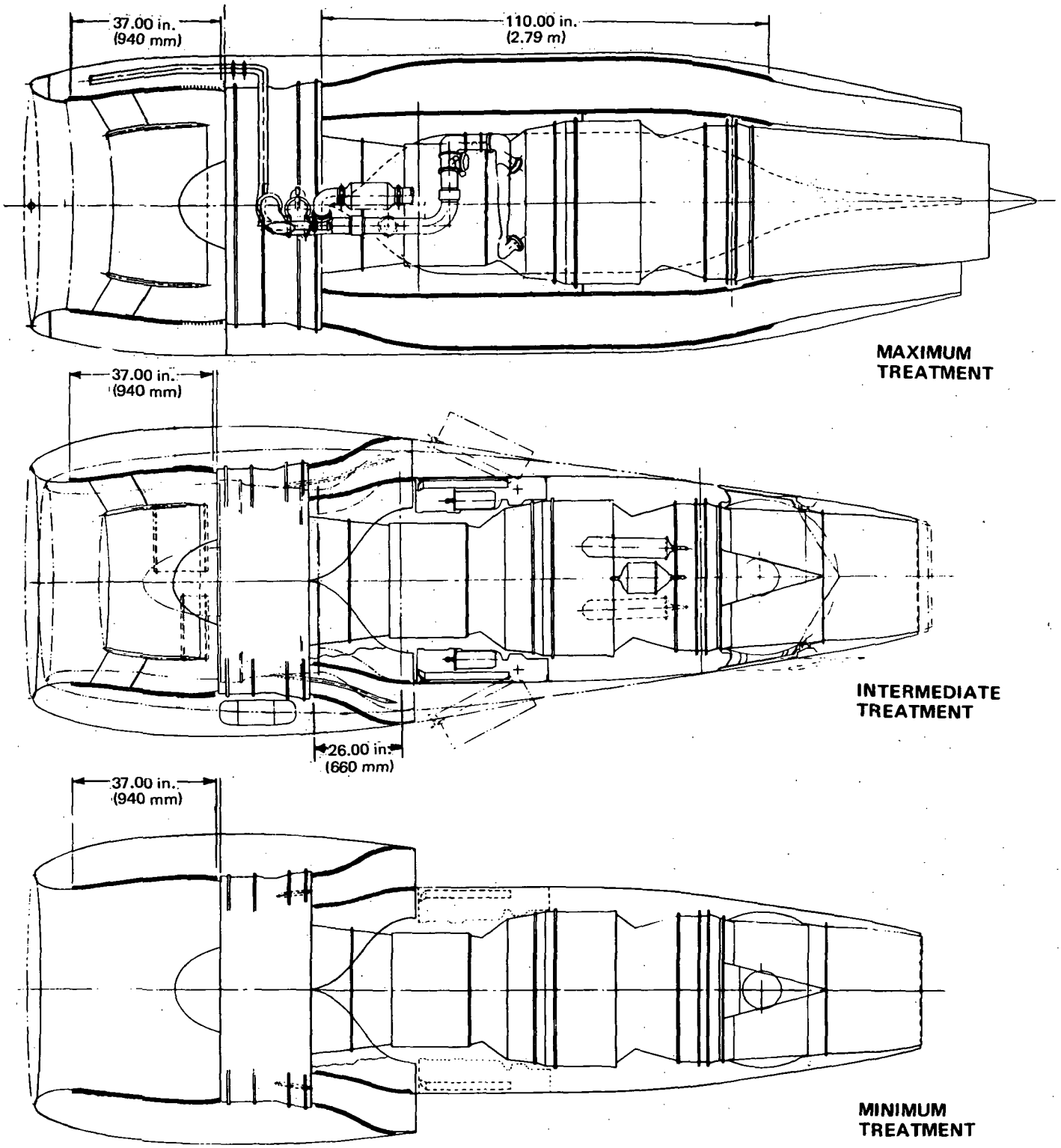

FIGURE D-17. DC-8-61 ACOUSTIC TREATMENT COMPARISON

TABLE D-10

DESCRIPTION OF NACELLE ACOUSTIC TREATMENT FOR DC-8

	MAXIMUM TREATED NACELLE	INTERMEDIATE TREATED NACELLE	MINIMUM TREATED NACELLE
Inlet	Cowl 37 in. (940 mm) plus one ring 18 in. (458 mm)	Cowl 37 in. (940 mm) plus one ring 18 in. (458 mm)	Cowl 37 in. (940 mm)
Fan Case	Inner Wall 19 in. (254 mm)	Inner Wall 10 in. (254 mm)	Inner Wall 10 in. (254 mm)
	Outer Wall 15 in. (381 mm)	Outer Wall 15 in. (381 mm)	Outer Wall 15 in. (381 mm)
	Splitter 6 in. (153 mm)	Splitter 6 in. (153 mm)	Splitter 6 in. (153 mm)
Fan Discharge Ducts	New Long Duct 110 in. (2.8 m)	New Short Duct 26 in. plus Splitter 16 in. (407 mm)	New Short Duct 26 in. (660 mm)

NOTE: 1. All acoustic treatment will be perforated aluminum sheet bonded to aluminum honeycomb core.

TABLE D-11

ESTIMATED EPNL'S FOR EXISTING AND MODIFIED DC-8-61 AIRCRAFT

Aircraft	Approach			Takeoff with Cutback			Takeoff without Cutback			Sideline		
		Δ EPNdB			Δ EPNdB			Δ EPNdB			EPNdB	
	EPNdB	Relative to Untreated Modified Aircraft	Relative to Existing Aircraft	EPNdB	Relative to Untreated Modified Aircraft	Relative to Existing Aircraft	EPNdB	Relative to Untreated Modified Aircraft	Relative to Existing Aircraft	EPNdB	Relative to Untreated Modified Aircraft	Relative to Existing Aircraft
Untreated Modified*	111	-	6	105	-	12	108	-	8	96	-	7
Maximum Treatment Modified	96	15	21	98	7	19	102	6	14	93	3	10
Intermediate Treatment Modified	100	11	17	102	3	15	107	1	9	96	0	7
Minimum Treatment Modified	104	7	13	103	2	14	107	1	9	96	0	7
FAR Part 36 Rule	106.2	-	-	103.6	-	-	103.6	-	-	106.2	-	-
Existing Aircraft	117	-	-	117	-	-	116	-	-	103	-	-

*Assumes aero performance of Untreated Modified Aircraft is the same as that of the Minimum Treated Modified Aircraft.

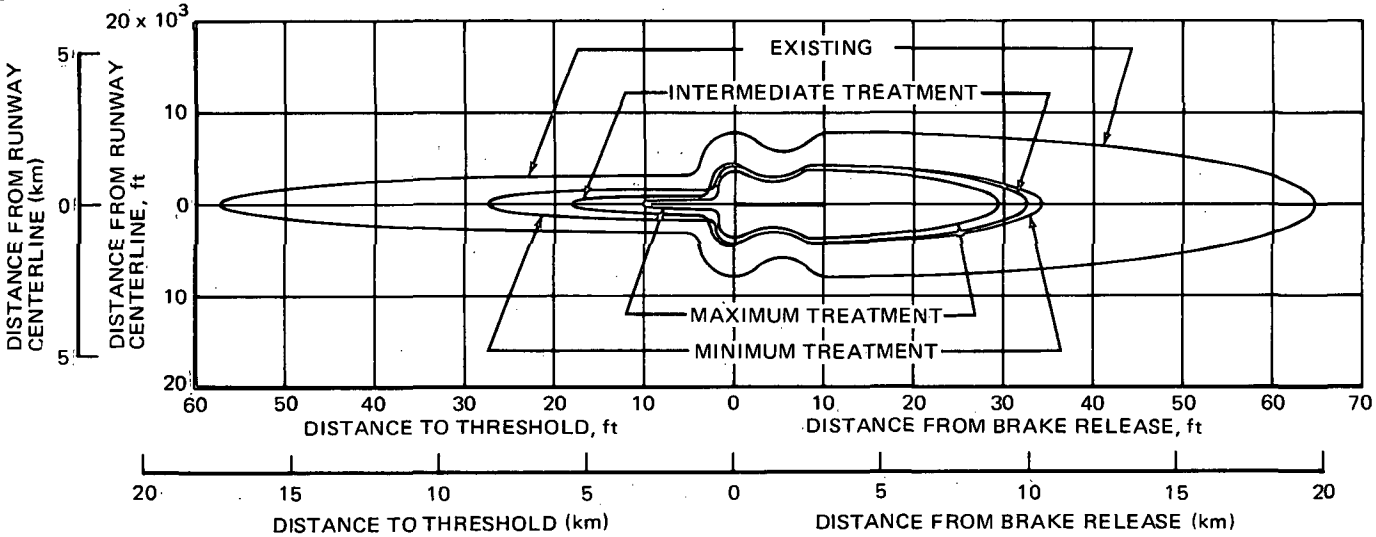

TREATMENT	AREA WITHIN CONTOUR	
	sq miles	(sq km)
EXISTING	40.2	104.0
MINIMUM	10.7	27.5
INTERMEDIATE	9.1	23.6
MAXIMUM	6.8	17.6

(A) APPROACH AND TAKEOFF WITHOUT CUTBACK

TREATMENT	AREA WITHIN CONTOUR	
	sq miles	(sq km)
EXISTING	49.1	127.0
MINIMUM	10.9	28.3
INTERMEDIATE	7.8	20.2
MAXIMUM	4.9	12.7

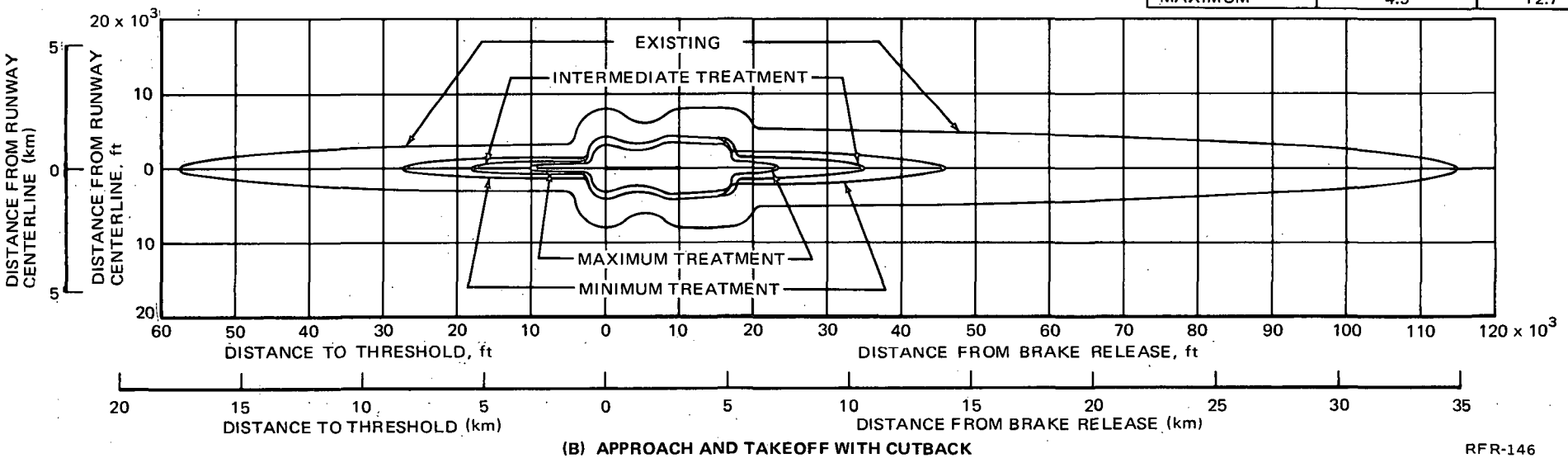

(B) APPROACH AND TAKEOFF WITH CUTBACK

RFR-146

FIGURE D-18. 90-EPNdB NOISE CONTOUR FOR EXISTING AND MODIFIED DC-8-61 AIRCRAFT FOR TYPICAL MISSION OPERATION

TABLE D-12

ESTIMATED EFFECTIVE PERCEIVED NOISE LEVELS (EPNdB)

AT FAR PART 36 CONDITIONS FOR

THE DELTA DC-8-51 INTERMEDIATE TREATED NACELLE

	APPROACH	TAKEOFF WITHOUT CUTBACK	TAKEOFF WITH CUTBACK	SIDELINE
Modified Aircraft (untreated)	110	103	98	97
Modified Aircraft (treated)	99	102	95	97
Existing Aircraft	117	110	109	104
FAR Part 36 Rule	105.8	102.4	102.4	105.8
Noise Reduction Relative to Untreated Modified Aircraft	11	1	3	0
Noise Reduction Relative to Existing Aircraft	18	8	14	7

NOTES: (1) For description of nacelle acoustic treatment for modified aircraft, see table D-10.

TABLE D-13

ESTIMATED EFFECTIVE PERCEIVED NOISE LEVELS (EPNdB)
AT FAR PART 36 CONDITIONS FOR THE
UAL DC-8-54F INTERMEDIATE TREATED NACELLE

	APPROACH	TAKEOFF WITHOUT CUTBACK	TAKEOFF WITH CUTBACK	SIDELINE
Modified Aircraft (untreated)	111	107	104	97
Modified Aircraft (treated)	100	106	101	97
Existing Aircraft	118	106	101	104
FAR Part 36 Rule	106.1	103.4	103.4	106.1
Noise Reduction Relative to Untreated Modified Aircraft	11	1	3	0
Noise Reduction Relative to Existing Aircraft	18	9	14	7

NOTES: (1) For description of nacelle acoustic treatment for modified aircraft, see table D-10.

gross weight of 125 194 kg (276,000 lb) and a maximum landing gross weight of 90 493 kg (199,500 lb). The weight of 142 884 kg (315,000 lb) and a maximum landing gross weight of 108 864 kg (240,000 lb).

Figures D-19 and D-20 present, for the Delta DC-8-51 and UAL DC-8-54F, respectively, 90 EPNdB noise contours and areas within contours, for the existing and modified (intermediate level of treatment) aircraft, for typical mission operations. A typical mission for the Delta DC-8-51 is defined here as a 55 percent payload and a 2.3 Mm (1,250 n. mi.) mission. A typical mission for the UAL DC-8-54 is defined here as a 70 percent payload, and 2.8 Mm (1,500 n. mi.) mission. Noise contours are presented for the following sets of power settings and flight paths: (1) approach and takeoff without cutback, and (2) approach and takeoff with cutback.

The modified nacelle which provides maximum noise suppression for the JT3D-9 engine on the DC-8 Model 63 retains the long fan duct concept and the undercut pylon of the existing airplane. The existing Douglas manufactured thrust reverser has been extensively modified to accommodate the increased fan and primary duct areas and the increased engine flow rates. Acoustic treatment has been incorporated in the nacelle in the form of wall treatment and one concentric ring in the inlet and wall treatment only in the fan discharge duct, figure D-21. Major nacelle accessories and subsystems of the existing DC-8-63 have been retained with little or no modification.

The minimum noise suppression nacelle design differs from the maximum suppression configuration primarily in the omission of the inlet ring and less treatment in the fan ducts, figure D-21. Engine and nacelle subsystems and accessories for this nacelle are essentially identical to the maximum treatment design, except for the ice protection system simplification resulting from elimination of the inlet ring.

The acoustic treatment for the maximum and minimum treated nacelles are summarized in table D-14. All acoustic treatment is perforated aluminum sheet bonded to honeycomb core.

The estimated EPNL's (and reduction in EPNL's relative to the untreated modified aircraft and the existing aircraft) at FAR Part 36 conditions are summarized in table D-15. These estimates are for an aircraft with a maximum takeoff gross weight of 158 760 kg (350,000 lb) and a maximum landing gross weight of 117 029 kg (258,000 lb).

Figure D-22 presents 90 EPNdB noise contours and areas within the contours for the existing and modified (maximum and minimum levels of treatment) DC-8-62 aircraft for typical mission operations. Both levels of treatment are shown here in order to provide a more comprehensive view of the relative change in area with change in treatment level. A typical mission is defined here as a 55 percent payload and 2.8 Mm (1,500 n. mi.) mission. Noise contours are presented for the following flight paths: (1) approach and takeoff without cutback ([A], figure D-22), and (2) approach and takeoff with cutback ([B], figure D-22).

Estimated noise levels at FAR Part 36 conditions are presented in table D-16. These estimates are for an aircraft with a maximum takeoff gross weight of 151 956 kg (335,000 lb) and a maximum landing gross weight of 108 864 kg (240,000 lb).

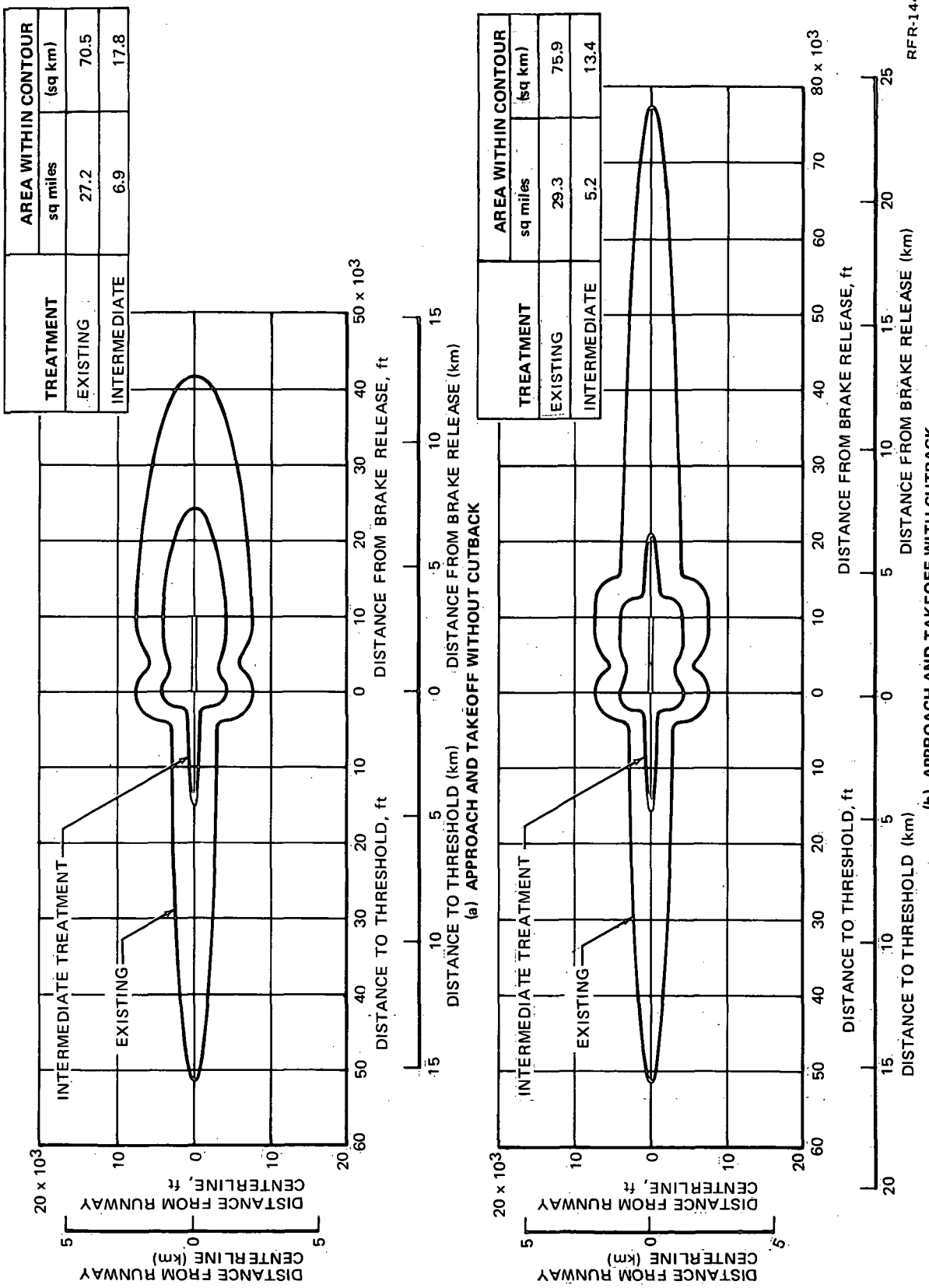

FIGURE D-19. 90 EPNdB NOISE CONTOURS FOR EXISTING AND MODIFIED DELTA DC-8-51 AIRCRAFT FOR TYPICAL MISSION OPERATIONS

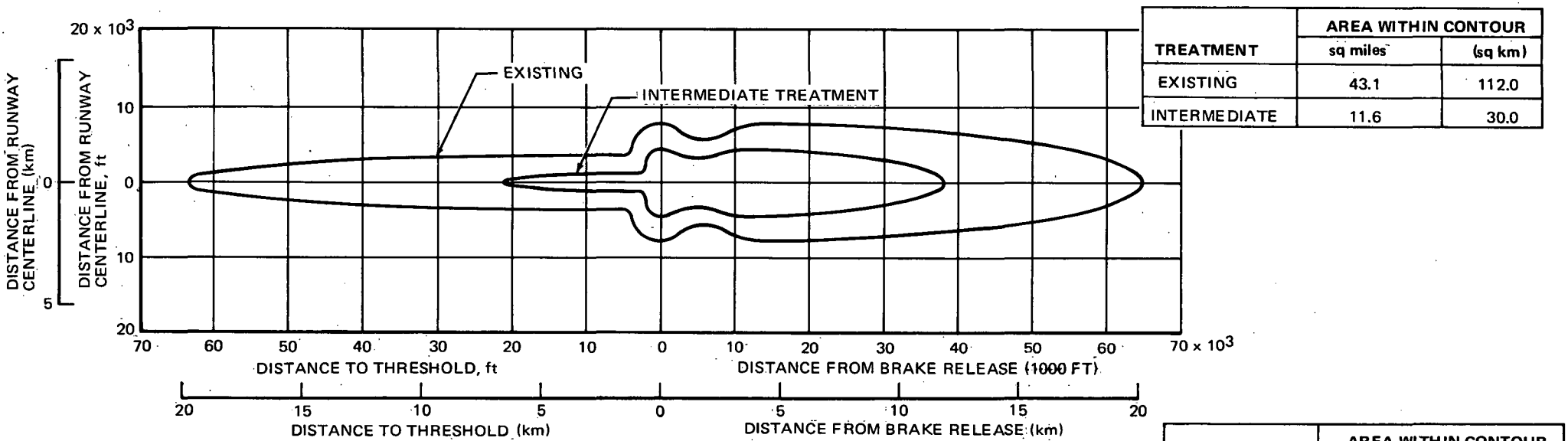

TREATMENT	AREA WITHIN CONTOUR	
	sq miles	(sq km)
EXISTING	43.1	112.0
INTERMEDIATE	11.6	30.0

(a) APPROACH AND TAKEOFF WITHOUT CUTBACK

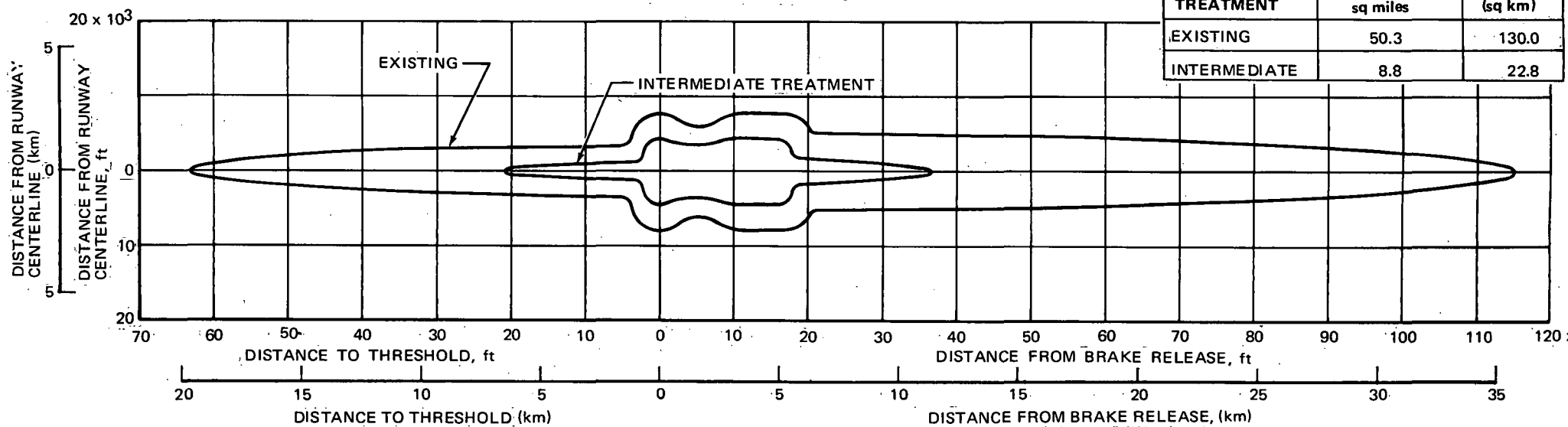

TREATMENT	AREA WITHIN CONTOUR	
	sq miles	(sq km)
EXISTING	50.3	130.0
INTERMEDIATE	8.8	22.8

(b) APPROACH AND TAKEOFF WITH CUTBACK

RFR-142

FIGURE D-20. 90 EPNdB NOISE CONTOURS FOR EXISTING AND MODIFIED UAL DC-8-54F AIRCRAFT FOR TYPICAL MISSION OPERATION

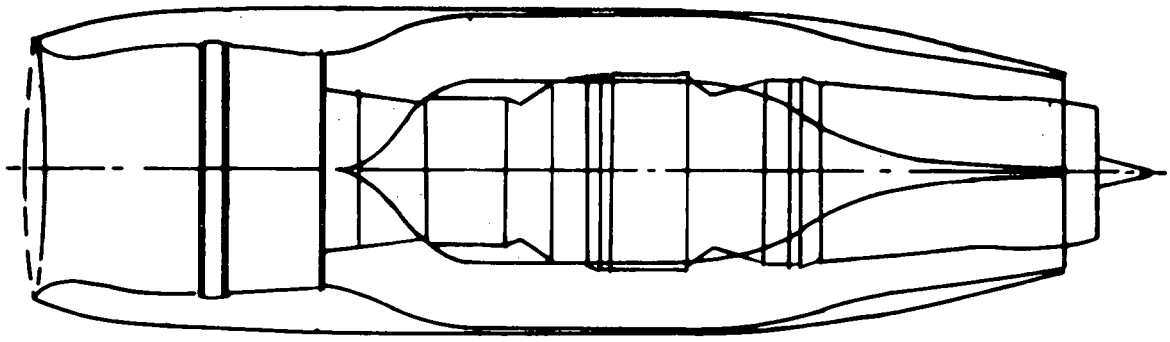

EXISTING JT3D-3B INSTALLATION

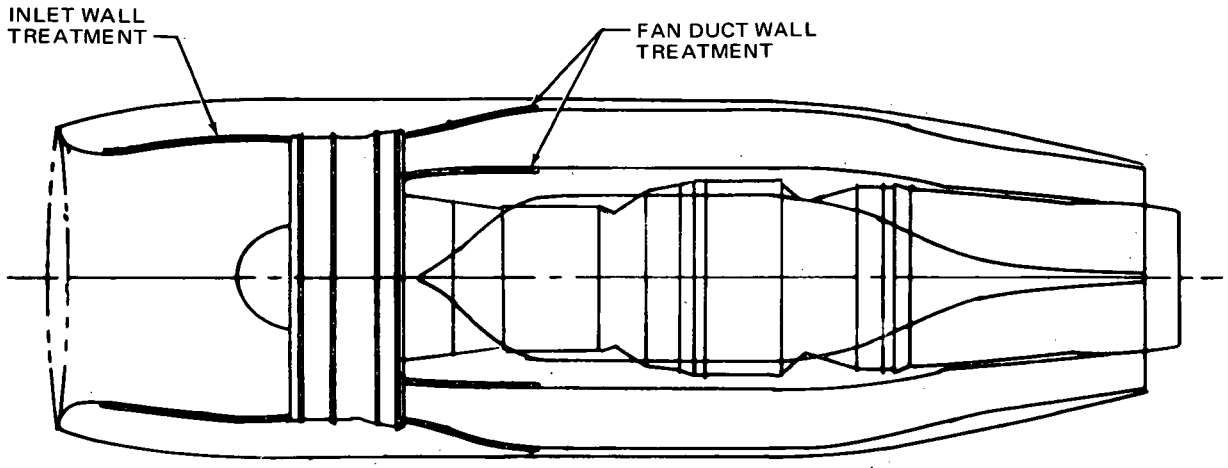

JT3D-9 MINIMUM ACOUSTIC TREATMENT INSTALLATION

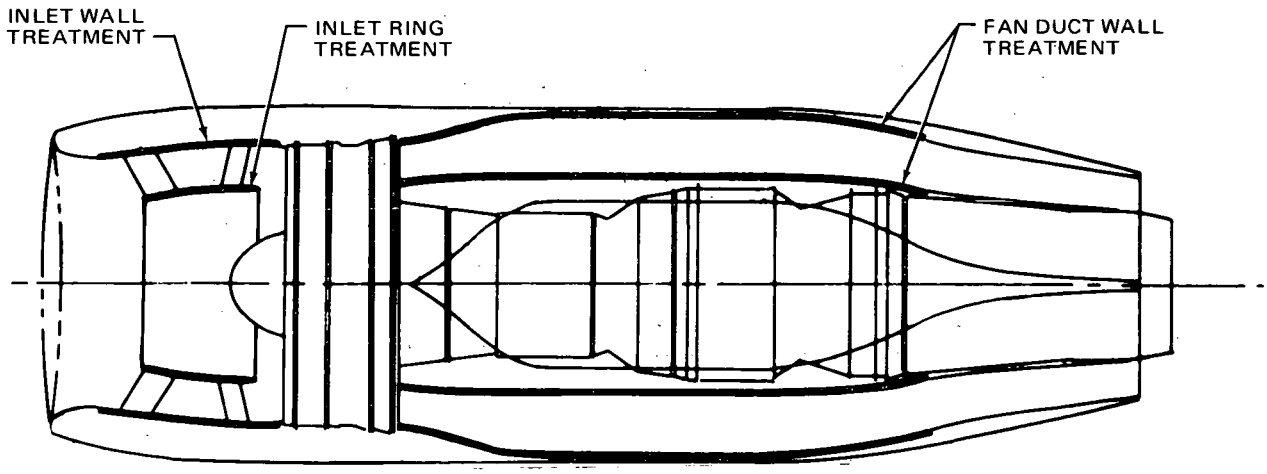

JT3D-9 MAXIMUM TREATMENT INSTALLATION

RFR-174

FIGURE D-21. DC-8-63 ACOUSTIC TREATMENT COMPARISON

TABLE D-14

DESCRIPTION OF NACELLE ACOUSTIC TREATMENT

	MAXIMUM TREATED NACELLE	MINIMUM TREATED NACELLE
Inlet	Cowl 37 in. (940 mm) plus one Ring 18 in. (458 mm)	Cowl 37 in. (940 mm)
Fan Case	Inner wall 10 in. (254 mm)	Inner Wall 10 in. (254 mm)
	Outer Wall 15 in. (381 mm)	Outer Wall 15 in. (381 mm)
	Splitter 6 in. (153 mm)	Splitter 6 in. (153 mm)
Fan Discharge Ducts	New Long Duct 110 in. (2.8 m)	New Long Duct 28 in. (711 mm)

NOTE: 1. All acoustic treatment will be perforated aluminum sheet bonded to aluminum honeycomb core.

2. For additional information see figure D-21.

TABLE D-15
ESTIMATED EPNL'S FOR EXISTING AND MODIFIED DC-8-63 AIRCRAFT
AT FAR PART 36 CONDITIONS

Aircraft	Approach			Takeoff with Cutback			Takeoff without Cutback			Sideline		
		Δ EPNdB			Δ EPNdB			Δ EPNdB			Δ EPNdB	
	EPNdB	Relative to Untreated Modified Aircraft	Relative to Existing Aircraft	EPNdB	Relative to Untreated Modified Aircraft	Relative to Existing Aircraft	EPNdB	Relative to Untreated Modified Aircraft	Relative to Existing Aircraft	EPNdB	Relative to Untreated Modified Aircraft	Relative to Existing Aircraft
Untreated Modified*	107	-	7	103	-	10	105	-	10	95	-	7
Maximum Treatment Modified	96	11	18	98	5	15	103	2	12	93	2	10
Minimum Treatment Modified	100	7	14	101	-	12	104	-	11	95	0	7
FAR Part 36 Rule	106.4	-	-	104.1	-	-	104.1	-	-	106.4	-	-
Existing Aircraft	114	-	-	113	-	-	115	-	-	102	-	-

*Assumes aero performance of Untreated Modified Aircraft is the same as that of the Minimum Treated Modified Aircraft.

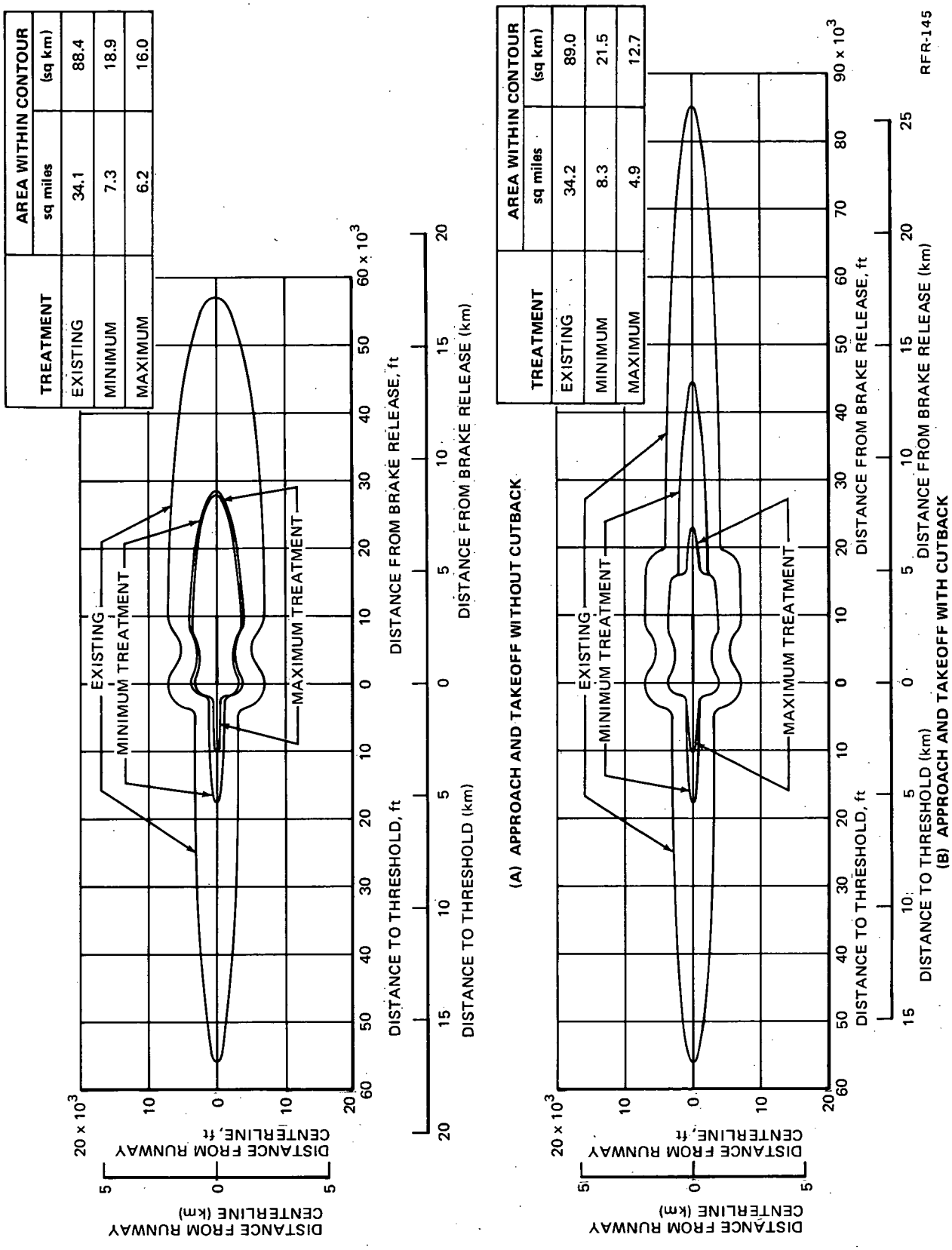

FIGURE D-22. 90-EPNdB NOISE CONTOUR FOR EXISTING AND MODIFIED DC-8-63 AIRCRAFT FOR TYPICAL MISSION OPERATIONS

TABLE D-16

ESTIMATED NOISE LEVELS AT FAR PART 36 CONDITIONS (EPNdB)
FOR DC-8-62

	APPROACH	TAKEOFF WITHOUT CUTBACK	TAKEOFF WITH CUTBACK	SIDELINE
Modified Aircraft (untreated)	106	104	102	97
Modified Aircraft (treated)	95	102	97	95
Existing Aircraft	114	113	112	103
FAR Part 36 Rule	106.3	103.8	103.8	106.3
Noise Reduction Relative to Untreated Modified Aircraft	11	2	5	2
Noise Reduction Relative to Existing Aircraft	19	11	15	8

Figure D-23 presents 90 EPNdB noise contours and areas within contours for the existing and modified aircraft for typical mission operations. A typical mission is defined here as a 55 percent payload and 2.8 Mm (1,500 n. mi.) mission. Noise contours are presented for the following sets of power settings and flight paths: (1) approach and takeoff without cutback, and (2) approach and takeoff with cutback. Noise contours were not developed for 2-segment .005 rad/.010 rad (3°/6°) approach operations.

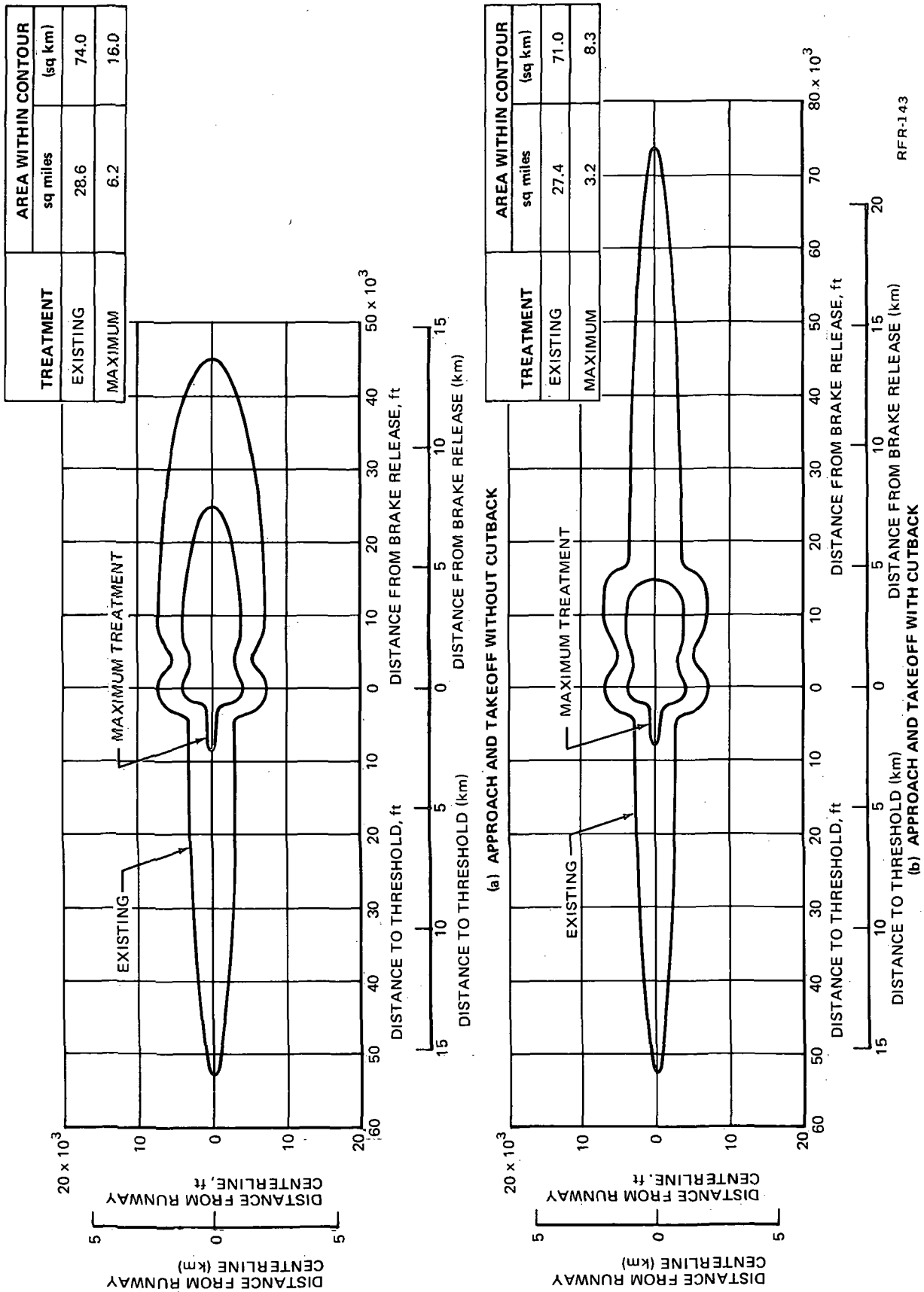

FIGURE D-23. 90 EPNdB NOISE CONTOURS FOR EXISTING AND MODIFIED BRANIFF DC-8-62 AIRCRAFT FOR TYPICAL MISSION OPERATION

APPENDIX D

MODEL TESTS

The following component and model tests were proposed for Phase I, but were deferred at the NASA's request to the Phase II program.

- DC-8 Nacelle Development Wind Tunnel Test
- DC-8 Short Duct Fan Reverser Test
- DC-8 and DC-9 Nacelle Inlet Protection Optimization and Verification Tests

Additional Phase II component and model tests included:

- Acoustic Materials Panel Tests for Mechanical Allowables and Sonic Fatigue
- Nacelle Composites Evaluation Program
- DC-8-61/-63 Flight-Type Nacelle Flutter Model Test
- DC-9 Scale Model Exhaust Duct Tests
- DC-8 and DC-9 Nozzle Thrust Coefficient Model Test
- DC-8 and DC-9 Inlet Bird Strike and Erosion Tests

Although the DC-8 Series 50 and 60 JT3D-9 refan engine portion of the NASA Phase I refan was terminated 15 January 1973, the high speed wind tunnel test on the DC-8-50 and -61 models, which was in progress, was completed and a summary of the results is presented.

DC-8-50 and -61 High Speed Wind Tunnel Test (Ref. 3)

The purpose of this test was to determine the feasibility of a common long duct refanned nacelle for all DC-8 models since serious consideration must be given to the aerodynamic design of the pylons for minimum interference drag. Previous wind tunnel and flight experience has shown the extreme sensitivity of the nacelle and pylon placement to severe interference drag penalties. These penalties are related to local Mach numbers in the wing/pylon/nacelle channel and are manifested as a wave drag associated with shocks in the channel and as a drag associated with a thickening and separation of the boundary layer on the nacelle pylon and wing. The existing long duct nacelle installation on the DC-8-62/-63 and the short duct nacelle installation on the DC-8-62/-63 and the short duct nacelle installation on the Series 50/61 are essentially interference-free installations.

Since the long duct nacelle on the Series 62/63 is well out in front of the wing, the refanned installation is not considered to be a problem. If the refanned nacelle were installed like Series 62/63 this would require re-skinning the wing on the Series 50/61 for flutter considerations. If, on the other hand, the long duct refanned nacelle were installed in the aft short duct position, a significant interference drag might result. The reason for this concern can be seen from a comparison of the wing/pylon/nacelle channel area distributions for the refanned installation with those for an essentially interference-free installation and an installation with a significant interference penalty (figure D-24). The latter two area distributions are for similar installation that were previously tested. The area distribution for the installation with an interference penalty corresponded closely to the development of supersonic flow and shocks in the channel. It can be seen from figure D-24 that the convergence-divergence of the refanned area distribution is worse that that of the interference-free installation.

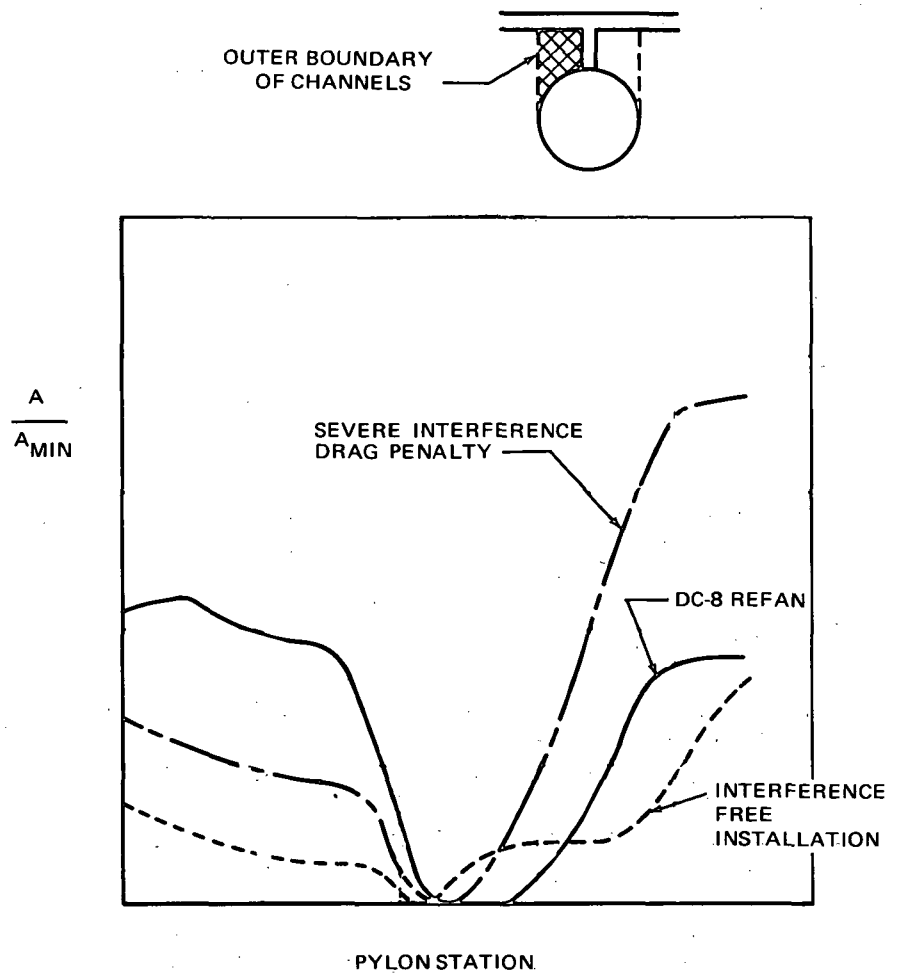

FIGURE D-24. DC-8 REFAN WING/NACELLE/PYLON CHANNEL AREA DISTRIBUTIONS

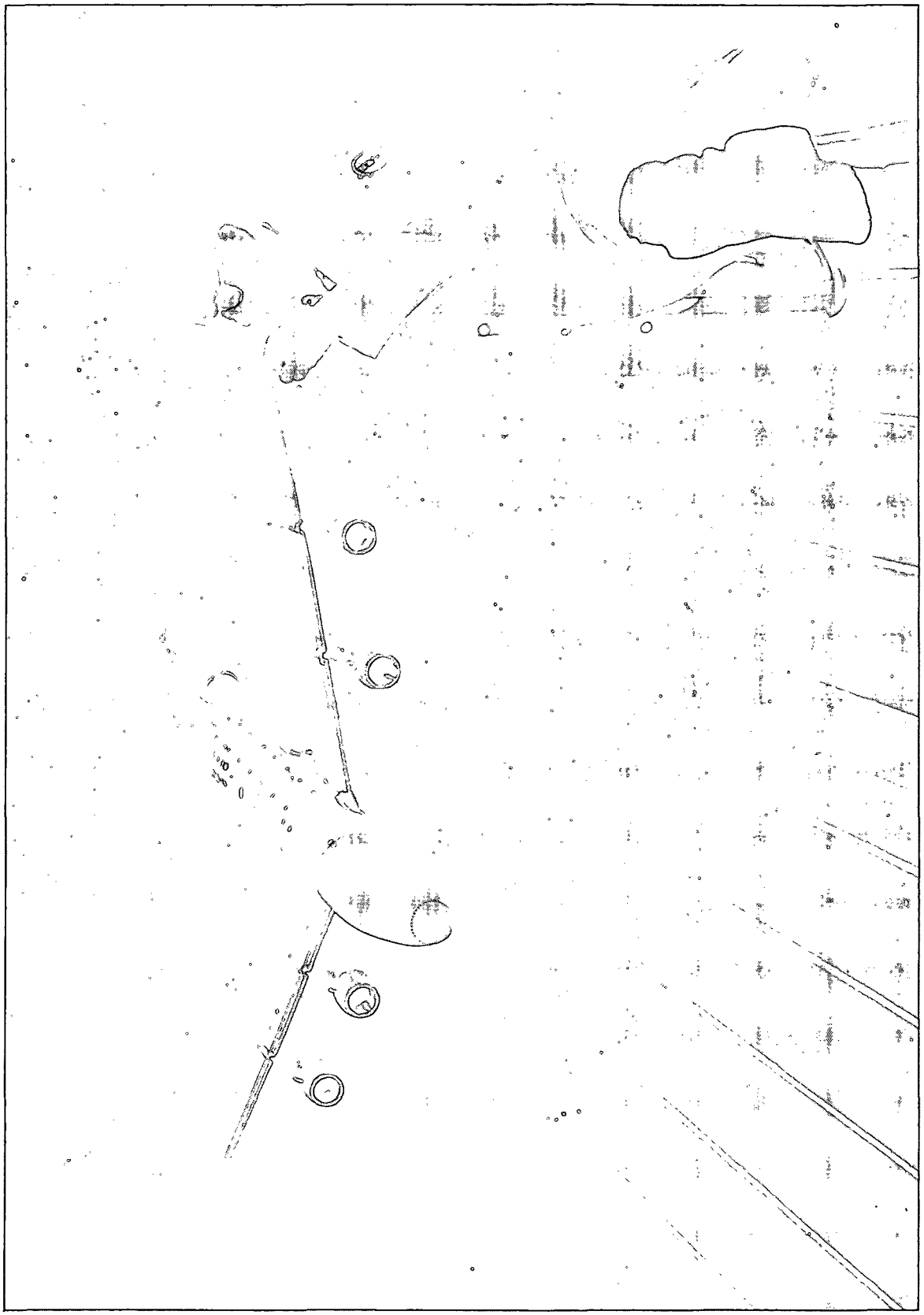

FIGURE D-25. MODEL IN AMES WIND TUNNEL

As a result of the concern expressed in the problem statement, a high speed wind tunnel test was conducted in the NASA Ames 11-foot transonic wind tunnel in January 1973. A photograph of the model installed in the Ames tunnel is presented in figure D-25. The purpose of this test was to determine if an interference drag penalty existed for the long duct refanned nacelle installation on the existing Series 50/61 short duct pylon, and if necessary to investigate potential fixes designed to minimize or eliminate the interference penalty. The potential fixes take the form of pylon bumps which are designed to improve the area distributions shown in figure D-26.

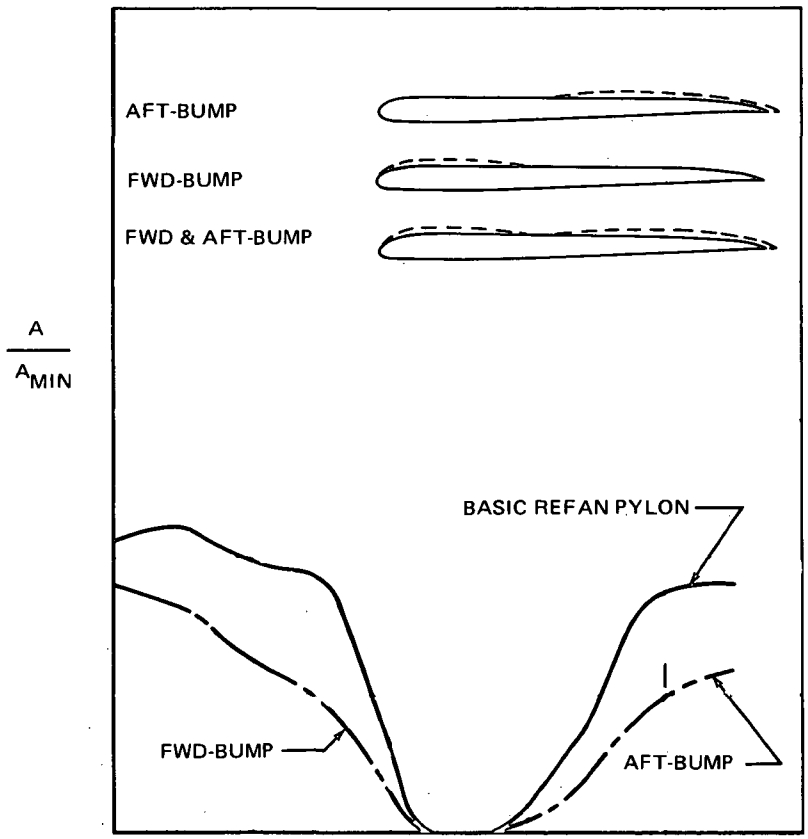

FIGURE D-26. DC-8 REFAN PYLON MODIFICATIONS

Three sets of modified pylons were designed and fabricated for this test. A sketch of these pylons and their effect on the channel area distribution is presented in figure D-26.

Analysis of the results from this test leads to the following conclusions:

(1) At a typical cruise condition there exists an interference drag penalty of less than one-percent of total cruise drag for the installation of the long duct refan nacelle on the existing

(minimum structural change) Series 50 and 61 short duct pylon. This very small penalty would, however, be much more than off-set by the large improvement, demonstrated on the existing DC-8, of a long duct nacelle over a short duct nacelle.

(2) At cruise conditions some supersonic flow is present in the inboard channel of the inboard refan nacelle installation, but it is not sufficient to cause any wave drag or boundary layer separation. The small interference drag penalty results from a general thickening in the boundary layer of some of the components when they are integrated.

(3) The one pylon modification tested resulted in a drag penalty because its design goal of eliminating shock-related interference drag was not required and the bump, thus, became a source of additional parasite drag.

(4) From aircraft performance considerations, a common long duct refan engine nacelle is certainly feasible for all DC-8 models.

Flutter Model Program

The installation of modified JT3D engines on the domestic DC-8 required detail study and tests to ensure that existing flutter margins for these aircraft were not jeopardized. The flutter mechanism of the DC-8 wing is complicated and sensitive to the engine pod weight and the stiffness of the supporting pylons. It was the purpose of the flutter model program to experimentally determine the flutter characteristics of the DC-8 Series -50, -61, and -63 airplanes as affected by the modified JT3D engines, and to ensure that these aircraft were free from flutter within the specified speed envelopes.

The existing 5% low speed full-span flutter model (LB 213) of the DC-8 is a complete model simulating the structural dynamic characteristics of the full scale vehicle. It is designed as an equivalent beam model with single spars to represent the structural stiffness with segmented fairings which are ballasted to simulate the mass properties. The model is mounted on a vertical rod system and is "flown" in the wind tunnel by remote control of the horizontal stabilizer. Main components of the model are interchangeable allowing it to be configured in the -50 Series as well as the -60 Series. The model parameters that can be studied are:

(1) Wing Fuel

(2) Pylon Stiffness

(3) Payload

(4) Aileron Restraint

(5) Aileron Mass Balance

(6) Engine Mass, c.g., Location, Inertia

(7) Engine Fore and Aft Location

The status of the DC-8 refanned flutter model (LB 213E) at 15 January 1973 was as follows:

- Vibration modes of -61 bare wing (cantilevered) were measured and compared with analytical model to re-establish a baseline in order to proceed with design of a wing spar to represent the -51 wing stiffness. Design values for the -51 wing spars were not established; however, preliminary drawings for "rough-cut" of wing spars had been released.
- Preliminary drawings for "rough-cut" of pylon flexures had been released; however, final design numbers had not been established.
- Preliminary sketches of the engine pods had been made; however, no final working drawings were started.
- Aileron springs drawings were re-released with minimum fabrication completed.
- New drawings for the revised ventral gear box (used for model yaw control) were released and parts purchased.
- Rudder springs drawings were re-released, but no fabrication was started.
- Fuselage repair had commenced with constant section mold finished for forming fiberglass skin for fuselage.
- Minor repair of wing fairing sections was completed.
- Left-hand aileron replacement for old damaged aileron was 50% complete.
- Wing spars were out to vendor with rough-cuts completed.
- Pylon flexure blanks (12 each) were completed.

JT3D Fanned Duct Internal Flow Tests

The purpose of this test program was to determine the internal flow performance characteristics of three basic flow duct configurations: (1) short duct with circumferential splitter, (2) short duct with circumferential and radial splitter, and (3) long duct. The performance of each configuration was to be determined using airflow, inlet and outlet total pressure surveys, wall static pressures and boundary flow visualization.

The test program was to be conducted on the Diane facility located at the McDonnell Aerophysics Laboratory. This facility allows a model of 100 square inch exit area to be tested up to pressure ratio of 2.1. This provides a duct model of 70% full scale. In addition to the mass flow instrumentation provided by the Diane facility, the model was to be instrumented to measure approximately 350 pressures. The inlet and exit station planes of the model were to be surveyed with six 6-probe total pressure rakes placed at centers of equal areas. Also, four boundary layer rakes were to be placed on the walls and one on the circumferential splitter.

The internal flow contours were established and loft lines defined, figure D-27. All detail drawings were completed for adapters, models and instrumentation. The fabrication of all tooling was completed, as well as the flow balancing screen, constant section adapter and inlet total pressure rakes. All parts and tooling was completed, as well as the flow balancing screen, constant section adapter and inlet total pressure rakes. All parts and tooling were stored.

RETROFIT AND ECONOMIC ANALYSES

Schedule and Market

The development and retrofit schedule and the estimated number of refanned DC-8 aircraft are closely related, and stretching the JT3D refan development schedule would reduce the total number of DC-8 aircraft which could be refanned. Since the fixed costs are constant, major schedule slippage would increase the unit cost and would, thereby, reduce the economic viability of the DC-8 retrofit program.

A series of schedule studies demonstrate retrofit could begin in an interval starting as early as January 1976. Risk could be reduced by avoiding concurrency and slipping retrofit initiation until January 1977. Beyond that, further schedule slippage would not appreciably reduce risk.

Start dates within the one-year interval provide a total estimated DC-8 retrofit market of 255 aircraft.

	Domestic	Foreign	Total
DC-8-61/-50	80	40	120
DC-8-63/-62	60	75	135
	140	115	255

The market estimate is based upon the domestic and worldwide fleets in mid-1980. This point provides an eight-year period for depreciating the retrofit costs. A three-year DC-8 retrofit program leads to an average retrofit rate of 6-1/2 to 7 aircraft per month for the worldwide fleet, or 3-1/2 to 4 per month for the domestic fleet. These average rates are high enough to provide a reasonable stable and efficient retrofit program.

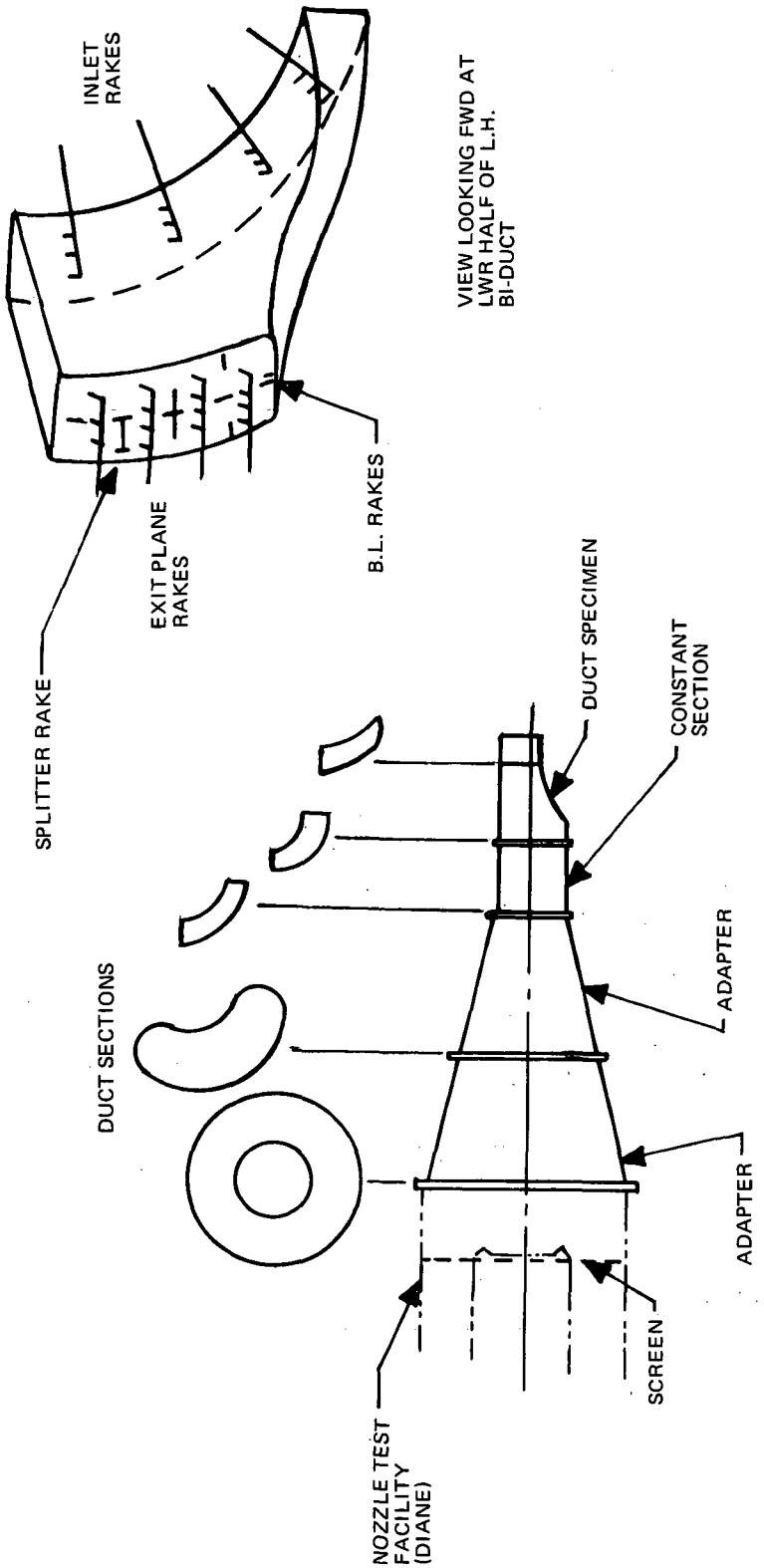

FIGURE D-27. DC-8 REFAN FAN DUCT EXHAUST MODEL TEST HARDWARE

Retrofit Unit Costs and Total Domestic Capital Costs

The quantities and rates cited earlier lead to estimated retrofit costs between $2.3 and $2.5 million per aircraft for the DC-8-61/-50's and between $2.1 and $2.3 million per aircraft for the DC-8-63/-62's depending upon the noise treatment level desired. The cost breakdown is shown in table D-17.

In addition to the retrofit modification, other capital or one-time expenditures will be required. Since the existing engines and airframes are modified, new spare parts inventories are required. Modification of the aircraft will require crew familiarization training before refanned aircraft can be used in scheduled service. When aircraft are removed from scheduled service some loss in gross revenue would be experienced during peak travel periods. These "out-of-service" costs represent a one-time loss in operating revenue which will eventually show up in the profit and loss statements of the various carriers and, therefore, represent an economic but not a recognized accounting cost. On the other hand, the value of the aircraft will be reduced by accounting charges which recognize the value of engine and airframe components, and their associated spares, discarded and obsoleted by the retrofit program. These are not an economic cost, but would be reflected in non-operating expense.

The costs cited earlier can be viewed in at least two ways. The first represents the estimated value in constant 1973 dollars while the second is in current dollars. Under the second approach, retrofit, training and out-of-service costs are included in 1977 to 1978 dollars while asset write-offs are included in 1968 to 1970 dollars. The magnitudes of the two approaches are:

	DOLLAR BASIS (MILLIONS)	
COST ITEM	1973	CURRENT
Retrofit	320	370
Spares	60	70
Training	5	5
Subtotal	385	445
Out-of-Service	45	52
Total Economic Cost	430	497
Subtotal (as above)	385	445
Asset Write-down	70	35
	455	480

The retrofit and spares costs are included in computation of direct operating costs. The DOC formula modifications used in the computation are based upon a retrofit depreciation period of eight years to 10 percent, and use Douglas maintenance experience.

TABLE D-17

RETROFIT UNIT COST BREAKDOWN

(IN MILLIONS OF 1973 DOLLARS)

AIRCRAFT SERIES QUANTITY TREATMENT LEVEL	DC-8-50/61 120			DC-8-63/62 135		
	MIN.	INT.	MAX. COMMON	MIN.	MAX. COMMON	MAX. UNIQUE
Engineering and Test	0.068	0.089	0.199	0.065	0.059	0.065
Manufacturing and Installation	0.132	0.132	0.133	0.112	0.112	0.112
Material and Equipment	1.004	1.109	1.048	0.979	0.879	1.058
Engine Kits	0.800	0.800	0.800	0.800	0.800	0.800
Total Cost	2.004	2.130	2.180	1.956	1.850	2.035
Profit	0.200	0.213	0.218	0.196	0.185	0.204
Total Cost & Profit	2.204	2.343	2.398	2.152	2.035	2.239
NASA Fee	0.090	0.094	0.096	0.087	0.081	0.092
TOTAL PRICE	2.294	2.437	2.494	2.239	2.116	2.331

The direct operating cost per aircraft mile increment would amount to between 7 and 8 percent depending upon the aircraft and treatment level:

Treatment Level Storage Length	Increased Direct Operating Costs DC-8-61/-50 1500 n. mi.	DC-8-63/-62 2800 n. mi.
Existing	0.0	0.0
Minimum	7.3	7.0
Intermediate	8.1	Not applicable
Maximum	7.7	7.0*/7.9

*Common DC-8-61 and DC-8-63 Pod.

Of the 7 to 8 percent, about 2 to 2-1/2 percent represent cash cost, the remainder is increased depreciation. Therefore, the primary financial issue is financing the cost of modification, additional spares, and the interest on the investment.

One possible financing scheme is rebating narrow-bodied federal ticket tax receipts to the airline operators, providing, in effect, a government guarantee of the capital cost. The rebate itself could consist of some part or all of the ticket tax receipts. Each DC-8 yields ticket taxes of about $1.25 million per year, or about $175 million for the DC-8 domestic fleet. A quick comparison of these receipts against the required expenditures shows that it is indeed financially feasible to guarantee this investiment over a relatively short recovery period. Figure D-28 shows the ticket tax percentages required to recover the DC-8 investment, including spares and 7 percent interest over a time period ranging from 3 to 13 years. At a simple interest rate of 7 percent, it would take 41% of the ticket tax receipts to liquidate the $445 million (current dollars) principal and interest over the 8-year period.

Benefits and Dominant Cases

The study covers four levels of DC-8-61 noise treatment: existing and refanned minimum, intermediate and maximum; and three levels of DC-8-63 noise treatment: existing, and refan minimum and maximum. In addition, both cutback and no cutback takeoff procedures are possible, making a total of 24 DC-8 possibilities. The cost of maximum treatment for the DC-8-61 (requiring a long duct pod) without also refanning the DC-8-63 would be exorbitant. Therefore, two possibilities were eliminated: cutback and no cutback for the maximum DC-8-61 and existing DC-8-63 cases.

The resulting reduction in the area of 90 EPNdB noise contours is shown on the abscissa of figure D-29, while the cost of attaining that area is

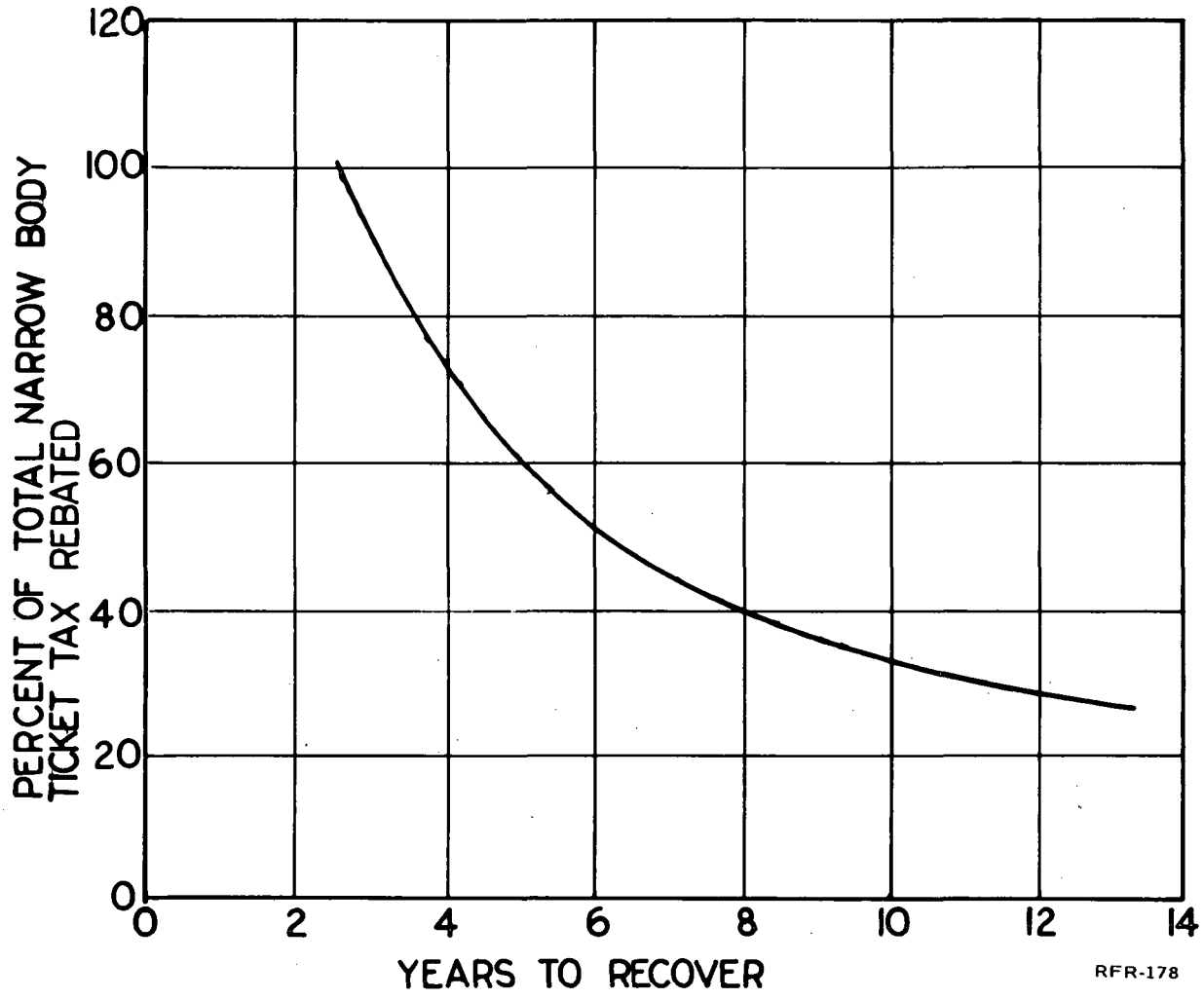

FIGURE D-28. DC-8 REFAN PROGRAM PERCENT FORECAST TICKET TAX REBATE VERSUS RECOVERY PERIOD FOR 7-PERCENT SIMPLE INTEREST

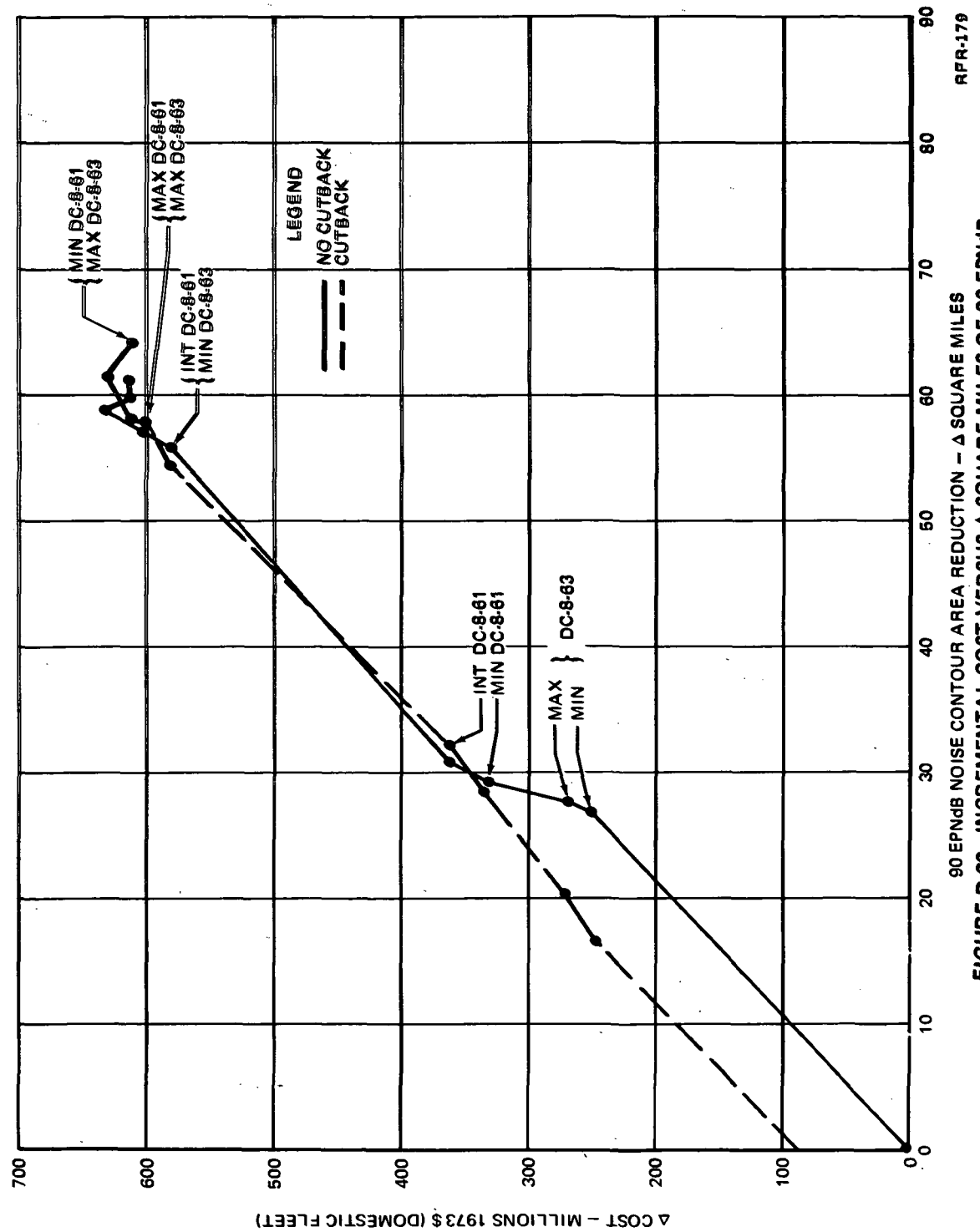

FIGURE D-28. INCREMENTAL COST VERSUS Δ SQUARE MILES OF 90 EPNdB

shown by the ordinate. Each refan combination generates a single cost and two reductions; one each for the takeoff cutback and no takeoff cutback cases. The plot shows that some cases clearly dominate others; e.g., the minimum and maximum DC-8-63 without cutback, while in most other cases the dominance is less clear cut. Nevertheless, the assumed 50-50 takeoff mix of DC-8-61's and DC-8-63's tends to eliminate many cases. The maximum treatment of both the DC-8-61 and DC-8-63 is both cheaper and more effective than combinations of intermediate DC-8-61 treatment and either level of DC-8-63 treatment. This occurs as a result of the commonality benefits of a common long duct pod. The other reasonable high area reduction cases are the minimum DC-8-61/maximum DC-8-63 case where the cutback procedure is slightly favored, and the minimum DC-8-61/minimum DC-8-63 where no cutback is slightly preferred. These results are summarized in table D-18.

The results have shown that it is technically feasible and economically viable, assuming low cost financing and no spillover effects, to refan the DC-8 fleet provided that the noise reductions really significantly contribute to improving the near airport noise environment.

TABLE D-18

SELECTED CONFIGURATIONS AND PROCEDURES

DC-8-63/-62 TREATMENT LEVEL	DC-8-61 TREATMENT LEVEL			
	Existing	Minimum	Intermediate	Maximum
Existing	No Cutback	No Cutback	Cutback	Not Applicable
Minimum	No Cutback	No Cutback	Out	Out
Maximum	No Cutback	Cutback	Out	Cutback

REFERENCES

1. Callaghan, J. T., Donelson, J. E., and Morelli, J. P., The Effects on Cruise Drag of Installing Refan-Engine Nacelles on the McDonnell-Douglas DC-9. NASA CR-121219, 1973.

2. Chrisenberry, H. E., Doss, P. G., Kressly, A. E., Prichard, R. D., and Thorndike, C. S., The Results of a Low Speed Wind Tunnel Test to Investigate the Effects of Installing Refan JT8D Engines on the McDonnell-Douglas DC-9-30. NASA CR-121220, 1973.

3. Callaghan, J. T., Donelson, J. E., and Morelli, J. P., The Effects on Cruise Drag of Installing Long-Duct Refan-Engine Nacelles on the McDonnell-Douglas DC-8-50 and -61. NASA CR-121218, 1973.

SYMBOLS

$\frac{A}{A_{min}}$	Ratio of local channel cross-sectional area to minimum value
AC	Alternating Current
ALT	Altitude
ATA	Air Transport Association
b/2	Wing semi-span normal to plane of symmetry
BPR	By-Pass Ratio
BRGW	Brake Release Gross Weight
C	Wing chord at location of pressure orifices
CB	Cutback
C_D	Airplane drag coefficient, Drag/q_o S_w
C_D	Incremental drag coefficient
$\bar{c}_e$	MAC of S_e
c.g.	Center of gravity
C_{H_e}	Elevator hinge moment coefficient $\frac{\text{hinge moment}}{q_o S_e \bar{c}_e}$, positive trailing edge down
C_L	Airplane lift coefficient, Lift/q_o S_w
C_m	Pitching moment coefficient, $\frac{\text{pitching moment}}{q_o S_w \bar{c}_w}$, positive airplane nose-up
C_{m_A}	Total airplane pitching moment coefficient
$C_{mc/4}$	C_m about the wing 1/4 MAC
ΔC_m	Incremental pitching moment coefficient
$C_{m_{C_L}}$	$\partial C_m / \partial C_L$
$C_{m_{\alpha_F}}$	$\partial C_m / \partial \alpha_F$

C_p	Pressure coefficient, $\frac{P_L - P_o}{qo}$
CP	Center of Pressure
CSD	Constant Speed Drive
$\bar{c}_w$	MAC of wing
CYC	Cycle
dB	Decibels
D_{BASE}	Base Drag
D_{NAC}	Nacelle Drag
D_{RAM}	Ram Drag
DOC	Direct Operating Cost
EFF	Fan Adiabatic Efficient
EPNdB	Effective Perceived Noise Levels in Decibels
EPNL	Effective Perceived Noise Level
EXT	Slats extended
FAR	Federal Aviation Regulations
FH	Flight Hours
F_N	Uninstalled Net Thrust
F_{NC}	Installed Net Thrust
FPR	Fan Pressure Ratio
HUB	Blade Hub
Hz	Hertz
IGV	Inlet Guide Vanes
i_H	Horizontal stabilizer incidence-positive trailing edge shown
ℓ_i	Inlet length (from engine face)
INT.	Intermediate
I_p	Pitch Moment of Inertia

L	Nozzle length
L/H	Nozzle length-to-height ratio
LPT	Low Pressure Turbine
M	Flight Mach Number
MAC	Mean Aerodynamic Chord
MAX	Maximum
M_{AXIAL}	Axial Mach Number
MEW	Manufacturer's Empty Weight
MIN	Minimum
M_L	Local Mach Number
MLW	Maximum Design Landing Weight
MMH	Maintenance Man Hour
M_o	Freestream Mach number
M_{REL}	Blade Row Relative Inlet Mach Number
MTOW	Maximum Takeoff Gross Weight
MTW	Maximum Design Taxi Weight
N_1	Low Speed Rotor rpm
$N_1\sqrt{\theta}$	Fan Corrected Rotor Speed
NEF	Noise Exposure Forecast
OEW	Operational Empty Weight
P_L	Local static pressure
PNdB	Units of PNL in Decibels
PNL	Perceived Noise Level
PNLT	Tone Corrected Perceived Noise Level
$P_{REV}dA_{FR}$	Induced Pressure Force
P_o	Freestream static pressure

P&WA	Pratt & Whitney Aircraft
q_o	Freestream dynamic pressure, $0.7\ P_o\ M_o^2$
RET	Slats retracted
rpm	Revolutions per minute
S_e	Elevator Area aft of hinge line
SFC	Specific Fuel Consumption
SL	Sea Level
SLS	Sea Level Static
S_w	Wing reference area
T	Sea Level Static Thrust
TIP	Blade Tip
TO	Takeoff
TMT	Treatment
TSFC	Thrust Specific Fuel Consumption
V	Speed, knots
V_C	Cruise Speed
V_{FAN}	Fan Jet Velocity
V_{MC}	Airplane Minimum Control Speed
V_{PRI}	Primary Jet Velocity
V_{s_i}	FAA certified stall speed
W_T	Total Fan inlet flow rate
W_c	Core Flow Rate
W_m	Windmilling
X	Aircraft Inboard-Outboard Station
Y	Aircraft Fore-Aft Station
Z	Aircraft Vertical Station

SUBSCRIPTS OF X, Y and Z

N	Nacelle
Ip	Inboard pylon
Op	Outboard pylon
α_F	Fuselage angle-of-attack
δe	Elevator deflection - positive trailing edge down
δF	Flap deflection
$\ddot{\Theta}$	Pitch Acceleration

Page Intentionally Left Blank

REPORT DISTRIBUTION LIST

Addressee			Number of Copies
1. NASA Lewis Research Center 21000 Brookpark Road Cleveland, Ohio 44135			
Attention:	Report Control Office	MS: 5-5	1
	Library	MS: 60-3	2
	Dr. B. Lubarsky	MS: 3-3	1
	A. A. Medeiros	MS: 501-7	25
	F. O. Driscoll	MS: 500-206	1
	N. T. Musual	MS: 500-113	1
	M. A. Beheim	MS: 86-1	1
	D. N. Bowditch	MS: 86-1	1
	R. J. Rulis	MS: 501-7	1
	U. H. von Glahn	MS: 501-4	1
	W. L. Stewart	MS: 501-5	1
	R. W. Schroeder	MS: 501-5	1
	R. W. Luidens	MS: 501-4	1
2. NASA Scientific and Technical Information Facility			10
Attention:	Acquisitions Branch P.O. Box 33 College Park, Maryland 20740		
3. NASA Headquarters 600 Independence Ave., S.W. Washington, DC 20546			
Attention:	Code RJ/William H. Roudebush		1
	Code RJ/Frederick P. Povinelli		5
	Code RL/Harry W. Johnson		1
	Code RO/Kenneth E. Hodge		1
	Code KSS-10/Library		1
4. Environmental Protection Agency 8th Floor 1835 K Street, N.W. Washington, DC 20460			
Attention:	John Schettino		1
	William Sperry		1
5. Federal Aviation Administration 800 Independence Ave., S.W. Washington, DC 20591			
Attention:	Robert J. Koenig (Code ARD-551)		1
	James F. Woodall (Code ARD-500)		1

Addressee			Number of Copies
6.	Office of Environmental Quality 800 Independence Ave., S.W. Washington, DC 20591		
	Attention: John O. Powers (Code AEQ-2)		1
	Richard P. Skully (Code AEQ-1)		1
7.	Department of Transportation 400 7th Street, S.W. Washington, DC 20590		
	Attention: Charles R. Foster		1
	Bernard Maggin (Code TST-51)		1
8.	NASA Langley Research Center Hampton, Virginia 23365		
	Attention: Harry T. Norton, Jr.	MS: 249A	1
	Tom F. Bonner, Jr.	MS: 257	1
9.	NASA Ames Research Center Moffett Field, Calif. 94035		
	Attention: Library	MS: 202-3	1
	Stuart Treon	MS: 227-5	1
	David Hickey	MS: 221-2	1
10.	NASA Flight Research Center P.O. Box 273 Edwards, Calif. 93523		
	Attention: Donal Bellman	Room 2106	1
	Library		1
11.	United Air Lines SFO EG San Francisco International Airport San Francisco, Calif. 94128		
	Attention: L. C. Ellis		1
	R. A. Gustafson		1
12.	American Airlines 633 Third Ave. New York, New York 10017		
	Attention: G. P. Sallee		1
13.	The Boeing Company Commercial Airplane Group P.O. Box 3707 Seattle, Washington 98124		
	Attention: K. P. Rice		1
	G. J. Schott		1
	R. W. Colebrook		1

Addressee	Number of Copies
14. Pratt & Whitney Aircraft 400 Main Street E. Hartford, Conn. 06108	
Attention: G. M. McRae	2
15. The Boeing Company 3801 S. Oliver Street Wichita, Kansas 67210	
Attention: Floyd Palmer	1
16. Rohr Corporation P.O. Box 878 Chula Vista, Calif. 92012	
Attention: F. A. Nickols	1
S. Beggs	1
17. General Electric Company Aircraft Engine Group - E198 Cincinnati, Ohio 45215	
Attention: John T. Kutney	1
18. LTV Aerospace Corporation P.O. Box 6267 Dallas, Texas 75222	
Attention: F. T. Esenwein	1
19. McDonnell Douglas Corporation Box 516 St. Louis, Mo. 63166	
Attention: Carl F. Schueller MS: 152, Bldg. 33	1
20. General Dynamics Corporation P.O. Box 748 Fort Worth, Texas 76101	
Attention: Gene Miller, Dept. 420 - Plant 35	1
21. Lockheed California Company P.O. Box 551 Burbank, Calif. 91503	
Attention: John Stroud	1
Harry Drell	1
22. Lockheed Georgia Company Marietta, Georgia 30060	
Attention: J. P. Hancock	1
J. M. Saylor	1

Addressee	Number of Copies
23. North American Rockwell 4300 E. Fifth Avenue Columbus, Ohio	
Attention: L. W. Throndson	1
24. AF Flight Dynamics Laboratory (FDMM) Wright-Patterson AFB, Ohio 45433	
Attention: J. A. Laughrey	1
25. Allison Division, GMC P.O. Box 894 Indianapolis, Indiana 46206	
Attention: Von D. Baker	1
26. North American Rockwell Los Angeles Division International Airport Los Angeles, Calif. 90009	
Attention: Leonard Rose	1